About the Book...

About the Author...

TAYLOR & FRANCIS
Founded 1798

ISBN 1-56032-712-X
90000>

MECHANICS OF COMPOSITE MATERIALS

MECHANICS OF COMPOSITE MATERIALS

Second Edition

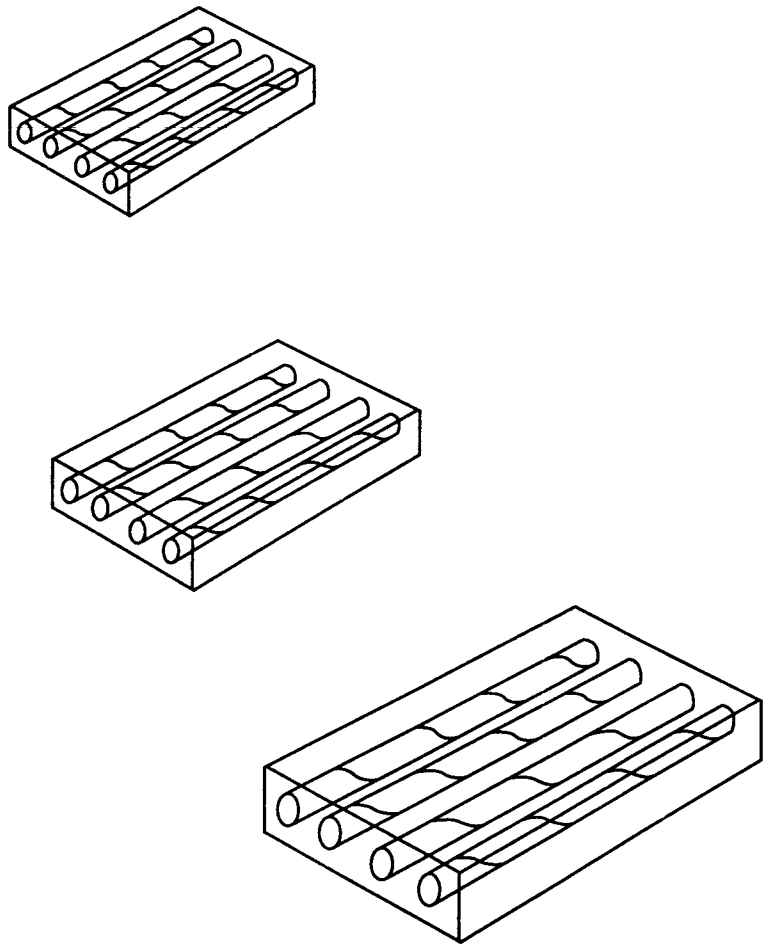

MECHANICS OF COMPOSITE MATERIALS

SECOND EDITION

MECHANICS OF COMPOSITE MATERIALS

SECOND EDITION

ROBERT M. JONES

Professor of Engineering Science and Mechanics
Virginia Polytechnic Institute and State University
Blacksburg, Virginia 24061-0219

USA Publishing Office: Taylor & Francis, Inc.
325 Chestnut Street
Philadelphia, PA 19106
Tel: (215) 625-8900
Fax: (215) 625-2940

Distribution Center: Taylor & Francis, Inc.
47 Runway Road, Suite G
Levittown, PA 19057-4700
Tel: (215) 629-0400
Fax: (215) 629-0363

UK Taylor & Francis Ltd.
1 Gunpowder Square
London EC4A 3DE
Tel: 171 583 0490
Fax: 171 583 0581

MECHANICS OF COMPOSITE MATERIALS, 2/E

1 2 3 4 5 6 7 8 9 0

This book was produced in IBM Generalized Markup Language by Robert M. Jones and Karen S. Devens. Cover design by Michelle Fleitz.
Printing by Edwards Brothers, Ann Arbor, MI, 1998.

A CIP catalog record for this book is available from the British Library.
♾ The paper in this publication meets the requirements of the ANSI Standard Z39.48-1984 (Permanence of Paper)

Library of Congress Cataloging-in-Publication Data

Jones, Robert M. (Robert Millard)
Mechanics of composite materials / Robert M. Jones --- 2nd ed.
p. cm.
Includes bibliographical references and index.
ISBN 1-56032-712-X (hardcover : alk. paper)
1. Composite materials --- Mechanical properties. 2. Laminated materials --- Mechanical properties. I. Title.
TA418.9.C6J59 1999
620.1'1892---dc21 98-18290
CIP

ISBN: 1-56032-712-X (hardcover)

CONTENTS

PREFACE TO THE SECOND EDITION

More than two decades have passed since the first edition of this book appeared in 1975. During that time, composite materials have progressed from almost an engineering curiosity to a widely used material in aerospace applications, as well as many other applications in everyday life. Accordingly, the contents of the first edition, although in most respects timeless fundamental mechanical behavior and mechanics analyses, must be expanded and updated.

The specific revisions include more thorough explanation of many concepts, enhanced comparisons between theory and experiment, more reader-friendly figures, figures that are more visually obvious in portrayal of fibers and deformations, description of experimental measurements of properties, expanded coverage of lamina failure criteria including an evaluation of how failure criteria are obtained, and more comprehensive description of laminated plate deflection, buckling, and vibration problems. Moreover, laminate design is introduced as part of the structural design process.

The 'latest' research results are deliberately not included. That is, this book is a fundamental teaching text, not a monograph on contemporary composite materials and structures topics. Thus, topics are chosen for their importance to the basic philosophy which includes simplicity of presentation and 'absorbability' by newcomers to composite materials and structures. More advanced topics as well as the nuances of covered topics can be addressed after this book is *digested*.

I have come to expect my students to interpret or transform the sometimes highly abbreviated, and thus relatively uninformative, problem set statements at the end of each section such as 'derive Equation (3.86)' to the more formal, descriptive, and revealing form:

Given:	A composite material is to be designed.
Required:	Find the critical fiber-volume fraction necessary to ensure that the composite material strength exceeds the matrix strength, i.e., derive Equation (3.86).

Moreover, I expect students to explain on a physical basis where they start and what objectives they're trying to meet. In doing so, they should carefully explain the nature of the problem as well as its solution. I want students to gain some perspective on the problem to more fully under-

stand the text. That is, I want them to focus on *The Why* of each problem so they will develop a feeling for the behavior of composite materials and structures. I also expect use of appropriate figures that are well discussed. Figures that have not been fully interpreted for the reader are of questionable value and certainly leave room for misinterpretation. Also, I expect students to explain and describe each step in the problem-solving process with physically based reasons and explanations. Moreover, I expect observations, comments, and conclusions about what they learned at the end of each problem. I feel such requirements are good training for survival in today's and tomorrow's more competitive world.

Completion of the problems will often require thoughtful analysis of the conditions and search for the correct solution. Thus, the problems are often not trivial or straightforward. The required mathematics are senior level except for the elasticity solutions in the micromechanics chapter where obviously the level must be higher (but the elasticity sections can be skipped in lower-level classes).

I am delighted to express my appreciation to the attendees of more than 80 short courses from 1971 through 1995 at government laboratories, companies, and open locations. They helped shape this second edition by their questions and comments, as did the more than twenty university classes I taught over the years.

I thank those who offered suggestions and corrections from their experience with the first edition. I am also delighted to express my appreciation to those who contributed to both editions: Patrick Barr (now M.D.!) for illustrations in the first edition, some of which are used in the second edition; Ann Hardell for Adobe Illustrator illustrations in the second edition; my daughter, Karen Devens, for IBM Script and GML text production; and my secretary, Norma Guynn, for miscellaneous typing.

Blacksburg, Virginia
April 1998

PREFACE TO THE FIRST EDITION

Composite materials are ideal for structural applications where high strength-to-weight and stiffness-to-weight ratios are required. Aircraft and spacecraft are typical weight-sensitive structures in which composite materials are cost-effective. When the full advantages of composite materials are utilized, both aircraft and spacecraft will be designed in a manner much different from the present.

The study of composite materials actually involves many topics, such as, for example, manufacturing processes, anisotropic elasticity, strength of anisotropic materials, and micromechanics. Truly, no one individual can claim a complete understanding of all these areas. Any practitioner will be likely to limit his attention to one or two subareas of the broad possibilities of analysis versus design, micromechanics versus macromechanics, etc.

The objective of this book is to introduce the student to the basic concepts of the mechanical behavior of composite materials. Actually, only an overview of this vast set of topics is offered. The balance of subject areas is intended to give a fundamental knowledge of the broad scope of composite materials. The mechanics of laminated fiber-reinforced composite materials are developed as a continuing example. Many important topics are ignored in order to restrict the coverage to a one-semester graduate course. However, the areas covered do provide a firm foundation for further study and research and are carefully selected to provide continuity and balance. Moreover, the subject matter is chosen to exhibit a high degree of comparison between theory and experiment in order to establish confidence in the derived theories.

The whole gamut of topics from micromechanics and macromechanics through lamination theory and examples of plate bending, buckling, and vibration problems is treated so that the physical significance of the concepts is made clear. A comprehensive introduction to composite materials and motivation for their use in current structural applications is given in Chapter 1. Stress-strain relations for a lamina are displayed with engineering material constants in Chapter 2. Strength theories are also compared with experimental results. In Chapter 3, micromechanics is introduced by both the mechanics of materials approach and the elasticity approach. Predicted moduli are compared with measured values. Lamination theory is presented in Chapter 4 with the aid of a new laminate classification scheme. Laminate stiffness predictions are compared with experimental results. Laminate strength con-

cepts, as well as interlaminar stresses and design, are also discussed. In Chapter 5, bending, buckling, and vibration of a simply supported plate with various lamination characteristics is examined to display the effects of coupling stiffnesses in a physically meaningful problem. Miscellaneous topics such as fatigue, fracture mechanics, and transverse shear effects are addressed in Chapter 6. Appendices on matrices and tensors, maxima and minima of functions of a single variable, and typical stress-strain curves are provided.

This book was written primarily as a graduate-level textbook, but is well suited as a guide for self-study of composite materials. Accordingly, the theories presented are simple and illustrate the basic concepts, although they may not be the most accurate. Emphasis is placed on analyses compared with experimental results, rather than on the most recent analysis for the material currently 'in vogue.' Accuracy may suffer, but educational objectives are better met. Many references are included to facilitate further study. The background of the reader should include an advanced mechanics of materials course or separate courses in which three-dimensional stress-strain relations and plate theory are introduced. In addition, knowledge of anisotropic elasticity is desirable, although not essential.

Many people have been most generous in their support of this writing effort. I would like to especially thank Dr. Stephen W. Tsai, of the Air Force Materials Laboratory, for his inspiration by example over the past ten years and for his guidance throughout the past several years. I deeply appreciate Steve's efforts and those of Dr. R. Bryon Pipes of the University of Delaware and Dr. Thomas Cruse of Pratt and Whitney Aircraft, who reviewed the manuscript and made many helpful comments. Still others contributed material for the book. My thanks to Marvin Howeth of General Dynamics, Forth Worth, Texas, for many photographs; to John Pimm of LTV Aerospace Corporation for the photograph in Section 4.7; to Dr. Nicholas Pagano of the Air Force Materials Laboratory for many figures; to Dr. R. Byron Pipes of the University of Delaware for many photographs and figures in Section 4.6; and to Dr. B. Walter Rosen of Materials Sciences Corporation, Blue Bell, Pennsylvania, for the photo in Section 3.5. I also appreciate the permission of the Technomic Publishing Company, Inc., of Westport, Connecticut, to reprint throughout the text many figures which have appeared in the various Technomic books and in the *Journal of Composite Materials* over the past several years. I am very grateful for support by the Air Force Office of Scientific Research (Directorate of Aerospace Sciences) and the Office of Naval Research (Structural Mechanics Program) of my research on laminated plates and shells discussed in Chapters 5 and 6. I am also indebted to several classes at the Southern Methodist Institute of Technology and the Naval Air Development Center, Warminister, Pennsylvania, for their patience and help during the development of class notes that led to this book. Finally, I must single out Harold S. Morgan for his numerous contributions and Marty Kunkle for her manuscript typing (although I did some of the typing myself!).

R.M.J.

First Edition:

To my neglected family:
Donna, Mark, Karen, and Christopher

Second Edition:

To Christopher:
He helped many others,
but he couldn't help himself

Chapter 1

INTRODUCTION TO COMPOSITE MATERIALS

1.1 INTRODUCTION

The objective of this chapter is to address the three basic questions of composite materials and structures in Figure 1-1: (1) What is a composite material? (2) Why are composite materials used instead of metals? and (3) How are composite materials used in structures? As part of The What, the general set of composite materials will be defined, classified, and characterized. Then, our attention will be focused on laminated fiber-reinforced composite materials for this book. Finally, to help us understand the nature of the material we are trying to model with mechanics equations, we will briefly describe manufacturing of composite materials and structures. In The Why, we will investigate the advantages of composite materials over metals from the standpoints of strength, stiffness, weight, and cost among others. Finally, in The How, we will look into examples and short case histories of important structural applications of composite materials to see even more reasons why composite materials play an ever-expanding role in today's and tomorrow's structures.

- **THE WHAT**

  WHAT IS A COMPOSITE MATERIAL?
- **THE WHY**

  WHY ARE COMPOSITE MATERIALS USED INSTEAD OF METALS?
- **THE HOW**

  HOW ARE COMPOSITE MATERIALS USED IN STRUCTURAL APPLICATIONS?

Figure 1-1 Basic Questions of Composite Materials and Structures

1.2 THE WHAT — WHAT IS A COMPOSITE MATERIAL?

The word *composite* in the term *composite material* signifies that two or more materials are combined on a macroscopic scale to form a useful third material. The key is the macroscopic examination of a material wherein the components can be identified by the naked eye. Different materials can be combined on a microscopic scale, such as in alloying of metals, but the resulting material is, for all practical purposes, macroscopically homogeneous, i.e., the components cannot be distinguished by the naked eye and essentially act together. The advantage of composite materials is that, if well designed, they usually exhibit the best qualities of their components or constituents and often some qualities that neither constituent possesses. Some of the properties that can be improved by forming a composite material are

- strength
- stiffness
- corrosion resistance
- wear resistance
- attractiveness
- weight
- fatigue life
- temperature-dependent behavior
- thermal insulation
- thermal conductivity
- acoustical insulation

Naturally, not all of these properties are improved at the same time nor is there usually any requirement to do so. In fact, some of the properties are in conflict with one another, e.g., thermal insulation versus thermal conductivity. The objective is merely to create a material that has only the characteristics needed to perform the design task.

Composite materials have a long history of usage. Their precise beginnings are unknown, but all recorded history contains references to some form of composite material. For example, straw was used by the Israelites to strengthen mud bricks. Plywood was used by the ancient Egyptians when they realized that wood could be rearranged to achieve superior strength and resistance to thermal expansion as well as to swelling caused by the absorption of moisture. Medieval swords and armor were constructed with layers of different metals. More recently, fiber-reinforced, resin-matrix composite materials that have high strength-to-weight and stiffness-to-weight ratios have become important in weight-sensitive applications such as aircraft and space vehicles.

1.2.1 Classification and Characteristics of Composite Materials

Four commonly accepted types of composite materials are:

(1) *Fibrous composite materials* that consist of fibers in a matrix
(2) *Laminated composite materials* that consist of layers of various materials
(3) *Particulate composite materials* that are composed of particles in a matrix
(4) Combinations of some or all of the first three types

These types of composite materials are described and discussed in the following subsections. I am indebted to Professor A. G. H. Dietz [1-1] for the character and much of the substance of the presentation.

1.2.1.1 Fibrous Composite Materials

Long fibers in various forms are inherently much stiffer and stronger than the same material in bulk form. For example, ordinary plate glass fractures at stresses of only a few thousand pounds per square inch (lb/in^2 or psi) (20 MPa), yet glass fibers have strengths of 400,000 to 700,000 psi (2800 to 4800 MPa) in commercially available forms and about 1,000,000 psi (7000 MPa) in laboratory-prepared forms. Obviously, then, the geometry and physical makeup of a fiber are somehow crucial to the evaluation of its strength and must be considered in structural applications. More properly, the paradox of a fiber having different properties from the bulk form is due to the more perfect structure of a fiber. In fibers, the crystals are aligned along the fiber axis. Moreover, there are fewer internal defects in fibers than in bulk material. For example, in materials that have dislocations, the fiber form has fewer dislocations than the bulk form.

Properties of Fibers

A fiber is characterized geometrically not only by its very high length-to-diameter ratio but by its near-crystal-sized diameter. Strengths and stiffnesses of a few selected fiber materials are arranged in increasing average S/ρ and E/ρ in Table 1-1. The common structural materials, aluminum, titanium, and steel, are listed for the purpose of comparison. However, a direct comparison between fibers and structural metals is not valid because fibers must have a surrounding matrix to perform in a structural member, whereas structural metals are 'ready-to-use'. Note that the density of each material is listed because the strength-to-density and stiffness-to-density ratios are commonly used as indicators of the effectiveness of a fiber, especially in weight-sensitive applications such as aircraft and space vehicles.

Table 1-1 Fiber and Wire Properties*

Fiber or Wire	Density, ρ lb/in^3 (kN/m^3)	Tensile Strength, S 10^3 lb/in^2 (GN/m^2)	S/ρ 10^5 in (km)	Tensile Stiffness, E 10^6 lb/in^2 (GN/m^2)	E/ρ 10^7 in (Mm)
Aluminum	.097 (26.3)	90 (.62)	9 (24)	10.6 (73)	11 (2.8)
Titanium	.170 (46.1)	280 (1.9)	16 (41)	16.7 (115)	10 (2.5)
Steel	.282 (76.6)	600 (4.1)	21 (54)	30 (207)	11 (2.7)
E-Glass	.092 (25.0)	500 (3.4)	54 (136)	10.5 (72)	11 (2.9)
S-Glass	.090 (24.4)	700 (4.8)	78 (197)	12.5 (86)	14 (3.5)
Carbon	.051 (13.8)	250 (1.7)	49 (123)	27 (190)	53 (14)
Beryllium	.067 (18.2)	250 (1.7)	37 (93)	44 (300)	66 (16)
Boron	.093 (25.2)	500 (3.4)	54 (137)	60 (400)	65 (16)
Graphite	.051 (13.8)	250 (1.7)	49 (123)	37 (250)	72 (18)

*Adapted from Dietz [1-1]

Graphite or carbon fibers are of high interest in today's composite structures. Both are made from rayon, pitch, or PAN (polyacrylonitrile) precursor fibers that are heated in an inert atmosphere to about 3100°F (1700°C) to carbonize the fibers. To get graphite fibers, the heating exceeds 3100°F (1700°C) to partially graphitize the carbon fibers. Actual processing is proprietary, but fiber tension is known to be a key processing parameter. Moreover, as the processing temperature is increased, the fiber modulus increases, but the strength often decreases. The fibers are typically far thinner than human hairs, so they can be bent quite easily. Thus, carbon or graphite fibers can be woven into fabric. In contrast, boron fibers are made by vapor depositing boron on a tungsten wire and coating the boron with a thin layer of boron carbide. The fibers are about the diameter of mechanical pencil lead, so they cannot be bent or woven into fabric.

Properties of Whiskers

A whisker has essentially the same near-crystal-sized diameter as a fiber, but generally is very short and stubby, although the length-to-diameter ratio can be in the hundreds. Thus, a whisker is an even more obvious example of the crystal-bulk-material-property-difference paradox. That is, a whisker is even more perfect than a fiber and therefore exhibits even higher properties. Whiskers are obtained by crystallization on a very small scale resulting in a nearly perfect alignment of crystals. Materials such as iron have crystalline structures with a theoretical strength of 2,900,000 psi (20 GPa), yet commercially available structural steels, which are mainly iron, have strengths ranging from 75,000 psi to about 100,000 psi (570 to 690 MPa). The discrepancy between theoretical and actual strength is caused by imperfections in the crystalline structure of steel. Those imperfections are called dislocations and are easily moved for ductile materials. The movement of dislocations changes the relation of the crystals and hence the strength and stiffness of the material. For a nearly perfect whisker, few dislocations exist. Thus, whiskers of iron have significantly higher strengths than steel in bulk form. A representative set of whisker properties is given in Table 1-2 along with three metals (as with fibers, whiskers cannot be used alone, so a direct comparison between whiskers and metals is not meaningful).

Table 1-2 Whisker Properties*

Whisker	Density, ρ lb/in^3 (kN/m^3)	Theoretical Strength, S_T 10^6 lb/in^2 (GN/m^2)	Experimental Strength S_E 10^6 lb/in^2 (GN/m^2)	S_E/ρ 10^5 in (km)	Tensile Stiffness, E 10^6 lb/in^2 (GN/m^2)	E/ρ 10^7 in (Mm)
Copper	.322 (87.4)	1.8 (12)	.43 (3.0)	13 (34)	18 (124)	6 (1.4)
Nickel	.324 (87.9)	3.1 (21)	.56 (3.9)	17 (44)	31 (215)	10 (2.5)
Iron	.283 (76.8)	2.9 (20)	1.9 (13)	67 (170)	29 (200)	10 (2.6)
B_4C	.091 (24.7)	6.5 (45)	.97 (6.7)	106 (270)	65 (450)	71 (18)
SiC	.115 (31.2)	12 (83)	1.6 (11)	139 (350)	122 (840)	106 (27)
Al_2O_3	.143 (38.8)	6 (41)	2.8 (19)	196 (490)	60 (410)	42 (11)
C	.060 (16.3)	14.2 (98)	3 (21)	500 (1300)	142 (980)	237 (60)

*Adapted from Sutton, Rosen, and Flom [1-2] *(Courtesy of Society of Plastic Engineers Journal).*

Properties of Matrix Materials

Naturally, fibers and whiskers are of little use unless they are bonded together to take the form of a structural element that can carry loads. The binder material is usually called a matrix (not to be confused with the mathematical concept of a matrix). The purpose of the matrix is manifold: support of the fibers or whiskers, protection of the fibers or whiskers, stress transfer between broken fibers or whiskers, etc. Typically, the matrix is of considerably lower density, stiffness, and strength than the fibers or whiskers. However, the combination of fibers or whiskers and a matrix can have very high strength and stiffness, yet still have low density. Matrix materials can be polymers, metals, ceramics, or carbon. The cost of each matrix escalates in that order as does the temperature resistance.

Polymers (poly ≡ many and mer ≡ unit or molecule) exist in at least three major forms: linear, branched, or cross-linked. A *linear polymer* is merely a chain of mers. A *branched polymer* consists of a primary chain of mers with other chains that are attached in three dimensions just like tree branches in Figure 1-2. Finally, a *cross-linked polymer* has a large number of three-dimensional highly interconnected chains as in Figure 1-2. Linear polymers have the least strength and stiffness, whereas cross-linked polymers have the most because of their inherently stiffer and stronger internal structure. The three main classes of structural polymers are rubbers, thermoplastics, and thermosets. Rubbers are cross-linked polymers that have a semicrystalline state well below room temperature, but act as the rubber we all know above room temperature (remember the Challenger rubber O-rings that failed so catastrophically!). Thermoplastics are polymers that branch, but generally do not cross-link very much, if at all. Thus, they usually can be repeatedly softened by heating and hardened by cooling. Examples of thermoplastics include nylon, polyethylene, and polysulfone. Thermosets are polymers that are chemically reacted until almost all the molecules are *irreversibly cross-linked* in a three-dimensional network. Thus, once an epoxy has 'set', it cannot be changed in form. Examples of thermosets include epoxies, phenolics, and polyimides. A typical organic epoxy matrix material such

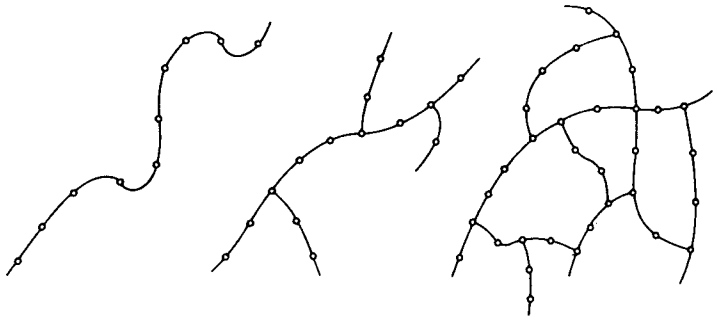

Figure 1-2 Polymer Structure

as Narmco 2387 [1-3] has a density of .044 lb/in^3 (11.9 kN/m^3), compressive strength of 23,000 psi (.158 GPa), compressive modulus of 560,000 psi (3.86 GPa), tensile strength of 4200 psi (.029 GPa), and tensile modulus of 490,000 psi (3.38 GPa).

Other matrix materials include metals that can be made to flow around an in-place fiber system by diffusion bonding or by heating and vacuum infiltration. Common examples include aluminum, titanium, and nickel-chromium alloys. Ceramic-matrix composite materials can be cast from a molten slurry around stirred-in fibers with random orientation or with preferred flow-direction orientation because of stirring or some other manner of introducing the ceramic. Alternatively, ceramic matrix material can be vapor deposited around a collection of already in-place fibers. Finally, carbon matrix material can be vapor deposited on an already in-place fiber system. Alternatively, liquid material can be infiltrated around in-place fibers and then carbonized in place by heating to high temperature. The process involving liquid infiltration and carbonization must be repeated many times because carbonizing the liquid results in decreased volume of the matrix. Until the voids can no longer be filled (they become disconnected as densification continues), the potential matrix strength and stiffness have not been achieved.

1.2.1.2 Laminated Composite Materials

Laminated composite materials consist of layers of at least two different materials that are bonded together. Lamination is used to combine the best aspects of the constituent layers and bonding material in order to achieve a more useful material. The properties that can be emphasized by lamination are strength, stiffness, low weight, corrosion resistance, wear resistance, beauty or attractiveness, thermal insulation, acoustical insulation, etc. Such claims are best represented by the examples in the following paragraphs in which bimetals, clad metals, laminated glass, plastic-based laminates, and laminated fibrous composite materials are described.

Bimetals

Bimetals are laminates of two different metals that usually have significantly different coefficients of thermal expansion. Under change in temperature, bimetals warp or deflect a predictable amount and are therefore well suited for use in temperature-measuring devices. For example, a simple thermostat can be made from a cantilever strip of two metals bonded together as shown in Figure 1-3. There, metal A has coefficient of thermal expansion α_A and metal B has α_B greater than α_A. Consider the two cases of (1) two unbonded metal strips of different coefficients of thermal expansion placed side by side but not bonded and (2) the same two strips bonded together. For case (1), at room temperature, the two strips are the same length. When they are heated, both strips elongate (their primary observable change, but they do also get wider and thicker). For case (2) at room temperature, the strips are also of the same length but bonded together. When the bonded bimetallic

strip is heated, strip B wants to expand more than strip A, but they are bonded, so strip B causes the bimetallic strip to bend! This bending under a loading that would otherwise seem to cause only extension is our first (qualitative) example of the *structural phenomenon of coupling between bending and extension* that we will study in more detail in Chapter 4.

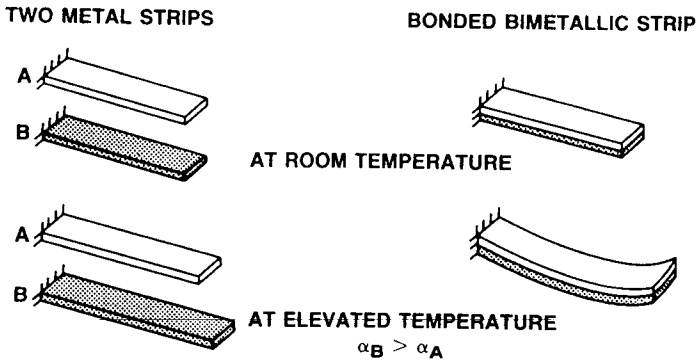

Figure 1-3 Cantilevered Bimetallic Strip (Thermostat)

Clad Metals

The cladding or sheathing of one metal with another is done to obtain the best properties of both. For example, high-strength aluminum alloys do not resist corrosion; however, pure aluminum and some aluminum alloys are very corrosion resistant but relatively weak. Thus, a high-strength aluminum alloy covered with a corrosion-resistant aluminum alloy is a composite material with both high strength and corrosion resistance which are unique and attractive advantages over the properties of its constituents.

In the 1960s, aluminum wire clad with about 10% copper was introduced as a replacement for copper wire in the electrical wiring market. Aluminum wire by itself is economical and lightweight, but overheats and is difficult to connect to terminals at wall switches and outlets. Aluminum wire connections expand and contract when the current is turned on or off so that fatigue breaks the wire causing shorts and, consequently, potential fires. On the other hand, copper wire is expensive and relatively heavy, but stays cool and can be connected easily to wall switches and outlets. The copper-clad aluminum wire is lightweight and connectable, stays cool, and is less expensive than copper wire. Moreover, copper-clad aluminum wire is nearly insusceptible to the usual construction-site problem of theft because of far lower salvage value than copper wire.

Laminated Glass

The concept of protection of one layer of material by another as described in the previous category, Clad Metals, has been extended in a rather unique way to automotive safety glass. Ordinary window glass

is durable enough to retain its transparency under the extremes of weather. However, glass is quite brittle and is dangerous because it can break into many sharp-edged pieces, especially in collisions. On the other hand, a plastic called polyvinyl butyral is very tough (deforms to high strains without fracture), but is very flexible and susceptible to scratching. Safety glass is a layer of polyvinyl butryal sandwiched between two layers of glass. The glass in the composite material protects the plastic from scratching and gives it stiffness. The plastic provides the toughness of the composite material. Thus, together, the glass and plastic protect each other in different ways and lead to a composite material with properties that are vastly improved over those of its constituents. In fact, the high-scratchability property of the plastic is totally eliminated because it is the *inner layer* of the composite laminate.

Plastic-Based Laminates

Many materials can be saturated with various plastics for a variety of purposes. The common product Formica is merely layers of heavy kraft paper impregnated with a phenolic resin overlaid by a plastic-saturated decorative sheet that, in turn, is overlaid with a plastic-saturated cellulose mat. Heat and pressure are used to bond the layers together. A useful variation on the theme is obtained when an aluminum layer is placed between the decorative layer and the kraft paper layer to quickly dissipate the heat of, for example, a burning cigarette or hot pan on a kitchen counter instead of leaving a burned spot. Formica is a good example of a compound composite material, i.e., one made of more than two constituents, each making an essential, but different, contribution to the resulting composite material.

Layers of glass or asbestos fabrics can be impregnated with silicones to yield a composite material with significant high-temperature properties. Glass, Kevlar, or nylon fabrics can be laminated with various resins to yield an impact- and penetration-resistant composite material that is uniquely suitable as lightweight personnel armor. The list of examples is seemingly endless, but the purpose of illustration is served by the preceding examples.

1.2.1.3 Particulate Composite Materials

Particulate composite materials consist of particles of one or more materials suspended in a matrix of another material. The particles can be either metallic or nonmetallic as can the matrix. The four possible combinations of these constituents are described in the following paragraphs.

Nonmetallic Particles in Nonmetallic Matrix Composite Materials

The most common example of a nonmetallic particle system in a nonmetallic matrix, indeed the most common composite material, is concrete. Concrete is particles of sand and gravel (rock particles) that are bonded together with a mixture of cement and water that has chemically reacted and hardened. The strength of the concrete is

normally that of the gravel because the cement matrix is stronger than the gravel. The accumulation of strength up to that of the gravel is varied by changing the type of cement in order to slow or speed the chemical reaction. Many books have been written on concrete and on a variation, reinforced concrete, that can be considered both a fibrous and a particulate composite material.

Flakes of nonmetallic materials such as mica or glass can form an effective composite material when suspended in a glass or plastic, respectively. Flakes have a primarily two-dimensional geometry with strength and stiffness in the two directions, as opposed to only one for fibers. Ordinarily, flakes are packed parallel to one another with a resulting higher density than fiber packing concepts. Accordingly, less matrix material is required to bond flakes than fibers. Flakes overlap so much that a flake composite material is much more impervious to liquids than an ordinary composite material of the same constituent materials. Mica-in-glass composite materials are extensively used in electrical applications because of good insulating and machining qualities. Glass flakes in plastic resin matrices have a potential similar to, if not higher than, that of glass-fiber composite materials. Even higher stiffnesses and strengths should be attainable with glass-flake composite materials than with glass-fiber composite materials because of the higher packing density. However, surface flaws reduce the strength of glass-flake composite materials from that currently obtained with more-perfect glass-fiber composite materials.

Metallic Particles in Nonmetallic Matrix Composite Materials

Solid-rocket propellants consist of inorganic particles such as aluminum powder and perchlorate oxidizers in a flexible organic binder such as polyurethane or polysulfide rubber. The particles comprise as much as 75% of the propellant leaving only 25% for the binder. The objective is a steadily burning reaction to provide controlled thrust. Thus, the composite material must be uniform in character and must not crack; otherwise, burning would take place in unsteady bursts that could actually develop into explosions that would, at the very least, adversely affect the trajectory of the rocket. The instantaneous thrust of a rocket is proportional to the burning surface area; thus, solid propellants are cast with, for example, a star-shaped hole instead of a circular hole. Many stress-analysis problems arise in connection with support of the solid propellant in a rocket-motor casing and with internal stresses due to dissimilar particle and binder stiffnesses. The internal stresses can be reduced by attempting to optimize the shape of the burning cross section; again, a reason for a noncircular hole.

Metal flakes in a suspension are common. For example, aluminum paint is actually aluminum flakes suspended in paint. Upon application, the flakes orient themselves parallel to the surface and give very good coverage. Similarly, silver flakes can be applied to give good electrical conductivity.

Cold solder is metal powder suspended in a thermosetting resin. The composite material is strong and hard and conducts heat and elec-

tricity. Inclusion of copper in an epoxy resin increases the conductivity immensely. Many metallic additives to plastic increase the thermal conductivity, lower the coefficient of thermal expansion, and decrease wear.

Metallic Particles in Metallic Matrix Composite Materials

Unlike an alloy, a metallic particle in a metallic matrix does not dissolve. Lead particles are commonly used in copper alloys and steel to improve the machinability (so that metal comes off in shaving form rather than in chip form). In addition, lead is a natural lubricant in bearings made from copper alloys.

Many metals are naturally brittle at room temperature, so must be machined when hot. However, particles of these metals, such as tungsten, chromium, molybdenum, etc., can be suspended in a ductile matrix. The resulting composite material is ductile, yet has the elevated-temperature properties of the brittle constituents. The actual process used to suspend the brittle particles is called liquid sintering and involves infiltration of the matrix material around the brittle particles. Fortunately, in the liquid sintering process, the brittle particles become rounded and therefore naturally more ductile.

Nonmetallic Particles in Metallic Matrix Composite Materials

Nonmetallic particles such as ceramics can be suspended in a metal matrix. The resulting composite material is called a cermet. Two common classes of cermets are oxide-based and carbide-based composite materials.

As a slight departure from the present classification scheme, oxide-based cermets can be either oxide particles in a metal matrix or metal particles in an oxide matrix. Such cermets are used in tool making and high-temperature applications where erosion resistance is needed.

Carbide-based cermets have particles of carbides of tungsten, chromium, and titanium. Tungsten carbide in a cobalt matrix is used in machine parts requiring very high hardness such as wire-drawing dies, valves, etc. Chromium carbide in a cobalt matrix has high corrosion and abrasion resistance; it also has a coefficient of thermal expansion close to that of steel, so is well-suited for use in valves. Titanium carbide in either a nickel or a cobalt matrix is often used in high-temperature applications such as turbine parts. Cermets are also used as nuclear reactor fuel elements and control rods. Fuel elements can be uranium oxide particles in stainless steel ceramic, whereas boron carbide in stainless steel is used for control rods.

1.2.1.4 Combinations of Composite Materials

Numerous multiphase composite materials exhibit more than one characteristic of the various classes, fibrous, laminated, or particulate composite materials, just discussed. For example, reinforced concrete is both particulate (because the concrete is composed of gravel in a cement-paste binder) and fibrous (because of the steel reinforcement).

Also, laminated fiber-reinforced composite materials are obviously both laminated and fibrous composite materials. Thus, any classification system is arbitrary and imperfect. Nevertheless, the system should serve to acquaint the reader with the broad possibilities of composite materials.

Laminated fiber-reinforced composite materials are a hybrid class of composite materials involving both fibrous composite materials and lamination techniques. Here, layers of fiber-reinforced material are bonded together with the fiber directions of each layer typically oriented in different directions to give different strengths and stiffnesses of the laminate in various directions. Thus, the strengths and stiffnesses of the laminated fiber-reinforced composite material can be tailored to the specific design requirements of the structural element being built. Examples of laminated fiber-reinforced composite materials include rocket motor cases, boat hulls, aircraft wing panels and body sections, tennis rackets, golf club shafts, etc.

1.2.2 Mechanical Behavior of Composite Materials

Composite materials have many mechanical behavior characteristics that are different from those of more conventional engineering materials. Some characteristics are merely modifications of conventional behavior; others are totally new and require new analytical and experimental procedures.

Most common engineering materials are both *homogeneous* and *isotropic:*

> A *homogeneous* body has uniform properties throughout, i.e., the properties are independent of *position* in the body.
>
> An *isotropic* body has material properties that are the same in every direction at a point in the body, i.e., the properties are independent of *orientation* at a point in the body.

Bodies with temperature-dependent isotropic material properties are not homogeneous when subjected to a temperature gradient, but still are isotropic.

In contrast, composite materials are often both *inhomogeneous* (or nonhomogeneous or heterogeneous — the three terms can be used interchangeably) and *nonisotropic* (orthotropic or, more generally, anisotropic, but the words are not interchangeable):

> An *inhomogeneous* body has nonuniform properties over the body, i.e., the properties depend on *position* in the body.
>
> An *orthotropic* body has material properties that are different in three mutually perpendicular directions at a point in the body and, further, has three mutually perpendicular planes of material property symmetry. Thus, the properties depend on orientation at a point in the body.

An *anisotropic* body has material properties that are different in all directions at a point in the body. No planes of material property symmetry exist. Again, the properties depend on *orientation* at a point in the body.

Some composite materials have very simple forms of inhomogeneity. For example, laminated safety glass has three layers, each of which is homogeneous and isotropic; thus, the inhomogeneity of the composite material is a step function in the direction perpendicular to the plane of the glass. Also, some particulate composite materials are inhomogeneous, yet isotropic, although some are orthotropic and others are anisotropic. Other composite materials are typically more complex, especially those with fibers placed at many angles in space.

Because of the inherently heterogeneous nature of composite materials, they are conveniently studied from two points of view: micromechanics and macromechanics:

Micromechanics is the study of composite material behavior wherein the *interaction* of the constituent materials is examined on a *microscopic* scale to determine their effect on the properties of the composite material.

Macromechanics is the study of composite material behavior wherein the material is presumed *homogeneous* and the effects of the constituent materials are detected only as *averaged apparent macroscopic properties* of the composite material.

In this book, attention will first be focused on macromechanics because it is the most readily appreciated of the two and the more important topic in structural design analysis. Subsequently, micromechanics will be investigated in order to gain an appreciation for how the constituents of composite materials can be proportioned and arranged to achieve certain specified strengths and stiffnesses.

Use of the two concepts of macromechanics and micromechanics allows the *tailoring* of a composite material to meet a particular structural requirement with little waste of material capability. The ability to tailor a composite material to its job is one of the most significant advantages of a composite material over an ordinary material. Perfect tailoring of a composite material yields only the stiffness and strength required in each direction, no more. In contrast, an isotropic material is, by definition, constrained to have excess strength and stiffness in any direction other than that of the largest required strength or stiffness.

The inherent anisotropy (most often only orthotropy) of composite materials leads to mechanical behavior characteristics that are quite different from those of conventional isotropic materials. The behavior of isotropic, orthotropic, and anisotropic materials under loadings of normal stress and shear stress is shown in Figure 1-4 and discussed in the following paragraphs.

For isotropic materials, application of normal stress causes extension in the direction of the stress and contraction in the perpendicular

directions, but no shearing deformation. Also, application of shear stress causes only shearing deformation, but no extension or contraction in any direction. Only two material properties, Young's modulus (the extensional modulus or slope of the material's stress-strain curve) and Poisson's ratio (the negative ratio of lateral contraction strain to axial extensional strain caused by axial extensional stress), are needed to quantify the deformations. The shear modulus (ratio of shear stress to shear strain at a point) could be used as an alternative to either Young's modulus or Poisson's ratio.

For orthotropic materials, like isotropic materials, application of normal stress in a principal material direction (along one of the intersections of three orthogonal planes of material symmetry) results in extension in the direction of the stress and contraction perpendicular to the stress. The magnitude of the extension in one principal material direction under normal stress in that direction is different from the extension in another principal material direction under the same normal stress in that other direction. Thus, different Young's moduli exist in the various principal material directions. In addition, because of different properties in the two principal material directions, the contraction can be either more or less than the contraction of a similarly loaded isotropic material with the same elastic modulus in the direction of the load. Thus, different Poisson's ratios are associated with different pairs of principal material directions (and with the order of the coordinate direction numbers designating the pairs). Application of shear stress causes shearing deformation, but the magnitude of the shearing deformation is totally independent of the various Young's moduli and Poisson's ratios. That is, the shear modulus of an orthotropic material is, unlike isotropic materials, not dependent on other material properties. Thus, at least five material properties are necessary to describe the mechanical behavior of orthotropic materials (we will find the correct number of properties in Chapter 2).

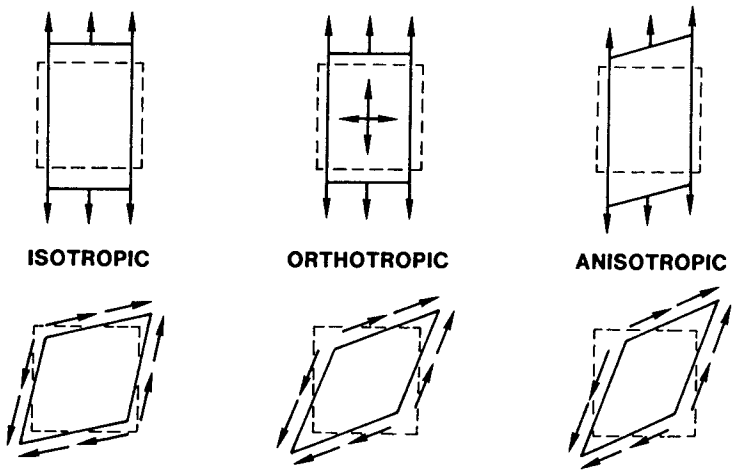

Figure 1-4 Mechanical Behavior of Various Materials

For anisotropic materials, application of a normal stress leads not only to extension in the direction of the stress and contraction perpendicular to it, but to shearing deformation. Conversely, application of shearing stress causes extension and contraction in addition to the distortion of shearing deformation. This coupling between both loading modes and both deformation modes, i.e., shear-extension coupling, is also characteristic of orthotropic materials subjected to normal stress in a non-principal material direction. For example, cloth is an orthotropic material composed of two sets of interwoven fibers at right angles to each other. If cloth is subjected to a normal stress at 45° to a fiber direction, both stretching and distortion occur, as can easily be demonstrated by the reader. Even more material properties than for orthotropic materials are necessary to describe the mechanical behavior of anisotropic materials because of the additional response characteristics.

Coupling between deformation modes and types of loading creates problems that are not easily overcome and, at the very least, cause a reorientation of thinking. For example, the conventional American Society for Testing and Materials (ASTM) dog-bone tensile specimen shown in Figure 1-5 obviously cannot be used to determine the tensile moduli of orthotropic materials loaded in non-principal material directions (nor of anisotropic materials). For an isotropic material, loading on a dog-bone specimen is actually a prescribed lengthening that is only coincidentally a prescribed stress because of the symmetry of an isotropic material. However, for an off-axis-loaded orthotropic material or an anisotropic material, only the prescribed lengthening occurs because of the lack of symmetry of the material about the loading axis and the clamped ends of the specimen. Accordingly, shearing stresses result in addition to normal stresses in order to counteract the natural tendency of the specimen to shear. Furthermore, the specimen has a tendency to bend. Thus, the strain measured in the specimen gage length in Figure 1-5 cannot be used with the axial load to determine the axial stiffness or modulus. Accordingly, techniques more sophisticated than the ASTM dog-bone test must typically be used to determine the mechanical properties of a composite material.

The foregoing characteristics of the mechanical behavior of composite materials have been presented in a qualitative manner without proof. In subsequent chapters, these characteristics will be demonstrated to exist, and further quantitative observations will be made.

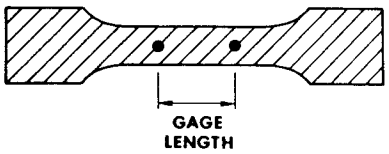

Figure 1-5 ASTM Dog-Bone Tensile Specimen

1.2.3 Basic Terminology of Laminated Fiber-Reinforced Composite Materials

For the remainder of this book, fiber-reinforced composite laminates will be emphasized. The fibers are long and continuous as opposed to whiskers. The concepts developed herein are applicable mainly to fiber-reinforced composite laminates, but are also valid for other laminates and whisker composites with some fairly obvious modifications. That is, fiber-reinforced composite laminates are used as a uniform example throughout this book, but concepts used to analyze their behavior are often applicable to other forms of composite materials. In many instances, the applicability will be made clear as an example complementary to the principal example of fiber-reinforced composite laminates.

The basic terminology of fiber-reinforced composite laminates will be introduced in the following paragraphs. For a lamina, the configurations and functions of the constituent materials, fibers and matrix, will be described. The characteristics of the fibers and matrix are then discussed. Finally, a laminate is defined to round out this introduction to the characteristics of fiber-reinforced composite laminates.

1.2.3.1 Laminae

The basic building block of a laminate is a *lamina* which is a flat (sometimes curved as in a shell) arrangement of unidirectional fibers or woven fibers in a matrix. Two typical flat laminae along with their principal material axes that are parallel and perpendicular to the fiber direction are shown in Figure 1-6. The fibers are the principal reinforcing or load-carrying agent and are typically strong and stiff. The matrix can be organic, metallic, ceramic, or carbon. The function of the matrix is to support and protect the fibers and to provide a means of distributing load among, and transmitting load between, the fibers. The latter function is especially important if a fiber breaks as in Figure 1-7. There, load from one portion of a broken fiber is transferred to the matrix and, subsequently, to the other portion of the broken fiber as well as to adjacent fibers. The mechanism for load transfer is the shearing stress developed in the matrix; the shearing stress resists the pulling out of the broken fiber. This load-transfer mechanism is the means by which whisker-reinforced composite materials carry any load at all above the inherent matrix strength.

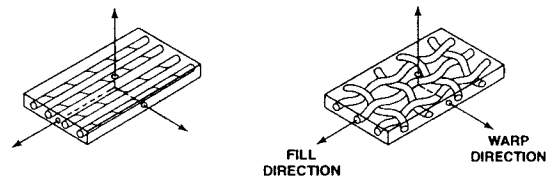

Figure 1-6 Two Principal Types of Laminae

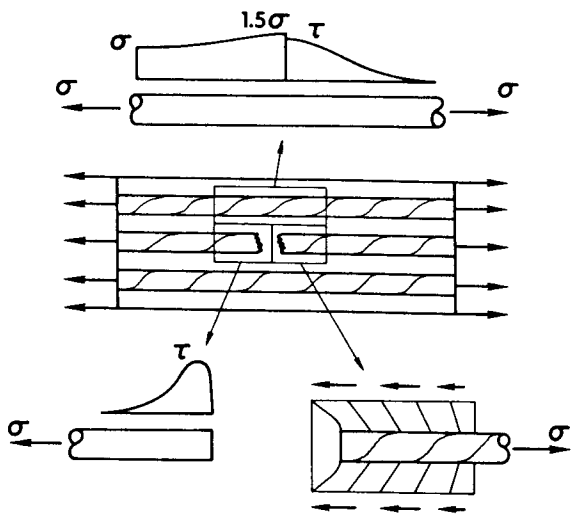

Figure 1-7 Effect of Broken Fiber on Matrix and Fiber Stresses

The properties of the lamina constituents, the fibers and the matrix, have been only briefly discussed so far. Their stress-strain behavior is typified as one of the four classes depicted in Figure 1-8. Fibers generally exhibit linear elastic behavior, although reinforcing steel bars in concrete are more nearly elastic–perfectly plastic. Aluminum, as well as

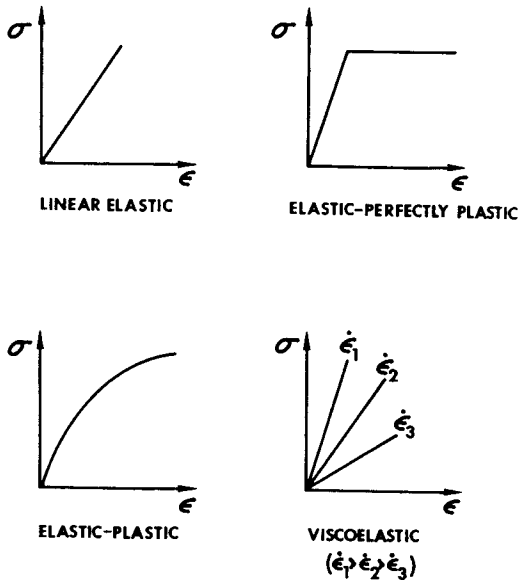

Figure 1-8 Various Stress-Strain Behaviors

many polymers, and some composite materials exhibit elastic-plastic behavior that is really nonlinear elastic behavior if there is no unloading. Commonly, resinous matrix materials are viscoelastic if not viscoplastic, i.e., have strain-rate dependence and linear or nonlinear stress-strain behavior. The various stress-strain relations are sometimes referred to as constitutive relations because they describe the mechanical constitution of the material.

Fiber-reinforced composite materials such as boron-epoxy and graphite-epoxy are usually treated as linear elastic materials because the essentially linear elastic fibers provide the majority of the strength and stiffness. Refinement of that approximation requires consideration of some form of plasticity, viscoelasticity, or both (viscoplasticity). Very little work has been done to implement those models or idealizations of composite material behavior in structural applications.

1.2.3.2 Laminates

A *laminate* is a bonded stack of laminae with various orientations of principal material directions in the laminae as in Figure 1-9. Note that the fiber orientation of the layers in Figure 1-9 is not symmetric about the middle surface of the laminate. The layers of a laminate are usually bonded together by the same matrix material that is used in the individual laminae. That is, some of the matrix material in a lamina coats the surfaces of a lamina and is used to bond the lamina to its adjacent laminae without the addition of more matrix material. Laminates can be composed of plates of different materials or, in the present context, layers of fiber-reinforced laminae. A laminated circular cylindrical shell can be constructed by winding resin-coated fibers on a removable core structure called a mandrel first with one orientation to the shell axis, then another, and so on until the desired thickness is achieved.

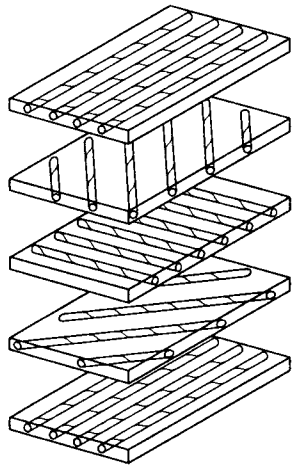

Figure 1-9 Unbonded View of Laminate Construction

A major purpose of lamination is to tailor the directional dependence of strength and stiffness of a composite material to match the loading environment of the structural element. Laminates are uniquely suited to this objective because the principal material directions of each layer can be oriented according to need. For example, six layers of a ten-layer laminate could be oriented in one direction and the other four at 90° to that direction; the resulting laminate then has a strength and extensional stiffness roughly 50% higher in one direction than the other. The ratio of the extensional stiffnesses in the two directions is approximately 6:4, but the ratio of bending stiffnesses is unclear because the order of lamination is not specified in the example. Moreover, if the laminae are not arranged symmetrically about the middle surface of the laminate, the result is stiffnesses that represent coupling between bending and extension. These characteristics are discussed on a firm quantitative basis in Chapter 4.

1.2.4 Manufacture of Laminated Fiber-Reinforced Composite Materials

Unlike most conventional materials, there is a very close relation between the manufacture of a composite material and its end use. The manufacture of the material is often actually part of the fabrication process for the structural element or even the complete structure. Thus, a complete description of the manufacturing process is not possible nor is it even desirable. The discussion of manufacturing of laminated fiber-reinforced composite materials is restricted in this section to how the fibers and matrix materials are assembled to make a lamina and how, subsequently, laminae are assembled and cured to make a laminate.

1.2.4.1 Initial Form of Constituent Materials

The fibers and matrix material can be obtained commercially in a variety of forms, both individually and as laminae. Fibers are available individually or as roving which is a continuous, bundled, but not twisted, group of fibers. The fibers can be unidirectional or interwoven. Fibers are often saturated or coated with resinous material such as epoxy which is subsequently used as a matrix material. The process is referred to as preimpregnation, and such forms of preimpregnated fibers are called 'prepregs'. For example, unidirectional fibers in an epoxy matrix are available in a tape form (prepreg tape) where the fibers run in the lengthwise direction of the tape (see Figure 1-10). The fibers are held in position not only by the matrix but by a removable backing that also prevents the tape from sticking together in the roll. The tape is very similar to the widely used glass-reinforced, heavy-duty package-strapping tape. Similarly, prepreg cloth or mats are available in which the fibers are interwoven and then preimpregnated with resin. Other variations on these principal forms of fibers and matrix exist.

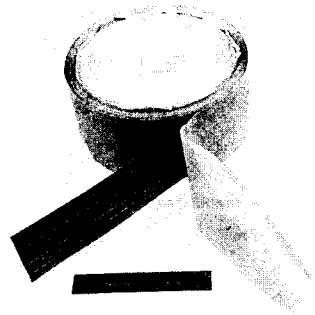

Figure 1-10 Boron-Epoxy Prepreg Tape
(Courtesy of General Dynamics)

1.2.4.2 Layup

Three principal layup processes for laminated fiber-reinforced composite materials are winding, laying, and molding. The choice of a layup process (as well as a curing process) depends on many factors: part size and shape, cost, schedule, familiarity with particular techniques, etc.

Winding and laying operations include filament winding, tape laying or wrapping, and cloth winding or wrapping. Filament winding consists of passing a fiber through a liquid resin and then winding it on a mandrel (see Figure 1-11). The fibers are wrapped at different orientations on the mandrel to yield strength and stiffness in many directions. Subsequently, the entire assembly, including the mandrel, is cured, after which the mandrel is removed. If the mandrel is a sand casting, then using a water hose to clean out the new pressure vessel dissolves the sand casting. Some mandrels are barrel-stave-like assemblies that must be disassembled through an opening in the new pressure vessel. Tape laying starts with a tape consisting of fibers in a preimpregnated form held together by a removable backing material. The tape is unwound and laid down to form the desired shape in the desired orientations of tape layers. Tape laying can be by hand or automated with an automated tape-laying machine shown in Figure 1-12. Cloth winding or laying begins with preimpregnated cloth that is unrolled and deposited in the desired form and orientation. Cloth winding or laying is more inflexible and inefficient than filament winding or tape laying in achieving specified goals of strength and stiffness because of the less efficient bidirectional character of the fibers in the cloth than in unidirectional tape or fibers. That is, the bidirectional character of the cloth does not permit the large strengths and stiffnesses obtainable with unidirectional tapes because the cloth always has two essentially (but not necessarily) equal strength and stiffness directions. Moreover, fibers that are woven are often damaged to some extent by the bending inherent to the weaving process. Cloth layers are often used as filler layers in laminates for which strength and stiffness are not critical.

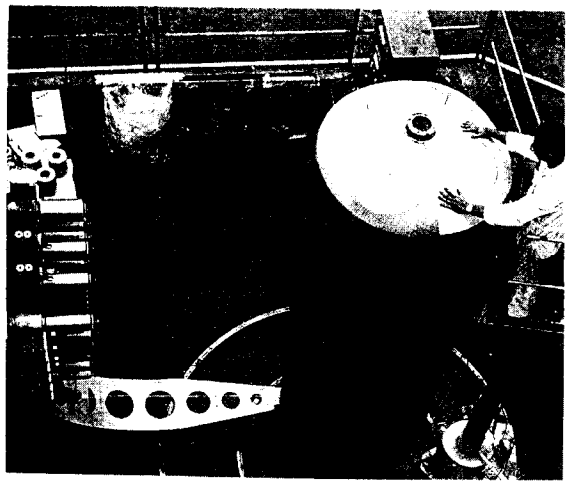

Figure 1-11 Filament Winding a Rocket Motor Case
(Courtesy Structural Composites Industries)

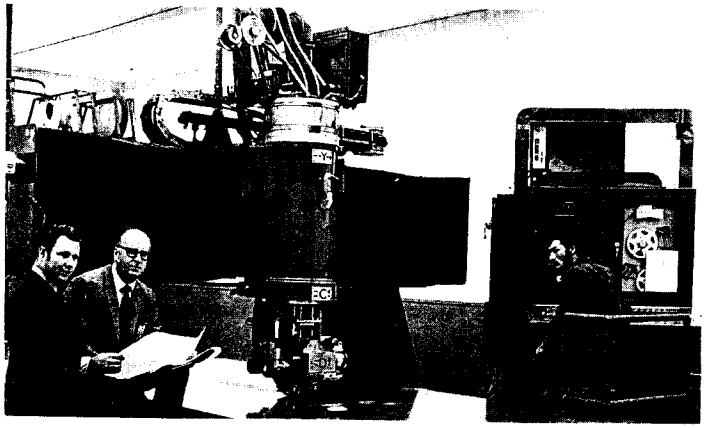

Figure 1-12 Automatic Tape-Laying Machine
(Courtesy General Dynamics)

Molding operations can begin with hand or automated deposition of preimpregnated fibers in layers. Often, the prepreg layers are also precut. Subsequently, the layers are compressed under elevated temperature to form the final laminate in a press as shown in Figure 1-13. Molding is used, for example, to fabricate radomes to close tolerances in thickness. Resin-transfer molding (RTM) is a process in which dry fiber or dry textile sheets and solid resin sheets are heated and formed on a mold or tool as in Figure 1-14. Thus, parts of complex shape can

be made quickly in a single step (avoiding the preimpregnation of fibers step). Effective use of such molding involves specification and control of a large number of material properties and processing parameters. The F-111 boron-epoxy fuselage frame assembly shown in Figure 1-15 is another molded composite part. Actually, the upper one-third of the frame is molded, and the lower two-thirds is laid-up tape.

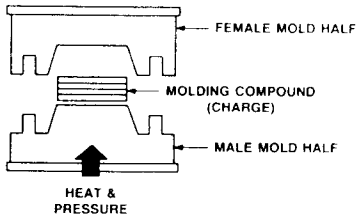

Figure 1-13 Compression Molding

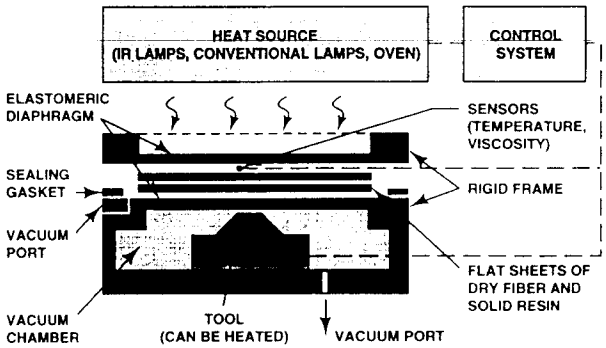

Figure 1-14 Resin-Transfer Molding

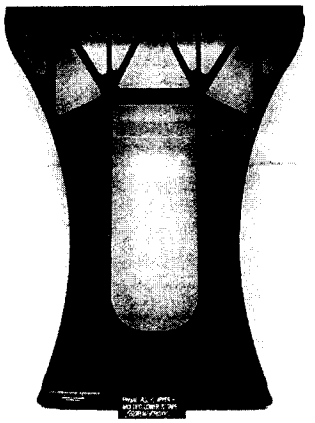

Figure 1-15 Molded F-111 Fuselage Frame Assembly
(Courtesy of General Dynamics)

Sheet molding compound (SMC) consists of randomly oriented chopped fibers in a matrix of resin and filler. SMC is produced in the continuous manner shown in Figure 1-16. Note that the polyethylene film protects the roller system from getting 'gummed up' with the resin-filler paste. The rug-like rolls of SMC are then used in compression molding machines to create large parts such as the sides of cars and trucks.

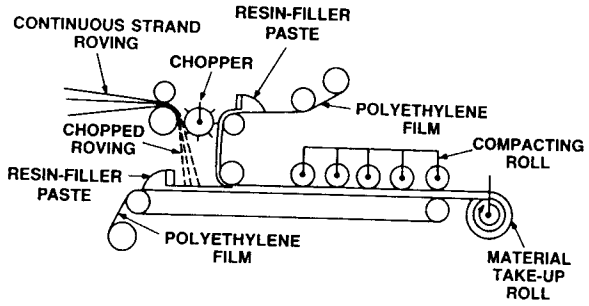

Figure 1-16 Sheet Molding Compound Machine

The roll-forming process can be used to directly produce long structural shapes in large quantities. The entering material form is rolls of variously orientated fiber-reinforced tape. The layers are consolidated and then formed into, e.g., a hat-shaped stiffener, as in Figure 1-17. Note the presence of a stiffer layer such as boron-epoxy in surrounding layers of glass-epoxy. Such an optimally placed stiff layer dramatically increases the bending stiffness, yet is easily made, unlike any metal stiffener.

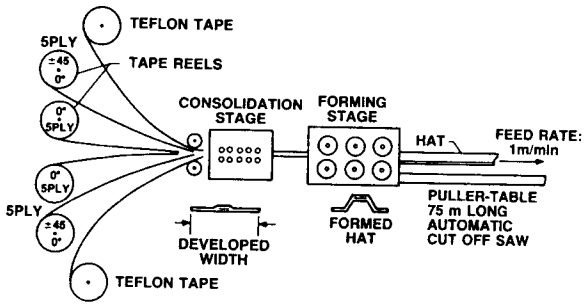

Figure 1-17 Roll-Forming Process

Pultrusion is also used to make structural shapes from composite materials. The incoming material is generally unidirectional and must be pulled through the pultrusion die because the uncured composite material is entirely too flexible to push (as in extrusion processes). The incoming material can be preshaped by various guides and rollers as in Figure 1-18.

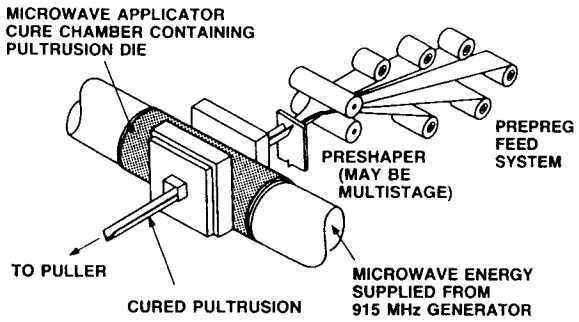

Figure 1-18 Pultrusion

We have seen a variety of manufacturing processes, but certainly not all possible processes. Those processes would likely be used to produce many different parts with different characteristics and purposes. The diversity of parts might well be combined to form a single structural part such as a wing in Figure 1-19. After each process, every part is nondestructively inspected.

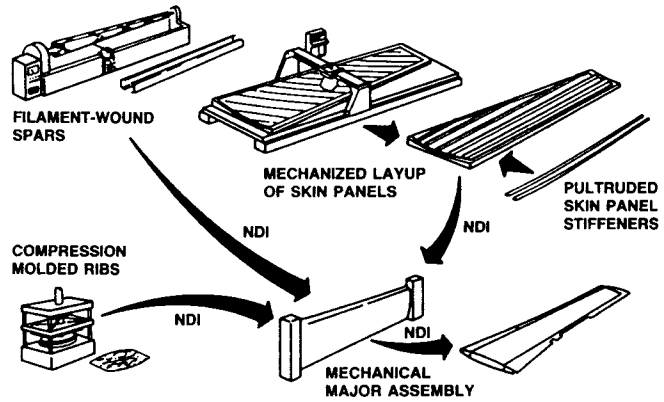

Figure 1-19 Combining Manufacturing Operations to Produce a Wing

1.2.4.3 Curing

Curing primarily refers to the process of solidification of polymer matrix materials. Metal matrix materials are simply heated and cooled around fibers to solidify. Ceramic matrix and carbon matrix materials are either vapor deposited, mixed with fibers in a slurry and hardened, or, in the case of carbon, subjected to repeated liquid infiltration followed by carbonization. Thus, we concentrate here on curing of polymers.

For thermoset-matrix materials, heat is usually added as a catalyst to speed the natural chemical reaction of polymerization. Two-part epoxies, such as found in your local hardware store, consist of a tube of epoxy and a tube of chemical hardener that react when mixed. Heat

is not added to a two-part epoxy, but is given off as a product of the reaction. For virtually all epoxies, volatile gases are given off during curing. Those volatile gases come from heating the solvents used to keep the epoxy from curing prior to assembly time.

In general, the higher the temperature during curing, the shorter the cure time (short of burning the material, of course). Heat is required because (1) some catalysts and/or hardeners do not react below a critical temperature; (2) molecular mobility is necessary for contact of reactive chemical groups; (3) heat drives off volatiles from solvents and water (otherwise, voids occur; note that volatiles will not outgas if pressure is also being applied); and (4) resin flows more easily to obtain uniform distribution. Pressure is required to consolidate (debulk) the fiber and matrix system and to squeeze out excess resin.

A typical curing cycle of temperature versus time with notes on other actions is shown in Figure 1-20. The time scale is several hours, and the temperature scale is hundreds of °F (also hundreds of °C). The curing cycle starts with a gradual temperature increase under vacuum conditions so that volatiles and water (vapor) can be driven off. Then, the temperature is gradually increased to the maximum curing temperature which is held for a couple of hours to develop a high degree of cross-linking along with pressure application to consolidate the laminae.

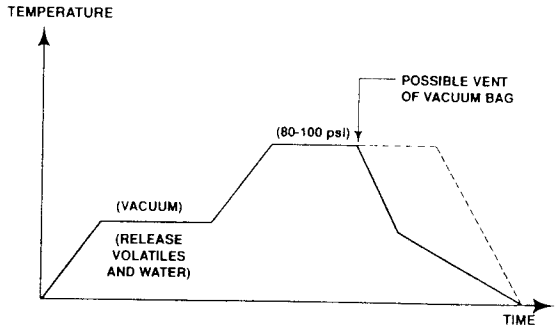

Figure 1-20 Typical Epoxy Cure Cycle

We should examine the resin behavior during the curing process. Before curing, the initial form of the laminate is laminae laid adjacently in a B-staged condition (partially cured to reduce resin flow during lamination or molding). The resin is a semi-solid with negligible strength and stiffness. As the temperature is gradually increased, resin cross-linking begins and is significant when the gel temperature is reached (the temperature at which the viscosity is so high that no further dimensional change occurs). The progressive cross-linking causes solidification, but the elevated temperature causes softening and hence lowers stiffness. At the highest temperature reached (if the proper prescribed cure cycle is followed which also means that the temperature must be held for a specified time), cross-linking is nearly complete. The resin is now solidified, but is of low stiffness because of the high temperature. Then,

the temperature is gradually decreased to room temperature over a period of about an hour to avoid thermal shock. The pressure can be released quickly. If postcuring is performed, no further cross-linking occurs unless the previous maximum temperature is exceeded and held for at least an hour (presuming the previous maximum temperature was held for an hour or so).

Curing can be performed in several devices: heated mold (Figure 1-13), hot press (heated plates that are forced together), and an autoclave which is essentially a very large version of an ordinary kitchen pressure cooker as in Figure 1-21.

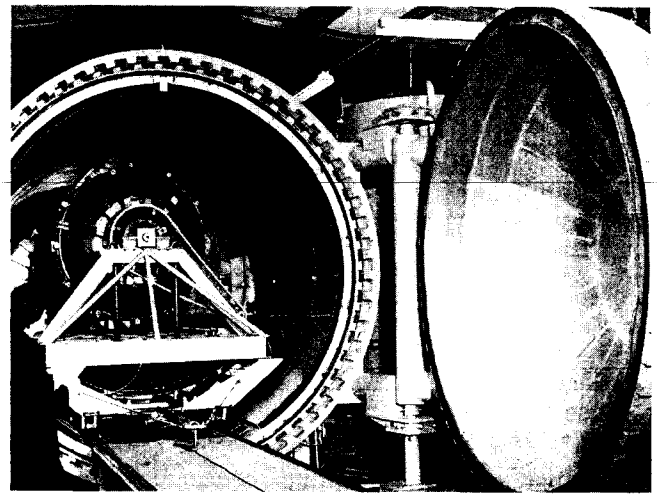

Figure 1-21 Autoclave *(Courtesy of Thiokol)*

The curing process for thermoplastic-matrix materials does not involve cross-linking but only melting and cooling. That is, a thermoplastic is already a solid that, like metals, can be heated to soften and cooled to stiffen. For some thermoplastic materials, a small degree of cross-linking occurs, so such thermoplastics cannot be cycled more than a few times through a heating-cooling cycle. Also, the time at elevated temperature [usually nearly 1000°F (500°C)] need not be but a few moments. Thus, the laser heating and roller for consolidation device in Figure 1-22 enables rapid simultaneous tape layup and curing.

The term *cocuring* means that two parts that must be fastened together are cured simultaneously and in contact to achieve permanent bonding between them. The process applies equally to thermoset-matrix composite materials and to thermoplastic-matrix composite materials (except the cocuring of two thermoplastic-matrix parts is not, of course, permanent).

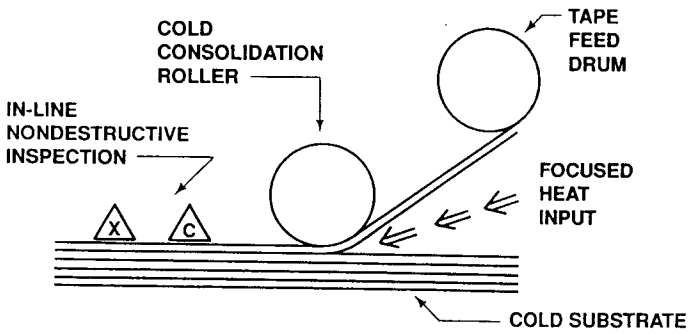

Figure 1-22 Thermoplastic-Matrix Layup and Curing Device

1.3 THE WHY — CURRENT AND POTENTIAL ADVANTAGES OF FIBER-REINFORCED COMPOSITE MATERIALS

The advent of advanced fiber-reinforced composite materials has been called the biggest technical revolution since the jet engine [1-4]. This claim is very striking because the tremendous impact of the jet engine on military aircraft performance is readily apparent. The impact on commercial aviation is even more striking because the airlines switched from propeller-driven planes to all-jet fleets within the span of just a few years because of superior performance and lower maintenance costs.

The adjective *advanced* in *advanced fiber-reinforced composite materials* is used to distinguish composite materials with ultrahigh strength and stiffness fibers such as boron and graphite from some of the more-familiar, but less-capable fibers such as glass. Such advanced composite materials have two major advantages, among many others: improved strength and stiffness, especially when compared with other materials on a unit weight basis. For example, composite materials can be made that have the same strength and stiffness as high-strength steel, yet are 70% lighter! Other advanced composite materials are as much as three times as strong as aluminum, the common aircraft structural material, yet weigh only 60% as much! Moreover, as has already been noted, composite materials can be tailored to efficiently meet design requirements of strength, stiffness, and other parameters, all in various directions. These advantages will lead to new aircraft and spacecraft designs that are radical departures from past efforts based on conventional materials. However, the aerospace industry was attracted to titanium in the 1950s for similar reasons, but found serious disadvantages after the investment of many millions of dollars in research, development, and tooling. That unfortunate experience with titanium caused a more cautious, yet more deliberately complete and well-balanced approach to composite materials development. The advantages of composite materials are so compelling that research and development is being conducted across broad fronts instead of just down the most obvious paths. Whole organizations have sprung up to analyze, design, and fabricate parts made of composite materials. The strength and stiffness advantages of advanced composite materials will be discussed in Section 1.3.1, cost advantages in Section 1.3.2, and weight advantages in Section 1.3.3.

1.3.1 Strength and Stiffness Advantages

One of the most common ways of expressing the effectiveness of strength or stiffness of a material is as a ratio of either of the quantities to the density, i.e., weight per unit volume. Such an index does not include the cost to achieve a certain strength or stiffness, but cost comparisons are probably not valid by themselves because many factors influence cost beyond raw material cost.

Consider some of the advantages of fiber-reinforced composite materials. Very high strength and stiffness are about the most common advantages that come to mind. We often express those strength and stiffness properties not in absolute terms, but in relative terms by dividing them by the density. Those strength-to-density and stiffness-to-density quotients are simply manners of expressing what we call specific strength and specific modulus or specific stiffness that are particularly attractive when weight-sensitive structures such as aircraft or spacecraft are addressed. That is, we are asking: what will this material do for us per unit of weight that we use?

First, we examine how the properties of the composite material constituents, fiber and matrix, generally contribute to the lamina properties and, subsequently, how lamina properties influence the laminate properties. We plot vertically the strength and horizontally the stiffness or the modulus in Figure 1-23 on translation from constituent properties of the composite material to the level of the lamina and then finally to the level of the laminate. Typically, the fibers used in advanced composite materials are very high in strength and often very high in modulus. Next, we put those fibers in a matrix material that is typically low in strength and low in stiffness to create a unidirectionally reinforced lamina. Such a lamina is a layer that has substantially different strengths and stiffnesses in different directions. The strength and stiffness in the fiber direction are the highest properties. However, perpendicular to the fibers, that is, at 90°, the lowest properties exist with some variation in between as the angle varies from 0° to 90°. In fact, it is possible to get even lower stiffness and strength properties than the 90° properties at some off-axis angle generally in the vicinity of 60° with some composite materials. At 90°, the lamina stiffness and strength are much more like the matrix properties than the fiber properties, whereas, at 0° to the fiber direction, the properties are fiber dominated.

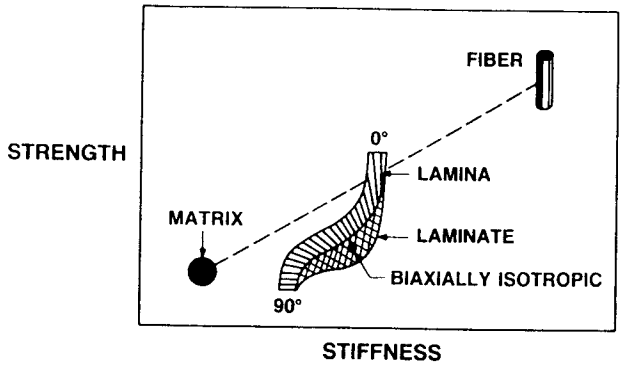

Figure 1-23 Translation from Constituent Properties to Lamina to Laminate Properties

A laminate is a bonded mixture of variously angled laminae, and we expect the laminate properties not to be as high as those of the 0° lamina nor as low as those of the 90° lamina, but some value in between. Actually, the zone marked laminate in Figure 1-23 must include both the 0° and the 90° cases because we can make a laminate, if we so choose, with all 0° fibers, i.e., all 0° layers. At some place in the zone labelled laminate, what is called an isotropic point or biaxially isotropic point exists as some measure of equal in-plane properties in at least two directions in terms of stiffness and strength. The so-called biaxially isotropic laminate is an artificial laminate that is simply used as a basis for comparison of one composite laminate to another or of a composite material to a metal. The type of properties plot in Figure 1-23 is the basic scheme that we will use for comparative purposes.

A representation of the strength and stiffness of many materials on the basis of effectiveness per unit weight is shown in Figure 1-24. The properties of common structural metals are denoted by open squares. Various forms of advanced composite materials are denoted by three types of circles: fibers alone are represented with open circles; laminae with unidirectional fibers are shown as circles with a vertical line in them; and laminae with equal numbers of fibers in two perpendicular directions are shown with circles with a horizontal and vertical line in them. Obviously, the most effective material lies in the upper right-hand corner of Figure 1-24. Fibers alone are stiffer and stronger than when placed in a matrix. However, as we have already seen, the fibers are not used without a matrix because of the important advantages of the combination of fibers in a matrix. Also, unidirectional configurations are stiffer and stronger in the fiber direction than biaxially isotropic configurations in either of the two directions. Practical laminates lie somewhere between unidirectional and biaxially isotropic configurations.

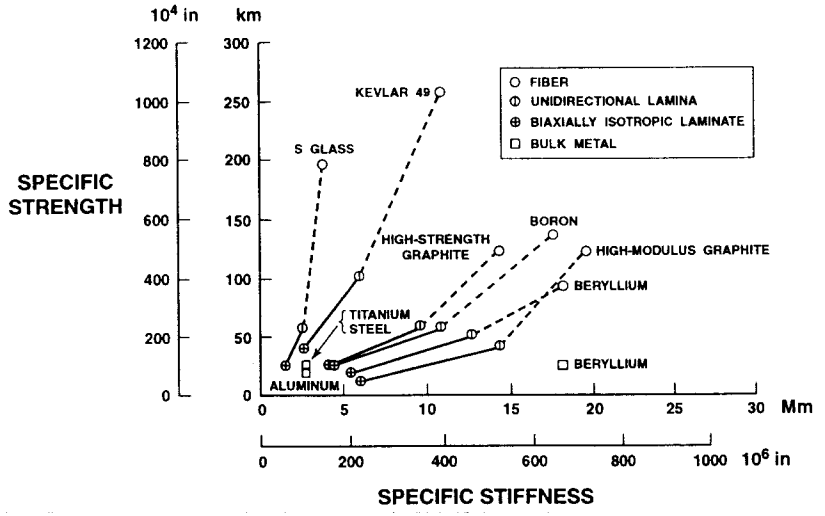

Figure 1-24 Strength and Stiffness of Composite Materials and Metals

Let's compare various forms of specific composite materials with structural-grade metals. The metals each occupy only one point on a specific strength versus specific stiffness curve, e.g., the open squares in Figure 1-24. We need not consider their constituents, and there are no orientation aspects, so only one point is necessary to represent their stiffness and, simultaneously, their strength. However, for composite materials, strong directionally dependent factors must be accounted for. The bulk metals considered for structural applications are steel, titanium, and aluminum in the lower left-hand corner of Figure 1-24 and beryllium in the lower right-hand corner. Now, contrast those bulk metal properties with the properties of a high-modulus graphite fiber which is up and to the right about as far as possible in Figure 1-24. Observe that the graphite looks terrific at first glance. However, we cannot use graphite in strictly a fiber form. We must drop back from the capabilities of the fiber form to the unidirectional laminate form at least, if not perhaps back more toward the biaxially isotropic laminate. And the real practical application is some place in between these two simple composite laminates.

A unidirectional laminate can be used in certain special applications. For example, all the fibers can be aligned in the axial direction of a strut or column to take advantage of every possible capability of a graphite-epoxy composite material in that particular loading environment. However, for aircraft wings, all the fibers cannot be oriented in one direction. Multiple fiber orientations must be used to achieve the proper balance of strength and stiffness necessary to accommodate loads from various directions. Certainly the loads might be larger in one direction than another, and we would then prejudice the fiber system to accommodate the higher load levels. We simply cannot do that prejudicing of

directional properties with a metal structure. We must accept uniform all-around properties with a metal structure (unless we add stiffeners).

A wide variety of materials is depicted in Figure 1-24, e.g., both high-strength graphite-epoxy and high-modulus graphite-epoxy which naturally is further to the right on the figure than is high-strength graphite-epoxy. Generally, high-modulus graphite-epoxy is obtained by a higher graphitization temperature of the graphite fibers than high-strength graphite. Boron falls fairly close to high-strength graphite. Beryllium is over to the right in fiber form and much lower on the chart in bulk metal form. The fiber form of beryllium is much stronger, i.e., up higher in the figure, than the bulk form of beryllium. Thus, a beryllium-fiber composite material has a significant advantage over bulk beryllium in strength. Beryllium fibers in a composite form lead to loss in stiffness to some extent because we have had to use a less-stiff matrix material to surround the beryllium fibers, but we still have a considerable strength advantage. In contrast, we see fiberglass to the left in the figure, which is extremely strong, but not very stiff. When we put the glass fibers in a usable form, namely a unidirectional composite material, we get the same specific stiffness as ordinary structural metals, but fiberglass does have a higher specific strength. Fiberglass in the biaxially isotropic form has about the same specific strength as steel or titanium, but higher than aluminum. However, fiberglass has a lower specific modulus than any of the conventional metals. Thus, we would typically use glass in a strength-critical application whereas any of the graphites, even the high-strength graphites, would be used in stiffness-critical applications. In summary, for a stiffness-critical application, we would use graphite-epoxy. For a strength-critical application, we might use glass-epoxy or Kevlar-epoxy.

For example, we might make a strength-critical pressure vessel with glass-epoxy. We would wind the fibers so that they are not unidirectional, but resist the variously oriented pressure vessel stresses. A pressure vessel has a biaxial state of stress, so we must do more than just circumferential fiber winding. In some cases, some axial windings are necessary, and we might also wind some fibers at ±45° or other angles. We can find the angle to optimize the strength of this highly biaxially loaded structure. Some pressure vessels are made of graphite-epoxy as well as of fiberglass or Kevlar-epoxy.

Kevlar 49®-epoxy fits between the set of lines for S-glass-epoxy and the high-strength graphite-epoxy in Figure 1-24. Kevlar-epoxy is another member of the family of materials that can be used for a particular design application. Actually, several grades of Kevlar have properties in the general vicinity labelled Kevlar in Figure 1-24. For a certain balance of strength and stiffness, you might want a material some place in the Kevlar to high-strength graphite region of materials rather than to go all the way to a fiberglass or all the way to a high-modulus graphite, for example. That is, you must look at your specific design requirements to determine what material you really need.

Boron fibers exhibit the highest stiffness and strength efficiencies in Figure 1-24. When placed in a lamina as unidirectional fibers, the relative strength of boron-epoxy drops significantly whereas the relative stiffness drops only a little. In a biaxially isotropic configuration, boron-epoxy is still stiffer than steel or titanium, although it is of the same relative strength. High-strength graphite fibers in composite materials exhibit similar behavior. However, high-modulus graphite fibers, although their stiffness is greater in all configurations than the other materials, have generally lower relative strengths (even lower than aluminum when placed in a biaxially isotropic configuration). S-glass-epoxy in a unidirectional layup has about 2 1/2 times the relative strength of steel or titanium, but is no stiffer (in fact, it is less stiff in a biaxially isotropic configuration than steel or titanium). Beryllium has about six times the relative stiffness of steel, titanium, or aluminum, but is no stronger. Beryllium wires are much stronger, but no stiffer, than bulk beryllium. Beryllium wires in a matrix exhibit some of the same general characteristics as other composite materials.

The duality of the plot in Figure 1-24 is important. That is, *stiffness is often equally important and sometimes even more important than strength.* Some people tend to say strength when they actually mean stiffness. We must carefully and completely distinguish between these two very different physical concepts.

Not all of the strength and stiffness advantages of fiber-reinforced composite materials can be transformed directly into structural advantages. Prominent among the reasons for this statement is the fact that the joints for members made of composite materials are typically more bulky than those for metal parts. These relative inefficiencies are being studied because they obviously affect the cost trade-offs for application of composite materials. Other limitations will be discussed subsequently.

1.3.2 Cost Advantages

Decreasing the cost of a material per pound of structure depends on increasing manufacturing experience in a given process and on developing new, more effective manufacturing technologies, among other factors. The raw material graphite fibers fell from several hundred dollars a pound ($600–800/kg) in the early 1970s to $20 per pound ($40/kg) in 1990 due to increased manufacturing experience and to the increased efficiencies of large-scale production. On the other hand, boron fibers, also several hundred dollars per pound ($600–800/kg) in the early 1970s, cost about $100 per pound ($200/kg) in 1980 because of inherent technological limitations. The latter prices are for boron that is deposited on a tungsten substrate. If a glass substrate could be used, one technological barrier would be overcome, and the cost of boron fibers could be as low as that of graphite fibers. In addition, smaller fibers could be produced by the glass substrate process. One difficulty in working with boron is that it reacts chemically with many matrix materials, as does carbon to a lesser extent. Thus, certain fiber coatings must be used which increase the cost and sometimes lower the potential effectiveness of the resulting composite material.

Various elements must be considered in the cost of a structure or an object. We first consider an element on which many people often focus too much attention, and that is the raw material cost. However, *raw material cost is only one small element in the whole process of determining the true cost of an object over its lifetime of use.* Different materials have different associated costs to design a structure. A certain amount of money is required to fabricate or manufacture the object. Different amounts of money are required to assemble parts that are made in various ways. Similar-appearing parts of different materials might require very different fastening techniques. The first three elements mentioned constitute the initial cost of the object. Whenever the object comes out the door of the factory, what we pay for it is the initial cost. When we add to that initial cost the operating and maintenance costs over the life cycle of the object as in Figure 1-25, then we begin to get a true picture of the *real cost* of the object. Using only the initial cost to govern all decisions is totally unrealistic; operating and maintenance costs must be taken into account.

Often the operating costs are lower for a composite structure than for a metallic structure. Thus, we can automatically afford to pay more for the initial cost of the composite structure in order to achieve those lower operating costs as long as the key element, the life-cycle cost, is lower for composite structures. The life-cycle cost is made up of those initial costs mentioned, plus operating costs and maintenance costs, but less the salvage value as in Figure 1-25. Then, we must perform a cost analysis of the whole system and ask: which is the least-expensive choice? Like the TV ad, 'you can pay me now, or you can pay me later'. And if we pay at the beginning, we might very well have a lower life-cycle cost in many situations with composite structures. The development of composite structures is getting to the point where some applications of composite structures have both a lower initial cost and a lower operating cost. Thus, the life-cycle cost is very much more favorable for composite structures than it is for some metal structures.

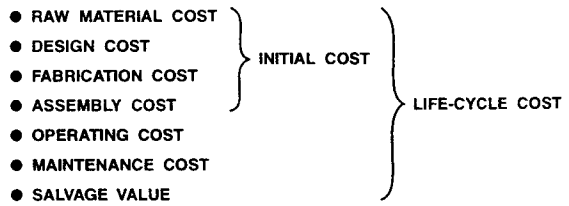

Figure 1-25 Life-Cycle Cost Elements

The operating cost includes items like fuel and other consumables. Maintenance costs are obviously repairs and periodic reworking of the structure. After the passage of years, nearly the entire aircraft structure has often been replaced part by part! The final category is the salvage value. What is the object worth at the end of its life? Consider an aluminum airplane for which some scrap value exists at the end of its useful life. When the structure is no longer suitable to be flown, and there we

sit with a pile of aluminum, we can retrieve some salvage value. Think of the plane as a big pile of aluminum beer cans! However, that value is not really significant in comparison to the original cost. Admittedly, with a composite structure, there is no salvage value at all if the structure is made entirely of some composite materials. There is *nothing* that we can do with the structure when we are through with it as a structure. If we made the object, for example, with graphite-epoxy, then after the epoxy matrix is cured (epoxy is a thermoset polymer which means that curing is a one-way process), the composite material takes that cured shape permanently. We cannot melt the structure down and make it into anything else. At that point, the plane is a pile of junk with zero salvage value (in fact, you would have to pay someone to take it away). However, even the salvage value of the aluminum aircraft is not enough higher than zero *relative to the initial cost* to make the salvage value a strong consideration in the overall economic analysis.

Why are the various cost elements being described? Because you need to have a feeling for the comparisons that you must make in structural design in order to decide which material is best for your particular application. One of the primary considerations in structural design is always cost. A material might appear very efficient when expressed in terms of weight, but we must usually think of cost as well. The cost-competitiveness of composite materials is generally best in applications to weight-sensitive structures simply because the specific strength and specific modulus of composite materials are typically very high when compared to ordinary structural metals. That is, composite materials are especially effective in weight-sensitive structures.

Cost advantages of composite materials are obtained when we have and recognize the sometimes easier fabrication concepts for advanced composite structures than exist for metals. Generally, all cost advantages or cost comparisons are becoming more favorable for composite structures with increasing production rates of composite raw materials and composite parts. Those advantages and production rates go hand in hand, so if we develop new technology for production of composite materials, that new technology will drive down the cost of composite structures.

Labor cost in a structure is directly related to part count. If part count can be reduced, then labor costs (and inventory costs) will decrease. Composite structures are generally composed of many fewer parts than are metal structures. Integral part design and fabrication techniques reduce fastener count and bonding operations. Thus, composite structures can have cost elements that are considerably lower than those for metal structures.

Often, the manufacturing processes involved for composite structures fabrication are greatly simplified as compared to those for metal structures. Reduced part count results in a much lower assembly cost and overall reduction in the factory labor hours.

Manufacturing efficiency embodies a wide variety of topics far beyond the scope of this book. However, a materials utilization factor will be defined and characterized for composite materials and metals as a

quantitative way of expressing how efficiently materials are used in a manufacturing process. That materials utilization factor is defined very simply to be the amount of raw material required at the beginning of the manufacturing process divided by the amount of material that exists in the final part:

$$\text{Materials Utilization Factor} = \frac{\text{raw material weight}}{\text{final part weight}}$$

The difference between the two weights is the amount of material removed in the manufacturing process. For some parts made of metals, the materials utilization factor can be as high as 15 to 25! Typically, that large number occurs when a lot of metal-removing operations are performed on an initially large block of metal. Those so-called 'hogging out' operations involve simply machining away much of the material, sweeping it up from the floor, putting it in a bin, and selling it back to the manufacturer for a small refund compared to what it cost originally. That process is a natural way of dealing with metals; *metals are often carved down from a big chunk to the final intricate shape.* And, the labor and machining costs associated with that carving-down operation are usually quite high.

In contrast, with composite materials, the materials utilization factor is rarely higher than 1.2 to 1.3. That is, only a maximum of 20–30% of the material is wasted with composite structures. Whereas obviously with a materials utilization factor for some metal parts of 15-25, the waste is 1500–2500%! Those are not individually typical numbers, but are the worst cases in both situations, i.e., for metals and composite materials. For metals, there are many, many operations for which the waste factor is very low. And for composite materials there are also many situations where the waste factor is much lower than 20–30%. The point is that the worst-case situations are totally different for these two kinds of materials based on the way objects are inherently created with the two different types of materials. *Composite materials are built up until the limits of the desired geometry are reached.* At that point, the layup operation simply ceases. Composite materials and structures are fabricated in as close to the final configuration as possible, i.e., so-called near-net shape.

An example of the contrast between these two situations is illustrated in the context of the part of a wing called the doubly tapered wing spar. What you see in the middle of Figure 1-26 is not just an I-beam drawn in perspective. The spar actually is deeper and wider on the left-hand end near the fuselage than it is on the right-hand end because the wing is tapered both in height and width toward the tip. That is, the spar gets thinner and narrower in the direction away from the fuselage of the aircraft. To make such a wing spar of titanium requires starting with a block of material, as in the upper left-hand corner of Figure 1-26, which is as high as the deepest part of the beam and as wide as the widest part of the flange. Then titanium is machined away, including the cutting of lightening holes in the middle of the web because the web does not carry a lot of shear, so it can be made lighter by removing metal.

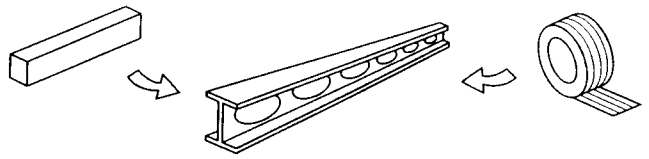

COST	TITANIUM	GRAPHITE-EPOXY
RAW MATERIAL COST	HIGH	HIGH
MACHINING COST	VERY HIGH	VERY LOW
SCRAPPAGE	VERY HIGH	VERY LOW
LAYUP COST	NONE	MODERATE

Figure 1-26 Doubly Tapered Wing Spar

For a composite wing spar, the starting point is a roll of tape as in the upper right-hand corner of Figure 1-26, and then the wing spar is *built up in layers* until the proper size is reached. Composite structures manufacturing is being contrasted here with a machining operation instead of, for example, a forging operation. Perhaps parts like this spar could be made of a titanium forging as well — in which case the materials utilization factor would be lower. However, the very high cost of the forging must be taken into account as well as the very considerable time in advance of production to obtain that forged spar.

Let's contrast four different categories of operations between the titanium on the left and the graphite-epoxy on the right in Figure 1-26. First, for raw material cost, titanium is not an inexpensive material, so the cost is labeled high, and graphite-epoxy might also be called high. The machining costs for the titanium spar are undoubtedly very high. However, little machining is required for the graphite-epoxy spar. The scrappage of material for titanium is very high. The wing spar involves one of those 'hogging-out' operations (very extensive machining away of significant amounts of material) where more than 1000% of the material is wasted relative to the final part weight. With graphite-epoxy, only approximately what material is needed is actually used. Hence, a very low scrappage rate exists. Another item in the budget is the layup costs. For titanium, there is no such cost. For a graphite-epoxy, such a part is not particularly difficult to layup. That layup is a moderate cost, certainly quite moderate in comparison to the extensive machining required for a titanium spar.

Specific numbers are not available for the final comparison in which all cost factors are weighed. First of all, a possibly higher raw material cost for graphite-epoxy is made up for, at least in a qualitative sense, by the fact that not as much machining is required for the graphite-epoxy spar. Essentially only as much graphite-epoxy as is needed is bought, whereas many times the amount of titanium that is needed in the final

part must be bought. The raw material cost per unit of weight for the titanium is high and perhaps somewhat higher for the graphite. But what is the cost of the raw material that must be bought to put into this object? The cost of the total amount of the titanium bought is likely greater than the cost of the graphite-epoxy. Moreover, the titanium spar has a very high machining cost. Thus, the bottom-line cost for the graphite-epoxy spar is expected to be lower than that for the titanium spar. Many other such comparisons are possible for various parts.

Composite materials are not claimed to be a cure-all for every application or even necessarily competitive with other materials. However, there are many instances in which composite materials are uniquely well-suited because of their peculiar fabrication processes. Thus, this 'special' case of a doubly tapered wing spar is not really special, but is actually a powerful example of the class of applications where composite materials offer significant advantages over conventional materials.

1.3.3 Weight Advantages

What are the benefits of saving weight in a structure? Generally, we can choose from several alternatives. First, we can directly transfer weight savings into savings of fuel so that more efficient operating conditions result. Or else we can carry a heavier load of fuel and increase the range of an aircraft or truck. Or some combination of the two is possible. Further consequences of decreased weight of an airplane are that engine thrust, wing area, and fuel can then be decreased. For example, for fighters, a 1-lb (.45 kg) decrease in a part could lead to a 2.5-lb (1.13 kg) total weight decrease! For spacecraft, the total weight decrease is even larger! An observation: every pound of structural weight saved in a satellite means more propellant can be carried, and that results in a longer-life satellite because the weight that can be put into orbit is usually fixed by the booster capacity. If we make a higher percentage of that satellite weight fuel rather than structure, then the satellite will serve longer.

Weight savings can also mean the difference between whether the structure we design can perform its mission or not. The current Space Shuttle payload is limited to 60,000 lb (27,200 kg). If we have an object that we wish to carry up into space that weighs 65,000 lb (29,500 kg), then we are out of luck. That object does not satisfy the Shuttle's weight limit. We must wait for a new-generation Space Shuttle, or sufficient weight in the object to be carried must be saved to fit within the current Space Shuttle limitations.

The potential weight savings in a variety of structures are displayed in Figure 1-27. There, the savings range from a modest $25/lb ($55/kg), barely justifying the use of some composite materials, to the enormous $15,000/lb ($33,000/kg) in the Space Shuttle. In the case of the Space Shuttle, use of composite materials fairly shouts for attention. In between those two extremes, composite materials have very strong justification for use.

• SMALL CIVIL AIRCRAFT	$25/lb	($55/kg)
• HELICOPTER	$50/lb	($110/kg)
• AIRCRAFT ENGINES	$200/lb	($440/kg)
• FIGHTERS	$200/lb	($440/kg)
• COMMERCIAL AIRCRAFT ($20/lb/yr x 20 yr)	$400/lb	($880/kg)
• SST	$500/lb	($1,100/kg)
• NEAR-ORBIT SATELLITES	$1,000/lb	($2,200/kg)
• SYNCHRONOUS SATELLITES	$10,000/lb	($22,000/kg)
• SPACE SHUTTLE	$15,000/lb	($33,000/kg)

Figure 1-27 Value of Weight Savings in Structures

The potential for weight savings is closely coupled to fuel savings for most vehicles. Recently, the impact of both aerodynamic improvements and structural weight savings via the use of composite structures was assessed. The basic conclusions were that composite secondary structures might save 10% but that composite primary structures might save more than 30%. In contrast, laminar flow control might save 20%, active controls for both tail and wing 10%, high-aspect-ratio wings 10%, and supercritical wings less than 5%. Thus, the importance of improvements in both aerodynamics and composite structures is about equal.

Potentially, the structural weight savings on current production military aircraft is limited to about 20% or less. That number is necessarily low without extensive redesign. Future commercial aircraft might have weight savings of 25% whereas military aircraft might have 35%. The difference is in the more extensive use of composite materials in the high-heating environments of military aircraft. Spacecraft might have weight savings as high as 40%.

1.4 THE HOW — APPLICATIONS OF COMPOSITE MATERIALS

1.4.1 Introduction

Currently, almost every aerospace company is developing products made with fiber-reinforced composite materials. The usage of composite materials has progressed through several stages since the 1960s. First, *demonstration pieces* were built with the philosophy 'let's see if we *can* build one'. There may never have been any intention to put the part on an airplane and flight-test it because the objective was to make a first step toward *learning* about composite structures. The second stage was *replacement pieces* where part of the objective was to flight-test a part that was designed to replace a metal part on an existing airplane. The third stage is actual *production pieces* where the plane is designed from the beginning to have various parts fabricated from fiber-reinforced composite materials. The final stage is the *all-composite airplane* that many people have dreamed of building for many years. This last goal has been approached in the deliberate, conservative, multistage fashion just outlined. A substantial composite materials technology and manufacturing base has been built and awaits further challenge.

The impact of composite materials use on jet-engine performance is also very substantial. Currently, with various metal alloys, thrust-to-

weight ratios of 5 to 1 are achieved. Fiber-reinforced plastics and metals might lead to ratios as high as 16 to 1. Ultimately, with advanced graphite-fiber composites, thrust-to-weight ratios on the order of 40 to 1 appear possible. An eightfold increase in the performance index of thrust-to-weight ratio should lead to drastically pyramided weight savings in an entire aircraft due to substantially lessened structural support requirements. However, the road to this goal can be perilous. For example, the Rolls-Royce bankruptcy of the 1970s appears to be closely tied to a lost gamble on the timely development of graphite-epoxy fan blades for the Lockheed L-1011 engines.

In the near future, aircraft will be built with a very high percentage of components made from composite materials. Only then will the full advantages of weight savings be realized because nearly all parts of a plane interact with or support other parts. Hence, the effect of weight reduction in one part of a plane pyramids over the entire plane. Weight reductions are well-motivated because the structure of a typical airplane might weigh 30% of the total weight with only about 10% being payload and the rest fuel, electronic gear, etc. Thus, if materials that are 50% more effective in stiffness and strength were used, then the weight would be reduced by the amount of the payload. The implications of such a significant reduction are manifold. The payload could be doubled, the range extended, operating efficiency improved, or some combination of these and other factors would occur. Obviously, such benefits are welcome improvements, but there is a sometimes more significant benefit from weight savings. In the case of the 1960s United States SuperSonic Transport (SST) project, the possibility of carrying any payload at all was in doubt right up to the time when the project was cancelled. Similarly, the economic feasibility of VTOL (Vertical TakeOff and Landing) craft depends on the extensive use of composite materials. In all applications, improved fatigue life and reliability of composite materials are welcome added attractions.

1.4.2 Military Aircraft

A variety of military aircraft projects have occurred over the years — far more than can be summarized in a short space here. Thus, only some of the significant milestones will be described.

1.4.2.1 General Dynamics F-111 Wing-Pivot Fitting

The F-111 is a swing-wing fighter-bomber made by General Dynamics (now Lockheed Martin) in Fort Worth, Texas. The wings are perpendicular to the fuselage during takeoff or landing, and they are swept back at high speeds. Early in the production, some of the planes crashed, and the cause was traced to premature fatigue cracks in the forged-steel wing-pivot fitting shown in Figure 1-28. There, we can see the primary pivot point and where an actuator arm is attached with a piston to cause the wing to pivot. In the area of the central plate, fatigue cracks were identified when some of the planes were taken apart for inspection.

The obvious solution is to thicken the metal in that region of the wing-pivot fitting where failures occur so the stress levels are reduced below the endurance limit of the material. As an alternative solution, Dial and Howeth [1-5] reported that a boron-epoxy doubler was applied to reduce the stress levels. This doubler could be called a 'boron-epoxy Band-Aid'. Like a Band-Aid, the doubler was glued on the lower surface of an already existing wing-pivot forging as a reinforcement. Let's look at two contrasting situations to see how that solution actually worked out.

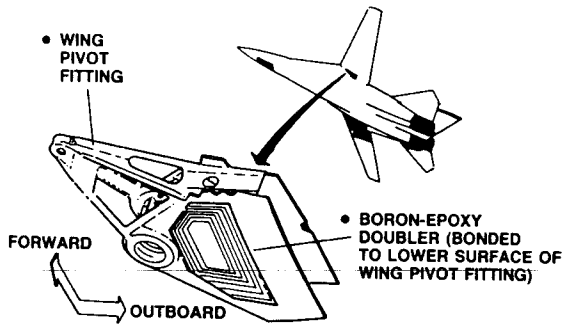

Figure 1-28 F-111 Wing-Pivot Fitting *(Courtesy of Lockheed Martin)*

Consider first the case of new aircraft. That is, the wing-pivot fitting crack problem was identified during the production run, so many airplanes had not yet been built. Obviously, the wing-pivot fittings on the unbuilt aircraft did not have any fatigue cracks. So General Dynamics put the doubler on the wing-pivot fitting before wing assembly. Let's compare the relative cost of the two different options. Suppose we had to redesign that steel wing-pivot fitting. The cost of the design modification and its fabrication and installation was in addition to the cost of the basic wing-pivot fitting which is the baseline or 100% relative cost for subsequent comparisons.

In contrast, if we take the already-designed wing-pivot fitting and simply put the boron-epoxy doubler on it (i.e., fabricate and install the doubler), the cost savings is 21%! That is a very worthwhile cost savings. That is, for all airplanes that had not yet been produced, the least-expensive approach was simply to put on the boron-epoxy Band-Aid. And that cost savings occurred at a time (the late 1960s) when boron-epoxy cost several hundred dollars per pound! This 21% savings in cost did not reflect one other very important issue. That issue is the long lead time to get such a large forging changed and back into production.

If General Dynamics had chosen to redesign the forging and request new forging production, they would have faced at least a year of production shutdown. The cost of that shutdown would far outweigh the 21% savings for a part. This 21% savings could actually have been a cost well above the original cost, and they would have been better off spending the money than stopping the production line. Thus, there are

various reasons why we choose alternative approaches, and they are not necessarily related to the cost of the part we are addressing. This 21% savings was a plus, both in the short-term and in the long-term cost of this essential aircraft modification.

The really big cost savings occurred for the aircraft that were already flying. In that case, the wing-pivot fitting that is not capable of doing the necessary job could be replaced with a redesigned wing-pivot fitting. However, we must pay for *two* wing-pivot fittings plus *disassembly* of the wing to remove the old wing-pivot fitting and then *reassembly* of the wing afterwards. That multiple assembly cost is very high. In contrast to that situation, as long as the existing wing-pivot fitting does not have fatigue cracks, then we can put on the boron-epoxy doubler and save about 60% over the alternative total replacement with a thickened steel forging in the region of the fatigue crack. That was the big savings, other than stopping the production line. This doubler was supposedly the first cost-effective application of advanced composite materials in about 1968. Some very important design trade-offs are prominent in this example.

1.4.2.2 Vought A-7 Speedbrake

The next example of military aircraft applications of composite materials is the Vought (now Northrop Grumman) A-7 speedbrake that drops from the bottom of the aircraft to decrease speed as in Figure 1-29. The A-7 is a diving fighter-bomber, so it must be able to slow down very rapidly by use of such a speedbrake. The metal design is a fairly intricate interlacing of longitudinal and lateral stiffeners in Figure 1-29 and weighs about 123 lb (56 kg). The composite speedbrake is a much simpler design with two bent (or jogged) struts that take loads in the different directions in Figure 1-30. Vought's all-composite-bonded structure with some molded fittings that were also laminated weighed 80 lb (36 kg), about a one-third weight savings. The simplicity of the composite speedbrake is readily apparent from comparison of Figures 1-29 and 1-30. The shape of the composite struts could not be duplicated with metal unless they were forged or machined, and both processes are quite expensive.

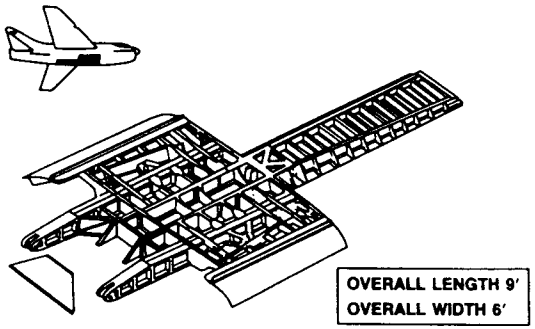

Figure 1-29 Metal A-7 Speedbrake *(Courtesy of Northrop Grumman)*

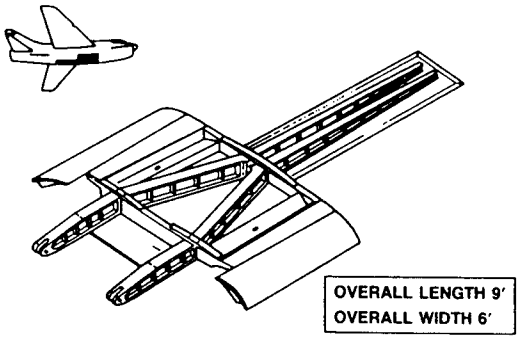

Figure 1-30 Composite A-7 Speedbrake *(Courtesy of Northrop Grumman)*

Some of the most significant problems in making this speedbrake with graphite-epoxy were in the regions where a hinge or pivot point is needed. We will examine this topic more in Section 7.5, but, for now, be aware that graphite-epoxy does not have a particularly high bearing strength. Any time a pivot, pin, or fastener exists, we must be concerned about the bearing strength of a composite structure, i.e., the ability of the composite material to support the pivot, pin, or fastener in direct bearing. Thus, Vought had to approach that problem cautiously, and, at the pivot point on the speed brake, they encapsulated some aluminum, which had adequate bearing strength, with graphite-epoxy as in Figure 1-31. Thus, this is a compound composite part with three constituents: graphite, epoxy, and aluminum. In a production environment, this speedbrake would not be made of aluminum next to graphite-epoxy because galvanic corrosion (discussed in Section 6.7) would exist between the two materials. But because this was a demonstration part and not intended for long-time flight use, the speedbrake pivot point area could be built with a material that is inexpensive such as aluminum because it is easy to machine. Vought was trying to demonstrate a principle, not to make a production part.

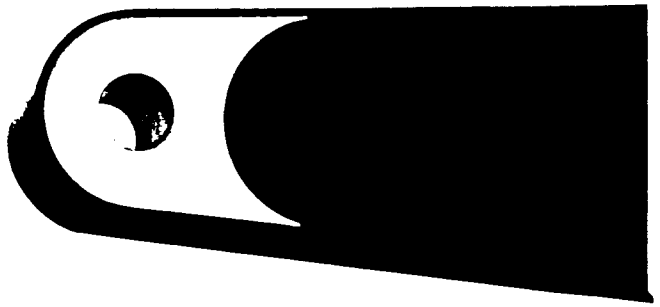

Figure 1-31 A-7 Speedbrake Bearing Pin Holder *(Courtesy of Northrop Grumman)*

1.4.2.3 Vought S-3A Spoiler

The next example is a spoiler made by Vought (now Northrop Grumman) for the Lockheed S-3A. The S-3A is a submarine search plane, and the spoiler is a relatively small flap-like object in the wing. In section A-A through the metal spoiler in Figure 1-32, we see that several machined extrusions are used as stiffeners internal to this structure. The spoiler skin has been chemically milled to change its thickness in various areas. Both machining extrusions and chem-milling are high-cost operations, so the spoiler looks quite simple, but is quite costly.

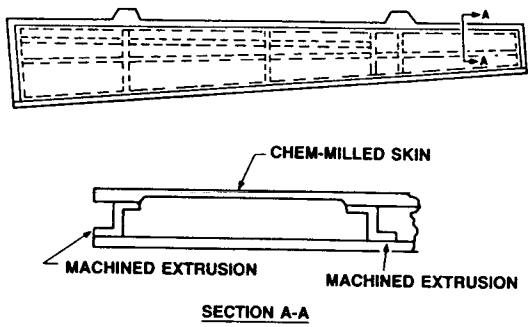

Figure 1-32 Metal S-3A Spoiler *(Courtesy of Lockheed Martin)*

For the composite spoiler design, the bottom is a variable-thickness skin on one side in Figure 1-33, but with composite materials that construction is not difficult. We do not have to chem-mill a composite material to change its thickness. All we do is stop building up the material in layers in the middle, but continue to build it up at the sides. That's a very natural process for composite materials and does not involve a costly machining operation. Instead of machined extruded stiffeners, a honeycomb core is placed on the inside of the laminae. That honeycomb

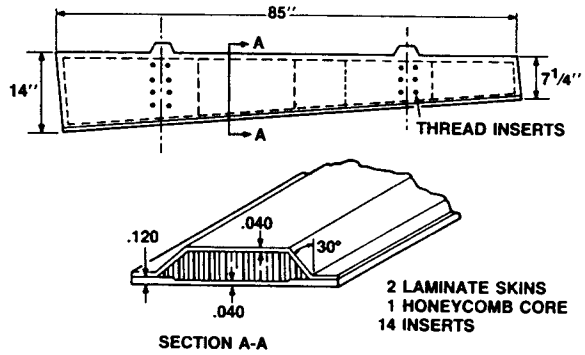

Figure 1-33 Composite S-3A Spoiler *(Courtesy of Lockheed Martin)*

core is simply band-sawed to shape and laid on the lower skin. The upper layer of skin is then draped over that band-sawed core, and the whole assembly is co-cured. Thus, the composite spoiler involves a very simple manufacturing procedure and a simple configuration.

The original metal spoiler weighs 13 lb (5.9 kg), and the graphite-epoxy with honeycomb-core spoiler weighs less than 8 lb (3.6 kg). Thus, Vought achieved a 41% weight savings. Contrast the high machining and chem-milling costs for the metal spoiler and its high weight with the graphite-epoxy design. Actual costs are not available, but from the weight savings and from the types of machining operations involved, the composite spoiler could be much more cost-effective than the metal spoiler. That conclusion is true even if the graphite-epoxy raw material cost is more than the aluminum cost because we are not comparing the designs based on raw material costs alone. Raw material cost is only the beginning of the true cost story. Fabrication costs can have a very strong, if not dominant, influence on the total cost of the structure.

1.4.2.4 Boeing F-18

Composite materials are used extensively in the F-18, an attack fighter made by McDonnell Douglas (now Boeing) and Northrop (now Northrop Grumman). The various speckled areas in Figure 1-34 are graphite-epoxy in primary structure: the vertical fin, the wings, and the horizontal tail surfaces. Also, graphite-epoxy is used in various small doors and other regions around the entire plane, which are secondary structures.

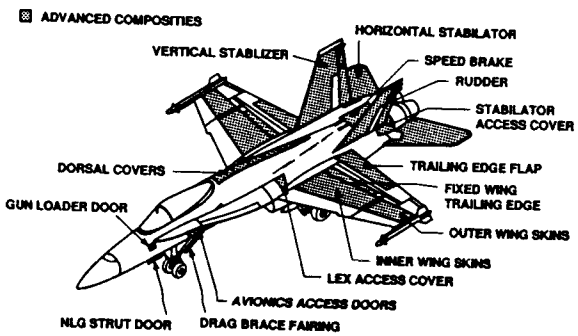

Figure 1-34 F-18C/D Composite Materials Usage *(Courtesy of Boeing)*

What are some of the important issues in the design and projected use of various second-generation part-composite aircraft, and why does graphite-epoxy play such an important role? If we consider aircraft weight alone, using graphite-epoxy can easily save approximately 10% of the total weight in Figure 1-35 over conventional metal aircraft design. For those specific structural elements made of composite materials as compared to if they had been made with metals, the percentage savings is much higher. Much larger savings, perhaps 30%, occur in the number

of parts in Figure 1-35. That savings in parts leads to yet another cost savings in the management system that must track all the parts through the production and assembly process to the final product and continue in the warehousing system to be able to replace parts in the future.

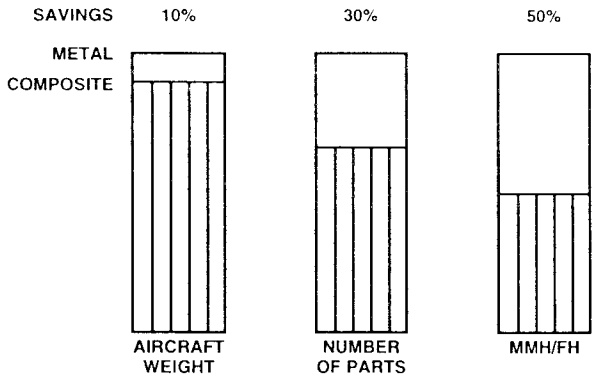

Figure 1-35 Typical Savings in Second-Generation Part-Composite Aircraft

The prospective savings in the ordinary maintenance that must be done in order to keep planes in the air, i.e., maintenance man-hours per flight hour, is 50% by using composite materials instead of metals in Figure 1-35. That percentage is enormous! And, the maintenance man-hours per flight hour issue is a very important indication of aircraft reliability and the cost of maintaining an aircraft over its lifetime. The main point is this: we cannot necessarily focus only on the issue of weight or on the issue of manufacturing costs. *All* of these costs must be examined at the same time to get a life-cycle cost estimate for a prospective aircraft.

1.4.2.5 Boeing AV-8B Harrier

On the AV-8B Harrier, also made by McDonnell Douglas (now Boeing) the shaded areas in Figure 1-36 are graphite-epoxy. The wing is 160 to 180 layers of graphite-epoxy at the thickest portion. About 1300 lb (590 kg) of graphite-epoxy are used in the entire structure. One of the reasons why we would like to use some of the advanced composite materials involves an issue that has not been mentioned so far. One of the alternative materials to some composite materials is titanium which is a strategic metal, i.e., a material of strategic importance in that it is not found naturally in the United States, yet it is necessary in some applications. If we can conserve strategic metals for applications where we absolutely must use them, then our concern about the strategic metal supply is lessened. We can make some substitutions for titanium with advanced composite materials, but not necessarily with graphite-epoxy. Some titanium is used in higher temperature situations than an epoxy is able to function. Other matrix materials for high-temperature applications are under development.

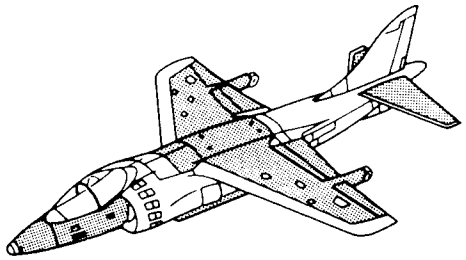

Figure 1-36 AV-8B Harrier Composite Material Applications *(Courtesy of Boeing)*

1.4.2.6 Grumman X-29A

The most unique feature of the Grumman X-29A is its forward-swept wings as seen in Figure 1-37. In metal aircraft, forward-swept wing structures must be especially stiffened at great weight penalty to avoid aerodynamic divergence. Only a few such aircraft have been built. In contrast, composite wing structures can be tailored layer by layer in laminate stiffnesses to successfully resist aerodynamic divergence and to simultaneously save weight over the usual rearward-swept wings! Such structural advances enable the use of the aerodynamically better performing forward-swept wings that offer the improved agility so essential to air-combat performance.

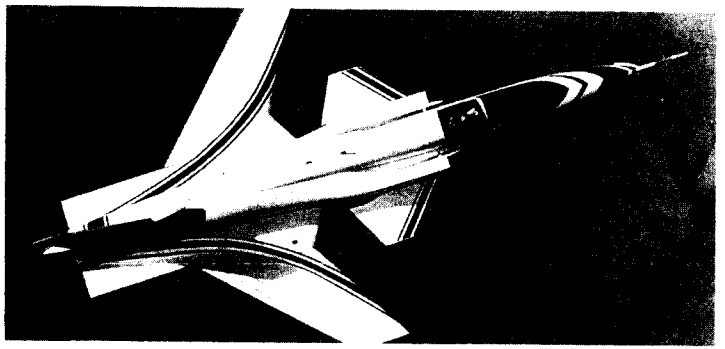

Figure 1-37 Grumman X-29A *(Courtesy of Northrop Grumman)*

1.4.2.7 Northrop Grumman B-2

The B-2 stealth bomber in Figure 1-38 is made by Northrop Grumman. Virtually all external parts are made of various composite materials because of their radar-absorption characteristics and/or their capability to be formed to shapes that naturally lower the radar cross section of the plane. However, the details are not publicly available, nor are they for the Lockheed Martin F-117A stealth fighter.

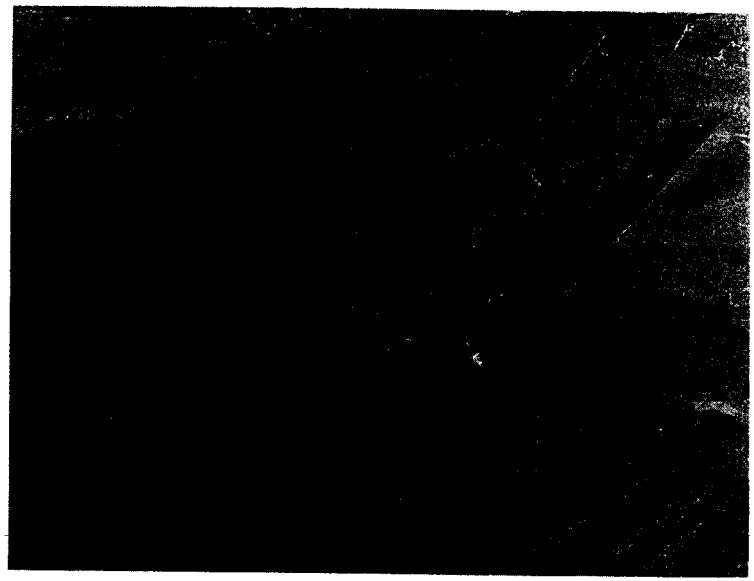

Figure 1-38 B-2 Stealth Bomber *(Courtesy of Northrop Grumman)*

1.4.2.8 Lockheed Martin F-22

The Lockheed Martin F-22 air-superiority fighter first flew in 1997 as in Figure 1-39. The plane has about 26% composite structures with two main manufacturing techniques used. Resin-transfer molding (RTM), as discussed in Section 1.2.4.2, permits thicker, more complexly shaped parts such as wing spars that are one-third the weight of a metal spar, 20% less expensive, and have half the rejection rate. Conventional tape layup for large flat pieces such as wings has no rivets so the flight-control surfaces are smooth leading to less drag.

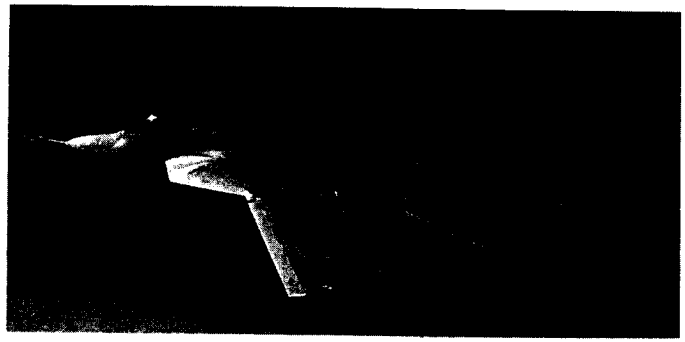

Figure 1-39 Lockheed Martin F-22 *(Courtesy of Lockheed Martin)*

1.4.3 Civil Aircraft

1.4.3.1 Lockheed L-1011 Vertical Fin

The vertical fin of the Lockheed L-1011 is shown in Figure 1-40 where the placement of the fin along with the internal structural members is apparent. The spar that goes up the entire fin is light enough to be picked up by one person even though it is over 20 ft (7 m) long. The main problem that was uncovered in the construction of this vertical fin was the difficulty to attach one composite part to another. And, in any structural test of the vertical fin, that is where the failures occurred. Reinforcements were then designed, and the fin achieved its design goal.

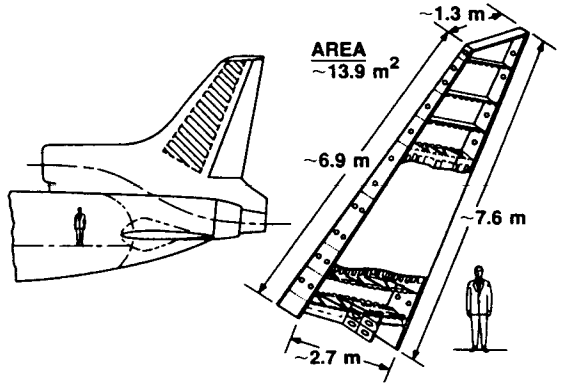

Figure 1-40 Lockheed L-1011 Vertical Fin *(After Jackson, et al. [1-6])*

The design goals of the vertical fin project were not only to achieve a lighter weight than with aluminum construction, but to reveal the cost implications of this kind of construction in comparison to metals. The cost of the aluminum fin on the left-hand side of Figure 1-41 is contrasted with the graphite-epoxy fin on the right-hand side. The cost is separated into various categories. For example, the aluminum fabrication material is about 5% of the total cost whereas graphite-epoxy is 14% of the total cost. Thus, the raw material cost would appear to be nearly three times as much for the graphite-epoxy as a percentage of the overall cost of the fin as for the aluminum. That comparison does not sound good, but *raw material cost is simply not the basis on which to make an initial, much less a final, cost judgement.* The other costs that are involved, such as support labor and structural assembly labor, are much lower for composite structures than they are for metallic structures as is seen in Figure 1-41. These costs are, in fact, so much lower that the other costs actually overwhelm that initial disadvantage of a higher raw material cost to the point where the bottom-line cost for the composite fin is 10% less than for the metal fin! Labor is the key issue in increased fabricability of composite materials which makes them much more cost-effective than metals in many applications, and that fact is becoming more evident every day.

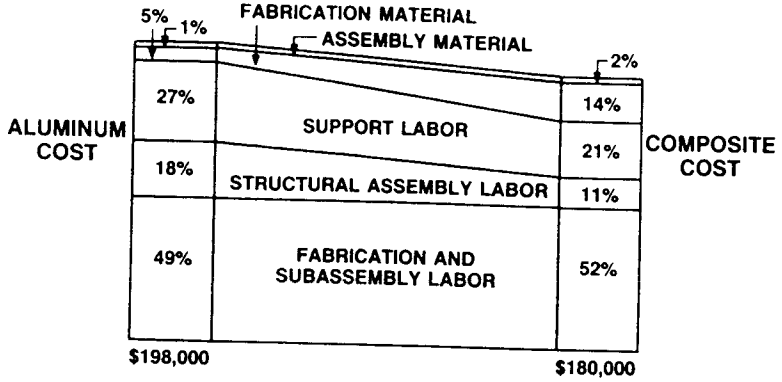

Figure 1-41 L-1011 Vertical Fin Cost *(After Alva, et al. [1-7])*

The point is that, despite a higher raw material cost, the *fabrication cost went down* enough to totally overwhelm the increased raw material cost! Obviously, the *labor costs far exceed the raw material cost, so small changes in labor costs are much more important than large changes in raw material costs.* A very important point: *do not think in terms of raw material cost alone.* We must integrate the fabrication costs in the total cost before we can make a valid comparison. Here, graphite-epoxy is more than competitive. Graphite-epoxy is the favored material in this application because it is more cost-effective than aluminum. That comparison is based on initial cost alone without taking into account the lower long-term operating and maintenance costs.

1.4.3.2 Rutan Voyager

One of the most significant recent aircraft is the Rutan Voyager, an all-composite plane in Figure 1-42 which was flown around the world non-stop in 1989. Burt Rutan of the Rutan Aircraft Factory created a seemingly endless line of all-composite aircraft in the 1980s and 1990s.

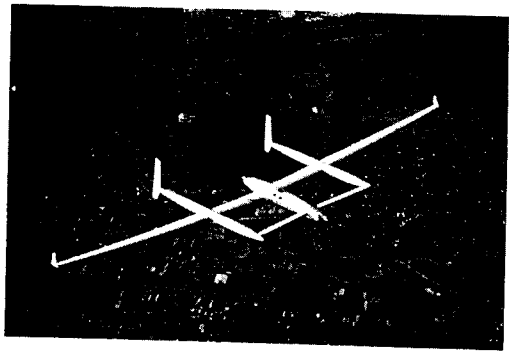

Figure 1-42 Rutan Voyager *(Courtesy of Scaled Composites)*

1.4.3.3 Boeing 777

The Boeing 777 large twin-engine wide-body aircraft in Figure 1-43 entered service in 1995 with more use of composite materials than any previous Boeing commercial aircraft. Approximately 18,500 lb (8,400 kg) of composite materials are used in each plane for both primary structure (a first for Boeing) and secondary structure for a total of 10% of the structural weight. Most notable is the large tail of carbon fibers in a toughened epoxy matrix with advantages of a 15-20% weight savings, enhanced corrosion resistance, improved aerodynamics, and surface detectability of impact damage. Production of the tail is highly automated, including tape layup, forming, and machining. The many fuselage floor beams in Figure 1-43 are also made with the toughened epoxy resin system. More ordinary carbon-epoxy is used in a variety of applications: tail rudder and elevators, inboard and outboard flaps, flaperons and ailerons, landing-gear doors, and engine cowlings. A hybrid of glass and carbon is used in the wing-to-body fairings. Lastly, the brakes are carbon-carbon.

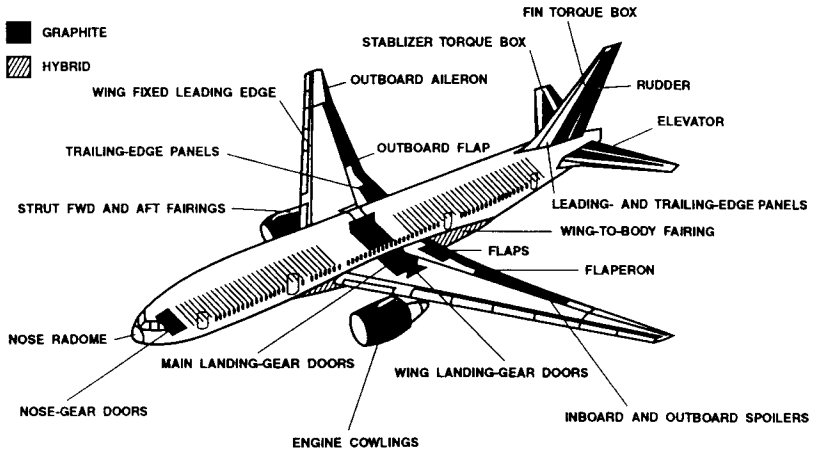

Figure 1-43 Boeing 777 *(Courtesy of Boeing)*

1.4.3.4 High-Speed Civil Transport

Much work is underway for the High-Speed Civil Transport (HSCT) as a successor to the various Supersonic Transports (SSTs) — the British-French Concorde, the Soviet Tupelov Tu-144, and the never-produced United States version. For the SSTs, the desired performance goals were attained at the expense of profitability. That is, the speed and range met the design requirements, but the structural weight to achieve them was so large as to preclude carrying a profitable payload. Advances in high-temperature structural concepts are the key to meeting profitability requirements for the HSCT as in Figure 1-44 to serve, for example, the Pacific-Rim market.

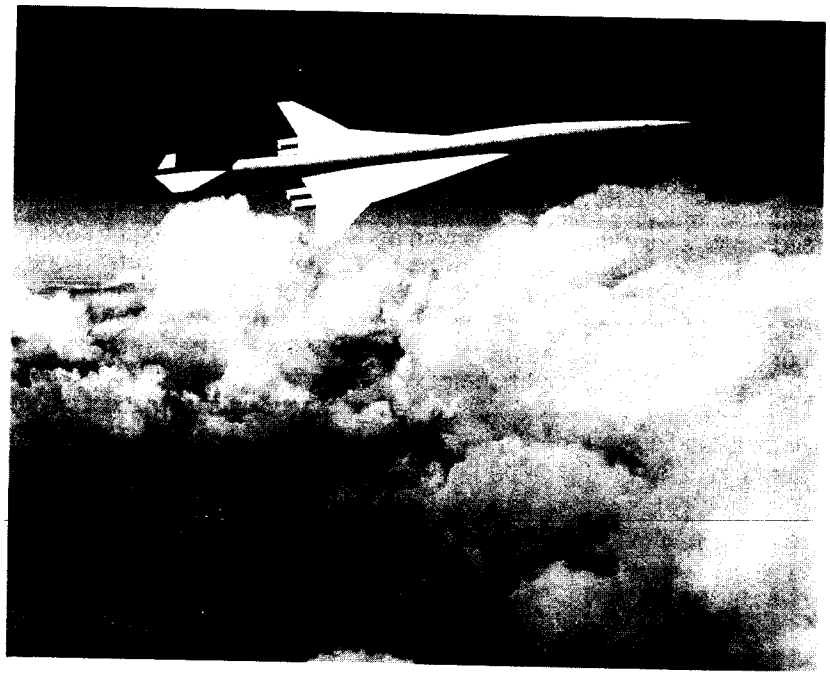

Figure 1-44 The High-Speed Civil Transport *(Courtesy of Boeing)*

1.4.4 Space Applications

Everyone is familiar, to some degree, with space activities. However, few are conversant with the role that various composite materials play in these activities. Weight savings are a crucial arena for space structures because of the enormous cost of boosting every structure from earth into space. Thus, composite materials are playing a compelling role in virtually all space structures, but not as much as they will in the future as more applications are developed.

Some graphite-epoxy structures can be tailored to have a zero coefficient of thermal expansion, a big advantage for large antennas that must pass in and out of the sun, yet maintain dimensional stability for accuracy of pointing the signal. For example, a graphite-epoxy truss is used to stabilize and support the Hubble Space Telescope.

1.4.5 Automotive Applications

Automotive applications of composite materials have an entirely new dimension — low-cost, high-rate production — compared to aircraft and space applications. This duality of the usual pair of economic factors of low-cost production coupled to high-rate production is essential to maintain the present vehicle cost at the current high rates of production yet attain the goal of increasing the current average gas mileage of 27.5 miles per gallon (11.7 km/l) to 80 miles per gallon (34 km/l). Economic

and marketing advisors suggest that the typical prospective car purchaser will act positively only if the initial cost of the car does not increase above the current cost. Simultaneously, the corresponding level of demand forces production rates that cannot be met with current manufacturing techniques. For example, tape-laying machines have production rates sufficient to manufacture all the needed aircraft per year. However, those same tape-laying machines are woefully inadequate to manufacture parts at the rates necessary to sustain automobile production that has a current rate per day which far exceeds the number of aircraft made in a decade! Furthermore, autoclave curing each such part would be a further bottleneck in the manufacturing problem because each part would take several hours to cure. Thus, new manufacturing techniques are essential before widespread use of composite parts in the automotive industry occurs. Moreover, the raw fiber cost of, for example, carbon fibers must be quite a lot less than currently to enable production of suitably low-cost parts.

Many attempts have been made to incorporate composite materials in automobile production starting with Henry Ford's 'corn cob car' in the late 1930s (not to mention earlier uses of wood!). The fiberglass-bodied Chevrolet Corvette, first introduced in 1953, is the only long-term success. Certain individual car parts, such as springs and driveshafts, have unique characteristics that have proven production records of low-cost, high-production rates, and high weight savings that can satisfy body-mass-reduction requirements to meet the fuel economy goals. For example, the steel springs for the 1980 Chevrolet Corvette weighed 41 lb (19 kg) whereas the 1981 and later composite springs weighed only 8 lb (3.6 kg).

In the 1970s and 1980s, many attempts were made to update the data base of information on then-current manufacturing techniques, costs, and part weights. Moreover, the normal composite materials manufacturing advantage of being able to replace a large number of interconnected metal parts with a far smaller number (as low as one) of composite parts was explored to assess impact on overall manufacturing cost. In 1979, a Ford LTD (full-size) sedan was produced slowly from $25,000 (1979 dollars) in raw material for a total project cost of $3.5 million with a weight reduction to 2500 lb (1100 kg) from the usual 3740 lb (1700 kg) of the equivalent steel car. The total project cost is quite irrelevant because any single car will always cost more than $1 million to produce. However, the raw material cost alone was greater than the equivalent economic value of the car, i.e., what you could have bought instead. Moreover, the manufacturing techniques were far too slow to keep up with the normal consumer demand. Accordingly, the checkpoint result of 1979 was unsatisfactory (although some individual parts such as springs and driveshafts did survive to somewhat standard production). The further checkpoint of 1997 reveals substantial progress toward faster manufacturing processes and lower-mass vehicles, but the cost of carbon fibers to achieve a low enough mass to meet fuel economy goals still precludes production at the cost of a typical 1997 passenger sedan. However, large-scale molding has been demonstrated by Ford to result

in one-fifth the number of body parts with molding composite parts being 60% less costly than stamping metal parts of similar shape. Thus, progress is being made year-by-year toward the goal of composite cars that cost the same as metal cars, yet use far less of our precious petroleum resources.

1.4.6 Commercial Applications

Some composite materials found their way into commercial applications very quickly if costs could be controlled or were not an issue. For example, fiberglass fishing rods were produced in the 1940s and became virtually the standard by the 1960s. Many other fiberglass products became popular: boats, cars to a limited extent, tennis rackets, skis, surf boards. More costly fiber systems such as boron-epoxy and graphite-epoxy are used in golf clubs and tennis rackets despite their high cost because highly competitive consumers are quite willing, and even anxious, to spend more money on an 'exotic' fiber system that just might give them an 'edge' in their game. In fact, the early use of graphite-epoxy on golf clubs was a significant factor in enhanced use in military aircraft because the increased production volume of graphite-epoxy lowered the cost for all users. Graphite-epoxy is quite effective in reinforcing already built columns of bridges in seismically active regions such as California and Japan. More and more applications will occur as the world's inventors use their imagination and cunning to improve old products and to create new products.

1.5 SUMMARY

The basic questions of The What, The Why, and The How of composite materials and structures have been addressed. Much more could be said about, for example, polymers, metals, ceramics, and carbon used as matrix materials. Also, many more composites manufacturing techniques are available. Moreover, many more examples of effective use of composite materials in structures do exist. However, an introduction to each topic has been provided, and hopefully, those introductions will suffice for the purpose of giving background on composite materials prior to studying their mechanics.

Lamina macromechanics will be studied thoroughly in Chapter 2. Then, lamina micromechanics will be introduced in Chapter 3. Next, how laminae are combined to form a laminate is treated in Chapter 4 along with laminate strength and how interlaminar stresses arise and affect strength and fatigue life. In Chapter 5, the structural performance of laminated plates is addressed with emphasis on deflections, buckling loads, and vibration modes and frequencies. A variety of miscellaneous analysis and behavior topics is introduced in Chapter 6. Finally, in Chapter 7, the broad topic of design of composite structures is briefly introduced. In all parts of the book, always expect surprises relative to the often-inapplicable intuition you have developed based on the relatively simple behavior of isotropic metals!

Problem Set 1

For each of the following questions, write mini-essays that are at least a page long and have figures that you discuss and describe. Use your imagination and available resources such as the library and the World Wide Web to get more information than is in the book. Properly cite each of your sources.

1.1 Define a composite material in a more extensive manner than the one-sentence version in Chapter 1.
1.2 Find a description of how carbon and graphite fibers are made and summarize it.
1.3 Describe and discuss thermoset-matrix and thermoplastic-matrix materials. Contrast their production times if you were to build a composite structure with both materials.
1.4 Find another example or type of laminated composite material than those mentioned in Chapter 1 and describe it.
1.5 Describe some other composite materials that are not addressed in Chapter 1.
1.6 Describe the kind of structural element that can be produced using each of the manufacturing layup processes that were studied in Chapter 1.
1.7 Find another manufacturing process for creating a composite structure than addressed in Chapter 1 or in class and describe it.
1.8 Find a description of an innovative composite structure, device, or object in a publication such as *Aviation Week and Space Technology, Mechanical Engineering, Civil Engineering*, etc. and write a synopsis of its important characteristics.

REFERENCES

1-1 Albert G. H. Dietz, Composite Materials, 1965 Edgar Marburg Lecture, American Society for Testing and Materials, 1965 (reprinted with permission).
1-2 Willard H. Sutton, B. Walter Rosen, and Donald G. Flom, Whisker-Reinforced Plastics for Space Applications, *SPE Journal*, November 1964, pp. 1203–1209.
1-3 *Structural Design Guide for Advanced Composite Applications*, Vol. 1, Material Characterization, 2nd edition, Advanced Composites Division, Air Force Materials Laboratory, January 1971.
1-4 John F. Judge, Composite Materials: The Coming Revolution, *Airline Management and Marketing*, September 1969, pp. 85, 90, and 91.
1-5 D. D. Dial and M. S. Howeth, Advanced Composites Cost Comparison, *16th National SAMPE Symposium and Exhibition*, Anaheim, California, 21-23 April 1971.
1-6 A. C. Jackson, J. F. Crocker, J. C. Ekvall, R. R. Eudaily, B. Mosesian, R. R. Van Cleave, and J. Van Hamersveld, *Advanced Manufacturing Development of a Composite Empennage for L-1011 Aircraft, Phase II Final Report, Design Analysis*, NASA CR 165634, Lockheed California Company, Burbank California, April 1981.
1-7 F. Alva, G. Brozovic, B. Carll, R. Eudaily, J. Henkel, A. Jackson, R. Johnson, B. Mosesian, and R. O'Brien, *Advanced Manufacturing Development of a Composite Empennage for L-1011 Aircraft, Phase IV Final Report, Manufacturing Development*, NASA CR 165885, Lockheed California Company, Burbank California, May 1982.

Chapter 2

MACROMECHANICAL BEHAVIOR OF A LAMINA

2.1 INTRODUCTION

The basic questions of lamina macromechanics are: (1) what are the characteristics of a lamina? and (2) how does a lamina respond to applied stresses as in Figure 2-1? A lamina is a flat (or curved as in a shell) arrangement of unidirectional or woven fibers in a supporting matrix. The concepts developed in this chapter apply equally to both types of lamina, but we will explicitly address only unidirectional laminae. A lamina is the basic building block in laminated fiber-reinforced composite materials. Thus, knowledge of the mechanical behavior of a lamina is essential to the understanding of laminated fiber-reinforced structures. This chapter is focused on macromechanical behavior, i.e., the behavior when only averaged apparent mechanical properties are considered, rather than the detailed interactions of the constituents of the composite material which will be addressed in Chapter 3. The basic restriction of both chapters is to linear elastic behavior. Both stiffnesses and strengths will be investigated for complex through simple materials in what follows.

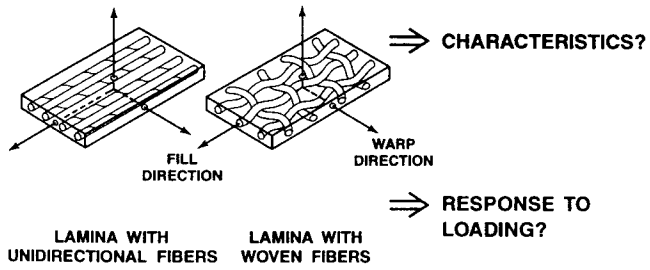

Figure 2-1 Basic Questions of Lamina Macromechanics

2.2 STRESS-STRAIN RELATIONS FOR ANISOTROPIC MATERIALS

The generalized Hooke's law relating stresses to strains can be written in contracted notation as

$$\sigma_i = C_{ij}\,\varepsilon_j \qquad i,j = 1, \ldots, 6 \tag{2.1}$$

where σ_i are the stress components shown on a three-dimensional cube in x, y, and z coordinates in Figure 2-2, C_{ij} is the stiffness matrix, and ε_j are the strain components. The contracted notation for three-dimensional stresses and strains is defined in comparison to the usual tensor notation in Table 2-1 for situations in which the stress and strain tensors are symmetric (the usual case when body forces are absent). Note that, by virtue of Table 2-1, the strains are therefore defined as

$$\varepsilon_1 = \frac{\partial u}{\partial x} \qquad \varepsilon_2 = \frac{\partial v}{\partial y} \qquad \varepsilon_3 = \frac{\partial w}{\partial z}$$
$$\gamma_{23} = \frac{\partial v}{\partial z} + \frac{\partial w}{\partial y} \qquad \gamma_{31} = \frac{\partial w}{\partial x} + \frac{\partial u}{\partial z} \qquad \gamma_{12} = \frac{\partial u}{\partial y} + \frac{\partial v}{\partial x} \tag{2.2}$$

where u, v, and w are displacements in the x, y, and z directions (or the 1, 2, and 3 directions).

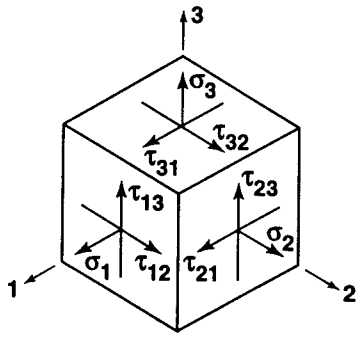

Figure 2-2 Stresses on an Element

Table 2-1 Tensor versus Contracted Notation for Stresses and Strains

Stresses		Strains	
Tensor Notation	Contracted Notation	Tensor Notation	Contracted Notation
σ_{11} (σ_1)	σ_1	ε_{11} (ε_1)	ε_1
σ_{22} (σ_2)	σ_2	ε_{22} (ε_2)	ε_2
σ_{33} (σ_3)	σ_3	ε_{33} (ε_3)	ε_3
$\tau_{23} = \sigma_{32}$	σ_4	$\gamma_{23} = 2\varepsilon_{23}$*	ε_4
$\tau_{31} = \sigma_{31}$	σ_5	$\gamma_{31} = 2\varepsilon_{31}$	ε_5
$\tau_{12} = \sigma_{12}$	σ_6	$\gamma_{12} = 2\varepsilon_{12}$	ε_6

*Note that γ_{ij} represents engineering shear strain whereas $\varepsilon_{ij}(i \neq j)$ represents tensor shear strain.

Note that the engineering shear strain, γ_{ij}, in Table 2-1 is the total angle of shearing under a state of simple shear in Figure 2-3. Also, the tensor shear strain, ε_{ij}, is half of the angle of shearing under pure shear stress in Figure 2-3. Engineering shear strain implies a rotation of the originally square element, whereas tensor shear strain does not have an accompanying rotation. These distinctions have little significance for the usual engineering calculations, but have crucial significance in what follows.

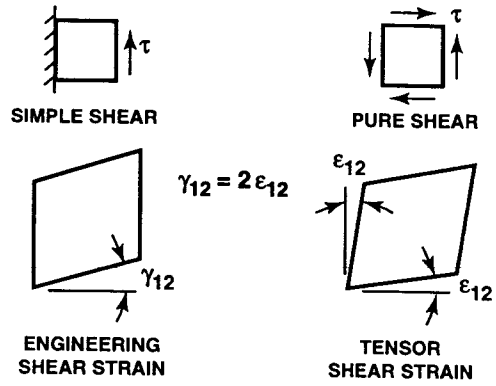

Figure 2-3 Engineering Shear Strain versus Tensor Shear Strain

The stiffness matrix, C_{ij}, has 36 constants in Equation (2.1). However, less than 36 of the constants can be shown to actually be independent for elastic materials when important characteristics of the strain energy are considered. Elastic materials for which an elastic potential or strain energy density function exists have incremental work per unit volume of

$$dW = \sigma_i d\varepsilon_i \tag{2.3}$$

when the stresses σ_i act through strains $d\varepsilon_i$. However, because of the stress-strain relations, Equation (2.1), the incremental work becomes

$$dW = C_{ij}\varepsilon_j d\varepsilon_j \tag{2.4}$$

Upon integration for all strains, the work per unit of volume is

$$W = \frac{1}{2} C_{ij}\varepsilon_i\varepsilon_j \tag{2.5}$$

However, Hooke's law, Equation (2.1), can be derived from Equation (2.5):

$$\frac{\partial W}{\partial \varepsilon_i} = C_{ij}\varepsilon_j \tag{2.6}$$

whereupon

$$\frac{\partial^2 W}{\partial \varepsilon_i \partial \varepsilon_j} = C_{ij} \tag{2.7}$$

Similarly,

$$\frac{\partial^2 W}{\partial \varepsilon_j \partial \varepsilon_i} = C_{ji} \tag{2.8}$$

But the order of differentiation of W is immaterial, so

$$C_{ij} = C_{ji} \tag{2.9}$$

Thus, the stiffness matrix is symmetric, so only 21 of the constants are independent.

In a similar manner, we can show that

$$W = \frac{1}{2} S_{ij} \sigma_i \sigma_j \tag{2.10}$$

where S_{ij} is the compliance matrix defined by the inverse of the stress-strain relations, namely the strain-stress relations:

$$\varepsilon_i = S_{ij} \sigma_j \qquad i, j = 1, \ldots, 6 \tag{2.11}$$

Reasoning similar to that in the preceding paragraph leads to

$$S_{ij} = S_{ji} \tag{2.12}$$

i.e., that the compliance matrix is symmetric and hence has only 21 independent constants. At this point, note that the stiffnesses and compliances are not described with mnemonic notation, but are unfortunately reversed in common usage. The stiffness and compliance components will be referred to as elastic constants (although they could be functions of temperature or moisture content).

With the foregoing reduction from 36 to 21 independent constants, the stress-strain relations are

$$\begin{bmatrix} \sigma_1 \\ \sigma_2 \\ \sigma_3 \\ \tau_{23} \\ \tau_{31} \\ \tau_{12} \end{bmatrix} = \begin{bmatrix} C_{11} & C_{12} & C_{13} & C_{14} & C_{15} & C_{16} \\ C_{12} & C_{22} & C_{23} & C_{24} & C_{25} & C_{26} \\ C_{13} & C_{23} & C_{33} & C_{34} & C_{35} & C_{36} \\ C_{14} & C_{24} & C_{34} & C_{44} & C_{45} & C_{46} \\ C_{15} & C_{25} & C_{35} & C_{45} & C_{55} & C_{56} \\ C_{16} & C_{26} & C_{36} & C_{46} & C_{56} & C_{66} \end{bmatrix} \begin{bmatrix} \varepsilon_1 \\ \varepsilon_2 \\ \varepsilon_3 \\ \gamma_{23} \\ \gamma_{31} \\ \gamma_{12} \end{bmatrix} \tag{2.13}$$

as the most general expression within the framework of linear elasticity. Actually, the relations in Equation (2.13) are referred to as characterizing *anisotropic* materials (anisotropic means without isotropy) because there are no planes of symmetry for the material properties. An alternative name for such an anisotropic material is a *triclinic* material (three axes of the material are all oblique to one another). Materials with more property symmetry than anisotropic materials will be described in the next few paragraphs. Proof of the form of the stress-strain relations for the various cases of material property symmetry is given, for example, by Tsai [2-1].

If there is one plane of material property symmetry, the stress-strain relations reduce to

$$\begin{bmatrix} \sigma_1 \\ \sigma_2 \\ \sigma_3 \\ \tau_{23} \\ \tau_{31} \\ \tau_{12} \end{bmatrix} = \begin{bmatrix} C_{11} & C_{12} & C_{13} & 0 & 0 & C_{16} \\ C_{12} & C_{22} & C_{23} & 0 & 0 & C_{26} \\ C_{13} & C_{23} & C_{33} & 0 & 0 & C_{36} \\ 0 & 0 & 0 & C_{44} & C_{45} & 0 \\ 0 & 0 & 0 & C_{45} & C_{55} & 0 \\ C_{16} & C_{26} & C_{36} & 0 & 0 & C_{66} \end{bmatrix} \begin{bmatrix} \varepsilon_1 \\ \varepsilon_2 \\ \varepsilon_3 \\ \gamma_{23} \\ \gamma_{31} \\ \gamma_{12} \end{bmatrix} \tag{2.14}$$

where the plane of symmetry is $z = 0$ (or the 1-2 plane). Such a material is termed *monoclinic* and has 13 independent elastic constants.

If there are two orthogonal planes of material property symmetry for a material, symmetry will exist relative to a third mutually orthogonal plane. The stress-strain relations in coordinates aligned with principal material directions[1] are

$$\begin{bmatrix} \sigma_1 \\ \sigma_2 \\ \sigma_3 \\ \tau_{23} \\ \tau_{31} \\ \tau_{12} \end{bmatrix} = \begin{bmatrix} C_{11} & C_{12} & C_{13} & 0 & 0 & 0 \\ C_{12} & C_{22} & C_{23} & 0 & 0 & 0 \\ C_{13} & C_{23} & C_{33} & 0 & 0 & 0 \\ 0 & 0 & 0 & C_{44} & 0 & 0 \\ 0 & 0 & 0 & 0 & C_{55} & 0 \\ 0 & 0 & 0 & 0 & 0 & C_{66} \end{bmatrix} \begin{bmatrix} \varepsilon_1 \\ \varepsilon_2 \\ \varepsilon_3 \\ \gamma_{23} \\ \gamma_{31} \\ \gamma_{12} \end{bmatrix} \tag{2.15}$$

and are said to define an *orthotropic* material. Note that there is no interaction between normal stresses σ_1, σ_2, σ_3 and shearing strains γ_{23}, γ_{31}, γ_{12} such as occurs in anisotropic materials (by virtue of the presence of, for example, C_{14}). Similarly, there is no interaction between shearing stresses and normal strains as well as none between shearing stresses and shearing strains in different planes. Note also that there are now only *nine* independent constants in the stiffness matrix.

If at every point of a material there is one plane in which the mechanical properties are equal in all directions, then the material is called *transversely isotropic*. If, for example, the 1-2 plane is the plane of isotropy, then the 1 and 2 subscripts on the stiffnesses are interchangeable. The stress-strain relations have only *five* independent constants:

[1] Principal material directions (PMD) are directions that are parallel to the intersections of the three orthogonal planes of material property symmetry. Principal material coordinates (PMC) are the set of axes in principal material directions.

$$\begin{bmatrix}\sigma_1\\ \sigma_2\\ \sigma_3\\ \tau_{23}\\ \tau_{31}\\ \tau_{12}\end{bmatrix}=\begin{bmatrix}C_{11} & C_{12} & C_{13} & 0 & 0 & 0\\ C_{12} & C_{11} & C_{13} & 0 & 0 & 0\\ C_{13} & C_{13} & C_{33} & 0 & 0 & 0\\ 0 & 0 & 0 & C_{44} & 0 & 0\\ 0 & 0 & 0 & 0 & C_{44} & 0\\ 0 & 0 & 0 & 0 & 0 & (C_{11}-C_{12})/2\end{bmatrix}\begin{bmatrix}\varepsilon_1\\ \varepsilon_2\\ \varepsilon_3\\ \gamma_{23}\\ \gamma_{31}\\ \gamma_{12}\end{bmatrix} \tag{2.16}$$

If there is an infinite number of planes of material property symmetry, then the foregoing relations simplify to the *isotropic* material relations with only *two* independent constants in the stiffness matrix:

$$\begin{bmatrix}\sigma_1\\ \sigma_2\\ \sigma_3\\ \tau_{23}\\ \tau_{31}\\ \tau_{12}\end{bmatrix}=\begin{bmatrix}C_{11} & C_{12} & C_{12} & 0 & 0 & 0\\ C_{12} & C_{11} & C_{12} & 0 & 0 & 0\\ C_{12} & C_{12} & C_{11} & 0 & 0 & 0\\ 0 & 0 & 0 & (C_{11}-C_{12})/2 & 0 & 0\\ 0 & 0 & 0 & 0 & (C_{11}-C_{12})/2 & 0\\ 0 & 0 & 0 & 0 & 0 & (C_{11}-C_{12})/2\end{bmatrix}\begin{bmatrix}\varepsilon_1\\ \varepsilon_2\\ \varepsilon_3\\ \gamma_{23}\\ \gamma_{31}\\ \gamma_{12}\end{bmatrix} \tag{2.17}$$

The strain-stress relations for the five most common material property symmetry cases are shown in Equations (2.18) to (2.22):

Anisotropic (21 independent constants):

$$\begin{bmatrix}\varepsilon_1\\ \varepsilon_2\\ \varepsilon_3\\ \gamma_{23}\\ \gamma_{31}\\ \gamma_{12}\end{bmatrix}=\begin{bmatrix}S_{11} & S_{12} & S_{13} & S_{14} & S_{15} & S_{16}\\ S_{12} & S_{22} & S_{23} & S_{24} & S_{25} & S_{26}\\ S_{13} & S_{23} & S_{33} & S_{34} & S_{35} & S_{36}\\ S_{14} & S_{24} & S_{34} & S_{44} & S_{45} & S_{46}\\ S_{15} & S_{25} & S_{35} & S_{45} & S_{55} & S_{56}\\ S_{16} & S_{26} & S_{36} & S_{46} & S_{56} & S_{66}\end{bmatrix}\begin{bmatrix}\sigma_1\\ \sigma_2\\ \sigma_3\\ \tau_{23}\\ \tau_{31}\\ \tau_{12}\end{bmatrix} \tag{2.18}$$

Monoclinic (13 independent constants) (for symmetry about z = 0):

$$\begin{bmatrix}\varepsilon_1\\ \varepsilon_2\\ \varepsilon_3\\ \gamma_{23}\\ \gamma_{31}\\ \gamma_{12}\end{bmatrix}=\begin{bmatrix}S_{11} & S_{12} & S_{13} & 0 & 0 & S_{16}\\ S_{12} & S_{22} & S_{23} & 0 & 0 & S_{26}\\ S_{13} & S_{23} & S_{33} & 0 & 0 & S_{36}\\ 0 & 0 & 0 & S_{44} & S_{45} & 0\\ 0 & 0 & 0 & S_{45} & S_{55} & 0\\ S_{16} & S_{26} & S_{36} & 0 & 0 & S_{66}\end{bmatrix}\begin{bmatrix}\sigma_1\\ \sigma_2\\ \sigma_3\\ \tau_{23}\\ \tau_{31}\\ \tau_{12}\end{bmatrix} \tag{2.19}$$

Orthotropic (9 independent constants):

$$\begin{bmatrix}\varepsilon_1\\ \varepsilon_2\\ \varepsilon_3\\ \gamma_{23}\\ \gamma_{31}\\ \gamma_{12}\end{bmatrix}=\begin{bmatrix}S_{11} & S_{12} & S_{13} & 0 & 0 & 0\\ S_{12} & S_{22} & S_{23} & 0 & 0 & 0\\ S_{13} & S_{23} & S_{33} & 0 & 0 & 0\\ 0 & 0 & 0 & S_{44} & 0 & 0\\ 0 & 0 & 0 & 0 & S_{55} & 0\\ 0 & 0 & 0 & 0 & 0 & S_{66}\end{bmatrix}\begin{bmatrix}\sigma_1\\ \sigma_2\\ \sigma_3\\ \tau_{23}\\ \tau_{31}\\ \tau_{12}\end{bmatrix} \tag{2.20}$$

Transversely Isotropic (5 independent constants):

$$\begin{bmatrix}\varepsilon_1\\ \varepsilon_2\\ \varepsilon_3\\ \gamma_{23}\\ \gamma_{31}\\ \gamma_{12}\end{bmatrix}=\begin{bmatrix}S_{11} & S_{12} & S_{13} & 0 & 0 & 0\\ S_{12} & S_{11} & S_{13} & 0 & 0 & 0\\ S_{13} & S_{13} & S_{33} & 0 & 0 & 0\\ 0 & 0 & 0 & S_{44} & 0 & 0\\ 0 & 0 & 0 & 0 & S_{44} & 0\\ 0 & 0 & 0 & 0 & 0 & 2(S_{11}-S_{12})\end{bmatrix}\begin{bmatrix}\sigma_1\\ \sigma_2\\ \sigma_3\\ \tau_{23}\\ \tau_{31}\\ \tau_{12}\end{bmatrix} \tag{2.21}$$

where the 1-2 plane is a symmetry plane in which the compliances are isotropic and in the 3-direction (transverse to the symmetry plane), the compliances are different.

Isotropic (2 independent constants):

$$\begin{bmatrix}\varepsilon_1\\ \varepsilon_2\\ \varepsilon_3\\ \gamma_{23}\\ \gamma_{31}\\ \gamma_{12}\end{bmatrix} = \begin{bmatrix} S_{11} & S_{12} & S_{12} & 0 & 0 & 0\\ S_{12} & S_{11} & S_{12} & 0 & 0 & 0\\ S_{12} & S_{12} & S_{11} & 0 & 0 & 0\\ 0 & 0 & 0 & 2(S_{11}-S_{12}) & 0 & 0\\ 0 & 0 & 0 & 0 & 2(S_{11}-S_{12}) & 0\\ 0 & 0 & 0 & 0 & 0 & 2(S_{11}-S_{12}) \end{bmatrix} \begin{bmatrix}\sigma_1\\ \sigma_2\\ \sigma_3\\ \tau_{23}\\ \tau_{31}\\ \tau_{12}\end{bmatrix} \tag{2.22}$$

One of the major objectives in studying the strain-stress relations is to be able to conclude what deformation response occurs because of a specific applied stress. The strain-stress relations can be written as

$$\begin{aligned}\varepsilon_1 &= S_{11}\sigma_1 + S_{12}\sigma_2 + S_{13}\sigma_3 + S_{14}\tau_{23} + S_{15}\tau_{31} + S_{16}\tau_{12}\\ &\vdots\\ \gamma_{12} &= S_{16}\sigma_1 + S_{26}\sigma_2 + S_{36}\sigma_3 + S_{46}\tau_{23} + S_{56}\tau_{31} + S_{66}\tau_{12}\end{aligned} \tag{2.23}$$

Accordingly, for an applied uniaxial stress $\sigma_1 = \sigma$ (all other stresses are zero):

$$\begin{aligned}\varepsilon_1 &= S_{11}\sigma \qquad \varepsilon_2 = S_{12}\sigma \qquad \varepsilon_3 = S_{13}\sigma\\ \gamma_{23} &= S_{14}\sigma \qquad \gamma_{31} = S_{15}\sigma \qquad \gamma_{12} = S_{16}\sigma\end{aligned} \tag{2.24}$$

The physical interpretation of these strains is that an originally equal-sided cube has many deformations. Specifically, each side deforms in length differently from any other side (because $S_{11} \neq S_{12} \neq S_{13}$), and each side of the cube undergoes a different shearing deformation (because $S_{14} \neq S_{15} \neq S_{16}$), as depicted imperfectly in Figure 2-4, where the dashed lines represent the undeformed cube and the solid lines represent the deformed cube. Try to imagine yourself in a room that undergoes these deformations! In contrast, an isotropic material would have the same change in side length in the 2- and 3-directions (because $S_{12} = S_{13}$) and no shearing deformation of any side (because $S_{14} = S_{15} = S_{16} = 0$). Thus, for an anisotropic material, significant coupling occurs between the applied stress and the various strain responses.

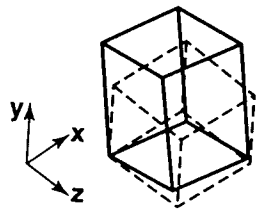

Figure 2-4 Deformation of an Anisotropic Cube under σ_y

Those various couplings are shown for an arbitrarily stressed body in Figure 2-5 where the physical significance of each compliance is labeled. There, the terms S_{11}, S_{22}, and S_{33} each represent extensional response to an individual applied stress, σ_1, σ_2, and σ_3, respectively, *in the same direction.* The terms S_{44}, S_{55}, and S_{66} represent shear strain response to an applied shear stress *in the same plane.* The terms S_{12}, S_{13}, and S_{23} represent coupling between dissimilar normal stresses and normal strains (*extension-extension coupling* more commonly known as the Poisson effect). The terms S_{14}, S_{15}, S_{16}, S_{24}, S_{25}, S_{26}, S_{34}, S_{35}, and S_{36} represent normal strain response to applied shear stress in a more complex manner than for the preceding compliances (*shear-extension coupling*). Finally, the terms S_{45}, S_{46}, and S_{56} represent shear strain response to shear stress applied in another plane (*shear-shear coupling*). In contrast, the only coupling that exists for an isotropic material is extension-extension coupling. Thus, the deformation response of an anisotropic material even to simple stress states can literally be in every direction and in every plane. We will see in Section 2.6 that orthotropic materials can exhibit apparent anisotropy when stressed in non-principal material coordinates. Moreover, we will see that S_{11}, S_{22}, and S_{33} are related to the Young's moduli in the 1-, 2-, and 3-directions, respectively. Also, S_{12}, S_{13}, and S_{14} will be related to the Poisson's ratios and Young's moduli. Finally, S_{44}, S_{55}, and S_{66} will be related to shear moduli in the 2-3, 3-1, and 1-2 planes, respectively.

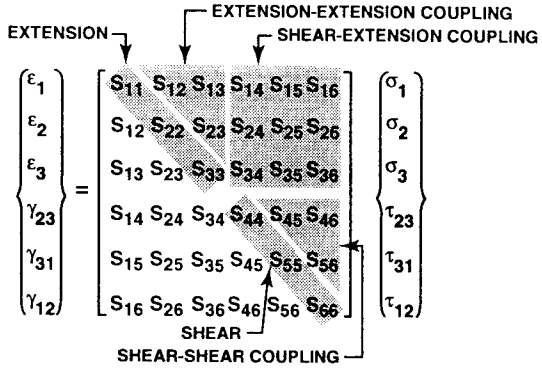

Figure 2-5 Physical Significance of the Anisotropic Stress-Strain Relations

2.3 STIFFNESSES, COMPLIANCES, AND ENGINEERING CONSTANTS FOR ORTHOTROPIC MATERIALS

Engineering constants (sometimes known as technical constants) are generalized Young's moduli, Poisson's ratios, and shear moduli as well as some other behavioral constants that will be discussed in Section 2.6. These constants are measured in simple tests such as uniaxial tension or pure shear tests. Thus, these constants with their obvious physical interpretation have more direct meaning than the components

of the relatively abstract compliance and stiffness matrices used in Section 2.2.

Most simple material characterization tests are performed with a known load or stress. The resulting displacement or strain is then measured. The engineering constants are generally the slope of a stress-strain curve (e.g., $E = \sigma/\varepsilon$) or the slope of a strain-strain curve (e.g., $\nu = -\varepsilon_y/\varepsilon_x$ for $\sigma_x = \sigma$ and all other stresses are zero). Thus, the components of the compliance (S_{ij}) matrix are determined more directly than those of the stiffness (C_{ij}) matrix. For an orthotropic material, the compliance matrix components in terms of the engineering constants are

$$[S_{ij}] = \begin{bmatrix} \frac{1}{E_1} & -\frac{\nu_{21}}{E_2} & -\frac{\nu_{31}}{E_3} & 0 & 0 & 0 \\ -\frac{\nu_{12}}{E_1} & \frac{1}{E_2} & -\frac{\nu_{32}}{E_3} & 0 & 0 & 0 \\ -\frac{\nu_{13}}{E_1} & -\frac{\nu_{23}}{E_2} & \frac{1}{E_3} & 0 & 0 & 0 \\ 0 & 0 & 0 & \frac{1}{G_{23}} & 0 & 0 \\ 0 & 0 & 0 & 0 & \frac{1}{G_{31}} & 0 \\ 0 & 0 & 0 & 0 & 0 & \frac{1}{G_{12}} \end{bmatrix} \tag{2.25}$$

where

E_1, E_2, E_3 = Young's (extension) moduli in the 1-, 2-, and 3-directions

ν_{ij} = Poisson's ratio (extension-extension coupling coefficient), i.e., the negative of the transverse strain in the j-direction over the strain in the i-direction when stress is applied in the i-direction, i.e.,

$$\nu_{ij} = -\frac{\varepsilon_j}{\varepsilon_i} \tag{2.26}$$

for $\sigma_i = \sigma$ and all other stresses are zero

G_{23}, G_{31}, G_{12} = shear moduli in the 2-3, 3-1, and 1-2 planes

Note that an orthotropic material that is stressed in principal material coordinates (the 1, 2, and 3 coordinates) does not exhibit either shear-extension or shear-shear coupling. Recall that an orthotropic material has nine independent constants because

$$S_{ij} = S_{ji} \tag{2.27}$$

and the compliance matrix is the inverse of the stiffness (C_{ij}) matrix that was shown to be symmetric in Equation (2.9). When engineering constants are substituted in Equation (2.27),

$$\frac{\nu_{ij}}{E_i} = \frac{\nu_{ji}}{E_j} \qquad i, j = 1, 2, 3 \qquad i \neq j \tag{2.28}$$

Thus, three reciprocal relations must be satisfied for an orthotropic material. Moreover, only ν_{12}, ν_{13}, and ν_{23} need be further considered because ν_{21}, ν_{31}, and ν_{32} can be expressed in terms of the first-mentioned group of Poisson's ratios and the Young's moduli. The latter group of Poisson's ratios should not be forgotten, however, because for some tests they are what is actually measured.

The difference between ν_{12} and ν_{21} for an orthotropic material is emphasized with the aid of Figure 2-6 where two cases of uniaxial stress are shown for a square element. First, stress is applied in the 1-direction in Figure 2-6. Then, from Equations (2.20) and (2.25), the strains are

$$^1\varepsilon_1 = \frac{\sigma}{E_1} \qquad ^1\varepsilon_2 = -\frac{\nu_{12}}{E_1}\sigma \tag{2.29}$$

where the direction of loading is denoted with the pre-superscript, the directions of strain and deformation are denoted with subscripts, and the deformations are

$$^1\Delta_1 = \frac{\sigma L}{E_1} \qquad ^1\Delta_2 = \frac{\nu_{12}}{E_1}\sigma L \tag{2.30}$$

Second, the same value of stress is applied in the 2-direction in Figure 2-6. The strains are

$$^2\varepsilon_1 = -\frac{\nu_{21}}{E_2}\sigma \qquad ^2\varepsilon_2 = \frac{\sigma}{E_2} \tag{2.31}$$

and the deformations are

$$^2\Delta_1 = \frac{\nu_{21}}{E_2}\sigma L \qquad ^2\Delta_2 = \frac{\sigma L}{E_2} \tag{2.32}$$

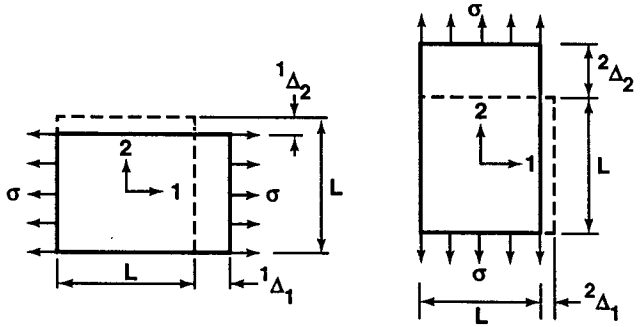

Figure 2-6 Distinction between ν_{12} and ν_{21}

Obviously, if $E_1 > E_2$ as is the case for a lamina reinforced with fibers in the 1-direction, then ${}^1\Delta_1 < {}^2\Delta_2$ as we would expect because the lamina is stiffer in the 1-direction than in the 2-direction. However, because of the reciprocal relations, irrespective of the values of E_1 and E_2,

$$ {}^1\Delta_2 = {}^2\Delta_1 \tag{2.33} $$

which is an obvious generalization of Betti's law to the treatment of orthotropic bodies. That is, the transverse deformation (and transverse strain) is the same when the stress is applied in the 2-direction as when it is applied in the 1-direction. Clearly, ν_{12} is not at all the same as ν_{21}.

Because the stiffness and compliance matrices are mutually inverse, it follows by matrix algebra that their components are related as follows for orthotropic materials:

$$ C_{11} = \frac{S_{22}S_{33} - S_{23}^2}{S} \quad C_{12} = \frac{S_{13}S_{23} - S_{12}S_{33}}{S} \quad C_{13} = \frac{S_{12}S_{23} - S_{13}S_{22}}{S} $$

$$ C_{22} = \frac{S_{33}S_{11} - S_{13}^2}{S} \quad C_{23} = \frac{S_{12}S_{13} - S_{23}S_{11}}{S} \quad C_{33} = \frac{S_{11}S_{22} - S_{12}^2}{S} $$

$$ C_{44} = \frac{1}{S_{44}} \quad C_{55} = \frac{1}{S_{55}} \quad C_{66} = \frac{1}{S_{66}} \tag{2.34} $$

where

$$ S = S_{11}S_{22}S_{33} - S_{11}S_{23}^2 - S_{22}S_{13}^2 - S_{33}S_{12}^2 + 2S_{12}S_{23}S_{13} \tag{2.35} $$

In Equation (2.34), the symbols C and S can be interchanged everywhere to provide the converse relationship.

The stiffness matrix, C_{ij}, for an orthotropic material in terms of the engineering constants is obtained by inversion of the compliance matrix, S_{ij}, in Equation (2.25) or by substitution in Equations (2.34) and (2.35). The nonzero stiffnesses in Equation (2.15) are

$$ C_{11} = \frac{1 - \nu_{23}\nu_{32}}{E_2E_3\Delta} \quad C_{22} = \frac{1 - \nu_{13}\nu_{31}}{E_1E_3\Delta} $$

$$ C_{12} = \frac{\nu_{21} + \nu_{31}\nu_{23}}{E_2E_3\Delta} = \frac{\nu_{12} + \nu_{32}\nu_{13}}{E_1E_3\Delta} \quad C_{23} = \frac{\nu_{32} + \nu_{12}\nu_{31}}{E_1E_3\Delta} = \frac{\nu_{23} + \nu_{21}\nu_{13}}{E_1E_2\Delta} $$

$$ C_{13} = \frac{\nu_{31} + \nu_{21}\nu_{32}}{E_2E_3\Delta} = \frac{\nu_{13} + \nu_{12}\nu_{23}}{E_1E_2\Delta} \quad C_{33} = \frac{1 - \nu_{12}\nu_{21}}{E_1E_2\Delta} \tag{2.36} $$

$$ C_{44} = G_{23} \quad C_{55} = G_{31} \quad C_{66} = G_{12} $$

where

$$ \Delta = \frac{1 - \nu_{12}\nu_{21} - \nu_{23}\nu_{32} - \nu_{31}\nu_{13} - 2\nu_{21}\nu_{32}\nu_{13}}{E_1E_2E_3} \tag{2.37} $$

in which Δ is identical to S in Equation (2.35).

Note especially that if a material is suspected to be orthotropic, mechanical tests at various angles will reveal whether there are coordinates for which shear-extension coupling does not exist. Hence, the orthotropy, isotropy, or lack thereof can be determined, although at a sometimes significant cost. The easiest way to determine principal material directions is visual observation. However, for visual observation to work, the characteristics of the material must obviously be readily seen by the naked eye. For example, in a fiber-reinforced lamina made from the boron-epoxy tape in Figure 1-10, the longitudinal direction is readily determined (and defined) to be the 1-direction along the fibers. Similarly, the 2-direction is in the plane of the tape transverse to the longitudinal direction. Finally, the 3-direction is defined to be perpendicular to the plane of the tape.

2.4 RESTRICTIONS ON ENGINEERING CONSTANTS

2.4.1 Isotropic Materials

For isotropic materials, certain relations between the engineering constants must be satisfied. For example, the shear modulus is defined in terms of the elastic modulus, E, and Poisson's ratio, ν, as

$$ G = \frac{E}{2(1 + \nu)} \tag{2.38} $$

Thus, in order that E and G always be positive, i.e., that a positive normal stress or shear stress times the respective positive normal strain or shear strain yield *positive* work,

$$ \nu > -1 \tag{2.39} $$

In a similar manner, if an isotropic body is subjected to hydrostatic pressure, p, i.e., $\sigma_x = \sigma_y = \sigma_z = -p$, then the volumetric strain, the sum of the three normal or extensional strains (the first-order approximation to the volume change), is

$$ \theta = \varepsilon_x + \varepsilon_y + \varepsilon_z = \frac{p}{E/3(1 - 2\nu)} = \frac{p}{K} \tag{2.40} $$

where K is the bulk modulus,

$$ K = \frac{E}{3(1 - 2\nu)} \tag{2.41} $$

Thus, K is positive only if E is positive and

$$ \nu < \frac{1}{2} \tag{2.42} $$

If the bulk modulus were negative, a hydrostatic pressure would cause expansion of a cube of isotropic material! Finally, for isotropic materials, Poisson's ratio is restricted to the range

$$ -1 < \nu < \frac{1}{2} \tag{2.43} $$

so shear or hydrostatic loading does not produce negative strain energy.

2.4.2 Orthotropic Materials

For orthotropic materials, the relations between engineering constants are more complex. Those relations must be rigorously investigated to avoid the pitfalls of an intuition built up on the basis of working with isotropic materials. First, the product of a stress and the corresponding strain represents work done by the stress. The sum of the work done by all stresses must be positive in order to avoid the creation of energy. This latter condition provides a *thermodynamic constraint* on the values of the engineering constants. What was previously accomplished for isotropic materials is, in reality, a consequence of such a constraint. The constraint was generalized for orthotropic materials by Lempriere [2-2]. Formally, he showed that the matrices relating stress to strain must be positive-definite, i.e., have positive principal values or invariants. Thus, both the stiffness and compliance matrices must be positive-definite.

This mathematical condition can be replaced by the following physical argument. If only one normal stress is applied at a time, the corresponding strain is determined by the diagonal elements of the compliance matrix. Thus, those elements must be positive, that is,

$$S_{11}, S_{22}, S_{33}, S_{44}, S_{55}, S_{66} > 0 \tag{2.44}$$

or, in terms of the engineering constants,

$$E_1, E_2, E_3, G_{23}, G_{31}, G_{12} > 0 \tag{2.45}$$

Similarly, under suitable constraints, deformation is possible in which only one extensional strain arises or is applied. Again, work is produced by the corresponding stress alone. Thus, because the work done is determined by the diagonal elements of the stiffness matrix, those elements must be positive, that is,

$$C_{11}, C_{22}, C_{33}, C_{44}, C_{55}, C_{66} > 0 \tag{2.46}$$

whereupon from Equation (2.34)

$$(1 - \nu_{23}\nu_{32}) > 0 \qquad (1 - \nu_{13}\nu_{31}) > 0 \qquad (1 - \nu_{12}\nu_{21}) > 0 \tag{2.47}$$

and

$$\bar{\Delta} = 1 - \nu_{12}\nu_{21} - \nu_{23}\nu_{32} - \nu_{31}\nu_{13} - 2\nu_{21}\nu_{32}\nu_{13} > 0 \tag{2.48}$$

because the determinant of a matrix must be positive for the matrix to be positive-definite. Also, from Equation (2.34), the positive nature of the stiffnesses leads to

$$|S_{23}| < \sqrt{S_{22}S_{33}} \qquad |S_{13}| < \sqrt{S_{11}S_{33}} \qquad |S_{12}| < \sqrt{S_{11}S_{22}} \tag{2.49}$$

Use the compliance symmetry condition, Equation (2.12), in the form

$$\frac{\nu_{ij}}{E_i} = \frac{\nu_{ji}}{E_j} \qquad i, j = 1, 2, 3 \tag{2.50}$$

to write the conditions of Equation (2.47) as

$$\begin{aligned} |\nu_{21}| &< \sqrt{\frac{E_2}{E_1}} & |\nu_{32}| &< \sqrt{\frac{E_3}{E_2}} & |\nu_{13}| &< \sqrt{\frac{E_1}{E_3}} \\ |\nu_{12}| &< \sqrt{\frac{E_1}{E_2}} & |\nu_{23}| &< \sqrt{\frac{E_2}{E_3}} & |\nu_{31}| &< \sqrt{\frac{E_3}{E_1}} \end{aligned} \tag{2.51}$$

Equations (2.51) can also be obtained from Equations (2.49) if the definitions for S_{ij} in terms of the engineering constants are substituted. Similarly, Equation (2.48) can be expressed as

$$\nu_{21}\nu_{32}\nu_{13} < \frac{1 - \nu_{21}^2\frac{E_1}{E_2} - \nu_{32}^2\frac{E_2}{E_3} - \nu_{13}^2\frac{E_3}{E_1}}{2} < \frac{1}{2} \tag{2.52}$$

and can be regrouped to read

$$\left[1 - \nu_{32}^2\frac{E_2}{E_3}\right]\left[1 - \nu_{13}^2\frac{E_3}{E_1}\right] - \left[\nu_{21}\sqrt{\frac{E_1}{E_2}} + \nu_{32}\nu_{13}\sqrt{\frac{E_2}{E_1}}\right]^2 > 0 \tag{2.53}$$

In order to obtain a constraint on one Poisson's ratio, ν_{21}, in terms of two others, ν_{32} and ν_{13}, Equation (2.53) can be further rearranged as

$$-\left[\nu_{32}\nu_{13}\frac{E_2}{E_1} + \sqrt{1 - \nu_{32}^2\frac{E_2}{E_3}}\sqrt{1 - \nu_{13}^2\frac{E_3}{E_1}}\sqrt{\frac{E_2}{E_1}}\right] < \nu_{21} < -\left[\nu_{32}\nu_{13}\frac{E_2}{E_1} - \sqrt{1 - \nu_{32}^2\frac{E_2}{E_3}}\sqrt{1 - \nu_{13}^2\frac{E_3}{E_1}}\sqrt{\frac{E_2}{E_1}}\right] \tag{2.54}$$

Similar expressions can be obtained for ν_{32} and ν_{13}.

The preceding restrictions on engineering constants for orthotropic materials are used to examine experimental data to see if they are physically consistent within the framework of the mathematical elasticity model. For boron-epoxy composite materials, Dickerson and DiMartino [2-3] measured Poisson's ratios as high as 1.97 for the negative of the strain in the 2-direction over the strain in the 1-direction due to loading in the 1-direction (ν_{12}). The reported values of the Young's moduli for the two directions are $E_1 = 11.86 \times 10^6$ psi (81.77 GPa) and $E_2 = 1.33 \times 10^6$ psi (9.17 GPa). Thus,

$$\sqrt{\frac{E_1}{E_2}} = 2.99 \tag{2.55}$$

(which is far greater than the value of one for an isotropic material), and the condition

$$|\nu_{12}| < \sqrt{\frac{E_1}{E_2}} \tag{2.56}$$

is satisfied. Accordingly, $\nu_{12} = 1.97$ is a reasonable number even though our intuition based on isotropic materials ($\nu < 1/2$) rejects such a large number. The data reported were insufficient to verify the determinant condition, Equation (2.48), that might be more stringent. Also, the 'converse' (or minor) Poisson's ratio, ν_{21}, was reported as .22. This value satisfies the reciprocal relations in Equation (2.50).

If the measured material properties satisfy the constraints in this section, then we can proceed with confidence to design structures with the material. Otherwise, we have reason to doubt either the material model or the experimental data or both!

The restrictions on engineering constants can also be used in the solution of practical engineering analysis problems. For example, consider a differential equation that has several solutions depending on the relative values of the coefficients in the differential equation. Those coefficients in a physical problem of deformation of a body involve the elastic constants. The restrictions on elastic constants can then be used to determine which solution to the differential equation is applicable.

Problem Set 2.4

2.4.1 Show that the determinant inequality in Equation (2.48) for orthotropic materials correctly reduces to $\nu < 1/2$ for isotropic materials.
2.4.2 Derive Equation (2.52) from the determinant inequality in Equation (2.48).
2.4.3 Derive Equation (2.53) from Equation (2.52).
2.4.4 Derive Equation (2.54) from Equation (2.53).
2.4.5 Show that Equation (2.54) reduces for isotropic materials to known bounds on ν.

2.5 STRESS-STRAIN RELATIONS FOR PLANE STRESS IN AN ORTHOTROPIC MATERIAL

For a unidirectionally reinforced lamina in the 1-2 plane as shown in Figure 2-7 or a woven lamina as in Figure 2-1, a plane stress state is defined by setting

$$\sigma_3 = 0 \qquad \tau_{23} = 0 \qquad \tau_{31} = 0 \tag{2.57}$$

so that

$$\sigma_1 \neq 0 \qquad \sigma_2 \neq 0 \qquad \tau_{12} \neq 0 \tag{2.58}$$

in the three-dimensional stress-strain relations given in Equations (2.18)-(2.22) for anisotropic, monoclinic, orthotropic, transversely isotropic, or isotropic materials. Note that a plane stress state on a lamina is not merely an idealization of reality, but instead is a practical and achievable objective of how we must use a lamina with fibers in its plane. After all, the lamina cannot withstand high stresses in any direction other than that of the fibers, so why would we subject it to unnatural stresses such as σ_3? That is, we expect to load a lamina *only* in plane stress because carrying in-plane stresses is its fundamental capability. A unidirectionally reinforced lamina would need 'help' carrying in-plane stress perpendicular to its fibers, but that help can be provided by other (parallel) layers that have their fibers in the direction of the stress. Thus, a laminate is needed, but we concentrate on the characteristics of a lamina in this chapter. Practical examples of in-plane loaded structural elements are most car body panels, aircraft wings and fuselages, etc.

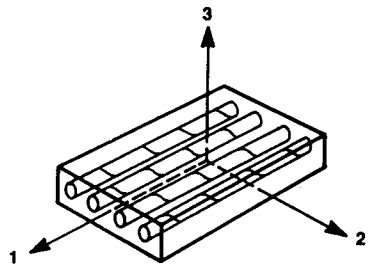

Figure 2-7 Unidirectionally Reinforced Lamina

For orthotropic materials, imposing a state of plane stress results in implied out-of-plane strains of

$$\varepsilon_3 = S_{13}\sigma_1 + S_{23}\sigma_2 \qquad \gamma_{23} = 0 \qquad \gamma_{31} = 0 \tag{2.59}$$

where

$$S_{13} = -\frac{\nu_{13}}{E_1} = -\frac{\nu_{31}}{E_3} \qquad S_{23} = -\frac{\nu_{23}}{E_2} = -\frac{\nu_{32}}{E_3} \tag{2.60}$$

Moreover, the strain-stress relations in Equation (2.20) reduce to

$$\begin{bmatrix} \varepsilon_1 \\ \varepsilon_2 \\ \gamma_{12} \end{bmatrix} = \begin{bmatrix} S_{11} & S_{12} & 0 \\ S_{12} & S_{22} & 0 \\ 0 & 0 & S_{66} \end{bmatrix} \begin{bmatrix} \sigma_1 \\ \sigma_2 \\ \tau_{12} \end{bmatrix} \tag{2.61}$$

supplemented by Equation (2.59) where

$$S_{11} = \frac{1}{E_1} \qquad S_{12} = -\frac{\nu_{12}}{E_1} = -\frac{\nu_{21}}{E_2} \qquad S_{22} = \frac{1}{E_2} \qquad S_{66} = \frac{1}{G_{12}} \tag{2.62}$$

Note that in order to determine ε_3 in Equation (2.59), ν_{13} and ν_{23} must be known in addition to the engineering constants in Equation (2.62). That is, ν_{13} and ν_{23} arise from S_{13} and S_{23} in Equation (2.59).

The strain-stress relations in Equation (2.61) can be inverted to obtain the stress-strain relations

$$\begin{bmatrix} \sigma_1 \\ \sigma_2 \\ \tau_{12} \end{bmatrix} = \begin{bmatrix} Q_{11} & Q_{12} & 0 \\ Q_{12} & Q_{22} & 0 \\ 0 & 0 & Q_{66} \end{bmatrix} \begin{bmatrix} \varepsilon_1 \\ \varepsilon_2 \\ \gamma_{12} \end{bmatrix} \tag{2.63}$$

where the Q_{ij} are the so-called reduced stiffnesses for a plane stress state in the 1-2 plane which are determined either (1) as the components of the inverted compliance matrix in Equation (2.61) or (2) from the C_{ij} directly by applying the condition $\sigma_3 = 0$ to the strain-stress relations to get an expression for ε_3 and simplifying the results to get

$$Q_{ij} = C_{ij} - \frac{C_{i3}C_{j3}}{C_{33}} \qquad i,j = 1, 2, 6 \tag{2.64}$$

The term C_{63} is zero because no shear-extension coupling exists for an orthotropic lamina in principal material coordinates. For the orthotropic lamina, the Q_{ij} are

$$Q_{11} = \frac{S_{22}}{S_{11}S_{22} - S_{12}^2} \qquad Q_{22} = \frac{S_{11}}{S_{11}S_{22} - S_{12}^2}$$
$$Q_{12} = \frac{S_{12}}{S_{11}S_{22} - S_{12}^2} \qquad Q_{66} = \frac{1}{S_{66}} \tag{2.65}$$

or, in terms of the engineering constants,

$$Q_{11} = \frac{E_1}{1 - \nu_{12}\nu_{21}} \qquad Q_{22} = \frac{E_2}{1 - \nu_{12}\nu_{21}}$$
$$Q_{12} = \frac{\nu_{12}E_2}{1 - \nu_{12}\nu_{21}} = \frac{\nu_{21}E_1}{1 - \nu_{12}\nu_{21}} \qquad Q_{66} = G_{12} \tag{2.66}$$

Note that there are four independent material properties, E_1, E_2, ν_{12}, and G_{12}, in Equations (2.61) and (2.63) when Equations (2.62) and (2.66) are considered in addition to the reciprocal relation

$$\frac{\nu_{12}}{E_1} = \frac{\nu_{21}}{E_2} \tag{2.67}$$

The preceding stress-strain and strain-stress relations are the basis for stiffness and stress analysis of an individual lamina subjected to forces in its own plane. Thus, the relations are indispensable in laminate analysis.

For plane stress on isotropic materials, the strain-stress relations are

$$\begin{bmatrix} \varepsilon_1 \\ \varepsilon_2 \\ \gamma_{12} \end{bmatrix} = \begin{bmatrix} S_{11} & S_{12} & 0 \\ S_{12} & S_{11} & 0 \\ 0 & 0 & 2(S_{11} - S_{12}) \end{bmatrix} \begin{bmatrix} \sigma_1 \\ \sigma_2 \\ \tau_{12} \end{bmatrix} \tag{2.68}$$

where

$$S_{11} = \frac{1}{E} \qquad S_{12} = -\frac{\nu}{E} \tag{2.69}$$

and the stress-strain relations are

$$\begin{bmatrix} \sigma_1 \\ \sigma_2 \\ \tau_{12} \end{bmatrix} = \begin{bmatrix} Q_{11} & Q_{12} & 0 \\ Q_{12} & Q_{11} & 0 \\ 0 & 0 & Q_{66} \end{bmatrix} \begin{bmatrix} \varepsilon_1 \\ \varepsilon_2 \\ \gamma_{12} \end{bmatrix} \tag{2.70}$$

where

$$Q_{11} = \frac{E}{1 - \nu^2} \qquad Q_{12} = \frac{\nu E}{1 - \nu^2} \qquad Q_{66} = \frac{E}{2(1 + \nu)} = G \tag{2.71}$$

The preceding isotropic relations can be obtained either from the orthotropic relations by equating E_1 to E_2 and G_{12} to G or by the same manner as the orthotropic relations were obtained.

Observing the physical symmetry of the fibers and matrix in a unidirectionally reinforced lamina enables us to deduce how some of the out-of-plane properties are related to the in-plane properties, E_1, E_2, ν_{12}, and G_{12}. Consider the cube-shaped portion of a unidirectionally reinforced lamina in principal material coordinates in Figure 2-8. First, $E_3 = E_2$ because both stiffnesses are measured across fibers in the same manner. That is, in general, the 3-direction can be treated just as if it were the 2-direction for a unidirectionally reinforced lamina. Second, $\nu_{31} = \nu_{21}$ (hence, $\nu_{13} = \nu_{12}$) for the same reason. Third, irrespective of whether the shear stress τ_{13} or τ_{12} is applied, the resulting deformations are identical because, by symmetry, the fibers have the same orientation to the applied shearing stress, so $G_{13} = G_{12}$. Even if the fiber distribution in the 2-3 plane of the cube in Figure 2-8 were random, the same conclusions would apply. That is, with either the fiber-spacing regularity in Figure 2-8 or random fiber distribution in the 2-3 plane, the 2-3 plane can be regarded as a plane of isotropy because all stiffnesses, E, in the plane are the same. When we account for the different E_1 from E_2 in the 1-2 plane, we recognize that the lamina is a transversely isotropic material in three dimensions. However, when we concentrate only on the 1-2 plane, we call the lamina orthotropic. If the lamina is compacted in the 3-direction during the curing process, then slight differences in the properties between the 2- and 3-directions would result, and the material would be orthotropic in the three-dimensional sense.

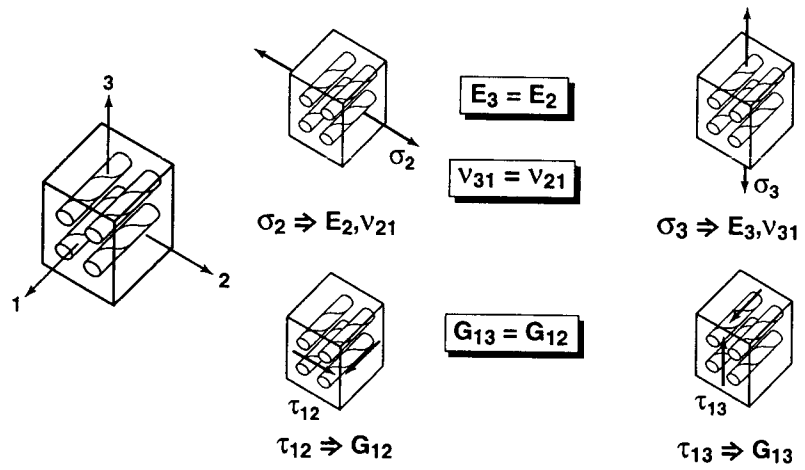

Figure 2-8 Physical Symmetry of a Unidirectionally Reinforced Lamina

2.6 STRESS-STRAIN RELATIONS FOR A LAMINA OF ARBITRARY ORIENTATION

In Section 2.5, the stresses and strains were defined in the principal material coordinates for an orthotropic material. However, the principal directions of orthotropy often do not coincide with coordinate directions that are geometrically natural to the solution of the problem. For example, consider the helically wound fiber-reinforced circular cylindrical shell in Figure 2-9. There, the coordinates natural to the solution of the shell problem are the shell coordinates x, y, z, whereas the principal material coordinates are x', y', z'. The filament-winding angle is defined by $\cos(y', y) = \cos\alpha$; also, $z' = z$. Other examples include laminated plates with different laminae at different orientations. Thus, a relation is needed between the stresses and strains in the principal material coordinates and those in the body coordinates. Then, a method of transforming stress-strain relations from one coordinate system to another is also needed.

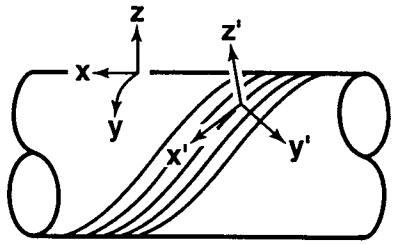

Figure 2-9 Helically Wound Fiber-Reinforced Circular Cylindrical Shell

At this point, we recall from elementary mechanics of materials the transformation equations for expressing stresses in an x-y coordinate system in terms of stresses in a 1-2 coordinate system,

$$\begin{bmatrix}\sigma_x\\ \sigma_y\\ \tau_{xy}\end{bmatrix} = \begin{bmatrix}\cos^2\theta & \sin^2\theta & -2\sin\theta\cos\theta\\ \sin^2\theta & \cos^2\theta & 2\sin\theta\cos\theta\\ \sin\theta\cos\theta & -\sin\theta\cos\theta & \cos^2\theta-\sin^2\theta\end{bmatrix}\begin{bmatrix}\sigma_1\\ \sigma_2\\ \tau_{12}\end{bmatrix} \tag{2.72}$$

where θ is the angle *from* the x-axis *to* the 1-axis (see Figure 2-10). Note especially that the transformation has nothing to do with the material properties but is merely a rotation of stress directions. Also, the *direction* of rotation is crucial.

Similarly, the strain-transformation equations are

$$\begin{bmatrix}\varepsilon_x\\ \varepsilon_y\\ \frac{\gamma_{xy}}{2}\end{bmatrix} = \begin{bmatrix}\cos^2\theta & \sin^2\theta & -2\sin\theta\cos\theta\\ \sin^2\theta & \cos^2\theta & 2\sin\theta\cos\theta\\ \sin\theta\cos\theta & -\sin\theta\cos\theta & \cos^2\theta-\sin^2\theta\end{bmatrix}\begin{bmatrix}\varepsilon_1\\ \varepsilon_2\\ \frac{\gamma_{12}}{2}\end{bmatrix} \tag{2.73}$$

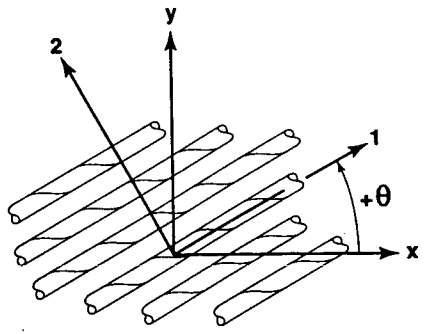

Figure 2-10 Positive Rotation of Principal Material Axes from x-y Axes

where we observe that strains do transform with the same transformation as stresses if the tensor definition of shear strain is used (which is equivalent to dividing the engineering shear strain by two).

The transformations are commonly written as

$$\begin{bmatrix}\sigma_x\\ \sigma_y\\ \tau_{xy}\end{bmatrix} = [T]^{-1}\begin{bmatrix}\sigma_1\\ \sigma_2\\ \tau_{12}\end{bmatrix} \tag{2.74}$$

$$\begin{bmatrix}\varepsilon_x\\ \varepsilon_y\\ \frac{\gamma_{xy}}{2}\end{bmatrix} = [T]^{-1}\begin{bmatrix}\varepsilon_1\\ \varepsilon_2\\ \frac{\gamma_{12}}{2}\end{bmatrix} \tag{2.75}$$

where the superscript –1 denotes the matrix inverse and

$$[T] = \begin{bmatrix}\cos^2\theta & \sin^2\theta & 2\sin\theta\cos\theta\\ \sin^2\theta & \cos^2\theta & -2\sin\theta\cos\theta\\ -\sin\theta\cos\theta & \sin\theta\cos\theta & \cos^2\theta-\sin^2\theta\end{bmatrix} \tag{2.76}$$

However, if the simple matrix

$$[R] = \begin{bmatrix}1 & 0 & 0\\ 0 & 1 & 0\\ 0 & 0 & 2\end{bmatrix} \tag{2.77}$$

due to Reuter [2-4] is introduced, then the engineering strain vectors

$$\begin{bmatrix}\varepsilon_1\\ \varepsilon_2\\ \gamma_{12}\end{bmatrix} = [R]\begin{bmatrix}\varepsilon_1\\ \varepsilon_2\\ \frac{\gamma_{12}}{2}\end{bmatrix} \tag{2.78}$$

$$\begin{bmatrix}\varepsilon_x\\ \varepsilon_y\\ \gamma_{xy}\end{bmatrix} = [R]\begin{bmatrix}\varepsilon_x\\ \varepsilon_y\\ \frac{\gamma_{xy}}{2}\end{bmatrix} \tag{2.79}$$

can be used instead of the tensor strain vectors in the strain transformations as well as in stress-strain law transformations. The beauty of Reuter's transformation is that concise matrix notation can then be used. As a result, the ordinary expressions for stiffness and compliance matrices with awkward factors of 1/2 and 2 in various rows and columns are avoided.

A so-called *specially orthotropic lamina* is an orthotropic lamina whose principal material axes are aligned with the natural body axes:

$$\begin{bmatrix}\sigma_x\\ \sigma_y\\ \tau_{xy}\end{bmatrix} = \begin{bmatrix}\sigma_1\\ \sigma_2\\ \tau_{12}\end{bmatrix} = \begin{bmatrix}Q_{11} & Q_{12} & 0\\ Q_{12} & Q_{22} & 0\\ 0 & 0 & Q_{66}\end{bmatrix}\begin{bmatrix}\varepsilon_1\\ \varepsilon_2\\ \gamma_{12}\end{bmatrix} \tag{2.80}$$

where the principal material axes are shown in Figure 2-7. These stress-strain relations were introduced in Section 2.5 and apply when the principal material directions of an orthotropic lamina are used as coordinates.

However, as mentioned previously, orthotropic laminae are often constructed in such a manner that the principal material coordinates do not coincide with the natural coordinates of the body. This statement is not to be interpreted as meaning that the material itself is no longer orthotropic; instead, we are just looking at an orthotropic material in an unnatural manner, i.e., in a coordinate system that is oriented at some angle to the principal material coordinate system. Then, the basic question is: given the stress-strain relations in the principal material coordinates, what are the stress-strain relations in x-y coordinates?

Accordingly, we use the stress and strain transformations of Equations (2.74) and (2.75) along with Reuter's matrix, Equation (2.77), after abbreviating Equation (2.80) as

$$\begin{bmatrix}\sigma_1\\ \sigma_2\\ \tau_{12}\end{bmatrix} = [Q]\begin{bmatrix}\varepsilon_1\\ \varepsilon_2\\ \gamma_{12}\end{bmatrix} \tag{2.81}$$

to obtain

$$\begin{bmatrix}\sigma_x\\ \sigma_y\\ \tau_{xy}\end{bmatrix} = [T]^{-1}\begin{bmatrix}\sigma_1\\ \sigma_2\\ \tau_{12}\end{bmatrix} = [T]^{-1}[Q][R][T][R]^{-1}\begin{bmatrix}\varepsilon_x\\ \varepsilon_y\\ \gamma_{xy}\end{bmatrix} \tag{2.82}$$

However, $[R][T][R]^{-1}$ can be shown to be $[T]^{-T}$ where the superscript T denotes the matrix transpose. Then, if we use the abbreviation

$$[\bar{Q}] = [T]^{-1}[Q][T]^{-T} \tag{2.83}$$

the stress-strain relations in x-y coordinates are

$$\begin{bmatrix}\sigma_x\\ \sigma_y\\ \tau_{xy}\end{bmatrix} = [\bar{Q}]\begin{bmatrix}\varepsilon_x\\ \varepsilon_y\\ \gamma_{xy}\end{bmatrix} = \begin{bmatrix}\bar{Q}_{11} & \bar{Q}_{12} & \bar{Q}_{16}\\ \bar{Q}_{12} & \bar{Q}_{22} & \bar{Q}_{26}\\ \bar{Q}_{16} & \bar{Q}_{26} & \bar{Q}_{66}\end{bmatrix}\begin{bmatrix}\varepsilon_x\\ \varepsilon_y\\ \gamma_{xy}\end{bmatrix} \tag{2.84}$$

in which

$$\begin{aligned}
\bar{Q}_{11} &= Q_{11}\cos^4\theta + 2(Q_{12}+2Q_{66})\sin^2\theta\cos^2\theta + Q_{22}\sin^4\theta\\
\bar{Q}_{12} &= (Q_{11}+Q_{22}-4Q_{66})\sin^2\theta\cos^2\theta + Q_{12}(\sin^4\theta+\cos^4\theta)\\
\bar{Q}_{22} &= Q_{11}\sin^4\theta + 2(Q_{12}+2Q_{66})\sin^2\theta\cos^2\theta + Q_{22}\cos^4\theta\\
\bar{Q}_{16} &= (Q_{11}-Q_{12}-2Q_{66})\sin\theta\cos^3\theta + (Q_{12}-Q_{22}+2Q_{66})\sin^3\theta\cos\theta\\
\bar{Q}_{26} &= (Q_{11}-Q_{12}-2Q_{66})\sin^3\theta\cos\theta + (Q_{12}-Q_{22}+2Q_{66})\sin\theta\cos^3\theta\\
\bar{Q}_{66} &= (Q_{11}+Q_{22}-2Q_{12}-2Q_{66})\sin^2\theta\cos^2\theta + Q_{66}(\sin^4\theta+\cos^4\theta)
\end{aligned} \tag{2.85}$$

where the bar over the $\bar{Q}_{ij}$ matrix denotes that we are dealing with the transformed reduced stiffnesses instead of the reduced stiffnesses, Q_{ij}.

Note that the transformed reduced stiffness matrix $\bar{Q}_{ij}$ has terms in all nine positions in contrast to the presence of zeros in the reduced stiffness matrix Q_{ij}. However, there are still only *four* independent material constants because the lamina is orthotropic. In the general case with body coordinates x and y, there is coupling between shear strain and normal stresses and between shear stress and normal strains, i.e., shear-extension coupling exists. Thus, in body coordinates, even an orthotropic lamina appears to be anisotropic. However, because such a lamina does have orthotropic characteristics in principal material coordinates, it is called a *generally orthotropic lamina* because it can be represented by the stress-strain relations in Equation (2.84). That is, a *generally orthotropic lamina* is an orthotropic lamina whose principal material axes are not aligned with the natural body axes.

The only advantage associated with generally orthotropic laminae as opposed to anisotropic laminae is that generally orthotropic laminae are easier to characterize experimentally. However, if we do not realize that principal material axes exist, then a generally orthotropic lamina is indistinguishable from an anisotropic lamina. That is, we cannot take away the inherent orthotropic character of a lamina, but we can orient the lamina in such a manner as to make that character quite difficult to recognize.

As an alternative to the foregoing procedure, we can express the strains in terms of the stresses in body coordinates by either (1) inversion of the stress-strain relations in Equation (2.84) or (2) transformation of the strain-stress relations in principal material coordinates from Equation (2.61),

$$\begin{bmatrix}\varepsilon_1\\ \varepsilon_2\\ \gamma_{12}\end{bmatrix}=\begin{bmatrix}S_{11} & S_{12} & 0\\ S_{12} & S_{22} & 0\\ 0 & 0 & S_{66}\end{bmatrix}\begin{bmatrix}\sigma_1\\ \sigma_2\\ \tau_{12}\end{bmatrix} \tag{2.86}$$

to body coordinates. We choose the second approach and apply the transformations of Equations (2.74) and (2.75) along with Reuter's matrix, Equation (2.77), to obtain

$$\begin{bmatrix}\varepsilon_x\\ \varepsilon_y\\ \gamma_{xy}\end{bmatrix}=[T]^T[S][T]\begin{bmatrix}\sigma_x\\ \sigma_y\\ \tau_{xy}\end{bmatrix}=\begin{bmatrix}\bar{S}_{11} & \bar{S}_{12} & \bar{S}_{16}\\ \bar{S}_{12} & \bar{S}_{22} & \bar{S}_{26}\\ \bar{S}_{16} & \bar{S}_{26} & \bar{S}_{66}\end{bmatrix}\begin{bmatrix}\sigma_x\\ \sigma_y\\ \tau_{xy}\end{bmatrix} \tag{2.87}$$

where $[R][T]^{-1}[R]^{-1}$ was found to be $[T]^T$ and

$$\begin{aligned}
\bar{S}_{11} &= S_{11}\cos^4\theta + (2S_{12}+S_{66})\sin^2\theta\cos^2\theta + S_{22}\sin^4\theta\\
\bar{S}_{12} &= S_{12}(\sin^4\theta+\cos^4\theta) + (S_{11}+S_{22}-S_{66})\sin^2\theta\cos^2\theta\\
\bar{S}_{22} &= S_{11}\sin^4\theta + (2S_{12}+S_{66})\sin^2\theta\cos^2\theta + S_{22}\cos^4\theta\\
\bar{S}_{16} &= (2S_{11}-2S_{12}-S_{66})\sin\theta\cos^3\theta - (2S_{22}-2S_{12}-S_{66})\sin^3\theta\cos\theta\\
\bar{S}_{26} &= (2S_{11}-2S_{12}-S_{66})\sin^3\theta\cos\theta - (2S_{22}-2S_{12}-S_{66})\sin\theta\cos^3\theta\\
\bar{S}_{66} &= 2(2S_{11}+2S_{22}-4S_{12}-S_{66})\sin^2\theta\cos^2\theta + S_{66}(\sin^4\theta+\cos^4\theta)
\end{aligned} \tag{2.88}$$

Recall that the S_{ij} are defined in terms of the engineering constants in Equation (2.62).

Because of the presence of $\bar{Q}_{16}$ and $\bar{Q}_{26}$ in Equation (2.84) and of S_{16} and S_{26} in Equation (2.87), the solution of problems involving so-called generally orthotropic laminae is more difficult than problems with so-called specially orthotropic laminae. That is, shear-extension coupling complicates the solution of practical problems. As a matter of fact, there

is no difference between solutions for generally orthotropic laminae and those for anisotropic laminae whose stress-strain relations, under conditions of plane stress, can be written as

$$\begin{bmatrix}\sigma_1\\ \sigma_2\\ \tau_{12}\end{bmatrix}=\begin{bmatrix}Q_{11} & Q_{12} & Q_{16}\\ Q_{12} & Q_{22} & Q_{26}\\ Q_{16} & Q_{26} & Q_{66}\end{bmatrix}\begin{bmatrix}\varepsilon_1\\ \varepsilon_2\\ \gamma_{12}\end{bmatrix} \tag{2.89}$$

or in inverted form as

$$\begin{bmatrix}\varepsilon_1\\ \varepsilon_2\\ \gamma_{12}\end{bmatrix}=\begin{bmatrix}S_{11} & S_{12} & S_{16}\\ S_{12} & S_{22} & S_{26}\\ S_{16} & S_{26} & S_{66}\end{bmatrix}\begin{bmatrix}\sigma_1\\ \sigma_2\\ \tau_{12}\end{bmatrix} \tag{2.90}$$

where the anisotropic compliances in terms of the engineering constants are

$$\begin{aligned}
S_{11} &= \frac{1}{E_1} & S_{22} &= \frac{1}{E_2} & S_{16} &= \frac{\eta_{12,1}}{E_1} = \frac{\eta_{1,12}}{G_{12}}\\
S_{12} &= -\frac{\nu_{12}}{E_1} = -\frac{\nu_{21}}{E_2} & S_{66} &= \frac{1}{G_{12}} & S_{26} &= \frac{\eta_{12,2}}{E_2} = \frac{\eta_{2,12}}{G_{12}}
\end{aligned} \tag{2.91}$$

Note that some new engineering constants have been used. The new constants are called *coefficients of mutual influence* by Lekhnitskii [2-5] and are defined as

$\eta_{i,ij}$ = coefficient of mutual influence of the first kind that characterizes stretching in the i-direction caused by shear stress in the ij-plane

$$\eta_{i,ij} = \frac{\varepsilon_i}{\gamma_{ij}} \tag{2.92}$$

for $\tau_{ij} = \tau$ and all other stresses are zero.

$\eta_{ij,i}$ = coefficient of mutual influence of the second kind characterizing shearing in the ij-plane caused by normal stress in the i-direction

$$\eta_{ij,i} = \frac{\gamma_{ij}}{\varepsilon_i} \tag{2.93}$$

for $\sigma_i = \sigma$ and all other stresses are zero.

Lekhnitskii defines the coefficients of mutual influence and the Poisson's ratios with subscripts that are reversed from the present notation. The coefficients of mutual influence are not named very effectively because the Poisson's ratios could also be called coefficients of mutual influence. Instead, the $\eta_{ij,j}$ and $\eta_{i,ij}$ are more appropriately called by the functional name shear-extension coupling coefficients.

Other anisotropic elasticity relations are used to define *Chentsov coefficients* that are to shearing stresses and shearing strains what Poisson's ratios are to normal stresses and normal strains. However, the Chentsov coefficients do not affect the in-plane behavior of laminae under plane stress because the coefficients are related to S_{45}, S_{46}, S_{56} in Equation (2.18). The Chentsov coefficients are defined as

$\mu_{ij,\,kl}$ = Chentsov coefficient that characterizes the shearing strain in the kl-plane due to shearing stress in the ij-plane, i.e.,

$$\mu_{ij,\,kl} = \frac{\gamma_{kl}}{\gamma_{ij}} \qquad (2.94)$$

for $\tau_{ij} = \tau$ and all other stresses are zero.

The Chentsov coefficients are subject to the reciprocal relations

$$\frac{\mu_{kl,\,ij}}{G_{kl}} = \frac{\mu_{ij,\,kl}}{G_{ij}} \qquad (2.95)$$

Note that the Chentsov coefficients are more effectively called the functional name of shear-shear coupling coefficients.

The out-of-plane shearing strains of an anisotropic lamina due to in-plane shearing stress and normal stresses are

$$\gamma_{13} = \frac{\eta_{1,\,13}\sigma_1 + \eta_{2,\,13}\sigma_2 + \mu_{12,\,13}\tau_{12}}{G_{13}}$$
$$\gamma_{23} = \frac{\eta_{1,\,23}\sigma_1 + \eta_{2,\,23}\sigma_2 + \mu_{12,\,23}\tau_{12}}{G_{23}} \qquad (2.96)$$

wherein both the shear-shear coupling coefficients and the shear-extension coupling coefficients are required. Note that neither of these shear strains arise in an orthotropic material unless it is stressed in coordinates other than the principal material coordinates. In such cases, the shear-shear coupling coefficients and the shear-extension coupling coefficients are obtained from the transformed compliances as in the following paragraph.

Compare the transformed orthotropic compliances in Equation (2.88) with the anisotropic compliances in terms of engineering constants in Equation (2.91). Obviously an *apparent* shear-extension coupling coefficient results when an orthotropic lamina is stressed in non-principal material coordinates. Redesignate the coordinates 1 and 2 in Equation (2.90) as x and y because, by definition, an anisotropic material has *no* principal material directions. Then, substitute the redesignated S_{ij} from Equation (2.91) in Equation (2.88) along with the orthotropic compliances in Equation (2.62). Finally, the apparent engineering constants for an orthotropic lamina that is stressed in non-principal x-y coordinates are

$$\frac{1}{E_x} = \frac{1}{E_1}\cos^4\theta + \left[\frac{1}{G_{12}} - \frac{2\nu_{12}}{E_1}\right]\sin^2\theta\cos^2\theta + \frac{1}{E_2}\sin^4\theta$$
$$\nu_{xy} = E_x\left[\frac{\nu_{12}}{E_1}(\sin^4\theta + \cos^4\theta) - \left[\frac{1}{E_1} + \frac{1}{E_2} - \frac{1}{G_{12}}\right]\sin^2\theta\cos^2\theta\right]$$
$$\frac{1}{E_y} = \frac{1}{E_1}\sin^4\theta + \left[\frac{1}{G_{12}} - \frac{2\nu_{12}}{E_1}\right]\sin^2\theta\cos^2\theta + \frac{1}{E_2}\cos^4\theta \qquad (2.97)$$
$$\frac{1}{G_{xy}} = 2\left[\frac{2}{E_1} + \frac{2}{E_2} + \frac{4\nu_{12}}{E_1} - \frac{1}{G_{12}}\right]\sin^2\theta\cos^2\theta + \frac{1}{G_{12}}(\sin^4\theta + \cos^4\theta)$$
$$\eta_{xy,\,x} = E_x\left[\left[\frac{2}{E_1} + \frac{2\nu_{12}}{E_1} - \frac{1}{G_{12}}\right]\sin\theta\cos^3\theta - \left[\frac{2}{E_2} + \frac{2\nu_{12}}{E_1} - \frac{1}{G_{12}}\right]\sin^3\theta\cos\theta\right]$$
$$\eta_{xy,\,y} = E_y\left[\left[\frac{2}{E_1} + \frac{2\nu_{12}}{E_1} - \frac{1}{G_{12}}\right]\sin^3\theta\cos\theta - \left[\frac{2}{E_2} + \frac{2\nu_{12}}{E_1} - \frac{1}{G_{12}}\right]\sin\theta\cos^3\theta\right]$$

An important implication of the presence of the shear-extension coupling coefficient is that off-axis (non-principal material direction) tensile loadings for composite materials result in shear deformation in addition to the usual axial extension. This subject is investigated further in Section 2.8. At this point, recognize that Equation (2.97) is a quantification of the foregoing implication for tensile tests and of the qualitative observations made in Section 1.2.

The apparent anisotropic moduli for an orthotropic lamina stressed at an angle θ to the principal material directions vary with θ as in Equation (2.97). To gain a visual appreciation for how the moduli vary, values typical of a glass-epoxy composite material are plotted from Equation (2.97) in Figure 2-11. Similarly, values for a boron-epoxy composite material are plotted in Figure 2-12. In both figures, E_x is divided by E_2 and G_{xy} is divided by G_{12}. This normalization is done to permit a convenient comparison of most of the moduli in a single figure. Note in both figures that G_{xy} is largest at $\theta = 45°$. The shear-extension coupling coefficient $\eta_{xy,x}$ is, of course, zero at $\theta = 0°$ and $\theta = 90°$, but achieves large values compared to ν_{xy} for intermediate angles. The modulus E_y behaves essentially like E_x, except E_y is, of course, small for θ near 0° and large when θ is near 90°. Similar comments could be made for ν_{yx} and $\eta_{xy,y}$.

The values in Figures 2-11 and 2-12 are not entirely typical of all composite materials. For example, follow the hints in Exercise 2.6.7 to demonstrate that E_x can actually exceed both E_1 and E_2 for some orthotropic laminae. Similarly, E_x can be shown to be smaller than both E_1 and E_2 (note that for boron-epoxy in Figure 2-12 E_x is slightly smaller than E_2 in the neighborhood of $\theta = 60°$). These results were summarized by Jones [2-6] as a simple theorem: the extremum (largest and smallest) material properties do not necessarily occur in principal material coordinates. The moduli G_{xy}, ν_{xy}, and $\eta_{xy,x}$ can exhibit similar peculiarities within the scope of Equation (2.97). Nothing should, therefore, be taken for granted with a new composite material: its moduli as a function of θ must be examined to truly understand its character.

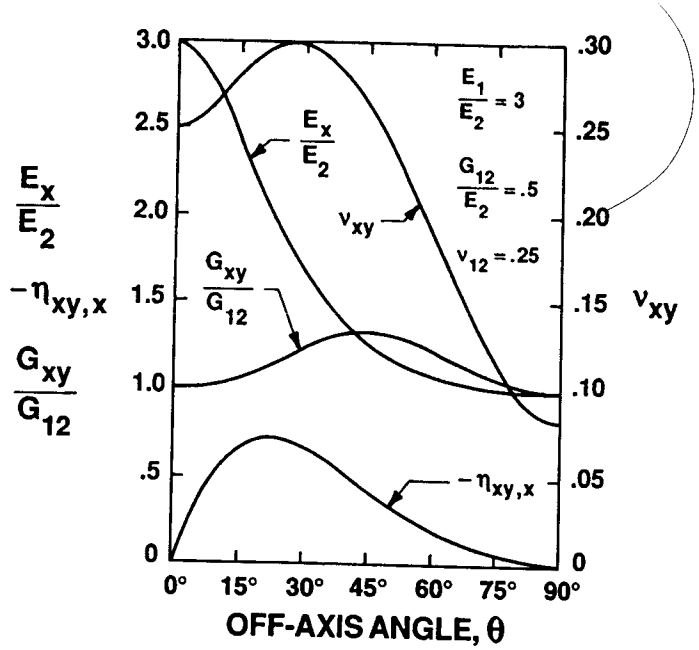

Figure 2-11 Normalized Moduli for Glass-Epoxy

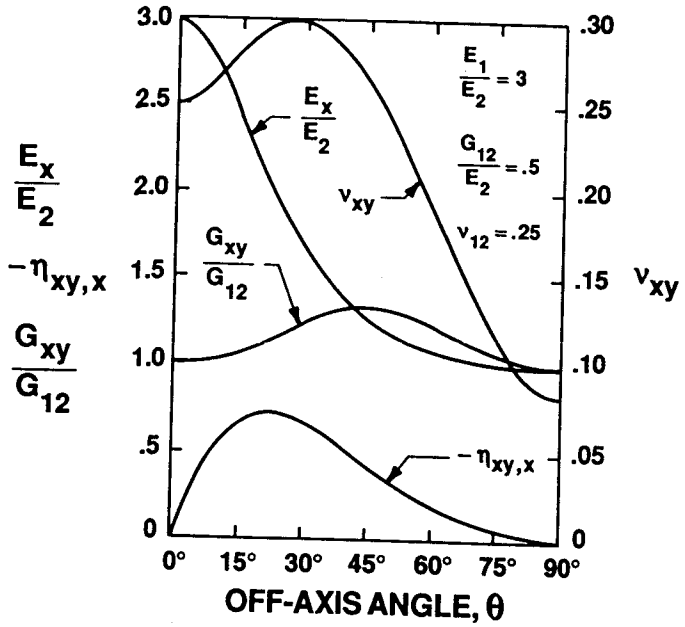

Figure 2-12 Normalized Moduli for Boron-Epoxy

Two observations are useful to rationalize why in Figures 2-11 and 2-12 (1) G_{xy} exceeds G_{12} and (2) $E_{45°}$ is less than E_1 for composite materials that have a fiber modulus much greater than the matrix modulus:

(1) Relation of G_{xy} to G_{12}

The response of an element to shearing stresses to measure E_1 is often better understood when the principal stress state at 45° to the shearing stresses is examined. For pure shear in principal material coordinates, the deformation response of the element on the bottom left-hand side of Figure 2-13 to normal stresses is clearly matrix-dominated. That is, the fibers cannot play a dominant role in the deformation process because they are not directly loaded (the action is more of a 'scooping' of the matrix). On the other hand, for pure shear in non-principal material coordinates on the right-hand side of Figure 2-13, the deformation response to the normal stresses in tension is fiber-dominated because the fibers are loaded directly, although the response to the normal stresses in compression is matrix-dominated because the matrix, which is less stiff than the fibers, deforms much more than the fibers. Thus, G_{xy} in any coordinates other than principal material coordinates is greater than G_{12}.

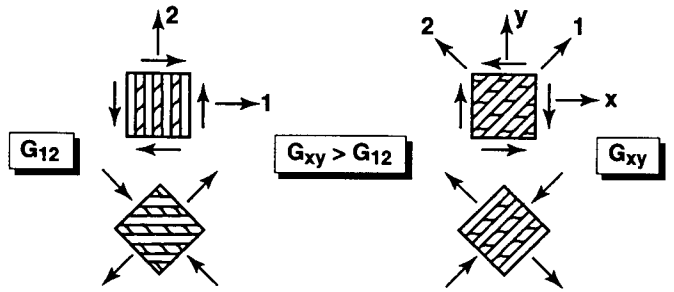

Figure 2-13 Unidirectional Lamina Shear Behavior

(2) Relation of $E_{45°}$ to E_1

A fiber-reinforced composite material that is woven of fibers in two perpendicular directions as in Figure 2-1 has principal material directions in those two directions. If such a material is loaded in a fiber direction, we measure E_1 as on the left-hand side of Figure 2-14. On the other hand, if such a woven material is loaded, for example, at 45° to principal material coordinates (so-called off-axis loading; also called on-the-bias loading), the measured $E_{45°}$ is far less than E_1. You can perform this experiment yourself with your shirt or blouse — a bidirectionally woven fibrous material essentially without a matrix (unless starched!). You can tell E_1 is higher than $E_{45°}$ because far more deformation results when you pull off-axis with your fingers than when you pull on-axis with the same force. A unidirectionally reinforced lamina has the same relation $E_1 > E_{45°}$ as the woven lamina, but a simple everyday object does not exist to demonstrate that fact.

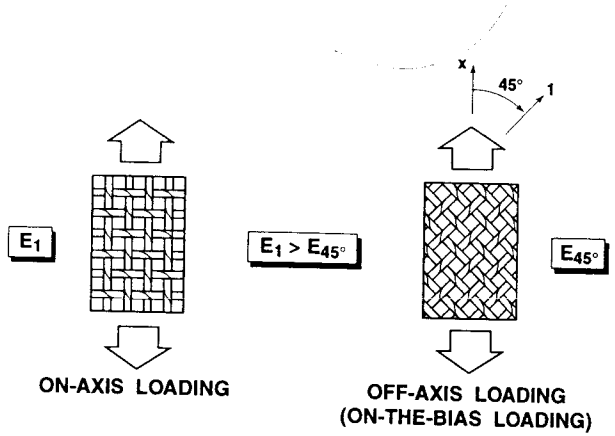

Figure 2-14 Effect of On-Axis versus Off-Axis Loading on Stiffness of a Woven Lamina

In summary, the engineering constants for anisotropic materials and orthotropic materials loaded in non-principal material coordinates can be most effectively thought of in strictly functional terms:

E_i Extensional moduli (Young's moduli)
G_{ij} Shear moduli
ν_{ij} Extension-extension coupling coefficients (Poisson's ratios)
$\eta_{i,ij}$ Shear-extension coupling coefficients (coefficients of mutual influence)
$\mu_{ij,kl}$ Shear-shear coupling coefficients (Chentsov coefficients)

Note that the functional names immediately and obviously call to mind the operational nature of the various engineering constants. In contrast, the non-functional names are a maze of either complicated non-obvious terms or names of people who do not bring to mind what the terms are supposed to mean. Thus, the functional names are preferred for ease of use and clarity of understanding.

Problem Set 2.6

2.6.1 Derive Equation (2.82).
2.6.2 Prove $[R][T][R]^{-1} = [T]^{-T}$.
2.6.3 Derive Equation (2.87).
2.6.4 Prove $[R][T]^{-1}[R]^{-1} = [T]^{T}$.
2.6.5 Identify Equation (2.97) by interpreting Equation (2.88) using Equation (2.90) as well as Equations (2.91) and (2.62). Explain the key logical step that enables you to use both Equations (2.90) and (2.91) for anisotropic materials and Equations (2.62) and (2.88) for orthotropic materials in this problem. That is, in what way can we interpret a material as satisfying both definitions of a material?
2.6.6 Plot the apparent engineering constants E_x, E_y, G_{xy}, ν_{xy}, $\eta_{xy,x}$, and $\eta_{xy,y}$ as functions of θ from $\theta = 0°$ to $\theta = 90°$ in the manner of Figures 2-11 and 2-12 for high-modulus graphite-epoxy, an orthotropic material with $E_1 = 30 \times 10^6$ psi (207 GPa), $E_2 = .75 \times 10^6$ psi (5.2 GPa), $G_{12} = .375 \times 10^6$ psi (2.59 GPa), and $\nu_{12} = .25$.
2.6.7 Show that the apparent extensional modulus of an orthotropic material as a function of θ [the first of Equations (2.97)] can be written as

$$\frac{E_1}{E_x} = (1 + a - 4b)\cos^4\theta + (4b - 2a)\cos^2\theta + a$$

where $a = E_1/E_2$ and $b = \frac{1}{4}(E_1/G_{12} - 2\nu_{12})$. Use the derivatives of E_x to find its maxima and minima in the manner of Appendix B. Hence, show that E_x is greater than both E_1 and E_2 for some values of θ if

$$G_{12} > \frac{E_1}{2(1 + \nu_{12})}$$

and that E_x is less than both E_1 and E_2 for some values of θ if

$$G_{12} < \frac{E_1}{2[(E_1/E_2) + \nu_{12}]}$$

That is, show that an orthotropic material can have an apparent Young's modulus that either exceeds or is less than the Young's moduli in both principal material directions. In doing so, derive the conditions for which each type of behavior exists, i.e., derive the inequalities. Plot E_x/E_1 for some contrived materials that exemplify these relations.

2.7 INVARIANT PROPERTIES OF AN ORTHOTROPIC LAMINA

The transformed reduced stiffnesses in Equation (2.85) are obviously very complicated functions of the four independent material properties E_1, E_2, ν_{12}, and G_{12} as well as the angle of rotation, θ. To understand the physical implications of the various rotations that occur in actual laminates would require considerable practical experience. Matching up the highest E of E_1 and E_2 with the laminate direction requiring the highest stiffness is easy. However, if the design situation includes requirements for various stiffnesses in several directions, then we must have a rationale for deciding the orientation of the laminae that make up a laminate. Obviously, then, we must understand how an individual lamina changes stiffness as it is reoriented at different angles to the reference direction. However, the present form of the transformation relations in Equation (2.85) is not particularly conducive to understanding their physical significance.

Tsai and Pagano [2-7] ingeniously recast the stiffness transformation equations to enable ready understanding of the consequences of rotating a lamina in a laminate. By use of various trigonometric identities between sin and cos to powers and sin and cos of multiples of the angle, the transformed reduced stiffnesses, Equation (2.85), can be written as

$$\begin{aligned}
\bar{Q}_{11} &= U_1 + U_2\cos 2\theta + U_3\cos 4\theta \\
\bar{Q}_{12} &= U_4 - U_3\cos 4\theta \\
\bar{Q}_{22} &= U_1 - U_2\cos 2\theta + U_3\cos 4\theta \\
\bar{Q}_{16} &= \frac{1}{2}U_2\sin 2\theta + U_3\sin 4\theta \\
\bar{Q}_{26} &= \frac{1}{2}U_2\sin 2\theta - U_3\sin 4\theta \\
\bar{Q}_{66} &= U_5 - U_3\cos 4\theta
\end{aligned} \qquad (2.98)$$

in which

$$U_1 = \frac{3Q_{11} + 3Q_{22} + 2Q_{12} + 4Q_{66}}{8}$$
$$U_2 = \frac{Q_{11} - Q_{22}}{2}$$
$$U_3 = \frac{Q_{11} + Q_{22} - 2Q_{12} - 4Q_{66}}{8} \qquad (2.99)$$
$$U_4 = \frac{Q_{11} + Q_{22} + 6Q_{12} - 4Q_{66}}{8}$$
$$U_5 = \frac{Q_{11} + Q_{22} - 2Q_{12} + 4Q_{66}}{8}$$

Note that Tsai and Pagano's angle of rotation is oppositely defined to that in Figure 2-10, so the sine terms in Equation (2.98) are also of opposite sign.

The advantage of writing the transformation equations in the form of Equation (2.98) is that parts of $\overline{Q}_{11}$, $\overline{Q}_{12}$, $\overline{Q}_{22}$, and $\overline{Q}_{66}$ are then obviously invariant under rotations about the z-axis (perpendicular to the lamina). This concept of invariance is useful when examining the prospect of orienting a lamina at various angles to achieve a certain stiffness profile. For example,

$$\overline{Q}_{11} = U_1 + U_2 \cos 2\theta + U_3 \cos 4\theta \qquad (2.100)$$

can be decomposed into its components in the graphical manner of Figure 2-15. There, we see that the value of $\overline{Q}_{11}$ is determined by a fixed constant, U_1, plus a quantity of low-frequency variation with θ plus another quantity of higher frequency variation with θ. Thus, U_1 is an effective measure of lamina stiffness in a design application because it is not affected by orientation. The concept of invariance will be more useful in the study of laminates because laminates are made of a collection of laminae at various orientations to achieve a certain stiffness. Such tailoring of the material and structural configuration, however, comes at the expense of capabilities in other directions. For example, from observation of the variable nature of $\overline{Q}_{11}$, apparently trying to meet a required stiffness in one direction leads to a lower stiffness in some other direction unless the requirement is as low as Q_{22} in this example.

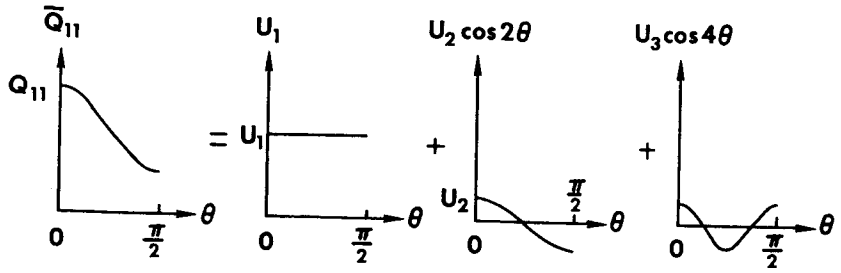

Figure 2-15 Decomposition of $\overline{Q}_{11}$ into Components

Similar invariance concepts for anisotropic materials were also developed by Tsai and Pagano [2-7]. For anisotropy, the following definitions

$$U_6 = \frac{Q_{16} + Q_{26}}{2} \qquad U_7 = \frac{Q_{16} - Q_{26}}{2} \qquad (2.101)$$

must be appended to Equation (2.99) and worked into Equation (2.98) in such a manner that Table 2-2 results, so the transformation equations can be written.

Table 2-2 Transformation Equations for $\overline{Q}_{ij}$ and $\overline{Q}'_{ij}$*

	Constant	cos 2θ	sin 2θ	cos 4θ	sin 4θ
$\overline{Q}'_{11}$	U_1	U_2	$-2U_6$	U_3	$-U_7$
$\overline{Q}'_{22}$	U_1	$-U_2$	$2U_6$	U_3	$-U_7$
$\overline{Q}'_{12}$	U_4	0	0	$-U_3$	U_7
$\overline{Q}'_{66}$	U_5	0	0	$-U_3$	U_7
$2\overline{Q}'_{16}$	0	$2U_6$	U_2	$2U_7$	$2U_3$
$2\overline{Q}'_{26}$	0	$2U_6$	U_2	$-2U_7$	$-2U_3$

*$\overline{Q}'_{ij}$ are for anisotropic materials. $\overline{Q}_{ij}$ for orthotropic materials are obtained by deleting U_6 and U_7 from the definitions of $\overline{Q}'_{ij}$.

The actual invariants in 'invariant properties of a lamina' include not only U_1, U_4, and U_5 because they are the constant terms in Equation (2.93) but functions related to U_1, U_4, and U_5 as shown in Problem Set 2.7. The terms U_2 and U_3 are not invariants. The only invariants of an orthotropic lamina can be shown to be

$$L_1 = Q_{11} + Q_{22} + 2Q_{12} = \overline{Q}_{11} + \overline{Q}_{22} + 2\overline{Q}_{12} = 2(U_1 + U_4)$$
$$L_2 = Q_{66} - Q_{12} = \overline{Q}_{66} - \overline{Q}_{12} = U_5 - U_4 \qquad (2.102)$$

Discussion of invariance concepts for laminates will be deferred until Chapter 7 after the development of lamination concepts in Chapter 4.

Problem Set 2.7

2.7.1 Show that $Q_{11} + Q_{22} + 2Q_{12}$ is invariant under rotation about the z-axis, i.e., that

$$\overline{Q}_{11} + \overline{Q}_{22} + 2\overline{Q}_{12} = Q_{11} + Q_{22} + 2Q_{12}$$

2.7.2 Show that $Q_{66} - Q_{12}$ is invariant under rotation about the z-axis, i.e., that

$$\overline{Q}_{66} - \overline{Q}_{12} = Q_{66} - Q_{12}$$

2.7.3 Show that $U_5 = (U_1 - U_4)/2$, i.e., that the quantities U_1, U_4, and U_5 are related and only two are independent because one can be expressed in terms of the other two.

2.8 STRENGTHS OF AN ORTHOTROPIC LAMINA

2.8.1 Strength Concepts

The strength characteristics of an orthotropic lamina are just as important a building block in the description of laminates as the stiffness characteristics. As review, from previous studies, the central issue here is that principal stresses and strains are the largest values irrespective of direction or orientation; however, direction of stress or strain has, by definition, absolutely no significance for isotropic materials. Because of orthotropy, the axes of principal stress do not coincide with the axes of principal strain. Moreover, because the strength is lower in one direction than another, the highest stress might not be the stress governing the design. A rational comparison of the actual stress field with the allowable stress field is therefore required, irrespective of any principal values.

What has been accomplished in preceding sections on stiffness relationships serves as the basis for determination of the actual stress field; what remains is the definition of the allowable stress field. The first step in such a definition is the establishment of allowable stresses or strengths in the principal material directions. Such information is basic to the study of strength of an orthotropic lamina.

For a lamina stressed in its own plane, there are three fundamental strengths if the lamina has equal strengths in tension and compression:

X = axial or longitudinal strength (in the 1-direction)
Y = transverse strength (in the 2-direction)
S = shear strength (in 1-2 coordinates)

(The units are force/area, that is, allowable stresses). The directions of each of these strengths are shown in Figure 2-16; obviously, the strengths result from *independent* application of the respective stresses, σ_1, σ_2, τ_{12}.

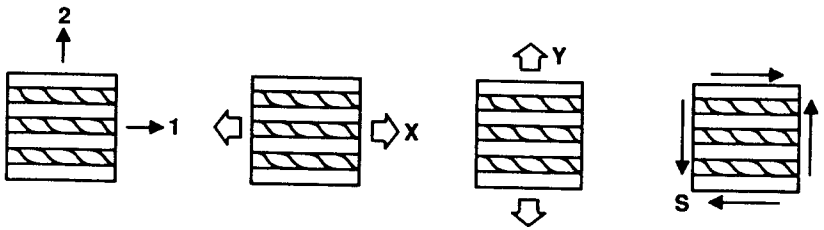

Figure 2-16 Fundamental Strengths for a Unidirectionally Reinforced Lamina

That the principal stresses are not of interest in determining the strength of an orthotropic lamina is illustrated with the following example. Consider the lamina with unidirectional fibers shown in Figure 2-16. Say that the hypothetical strengths of the lamina in the 1-2 plane are

X = 50,000 psi (350 MPa)
Y = 1,000 psi (7 MPa)
S = 2,000 psi (14 MPa)

The stiffness would also be high in the 1-direction and low in the 2-direction, as is easily imagined on the physical basis of the fiber orientation. Imagine that, in the 1-2 plane, the stresses are

σ_1 = 45,000 psi (315 MPa)
σ_2 = 2,000 psi (14 MPa)
τ_{12} = 1,000 psi (7 MPa)

Then, obviously the maximum principal stress is lower than the largest strength. However, σ_2 is greater than Y, so the lamina must fail under the imposed stresses (perhaps by cracking parallel to the fibers, but not necessarily). The key observation is that strength is a function of *orientation* of stresses relative to the principal material coordinates of an orthotropic lamina. In contrast, for an isotropic material, strength is independent of material orientation relative to the imposed stresses (the isotropic material has *no* orientation).

If the material has different properties in tension and compression as do most composite materials, then the following strengths are required:

X_t = axial or longitudinal strength in tension
X_c = axial or longitudinal strength in compression
Y_t = transverse strength in tension
Y_c = transverse strength in compression
S = shear strength

Remember that the preceding strengths must be defined in principal material coordinates.

The shear strength in the principal material coordinates is seen to be independent of differences in tensile and compressive behavior, as it must be by definition of a pure shear stress. That is, the shear stress, whether 'positive' or 'negative', has the same maximum value in principal material coordinates for materials that exhibit different behavior in tension than in compression. This statement is rationalized by observation of Figure 2-17 wherein positive and negative shear stresses are applied to a unidirectionally reinforced lamina. The convention of which shear stress is positive is consistent with Pagano and Chou's convention that a positive shear stress τ_{12} is directed in the positive 2-direction on a positive 1-direction face [2-8]. Note in Figure 2-17 that there is no real difference between the stress fields labeled positive and negative shear stress. The two stress fields are perfect mirror images of each other, even when the principal stresses are examined as in the lower half of Figure 2-17. Thus, the maximum value of shear stress is the same in both cases because the action of the stresses on the two pieces of material is identical.

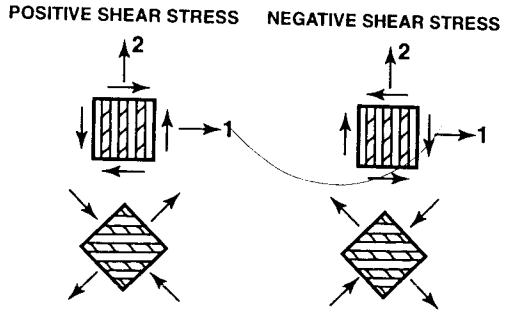

Figure 2-17 Shear Stress in Principal Material Coordinates

However, the maximum value of shear stress in other than principal material coordinates depends on the sign of the shear stress. For example, at 45° to the principal material axes, positive and negative shear stresses result in normal stresses of opposite signs on the fibers as in Figure 2-18. There, for positive shear stress, tensile stresses result in the fiber direction, and compressive stresses arise perpendicular to the fibers. For negative shear stress, compressive stresses exist in the fiber direction and tensile stresses occur transverse to the fibers. However, both the normal strengths and normal stiffnesses for the material are different under tension loading than under compression loading. Thus, the apparent shear strengths and shear stiffnesses are different for positive and negative shear stresses applied at 45° to the principal material coordinates. This rationale can readily be extended from the simple unidirectionally reinforced lamina to woven materials.

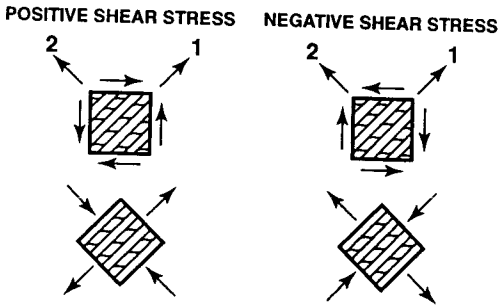

Figure 2-18 Shear Stress at 45° to Principal Material Coordinates

The foregoing example is but one of the difficulties encountered in analysis of orthotropic materials with different properties in tension and compression. The example is included to illustrate how basic information in principal material coordinates can be transformed to other useful coordinate directions, depending on the stress field under consideration. Such transformations are simply indications that the basic information, whether strengths or stiffnesses, is in tensor form and therefore is subject to the rules governing tensor transformations given in Appendix A.

The topic of materials with different strengths and stiffnesses in tension than in compression will not be covered further in much depth (except to report different strengths) because research on such materials is still in its infancy. However, the topic is very important for the general class of composite materials, if not fiber-reinforced laminated composites. Ambartsumyan and his associates first reported research on this topic in 1965 [2-9]. A few Americans have also investigated some aspects of the mechanics of these materials (see Jones [2-10], Bert [2-11], and Bert and Reddy [2-12]).

2.8.2 Experimental Determination of Strength and Stiffness

For orthotropic materials, certain basic experiments can be performed to measure the properties in the principal material coordinates. The experiments, if conducted properly, generally reveal both the strength and stiffness characteristics of the material. Recall that the stiffness characteristics are

E_1 = Young's modulus in the 1-direction

E_2 = Young's modulus in the 2-direction

$\nu_{12} = -\dfrac{\varepsilon_2}{\varepsilon_1}$ for $\sigma_1 = \sigma$ and all other stresses are zero

$\nu_{21} = -\dfrac{\varepsilon_1}{\varepsilon_2}$ for $\sigma_2 = \sigma$ and all other stresses are zero

G_{12} = shear modulus in 1-2 coordinates

where only three of $E_1, E_2, \nu_{12}, \nu_{21}$ are independent, and the strength characteristics are

X = axial or longitudinal strength (1-direction)

Y = transverse strength (2-direction)

S = shear strength (1-2 coordinates)

where X and Y can have different values in tension and compression.

Several experiments will now be described from which the foregoing basic stiffness and strength information can be obtained. For many, but not all, composite materials, the stress-strain behavior is linear from zero load to the ultimate or fracture load. Such linear behavior is typical for glass-epoxy composite materials and is quite reasonable for boron-epoxy and graphite-epoxy composite materials except for the shear behavior that is very nonlinear to fracture.

A key element in the experimental determination of the stiffness and strength characteristics of a lamina is the imposition of a uniform stress state in the specimen. Such loading is relatively easy for isotropic materials. However, for composite materials, the orthotropy introduces coupling between normal stresses and shear strains and between shear stresses and normal and shear strains when loaded in non-principal material coordinates for which the stress-strain relations are given in Equation (2.88). Thus, special care must be taken to ensure obtaining

the desired information. This care typifies the knowledge required to treat composite materials.

Before we examine any specific tests, we need to examine the 'testing' or measurement process itself. After all, testing is no substitute for thinking! Tests are, quite often, subtle in their implications. Thus, we must

- understand the purpose of the test
- visualize the expected results
- know opportunities for errors
- question the validity of 'standard' tests for metals when used for composite materials

We would probably agree on the following criteria for a good test specimen:

(1) The highest stress must occur in the gage section (region of smallest cross-sectional area) so that failure occurs in the gage section.
(2) A uniform stress field must exist over the entire gage-section volume to eliminate volume-based statistical failure effects (e.g., a realistic distribution of ordinary defects must exist for the test to be representative of the actual material).
(3) Unwanted 'other' stresses must be eliminated from the gage section (e.g., eliminate bending stresses induced by load-application mechanisms such as misalignment of loading grips).
(4) Alternatively to (3), *account for* certain end and edge effects (e.g., shear-extension coupling) in the data-reduction process.
(5) The specimen material and the test procedure must be representative of the intended application from the standpoint of
   (a) fabrication (a tape-laid specimen does not in any way represent a filament-wound structure!)
   (b) size effects (the characteristic dimensions of the specimen, e.g., thickness, cannot approach any characteristic material dimension such as void size, fiber diameter, etc.)
   (c) environment (the loading rate, moisture content, and temperature of the specimen must be similar to, if not identical with, the actual structural application)

These criteria will be used in the evaluation of several test specimens.

Further, with any test specimen, there are certain natural 'regions of concern'. For example, consider the tension specimen depicted schematically in Figure 2-19. There, three regions are shown: (1) loading region where load is applied to the specimen, (2) gage region that must be uniformly stressed and that must be the location of failure under maximum load, and (3) transition region that provides a smooth transition (without stress concentrations) from the loading region to the gage region. We will examine several tests that have been designed to measure the strengths and stiffnesses of composite materials. At all times, we must be conscious of both the test specimen criteria and the specimen regions of concern.

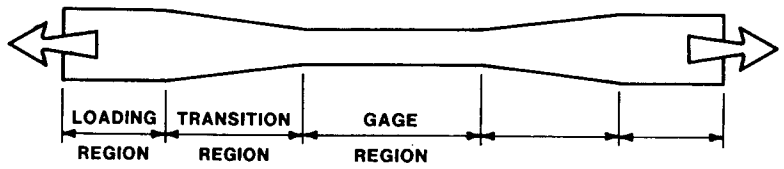

Figure 2-19 Test Specimen Regions of Concern

First, consider uniaxial tension loading in the 1-direction on a flat piece of unidirectionally reinforced lamina where only the gage section is shown in Figure 2-20. The specimen thickness is not just one lamina, but several laminae all of which are at the same orientation (a single lamina would be too fragile to handle). The strains ε_1 and ε_2 are measured so, by definition,

$$\sigma_1 = \frac{P}{A} \qquad E_1 = \frac{\sigma_1}{\varepsilon_1} \qquad \nu_{12} = -\frac{\varepsilon_2}{\varepsilon_1} \qquad X = \frac{P_{ult}}{A} \tag{2.103}$$

where A is the gage section cross-sectional area perpendicular to the applied load and P_{ult} is the ultimate load on the specimen. But, how do we achieve a reasonable gage section given the test specimen criteria? Let's examine several specific test specimens to see how well they satisfy the criteria.

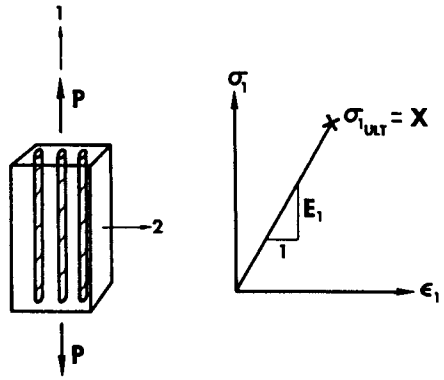

Figure 2-20 Uniaxial Loading in the 1-Direction

The ASTM D 638 tension test specimen is a fairly simple specimen that requires some machining to create the rounded transition from a wide loading region to a narrow gage region. The gage region is about one-quarter of the specimen length as shown in Figure 2-21. The typical failure occurs in the transition region. Thus, this specimen does not meet the criterion of failure in the gage region. However, because the failure strengths achieved with this specimen are underestimates of the real strength, this specimen is considered practical.

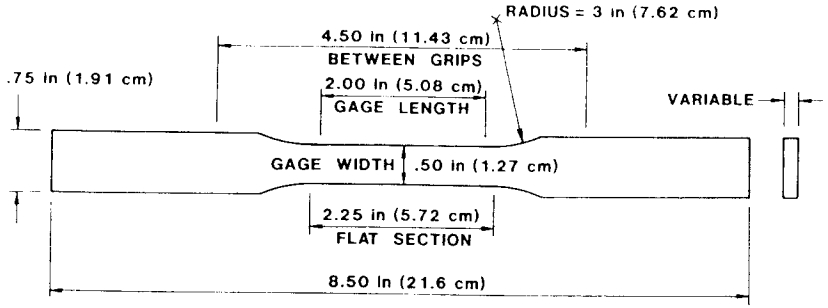

Figure 2-21 ASTM D 638 Tension Specimen

Next, the straight-sided tension specimen has a transition region that is created by thickness change (instead of the width change of the ASTM D 638 specimen) as shown in Figure 2-22. Failures typically occur either in the bonded tabs or in the gage section. If the bonded tabs fail, then the failure load is never a measure of the subject material's strength!

Finally, the bow-tie tension specimen has considerable machining required to create a very gradual transition region as in Figure 2-23. Moreover, this specimen is much longer than the previous two. However, failure consistently occurs in the gage region, so the bow-tie specimen is the only specimen of the three that satisfies the main criterion for a good specimen.

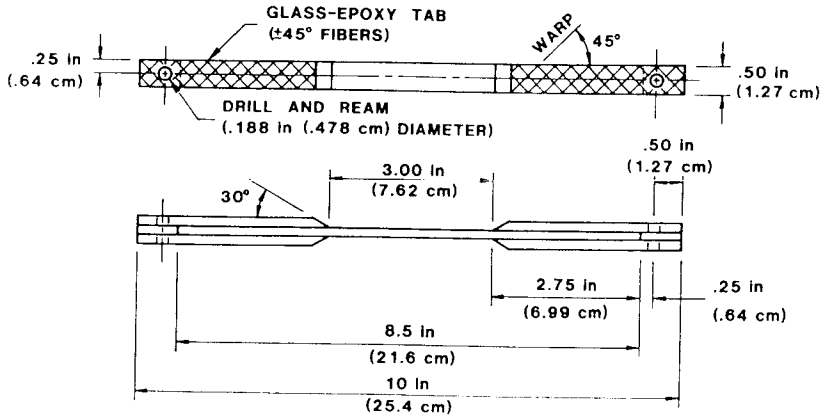

Figure 2-22 Straight-Sided Tension Specimen

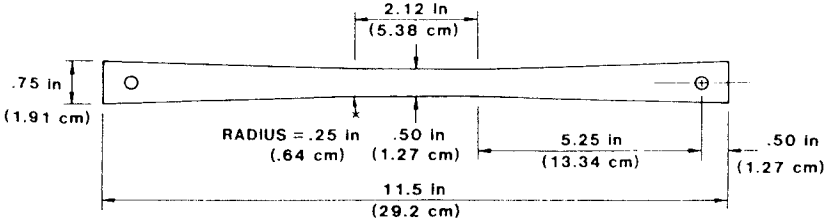

Figure 2-23 Bow-Tie Tension Specimen

Under compression loading, the long flexible tension specimens would simply buckle. Thus, lateral support to prevent buckling is necessary as shown in the compression test fixture with side-support plates in Figure 2-24. There, the specimen is essentially as long as the fixture is tall, and only a small portion of the specimen can be seen where it is not supported.

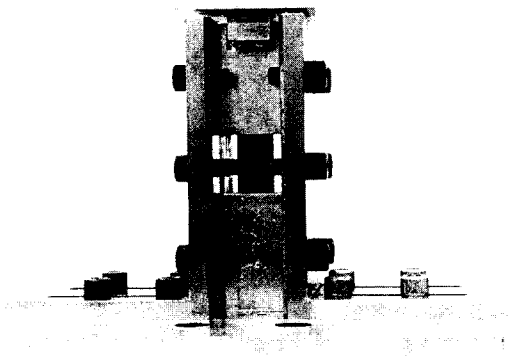

Figure 2-24 Compression Test Fixture

As the second major measurement, consider uniaxial tension loading in the 2-direction on a flat piece of unidirectionally reinforced lamina as in Figure 2-25. As in the first experiment, ε_1 and ε_2 are measured so

$$\sigma_2 = \frac{P}{A} \qquad E_2 = \frac{\sigma_2}{\varepsilon_2} \qquad \nu_{12} = -\frac{\varepsilon_1}{\varepsilon_2} \qquad Y = \frac{P_{ult}}{A} \tag{2.104}$$

where again A is the cross-sectional area of the gage section and P_{ult} is the ultimate load on the specimen.

The stiffness properties should satisfy the reciprocal relations

$$\frac{\nu_{12}}{E_1} = \frac{\nu_{21}}{E_2} \tag{2.105}$$

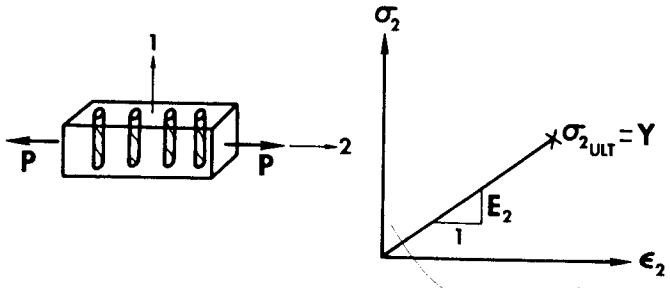

Figure 2-25 Uniaxial Loading in the 2-Direction

or else one of three possibilities exists:

(1) The data were measured incorrectly
(2) The calculations were performed incorrectly
(3) The material cannot be described with linear elastic stress-strain relations

As the third major measurement to try to determine the remaining properties G_{12} and S, consider uniaxial tension loading at 45° to the 1-direction on a flat piece of lamina, i.e., a 45° off-axis test, as shown in Figure 2-26. By measurement of ε_x alone, obviously

$$E_x = \frac{P/A}{\varepsilon_x} \tag{2.106}$$

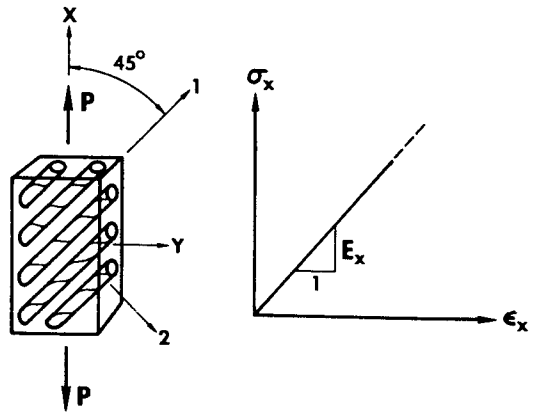

Figure 2-26 Uniaxial Loading at 45° to the 1-Direction

Then, by use of the modulus transformation relations in Equation (2.97)

$$\frac{1}{E_x} = \frac{1}{4}\left[\frac{1}{E_1} - \frac{2\nu_{12}}{E_1} + \frac{1}{G_{12}} + \frac{1}{E_2}\right] \tag{2.107}$$

wherein G_{12} is the only unknown. Thus,

$$G_{12} = \frac{1}{\frac{4}{E_x} - \frac{1}{E_1} - \frac{1}{E_2} + \frac{2\nu_{12}}{E_1}} \tag{2.108}$$

Accordingly, we have supposedly found the shear modulus G_{12}. However, a relationship such as Equation (2.107) does not exist for strengths because strengths do not transform like stiffnesses. Thus, this experiment cannot be relied upon to determine S, the ultimate shear stress (shear strength), because a pure shear deformation mode has not been excited with accompanying failure in shear. Accordingly, other approaches to obtain S must be used.

Before consideration of other approaches to determination of the shear strength, however, it is appropriate to comment on the ease of performing the 45° off-axis test. From Equation (2.87), it is apparent that because of the presence of $\bar{S}_{16}$ there is coupling between the normal stress σ_x and shear strain γ_{xy}. Thus, although just a force P is indicated in Figure 2-26, the experiment cannot be properly conducted unless the force is applied uniformly across the end and, in addition, unless the ends of the lamina are free to deform in the manner shown on the left of Figure 2-27. Otherwise, if for example the end edges of the lamina were clamped in the jaws of a load frame and a resultant force P were applied, then the lamina would be restrained from shearing deformation, so it would deform in the fashion shown on the right in Figure 2-27 [2-13]. In the center of such a specimen, if it is long enough as compared to its width, the deformation is similar to the shearing and extension of the unrestrained lamina in Figure 2-27. That is, away from Saint-Venant end effects,[2] the type of test does not matter. However, normally we do not choose to use enough material to have a useful gage section that does not have Saint-Venant effects.

An additional characteristic of the off-axis test displayed in Figures 2-26 and 2-27 is that the modulus $\bar{E}_x$ is not actually measured. Instead, the transformed reduced stiffness $\bar{Q}_{11}$ is measured unless the specimen has a high length-to-width ratio. The reason for this discrepancy is that the geometrically admissible state of strain in the specimen depends strongly on the geometry. If the specimen is long and slender, the boundary conditions at the specimen end grips are of no consequence à la Saint-Venant. Accordingly, a pure uniaxial strain is obtained and

$$\sigma_x = E_x \varepsilon_x \tag{2.109}$$

However, if the specimen is short and wide, the end restraint of $\sigma_x \neq 0$ and $\varepsilon_y = \gamma_{xy} = 0$ leads to a stress-strain relation

$$\sigma_x = \bar{Q}_{11}\varepsilon_x \tag{2.110}$$

[2] Saint-Venant stated that two different loadings that are statically equivalent produce the same stresses and deformations at a distance sufficiently far removed from the area of application of the loadings. Thus, if two statically equivalent loadings are applied and the observation point is near the end where the loading is applied, then the stresses and deformations will be different for each loading. Hence the name Saint-Venant end effects.

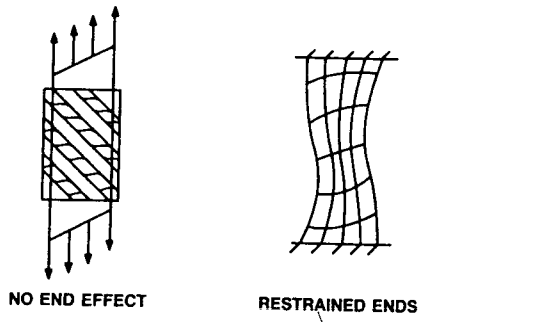

Figure 2-27 Deformation of a Unidirectionally Reinforced Lamina Loaded at 45° to the Fibers

that is consistent with Equation (2.84). The reader should verify Equations (2.109) and (2.110) by imposing the stated conditions and deriving the relation for σ_x. That the difference between E_x in Equation (2.109) and $\bar{Q}_{11}$ in Equation (2.110) is significant is best illustrated with Figure 2-28 for graphite-epoxy specimens. There, for off-axis loading at 30° to the fiber direction, the value of $\bar{Q}_{11}$ is 10.4 times as great as E_x! Similar differences exist for $\bar{Q}_{66}$ versus G_{xy}. For materials with lower values of E_1/E_2, the difference between $\bar{Q}_{11}$ and E_x is smaller than for graphite-epoxy. The practical significance of the difference between $\bar{Q}_{11}$ and E_x is that the length-to-width ratio of off-axis specimens must be large enough to ensure that we are measuring E_x and not $\bar{Q}_{11}$. Pagano and Halpin [2-13] present a quantitative analysis of the effect of length-to-width ratio on the apparent E_x. Note, at this point, that even

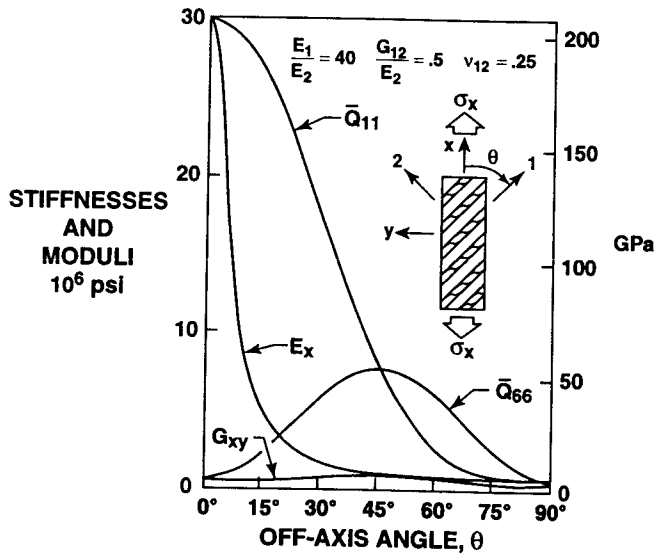

Figure 2-28 Stiffnesses $\bar{Q}_{11}$ and $\bar{Q}_{66}$ versus Moduli E_x and G_{xy}

though we thought we had measured G_{12} with the procedure leading to Equation (2.108), the value of E_x was seriously overestimated. Thus, the value of G_{12} from Equation (2.108) is also seriously overestimated and hence unreliable.

The continuing search to determine the shear modulus and shear strength consists of a collection of tests. Several tests are discussed because each has faults, as will be seen, and because, to some extent, there is no universal agreement on the best way to measure the shear properties.

The *torsion-tube test* described by Whitney, Pagano, and Pipes [2-14] involves a thin circular tube subjected to a torque, T, at the ends as in Figure 2-29. The tube is made of multiple laminae with their fiber directions aligned either all parallel to the tube axis or all circumferentially. Reasonable assurance of a constant stress state through the tube thickness exists if the tube is only a few laminae thick. However, then serious end-grip difficulties can arise because of the flimsy nature of the tube. Usually, the thickness of the tube ends must be built up by bonding on additional layers to introduce the load so that failure occurs in the central uniformly stressed portion of the tube (recall the test specimen criteria). Torsion tubes are expensive to fabricate and require relatively sophisticated instrumentation. If the shearing strain γ_{12} is measured under shear stress τ_{12}, then

$$\tau_{12} = \frac{T}{2\pi r^2 t} \tag{2.111}$$

$$S = \tau_{12_{ult}} = \frac{T_{ult}}{2\pi r^2 t} \tag{2.112}$$

Also, the shear modulus is

$$G_{12} = \frac{\tau_{12}}{\gamma_{12}} \tag{2.113}$$

for the linear portion of the stress-strain curve. However, a typical shear stress–shear strain curve is quite nonlinear as in Figure 2-29. Accordingly, the whole stress-strain curve instead of the initial 'elastic' modulus should be used in practical analyses as done by Hahn and Tsai [2-15] and Jones and Morgan [2-16]. Nevertheless, most composite materials analyses are performed with the initial elastic modulus from Equation (2.113).

Another test used to determine the shear modulus and shear strength of a composite material is the *sandwich cross-beam test* due to Shockey and described by Waddoups [2-17]. The composite lamina

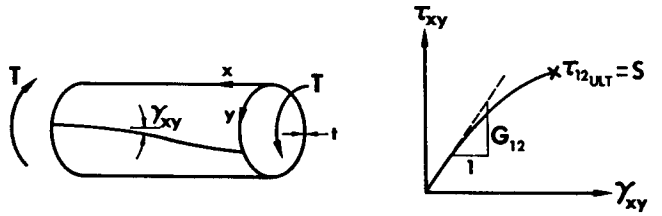

Figure 2-29 Torsion-Tube Test

being evaluated is the facing of a sandwich beam whose core elastic modulus is about two orders of magnitude less than that of the lamina. A cross-shaped beam configuration is subjected to the loads shown in Figure 2-30. A state of plane stress results which at 45° to the x-axis is supposedly a uniform pure shear stress. However, because of inevitable stress concentrations at the corners of the cross, a uniform stress state is approached only in the very center of the cross. Failure initiates in the corners of the cross; thus, the cross-beam test, even with rounded corners, is no longer regarded as an adequate measuring tool for shear strength and shear stiffness.

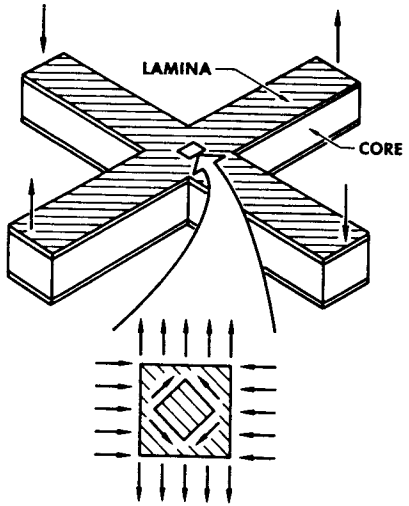

Figure 2-30 Sandwich Cross-Beam Test

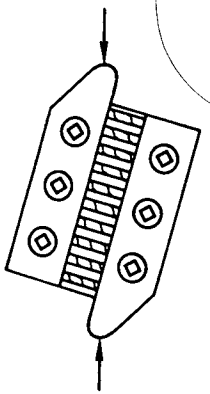

Figure 2-31 Rail Shear Test

Yet another shear strength and shear modulus test is the *rail shear test* as described by Whitney, Stansbarger, and Howell [2-18]. Basically, four pieces of rail are bolted together along two opposite edges of a lamina as shown schematically in Figure 2-31. One pair of rails protrudes at the top of the laminate, and the other pair at the bottom. The assembly is placed between the heads of a loading frame and compressed. Thus, shear is induced in the lamina. However, the geometry of such a specimen must be carefully selected to account for end effects such as the free edges at the top and bottom of the lamina. These and other effects could lead to strength evaluations that are lower than physical reality. Nevertheless, the rail shear test is widely used in the aerospace industry because it is simple, inexpensive, and can be used for tests at both higher and lower than room temperature.

2.8.3 Summary of Mechanical Properties

As an illustration of the results of the measurements just described, the mechanical properties for four unidirectionally reinforced composite materials, glass-epoxy, boron-epoxy, graphite-epoxy, and Kevlar 49®-epoxy, are given in Table 2-3. These values are representative of the strengths and initial stiffnesses that can be obtained with such materials (except for graphite-epoxy of which many variations are available). However, these values are for purposes of illustration only and should not be used for design of composite structures. Only up-to-date information of the specific fiber and matrix system should be used in design. Again, recall the essential linearity of the normal stress–normal strain results and the nonlinearity of the shear stress–shear strain results (especially for boron-epoxy and graphite-epoxy). Typical stress-strain curves for the first three materials are shown in Appendix C. The specific values will change when the fiber and matrix content of the composite material changes. The rationale for changing those values will be described in Chapter 3 on micromechanics of a lamina. The values in Table 2-3 will be used in example problems and homework problems throughout the book, and, as a matter of fact, were already used to obtain Figures 2-11 and 2-12.

Table 2-3a Typical Mechanical Properties of Some Composite Materials (U. S. Standard Units)

Property	Unidirectionally Reinforced Composite Material			
	Glass-Epoxy	Boron-Epoxy	Graphite-Epoxy	Kevlar®-Epoxy
E_1	7.8×10^6 psi	30×10^6 psi	30×10^6 psi	11×10^6 psi
E_2	2.6×10^6 psi	3×10^6 psi	$.75 \times 10^6$ psi	$.8 \times 10^6$ psi
ν_{12}	.25	.3	.25	.34
G_{12}	1.3×10^6 psi	1×10^6 psi	$.375 \times 10^6$ psi	$.3 \times 10^6$ psi
X_t	150×10^3 psi	200×10^3 psi	150×10^3 psi	200×10^3 psi
Y_t	4×10^3 psi	12×10^3 psi	6×10^3 psi	4×10^3 psi
S	6×10^3 psi	18×10^3 psi	10×10^3 psi	6.4×10^3 psi
X_c	150×10^3 psi	400×10^3 psi	100×10^3 psi	40×10^3 psi
Y_c	20×10^3 psi	40×10^3 psi	17×10^3 psi	20×10^3 psi

Table 2-3b Typical Mechanical Properties of Some Composite Materials (SI Units)

Property	Unidirectionally Reinforced Composite Material			
	Glass-Epoxy	Boron-Epoxy	Graphite-Epoxy	Kevlar®-Epoxy
E_1	54 GPa	207 GPa	207 GPa	76 GPa
E_2	18 GPa	21 GPa	5 GPa	5.5 Gpa
ν_{12}	.25	.3	.25	.34
G_{12}	9 GPa	7 GPa	2.6 GPa	2.1 GPa
X_t	1035 MPa	1380 MPa	1035 MPa	1380 MPa
Y_t	28 MPa	83 MPa	41 MPa	28 MPa
S	41 MPa	124 MPa	69 MPa	44 MPa
X_c	1035 MPa	2760 MPa	689 MPa	276 MPa
Y_c	138 MPa	276 MPa	117 MPa	138 MPa

Now that the basic stiffnesses and strengths have been defined for the principal material coordinates, we can proceed to determine how an orthotropic lamina behaves under biaxial stress states in Section 2.9. There, we must combine the information in principal material coordinates in order to define the stiffness and strength of a lamina at arbitrary orientations under arbitrary biaxial stress states.

Problem Set 2.8

2.8.1 Find, read, and summarize the ASTM specification for two of the tension measurements described in Section 2.8.

2.8.2 Find and describe two other tests to determine the shear stiffness and strength of an orthotropic fiber-reinforced lamina.

2.9 BIAXIAL STRENGTH CRITERIA FOR AN ORTHOTROPIC LAMINA

Most measurements of the strength of a material are based on uniaxial stress states. However, the general practical design problem involves at least a biaxial if not a triaxial state of stress. Thus, a logical method of using uniaxial strength information obtained in principal material coordinates is required for analysis of multiaxial loading problems. Obtaining the strength characteristics of a lamina at all possible orientations is physically impossible, so a method must be determined for obtaining the characteristics at any orientation in terms of characteristics in the principal material coordinates. In such an extension of the information obtained in principal material coordinates, the well-known concepts of principal stresses and principal strains are of no value. A multitude of possible microscopic failure mechanisms exists, so a tensor transformation of strengths is very difficult. Moreover, tensor transformations of strength properties are much more complicated than the tensor transformation of stiffness properties. (The strength tensor, if one even exists, must be of higher order than the stiffness tensor.) Nevertheless, tensor transformations of strength are performed and used as a phenomenological failure criterion (phenomenological because only the occurrence of failure is predicted, not the actual mode of failure). A somewhat empirical approach will be adopted: the actual failure envelopes in stress space will be compared with simplified failure envelopes.

The simplified failure envelopes are not derived from physical theories of failure in which the actual physical processes that cause failure on a microscopic level are 'integrated' to obtain a failure theory. We, instead, deal with phenomenological theories in which we ignore the actual failure mechanisms and concentrate on the gross macroscopic events of failure. Phenomenological theories are based on curve-fitting, so they are *failure criteria* and not theories of any kind (the term theory implies a formal derivation process).

The simplified failure envelopes differ little from the concept of yield surfaces in the theory of plasticity. Both the failure envelopes (or surfaces) and the yield surfaces (or envelopes) represent the end of linear elastic behavior under a multiaxial stress state. The limits of linear elastic

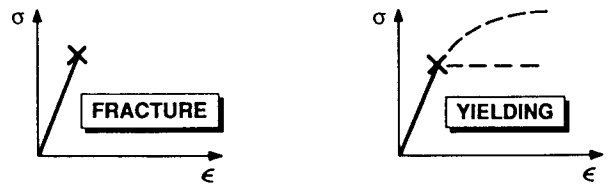

Figure 2-32 Failure (Fracture) versus Yielding

behavior are shown with the symbol x in the stress-strain curves for a fracture condition and two types of yielding conditions in Figure 2-32. Actually, the failure envelopes are not restricted to be the limit of multiaxial linear elastic behavior (although they are for brittle materials). The envelopes mask the actual material phenomena that are occurring and merely represent the levels of stresses at which failure occurs, even though other events such as yielding took place at lower stress levels.

Our objective is the analytical definition of the failure surface or envelope in stress space that can be conveniently used in design. For example, the failure data for a hypothetical material are shown in two dimensions in Figure 2-33. There, the material has unequal strengths in tension and compression. We must, in some manner, describe those data with a curve or set of curves, each of which has an equation that is suitable for design use. That is, we must *curve-fit* the failure data with an equation that is a reasonable fit for design purposes. However, we must be fully aware that a single failure curve is merely an approximate or averaging process for all the events that actually cause failure. Thus, we are oversimplifying the actual failure process.

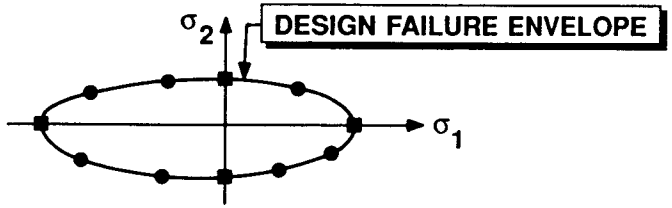

Figure 2-33 Hypothetical Two-Dimensional Failure Data and Design Curve

Unfortunately, with curve-fitting, we lose the ability to determine the failure mode. That is, curve-fit failure criteria are generally disassociated from knowledge of precisely how the material fails. Perhaps the best description of the curve-fitting procedure is that by John Hart-Smith "most failure criteria are meaningless curves passed through unrelated data points" [2-19]. Think about it! Each of the principal material direction strengths, X_t, X_c, Y_t, Y_c, that correspond to the solid squares in Figure 2-33 represents a totally different failure mode, so why should they be connected with a single curve? That is, as we will see later, X_t corresponds to fiber fracture, X_c to fiber buckling, Y_t to matrix fracture, and Y_c to matrix compression failure. And, the material behavior (or structural behavior in the case of X_c) corresponding to each failure is drastically

different. Thus, there is no physical reason to justify connecting the various failure points with a single continuous curve. In fact, there is reason *not* to connect the principal material strength data points with a continuous curve. Nevertheless, designers need something simple enough to use every day, so we pursue the curve-fitting approach.

For conventional engineering metals, the curve-fitting process works fairly well. Note, however, that the curve-fitting process is less challenged than for orthotropic materials because metals are isotropic, so they don't have different strengths in different directions. Failure data for cast iron, steel, copper, and aluminum are shown on Figure 2-34 along with three common failure criteria. There, the cast iron data are best fit with the maximum normal stress failure criterion. That is, cast iron apparently fails in a brittle manner when the largest principal stress reaches the uniaxial failure stress irrespective of the value of the other principal stresses. In contrast, the other metals, steel, copper, and aluminum, fail in a ductile manner — perhaps by yielding. All their failure data are grouped essentially on or between the maximum shearing stress failure criterion and the maximum distortional energy failure criterion (also known as the von Mises failure criterion). The maximum shearing stress criterion is identical to the maximum normal stress criterion in the first and third quadrants in Figure 2-34, but different in the second and fourth quadrants. The maximum distortional energy failure criterion represents an interaction between principal normal stresses so that both normal stresses influence failure, not just one as in the maximum normal stress criterion. One of the obvious conclusions to be drawn from Figure 2-34 is that different metals fail in different manners and thereby require correspondingly different failure criteria. Shouldn't we expect the same for composite materials?

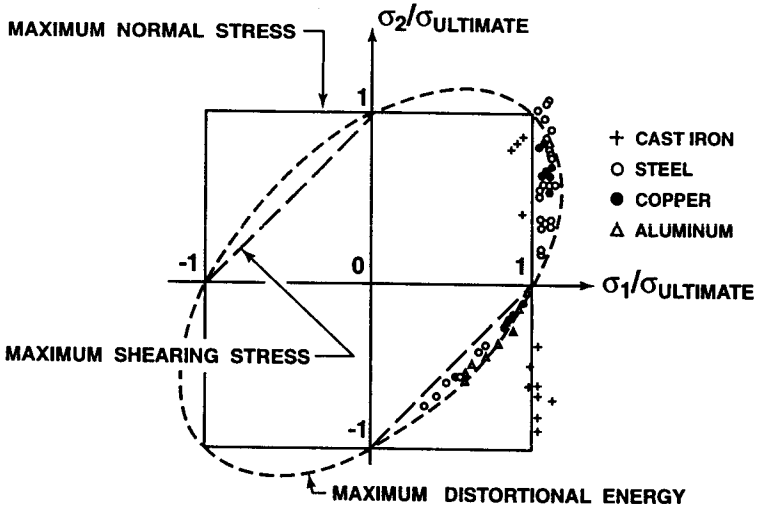

Figure 2-34 Failure Criteria for Metals
(data compiled from various sources by Murphy [2-20])

Our attention in this section is restricted to biaxial loading. We will examine the following biaxial strength criteria: (1) maximum stress failure criterion, (2) maximum strain failure criterion, (3) Tsai-Hill failure criterion, (4) Hoffman failure criterion, and (5) Tsai-Wu tensor failure criterion. In all failure criteria, the material, although orthotropic, is regarded as homogeneous. Thus, we inherently cannot account for some of the failure mechanisms at the microscopic level. At the same time, the failure criteria tend to be smoother than the actual behavior that often exhibits considerable data scatter because of testing technique, manufacturing nonuniformities, etc. The final goal of a failure criterion envelope that is in agreement with an actual strength envelope would readily enable designing structural elements made with composite materials.

For each of the failure criteria, we will generate biaxial stresses by off-axis loading of a unidirectionally reinforced lamina. That is, the uniaxial off-axis stress σ_x at θ to the fibers is transformed into biaxial stresses in the principal material coordinates as shown in Figure 2-35. From the stress-transformation equations in Figure 2-35, a uniaxial loading obviously cannot produce a state of mixed tension and compression in principal material coordinates. Thus, some other loading state must be applied to test any failure criterion against a condition of mixed tension and compression.

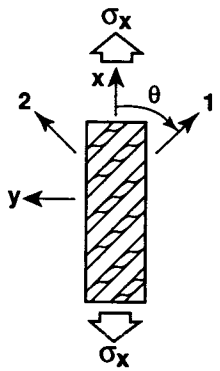

$$\sigma_1 = \sigma_x \cos^2\theta$$

$$\sigma_2 = \sigma_x \sin^2\theta$$

$$\tau_{12} = -\sigma_x \sin\theta\cos\theta$$

Figure 2-35 Biaxial Stresses from Off-Axis Uniaxial Loading

Most comparisons of a failure criterion with failure data will be for the glass-epoxy data shown in Figure 2-36 as a function of off-axis angle θ for both tension and compression loading [2-21]. The tension data are denoted by solid circles, and the compression data by solid squares. The tension data were obtained by use of dog-bone-shaped specimens, whereas the compression data were obtained by use of specimens with uniform rectangular cross sections. The shear strength for this glass-epoxy is 8 ksi (55 MPa) instead of the 6 ksi (41 MPa) in Table 2-3.

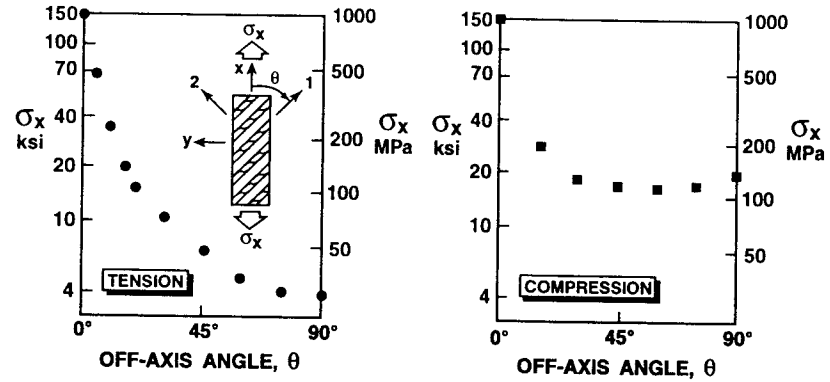

Figure 2-36 Measured Failure Data for Glass-Epoxy *(After Tsai [2-21])*

2.9.1 Maximum Stress Failure Criterion

In the maximum stress failure criterion, each and every one of the stresses in principal material coordinates must be less than the respective strengths; otherwise, fracture is said to have occurred. That is, for tensile stresses,

$$\sigma_1 < X_t \qquad \sigma_2 < Y_t \tag{2.114}$$

and for compressive stresses,

$$\sigma_1 > X_c \qquad \sigma_2 > Y_c \tag{2.115}$$

Also,

$$|\tau_{12}| < S \tag{2.116}$$

Note that the shear strength is independent of the sign of τ_{12} as discussed in Section 2.8. If any one of the foregoing inequalities is not satisfied, then the *assumption* is made that the material has failed by the failure mechanism associated with X_t, X_c, Y_t, Y_c, or S, respectively. Note that there is *no interaction* between modes of failure in this criterion — there are actually five subcriteria and five failure mechanisms.

In applications of the maximum stress criterion, the stresses in the body under consideration must be transformed to stresses in the principal material coordinates. For example, Tsai [2-21] considered a unidirectionally reinforced composite lamina subjected to uniaxial load at angle θ to the fibers as shown in Figure 2-35. The biaxial stresses in the principal material coordinates are obtained by transformation of the uniaxial stress, σ_x, as

$$\sigma_1 = \sigma_x \cos^2\theta \qquad \sigma_2 = \sigma_x \sin^2\theta \qquad \tau_{12} = -\sigma_x \sin\theta \cos\theta \tag{2.117}$$

Then by inversion of Equation (2.117) and substitution of Equations (2.114)-(2.116), the maximum uniaxial stress, σ_x, is the smallest of

$$\frac{X_c}{\cos^2\theta} < \sigma_x < \frac{X_t}{\cos^2\theta} \qquad \frac{Y_c}{\sin^2\theta} < \sigma_x < \frac{Y_t}{\sin^2\theta} \qquad |\sigma_x| < \left| \frac{S}{\sin\theta \cos\theta} \right| \tag{2.118}$$

This criterion is illustrated in Figure 2-37 where the tension and compression behaviors have been plotted simultaneously for an E-glass-epoxy composite material with the properties in Table 2-3 except for the shear strength as already noted. The uniaxial strength of the unidirectional composite material is plotted in Figure 2-37 versus the angle θ between the loading direction and the principal material directions. The maximum stress criterion is shown as several solid curves, the lowest curve of which governs the strength. The 'theoretical' cusps in the strength variation are not seen in the experimental data. Moreover, the 'theoretical' strength variation does not adequately represent the experimental strength variation. Thus, another biaxial strength criterion must be sought.

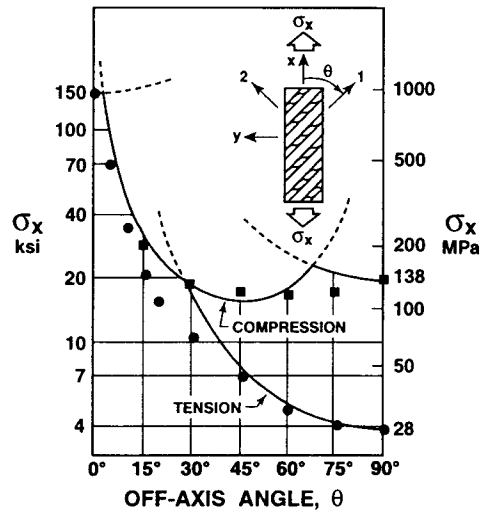

Figure 2-37 Maximum Stress Failure Criterion *(After Tsai [2-21])*

2.9.2 Maximum Strain Failure Criterion

The maximum strain failure criterion is quite similar to the maximum stress failure criterion. However, here strains are limited rather than stresses. Specifically, the material is said to have failed if one or more of the following inequalities is not satisfied:

$$\varepsilon_1 < X_{\varepsilon_t} \qquad \varepsilon_2 < Y_{\varepsilon_t} \qquad |\gamma_{12}| < S_\varepsilon \tag{2.119}$$

including for materials with different strength in tension and compression

$$\varepsilon_1 > X_{\varepsilon_c} \qquad \varepsilon_2 > Y_{\varepsilon_c} \tag{2.120}$$

where

$X_{\varepsilon_t}(X_{\varepsilon_c})$ = maximum tensile (compressive) normal strain in the 1-direction

$Y_{\varepsilon_t}(Y_{\varepsilon_c})$ = maximum tensile (compressive) normal strain in the 2-direction

S_ε = maximum shear strain in the 1-2 coordinates

As with the shear strength, the maximum shear strain is unaffected by the sign of the shear stress. The strains in principal material coordinates, $\varepsilon_1, \varepsilon_2, \gamma_{12}$, must be found from the strains in body coordinates by transformation before the criterion can be applied.

For a unidirectionally reinforced composite material subject to uniaxial load at angle θ to the fibers (the example problem in Section 2.9.1 on the maximum stress criterion), the allowable stresses can be found from the allowable strains X_{ε_t}, Y_{ε_t}, etc., in the following manner.

First, given that the strain-stress relations are

$$\begin{aligned}\varepsilon_1 &= \frac{1}{E_1}(\sigma_1 - \nu_{12}\sigma_2)\\ \varepsilon_2 &= \frac{1}{E_2}(\sigma_2 - \nu_{21}\sigma_1)\\ \gamma_{12} &= \frac{\tau_{12}}{G_{12}}\end{aligned} \tag{2.121}$$

upon substitution of the stress-transformation equations,

$$\begin{aligned}\sigma_1 &= \sigma_x \cos^2\theta\\ \sigma_2 &= \sigma_x \sin^2\theta\\ \tau_{12} &= -\sigma_x \sin\theta\cos\theta\end{aligned} \tag{2.122}$$

in the strain-stress relations, Equation (2.121), the strains are

$$\begin{aligned}\varepsilon_1 &= \frac{1}{E_1}(\cos^2\theta - \nu_{12}\sin^2\theta)\,\sigma_x\\ \varepsilon_2 &= \frac{1}{E_2}(\sin^2\theta - \nu_{21}\cos^2\theta)\,\sigma_x\\ \gamma_{12} &= -\frac{1}{G_{12}}(\sin\theta\cos\theta)\,\sigma_x\end{aligned} \tag{2.123}$$

Finally, if the usual restriction to linear elastic behavior to failure is made,

$$X_{\varepsilon_t} = \frac{X_t}{E_1} \quad Y_{\varepsilon_t} = \frac{Y_t}{E_2} \quad S_\varepsilon = \frac{S}{G_{12}} \quad X_{\varepsilon_c} = \frac{X_c}{E_1} \quad Y_{\varepsilon_c} = \frac{Y_c}{E_2} \tag{2.124}$$

(which could equally well come from measured values), then the maximum strain failure criterion for uniaxial off-axis loading can be written as

$$\begin{aligned}\frac{X_c}{\cos^2\theta - \nu_{12}\sin^2\theta} < \sigma_x < \frac{X_t}{\cos^2\theta - \nu_{12}\sin^2\theta}\\ \frac{Y_c}{\sin^2\theta - \nu_{21}\cos^2\theta} < \sigma_x < \frac{Y_t}{\sin^2\theta - \nu_{21}\cos^2\theta}\\ |\sigma_x| < \left|\frac{S}{\sin\theta\cos\theta}\right|\end{aligned} \tag{2.125}$$

The only difference between the maximum strain failure criterion, Equation (2.125), and the maximum stress failure criterion, Equation (2.118), is the inclusion of Poisson's ratio terms in the maximum strain failure criterion.

As with the maximum stress failure criterion, the maximum strain failure criterion can be plotted against available experimental results for uniaxial loading of an off-axis composite material. The discrepancies between experimental results and the prediction in Figure 2-38 are similar to, but even more pronounced than, those for the maximum stress failure criterion in Figure 2-37. Thus, the appropriate failure criterion for this E-glass-epoxy composite material still has not been found.

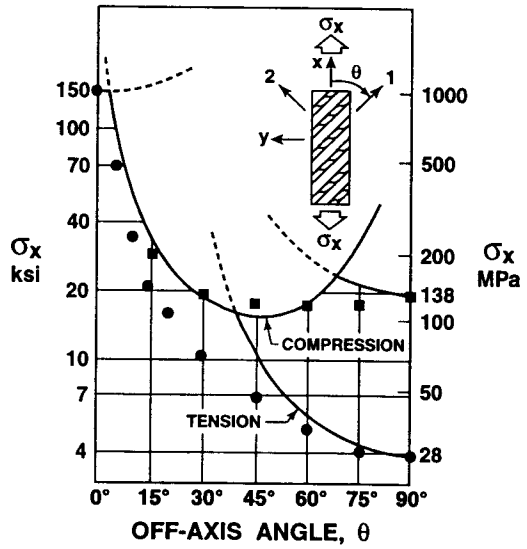

Figure 2-38 Maximum Strain Failure Criterion *(After Tsai [2-21])*

2.9.3 Tsai-Hill Failure Criterion

Hill [2-22] proposed a yield criterion for orthotropic materials:

$$\begin{aligned}(G+H)\sigma_1^2 + (F+H)\sigma_2^2 + (F+G)\sigma_3^2 - 2H\sigma_1\sigma_2 - 2G\sigma_1\sigma_3 - 2F\sigma_2\sigma_3\\ + 2L\tau_{23}^2 + 2M\tau_{13}^2 + 2N\tau_{12}^2 = 1\end{aligned} \tag{2.126}$$

This orthotropic yield criterion will be used as an orthotropic strength or failure criterion in the spirit of both criteria being limits of linear elastic behavior. Thus, Hill's yield stresses F, G, H, L, M, and N will be regarded as failure strengths. Hill's criterion is an extension of von Mises' yield criterion. The von Mises criterion, in turn, can be related to the amount of energy that is used to distort the isotropic body rather than to change its volume. However, distortion cannot be separated from dilatation in orthotropic materials, so Equation (2.126) is not related to distortional energy. Unfortunately, some authors still mistakenly call the criterion of this section a distortional energy failure criterion.

The failure strength parameters F, G, H, L, M, and N were related to the usual failure strengths X, Y, and S for a lamina by Tsai [2-21]. If only τ_{12} acts on the body, then, because its maximum value is S,

$$2N = \frac{1}{S^2} \tag{2.127}$$

Similarly, if only σ_1 acts on the body, then

$$G + H = \frac{1}{X^2} \tag{2.128}$$

and if only σ_2 acts, then

$$F + H = \frac{1}{Y^2} \tag{2.129}$$

If the strength in the 3-direction is denoted by Z and only σ_3 acts, then

$$F + G = \frac{1}{Z^2} \tag{2.130}$$

Then, upon combination of Equations (2.128), (2.129), and (2.130), the following relations between F, G, H and X, Y, Z result:

$$2F = \frac{1}{Y^2} + \frac{1}{Z^2} - \frac{1}{X^2} \quad 2G = \frac{1}{X^2} + \frac{1}{Z^2} - \frac{1}{Y^2} \quad 2H = \frac{1}{X^2} + \frac{1}{Y^2} - \frac{1}{Z^2} \tag{2.131}$$

For plane stress in the 1-2 plane of a unidirectional lamina with fibers in the 1-direction, $\sigma_3 = \tau_{13} = \tau_{23} = 0$. However, from the cross section of such a lamina in Figure 2-39, Y = Z from the obvious geometrical symmetry of the material construction. Thus, Equation (2.126) leads to

$$\frac{\sigma_1^2}{X^2} - \frac{\sigma_1\sigma_2}{X^2} + \frac{\sigma_2^2}{Y^2} + \frac{\tau_{12}^2}{S^2} = 1 \tag{2.132}$$

as the governing failure criterion in terms of the familiar lamina principal strengths X, Y, and S. And, the appropriate values of X_t or X_c and Y_t or Y_c must be used depending on the signs of σ_1 and σ_2. Thus, a different surface is generated in each portion of three-dimensional stress space σ_1, σ_2, τ_{12} (except that the surface is symmetrical about the plane $\tau_{12} = 0$ because S has only one value).

Finally, for the off-axis composite material example of this section, substitution of the stress-transformation equations,

$$\begin{aligned} \sigma_1 &= \sigma_x \cos^2\theta \\ \sigma_2 &= \sigma_x \sin^2\theta \\ \tau_{12} &= -\sigma_x \sin\theta \cos\theta \end{aligned} \tag{2.133}$$

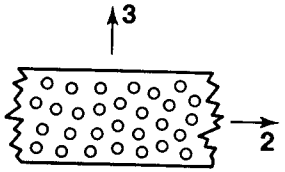

Figure 2-39 Cross Section of a Unidirectional Lamina with Fibers in the 1-Direction

in Equation (2.132) yields the Tsai-Hill failure criterion for uniaxial off-axis strength,

$$\frac{\cos^4\theta}{X^2} + \left[\frac{1}{S^2} - \frac{1}{X^2}\right]\cos^2\theta \sin^2\theta + \frac{\sin^4\theta}{Y^2} = \frac{1}{\sigma_x^2} \tag{2.134}$$

which is *one* criterion, not three as in previous failure criteria. Because a composite lamina usually has different strengths in tension and compression, the values of X and Y must take on the appropriate values depending on the quadrant of stress space in which the stresses lie. Thus, the failure envelope in stress space consists of four different segments that are continuous in value but not in slope at the uniaxial strengths.

Results for this criterion are plotted in Figure 2-40 along with the experimental data for E-glass-epoxy. The agreement between the Tsai-Hill failure criterion and experiment is quite good. Thus, a suitable failure criterion has apparently been found for E-glass-epoxy laminae at various orientations in biaxial stress fields.

The Tsai-Hill failure criterion appears to be much more applicable to failure prediction for this E-glass-epoxy composite material than either the maximum stress criterion or the maximum strain failure criterion. Other less obvious advantages of the Tsai-Hill failure criterion are:

(1) The variation of strength with angle of lamina orientation is smooth rather than having cusps that are not seen in experimental results.

(2) The strength continuously decreases as θ grows from 0° rather than the rise in uniaxial strength that is characteristic of both the maximum stress and the maximum strain criteria.

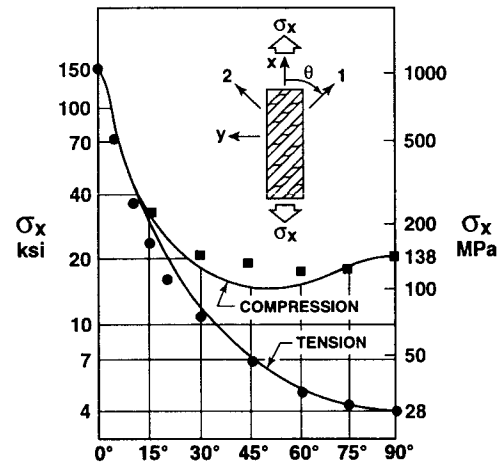

Figure 2-40 Tsai-Hill Failure Criterion *(After Tsai [2-21])*

(3) The agreement between the criterion and experiment is even better than that at first glance because Figures 2-37, 2-38, and 2-40 are plotted at a logarithmic scale. The maximum stress and strain criteria are incorrect by 100% at 30°!
(4) Considerable *interaction* exists between the failure strengths X, Y, S in the Tsai-Hill criterion, but *none* exists in the previous criteria where axial, transverse, and shear failures are presumed to occur independently.

For E-glass-epoxy, the Tsai-Hill failure criterion seems the most accurate of the criteria discussed. However, the applicability of a particular failure criterion depends on whether the material being studied is ductile or brittle. Other composite materials might be better treated with the maximum stress or the maximum strain criteria or even some other criterion.

2.9.4 Hoffman Failure Criterion

To account for different strengths in tension and compression, Hoffman added linear terms to Hill's equation (the basis for the Tsai-Hill criterion) [2-23]:

$$C_1(\sigma_2-\sigma_3)^2+C_2(\sigma_3-\sigma_1)^2+C_3(\sigma_1-\sigma_2)^2 + C_4\sigma_1+C_5\sigma_2+C_6\sigma_3+C_7\tau_{23}^2+C_8\tau_{31}^2+C_9\tau_{12}^2=1 \quad (2.135)$$

where the 9 C_i are determined from the 9 strengths in principal material coordinates: X_t, X_c, Y_t, Y_c, Z_t, Z_c, S_{23}, S_{31}, and S_{12}. For plane stress in the 1-2 plane ($\sigma_3=\tau_{23}=\tau_{31}=0$) and transverse isotropy in the 2-3 plane as in Figure 2-39 ($Z_t=Y_t$, $Z_c=Y_c$, $S_{31}=S_{12}$), the failure criterion in Equation (2.135) simplifies to

$$-\frac{\sigma_1^2}{X_cX_t}+\frac{\sigma_1\sigma_2}{X_cX_t}-\frac{\sigma_2^2}{Y_cY_t}+\frac{X_c+X_t}{X_cX_t}\sigma_1+\frac{Y_c+Y_t}{Y_cY_t}\sigma_2+\frac{\tau_{12}^2}{S_{12}^2}=1 \quad (2.136)$$

in which X_c is an inherently negative number, e.g., $X_c=-100$ ksi (or -690 MPa), unlike in Hoffman's paper, but consistent with usage in this book. For equal strengths in tension and compression ($X_c=-X_t=-X$ and $Y_c=-Y_t=-Y$), the Hoffman failure criterion reduces to the Tsai-Hill criterion in Equation (2.132). Both criteria are ellipsoids in σ_1, σ_2, τ_{12} space as in Figure 2-41. The Hoffman ellipsoid is symmetric about the σ_1-σ_2 plane, has principal axes at

$$\beta=\frac{1}{2}\cot^{-1}\left[\frac{Y_cY_t}{X_cX_t}-1\right] \quad (2.137)$$

and center at

$$\sigma_1=\frac{X_t+X_c}{2}+\frac{Y_t+Y_c}{2} \qquad \sigma_2=\frac{Y_t+Y_c}{2}+\frac{(X_t+X_c)Y_tY_c}{4X_tX_c} \quad (2.138)$$

Note for materials with equal strengths in tension and compression that β is 45° and the center of the ellipsoid is at the origin.

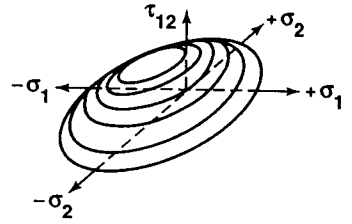

Figure 2-41 Hoffman Failure Surface

The Hoffman failure criterion is in very good agreement with glass-epoxy failure data [2-21] in Figure 2-42, with graphite-epoxy data [2-24] in Figure 2-43, and with boron-epoxy data [2-25] in Figure 2-44. The fact that the Hoffman failure criterion is a single curve in all quadrants of σ_1-σ_2 space implies that the curve in any single quadrant shifts from the corresponding Tsai-Hill failure criterion segment. However, that result is a normal consequence of using only one curve in all four quadrants.

Attractive features of the Hoffman failure criterion are

(1) Interaction between failure modes is treated instead of separate criteria for failure like the maximum stress or maximum strain failure criteria.
(2) A single failure criterion is used in all quadrants of σ_1-σ_2 space instead of the segments in separate quadrants for the Tsai-Hill failure criterion because of different strengths in tension and compression.
(3) In design use, the Hoffman criterion is the simplest criterion of all criteria discussed.

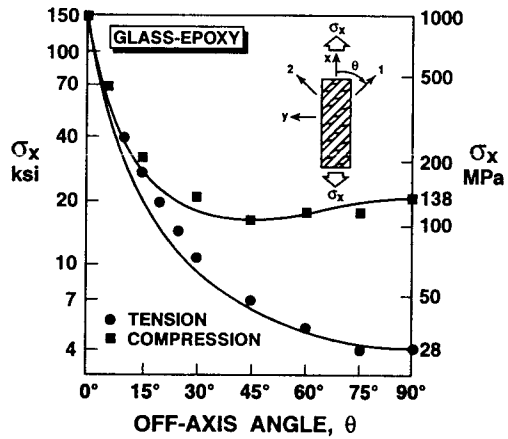

Figure 2-42 Hoffman Failure Criterion for Glass-Epoxy *(Data from Tsai [2-21])*

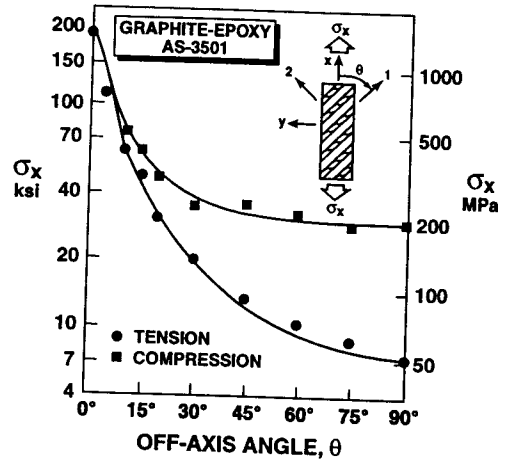

Figure 2-43 Hoffman Failure Criterion for Graphite-Epoxy *(Data from Kim [2-24])*

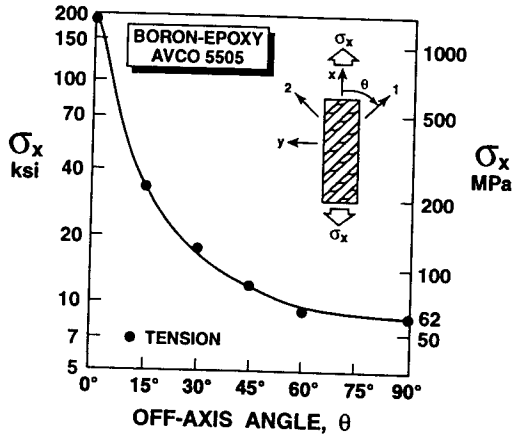

Figure 2-44 Hoffman Failure Criterion for Boron-Epoxy *(Data from Pipes and Cole [2-25])*

2.9.5 Tsai-Wu Tensor Failure Criterion

The preceding biaxial failure criteria suffer from various inadequacies in their representation of experimental data. One obvious way to improve the correlation between a criterion and experiment is to increase the number of terms in the prediction equation. This increase in curve-fitting ability plus the added feature of representing the various strengths in tensor form was used by Tsai and Wu [2-26]. In the process, a new strength definition is required to represent the interaction between stresses in two directions.

Tsai and Wu postulated that a failure surface in six-dimensional stress space exists in the form

$$F_i \sigma_i + F_{ij} \sigma_i \sigma_j = 1 \qquad i, j = 1, \ldots, 6 \tag{2.139}$$

wherein F_i and F_{ij} are strength tensors of the second and fourth rank, respectively, and the usual contracted stress notation is used ($\sigma_4 = \tau_{23}$, $\sigma_5 = \tau_{31}$, and $\sigma_6 = \tau_{12}$). Equation (2.139) is obviously very complicated; we will restrict our attention to the reduction of Equation (2.139) to the case of an orthotropic lamina under plane stress conditions:

$$F_1\sigma_1 + F_2\sigma_2 + F_6\sigma_6 + F_{11}\sigma_1^2 + F_{22}\sigma_2^2 + F_{66}\sigma_6^2 + 2F_{12}\sigma_1\sigma_2 = 1 \tag{2.140}$$

The terms that are linear in the stresses are useful in representing different strengths in tension and compression. The terms that are quadratic in the stresses are the more or less usual terms to represent an ellipsoid in stress space. However, the independent parameter F_{12} is new and quite unlike the dependent coefficient $2H = 1/X^2$ in the Tsai-Hill failure criterion on the term involving interaction between normal stresses in the 1- and 2-directions.

Most components of the strength tensors are defined in terms of the engineering strengths already discussed. For example, consider a uniaxial load on a specimen in the 1-direction. Under tensile load, the engineering strength is X_t, whereas under compressive load, it is X_c (for example, $X_c = -400$ ksi (–2760 MPa) for boron-epoxy). Thus, under tensile load,

$$F_1 X_t + F_{11} X_t^2 = 1 \tag{2.141}$$

and under compressive load,

$$F_1 X_c + F_{11} X_c^2 = 1 \tag{2.142}$$

Upon simultaneous solution of Equations (2.141) and (2.142),

$$F_1 = \frac{1}{X_t} + \frac{1}{X_c} \qquad F_{11} = -\frac{1}{X_t X_c} \tag{2.143}$$

Similarly,

$$F_2 = \frac{1}{Y_t} + \frac{1}{Y_c} \qquad F_{22} = -\frac{1}{Y_t Y_c} \tag{2.144}$$

Similar reasoning, along with our observation that the shear strength in principal material coordinates is independent of shear stress sign, leads to

$$F_6 = 0 \qquad F_{66} = \frac{1}{S^2} \tag{2.145}$$

Note that for equal strengths in tension and compression ($X_t = -X_c$ and $Y_t = -Y_c$),

$$F_1 = 0 \qquad F_{11} = \frac{1}{X^2} \qquad F_2 = 0 \qquad F_{22} = \frac{1}{Y^2} \tag{2.146}$$

leaving us with a failure criterion

$$\frac{\sigma_1^2}{X^2} + 2F_{12}\sigma_1\sigma_2 + \frac{\sigma_2^2}{Y^2} + \frac{\tau_{12}^2}{S^2} = 1 \tag{2.147}$$

which is remarkably similar to the Tsai-Hill failure criterion except for the value of F_{12}, which is not $-1/X^2$.

Determination of the fourth-rank tensor term F_{12} remains. Basically, F_{12} cannot be found from any uniaxial test in the principal material directions. Instead, a biaxial test must be used. This fact should not be surprising because F_{12} is the coefficient of the *product* of σ_1 *and* σ_2 in the failure criterion, Equation (2.140). Thus, for example, we can impose a state of biaxial tension described by $\sigma_1 = \sigma_2 = \sigma$ and all other stresses are zero. Accordingly, from Equation (2.140),

$$(F_1 + F_2)\sigma + (F_{11} + F_{22} + 2F_{12})\sigma^2 = 1 \tag{2.148}$$

Now solve for F_{12} after substituting the definitions just derived for F_1, F_2, F_{11}, and F_{22}:

$$F_{12} = \frac{1}{2\sigma^2}\left[1 - \left[\frac{1}{X_t} + \frac{1}{X_c} + \frac{1}{Y_t} + \frac{1}{Y_c}\right]\sigma + \left[\frac{1}{X_t X_c} + \frac{1}{Y_t Y_c}\right]\sigma^2\right] \tag{2.149}$$

The value of F_{12} then depends on the various engineering strengths plus the biaxial tensile failure stress, σ. Tsai and Wu also discuss the use of off-axis uniaxial tests to determine the interaction strengths such as F_{12} [2-26].

At this point, recall that all interaction between normal stresses σ_1 and σ_2 in the Tsai-Hill failure criterion is related to the strength in the 1-direction:

$$\frac{\sigma_1^2}{X^2} - \frac{\sigma_1\sigma_2}{X^2} + \frac{\sigma_2^2}{Y^2} + \frac{\tau_{12}^2}{S^2} = 1 \tag{2.150}$$

Thus, the Tsai-Wu tensor failure criterion is obviously of more general character than the Tsai-Hill or Hoffman failure criteria. Specific advantages of the Tsai-Wu failure criterion include (1) invariance under rotation or redefinition of coordinates; (2) transformation via known tensor-transformation laws (so data interpretation is eased); and (3) symmetry properties similar to those of the stiffnesses and compliances. Accordingly, the mathematical operations with this tensor failure criterion are well-known and relatively straightforward.

Pipes and Cole [2-25] measured the interaction term F_{12} in various off-axis tests for boron-epoxy. They reported significant variation of F_{12} for off-axis tension tests and acceptable variation for off-axis compression tests. However, compression tests are much more difficult to perform than 'simple' off-axis tension tests on a flat specimen with a high length-to-width ratio. A compression specimen with a high length-to-width ratio to avoid shear-extension coupling effects is extremely susceptible to buckling. Hence, a tubular specimen (with a rotating end to avoid shear-extension coupling effects) must be used. Although the determination of F_{12} was not precise, Pipes and Cole obtained the excellent agreement between the Tsai-Wu tensor failure criterion and the experimental data shown in Figure 2-45. Changes of F_{12} by a factor of eight resulted in only slight changes in predicted strength over the range $5° < \theta < 25°$. Also, the difference between the Tsai-Wu tensor failure criterion and the Tsai-Hill failure criterion was less than 5% over the range $5° < \theta < 75°$.

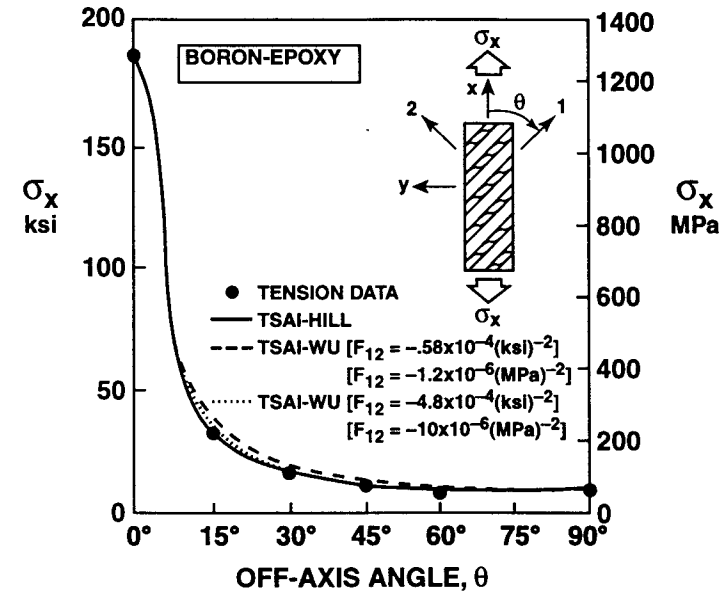

Figure 2-45 Tsai-Wu Tensor Failure Criterion *(After Pipes and Cole [2-25])*

The Tsai-Wu failure criterion has several important characteristics:

(1) Increased curve-fitting capability over the Tsai-Hill and Hoffman criteria because of an additional term in the equation.
(2) The additional term, F_{12}, can be determined only with an expensive and difficult-to-perform biaxial test.
(3) Graphical interpretations of the results are facilitated by the tensor formulation.

Because of the difficulty and expense of obtaining a reliable value of F_{12} and the fact that F_{12} seems to have little influence on the final results, Narayanaswami and Adelman [2-27] suggested that F_{12} simply be regarded as zero. This practical approach avoids the expense of the biaxial test.

2.9.6 Summary of Failure Criteria

Other strength criteria are described by Sendeckyj [2-28]. Tennyson, MacDonald, and Nanyaro addressed the next logical step in a curve-fitting procedure, namely a third-order polynomial fit to failure data [2-29]. However, the added complexity of their criterion has limited its use even though they identified some loading conditions under which their criterion is necessary to properly describe the actual failure behavior.

Problem Set 2.9

2.9.1 Identify which subcriterion for failure applies for each segment of the multisegmented maximum stress and maximum strain failure criteria curves in Figures 2-37 and 2-38 for uniaxial off-axis loading σ_x.

2.9.2 Derive Equation (2.131) from Equations (2.128), (2.129), and (2.130).

2.9.3 Derive Equation (2.132) from Equations (2.131) and (2.126).

2.9.4 Derive Equation (2.134) from Equations (2.132) and (2.133).

2.9.5 What is the Tsai-Hill failure criterion when the fibers of a unidirectional lamina in the 1-2 plane are aligned in the 2-direction? Denote the lamina strength in the fiber direction by X as usual; thus, the strength in the 1-direction is Y. Compare this criterion with Equation (2.132).

2.9.6 Find the Tsai-Hill failure criterion for pure shear loading at various angles θ to the principal material directions, i.e., the shear analog of Equation (2.134).

2.9.7 Note for Tsai's E-glass-epoxy data in Figure 2-36 that the uniaxial compressive strength at some angles between 0° and 90° is actually less than Y_c (not true for uniaxial tensile strength). The correct inference to be made is that E-glass-epoxy has a low shear strength. This situation is the strength analog for the Tsai-Hill failure criterion in Equation (2.134) of the stiffness variation studied in Problem 2.6.7. Find the relation between S, X, and Y such that such low values of off-axis uniaxial strength occur and also the relation for the case where values of off-axis uniaxial strength higher than X occur.

2.9.8 Determine the character of the Tsai-Hill failure criterion for pure shear loading between off-axis angles of 0° and 90° by examining the characteristics of the result from Problem 2.9.6 using the techniques of Appendix B. That is, this is the shear analog of Problem 2.9.7.

2.10 SUMMARY

In Section 2.2, the stress-strain relations (generalized Hooke's law) for anisotropic and orthotropic as well as isotropic materials are discussed. These relations have two commonly accepted manners of expression: compliances and stiffnesses as coefficients (elastic constants) of the stress-strain relations. The most attractive form of the stress-strain relations for orthotropic materials involves the engineering constants described in Section 2.3. The engineering constants are particularly helpful in describing composite material behavior because they are defined by the use of very obvious and simple physical measurements. Restrictions in the form of bounds are derived for the elastic constants in Section 2.4. These restrictions are useful in understanding the unusual behavior of composite materials relative to conventional isotropic materials. Attention is focused in Section 2.5 on stress-strain relations for an orthotropic material under plane stress conditions, the most common use of a composite lamina. These stress-strain relations are transformed in Section 2.6 to coordinate systems that are not aligned with the principal material

directions of the lamina. This transformation is necessary in order to describe the behavior of composite materials that have fibers running in directions other than the natural geometrical directions of the structural element (e.g., a helically wound circular cylindrical shell has helical coordinates in which the fibers are arranged in contrast to the axial and circumferential coordinates of the circular cylindrical shell). The stress-strain relations for an orthotropic lamina with principal material directions that are not aligned with the obvious geometrical directions are further related to generalized engineering constants and anisotropic materials. The transformed reduced stiffnesses derived in Section 2.6 are shown in Section 2.7 to have certain combinations that are invariant with respect to rotation of coordinates in the plane of the lamina. The invariants are useful in design of laminated composite structures. Next, in Section 2.8, the important topic of lamina strength is addressed. There, the common approach for conventional isotropic materials of comparing the maximum principal stress with the maximum allowable stress is rejected for composite materials. Tests are described to measure the stiffnesses and strengths of orthotropic composite laminae in principal material coordinates. The procedures for estimating the strength in non-principal material coordinates and the strength under biaxial loading conditions are discussed in Section 2.9. There, a failure criterion that is quadratic in the biaxial stresses is seen to agree well with experimental data.

REFERENCES

2-1 Stephen W. Tsai, *Mechanics of Composite Materials, Part II, Theoretical Aspects*, Air Force Materials Laboratory Technical Report AFML-TR-66-149, November 1966.

2-2 B. M. Lempriere, Poisson's Ratio in Orthotropic Materials, *AIAA Journal*, November 1968, pp. 2226–2227.

2-3 E. O. Dickerson and B. DiMartino, Off-Axis Strength and Testing of Filamentary Materials for Aircraft Application, in *Advanced Fibrous Reinforced Composites*, Vol. 10, Society of Aerospace Materials and Process Engineers, 1966, p. H-23.

2-4 Robert C. Reuter, Jr., Concise Property Transformation Relations for an Anisotropic Lamina, *Journal of Composite Materials*, April 1971, pp. 270–272.

2-5 S. G. Lekhnitskii, *Theory of Elasticity of an Anisotropic Elastic Body*, Holden-Day, San Francisco, 1963.

2-6 Robert M. Jones, Stiffness of Orthotropic Materials and Laminated Fiber-Reinforced Composites, *AIAA Journal*, January 1974, pp. 112–114.

2-7 Stephen W. Tsai and Nicholas J. Pagano, Invariant Properties of Composite Materials, in *Composite Materials Workshop*, S. W. Tsai, J. C. Halpin, and Nicholas J. Pagano (Editors), St. Louis, Missouri, 13–21 July 1967, Technomic, Westport, Connecticut, 1968, pp. 233–253. Also AFML-TR-67-349, March 1968.

2-8 N. J. Pagano and P. C. Chou, The Importance of Signs of Shear Stress and Shear Strain in Composites, *Journal of Composite Materials*, January 1969, pp. 166–173.

2-9 S. A. Ambartsumyan, The Axisymmetric Problem of a Circular Cylindrical Shell Made of Material with Different Stiffness in Tension and Compression, *Izvestiya Akademii Nauk SSSR Mekhanika*, No. 4, 1965, pp. 77–85; English translation N69-11070, STAR.

2-10 Robert M. Jones, Buckling of Stiffened Multilayered Circular Cylindrical Shells with Different Orthotropic Moduli in Tension and Compression, *AIAA Journal*, May 1971, pp. 917–923.

2-11 Charles W. Bert, Models for Fibrous Composites with Different Properties in Tension and Compression, *Journal of Engineering Materials and Technology*, October 1977, pp. 344–349.

2-12 C. W. Bert and J. N. Reddy, Mechanics of Bimodular Composite Structures, in *Mechanics of Composite Materials - Recent Advances*, Proceedings of the IUTAM

Symposium on Mechanics of Composite Materials, Zvi Hashin and Carl T. Herakovich (Editors), Blacksburg, Virginia, 16–19 August 1982, Pergamon Press, New York, 1983, pp. 323–337.

2-13 N. J. Pagano and J. C. Halpin, Influence of End Constraint in the Testing of Anisotropic Bodies, *Journal of Composite Materials*, January 1968, pp. 18–31.

2-14 J. M. Whitney, N. J. Pagano, and R. B. Pipes, Design and Fabrication of Tubular Specimens for Composite Characterization, in *Composite Materials: Testing and Design (Second Conference)*, H. T. Corten (Chairman), Anaheim, California, 20–22 April 1971, ASTM STP 497, American Society for Testing and Materials, 1972, pp. 52–67.

2-15 Hong T. Hahn and Stephen W. Tsai, Nonlinear Elastic Behavior of Unidirectional Composite Laminae, *Journal of Composite Materials*, January 1973, pp. 102–118.

2-16 Robert M. Jones and Harold S. Morgan, Analysis of Nonlinear Stress-Strain Behavior of Fiber-Reinforced Composite Materials, *AIAA Journal*, December 1977, pp. 1669–1676.

2-17 Max E. Waddoups, Characterization and Design of Composite Materials, in *Composite Materials Workshop*, S. W. Tsai, J. C. Halpin, and Nicholas J. Pagano (Editors), St. Louis, Missouri, 13–21 July 1967, Technomic, Westport, Connecticut, 1968, pp. 254–308.

2-18 J. M. Whitney, D. L. Stansbarger, and H. B. Howell, Analysis of the Rail Shear Test - Applications and Limitations, *Journal of Composite Materials*, January 1971, pp. 24–34.

2-19 John Hart-Smith, Douglas Aircraft Company, Long Beach, California, personal communication.

2-20 Glenn Murphy, *Advanced Mechanics of Materials*, McGraw-Hill, New York, 1946, p. 83.

2-21 Stephen W. Tsai, Strength Theories of Filamentary Structures, in *Fundamental Aspects of Fiber Reinforced Plastic Composites*, Conference Proceedings, R. T. Schwartz and H. S. Schwartz (Editors), Dayton, Ohio, 24–26 May 1966, Wiley Interscience, New York, 1968, pp. 3–11.

2-22 R. Hill, *The Mathematical Theory of Plasticity*, Oxford University Press, London, 1950, p. 318.

2-23 Oscar Hoffman, The Brittle Strength of Orthotropic Materials, *Journal of Composite Materials*, April 1967, pp. 200–206.

2-24 Ran Y. Kim, personal communication, 8 April 1981. For additional information, see Ran Y. Kim, On the Off-Axis and Angle-Ply Strength of Composites, in *Test Methods and Design Allowables for Fibrous Composites*, C. C. Chamis (Editor), Dearborn, Michigan, 2–3 October 1979, ASTM STP 734, American Society for Testing and Materials, 1981, pp. 91–108 (reprinted with permission).

2-25 R. Byron Pipes and B. W. Cole, On the Off-Axis Strength Test for Anisotropic Materials, *Journal of Composite Materials*, April 1973, pp. 246–256.

2-26 Stephen W. Tsai and Edward M. Wu, A General Theory of Strength for Anisotropic Materials, *Journal of Composite Materials*, January 1971, pp. 58–80.

2-27 R. Narayanaswami and Howard M. Adelman, Evaluation of the Tensor Polynomial and Hoffman Strength Theories for Composite Materials, *Journal of Composite Materials*, October 1977, pp. 366–377.

2-28 G. P. Sendeckyj, A Brief Survey of Empirical Multiaxial Strength Criteria for Composites, in *Composite Materials: Testing and Design (Second Conference)*, H. T. Corten (Chairman), Anaheim, California, 20–22 April 1971, ASTM STP 497, American Society for Testing and Materials, 1972, pp. 41–51.

2-29 R. C. Tennyson, D. MacDonald, and A. P. Nanyaro, Evaluation of the Tensor Polynomial Failure Criterion for Composite Materials, *Journal of Composite Materials*, January 1978, pp. 63–75.

Chapter 3

MICROMECHANICAL BEHAVIOR OF A LAMINA

3.1 INTRODUCTION

We addressed the 'apparent' properties of a lamina in Chapter 2. That is, a large enough piece of the lamina was considered so that the fact that the lamina is made of two or more constituent materials cannot be detected. Thus, almost magically, we were able to say that a boron-epoxy composite material of unidirectional boron fibers in epoxy has certain stiffnesses and strengths that we measured in various directions. However, this question has not been asked: how can the stiffnesses and strengths of a graphite-epoxy composite material be varied by changing the proportion of graphite fibers to epoxy matrix? That is, the basic question of micromechanics is: what is the relationship of the composite material properties to the properties of the constituents as in Figure 3-1?

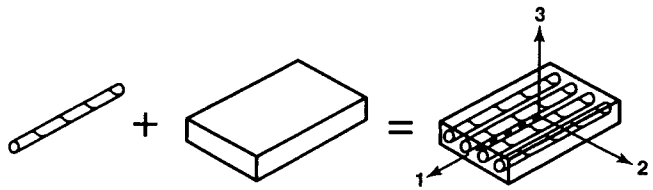

Figure 3-1 Basic Question of Micromechanics

Just as there must be some rationale for selecting a particular stiffness and/or strength of material for a specific structural application, there must also be a rationale for determining how best to achieve that stiffness and strength for a composite of two or more materials. That is, how can the percentages of the constituent materials be varied so as to arrive at the desired composite stiffness and strength?

An appropriate division of the efforts just mentioned is helped by defining two areas of composite material behavior, micromechanics and macromechanics:

Micromechanics — The study of composite material behavior wherein the *interaction* of the constituent materials is examined in detail as part of the definition of the behavior of the *heterogeneous* composite material.

Macromechanics — The study of composite material behavior wherein the material is assumed *homogeneous* and the effects of the constituent materials are detected only as averaged apparent properties of the composite material.

Thus, the properties of a lamina can be experimentally determined in the 'as made' state or can be mathematically estimated on the basis of the properties of the constituent materials. That is, we can *predict* lamina properties by the procedures of *micromechanics*, and we can *measure* lamina properties by physical means and use the properties in a *macromechanical* analysis of the structure. Knowledge of how to predict properties is essential to making composite materials that must have certain apparent or macroscopic properties. Thus, micromechanics is a natural adjunct to macromechanics when viewed in a *materials design* rather than a *structural analysis* environment. Real design power is demonstrated when the micromechanical predictions of the properties of a lamina agree with the measured properties. However, recognize that a micromechanical analysis has significant, inherent limitations. For example, a perfect bond between fibers and matrix is a usual analysis restriction that might well not be satisfied by some composite materials. An imperfect bond would presumably yield a material with properties degraded from those of the micromechanical analysis. Thus, micromechanical theories must be validated by careful experimental work. With such broad statements as background, let us now turn to the study of some specific micromechanics theories.

The two basic approaches to the micromechanics of composite materials are

(1) Mechanics of Materials
(2) Elasticity

The mechanics of materials (or strength of materials or resistance of materials) approach embodies the usual concept of vastly simplifying assumptions regarding the hypothesized behavior of the mechanical system. The elasticity approach actually is at least three approaches: (1) bounding principles, (2) exact solutions, and (3) approximate solutions.

All approaches are characterized by more rigorous satisfaction of physical laws (equilibrium, deformation continuity and compatibility, and stress-strain relations) than in mechanics of materials. Both basic approaches will be discussed in this chapter.

The objective of all micromechanics approaches is to determine the elastic moduli or stiffnesses or compliances of a composite material in terms of the elastic moduli of the constituent materials. For example, the elastic moduli of a fiber-reinforced composite material must be determined in terms of the properties of the fibers and the matrix and in terms of the relative volumes of fibers and matrix:

$$C_{ij} = C_{ij}(E_f, \nu_f, V_f, E_m, \nu_m, V_m)$$

where

E_f = Young's modulus for an isotropic fiber

ν_f = Poisson's ratio for an isotropic fiber

$$V_f = \frac{\text{Volume of Fibers}}{\text{Total Volume of Composite Material}}$$

with analogous definitions applying for the matrix material.

An additional and complementary objective of micromechanics approaches to composite materials analysis is to determine the strengths of the composite material in terms of the strengths of the constituent materials. For example, the strength of a fiber-reinforced composite material must be determined in terms of the strengths of the fibers and the matrix and their relative volumes (relative to the total volume of the composite material). In functional form,

$$X_i = X_i(X_{if}, V_f, X_{im}, V_m)$$

where

$X_i = X, Y, S$ = Composite Material Strengths

$X_{if} = X_f, Y_f, S_f$ = Fiber Strengths

$$V_f = \frac{\text{Volume of Fibers}}{\text{Total Volume of Composite Material}}$$

with analogous definitions applying for the matrix material. The foregoing definitions could be modified to account for different strengths under tensile and compressive loading. Also, the definitions could be simplified for isotropic fibers and/or isotropic matrix materials. Actually, we might be surprised at the form of the actual functional relationship for composite material strength in compression—more on this later.

Not much work is available regarding micromechanical theories of strength. However, considerable work as been done on micromechanical theories of stiffness. We will concentrate on those aspects of stiffness theory that are most prominent in usage (e.g., the Halpin-Tsai equations) in addition to those aspects that clearly illustrate the thrust of micromechanics. Available strength information will be summarized with the same intent as for stiffness theories.

Irrespective of the micromechanical stiffness approach used, the basic restrictions on the composite material that can be treated are:

- The lamina is
  - initially stress-free
  - linearly elastic
  - macroscopically homogeneous
  - macroscopically orthotropic
- The fibers are
  - homogeneous
  - linearly elastic
  - isotropic
  - regularly spaced
  - perfectly aligned
  - perfectly bonded
- The matrix is
  - homogeneous
  - linearly elastic
  - isotropic
  - void-free

In addition, no voids can exist in the fibers or matrix or in between them (i.e., the bonds between the fibers and matrix are perfect). These restrictive conditions should be at least somewhat suspicious. That is, some of them look perfectly plausible, but others should be readily apparent as somewhat unlikely to occur. For example, the matrix might very well have few voids such that it can be considered void-free, but the bonds between fibers and matrix surely are not perfect.

Basic to the discussion of micromechanics is the representative volume element that is the smallest region or piece of material over which the stresses and strains can be regarded as macroscopically uniform and yet the volume still has the correct proportions of fiber and matrix, i.e., is still *representative* of the composite material and its constituents *by volume*. Microscopically, however, the stresses and strains are nonuniform because of the heterogeneity of the material. Thus, scale of the volume element is very important. Generally, only a single fiber appears in a representative volume element, but more than one fiber can be required. The fiber spacing in a composite lamina with unidirectional fibers constitutes one dimension of the representative volume element. One of the other two dimensions is the lamina thickness or fiber spacing in the thickness direction if the lamina is more than one fiber thick. The third dimension is arbitrary. A typical representative volume element for a lamina with unidirectional fibers is shown in Figure 3-2.

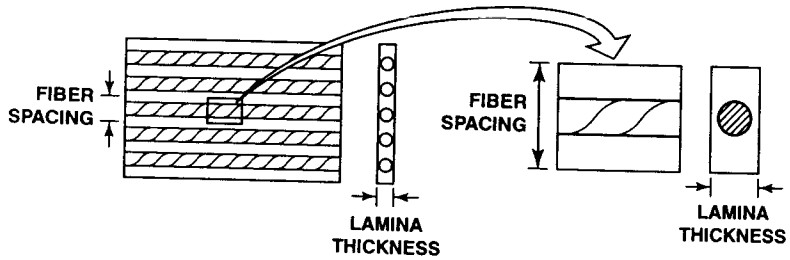

Figure 3-2 Representative Volume Element – Lamina with Unidirectional Fibers

For a lamina with fibers woven in two directions, the representative volume element must be much more complex than that for a lamina with unidirectional fibers. If the weaving geometry is neglected, two of the dimensions of the representative volume element are the spacings of the respective fibers. Finally, the third dimension is governed by the number of fibers in the thickness. If the actual weave geometry (curved fibers) is to be considered, finite element representation of the representative volume element, as in Figure 3-3, might be desirable. There, finite elements in the shape of triangles and quadrilaterals, including squares, are used to represent both the fiber and the surrounding matrix, and the matrix is presumed perfect.

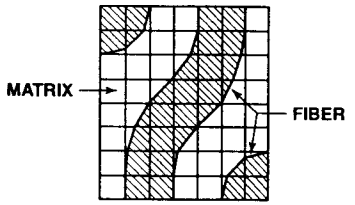

Figure 3-3 Finite Element Model of a Representative Volume Element for a Woven Lamina

Irrespective of the analysis approach, the representative volume element must be carefully defined and used. In fact, the representative volume element is crucial to the analysis and is the micromechanics analog of the free-body diagram in statics and dynamics. The representative volume element is of higher order than the free-body diagram because deformations and stresses are addressed in addition to forces.

The results of the micromechanics studies of composite materials with unidirectional fibers will be presented as plots of an individual mechanical property versus the fiber-volume fraction. A schematic representation of several possible functional relationships between a property and the fiber-volume fraction is shown in Figure 3-4. In addition, both upper and lower bounds on those functional relationships will be obtained.

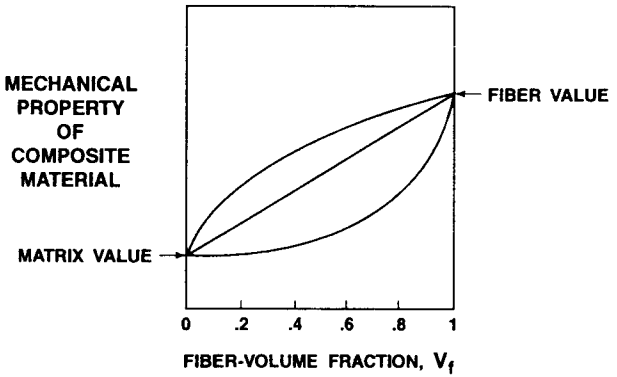

Figure 3-4 Typical Forms of Micromechanics Results

The mechanics of materials approach to the micromechanics of material stiffnesses is discussed in Section 3.2. There, simple approximations to the engineering constants E_1, E_2, ν_{12}, and G_{12} for an orthotropic material are introduced. In Section 3.3, the elasticity approach to the micromechanics of material stiffnesses is addressed. Bounding techniques, exact solutions, the concept of contiguity, and the Halpin-Tsai approximate equations are all examined. Next, the various approaches to prediction of stiffness are compared in Section 3.4 with experimental data for both particulate composite materials and fiber-reinforced composite materials. Parallel to the study of the micromechanics of material stiffnesses is the micromechanics of material strengths which is introduced in Section 3.5. There, mechanics of materials predictions of tensile and compressive strengths are described.

3.2 MECHANICS OF MATERIALS APPROACH TO STIFFNESS

The key feature of the mechanics of materials approach is that certain *simplifying assumptions* must be made regarding the mechanical behavior of a composite material in order to get an effective solution. Each assumption must be plausible, i.e., there must be a *reason* why the assumption *might* be true (in mechanics, assumptions cannot be arbitrary!). The most prominent assumption is that the strains in the fiber direction of a unidirectional fiber-reinforced composite material are the same in the fibers as in the matrix as shown in Figure 3-5. If the strains were not the same, then a fracture between the fibers and the matrix is implied. Thus, the assumption has a plausible reason. Because the strains in both the matrix and fiber are the same, then it is obvious that sections normal to the 1-axis, which were plane before being stressed, remain plane after stressing. The foregoing is a prominent assumption in the usual mechanics of materials approaches such as in beam, plate, and shell theories. We will derive, on that basis, the mechanics of materials predictions for the apparent orthotropic moduli of a unidirectionally fiber-reinforced composite material, namely, E_1, E_2, ν_{12}, and G_{12}. Note that the basis for the simplifying assumptions for each prediction is firm, and not wishful thinking.

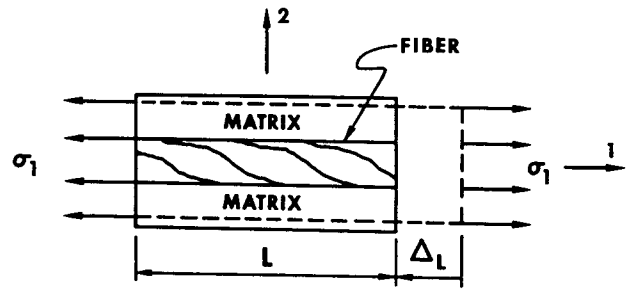

Figure 3-5 Representative Volume Element Loaded in the 1-Direction

3.2.1 Determination of E_1

The first modulus to be determined is that of the composite material in the 1-direction, that is, in the fiber direction. From Figure 3-5,

$$\varepsilon_1 = \frac{\Delta_L}{L} \tag{3.1}$$

where ε_1 applies for both the fibers and the matrix according to the basic assumption. Then, if both constituent materials behave elastically, the stresses in the fiber direction are

$$\sigma_f = E_f \varepsilon_1 \qquad \sigma_m = E_m \varepsilon_1 \tag{3.2}$$

The average stress σ_1 acts on cross-sectional area A of the representative volume element, σ_f acts on the cross-sectional area of the fibers A_f, and σ_m acts on the cross-sectional area of the matrix A_m. Thus, the resultant force on the representative volume element of composite material is

$$P = \sigma_1 A = \sigma_f A_f + \sigma_m A_m \tag{3.3}$$

By substitution of Equation (3.2) in Equation (3.3) and recognition from macromechanics that

$$\sigma_1 = E_1 \varepsilon_1 \tag{3.4}$$

apparently

$$E_1 = E_f \frac{A_f}{A} + E_m \frac{A_m}{A} \tag{3.5}$$

But the volume fractions of fibers and matrix can be written as

$$V_f = \frac{A_f}{A} \qquad V_m = \frac{A_m}{A} \tag{3.6}$$

Thus,

$$E_1 = E_f V_f + E_m V_m \tag{3.7}$$

which is known as the *rule of mixtures* for the apparent Young's modulus of the composite material in the direction of the fibers and is graphically depicted in Figure 3-6. The rule of mixtures represents a simple linear variation of apparent Young's modulus E_1 from E_m to E_f as V_f goes from 0 to 1. The fiber modulus is typically many times the matrix modulus. Thus, at usual practical fiber-volume fractions around .6, the fiber modulus dominates the composite modulus E_1. Even large changes in E_m have very little effect on E_1 (certainly not in proportion to the change in E_m) as long as the fiber-volume fraction is not close to zero. Thus, we regard E_1 as a fiber-dominated property.

The load sharing between fiber and matrix can be viewed as a simple springs-in-parallel model as in Figure 3-7. There, if all springs deform the same amount (the equal-strains assumption) and $k_f >> k_m$, then the fiber spring takes most of the applied load.

To appreciate the practical value of this analysis for E_1, examine the experimental results relative to the predicted straight line in Figure 3-8. The agreement is excellent!

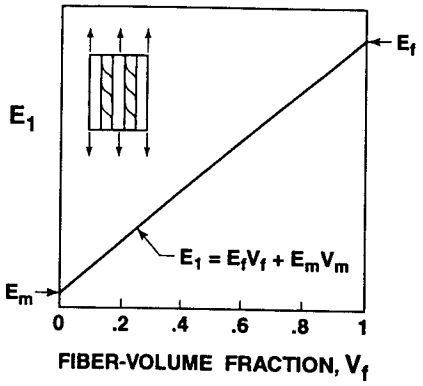

Figure 3-6 Variation of E_1 with Fiber-Volume Fraction

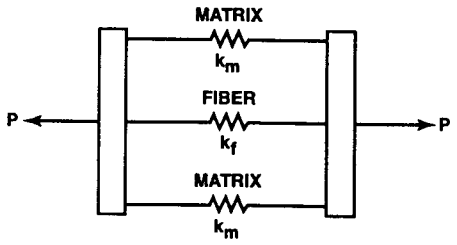

Figure 3-7 Load Sharing in a Fiber-Reinforced Lamina

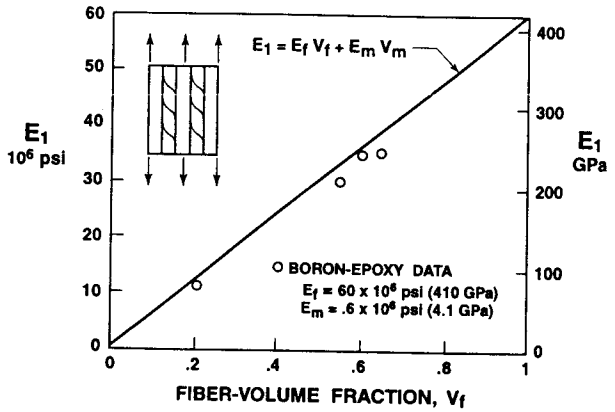

Figure 3-8 Predicted versus Measured E_1

3.2.2 Determination of E_2

The apparent Young's modulus, E_2, of the composite material in the direction transverse to the fibers is considered next. In the mechanics of materials approach, the same transverse stress, σ_2, is assumed to be applied to both the fiber and the matrix as in Figure 3-9. That is, equilibrium of adjacent elements in the composite material (fibers and matrix) must occur (certainly plausible). However, we cannot make any plausible approximation or assumption about the strains in the fiber and in the matrix in the 2-direction.

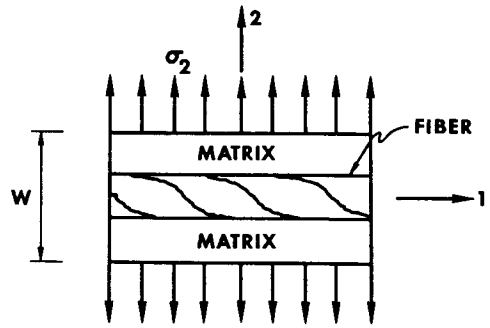

Figure 3-9 Representative Volume Element Loaded in the 2-Direction

The strains in the fiber and in the matrix are, therefore, found from the stresses:

$$\varepsilon_f = \frac{\sigma_2}{E_f} \qquad \varepsilon_m = \frac{\sigma_2}{E_m} \tag{3.8}$$

The transverse dimension over which, on average, ε_f acts is approximately $V_f W$, whereas ε_m acts on $V_m W$. Thus, the total transverse deformation is

$$\Delta W = \varepsilon_2 W = V_f W \varepsilon_f + V_m W \varepsilon_m \tag{3.9}$$

or

$$\varepsilon_2 = V_f \varepsilon_f + V_m \varepsilon_m \tag{3.10}$$

which becomes, upon substitution of the strains from Equation (3.8),

$$\varepsilon_2 = V_f \frac{\sigma_2}{E_f} + V_m \frac{\sigma_2}{E_m} \tag{3.11}$$

but from the macroscopic stress-strain relation

$$\sigma_2 = E_2 \varepsilon_2 = E_2 \left[\frac{V_f \sigma_2}{E_f} + \frac{V_m \sigma_2}{E_m} \right] \tag{3.12}$$

whereupon

$$E_2 = \frac{E_f E_m}{V_m E_f + V_f E_m} \tag{3.13}$$

which is the mechanics of materials expression for the apparent Young's modulus in the direction transverse to the fibers. Equation (3.13) can be nondimensionalized as

$$\frac{E_2}{E_m} = \frac{1}{V_m + V_f (E_m/E_f)} \tag{3.14}$$

Values of E_2/E_m are given in Table 3-1 for three values of the fiber-to-matrix modulus ratio.

Table 3-1 Values for E_2/E_m for Various E_f/E_m and V_f

$\frac{E_f}{E_m}$	V_f							
	0	.2	.4	.5	.6	.8	.9	1
1	1	1	1	1	1	1	1	1
10	1	1.22	1.56	1.82	2.17	3.56	5.26	10
100	1	1.25	1.66	1.98	2.46	4.80	9.17	100

Predicted results for E_2 are plotted in Figure 3-10 for three values of the fiber-to-matrix-modulus ratio. Note that if $V_f = 1$, the modulus predicted is that of the fibers. However, recognize that a perfect bond between fibers is then implied if a tensile σ_2 is applied. No such bond is implied if a compressive σ_2 is applied. Observe also that more than 50% by volume of fibers is required to raise the transverse modulus E_2 to twice the matrix modulus even if $E_f = 10 \times E_m$! That is, the fibers do not contribute much to the transverse modulus unless the percentage of fibers is impractically high. Thus, the composite material property E_2 is matrix-dominated.

A simple springs-in-series model represents the representative volume element loaded in the 2-direction as in Figure 3-11. There, the matrix is the soft link in the chain of stiffnesses. Thus, the spring stiffness for the matrix is quite low. We would expect, on this basis, that the matrix deformation dominates the deformation of the composite material.

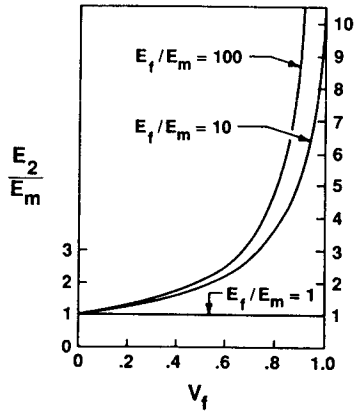

Figure 3-10 Variation of E_2 with Fiber-Volume Fraction

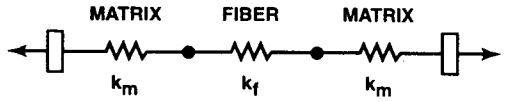

Figure 3-11 Deformation Sharing in a Fiber-Reinforced Lamina

Obviously, the assumptions involved in the foregoing derivation are not entirely consistent. A transverse strain mismatch exists at the boundary between the fiber and the matrix by virtue of Equation (3.8). Moreover, the transverse stresses in the fiber and in the matrix are not likely to be the same because ν_f is not equal to ν_m. Instead, a complete match of displacements across the boundary between the fiber and the matrix would constitute a rigorous solution for the apparent transverse Young's modulus. Such a solution can be found only by use of the theory of elasticity. The seriousness of such inconsistencies can be determined only by comparison with experimental results.

Another observation on this solution is that if the Poisson's ratios of the fiber and the matrix are not the same (they are likely different), then longitudinal stresses are induced in the fiber and matrix (with a net resultant longitudinal force of zero) with accompanying shearing stresses at the fiber-matrix boundary. Such shearing stresses will naturally arise under some stress states. Thus, this material characteristic cannot be regarded as undesirable or indicative of an inappropriate solution.

The predictions for E_2 from Equation (3.13) are shown along with measured values for E_2 in Figure 3-12. There, obviously this approach is an underestimate of the contribution of the flexible matrix material to E_2. As we will see in Section 3.4, better approaches are available for prediction of E_2, but at the cost of far more complexity.

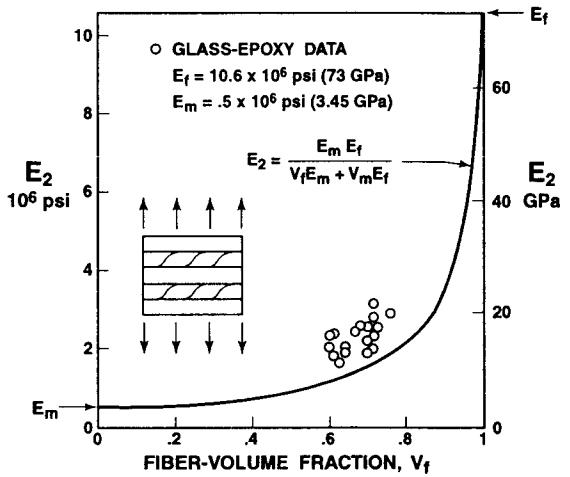

Figure 3-12 Predicted versus Measured E_2 *(Data from Tsai [3-1])*

3.2.3 Determination of ν_{12}

The so-called major Poisson's ratio, ν_{12}, is obtained by an approach similar to the analysis for E_1. First, the major Poisson's ratio is

$$\nu_{12} = -\frac{\varepsilon_2}{\varepsilon_1} \tag{3.15}$$

for the stress state $\sigma_1 = \sigma$ and all other stresses are zero. Then, the deformations are depicted in the representative volume element of Figure 3-13. There, the fundamental simplifying assumption is that the fiber strains are identical to the matrix strains in the fiber direction, as in the approach to E_1. The transverse deformation Δ_W is macroscopically

$$\Delta_W = -W\varepsilon_2 = W\nu_{12}\varepsilon_1 \tag{3.16}$$

but is also microscopically

$$\Delta_W = \Delta_{mW} + \Delta_{fW} \tag{3.17}$$

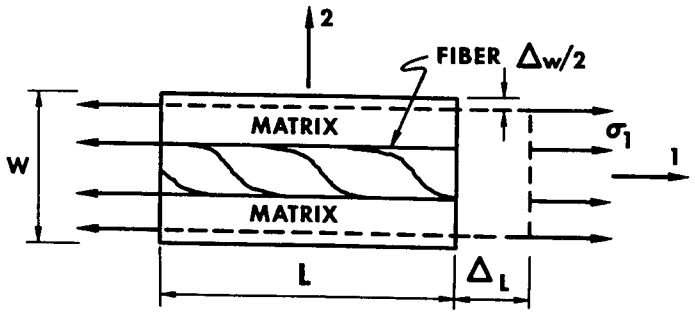

Figure 3-13 Representative Volume Element Loaded in the 1-Direction

In the manner of the analysis for the transverse Young's modulus, E_2, the transverse deformations Δ_{mW} and Δ_{fW} are approximately

$$\Delta_{mW} = WV_m\nu_m\varepsilon_1 \qquad \Delta_{fW} = WV_f\nu_f\varepsilon_1 \tag{3.18}$$

Combine Equations (3.16)-(3.18) and divide by $\varepsilon_1 W$ to get

$$\nu_{12} = \nu_m V_m + \nu_f V_f \tag{3.19}$$

which is a rule of mixtures for the major Poisson's ratio and is plotted in a manner similar to that for E_1 in Figure 3-14. Because the Poisson's ratios ν_m and ν_f are not significantly different from each other, the composite material major Poisson's ratio ν_{12} is neutral, i.e., neither matrix-dominated nor fiber-dominated. Experimental results for ν_{12} are presented in Section 3.4.2.

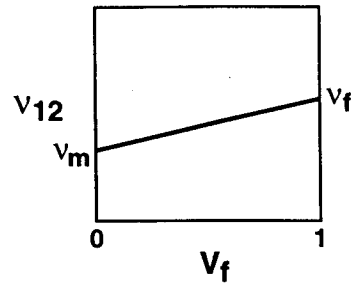

Figure 3-14 Variation of ν_{12} with Fiber-Volume Fraction

3.2.4 Determination of G_{12}

The in-plane shear modulus of a lamina, G_{12}, is determined in the mechanics of materials approach by presuming that the shearing stresses on the fiber and on the matrix are the same (clearly, the shear deformations cannot be the same!). The loading is shown in the representative volume element of Figure 3-15. By virtue of the basic presumption,

$$\gamma_m = \frac{\tau}{G_m} \qquad \gamma_f = \frac{\tau}{G_f} \tag{3.20}$$

The nonlinear shear stress–shear strain behavior typical of fiber-reinforced composite materials is ignored, i.e., the behavior is regarded as linear.

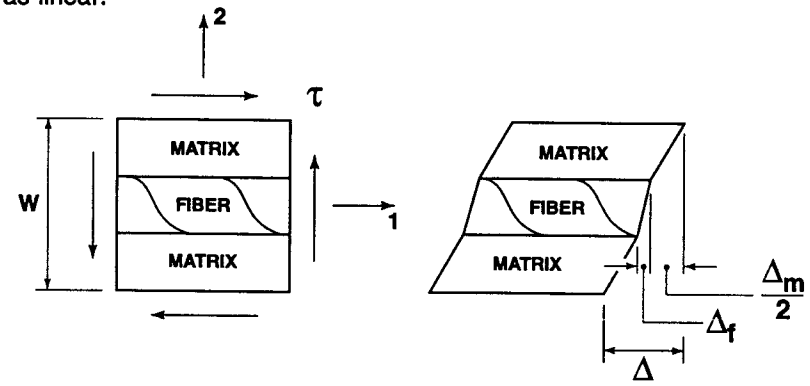

a Shear Stress Loading b Shear Deformation

Figure 3-15 Representative Volume Element Loaded in Shear

On a microscopic scale, the deformations are shown in Figure 3-15. Note that the matrix deforms more than the fiber in shear because the matrix has a lower shear modulus. The total shearing deformation is

$$\Delta = \gamma W \tag{3.21}$$

and is made up of, approximately, microscopic deformations

$$\Delta_m = V_m W \gamma_m \qquad \Delta_f = V_f W \gamma_f \tag{3.22}$$

Then, because $\Delta = \Delta_m + \Delta_f$, division by W yields

$$\gamma = V_m \gamma_m + V_f \gamma_f \tag{3.23}$$

or upon substitution of Equation (3.20) and realization that macroscopically

$$\gamma = \frac{\tau}{G_{12}} \tag{3.24}$$

Equation (3.23) can be written as

$$\frac{\tau}{G_{12}} = V_m \frac{\tau}{G_m} + V_f \frac{\tau}{G_f} \tag{3.25}$$

Finally,

$$G_{12} = \frac{G_m G_f}{V_m G_f + V_f G_m} \tag{3.26}$$

which is the same type of expression as was obtained for the transverse Young's modulus, E_2. As with E_2, the expression for G_{12} can be normalized by a modulus related to the matrix, that is,

$$\frac{G_{12}}{G_m} = \frac{1}{V_m + V_f(G_m/G_f)} \tag{3.27}$$

which is plotted in Figure 3-16 for several values of G_f/G_m. Only for a fiber volume of greater than 50% of the total volume does G_{12} rise above twice G_m even when $G_f/G_m = 10$! As with E_2, the composite material shear modulus G_{12} is matrix-dominated. Measured values of G_{12} have a relation to the predicted values similar to those for E_2 in Figure 3-12 (see Section 3.4.2).

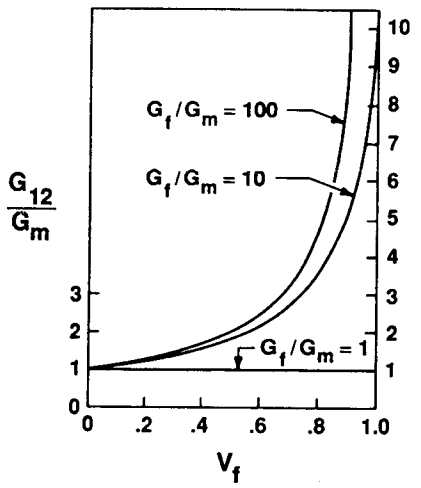

Figure 3-16 Variation of G_{12} with Fiber-Volume Fraction

3.2.5 Summary Remarks

The foregoing are but examples of the types of mechanics of materials approaches that can be used. Other assumptions of physical behavior lead to different expressions for the four elastic moduli for a unidirectionally reinforced lamina. For example, Ekvall [3-2] obtained a modification of the rule-of-mixtures expression for E_1 and of the expression for E_2 in which the triaxial stress state in the matrix due to fiber restraint is accounted for:

$$E_1 = V_f E_f + V_m E'_m \tag{3.28}$$

$$E_2 = \frac{E_f E'_m}{V_f E'_m + V_m E_f (1 - \nu_m^2)} \tag{3.29}$$

where

$$E'_m = \frac{E_m}{1 - 2\nu_m^2} \tag{3.30}$$

However, these modifications of the previously derived expressions are not significant for $\nu_m < 1/4$. Ekvall made other modifications to account for such features as square or rectangular versus round fibers and for stress concentrations due to fibers [3-3].

Problem Set 3.2

3.2.1 Use a mechanics of materials approach to determine the apparent Young's modulus for a composite material with an 'inclusion' of arbitrary shape in a cubic element of equal unit-length sides as in the representative volume element (RVE) of Figure 3-17. Fill in the details to show that the modulus is

$$E = \frac{\sigma}{\varepsilon} = \frac{F/A}{\delta/L} = \frac{F/(1[L] \times 1[L])}{\delta/(1[L])} = \frac{F}{\delta[L]}$$

where [L] represents units of length and can be written as

$$\frac{1}{E} = \int_0^1 \frac{dx}{E_1 + (E_2 - E_1)A_2(x)}$$

where $A_2(x)$ is the distribution of the inclusion. Note that the slice dx long of the RVE represents a microscopic portion of the RVE, i.e., recognize the difference between what happens for a slice and what happens for the entire RVE. Use this result in Problems 3.2.2 through 3.2.4.

3.2.2 Verify that the general expression for the modulus of a dispersion-stiffened composite material reduces to

$$\frac{E}{E_m} = \frac{E_m + (E_d - E_m)V_d^{2/3}}{E_m + (E_d - E_m)V_d^{2/3}\left[1 - V_d^{1/3}\right]}$$

for a cubic particle of modulus E_d in a matrix with modulus E_m. The volume fraction of the cubic particles is V_d and that of the matrix is V_m or $1 - V_d$. Hint: the representative volume element is a cube within a cube.

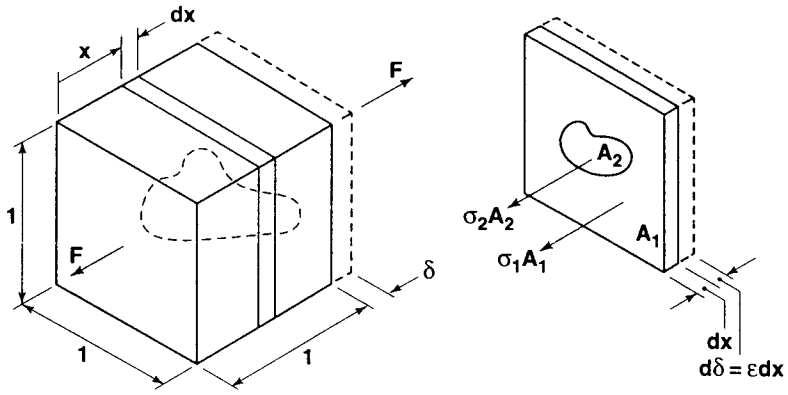

Figure 3-17 Particulate Reinforcement *(After Paul [3-4])*

3.2.3 Determine the expression for the modulus of a composite material stiffened by particles of any cross section but prismatic along the direction in which the modulus is desired as in Figure 3-18.

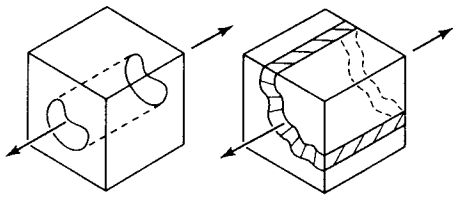

Figure 3-18 Prismatic Reinforcement *(After Paul [3-4])*

3.2.4 Determine the expression for the modulus of a composite material that consists of matrix material reinforced by a slab of constant thickness in the direction in which the modulus is desired as in Figure 3-19.

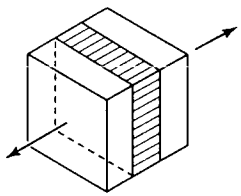

Figure 3-19 Slab Reinforcement *(After Paul [3-4])*

3.2.5 To what conclusion are you led if you assume for the determination of E_2 in Section 3.2.2 equal strains in the fiber and the matrix instead of equal stresses in the direction perpendicular to the fibers?

3.2.6 Develop a schematic model with fiber springs and matrix springs in which the actual surrounding of the fiber with matrix material is taken into account, i.e., for a cross section such as that with the dimension 'lamina thickness' in Figure 3-2, except make the fiber cross section square instead of round.

3.3 ELASTICITY APPROACH TO STIFFNESS

3.3.1 Introduction

The division of micromechanics stiffness evaluation efforts into the mechanics of materials approach and the elasticity approach with its many subapproaches is rather arbitrary. Chamis and Sendeckyj [3-5] divide micromechanics stiffness approaches into many more classes: netting analyses,[1] mechanics of materials approaches, self-consistent models, variational techniques using energy-bounding principles, exact solutions, statistical approaches, finite element methods, semiempirical approaches, and microstructure theories. All approaches have the common objective of the prediction of composite materials stiffnesses. All except the first two approaches use some or all of the principles of elasticity theory to varying degrees so are here classed as elasticity approaches. This simplifying and arbitrary division is useful in this book because the objective here is to merely become acquainted with advanced micromechanics theories after the basic concepts have been introduced by use of typical mechanics of materials reasoning. The reader who is interested in micromechanics should supplement this chapter with the excellent critique and extensive bibliography of Chamis and Sendeckyj [3-5].

The variational energy principles of classical elasticity theory are used in Section 3.3.2 to determine upper and lower bounds on lamina moduli. However, that approach generally leads to bounds that might not be sufficiently close for practical use. In Section 3.3.3, all the principles of elasticity theory are invoked to determine the lamina moduli. Because of the resulting complexity of the problem, many advanced analytical techniques and numerical solution procedures are necessary to obtain solutions. However, the assumptions made in such analyses regarding the interaction between the fibers and the matrix are not entirely realistic. An interesting approach to more realistic fiber-matrix interaction, the contiguity approach, is examined in Section 3.3.4. The widely used Halpin-Tsai equations are displayed and discussed in Section 3.3.5.

3.3.2 Bounding Techniques of Elasticity

Paul [3-4] was apparently the first to use the bounding (variational) techniques of linear elasticity to examine the bounds on the moduli of multiphase materials. His work was directed toward analysis of the elastic moduli of alloyed metals rather than toward fiber-reinforced composite materials. Accordingly, the treatment is for an isotropic composite material made of different isotropic constituents. The composite material is isotropic because the alloyed constituents are uniformly dispersed and have no preferred orientation. The modulus of the matrix material is E_m

[1] The basic assumption in netting analysis is that the fibers provide all the longitudinal stiffness and the matrix provides all the transverse and shear stiffness as well as the Poisson effect. On the basis of our observations of mechanics of materials results, we recognize the netting analysis assumption to be grossly conservative. Hence, netting analysis will be ignored in this book, and more useful theories will be addressed.

and the modulus of the dispersed material is E_d, whereas the modulus of the composite material is E. The volume fractions of the constituents are V_m and V_d such that

$$V_m + V_d = 1 \tag{3.31}$$

Obviously, any relationship for the composite modulus, E, must yield $E = E_m$ for $V_m = 1$ and $E = E_d$ for $V_d = 1$.

One of the simplest relationships that satisfies the foregoing restrictions is the rule of mixtures

$$E = E_m V_m + E_d V_d \tag{3.32}$$

wherein the constituents of the composite material are presumed to contribute to the composite stiffness in direct proportion to their own stiffnesses and volume fractions. The rule of mixtures will be shown to provide an upper bound on the composite modulus E for the special case in which

$$\nu_m = \nu_d = \nu \tag{3.33}$$

Another simple relationship between the constituent moduli results from the observation that the compliance of the composite material, 1/E, must agree with the compliance of the matrix, $1/E_m$, when $V_m = 1$ and with the compliance of the dispersed material when $V_d = 1$. The resulting rule of mixtures for compliances is

$$\frac{1}{E} = \frac{V_m}{E_m} + \frac{V_d}{E_d} \tag{3.34}$$

which will be shown to yield a lower bound on the composite material modulus, E.

In a uniaxial tension test to determine the elastic modulus of the composite material, E, the stress and strain states will be assumed to be macroscopically uniform in consonance with the basic presumption that the composite material is macroscopically isotropic and homogeneous. However, on a microscopic scale, both the stress and strain states will be nonuniform. In the uniaxial tension test,

$$E = \frac{\sigma}{\varepsilon} \tag{3.35}$$

where σ is the applied uniaxial stress and ε is the resulting axial strain. The resulting strain energy can be written in two equivalent forms:

$$U = \frac{1}{2}\frac{\sigma^2}{E} V \tag{3.36}$$

$$U = \frac{1}{2} E \varepsilon^2 V \tag{3.37}$$

Lower Bound on Apparent Young's Modulus

The basis for the determination of a lower bound on the apparent Young's modulus is application of the *principle of minimum complementary energy* which can be stated as: Let the *tractions* (forces and moments) be specified over the surface of a body. Let σ_x°, σ_y°, σ_z°, τ_{xy}°, τ_{yz}°, τ_{zx}° be a state of stress that satisfies the stress equations of equilibrium

and the specified boundary conditions, i.e., an admissible stress field. Let U° be the strain energy for the stress state σ_x°, σ_y°, σ_z°, τ_{xy}°, τ_{yz}°, τ_{zx}° given by use of the stress-strain relations (a simple rearrangement of the isotropic stress-strain relations in Equation (2.17) in terms of E and ν)

$$\begin{aligned} \sigma_x &= \frac{\nu E}{(1+\nu)(1-2\nu)}(\varepsilon_x + \varepsilon_y + \varepsilon_z) + \frac{E}{(1+\nu)}\varepsilon_x \\ &\vdots \\ \tau_{xy} &= G\gamma_{xy} = \frac{E}{2(1+\nu)}\gamma_{xy} \end{aligned} \tag{3.38}$$

and the expression for the strain energy

$$U = \frac{1}{2}\int_V (\sigma_x\varepsilon_x + \sigma_y\varepsilon_y + \sigma_z\varepsilon_z + \tau_{xy}\gamma_{xy} + \tau_{yz}\gamma_{yz} + \tau_{zx}\gamma_{zx})dV \tag{3.39}$$

Then, the actual strain energy U in the body due to the specified loads cannot exceed U°, that is,

$$U \le U^\circ \tag{3.40}$$

For a lower bound on the apparent Young's modulus, E, load the basic uniaxial test specimen with normal stress on the ends. The internal stress field that satisfies this loading and the stress equations of equilibrium is

$$\sigma_x^\circ = \sigma \qquad \sigma_y^\circ = \sigma_z^\circ = \tau_{xy}^\circ = \tau_{yz}^\circ = \tau_{zx}^\circ = 0 \tag{3.41}$$

We know full well that such a uniform stress state cannot exist throughout the *composite* material, yet we seek the implication of such an approximation. The strain energy for the stresses in Equation (3.41) is

$$U^\circ = \frac{1}{2}\int_V \frac{(\sigma_x^\circ)^2}{E} dV = \frac{\sigma^2}{2}\int_V \frac{dV}{E} \tag{3.42}$$

But E is obviously not constant over the volume because the matrix has modulus E_m over volume $V_m V$ and the dispersed material has modulus E_d over volume $V_d V$ where V is the total volume. Thus,

$$\int_V \frac{dV}{E} = \int_{V_m V} \frac{dV}{E_m} + \int_{V_d V} \frac{dV}{E_d} = \frac{V_m V}{E_m} + \frac{V_d V}{E_d} \tag{3.43}$$

whereupon

$$U^\circ = \frac{\sigma^2}{2}\left[\frac{V_m}{E_m} + \frac{V_d}{E_d}\right] V \tag{3.44}$$

However, by virtue of the inequality $U \le U^\circ$ and the definition of U in Equation (3.36),

$$\frac{1}{2}\frac{\sigma^2}{E} V \le \frac{\sigma^2}{2}\left[\frac{V_m}{E_m} + \frac{V_d}{E_d}\right] V \tag{3.45}$$

or

$$\frac{1}{E} \le \frac{V_m}{E_m} + \frac{V_d}{E_d} \tag{3.46}$$

Finally,

$$E \ge \frac{E_m E_d}{V_m E_d + V_d E_m} \tag{3.47}$$

which is a lower bound on the apparent Young's modulus, E, of the composite material in terms of the moduli and volume fractions of the constituent materials. Note that this bound coincides with the value for the modulus transverse to the fibers by the mechanics of materials approach.

Upper Bound on Apparent Young's Modulus

The basis for the determination of an upper bound on the apparent Young's modulus is the *principle of minimum potential energy* which can be stated as: Let the *displacements* be specified over the surface of the body except where the corresponding traction is zero. Let $\varepsilon_x^*, \varepsilon_y^*, \varepsilon_z^*, \gamma_{xy}^*, \gamma_{yz}^*, \gamma_{zx}^*$ be any compatible state of strain that satisfies the specified displacement boundary conditions, i.e., an admissible strain field. Let U^* be the strain energy of the strain state ε_x^*, etc., by use of the stress-strain relations

$$\begin{aligned} \sigma_x &= \frac{\nu E}{(1+\nu)(1-2\nu)}(\varepsilon_x + \varepsilon_y + \varepsilon_z) + \frac{E}{(1+\nu)}\varepsilon_x \\ &\vdots \\ \tau_{xy} &= G\gamma_{xy} = \frac{E}{2(1+\nu)}\gamma_{xy} \end{aligned} \tag{3.48}$$

and the expression for the strain energy

$$U = \frac{1}{2}\int_V (\sigma_x\varepsilon_x + \sigma_y\varepsilon_y + \sigma_z\varepsilon_z + \tau_{xy}\gamma_{xy} + \tau_{yz}\gamma_{yz} + \tau_{zx}\gamma_{zx})dV \tag{3.49}$$

Then, the actual strain energy U in the body due to the specified displacements cannot exceed U^*, that is,

$$U \le U^* \tag{3.50}$$

To find an upper bound on the apparent Young's modulus, E, subject the basic uniaxial test specimen to an elongation εL where ε is the average strain and L is the specimen length. The internal strain field that corresponds to the average strain at the boundaries of the specimen is

$$\varepsilon_x^* = \varepsilon \qquad \varepsilon_y^* = \varepsilon_z^* = -\nu\varepsilon \qquad \gamma_{xy}^* = \gamma_{yz}^* = \gamma_{zx}^* = 0 \tag{3.51}$$

where ν is the apparent Poisson's ratio of the composite material. We know full well that such a uniform strain state cannot exist throughout the *composite* material, yet we seek the implication of such an approximation. By use of the stress-strain relations, Equation (3.48), the stresses in the matrix for the given strain field are

$$\begin{aligned} \sigma_{x_m}^* &= \frac{1-\nu_m-2\nu_m\nu}{1-\nu_m-2\nu_m^2}E_m\varepsilon \\ \sigma_{y_m}^* &= \sigma_{z_m}^* = \frac{\nu_m-\nu}{1-\nu_m-2\nu_m^2}E_m\varepsilon \\ \tau_{xy_m}^* &= \tau_{yz_m}^* = \tau_{zx_m}^* = 0 \end{aligned} \tag{3.52}$$

and the stresses in the dispersed material are

$$\begin{aligned} \sigma_{x_d}^* &= \frac{1-\nu_d-2\nu_d\nu}{1-\nu_d-2\nu_d^2}E_d\varepsilon \\ \sigma_{y_d}^* &= \sigma_{z_d}^* = \frac{\nu_d-\nu}{1-\nu_d-2\nu_d^2}E_d\varepsilon \\ \tau_{xy_d}^* &= \tau_{yz_d}^* = \tau_{zx_d}^* = 0 \end{aligned} \tag{3.53}$$

The strain energy in the composite material is obtained by substituting the strains, Equation (3.51), and the stresses, Equations (3.52) and (3.53), in the strain energy, Equation (3.49):

$$U^* = \frac{\varepsilon^2}{2}\int_{V_d}\frac{1-\nu_d-4\nu_d\nu+2\nu^2}{1-\nu_d-2\nu_d^2}E_d dV + \frac{\varepsilon^2}{2}\int_{V_m}\frac{1-\nu_m-4\nu_m\nu+2\nu^2}{1-\nu_m-2\nu_m^2}E_m dV \tag{3.54}$$

or

$$U^* = \frac{\varepsilon^2}{2}\left[\frac{1-\nu_d-4\nu_d\nu+2\nu^2}{1-\nu_d-2\nu_d^2}E_dV_d + \frac{1-\nu_m-4\nu_m\nu+2\nu^2}{1-\nu_m-2\nu_m^2}E_mV_m\right]V \tag{3.55}$$

However, by virtue of the inequality $U \le U^*$ and the definition of U in Equation (3.37),

$$\frac{1}{2}E\varepsilon^2 V \le \frac{\varepsilon^2}{2}\left[\frac{1-\nu_d-4\nu_d\nu+2\nu^2}{1-\nu_d-2\nu_d^2}E_dV_d + \frac{1-\nu_m-4\nu_m\nu+2\nu^2}{1-\nu_m-2\nu_m^2}E_mV_m\right]V \tag{3.56}$$

whereupon the upper bound on E is, by simple cancellation of terms in Equation (3.56),

$$E \le \frac{1-\nu_d-4\nu_d\nu+2\nu^2}{1-\nu_d-2\nu_d^2}E_dV_d + \frac{1-\nu_m-4\nu_m\nu+2\nu^2}{1-\nu_m-2\nu_m^2}E_mV_m \tag{3.57}$$

The value of Poisson's ratio, ν, for the composite material is *unknown* at this stage of the analysis, so the upper bound on E is inspecific. In accordance with the principle of minimum potential energy, the expres-

sion for the strain energy U^* must be minimized[2] with respect to the unspecified constant ν to specify the bound on E. The minimization procedure consists of determining where

$$\frac{\partial U^*}{\partial \nu} = 0 \tag{3.58}$$

and at the same time verifying that

$$\left.\frac{\partial^2 U^*}{\partial \nu^2}\right|_{\frac{\partial U^*}{\partial \nu}=0} > 0 \tag{3.59}$$

First,

$$\frac{\partial U^*}{\partial \nu} = \frac{\varepsilon^2 V}{2}\left[\frac{-4\nu_d + 4\nu}{1-\nu_d-2\nu_d^2}E_d V_d + \frac{-4\nu_m + 4\nu}{1-\nu_m-2\nu_m^2}E_m V_m\right] \tag{3.60}$$

which is zero when

$$\nu = \frac{(1-\nu_m-2\nu_m^2)\nu_d E_d V_d + (1-\nu_d-2\nu_d^2)\nu_m E_m V_m}{(1-\nu_m-2\nu_m^2)E_d V_d + (1-\nu_d-2\nu_d^2)E_m V_m} \tag{3.61}$$

The second derivative of U^* is

$$\frac{\partial^2 U^*}{\partial \nu^2} = \frac{\varepsilon^2 V}{2}\left[\frac{4E_d V_d}{1-\nu_d-2\nu_d^2} + \frac{4E_m V_m}{1-\nu_m-2\nu_m^2}\right] \tag{3.62}$$

However, the matrix and dispersed material are isotropic, so $\nu_m < 1/2$ and $\nu_d < 1/2$ (the usual limit on Poisson's ratio for an isotropic material as seen in Section 2.4). Thus, upon substitution of these values for ν_m and ν_d, the value of $\partial^2 U^*/\partial \nu^2$ is seen to be always positive (even when $\partial U^*/\partial \nu$ is not zero) because the typical term $(1-b-2b^2)$ is always positive when $b < 1/2$. Finally, because $\partial^2 U^*/\partial \nu^2$ is always positive, the value of U^* when Equation (3.61) is used, corresponding to a minimum, maximum, or inflection point on the curve for U^* as a function of ν, is proved to be a minimum, and in fact, the absolute minimum.

The value of Poisson's ratio, ν, for the composite material has been derived explicitly as Equation (3.61). Thus, the upper bound on E can be obtained by substituting the expression for ν, Equation (3.61), in the expression for the upper bound on E in terms of ν, Equation (3.57). However, the algebra is quite messy, so an explicit expression for the upper bound on E is not presented. In practical applications, the value of ν can be calculated from Equation (3.61) and then substituted in Equation (3.57) to obtain E. For the special case in which $\nu_m = \nu_d$, the expression for ν, Equation (3.61), reduces to

[2]Note at this point that the potential energy of external forces is independent of material properties. Thus, its derivatives with respect to ν are zero, and only U^* affects the minimization.

$$E \le E_d V_d + E_m V_m \tag{3.63}$$

which is the value of the apparent Young's modulus, E_1, in the fiber direction of a fiber-reinforced composite material derived by the mechanics of materials approach. Thus, the expression for E_1 is an upper bound on the actual E_1. In addition, the mechanics of materials solution obviously includes an implicit equality of the Poisson's ratios of the constituent materials.

Paul's work [3-4] is primarily applicable to isotropic composite materials, but it can be interpreted in terms of fibrous composite materials. For example, Equation (3.63) is the upper bound on the transverse modulus, E_2, of a fiber-reinforced composite material, whereas Equation (3.47) is the lower bound. Obviously, the bounds, as plotted in Figure 3-20 for a glass-epoxy composite material [$E_f = 10.6 \times 10^6$ psi (73 GPa) and $E_m = .5 \times 10^6$ psi (3.5 GPa)], are far apart. Bounds on other moduli can be obtained in a similar manner (see Problem Set 3.3).

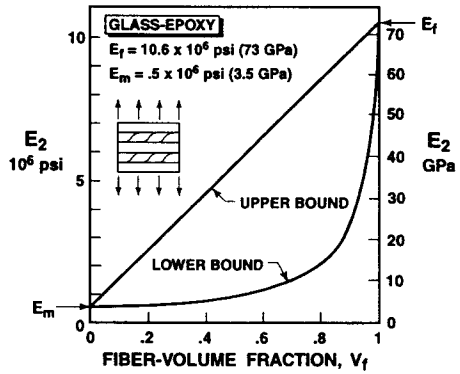

Figure 3-20 Bounds on E_2 for a Glass-Epoxy Composite Material

Hashin [3-6] and Hashin and Shtrikman [3-7] attempted to tighten Paul's bounds to obtain more useful estimates of moduli for isotropic heterogeneous materials. Their approach was to use a concentric-spheres model to treat the heterogeneous material as an elastic sphere inside a concentric-spherical portion of elastic matrix material in proportion to the volume content of spherical inclusions in the total volume of the composite material. The included spheres never touch one another in the model, although clearly as the volume percentage of particles increases, so does the likelihood of particle contact. Moreover, lack of contact might imply perfect particle spacing, an unlikely situation from the practical standpoint.

Hashin and Rosen [3-8] extended Hashin's work to fiber-reinforced composite materials. The fibers have a circular cross section and can be hollow or solid. Two cases were treated: (1) identical fibers in a hexagonal array and (2) fibers of various diameters (but same ratio of inside to outside diameter, if hollow) in a random array. The two types of arrays are depicted in Figure 3-21. In both cases, the basic analysis

element is a set of concentric cylinders with their axes in the fiber direction. For the random array, in analogy to Hashin's concentric-spheres model, the concentric-cylinder model consists of the fiber with matrix material around it in proportion to the volume content of matrix in the total volume. An additional matrix volume term is needed in the hexagonal array case to account for the volume left over when the circles of radius r_m are drawn around each fiber in Figure 3-21a. The concentric-cylinder model itself is displayed in Figure 3-21a. The Young's modulus in the fiber direction turns out to be, for all practical purposes, the rule of mixtures. The expressions for the transverse Young's modulus for a random array or a hexagonal array of solid or hollow fibers are more complex than the objectives of this book leave room for. Some of the expressions will be plotted later when experimental data are compared with various theoretical predictions. At any rate, the bounds on moduli for fibers in a hexagonal array are rather far apart for large values of the ratio of fiber modulus to matrix modulus in the composite material, a typical situation for practical composite materials. On the other hand, this random-array model is not an accurate representation of most practical fiber-reinforced composite materials. If, however, many different sizes of fibers were included to fill the matrix voids between the various concentric cylinders as in Figure 3-21b, the model would presumably be accurate.

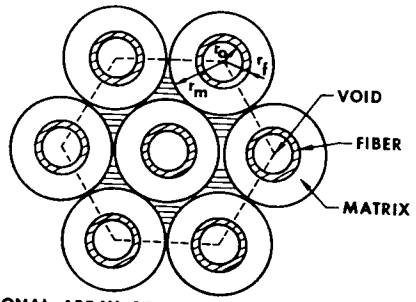

a HEXAGONAL ARRAY OF REGULAR HOLLOW FIBERS

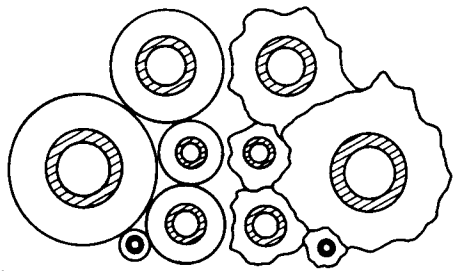

b RANDOM ARRAY OF IRREGULAR HOLLOW FIBERS

Figure 3-21 Hashin and Rosen's Fiber-Reinforcement Geometries and Composite-Cylinder Model *(After Hashin and Rosen [3-8])*

3.3.3 Exact Solutions

The problem of determining exact solutions to various cases of elastic inclusions in an elastic matrix is very difficult and well beyond the scope of this book. However, it is appropriate to indicate the types of solutions that are available and to compare them with the mechanics of materials results (in a later section). As in many other elasticity problems, the Saint-Venant semi-inverse method is prominent among the available techniques. In brief, the semi-inverse method consists of 'dreaming up' or assuming a part of the solution, i.e., some of the components of stress, strain, or displacement, and then seeing if the assumed solution satisfies the governing differential equations of equilibrium and the boundary conditions. The assumed solution must not be so rigorously specified that the equilibrium and compatibility equations cannot be satisfied. As an example, the assumption that plane sections remain plane is a semi-inverse method approach. In combination with the bounding theorem of elasticity, the semi-inverse method is quite effective.

Problems of inclusions in solids are also treated by exact elasticity approaches such as Muskhelishvili's complex-variable-mapping techniques [3-9]. In addition, numerical solution techniques such as finite elements and finite differences have been used extensively.

A strong background in elasticity is required for solution of problems in micromechanics of composite materials. Many of the available papers are quite abstract and of little direct applicability to practical analysis at this stage of development of elasticity approaches to micromechanics. Even the more sophisticated bounding approaches are a bit obscure.

The elasticity approaches depend to a great extent on the specific geometry of the composite material as well as on the characteristics of the fibers and the matrix. The fibers can be hollow or solid, but are usually circular in cross section, although rectangular-cross-section fibers are not uncommon. In addition, fibers are usually isotropic, but can have more complex material behavior, e.g., graphite fibers are transversely isotropic.

The fibers can exist in many types of cross-sectional arrays. Several typical arrays with various fiber types are shown in Figures 3-22 through 3-25. There, the representative volume element for each array is shown along with a simplified representative volume element that is just as representative by virtue of symmetry, but does not include a whole fiber (nor does it need to). Note in Figure 3-24 that if the rows of the staggered array with round fibers are offset by one-half the fiber spacing, the representative volume element is the same as for the square array, but with principal loading directions rotated by 45°. Also, the staggered array of rectangular cross-section fibers in Figure 3-25 is sometimes called a diamond array. Herrmann and Pister [3-10] were apparently the first to use the representative volume element and recognize its inherent symmetry.

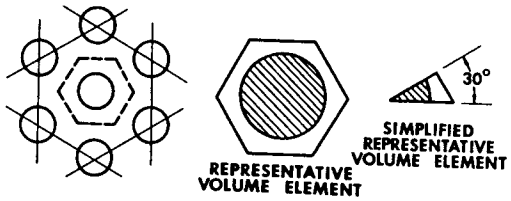

Figure 3-22 Hexagonal Array and Representative Volume Elements

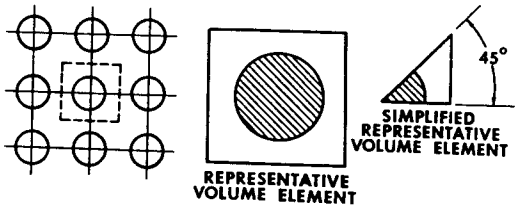

Figure 3-23 Square Array and Representative Volume Elements

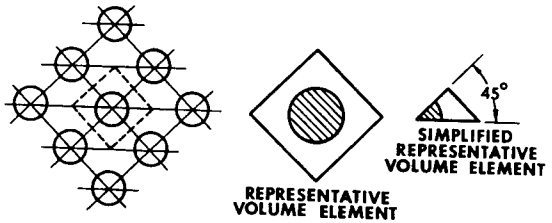

Figure 3-24 Staggered Square Array of Round Fibers and Representative Volume Elements

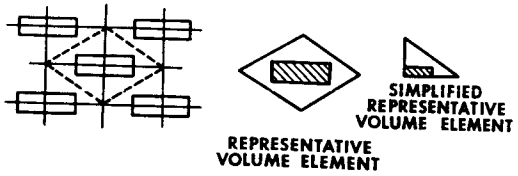

Figure 3-25 Staggered Square Array of Rectangular Fibers and Representative Volume Elements

Adams and Tsai [3-11] studied random arrays of two types: (1) square random arrays and (2) hexagonal random arrays. Both arrays have repeating elements so are not truly random. However, results of the hexagonal random-array analysis agree better with experiments than do results of the square random-array analysis. This observation is more satisfying than a previous result that (nonrandom) square-array analyses

agreed better with experiments than the more physically realistic hexagonal array analyses.

A variation on the exact solutions is the so-called self-consistent model that is explained in simplest engineering terms by Whitney and Riley [3-12]. Their model has a single hollow fiber embedded in a concentric cylinder of matrix material as in Figure 3-26. That is, only one inclusion is considered. The volume fraction of the inclusion in the composite cylinder is the same as that of the entire body of fibers in the composite material. Such an assumption is not entirely valid because the matrix material might tend to coat the fibers imperfectly and hence leave voids. Note that there is no association of this model with any particular array of fibers. Also recognize the similarity between this model and the concentric-cylinder model of Hashin and Rosen [3-8]. Other more complex self-consistent models include those by Hill [3-13] and Hermans [3-14] which are discussed by Chamis and Sendeckyj [3-5]. Whitney extended his model to transversely isotropic fibers [3-15] and to twisted fibers [3-16].

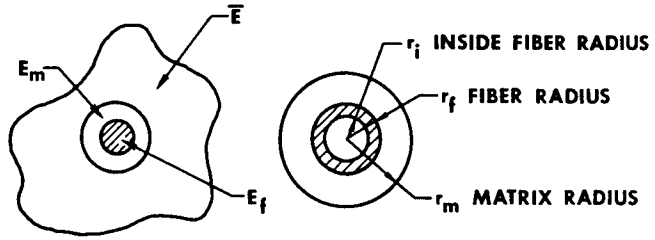

Figure 3-26 Self-Consistent Composite Cylinder Model

3.3.4 Elasticity Solutions with Contiguity

In the fabrication of fibrous composite materials, the fibers are often somewhat randomly placed rather than being packed in a regular array (see Figure 3-27). (This random nature is much more typical of small-diameter-fiber graphite-epoxy composite materials than of larger-diameter-fiber boron-epoxy composite materials.) Thus, the analyses for the moduli of composite materials with regular arrays must be modified to account for the fact that fibers are contiguous, i.e., that fibers touch each other rather than being entirely surrounded by matrix material. But, the fibers do not touch in many instances. Rather, some are contiguous and some are not. From an analytical point of view, a linear combination of (1) a solution in which all fibers are isolated from one another and (2) a solution in which all fibers contact each other provides the correct modulus. If C denotes degree of contiguity, then $C = 0$ corresponds to no contiguity (isolated fibers) and $C = 1$ corresponds to perfect contiguity (all fibers in contact) as in Figure 3-28. Naturally, with high volume fractions of fibers, C should approach $C = 1$. This approach is an example of what Chamis and Sendeckyj [3-5] call a semiempirical method, but it could also be classified as a bounding technique.

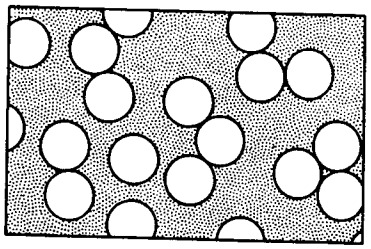

Figure 3-27 Schematic Diagram of Actual Fiber Arrangement

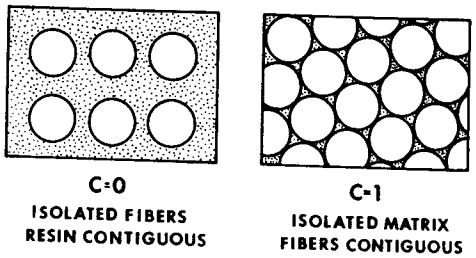

Figure 3-28 Extremes of Fiber Contiguity *(After Tsai [3-1])*

For the elasticity approach in which the contiguity is considered, Tsai [3-1] obtains for the modulus transverse to the fibers

$$E_2 = 2[1 - \nu_f + (\nu_f - \nu_m)V_m]\left[(1 - C)\frac{K_f(2K_m + G_m) - G_m(K_f - K_m)V_m}{(2K_m + G_m) + 2(K_f - K_m)V_m} + C\frac{K_f(2K_m + G_f) + G_f(K_m - K_f)V_m}{(2K_m + G_f) - 2(K_m - K_f)V_m}\right] \quad (3.64)$$

where

$$K_f = \frac{E_f}{2(1-\nu_f)} \quad G_f = \frac{E_f}{2(1+\nu_f)} \quad K_m = \frac{E_m}{2(1-\nu_m)} \quad G_m = \frac{E_m}{2(1+\nu_m)} \quad (3.65)$$

and C lies between 0 and 1. From a practical point of view, C would be determined by comparison of theoretical curves of E_2 versus V_f (or V_m) for various values of C with experimental results. The value of C for the prediction that best agrees with experiment is then the appropriate design value for the given material. Because C = 0 corresponds to the case where each fiber is isolated and C = 1 corresponds to the much less likely case where all fibers are in contact, low values of C should be expected.

Tsai also obtains

$$\nu_{12} = (1 - C)\frac{K_f\nu_f(2K_m + G_m)V_f + K_m\nu_m(2K_f + G_m)V_m}{K_f(2K_m + G_m) - G_m(K_f - K_m)V_m} + C\frac{K_m\nu_m(2K_f + G_f)V_m + K_f\nu_f(2K_m + G_f)V_f}{K_f(2K_m + G_m) + G_f(K_m - K_f)V_m} \quad (3.66)$$

$$G_{12} = (1 - C)G_m\frac{2G_f - (G_f - G_m)V_m}{2G_m + (G_f - G_m)V_m} + CG_f\frac{(G_f + G_m) - (G_f - G_m)V_m}{(G_f + G_m) + (G_f - G_m)V_m} \quad (3.67)$$

wherein the definitions of Equation (3.65) apply and C has the same value as in Equation (3.64).

For the modulus in the direction of the fibers, Tsai modified the rule of mixtures to account for imperfections in fiber alignment:

$$E_1 = k(V_fE_f + V_mE_m) \quad (3.68)$$

The fiber misalignment factor, k, ordinarily varies from .9 to 1, so Equation (3.68) does not represent a very significant departure from the rule of mixtures. Of course, k is an experimentally determined constant and is highly dependent on the manufacturing process.

Tsai [3-1] performed some interesting parametric studies for the values of E_1, E_2, ν_{12}, and G_{12} for glass-fiber–epoxy-resin composite materials. The baseline constituents have properties $E_f = 10.6 \times 10^6$ psi (73 GPa), $\nu_f = .22$, $E_m = .5 \times 10^6$ psi (3.5 GPa), and $\nu_m = .35$. By use of Equations (3.68), (3.64), (3.66), and (3.67), E_1, E_2, ν_{12}, and G_{12} are plotted in Figures 3-29 through 3-31 for the baseline composite material. In addition, the influence of fiber modulus is assessed by using $E_f = 16 \times 10^6$ psi (110 GPa) and $E_f = 6 \times 10^6$ psi (41 GPa) in the governing equations and is shown graphically in Figure 3-29. Similarly, the influence of the matrix modulus is shown in Figure 3-30 and that of the matrix and fiber Poisson's ratios in Figure 3-31. In all figures, the fiber misalignment factor, k, is unity and the fiber contiguity factor, C, is .2. Both values were found to be reasonable by comparison with experimental data (see Section 3.4, Comparison of Approaches to Stiffness).

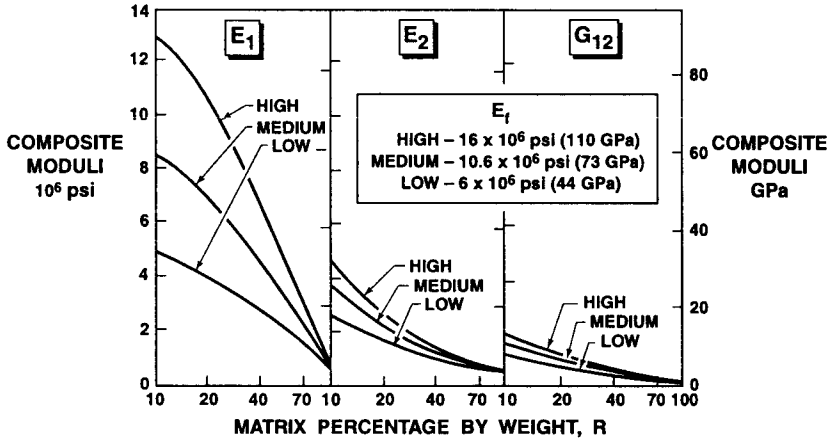

Figure 3-29 Contribution of E_f to E_1, E_2, and G_{12} *(After Tsai [3-1])*

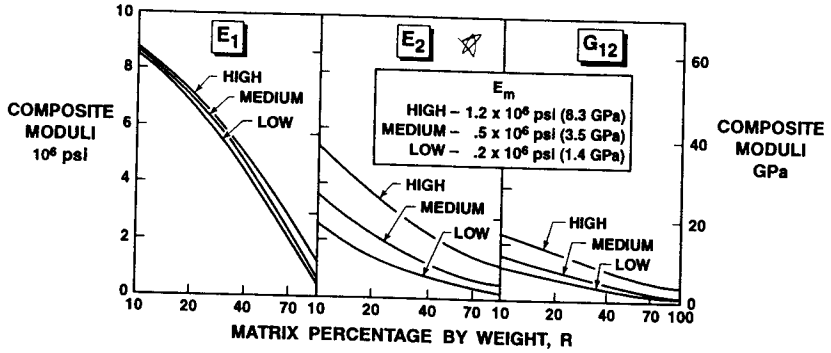

Figure 3-30 Contribution of E_m to E_1, E_2, and G_{12} *(After Tsai [3-1])*

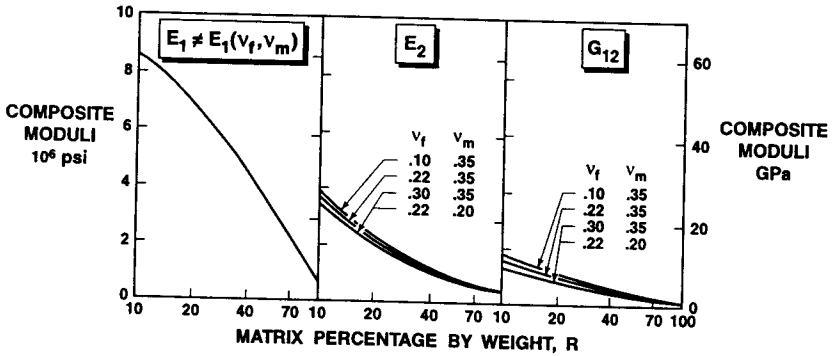

Figure 3-31 Contribution of v_f and v_m to E_1, E_2, and G_{12} *(After Tsai [3-1])*

The influence of the fiber modulus is felt most by the composite modulus in the fiber direction, E_1, as evidenced by Figure 3-29. The composite modulus transverse to the fiber direction, E_2, is most strongly influenced by the matrix modulus as seen in Figure 3-30 where E_m takes on values of 1.2×10^6 psi (8.3 GPa) and $.2 \times 10^6$ psi (1.4 GPa) in addition to the baseline value. The composite shearing modulus, G_{12} appears to be more strongly influenced by the matrix modulus than by the fiber modulus when Figures 3-29 and 3-30 are compared. From Figure 3-31, clearly the Poisson's ratios of the fiber and the matrix have little effect on the composite moduli for practical values of the Poisson's ratios. In fact, they have no effect on the composite modulus in the direction of the fibers, E_1, because they do not appear in the expression for that modulus. No study similar to that shown in Figures 3-29 through 3-31 was performed for the composite material major Poisson's ratio, v_{12}.

The contiguity factor, C, is actually a so-called 'fudge factor' used to make sense out of the comparison of experimental data with theoretical predictions. This correlation factor is useful only when the data fall between the theoretical bounds. The concept of a contiguity factor, i.e.,

some expression of the continuity of one phase of a composite material relative to another, is more easily seen to affect the tensile properties of a lamina than the compressive properties. There might be some interesting relation of contiguity to granule and fiber stiffnesses in tension and compression.

3.3.5 The Halpin-Tsai Equations

All of the preceding micromechanics results are represented by complicated equations and/or curves. The equations are usually somewhat awkward to use. The curves are generally restricted to a relatively small portion of the potential design regime. Thus, a need clearly exists for simple results to be used in the design of composite materials.

Halpin and Tsai [3-17] developed an interpolation procedure that is an approximate representation of more complicated micromechanics results. The beauty of the procedure is twofold. First, it is simple, so it can readily be used in the design process. Second, it enables the generalization of usually limited, although more exact, micromechanics results. Moreover, the procedure is apparently quite accurate if the fiber-volume fraction (V_f) does not approach one.

The essence of the procedure is that Halpin and Tsai [3-17] showed that Hermans' solution [3-14] generalizing Hill's self-consistent model [3-13] can be reduced to the approximate form

$$E_1 \cong E_f V_f + E_m V_m \tag{3.69}$$

$$v_{12} = v_f V_f + v_m V_m \tag{3.70}$$

and

$$\frac{M}{M_m} = \frac{1 + \xi \eta V_f}{1 - \eta V_f} \tag{3.71}$$

where

$$\eta = \frac{(M_f/M_m) - 1}{(M_f/M_m) + \xi} \tag{3.72}$$

in which

M = composite material modulus E_2, G_{12}, or v_{23}
M_f = corresponding fiber modulus E_f, G_f, or v_f
M_m = corresponding matrix modulus E_m, G_m, or v_m

and ξ is a measure of fiber reinforcement of the composite material that depends on the fiber geometry, packing geometry, and loading conditions. The values of ξ are obtained by comparing Equation (3-72) and another approximation, Equation (3-73), with exact elasticity solutions and assessing a value of, or function for, ξ by curve-fitting techniques.

Note that the expressions for E_1 and v_{12} are the generally accepted rule-of-mixtures results. The Halpin-Tsai equations are equally applicable to fiber, ribbon, or particulate composites. For example, Halpin and

Thomas [3-18] successfully applied Equations (3-72) and (3-73) to analysis of the stiffness of glass-ribbon-reinforced composite materials.

The only difficulty in using the Halpin-Tsai equations seems to be in the determination of a suitable value for ξ. Halpin and Tsai obtained excellent agreement with Adams and Doner's results [3-19] and [3-20] for circular fibers in a square array when $\xi = 2$ for calculation of E_2 and $\xi = 1$ for calculation of G_{12} at a fiber-volume fraction of .55 (see Figures 3-32 and 3-33). For the same values of ξ, excellent agreement was also obtained with Foye's results [3-21] and [3-22] for fibers with square cross sections in a diamond array when the fiber-volume fraction ranged up through .9 as in Figures 3-34 and 3-35. When Foye's rectangular cross-section fibers were addressed, Halpin and Tsai found that correlation with their equations required the value of ξ for transverse modulus calculations to be

$$\xi_{E_2} = 2\frac{a}{b} \tag{3.73}$$

where a/b is the rectangular cross-section aspect ratio. Also, the value of ξ for shear modulus calculations had to be

$$\log \xi_{G_{12}} = 1.73 \log \frac{a}{b} \tag{3.74}$$

to obtain the agreement with Foye's results shown in Figures 3-34 and 3-35.

Predictions of the Halpin-Tsai equations for glass-epoxy and boron-epoxy composite materials are shown in Figures 3-36 and 3-37. There, Foye's solutions for square arrays and hexagonal arrays are plotted in addition to Hermans' solution (to which the Halpin-Tsai equations are, of course, related). Note that the Halpin-Tsai predictions with $\xi = 2$ generally fall below the square-array results but above the hexagonal array results for $V_f > .65$. Below that fiber-volume fraction, the Halpin-Tsai results are quite close to Foye's square-array results.

However, Hewitt and de Malherbe [3-23] point out that the Halpin-Tsai equations yield an underestimate of the shear modulus G_{12} of composite materials with circular fibers in a square array for fiber-volume fractions greater than .5. Specifically, the underestimate is 30% at $V_f = .75$ for $G_f/G_m = 20$, a realistic value for both glass-epoxy and graphite-epoxy composite materials. They suggested that, instead of Halpin and Tsai's value of one for ξ, the value determined from

$$\xi = 1 + 40V_f^{10} \tag{3.75}$$

correlates better in the Halpin-Tsai equations with Adams and Donner's numerical solution as shown in Figure 3-38. Such a relation for ξ, like any other, is empirically determined. More refined estimates of ξ could be found, but care must be taken not to fall into the pit of deriving an expression that exceeds both the necessary accuracy requirements and defeats the original intent of a simple design tool that is easy to use.

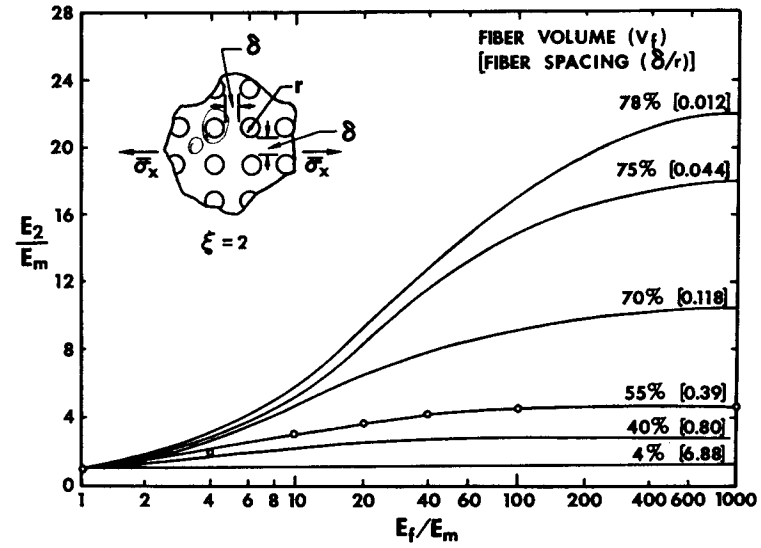

Figure 3-32 Halpin-Tsai Calculations (Circles) versus Adams and Doner's Calculations for E_2 of Circular Fibers in a Square Array *(After Halpin and Tsai [3-17])*

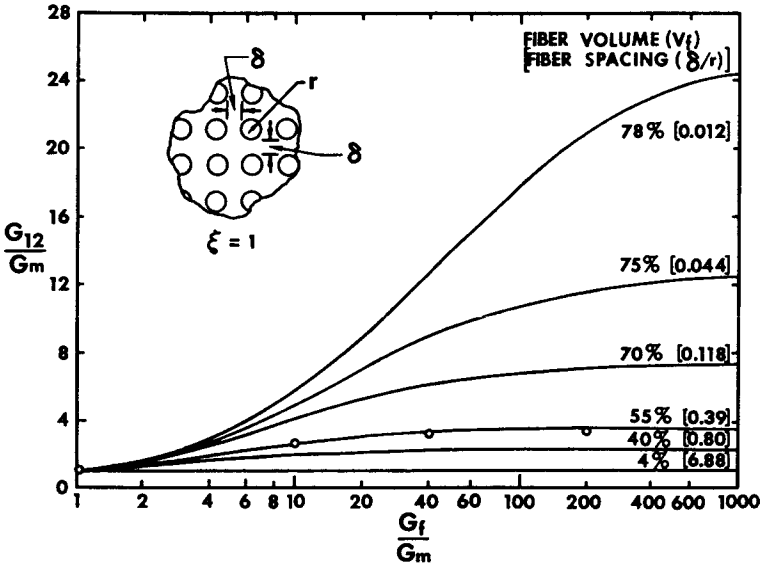

Figure 3-33 Halpin-Tsai Calculations (Circles) versus Adams and Doner's Calculations for G_{12} of Circular Fibers in a Square Array *(After Halpin and Tsai [3-17])*

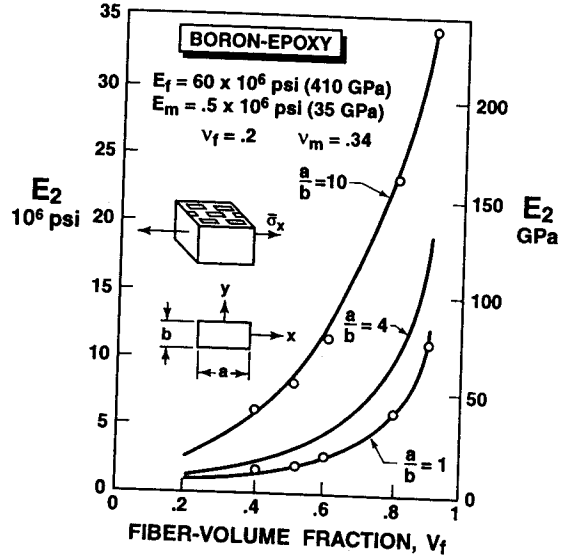

Figure 3-34 Halpin-Tsai Calculations (Circles) versus Foye's Calculations for E_2 of Rectangular Cross-Section Fibers in a Diamond Array *(After Halpin and Tsai [3-17])*

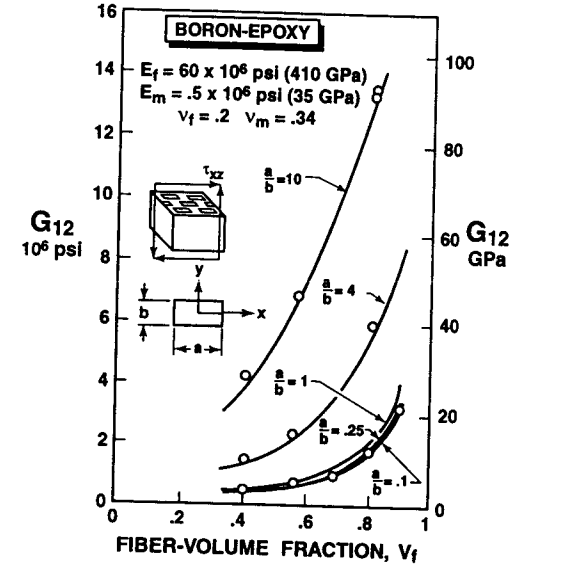

Figure 3-35 Halpin-Tsai Calculations (Circles) versus Foye's Calculations for G_{12} of Rectangular Cross-Section Fibers in a Diamond Array *(After Halpin and Tsai [3-17])*

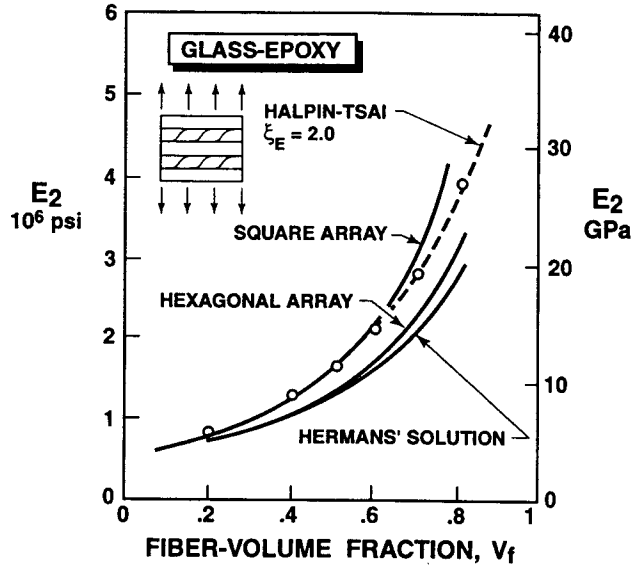

Figure 3-36 E_2 Calculations for a Glass-Epoxy Composite Material *(After Halpin and Tsai [3-17])*

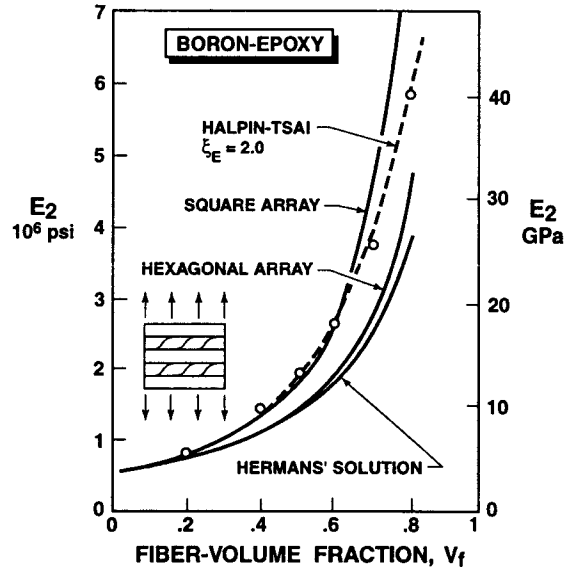

Figure 3-37 E_2 Calculations for a Boron-Epoxy Composite Material *(After Halpin and Tsai [3-17])*

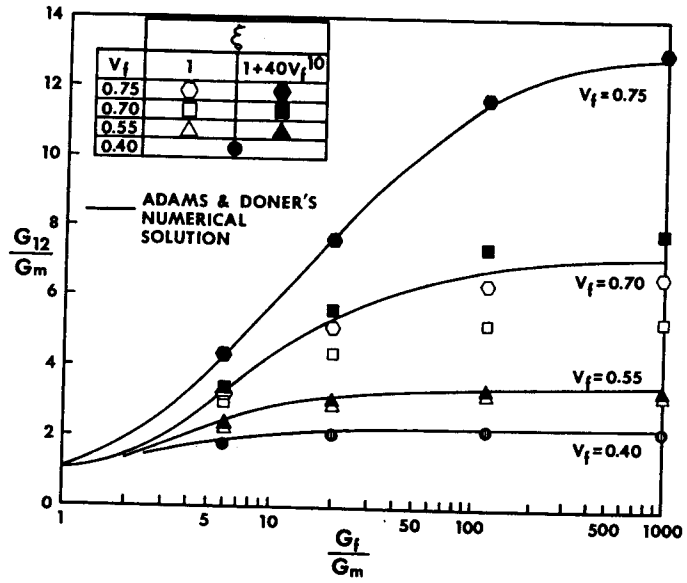

Figure 3-38 Modified Halpin-Tsai Calculations versus Adams and Donner's Calculations for G_{12} of Circular Fibers in a Square Array *(After Hewitt and de Malherbe [3-23])*

The mere existence of different predicted stiffnesses for different arrays leads to an important physical observation: Variations in composite material manufacturing will always yield variations in array geometry and hence in composite moduli. Thus, we cannot hope to predict composite moduli precisely, *nor is there any need to!* Approximations such as the Halpin-Tsai equations should satisfy all practical requirements.

Some physical insight into the Halpin-Tsai equations can be gained by examining their behavior for the ranges of values of ξ and η. First, although it is not obvious, ξ can range from 0 to ∞. When $\xi = 0$,

$$\frac{1}{M} = \frac{V_f}{M_f} + \frac{V_m}{M_m} \tag{3.76}$$

which is the series-connected model generally associated with a lower bound of a composite material modulus. When $\xi = \infty$,

$$M = V_f M_f + V_m M_m \tag{3.77}$$

which is the parallel-connected model, known as the rule of mixtures, generally associated with an upper bound of a composite material modulus. Thus, ξ is a measure of the reinforcement of the composite material by the fibers. For small values of ξ, the fibers are not very effective, whereas for large values of ξ, the fibers are extremely effective in increasing the composite stiffness above the matrix stiffness. Next, the limiting values of η can be shown to be: for rigid inclusions,

$$\eta = 1 \tag{3.78}$$

for homogeneous materials,

$$\eta = 0 \tag{3.79}$$

and for voids,

$$\eta = -\frac{1}{\xi} \tag{3.80}$$

The term ηV_f in Equation (3.71) can be interpreted as a reduced fiber-volume fraction. The word 'reduced' is used because $\eta \leq 1$. Moreover, it is apparent from Equation (3.72) that η is affected by the constituent material properties as well as by the reinforcement geometry factor ξ. To further assist in gaining appreciation of the Halpin-Tsai equations, the basic equation, Equation (3.71), is plotted in Figure 3-39 as a function of ηV_f. Curves with intermediate values of ξ can be quickly generated. Note that all curves approach infinity as ηV_f approaches one. Obviously, practical values of ηV_f are less than about .6, but most curves are shown in Figure 3-39 for values up to about .9. Such master curves for various values of ξ can be used in design of composite materials.

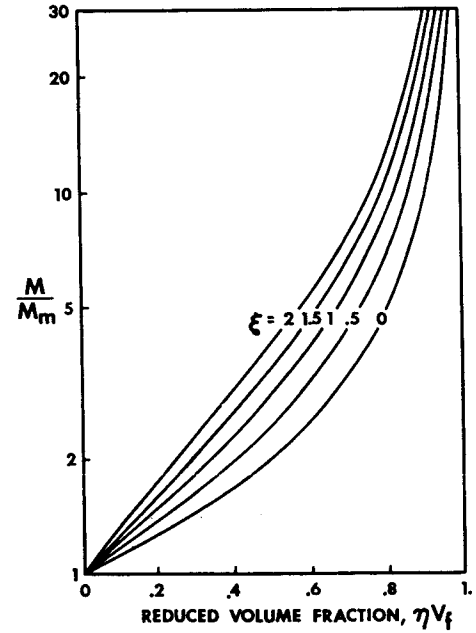

Figure 3-39 Master M/M_m Curves for Various ξ

3.3.6 Summary Remarks

There is much controversy associated with micromechanical analyses and predictions. Much of the controversy has to do with which approximations should be used. The Halpin-Tsai equations seem to be a commonly accepted approach.

One of the important conclusions of some of the microstructure work (see Chamis and Sendeckyj [3-5]) is that macroscopic homogeneity may *not* exist for composite materials. That is, microstructural considerations might be required.

Problem Set 3.3

3.3.1 Derive Equations (3.52) and (3.53), and use them to derive Equation (3.54).

3.3.2 Consider a dispersion-stiffened composite material. Determine the influence on the upper bound for the apparent Young's modulus of different Poisson's ratios in the matrix and in the dispersed material. Consider the following three combinations of material properties of the constituent materials:

Case	E_m	ν_m	E_d	ν_d
1	5×10^6 psi (34.5 GPa)	0	50×10^6 psi (345 GPa)	.3
2	5×10^6 psi (34.5 GPa)	.3	50×10^6 psi (345 GPa)	.3
3	5×10^6 psi (34.5 GPa)	.3	50×10^6 psi (345 GPa)	0

The values of E for values of $V_d = 0, .2, .4, .6, .8$, and 1.0 (and any values in between necessary to plot representative curves) should be tabulated and plotted as E versus V_d so that both specific numerical and visual differences can be examined.

3.3.3 Use the bounding techniques of elasticity to determine upper and lower bounds on the shear modulus, G, of a dispersion-stiffened composite material. Express the results in terms of the shear moduli of the constituents (G_m for the matrix and G_d for the dispersed particles) and their respective volume fractions (V_m and V_d). The representative volume element of the composite material should be subjected to a macroscopically uniform shear stress τ which results in a macroscopically uniform shear strain γ.

3.3.4 Determine the bounds on E for a dispersion-stiffened composite material of more than two constituents, i.e., more than one type of particle is dispersed in a matrix material.

3.3.5 Derive Equation (3.76).

3.3.6 Derive Equation (3.77).

3.3.7 Show that the limiting values of η are given correctly by Equations (3.78)–(3.80).

3.4 COMPARISON OF APPROACHES TO STIFFNESS

3.4.1 Particulate Composite Materials

The mechanics of materials approach to the estimation of stiffness of a composite material has been shown to be an upper bound on the actual stiffness. Paul [3-4] compared the upper and lower bound stiffness predictions with experimental data [3-24 and 3-25] for an alloy of tungsten carbide in cobalt. Tungsten carbide (WC) has a Young's modulus of 102×10^6 psi (703 GPa) and a Poisson's ratio of .22. Cobalt (Co) has a Young's modulus of 30×10^6 psi (207 GPa) and a Poisson's ratio of .3.

The constituent material properties are substituted in Equations (3.61) and (3.57) to obtain the upper bound on E of the composite material and in Equation (3.47) to obtain the lower bound on E. In addition, the mechanics of materials approach studied in Problems 3.2.1 through 3.2.4 is also compared with the experimental data. Specifically, the result

for the modulus of a composite material that is stiffened by dispersion of cube-shaped particles is used, that is

$$\frac{E}{E_m} = \frac{E_m + (E_d - E_m)V_d^{2/3}}{E_m + (E_d - E_m)V_d^{2/3}\left(1 - V_d^{1/3}\right)} \tag{3.81}$$

The predictions of the various approaches are plotted along with experimental data in Figure 3-40. Note that the upper bound on Young's modulus, E, is indistinguishable from a straight line. Thus, the effect of Poisson's ratio, ν, in Equation (3.61) on the result of Equation (3.57) is negligible for the Poisson's ratios and Young's moduli of cobalt and tungsten carbide. For practical purposes, the upper bound is given by the simple mechanics of materials expression known as the rule of mixtures:

$$E = E_m V_m + E_d V_d \tag{3.82}$$

in which $\nu_m = \nu_d$. The experimental data for E fall between the upper and lower bounds for E as they must for the bounds to be true bounds. Moreover, the approximate mechanics of materials prediction, Equation (3.81), appears to agree very well with the experimental data indicated with the triangles. The data indicated with open circles do not correlate particularly well with the approximate prediction of Equation (3.81). However, no information is available regarding the shape of the dispersed particles. In addition, the constituent materials might not be precisely the same in both sets of experimental data. Hashin and Shtrikman [3-7] obtained much closer bounds on the same experimental data.

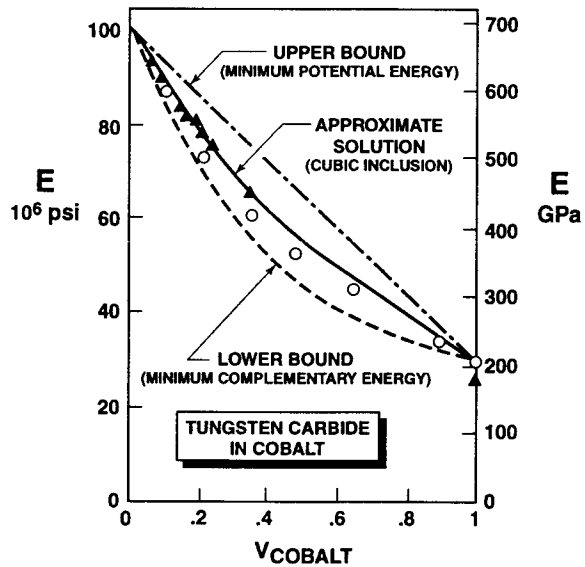

Figure 3-40 Predicted Modulus Bounds and Experimental Data for Tungsten Carbide in Cobalt *(After Paul [3-4])*

3.4.2 Fiber-Reinforced Composite Materials

Tsai conducted experiments to measure the various moduli of glass-fiber–epoxy-resin composite materials [3-1]. The glass fibers and epoxy resin had a Young's modulus and Poisson's ratio of 10.6×10^6 psi (73 GPa) and .22 and $.5 \times 10^6$ psi (3.5 GPa) and .35, respectively.

For various volume fractions of fibers, the experimental results are compared with the theoretical results in Equations (3.68), (3.64), (3.66), and (3.67) for E_1, E_2, ν_{12}, and G_{12}, respectively. The theoretical results depend on k, the fiber misalignment factor, and C, the contiguity factor, so theoretical curves can be drawn for a wide range of values of k and C. The objective of the comparison of theoretical and experimental results is to demonstrate both qualitative and quantitative agreement in order to validate a theoretical prediction. If the theoretical results have the same shape as the experimental results, then the agreement is termed qualitative. Further, if, by consistent adjustment of the parameters k and C, the two sets of results agree in value as well, then the agreement is termed quantitative. Thus, the concepts of fiber misalignment factor and a contiguity factor will be investigated.

The experimental and theoretical results for E_1 are shown in Figure 3-41 for a resin content by weight ranging from 10% to 100%. Because E_1 is not a function of C, only k was varied — two values were chosen: $k = 1$ and $k = .9$. Some experimental results in Figure 3-41 lie above the curve for $k = 1$ (i.e., above the upper bound!); some results lie below $k = .9$. However, most results lie between $k = .9$ and $k = 1$ with $k = .9$ being a conservative estimate of the behavior. The actual specimens were handmade, so the resin content might not be precise, and fiber misalignment is not unexpected. Thus, the results above the upper bound are not unusual nor is the basic fact of variation in E_1.

The theoretical and measured results for E_2 are shown in Figure 3-41 as a function of resin content by weight. Theoretical results from Equation (3.64) are shown for $C = 0, .2, .4$, and 1, and the data are bounded by the curves for $C = 0$ and $C = .4$. The theoretical curve labeled 'glass-resin connected in series' is a lower, lower bound than the $C = 0$ curve and is an overly conservative estimate of the stiffness.

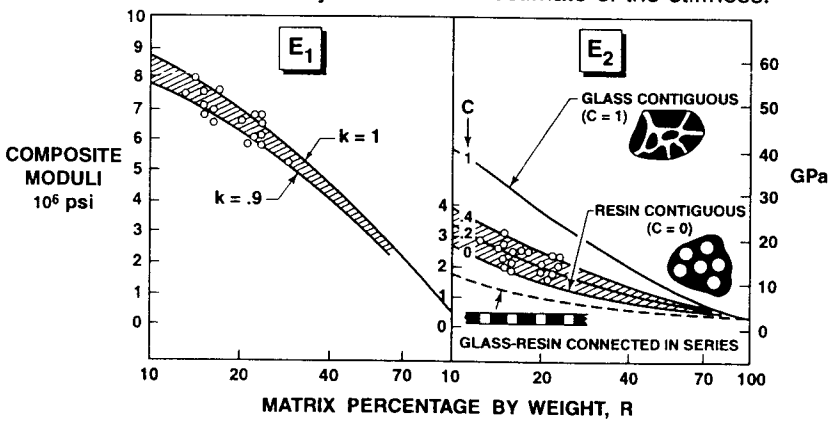

Figure 3-41 E_1 and E_2 versus Resin Content *(After Tsai [3-1])*

The existence of a contiguity factor, C, has been reasonably well demonstrated by the results of Figure 3-41. However, a more critical examination of the concept of a contiguity factor is in order. For this purpose, some special experiments were devised in which steel-epoxy composite materials were used. In order to obtain a composite material with $C = 0$ (no contiguity of fibers, i.e., no fibers touch), steel rods were inserted in holes in an epoxy bar. For a composite material with $C = 1$ (perfect contiguity of fibers, i.e., all fibers touch), epoxy resin was placed in holes in a steel bar. In both cases, there were 54 holes transverse to the longitudinal axis of the bar. Thus, when the bars in Figure 3-42 are pulled in their longitudinal direction, the modulus E_2 can be measured. The steel is always regarded as the fiber, so $E_f = 30 \times 10^6$ psi (207 GPa) and $\nu_f = .3$. The epoxy material has values $E_m = .45 \times 10^6$, $.60 \times 10^6$, and $.50 \times 10^6$ psi (3.1, 4.1, and 3.5 GPa) for three successive cases in addition to $\nu_m = .35$. The results for E_2 in the three cases are summarized in Figure 3-43. Note that the range of matrix content for the right-hand panel of Figure 3-43 is one-tenth the range of the left-hand and center panels. Moreover, the vertical scale of the right-hand panel is ten times that of the left-hand and center panels. Obviously, the experimental data agree very well with the results from Equation (3.64) for the cases $C = 0$ and $C = 1$. The data for $C = 1$ are fairly close to the theoretical results, but recognize that such small percentages of matrix are involved that the comparison is difficult. On the other hand, the data for $C = 0$ agree to an extent that is a little surprising. Thus, the physical significance of the contiguity factor has been established.

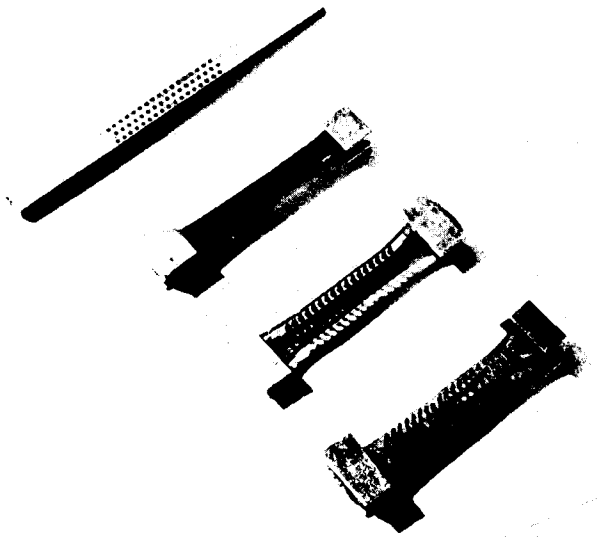

Figure 3-42 Steel-Epoxy Specimens *(After Tsai [3-1])*

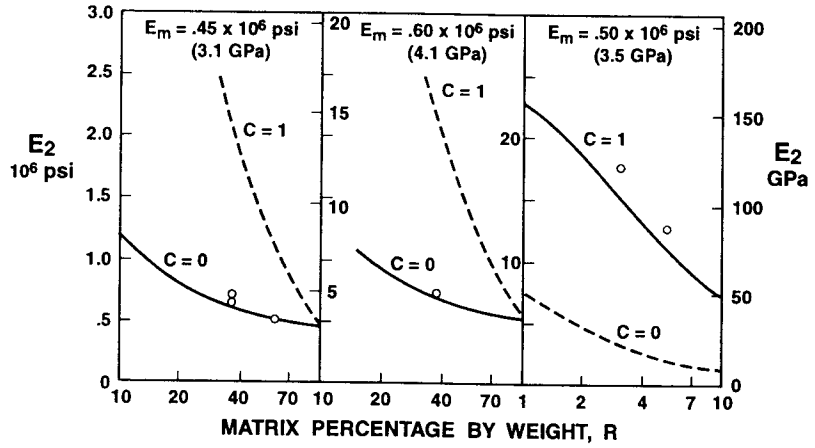

Figure 3-43 E_2 of Steel-Epoxy Composite Materials with C = 0 and C = 1 *(After Tsai [3-1])*

The experimental results for ν_{12} of a glass-epoxy composite material are shown along with the theoretical prediction from Equation (3.66) as a function of resin content by weight in Figure 3-44. Theoretical results are shown for contiguity factors of C = 0, .2, .4, and 1. Apparently, C = 0 is the upper limit of the data whereas C = .4 is the lower limit. Thus, the concept of contiguity factor is further reinforced.

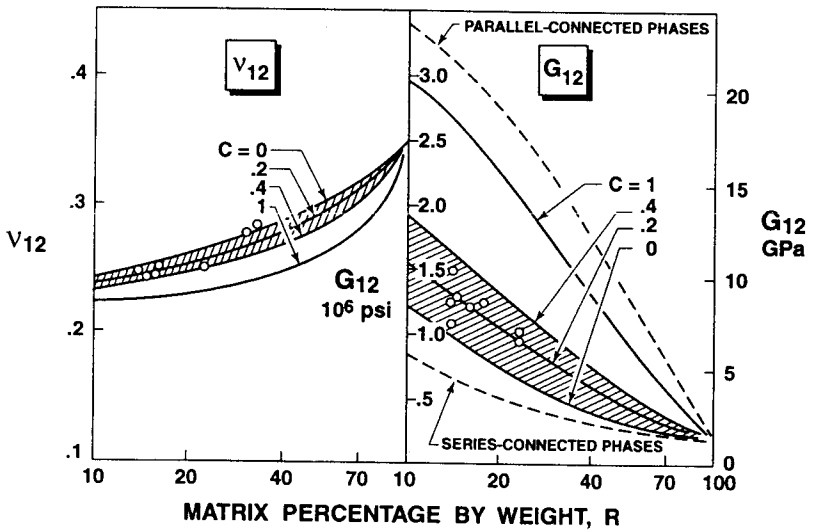

Figure 3-44 ν_{12} and G_{12} of a Glass-Epoxy Composite Material *(After Tsai [3-1])*

The experimental results for G_{12} are also shown in Figure 3-44, along with theoretical results from Equation (3.67) for C = 0, .2, .4, and 1. As with the previous moduli, the experimental data are bounded by curves for C = 0 and C = .4. The upper (parallel-connected phases) and lower (series-connected phases) bounds due to Paul (see Section 3.3) are shown to demonstrate the accuracy of the bounds in the present case where E_f is much greater than E_m. The lower bound results of Hashin and Rosen [3-8] correspond to C = 0, but their upper bound is below some of the experimental data in Figure 3-44.

3.4.3 Summary Remarks

For particulate-reinforced composite materials, Paul derived upper and lower bounds on the composite modulus [3-4]. His approximate mechanics of materials solution agrees fairly well with experimental data for tungsten carbide particles in cobalt.

For fiber-reinforced composite materials, Tsai gives expressions for E_1, E_2, ν_{12}, and G_{12} that are in good agreement with experimental data for a glass-fiber-reinforced–epoxy-resin composite material [3-1]. A contiguity factor, C, is the key to the agreement. Thus, the constituent material properties have the following effects on the properties of the composite material:

(1) E_f makes a significant contribution to E_1
(2) E_m makes a significant contribution to E_2 and G_{12}
(3) ν_f and ν_m have little effect on E_2 and G_{12} and no effect on E_1

The contiguity factor is very important for glass-fiber-reinforced composite materials for which $E_f/E_m = 20$. However, for composite materials for which E_f/E_m is close to unity, contiguity is probably not important. This latter conclusion is deduced from the results for C = 0 and C = 1 in Figure 3-45 where a fictitious glass-epoxy composite material is considered. There, a fictitious matrix with $E_m = 5 \times 10^6$ psi (34.5 GPa) is combined with a high-modulus glass fiber ($E_f = 16 \times 10^6$ psi) (110 GPa) to give $E_f/E_m = 3.2$. Note in Figure 3-45 that E_2, as calculated from Equation (3.64), changes very little between C = 0 and C = 1.

3.5 MECHANICS OF MATERIALS APPROACH TO STRENGTH

3.5.1 Introduction

Prediction of the strength of fiber-reinforced composite materials has not achieved the near-esoteric levels of the stiffness predictions studied in the preceding sections. Nevertheless, there are many interesting physical models for the strength characteristics of a matrix reinforced by fibers. Most of the models represent a very high degree of integration of physical observation with the mechanical description of a phenomenon.

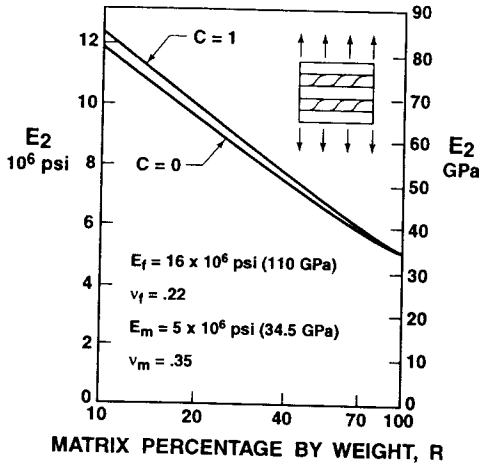

Figure 3-45 E_2 of a Fictitious Glass-Epoxy Composite Material *(After Tsai [3-1])*

Two major topics will be addressed in this section: tensile strength and compressive strength of a unidirectionally reinforced lamina in the fiber direction. The tensile strength will be examined in Section 3.5.2 by use of a model with fibers that all have the same strength in addition to a model in which the fibers have a statistical strength distribution. The compressive strength will be examined in Section 3.5.3 by use of a model for buckling of fibers surrounded by a matrix. These two topics occupied the attention of many fine investigators for ten years or so. However, to date, little work has been done on other topics of obvious importance such as prediction of shear strength.

3.5.2 Tensile Strength in the Fiber Direction

A unidirectional fiber-reinforced composite material deforms as the load increases in the following four stages, more or less, depending on the relative brittleness or ductility of the fibers and the matrix:

(1) Both fibers and matrix deform elastically
(2) The fibers continue to deform elastically, but the matrix deforms plastically
(3) Both the fibers and the matrix deform plastically
(4) The fibers fracture followed by fracture of the composite material

These stages are illustrated in Figure 3-46 for generic stress-strain curves for the fibers, matrix, and composite material. Note that the fibers are generally the stiffer, stronger, and less ductile of the two composite material constituents. as implied in Figure 3-46. Of course, for brittle fibers, stage 3 might not be realized. Similarly, a brittle matrix might not achieve either stage 2 or 3. Whether fracture of the composite material occurs as a fiber failure or as a matrix failure depends on the relative ductility of the fibers versus matrix as well as on the fiber-volume fraction.

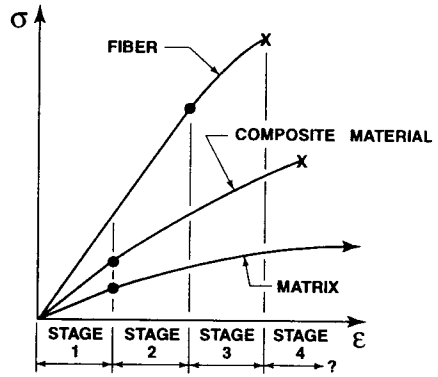

Figure 3-46 Deformation Stages of a Fiber-Reinforced Composite Material

Fibers of Equal Strength

Consider fibers that all have the same strength and are relatively brittle in comparison to the matrix as studied by Kelly and Davies [3-26]. Moreover, both the fibers and matrix are active only in the linear elastic range (stage 1 in Figure 3-46). If the composite material has more than a certain minimum volume fraction of fibers, V_f, the ultimate strength is achieved when the fibers are strained to correspond to their maximum (ultimate) stress. That is, in terms of strains,

$$\varepsilon_{c_{max}} = \varepsilon_{f_{max}} \tag{3.83}$$

Because the fibers are more brittle than the matrix, they cannot elongate as much as the matrix. Thus, the fibers are the weak link, from the strain viewpoint, in the strength chain that the composite material comprises.

The schematic stress-strain curves for the fibers and the matrix shown in Figure 3-47 (again, stage 1 only of Figure 3-46) are useful in interpreting the reasoning to obtain the composite material strength. Thus, if the fiber strain is presumed equal to the matrix strain in the direction of the fibers (as in the micromechanics prediction for E_1), then the strength of the composite material is

$$\sigma_{c_{max}} = \sigma_{f_{max}} V_f + (\sigma_m)_{\varepsilon_{f_{max}}} (1 - V_f) \tag{3.84}$$

where

$\sigma_{f_{max}}$ = maximum fiber tensile stress

$(\sigma_m)_{\varepsilon_{f_{max}}}$ = matrix stress at a matrix strain equal to the maximum tensile strain in the fibers

Obviously, if fiber reinforcement is to lead to a greater strength than can be obtained with the matrix alone, then

$$\sigma_{c_{max}} > \sigma_{m_{max}} \tag{3.85}$$

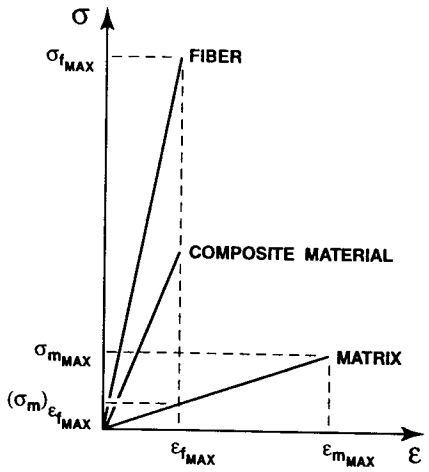

Figure 3-47 Schematic Stress-Strain Curves for Fibers and Matrix

Equations (3.84) and (3.85) can be solved for the critical V_f that must be exceeded to obtain fiber strengthening of the composite material:

$$V_{f_{critical}} = \frac{\sigma_{m_{max}} - (\sigma_m)_{\varepsilon_{f_{max}}}}{\sigma_{f_{max}} - (\sigma_m)_{\varepsilon_{f_{max}}}} \tag{3.86}$$

For smaller values of V_f, the behavior of the composite material might not follow Equation (3.84) because there might not be enough fibers to control the matrix elongation. That is, the matrix dominates the composite material and 'carries the fibers along for the ride'. Thus, the fibers would be subjected to high strains with only small loads and would fracture. If all fibers break at the same strain (an occurrence that is quite unlikely from a statistical standpoint), then the composite material will fracture unless the matrix (which occupies only V_m of the representative volume element) can take the entire load imposed on the composite material, that is,

$$\sigma_{c_{max}} < \sigma_{m_{max}} V_m \tag{3.87}$$

Thus, in this case, the matrix is the only contributor to the composite material strength. In fact, the composite material acts as matrix of amount V_m and *holes*, not fibers, of amount V_f! Finally, the entire composite material fails after fracture of the fibers if

$$\sigma_{c_{max}} = \sigma_{f_{max}} V_f + (\sigma_m)_{\varepsilon_{f_{max}}} (1 - V_f) \geq \sigma_{m_{max}} (1 - V_f) \tag{3.88}$$

from which a minimum V_f for validity of Equation (3.88) can be obtained as

$$V_{f_{minimum}} = \frac{\sigma_{m_{max}} - (\sigma_m)_{\varepsilon_{f_{max}}}}{\sigma_{f_{max}} + \sigma_{m_{max}} - (\sigma_m)_{\varepsilon_{f_{max}}}} \tag{3.89}$$

The preceding expressions, Equations (3.84) through (3.89), are more easily understood when they are plotted as in Figure 3-48. There, the composite material strength (i.e., the maximum composite material stress) is plotted as a function of the fiber-volume fraction. When V_f is less than $V_{f_{minimum}}$, the composite material strength is controlled by the matrix deformation and is actually less than the matrix strength. When V_f is greater than $V_{f_{minimum}}$, but less than $V_{f_{critical}}$, the composite material strength is controlled by the fiber deformation, but the composite material strength is still less than the inherent matrix strength. Only when V_f exceeds $V_{f_{critical}}$ does the composite material gain strength from having fiber reinforcement. Then, the composite material strength is controlled by the fiber deformations because V_f is greater than $V_{f_{minimum}}$. Note that the shape of Figure 3-48 will vary as $V_{f_{critical}}$ varies. Also, from Equation (3.86), $V_{f_{critical}}$ is small when

$$\sigma_{m_{max}} \cong (\sigma_m)_{\varepsilon_{f_{max}}} \tag{3.90}$$

as is the case for glass fibers reinforcing a resin matrix. In the latter case, the composite material strength is always fiber-controlled because $V_{f_{critical}}$ always exceeds $V_{f_{minimum}}$.

The preceding analysis is premised on having continuous fibers of equal strength all of which fracture at the same longitudinal position. However, fibers under tension do not all have the same fracture strength nor do they fracture in the same place. Rather, because surface imperfections vary from fiber to fiber, the individual fibers have different fracture strengths. A statistical analysis is then necessary to rationally define the strength of a composite material.

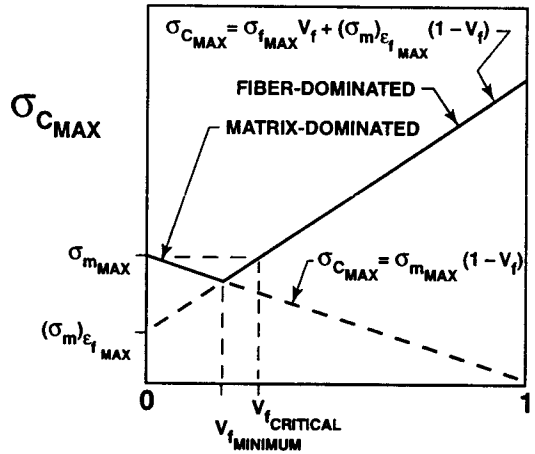

Figure 3-48 Composite Tensile Strength versus Fiber-Volume Fraction *(After Kelly and Davies [3-26])*

Fibers with a Statistical Strength Distribution

Rosen analyzed the strength of composite materials reinforced by fibers with a statistical strength distribution by use of the model shown in Figure 3-49 [3-27]. There, the representative volume element includes several fibers that are not broken and one fiber that is broken. Obviously, the representative volume element either changes size during loading and subsequent fiber fracture or else the number of fiber fractures in a fixed-size volume element increases. The broken fiber has presumably been subjected to a stress high enough to initiate fracture at a surface imperfection. The broken fiber causes redistribution of stresses around the fracture. Stress must then pass from one end of the broken fiber past the break to the other end. The mechanism for accomplishing this stress transfer is the development of high shear stresses in the matrix over a short distance from the fiber break as shown in Figure 3-49. The longitudinal fiber stress is thereby increased from zero at the break to the stress level, σ_f, of any other fiber in the composite material far from the break. Thus, the fiber-tension problem is transformed into a fiber-pull-out problem after fiber fracture.

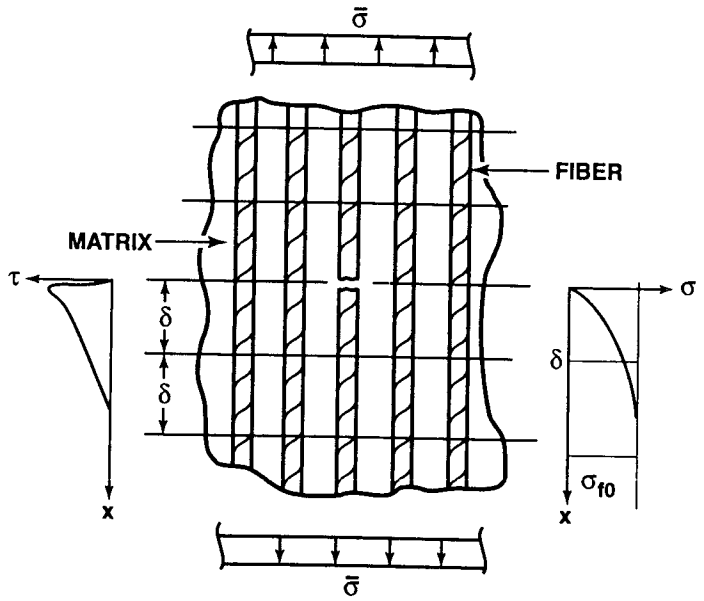

Figure 3-49 Rosen's Tensile Failure Model *(After Rosen [3-27])*

Failure of the composite material can then occur in two ways. First, the matrix shear stress around the fiber could exceed the allowable matrix shear stress. More precisely, the bond between the fiber and the matrix might be broken due to high shear stress in the aforementioned mechanism for transfer of stress between broken fibers. Second, the fiber fracture could actually propagate across the matrix through other fibers and hence cause overall fracture of the composite material. If a good bond is achieved between the fiber and the matrix and if the matrix fracture toughness is high, then the fiber fractures can continue until the statistical accumulation is sufficient to cause gross composite material fracture.

By use of statistical analysis, Dow and Rosen [3-28] obtained

$$\sigma_{c_{max}} = \sigma_{ref} V_f \left[\frac{1 - V_f^{1/2}}{V_f^{1/2}} \right]^{-1/(2\beta)} \tag{3.91}$$

where σ_{ref} is a reference stress level that is a function of the fiber and matrix properties and β is a statistical parameter in the Weibull distribution of fiber strength.

Rosen's results are plotted in Figure 3-50 for $\beta = 7.7$, a representative value for commercial E-glass fibers. Also plotted in Figure 3-50 is the rule-of-mixtures expression

$$\sigma_{c_{max}} = \sigma_{ref} V_f \tag{3.92}$$

in which the tensile strength of the matrix has been ignored because it is much less than the fiber tensile strength. Thus, σ_{ref} must be interpreted as essentially the fiber tensile strength, but with some statistical implications. Note in Figure 3-50 that Rosen's results from Equation (3.91) do not go to one at $V_f = 1$. This behavior occurs because the fiber packing has a maximum density as a hexagonal array of uniform-diameter fibers for which $V_f = .904$. Note that Rosen's results are close to the rule-of-mixtures expression. However, the two expressions are based on such widely differing approaches that it is fallacious to infer from mere agreement with each other and with experimental data that the correct physical theory has been found.

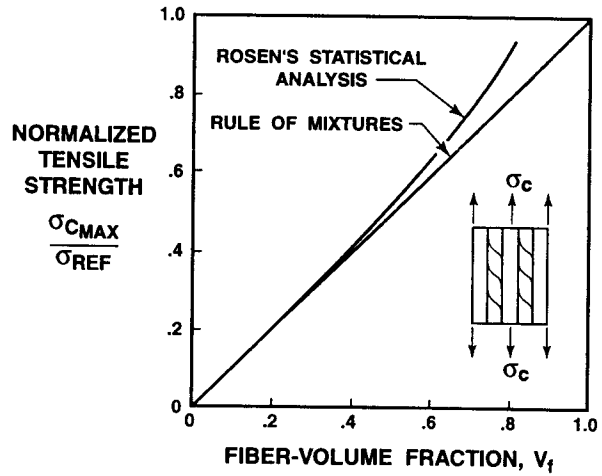

Figure 3-50 Composite Tensile Strength versus Fiber-Volume Fraction *(After Dow and Rosen [3-28])*

Several interesting conclusions can be drawn from observation of Figure 3-50. Basically, the fracture strength of the composite material exceeds that of an individual fiber because Rosen's results lie above the rule-of-mixtures expression. Moreover, the energy-absorption capacity of the composite material also exceeds that of the fibers. These characteristics follow from observation of Figures 3-51 and 3-52 where, first, fiber strength (E-glass fibers) is shown to be inversely proportional to fiber length and, second, the number of fiber fractures is seen to increase as the ultimate load for the composite material is approached. Note in Figure 3-52 that fibers actually fracture at half the ultimate load and that the number of fractures rapidly accumulates until the overall composite material fractures. Figure 3-51 on fiber strength versus length can be rationalized by likening a fiber with surface imperfections to a chain; the longer the chain (fiber), the higher the probability of a weak link (surface imperfection).

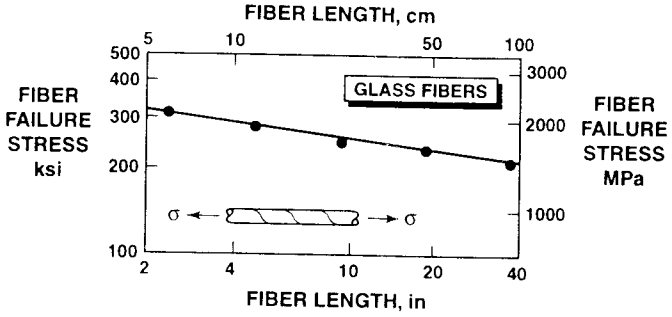

Figure 3-51 Fiber Tensile Strength versus Fiber Length
(After Dow and Rosen [3-28])

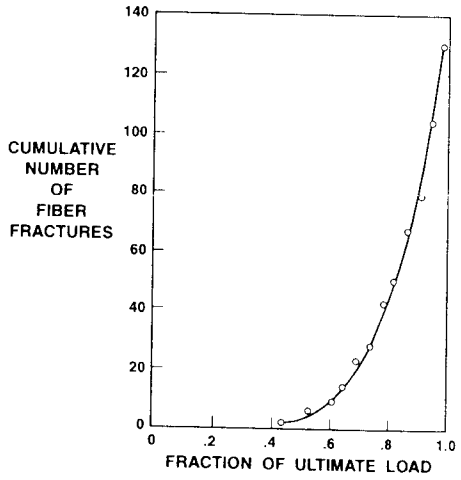

Figure 3-52 Cumulative Number of Fiber Fractures versus Percentage of Ultimate Composite Load
(After Rosen, Dow, and Hashin [3-29])

Definitive studies of composite material tensile strength from a micromechanics viewpoint simply do not exist. Obviously, much work remains in this area before composite materials can be accurately designed, i.e., constituents chosen and proportioned to resist a specified tensile stress.

3.5.3 Compressive Strength in the Fiber Direction

When fiber-reinforced composite materials are loaded in compression, Dow and Rosen speculate that the mode of failure appears to be fiber buckling within the restraint of the matrix material [3-28]. One indication of such failures is the periodic nature of the photoelastic stress pattern for the E-glass fibers of three different diameters in an epoxy matrix shown in Figure 3-53. If fiber buckling were to occur in the matrix, then a column on an elastic foundation model would appear to be reasonable. For such a model, the buckle wavelength can be shown to be directly proportional to the fiber diameter. This theoretical result is verified by the experimental data shown in Figure 3-54 where a best-fit linear relation is represented as a 45° line on the log-log plot. Moreover, those data further strengthen the overall hypothesis that fiber buckling is responsible for compressive failure. This mode of failure was called microbuckling by Greszczuk [3-30]. Note that, thus far, we have avoided making arbitrary assumptions, but instead are attempting to make effective approximations that are guided by careful observations of actual behavior.

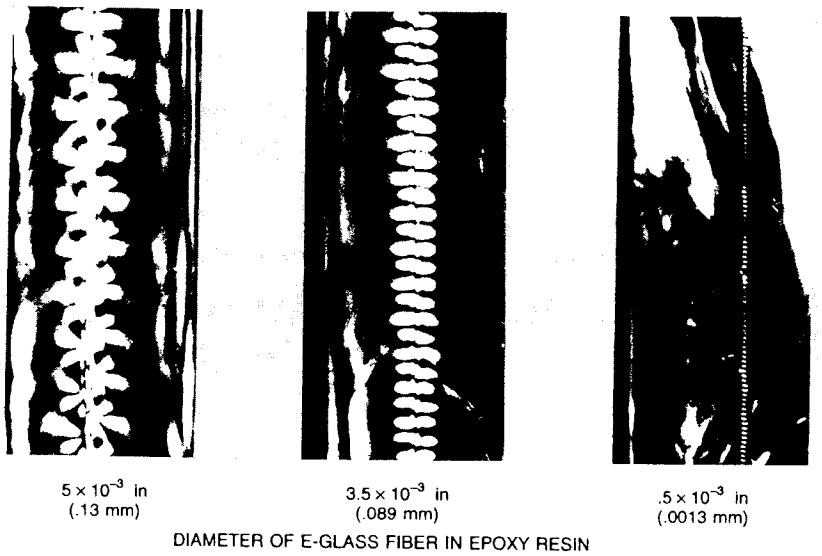

Figure 3-53 Photoelastic Stress Patterns for Three E-glass Fibers Embedded in an Epoxy Matrix
(Courtesy of Materials Sciences Corporation)

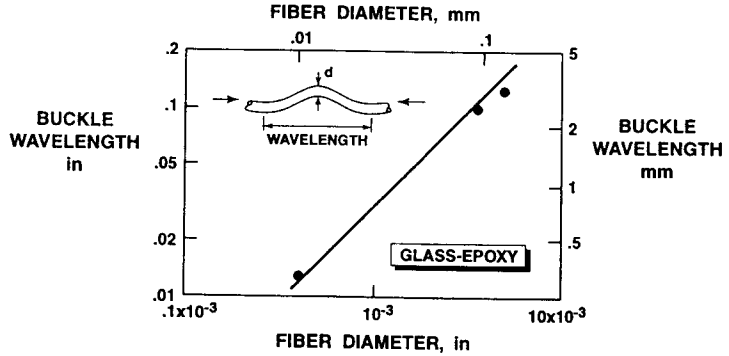

Figure 3-54 Experimental Results for Fiber Buckle Wavelength versus Fiber Diameter *(After Dow and Rosen [3-28])*

In addition to being caused by mechanical compressive loads, fiber buckling can be caused by shrinkage stresses developed during curing of the composite material. The shrinkage stresses result from the matrix having a higher thermal coefficient of expansion than the fibers. As a matter of fact, the photoelastic stress patterns in Figure 3-53 were due to matrix shrinkage during curing of a single glass fiber embedded in an epoxy matrix.

Two modes of fiber buckling are possible in the representative volume element of Figure 3-55a. First, the fibers can buckle out of phase relative to one another (symmetric about a line halfway between the fibers) to give the 'transverse' or 'extensional' buckling mode in Figure 3-55b. There, an originally vertical line in the matrix midway between each fiber (the dashed vertical lines in Figure 3-55b) does not move. All other originally vertical lines change to sine waves with an amplitude that increases as the distance from the midpoint between each fiber increases to a maximum at the fiber. Moreover, horizontal lines of original length 2c extend or contract as in Figure 3-55b. Thus, the matrix extends or contracts in the y-direction transverse to the x-direction. Hence, the name *transverse mode* or *extension mode* is used. The second mode, the *shear mode* , is so named because the matrix is subjected to shearing deformation because the fibers buckle in phase with one another (antisymmetrically with respect to the line halfway between the fibers) as shown in Figure 3-55c. There, all originally vertical lines in the matrix shear first to the right and then to the left of their originally straight position in the form of a sine wave. Also, originally horizontal lines do not change orientation or length during buckling, but do translate in the y-direction. Thus, the matrix shears in the x-y plane with all the shear being relative to the x-axis. Hence, the name shear mode is used.

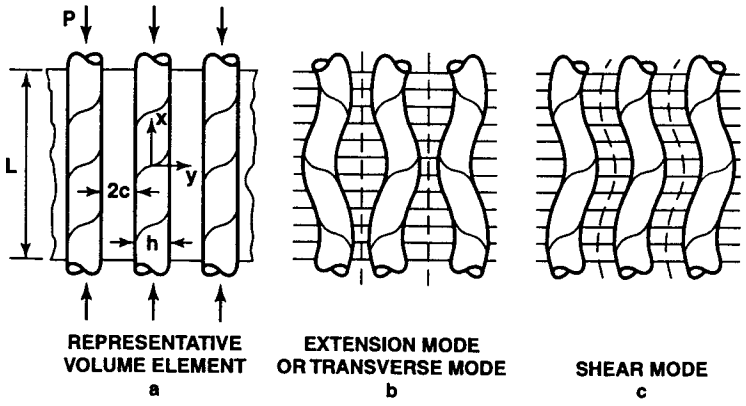

Figure 3-55 Extensional Mode and Shear Mode of Fiber Buckling

In the model for both buckling modes, the fibers are regarded as plates L long, infinitely wide, and h thick separated by matrix 2c wide. Thus, the problem is made two-dimensional because the dimension perpendicular to the x-y plane in the figure is disregarded. The two-dimensional buckling model result should be an upper bound on the real three-dimensional fiber buckling problem (in which the fiber buckles into a helix at a lower load than that corresponding to sinusoidal buckling in a plane). Each fiber is subjected to axial compressive load P. The fibers are also regarded as being much stiffer than the matrix (that is, $G_f >> G_m$), so the fiber-shearing deformations are neglected. Of course, the buckling load of a fiber that is surrounded by supporting matrix material is significantly higher than if no matrix material were present. In essence, the lateral support of the continuous matrix material is analogous to increasing the number of discrete lateral supports for an Euler Column. That is,

$$P = m^2\pi^2 \frac{EI}{L^2} \tag{3.93}$$

has results for buckling mode dependent on the number of lateral supports (m – 1) in Figure 3-56. For high values of m, the buckling load is enormously larger than if m is only one (a column without lateral support). However, note that the matrix support is elastic, i.e., a deforming support like a spring, not the rigid support of the Euler column with discrete supports.

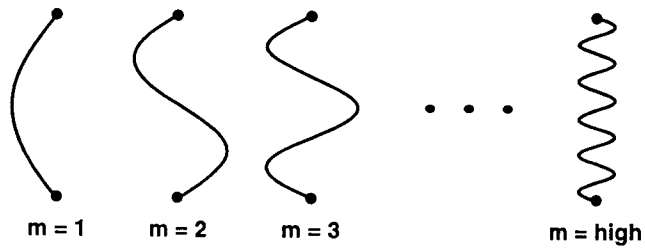

Figure 3-56 Buckling of a Discretely Supported Euler Column

The analysis to find the fiber buckling load in each mode is based on the energy method described by Timoshenko and Gere [3-31]. The buckling criterion is that the change in strain energy for the fiber, ΔU_f, and for the associated matrix material, ΔU_m, is equated to the work done by the fiber force, ΔW, during deformation to a buckled state, that is,

$$\Delta U_f + \Delta U_m = \Delta W \tag{3.94}$$

In the energy method, buckle deflection configurations are approximated for the various buckle modes. The corresponding buckling loads are then calculated by use of Equation (3.94). An important feature of the energy method is that calculated buckling loads are an upper bound to the actual buckling load for the problem considered. Thus, if the unknown buckling displacement, v, of an individual fiber in the y-direction (transverse to the fibers in Figure 3-55) is represented by the Fourier sine series

$$v = \sum_{n=1}^{\infty} a_n \sin \frac{n\pi x}{L} \tag{3.95}$$

then a buckling load will be obtained that is higher than the actual buckling load. If Equation (3.95) is used in energy expressions for transverse buckling and for shear buckling of the fiber-reinforced composite material, then the lowest of the two buckling loads governs the fiber buckling of the composite material. A buckling mode having deformations intermediate to the transverse and shear modes (i.e., fiber deformations that are neither in phase nor perfectly out of phase) would be expected to have a higher buckling load than either of the two simple modes.

Transverse or Extension Mode

For the transverse buckling mode in Figure 3-55, the matrix material expands or contracts in the y-direction. However, the matrix strain in the y-direction (transverse to the fibers) is presumed to be independent of y, i.e., simply twice the two adjacent fiber displacements, v, divided by the original distance between the fibers:

$$\varepsilon_y = \frac{\Delta L}{L} = \frac{2v}{2c} \tag{3.96}$$

whereupon from the stress-strain relations the matrix stress is

$$\sigma_y = E_m \frac{v}{c} \tag{3.97}$$

Any deformation of the matrix material in the x-direction is ignored. Thus, the change in strain energy is presumed to be dominated by the energy of transverse (extensional) stresses. Thus, for the matrix,

$$\Delta U_m = \frac{1}{2} \int_V \sigma_y \varepsilon_y dV \tag{3.98}$$

Substitute Equations (3.96) and (3.97) to get

$$\Delta U_m = \frac{E_m}{2c^2} \int_V v^2 dV \tag{3.99}$$

Substitute Equation (3.95) for the transverse deflection to get

$$\Delta U_m = \frac{E_m}{2c^2} \int_V \sum_{m=1}^{\infty} \sum_{n=1}^{\infty} a_m a_n \sin \frac{m\pi x}{L} \sin \frac{n\pi x}{L} dxdy \tag{3.100}$$

where the dimension of the representative volume element in the z-direction is unity. Now interchange integration and summation to get

$$\Delta U_m = \frac{E_m}{2c^2} \sum_{m=1}^{\infty} \sum_{n=1}^{\infty} \int_0^{2c} \int_0^{L} a_m a_n \sin \frac{m\pi x}{L} \sin \frac{n\pi x}{L} dxdy \tag{3.101}$$

However, the sine function is orthogonal to itself, i.e.,

$$\int_0^L \sin \frac{m\pi x}{L} \sin \frac{n\pi x}{L} dxdy = \begin{cases} 0, & m \neq n \\ \frac{L}{2}, & m = n \end{cases} \tag{3.102}$$

Thus, we get

$$\Delta U_m = \frac{E_m L}{2c} \sum_n a_n^2 \tag{3.103}$$

For the fibers, the change in strain energy is related to the curvature of the bent fiber, v", considered as a column in the manner of Timoshenko and Gere [3-31],

$$\Delta U_f = \frac{E_f I_f}{2} \int_0^L (v'')^2 dx \tag{3.104}$$

but $I_f = h^3/12$ for a fiber of thickness h and unit depth (because the dimension perpendicular to the x-y plane in Figure 3-55 is infinite and hence disregarded). Substitute the series for the deflection (after differentiation) to get

$$\Delta U_f = \frac{E_f h^3}{24} \int_0^L \sum_{m=1}^{\infty} \sum_{n=1}^{\infty} a_m a_n \left(\frac{m\pi}{L}\right)^2 \left(\frac{n\pi}{L}\right)^2 \sin \frac{m\pi x}{L} \sin \frac{n\pi x}{L} dxdy \tag{3.105}$$

Interchange integration with summation and use the orthogonality result in Equation (3.102) to get

$$\Delta U_f = \frac{\pi^4 E_f h^3}{48L^3} \sum_n n^4 a_n^2 \tag{3.106}$$

Finally, the work done by the external force P during buckling is

$$\Delta W = P\delta \tag{3.107}$$

where δ is the distance that P moves during buckling of a fiber from its originally straight position in Figure 3-57. Note that the column (fiber) does not change length during the buckling process (but must, of course, shorten as P increases from zero to the buckling load).

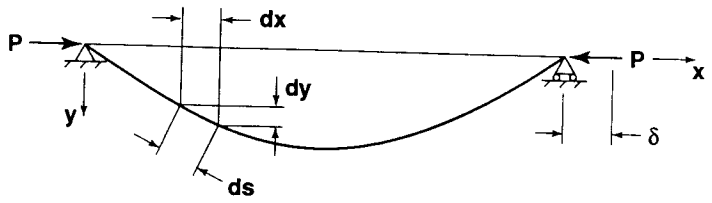

Figure 3-57 Deformation of a Simply Supported Column during Buckling

The differential movement, $d\delta$, of the force P is the difference between the differential arc length of the column, ds, and the x-direction differential length, dx. Thus, from the triangle of differential distances in Figure 3-57,

$$d\delta = ds - dx = \sqrt{dx^2 + dy^2} - dx = dx\sqrt{1 + \left[\frac{dy}{dx}\right]^2} - dx$$
$$= dx\left[\frac{1}{2}\left[\frac{dy}{dx}\right]^2 + \cdots\right] \approx \frac{1}{2}\left[\frac{dy}{dx}\right]^2 \tag{3.108}$$

Accordingly,

$$\delta = \frac{1}{2}\int_0^L \left[\frac{dy}{dx}\right]^2 dx \tag{3.109}$$

Then, upon substitution of the derivative of the transverse deflection, v, for y, Equation (3.95), in the work expression, Equation (3.107),

$$\Delta W = \frac{P}{2}\int_0^L \sum_{m=1}^{\infty}\sum_{n=1}^{\infty} a_m a_n \frac{m\pi}{L}\frac{n\pi}{L}\cos\frac{m\pi x}{L}\cos\frac{n\pi x}{L}\,dxdy \tag{3.110}$$

Interchange integration with summation and use the cosine analog of the sine orthogonality result in Equation (3.102) to get

$$\Delta W = \frac{P\pi^2}{4L}\sum_n n^2 a_n^2 \tag{3.111}$$

in which, for this two-dimensional problem, the fiber load per unit of width perpendicular to the plane of Figure 3-55 is

$$P = \sigma_f h \tag{3.112}$$

i.e., the fiber axial stress times the fiber thickness. Upon substitution of the foregoing energy expressions in the buckling criterion, Equation (3.94), the fiber buckling load is

$$P = \frac{\pi^2 E_f h^3}{12L^2}\,\frac{\sum_n n^4 a_n^2 + \dfrac{24L^4 E_m}{\pi^4 ch^3 E_f}\sum_n a_n^2}{\sum_n n^2 a_n^2} \tag{3.113}$$

Now presume that P achieves a minimum for a particular sine wave, say the m^{th} wave. Thus,

$$\sigma_{f_{cr}} = \frac{\pi^2 E_f h^2}{12L^2}\left[m^2 + \frac{24L^4 E_m}{\pi^4 ch^3 E_f}\frac{1}{m^2}\right] \tag{3.114}$$

where m is the number of half waves in the buckled column shape. From the aforementioned photoelasticity investigations [3-28], m is obviously a very large number. Thus, $\sigma_{f_{cr}}$ can be treated as a continuous function of m and the minimum of $\sigma_{f_{cr}}$ is obtained from the stationary value condition

$$\frac{\partial \sigma_{f_{cr}}}{\partial m} = 0 \tag{3.115}$$

subject to the condition for a minimum that

$$\left.\frac{\partial^2 \sigma_{f_{cr}}}{\partial m^2}\right|_{\frac{\partial \sigma_{f_{cr}}}{\partial m} = 0} > 0 \tag{3.116}$$

If m were small, the minimum $\sigma_{f_{cr}}$ must be found for *discrete* (integer) values of m. The following reasoning is offered in support of the preceding contention. Consider a hypothetical plot of $\sigma_{f_{cr}}$ versus m where $\sigma_{f_{cr}}$ has values only at integer values of m in Figure 3-58 because there must be an integer number of buckle half waves to satisfy column end conditions. The buckling load for the indicated lowest minimum at m = 2.7 does not physically exist and deviates substantially in value from the physical minimum at m = 3 because the mode number is squared in the buckling expression. However, the buckling load for the second minimum at m = 37.5, although it does not physically exist, is a reasonably close approximation to the actual minimum because the percentage difference between the buckling load for m = 37.5 and that for m = 37 or 38 is negligible. The minimum of $\sigma_{f_{cr}}$ as a continuous function of m is

$$\sigma_{f_{cr}} = 2\sqrt{\frac{V_f E_m E_f}{3(1 - V_f)}} \tag{3.117}$$

as can easily be verified (Problem 3.5.4). In the preceding derivation, recognize that

$$V_f = \frac{h}{h + 2c} \tag{3.118}$$

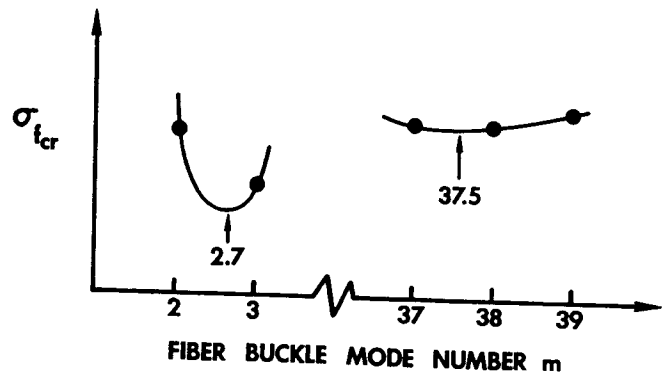

Figure 3-58 Hypothetical Relative Minima of $\sigma_{f_{cr}}$

The buckling stress in the composite material is then

$$\sigma_{c_{max}} = V_f \sigma_{f_{cr}} = 2V_f \sqrt{\frac{V_f E_m E_f}{3(1 - V_f)}} \tag{3.119}$$

wherein the matrix is assumed to be essentially unstressed in the x-direction in comparison to the fibers.

Alternatively, the x-direction strain at buckling can be calculated from Equation (3.117) and the uniaxial stress-strain relation as

$$\varepsilon_{f_{cr}} = 2\sqrt{\frac{V_f}{3(1 - V_f)}}\sqrt{\frac{E_m}{E_f}} \tag{3.120}$$

If the matrix is assumed to have the same strain in the fiber direction as the fiber (the fundamental approximation for strains in the determination of E_1 in Section 3.2.1, which is reasonable if no fractures occur), then

$$\sigma_m = E_m \varepsilon_{f_{cr}} \tag{3.121}$$

whereupon the maximum composite material stress is

$$\sigma_{c_{max}} = V_f \sigma_{f_{cr}} + V_m \sigma_m \tag{3.122}$$

or

$$\sigma_{c_{max}} = \left[V_f + (1 - V_f) \frac{E_m}{E_f} \right] \sigma_{f_{cr}} \tag{3.123}$$

Finally,

$$\sigma_{c_{max}} = 2\left[V_f + (1 - V_f) \frac{E_m}{E_f} \right] \sqrt{\frac{V_f E_m E_f}{3(1 - V_f)}} \tag{3.124}$$

The difference between Equations (3.119) and (3.124) is slight for high ratios of E_f to E_m as in practical fiber-reinforced composite materials.

Shear Mode

For the shear buckling mode in Figure 3-55, the fiber displacements are equal and in phase with one another. The matrix material is alternately sheared in one direction and then the other as the x-direction is traversed. However, changes in deformation in the y-direction are ignored. Thus, the shear strains are presumed to be a function of the fiber-direction coordinate alone. The matrix is sheared according to

$$\gamma_{xy} = \frac{\partial v}{\partial x} + \frac{\partial u}{\partial y} \tag{3.125}$$

where v is the displacement in the y-direction and u is the displacement in the x-direction. Then, because the transverse displacement is independent of the transverse coordinate y,

$$\left.\frac{dv}{dx}\right|_{matrix} = \left.\frac{dv}{dx}\right|_{fiber} \tag{3.126}$$

Because the shear strain is independent of y,

$$\frac{\partial u}{\partial y} = \frac{1}{2c}[u(c) - u(-c)] \tag{3.127}$$

as can be verified by examination of Figure 3-59. Next, because the shear deformation of the fiber is ignored,

$$u(c) = \frac{h}{2} \left.\frac{dv}{dx}\right|_{fiber} \tag{3.128}$$

But, from substitution of Equation (3.128) in Equation (3.127),

$$\frac{\partial u}{\partial y} = \frac{h}{2c} \left.\frac{dv}{dx}\right|_{fiber} \tag{3.129}$$

Now substitute Equations (3.129) and (3.126) in Equation (3.125) to get

$$\gamma_{xy} = \left[1 + \frac{h}{2c}\right] \left.\frac{dv}{dx}\right|_{fiber} \tag{3.130}$$

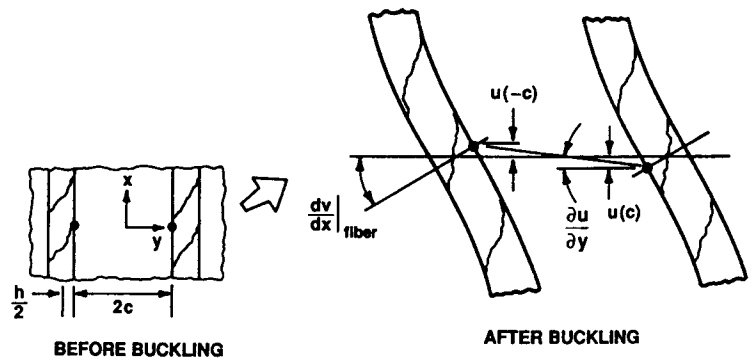

Figure 3-59 Fiber Deformations During Shear Mode Buckling

Recall the basic stress-strain relation

$$\tau_{xy} = G_m \gamma_{xy} \tag{3.131}$$

The change in strain energy of the matrix is merely that due to shear:

$$\Delta U_m = \frac{1}{2} \int_V \tau_{xy} \gamma_{xy} dV \tag{3.132}$$

Substitute the deflection function, Equation (3.95), the shear strain expression, Equation (3.130), and the stress-strain relation, Equation (3.131), in Equation (3.132) to get

$$\Delta U_m = G_m c \left[1 + \frac{h}{2c} \right]^2 \frac{\pi^2}{2L} \sum_n n^2 a_n^2 \tag{3.133}$$

The change in strain energy of the fiber is still given as Equation (3.106), and the work done is still that in Equation (3.111). Thus, upon application of the buckling criterion, Equation (3.94),

$$\sigma_{f_{cr}} = \frac{G_m}{V_f (1 - V_f)} + \frac{\pi^2 E_f}{12} \left[\frac{mh}{L} \right]^2 \tag{3.134}$$

Because the buckle wavelength is L/m, the second term in Equation (3.134) is small when the buckle wavelength is large relative to the fiber diameter, h. Thus, the fiber buckling stress is approximately

$$\sigma_{f_{cr}} = \frac{G_m}{V_f (1 - V_f)} \tag{3.135}$$

The maximum composite material stress (i.e., the strength) is then

$$\sigma_{c_{max}} = \frac{G_m}{1 - V_f} \tag{3.136}$$

and the strain at buckling is

$$\varepsilon_{cr} = \frac{1}{V_f (1 - V_f)} \left[\frac{G_m}{E_f} \right] \tag{3.137}$$

Predicted versus Measured Strength

The maximum stress expressions, Equations (3.119) and (3.136), are plotted in Figure 3-60 for a glass-epoxy composite material. Note that the shear mode has the lowest strength for the composite material over a wide range of fiber-volume fractions. However, the transverse or extensional mode does govern the composite material strength for low fiber-volume fractions. For fiber-volume fractions of between .6 and .7, the predicted compressive strength is between 450 and 600 ksi (3100 and 4100 MPa). These high strength levels have not been obtained for glass-epoxy composite materials. If such a composite material were to have a strength of 500 ksi (3400 MPa), the strain would have to exceed 5%. Under these conditions, the matrix would deform plastically. Thus, the predicted strength should be below the curve labeled 'elastic shear

mode' in Figure 3-60. As an approximation to the inelastic behavior, Dow and Rosen [3-28] replaced the matrix shear modulus in Equation (3.136) by a shear modulus that varies linearly from the elastic value at 1% strain to a zero value at 5% strain as in Figure 3-61. The resulting strength curve is labeled 'inelastic shear mode' in Figure 3-60. The predicted compressive strengths then appear more reasonable for glass-epoxy composite materials, but are still not as low as actual values. That these predicted strengths are too high should not be surprising in view of the fact that the analysis is only two-dimensional instead of the actual three-dimensional fiber buckling problem.

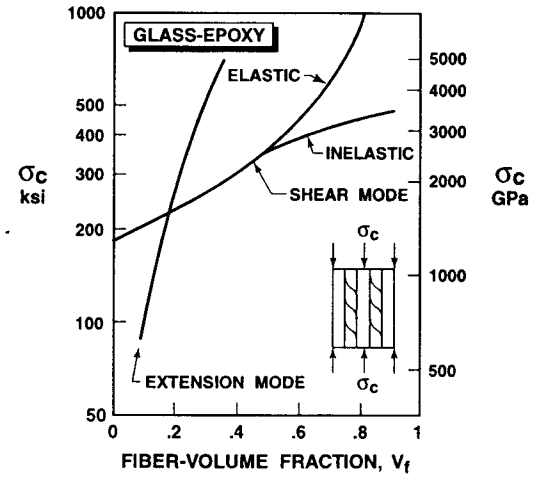

Figure 3-60 Compressive Strength of Glass-Epoxy Composite Materials *(After Dow and Rosen [3-28])*

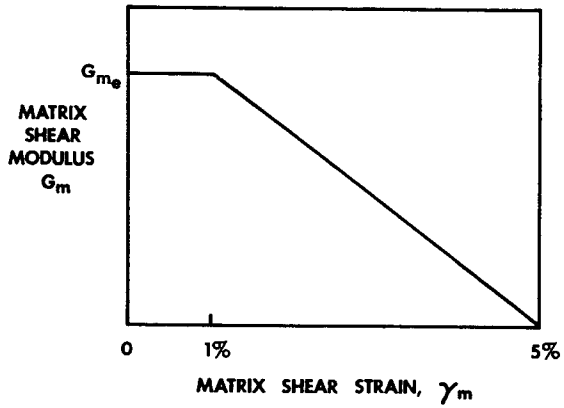

Figure 3-61 Variation of Matrix Shear Modulus with Shear Strain *(After Dow and Rosen [3-28])*

Dow and Rosen's results are plotted in another form, composite material strain at buckling versus fiber-volume fraction, in Figure 3-62. These results are Equation (3.137) for two values of the ratio of fiber Young's modulus to matrix shear modulus (E_f/G_m) at a matrix Poisson's ratio of .25. As in the previous form of Dow and Rosen's results, the shear mode governs the composite material behavior for a wide range of fiber-volume fractions. Moreover, note that a factor of 2 change in the ratio E_f/G_m causes a factor of 2 change in the maximum composite material compressive strain. Thus, the importance of the matrix shear modulus reduction due to inelastic deformation is quite evident.

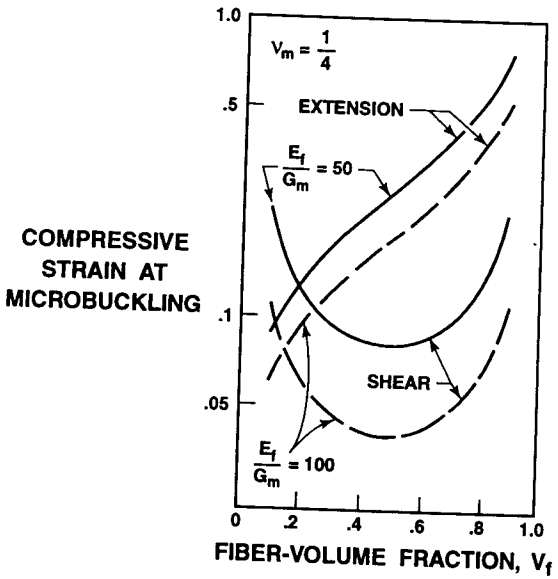

Figure 3-62 Compressive Strain at Microbuckling for Fiber-Reinforced Composite Materials *(After Dow and Rosen [3-28])*

Schuerch examined boron-fiber–metal-matrix composite materials parametrically with Rosen's equations and found them to require plastic buckling analysis [3-32]. Moreover, so do S-glass-epoxy composite materials, but boron-epoxy composite materials apparently buckle elastically according to Schuerch. Greszczuk studied the shear mode of microbuckling and determined that as the matrix shear modulus increases, the mode of failure changes from microbuckling to gross compression failure of the fibers [3-30].

Lager and June compared Dow and Rosen's theoretical predictions with experimental results for boron-epoxy composite materials that have two different matrix materials [3-33]. The theory appears to correlate well with the data if the matrix moduli in Equations (3.119) and (3.136) are multiplied by .63, that is,

$$(\sigma_{c_{max}})_{extension} = 2V_f\sqrt{\frac{V_f(.63E_m)E_f}{3(1-V_f)}} \tag{3.138}$$

$$(\sigma_{c_{max}})_{shear} = \frac{.63G_m}{1-V_f} \tag{3.139}$$

The fibers were laid up in a near-perfect square array as verified by inspection of magnified pictures of machined cross sections. The theoretical results in Equations (3.138) and (3.139) as well as the data are shown in Figure 3-63. Note that the initial (elastic) modulus was used with the reduction factor of .63. The 'influence' coefficient of .63 is apparently due to the matrix not becoming plastic to the same degree in all directions. (That is, Lager and June disagree with Schuerch's contention that boron-epoxy composite materials buckle elastically.) The influence coefficient is believed to be a strong function of the matrix modulus. For example, if reinforcing cloth such as fiberglass cloth is added to the matrix, the influence coefficient increases to .97.

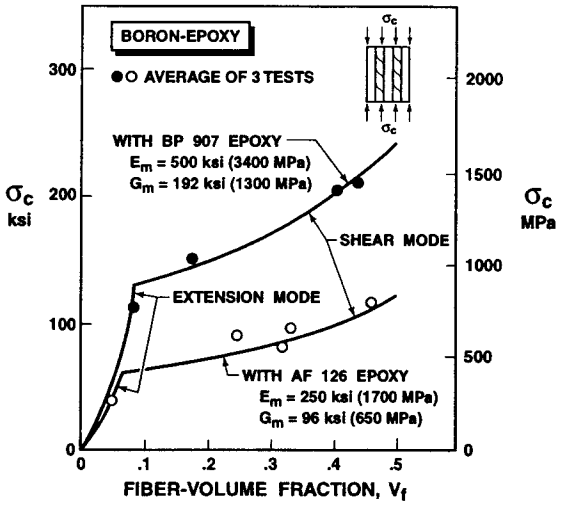

Figure 3-63 Compressive Strength of Boron-Epoxy Composite Materials *(After Lager and June [3-33])*

Zhang and Latour [3-34] used a more refined mechanics of materials model than Rosen to demonstrate that the shear mode and the extension mode of microbuckling must coincide at zero fiber-volume fraction, unlike Rosen's results that diverge as $V_f = 0$ is approached in Figure 3-60. At low V_f, the sparseness of fibers dictates that they are incapable of interacting with one another during buckling, so there can be no difference in buckling load between the shear mode and the extension mode. Moreover, they explain that at high V_f the theoretical results are for long wavelength buckling whereas experimental results clearly have short wavelength buckling. They describe other factors that could result in short wavelength fiber buckling.

Problem Set 3.5

3.5.1 Derive Equation (3.86).
3.5.2 Derive Equation (3.89).
3.5.3 Derive Equation (3.113).
3.5.4 Derive Equation (3.117) and verify that it is a minimum.
3.5.5 Derive Equation (3.133).
3.5.6 Derive Equation (3.134).

3.6 SUMMARY REMARKS ON MICROMECHANICS

The micromechanics approaches presented in this book are an attempt to *predict* the mechanical properties of a composite material based on the mechanical properties of its constituent materials. In nearly all fiber-reinforced composite materials, there is considerable difference between expectation and reality. Thus, we must ask: what is the usefulness of micromechanical analysis beyond gaining a feeling for why composite materials behave as they do? Basically, there are two answers: one related to designing a material and one related to designing a structure.

First, if we are designing a composite material to achieve certain properties, we must have a design rationale that can only be micromechanics. However, obviously adjustments (perhaps empirical) must be made to the rationale to obtain agreement between predicted and actual properties for given constituent properties and volume percentages. That is, something must be done to make up for the quantitative shortcomings of micromechanics theories used in the design of materials for specified properties. The actual properties of a composite material result from processing variables that are often difficult to assess, even qualitatively:

- nonuniform curing
- residual stresses
- voids
- cracks
- fiber damage
- random fiber packing
- contiguous fibers
- misaligned fibers

Thus, it seems inevitable that micromechanics predictions of properties will always be imprecise.

Second, if we are designing a structure made of composite materials, we might ideally wish to have the freedom to design the material for the structure as well as the structure itself. In such a situation, we would need micromechanics in the sense of answer number one (material design). However, we would much more likely be obliged to standardize the material (e.g., use a particular graphite-epoxy tape) and concentrate on how to use the standard material to best advantage. Specifically, how to orient laminae of known (*measured*, not predicted!) properties to achieve design goals would be the thrust of our efforts. Thus, the second possible answer to the question of the usefulness of micromechanics is that in many cases there is virtually *no* need for micromechanics. That is, the structural designer will probably rely almost exclusively on the results of mechanical tests for his material property data. He cannot risk using unsubstantiated micromechanics predictions that are often considerably in error.

The reader should be exposed to both micromechanics and macromechanics in order to function effectively in either material design or structural design. The main thrust of this book is in line with structural design and analysis requirements. Thus, the point of our addressing micromechanics is to better understand how and why composite materials function.

REFERENCES

3-1 Stephen W. Tsai, *Structural Behavior of Composite Materials*, NASA CR-71, July 1964.

3-2 J. C. Ekvall, Structural Behavior of Monofilament Composites, *Proceedings of the AIAA 6th Structures and Materials Conference*, Palm Springs, California, 5–7 April 1965, AIAA, New York, April 1965.

3-3 J. C. Ekvall, Elastic Properties of Orthotropic Monofilament Laminates, ASME Paper 61-AV-56, Aviation Conference, Los Angeles, California, 12–16 March 1961.

3-4 B. Paul, Prediction of Elastic Constants of Multiphase Materials, *Transactions of the Metallurgical Society of AIME*, February 1960, pp. 36–41.

3-5 C. C. Chamis and G. P. Sendeckyj, Critique on Theories Predicting Thermoelastic Properties of Fibrous Composites, *Journal of Composite Materials*, July 1968, pp. 332–358.

3-6 Zvi Hashin, The Elastic Moduli of Heterogeneous Materials, *Journal of Applied Mechanics*, March 1962, pp. 143–150.

3-7 Zvi Hashin and S. Shtrikman, A Variational Approach to the Theory of the Elastic Behaviour of Multiphase Materials, *Journal of the Mechanics and Physics of Solids*, March–April 1963, pp. 127–140.

3-8 Zvi Hashin and B. Walter Rosen, The Elastic Moduli of Fiber-Reinforced Materials, *Journal of Applied Mechanics*, June 1964, pp. 223–232. Errata, March 1965, p. 219.

3-9 N. I. Muskhelishvili, *Some Basic Problems of the Mathematical Theory of Elasticity*, P. Noordhoff, Groningen, The Netherlands, 1953.

3-10 L. R. Herrmann and K. S. Pister, Composite Properties of Filament-Resin Systems, ASME Paper 63-WA-239, ASME Winter Annual Meeting, Philadelphia, Pennsylvania, 17–22 November 1963.

3-11 Donald F. Adams and Stephen W. Tsai, The Influence of Random Filament Packing on the Elastic Properties of Composite Materials, *Journal of Composite Materials*, July 1969, pp. 368–381.

3-12 J. M. Whitney and M. B. Riley, Elastic Properties of Fiber Reinforced Composite Materials, *AIAA Journal*, September 1966, pp. 1537–1542.

3-13 R. Hill, Theory of Mechanical Properties of Fibre-Strengthened Materials - III. Self-Consistent Model, *Journal of the Mechanics and Physics of Solids*, August 1965, pp. 189–198.

3-14 J. J. Hermans, The Elastic Properties of Fiber Reinforced Materials when the Fibers are Aligned, *Proceedings of the Koninklijke Nederlandse Akademie van Wetenschappen*, Amsterdam, Series B, Volume 70, Number 1, 1967, pp. 1–9.

3-15 J. M. Whitney, Elastic Moduli of Unidirectional Composites with Anisotropic Filaments, *Journal of Composite Materials*, April 1967, pp. 188–193.

3-16 James M. Whitney, Geometrical Effects of Filament Twist on the Modulus and Strength of Graphite Fiber-Reinforced Composites, *Textile Research Journal*, September 1966, pp. 765–770.

3-17 J. C. Halpin and S. W. Tsai, *Effects of Environmental Factors on Composite Materials*, AFML-TR-67-423, June 1969.

3-18 J. C. Halpin and R. L. Thomas, Ribbon Reinforcement of Composites, *Journal of Composite Materials*, October 1968, pp. 488–497.

3-19 D. F. Adams and D. R. Doner, Transverse Normal Loading of a Unidirectional Composite, *Journal of Composite Materials*, April 1967, pp. 152–164.

3-20 D. F. Adams and D. R. Doner, Longitudinal Shear Loading of a Unidirectional Composite, *Journal of Composite Materials*, January 1967, pp. 4–17.

3-21 R. L. Foye, An Evaluation of Various Engineering Estimates of the Transverse Properties of Unidirectional Composites, *Proceedings of the 10th National Sympo-*

sium of the Society of Aerospace Materials and Process Engineers, San Diego, California, 9-11 November 1966, pp. G-31–42.

3-22 R. L. Foye, *Structural Composites*, Quarterly Progress Report Numbers 1 and 2, AFML Contract Number AF 33(615)-5150, 1966.

3-23 R. L. Hewitt and M. C. de Malherbe, An Approximation for the Longitudinal Shear Modulus of Continuous Fibre Composites, *Journal of Composite Materials*, April 1970, pp. 280–282.

3-24 C. Nishimatsu and J. Gurland, *Experimental Survey of the Deformation of a Hard-Ductile Two-Phase Alloy System, WC-Co*, Brown University Division of Engineering Technical Report Number 2, September 1958.

3-25 R. Kieffer and P. Schwartzkopf, *Hartstoffe und Hartmetalle*, Springer, Vienna, 1953.

3-26 A. Kelly and G. J. Davies, The Principles of the Fibre Reinforcement of Metals, *Metallurgical Reviews*, Volume 10, Number 37, 1965, pp. 1–77.

3-27 B. Walter Rosen, Tensile Failure of Fibrous Composites, *AIAA Journal*, November 1964, pp. 1985–1991.

3-28 Norris F. Dow and B. Walter Rosen, *Evaluations of Filament-Reinforced Composites for Aerospace Structural Applications*, NASA CR-207, April 1965.

3-29 B. Walter Rosen, Norris F. Dow, and Zvi Hashin, *Mechanical Properties of Fibrous Composites*, NASA CR-31, April 1964.

3-30 L. B. Greszczuk, Microbuckling Failure of Circular Fiber-Reinforced Composites, *AIAA Journal*, October 1975, pp. 1311–1318.

3-31 S. P. Timoshenko and J. M. Gere, *Theory of Elastic Stability*, 2nd edition, McGraw-Hill, New York, 1961.

3-32 H. Schuerch, *Compressive Strength of Boron-Metal Composites*, NASA CR-202, April 1965.

3-33 John R. Lager and Reid R. June, Compressive Strength of Boron-Epoxy Composites, *Journal of Composite Materials*, January 1969, pp. 48–56.

3-34 Guigen Zhang and Robert A. Latour, Jr., An Analytical and Numerical Study of Fiber Microbuckling, *Composites Science and Technology*, Volume 51, Number 1, 1994, pp. 95–109.

Chapter 4

MACROMECHANICAL BEHAVIOR OF A LAMINATE

4.1 INTRODUCTION

A laminate is two or more laminae bonded together to act as an integral structural element (see, for example, Figure 4-1). The two basic questions of laminate analysis are: (1) what are the conditions that the laminae must meet to be a laminate? and (2) how will a laminate respond to loading, i.e., imposed forces and moments? The various laminae are oriented with (local) principal material directions at different angles to the global laminate axes to produce a structural element capable of resisting load in several directions. The stiffnesses and strengths of such a composite material structural configuration are obtained from the properties of the constituent laminae by procedures derived in this chapter. Those procedures enable the analysis of laminates that have individual laminae with principal material directions oriented at arbitrary angles to the chosen or natural axes of the laminate. As a consequence of the arbitrary laminae orientations, the laminate might not have definable principal directions.

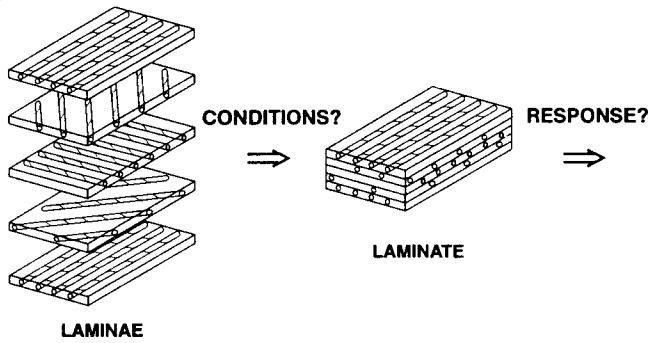

Figure 4-1 The Basic Questions of Laminate Analysis

The reason laminae are combined to create a laminate is to achieve the largest possible bending stiffness for the materials used. Recall the 'two-beam' problem from basic mechanics of materials. First, consider the two beams as not fastened together and loaded at midspan by a concentrated force as in Figure 4-2a. In contrast, the same two beams could be fastened together by nails, screws, or bonding as in Figure 4-2b. The deflection is less for the bonded beams than the unbonded beams by a factor of four! Thus, bonding laminae together results in a compellingly large increase in bending resistance.

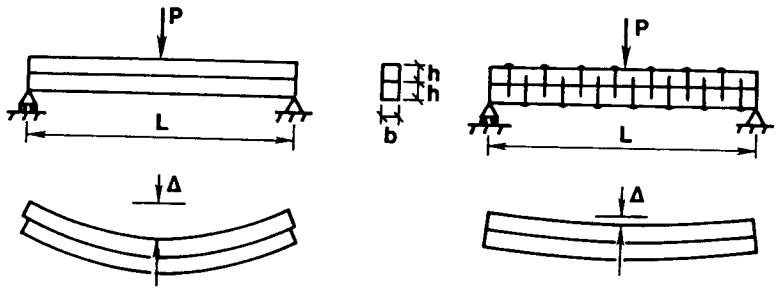

$$\Delta = \frac{PL^3}{48EI} = \frac{PL^3}{48E(2)\frac{1}{12}bh^3} = \frac{PL^3}{8Ebh^3} \qquad \Delta = \frac{PL^3}{48EI} = \frac{PL^3}{48E\frac{1}{12}b(2h)^3} = \frac{PL^3}{32Ebh^3}$$

$$\Delta_{unbonded} = 4\Delta_{bonded}$$

a Unbonded Beams b Bonded Beams

Figure 4-2 Reason for Lamination: The Two-Beam Problem

The fundamental analysis of a laminate can be explained, in principle, by use of a simple two-layered cross-ply laminate (a layer with fibers at 0° to the x-direction on top of an equal-thickness layer with fibers at 90° to the x-direction). We will analyze this laminate approximately by considering what conditions the two unbonded layers in Figure 4-3 must satisfy in order for the two layers to be bonded to form a laminate. Imagine that the layers are separate but are subjected to a load N_x in the x-direction. The force N_x is divided between the two layers such that the x-direction deformation of each layer is identical. That is, the laminae in a laminate must deform alike along the interface between the layers or else fracture must exist! Accordingly, deformation compatibility of layers is a requirement for a laminate. Because of the equal x-direction deformation of each layer, the top (0°) layer has the most x-direction stress because it is stiffer than the bottom (90°) layer in the x-direction. The x-direction stresses in the top and bottom layers can be shown to have the relation

$$\sigma_x^T = \frac{E_1}{E_2}\sigma_x^B \tag{4.1}$$

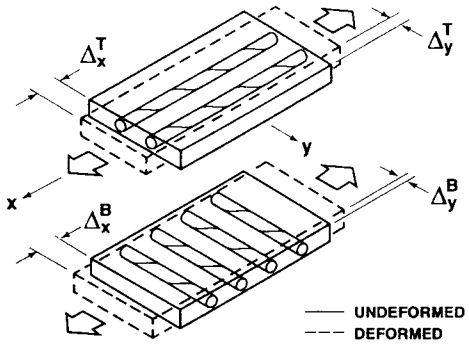

Figure 4-3 Analysis of a Two-Layered Laminate

Now consider the lateral (y-direction) displacements of both layers in Figure 4-3. Without bonding of the two laminae, the lateral displacements can be shown by use of the strain-stress relations and the relation of strain to displacement to have the relation

$$\Delta_y^T = \frac{E_1}{E_2}\Delta_y^B \tag{4.2}$$

That is, although we required equal x-direction displacements of the two layers (the proportion of N_x in each layer was adjusted to create that equal-displacement condition), the lateral displacements are quite different. Those different displacements are a violation of the required deformation compatibility of laminae in a laminate. To remedy this violation, the top layer must get wider by application of a lateral *tensile* stress σ_y^T, and the bottom layer must get narrower by application of a *compressive* stress σ_y^B. The two deformations must result in equal-width laminae to satisfy deformation compatibility. Moreover, the lateral stresses in each layer must satisfy force equilibrium in the y-direction, i.e.,

$$\sigma_y^T L\,t + \sigma_y^B L\,t = 0 \tag{4.3}$$

where L is the length and t is the lamina thickness. Thus, the forces corresponding to the lateral stresses, σ_y^T and σ_y^B, must be self-equilibrating — in this case, equal and opposite — because no load N_y is applied in the y-direction.

Next, observe that the x-direction displacements of each layer are also affected by the lateral stresses σ_y^T and σ_y^B and hence Δ_x^T and Δ_x^B are no longer equal. Thus, the x-direction stresses σ_x^T and σ_x^B must be adjusted to reimpose deformation compatibility of the two layers in the x-direction.

This step-by-step imposition of conditions of

- deformation compatibility
- stress-strain relations
- equilibrium

seemingly results in a never-ending succession of adjustments in x- and y-direction stresses until all conditions are simultaneously met. This approach to laminate analysis has revealed the essential character of, and principles used in, laminate analysis. The example of a two-layered laminate is understandable, yet the method seems hopeless for a many-layered laminate, especially if laminae at some arbitrary angle relative to the laminate x-direction are considered. Thus, we adopt a different approach to simultaneously satisfy all the required conditions, namely classical lamination theory. Moreover, we will discover that this 'simple' two-layered cross-ply laminate has another important characteristic that might surprise us.

Classical lamination theory is derived in Section 4.2. Then, special stiffnesses of practical interest are classified and examined in Section 4.3. Next, the theoretical stiffnesses obtained by classical lamination theory are compared with experimental results in Section 4.4. In Section 4.5, the strengths of various laminates are predicted. Finally, the stresses between the laminae of a laminate are examined in Section 4.6 and found to be a probable cause of delamination of some laminates.

Problem Set 4.1

4.1.1 Use the strain-stress relations, Equation (2.61), and the definition of deformation = εL to find the stresses in Equations (4.1) and (4.2).

4.1.2 Did we leave out any behavioral phenomenon in the discussion of Equations (4.1) and (4.2)? If so, what is it? Describe its effect on the results we obtained.

4.2 CLASSICAL LAMINATION THEORY

Classical lamination theory consists of a collection of mechanics-of-materials type of stress and deformation hypotheses that are described in this section. By use of this theory, we can consistently proceed directly from the basic building block, the lamina, to the end result, a structural laminate. The whole process is one of finding effective and reasonably accurate simplifying assumptions that enable us to reduce our attention from a complicated three-dimensional elasticity problem to a solvable two-dimensional mechanics of deformable bodies problem.

Actually, because of the stress and deformation hypotheses that are an inseparable part of classical lamination theory, a more correct name would be classical thin lamination theory, or even classical laminated plate theory. We will use the common term classical lamination theory, but recognize that it is a convenient oversimplification of the rigorous nomenclature. In the composite materials literature, classical lamination theory is often abbreviated as CLT.

First, the stress-strain behavior of an individual lamina is reviewed in Section 4.2.1, and expressed in equation form for the k^{th} lamina of a laminate. Then, the variations of stress and strain through the thickness of the laminate are determined in Section 4.2.2. Finally, the relation of the laminate forces and moments to the strains and curvatures is found in Section 4.2.3 where the laminate stiffnesses are the link from the

forces and moments to the strains and curvatures. The derivations in this section are quite similar to the classical work by Pister and Dong [4-1] and Reissner and Stavsky [4-2].

4.2.1 Lamina Stress-Strain Behavior

The stress-strain relations in principal material coordinates for a lamina of an orthotropic material under plane stress are

$$\begin{bmatrix}\sigma_1\\ \sigma_2\\ \tau_{12}\end{bmatrix}=\begin{bmatrix}Q_{11} & Q_{12} & 0\\ Q_{12} & Q_{22} & 0\\ 0 & 0 & Q_{66}\end{bmatrix}\begin{bmatrix}\varepsilon_1\\ \varepsilon_2\\ \gamma_{12}\end{bmatrix} \tag{4.4}$$

The reduced stiffnesses, Q_{ij}, are defined in terms of the engineering constants in Equation (2.66). In any other coordinate system in the plane of the lamina, the stresses are

$$\begin{bmatrix}\sigma_x\\ \sigma_y\\ \tau_{xy}\end{bmatrix}=\begin{bmatrix}\overline{Q}_{11} & \overline{Q}_{12} & \overline{Q}_{16}\\ \overline{Q}_{12} & \overline{Q}_{22} & \overline{Q}_{26}\\ \overline{Q}_{16} & \overline{Q}_{26} & \overline{Q}_{66}\end{bmatrix}\begin{bmatrix}\varepsilon_x\\ \varepsilon_y\\ \gamma_{xy}\end{bmatrix} \tag{4.5}$$

where the transformed reduced stiffnesses, $\overline{Q}_{ij}$, are given in terms of the reduced stiffnesses, Q_{ij}, in Equation (2.85).

The stress-strain relations in arbitrary in-plane coordinates, namely Equation (4.5), are useful in the definition of the laminate stiffnesses because of the arbitrary orientation of the constituent laminae. Both Equations (4.4) and (4.5) can be thought of as stress-strain relations for the k^{th} layer of a multilayered laminate. Thus, Equation (4.5) can be written as

$$\{\sigma\}_k=[\overline{Q}]_k\{\varepsilon\}_k \tag{4.6}$$

We will proceed in the next section to define the strain and stress variations through the thickness of a laminate. The resultant forces and moments on a laminate will then be obtained in Section 4.2.3 by integrating the stress-strain relations for each layer, Equation (4.6), through the laminate thickness subject to the stress and strain variations determined in Section 4.2.2.

4.2.2 Strain and Stress Variation in a Laminate

Knowledge of the variation of stress and strain through the laminate thickness is essential to the definition of the extensional and bending stiffnesses of a laminate. The laminate is presumed to consist of per-

fectly bonded laminae.[1] Moreover, the bonds are presumed to be infinitesimally thin as well as non-shear-deformable. That is, the displacements are continuous across lamina boundaries so that no lamina can slip relative to another. Thus, the laminate acts as a single layer with very *special* properties that later we will see constitute a structural element.

Accordingly, if the laminate is thin, a line originally straight and perpendicular to the middle surface of the laminate, i.e., a normal to the middle surface, is assumed to remain straight and perpendicular to the middle surface when the laminate is deformed, e.g., bent, extended, contracted, sheared, or twisted. Requiring the normal to the middle surface to remain straight and normal under deformation is equivalent to ignoring the shearing strains in planes perpendicular to the middle surface, that is, $\gamma_{xz} = \gamma_{yz} = 0$ where z is the direction of the normal to the middle surface in Figure 4-4 (note that γ_{xz} and γ_{yz} are the angles that a *deformed* normal would make with the deformed middle surface). In addition, the normals are presumed to have constant length so that the strain perpendicular to the middle surface is ignored as well, that is, $\varepsilon_z = 0$. The foregoing collection of assumptions of the behavior of the single layer that represents the laminate constitutes the familiar Kirchhoff hypothesis for plates and the Kirchhoff-Love hypothesis for shells (and is the two-dimensional analog of the ordinary one-dimensional beam theory assumption that plane sections, i.e., sections normal to the beam axis, remain plane after bending — thus, the physical justification of the collection of assumptions should be obvious). Note that no restriction has been made to flat laminates; the laminates can, in fact, be curved or shell-like.

The implications of the Kirchhoff hypothesis on the laminate displacements u, v, and w in the x-, y-, and z-directions are derived by use of the laminate cross section in the x-z plane shown in Figure 4-4. The displacement in the x-direction of point B from the undeformed middle surface to the deformed middle surface is u_o (the symbol 'nought' (°) is used to designate middle-surface values of a variable). Because line ABCD remains straight under deformation of the laminate, the displacement at point C is

[1] That the layers are perfectly bonded is *not* an idealization that cannot be realized in a practical sense. In fact, tests exist to determine whether layers are bonded to one another. Those tests are an integral part of current manufacturing technology for composite structures. One such test is the simple coin tap that anyone can perform. The noise from tapping a coin on a laminate changes pitch from regions of perfect bonding to regions where disbonds exist. Accordingly, effective bonds between laminae are *ensured by suitable inspection*. Thus, the usual (correct) perception that bonds between fiber and matrix at the microscopic level are never perfect has no analog at the (macroscopic) laminate level. Laminates that are not completely bonded will likely be rejected (or repaired, if possible) in usual manufacturing practice. The reason for this insistence on good bonds is that nearly perfect bonds are *required* in all laminates to ensure that the laminae work together as a *unit* as in Figure 4-2 instead of separately (If the laminae are not bonded, then we don't have a laminate!).

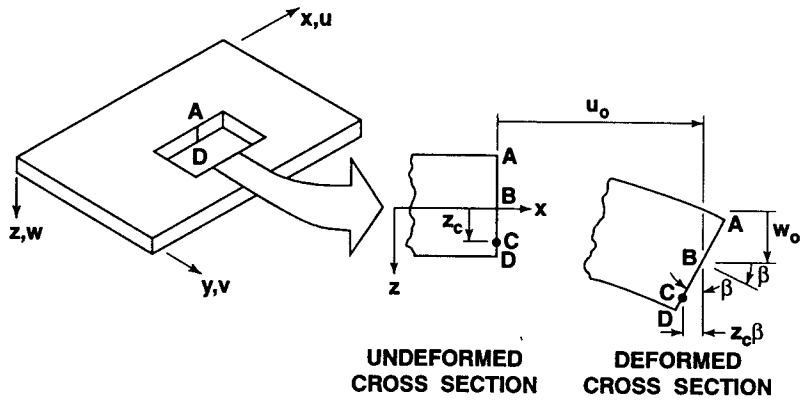

Figure 4-4 Geometry of Deformation in the x-z Plane

$$u_c = u_o - z_c \beta \tag{4.7}$$

But because, under deformation, line ABCD further remains perpendicular to the middle surface, β is the slope of the laminate middle surface in the x-direction, that is,

$$\beta = \frac{\partial w_o}{\partial x} \tag{4.8}$$

Then, the displacement, u, at any point z through the laminate thickness is

$$u = u_o - z\frac{\partial w_o}{\partial x} \tag{4.9}$$

By similar reasoning, the displacement, v, in the y-direction is

$$v = v_o - z\frac{\partial w_o}{\partial y} \tag{4.10}$$

The laminate strains have been reduced to ε_x, ε_y, and γ_{xy} by virtue of the Kirchhoff hypothesis. That is, $\varepsilon_z = \gamma_{xz} = \gamma_{yz} = 0$. For small strains (linear elasticity), the remaining strains are defined in terms of displacements as

$$\begin{aligned} \varepsilon_x &= \frac{\partial u}{\partial x} \\ \varepsilon_y &= \frac{\partial v}{\partial y} \\ \gamma_{xy} &= \frac{\partial u}{\partial y} + \frac{\partial v}{\partial x} \end{aligned} \tag{4.11}$$

Thus, for the derived displacements u and v in Equations (4.9) and (4.10), the strains are

$$\varepsilon_x = \frac{\partial u_o}{\partial x} - z\frac{\partial^2 w_o}{\partial x^2} \qquad \varepsilon_y = \frac{\partial v_o}{\partial y} - z\frac{\partial^2 w_o}{\partial y^2} \qquad \gamma_{xy} = \frac{\partial u_o}{\partial y} + \frac{\partial v_o}{\partial x} - 2z\frac{\partial^2 w_o}{\partial x \partial y} \tag{4.12}$$

or

$$\begin{bmatrix} \varepsilon_x \\ \varepsilon_y \\ \gamma_{xy} \end{bmatrix} = \begin{bmatrix} \varepsilon_x^o \\ \varepsilon_y^o \\ \gamma_{xy}^o \end{bmatrix} + z \begin{bmatrix} \kappa_x \\ \kappa_y \\ \kappa_{xy} \end{bmatrix} \tag{4.13}$$

where the middle-surface strains are

$$\begin{bmatrix} \varepsilon_x^o \\ \varepsilon_y^o \\ \gamma_{xy}^o \end{bmatrix} = \begin{bmatrix} \dfrac{\partial u_o}{\partial x} \\ \dfrac{\partial v_o}{\partial y} \\ \dfrac{\partial u_o}{\partial y} + \dfrac{\partial v_o}{\partial x} \end{bmatrix} \tag{4.14}$$

and the middle-surface curvatures are

$$\begin{bmatrix} \kappa_x \\ \kappa_y \\ \kappa_{xy} \end{bmatrix} = -\begin{bmatrix} \dfrac{\partial^2 w_o}{\partial x^2} \\ \dfrac{\partial^2 w_o}{\partial y^2} \\ 2\dfrac{\partial^2 w_o}{\partial x \partial y} \end{bmatrix} \tag{4.15}$$

(The last term in Equation (4.15) is the twist curvature of the middle surface.) We refer only to curvatures of the middle surface as a reference surface and not of any other surface, so nought superscripts are not needed on κ_x, κ_y, and κ_{xy}. Thus, the Kirchhoff hypothesis has been readily verified to imply a linear variation of strain through the laminate thickness because the strains in Equation (4.13) have the form of a straight line, i.e., $y = mx + b$. The foregoing strain analysis is valid only for plates because of the strain-displacement relations in Equation (4.11). For circular cylindrical shells, the ε_y term in Equation (4.11) must be supplemented by w_o/r where r is the shell radius; other shells have more complicated strain-displacement relations.

By substitution of the strain variation through the thickness, Equation (4.13), in the stress-strain relations, Equation (4.6), the stresses in the k^{th} layer can be expressed in terms of the laminate middle-surface strains and curvatures as

$$\begin{bmatrix} \sigma_x \\ \sigma_y \\ \tau_{xy} \end{bmatrix}_k = \begin{bmatrix} \overline{Q}_{11} & \overline{Q}_{12} & \overline{Q}_{16} \\ \overline{Q}_{12} & \overline{Q}_{22} & \overline{Q}_{26} \\ \overline{Q}_{16} & \overline{Q}_{26} & \overline{Q}_{66} \end{bmatrix}_k \left(\begin{bmatrix} \varepsilon_x^o \\ \varepsilon_y^o \\ \gamma_{xy}^o \end{bmatrix} + z \begin{bmatrix} \kappa_x \\ \kappa_y \\ \kappa_{xy} \end{bmatrix} \right) \tag{4.16}$$

The $\overline{Q}_{ij}$ can be different for each layer of the laminate, so the stress variation through the laminate thickness is not necessarily linear, even though the strain variation is linear. Instead, typical strain and stress variations are shown in Figure 4-5 where the stresses are piecewise linear (i.e., linear in each layer, but discontinuous at boundaries between laminae).

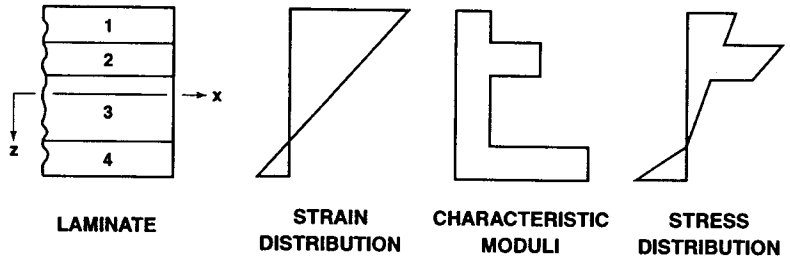

Figure 4-5 Hypothetical Variation of Strain and Stress through the Laminate Thickness

4.2.3 Resultant Laminate Forces and Moments

The resultant forces and moments acting on a laminate are obtained by integration of the stresses in each layer or lamina through the laminate thickness, for example,

$$N_x = \int_{-t/2}^{t/2} \sigma_x \, dz \qquad M_x = \int_{-t/2}^{t/2} \sigma_x \, z \, dz \tag{4.17}$$

Note in Figure 4-5 that the stresses vary within each lamina as well as from lamina to lamina, so the integration is not trivial. Actually, N_x is a force per unit width of the cross section of the laminate as shown in Figure 4-6.

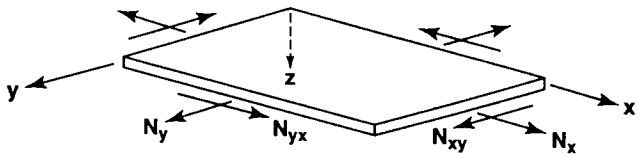

Figure 4-6 In-Plane Forces on a Flat Laminate

Similarly, M_x is a moment per unit width as shown in Figure 4-7. However, N_x, etc., and M_x, etc., will be referred to as forces and moments with the stipulation of 'per unit width' being dropped for convenience. The entire collection of force and moment resultants for an N-layered laminate is depicted in Figures 4-6 and 4-7 and is defined as

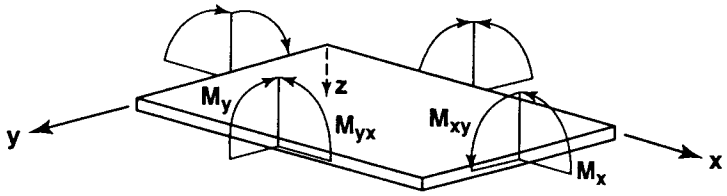

Figure 4-7 Moments on a Flat Laminate

$$\begin{bmatrix} N_x \\ N_y \\ N_{xy} \end{bmatrix} = \int_{-t/2}^{t/2} \begin{bmatrix} \sigma_x \\ \sigma_y \\ \tau_{xy} \end{bmatrix} dz = \sum_{k=1}^{N} \int_{z_{k-1}}^{z_k} \begin{bmatrix} \sigma_x \\ \sigma_y \\ \tau_{xy} \end{bmatrix}_k dz \qquad (4.18)$$

and

$$\begin{bmatrix} M_x \\ M_y \\ M_{xy} \end{bmatrix} = \int_{-t/2}^{t/2} \begin{bmatrix} \sigma_x \\ \sigma_y \\ \tau_{xy} \end{bmatrix} z\, dz = \sum_{k=1}^{N} \int_{z_{k-1}}^{z_k} \begin{bmatrix} \sigma_x \\ \sigma_y \\ \tau_{xy} \end{bmatrix}_k z\, dz \qquad (4.19)$$

where z_k and z_{k-1} are defined in the basic laminate geometry of Figure 4-8. Note there that the z_i are directed distances (coordinates) in accordance with the convention that z is positive downward. That is, z_k is the directed distance to the bottom of the k^{th} layer, and z_{k-1} is the directed distance to the top of the k^{th} layer. Moreover, $z_o = -t/2$, $z_1 = -t/2 + t_1$, etc., whereas $z_N = +t/2$, $z_{N-1} = +t/2 - t_N$, etc. These force and moment resultants do not depend on z after integration, but are functions of x and y, the coordinates in the plane of the laminate middle surface.

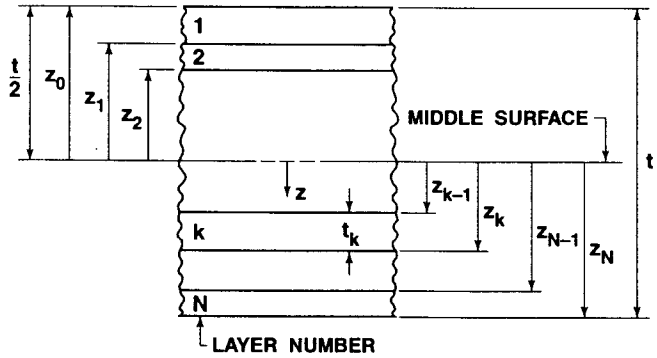

Figure 4-8 Geometry of an N-Layered Laminate

Equations (4.18) and (4.19) can be rearranged to take advantage of the fact that the stiffness matrix for a lamina is often constant within the lamina (unless the lamina has temperature-dependent or moisture-dependent properties and a temperature gradient or a moisture gradient exists across the lamina). If the elevated temperature or moisture is constant through the thickness of the lamina (a 'soaked' condition), then the values of $[\bar{Q}_{ij}]_k$ are constant in the layer but probably degraded because of the presence of temperature and/or moisture. Thus, the stiffness matrix goes outside the integration over each layer, but is within the summation of force and moment resultants for each layer. When the lamina stress-strain relations, Equation (4.16), are substituted, the forces and moments become

$$\begin{bmatrix} N_x \\ N_y \\ N_{xy} \end{bmatrix} = \sum_{k=1}^{N} \begin{bmatrix} \bar{Q}_{11} & \bar{Q}_{12} & \bar{Q}_{16} \\ \bar{Q}_{12} & \bar{Q}_{22} & \bar{Q}_{26} \\ \bar{Q}_{16} & \bar{Q}_{26} & \bar{Q}_{66} \end{bmatrix}_k \left[\int_{z_{k-1}}^{z_k} \begin{bmatrix} \varepsilon_x^o \\ \varepsilon_y^o \\ \gamma_{xy}^o \end{bmatrix} dz + \int_{z_{k-1}}^{z_k} \begin{bmatrix} \kappa_x \\ \kappa_y \\ \kappa_{xy} \end{bmatrix} z\, dz \right] \qquad (4.20)$$

$$\begin{bmatrix} M_x \\ M_y \\ M_{xy} \end{bmatrix} = \sum_{k=1}^{N} \begin{bmatrix} \bar{Q}_{11} & \bar{Q}_{12} & \bar{Q}_{16} \\ \bar{Q}_{12} & \bar{Q}_{22} & \bar{Q}_{26} \\ \bar{Q}_{16} & \bar{Q}_{26} & \bar{Q}_{66} \end{bmatrix}_k \left[\int_{z_{k-1}}^{z_k} \begin{bmatrix} \varepsilon_x^o \\ \varepsilon_y^o \\ \gamma_{xy}^o \end{bmatrix} z\, dz + \int_{z_{k-1}}^{z_k} \begin{bmatrix} \kappa_x \\ \kappa_y \\ \kappa_{xy} \end{bmatrix} z^2\, dz \right] \qquad (4.21)$$

Sometimes the stiffness matrix for a lamina, $[\bar{Q}_{ij}]_k$, is not constant through the thickness of the lamina. For example, if a temperature gradient or moisture gradient exists in the lamina and the lamina material properties are temperature dependent and/or moisture dependent, then $[\bar{Q}_{ij}]_k$ is a function of z and must be left inside the integral. In such cases,

the laminate is nonhomogeneous within each layer, so a more complicated numerical solution is required than is addressed here.

We should now recall that ε_x°, ε_y°, γ_{xy}°, κ_x, κ_y, and κ_{xy} are not functions of z, but are middle-surface values so they can be removed from within the summation signs. Thus, Equations (4.20) and (4.21) can be written as

$$\begin{bmatrix} N_x \\ N_y \\ N_{xy} \end{bmatrix} = \begin{bmatrix} A_{11} & A_{12} & A_{16} \\ A_{12} & A_{22} & A_{26} \\ A_{16} & A_{26} & A_{66} \end{bmatrix} \begin{bmatrix} \varepsilon_x^\circ \\ \varepsilon_y^\circ \\ \gamma_{xy}^\circ \end{bmatrix} + \begin{bmatrix} B_{11} & B_{12} & B_{16} \\ B_{12} & B_{22} & B_{26} \\ B_{16} & B_{26} & B_{66} \end{bmatrix} \begin{bmatrix} \kappa_x \\ \kappa_y \\ \kappa_{xy} \end{bmatrix} \tag{4.22}$$

$$\begin{bmatrix} M_x \\ M_y \\ M_{xy} \end{bmatrix} = \begin{bmatrix} B_{11} & B_{12} & B_{16} \\ B_{12} & B_{22} & B_{26} \\ B_{16} & B_{26} & B_{66} \end{bmatrix} \begin{bmatrix} \varepsilon_x^\circ \\ \varepsilon_y^\circ \\ \gamma_{xy}^\circ \end{bmatrix} + \begin{bmatrix} D_{11} & D_{12} & D_{16} \\ D_{12} & D_{22} & D_{26} \\ D_{16} & D_{26} & D_{66} \end{bmatrix} \begin{bmatrix} \kappa_x \\ \kappa_y \\ \kappa_{xy} \end{bmatrix} \tag{4.23}$$

where

$$\begin{aligned} A_{ij} &= \sum_{k=1}^{N} (\bar{Q}_{ij})_k (z_k - z_{k-1}) \\ B_{ij} &= \frac{1}{2} \sum_{k=1}^{N} (\bar{Q}_{ij})_k (z_k^2 - z_{k-1}^2) \\ D_{ij} &= \frac{1}{3} \sum_{k=1}^{N} (\bar{Q}_{ij})_k (z_k^3 - z_{k-1}^3) \end{aligned} \tag{4.24}$$

In Equations (4.22), (4.23), and (4.24), the A_{ij} are extensional stiffnesses, the B_{ij} are bending-extension coupling stiffnesses, and the D_{ij} are bending stiffnesses. The mere presence of the B_{ij} implies coupling between bending and extension of a laminate [because both forces and curvatures as well as moments and strains simultaneously exist in Equations (4.22) and (4.23)]. Thus, it is impossible to pull on a laminate that has B_{ij} terms without at the same time bending and/or twisting the laminate. That is, an extensional force results in not only extensional deformations, but bending and/or twisting of the laminate. Also, such a laminate cannot be subjected to moment without at the same time suffering extension of the middle surface. The first observation is borne out for the two-layered, nylon-reinforced rubber laminate depicted in Figure 4-9. Without load, the laminate is flat as in Figure 4-9a. Subject the laminate to the force resultant N_x and, because of the manner of support and loading, $N_y = N_{xy} = M_x = M_{xy} = 0$. When the principal material directions of the two laminae are oriented at $+\alpha$ and $-\alpha$, respectively, to the laminate x-axis, we can show that the general expression for N_x is specialized to

$$N_x = A_{11}\varepsilon_x^\circ + A_{12}\varepsilon_y^\circ + B_{16}\kappa_{xy} \tag{4.25}$$

Thus, the force resultant N_x produces twisting of the laminate as evidenced by the κ_{xy} term in addition to the usual normal strains ε_x° (extension) and ε_y° (contraction) as readily seen in Figure 4-9a.

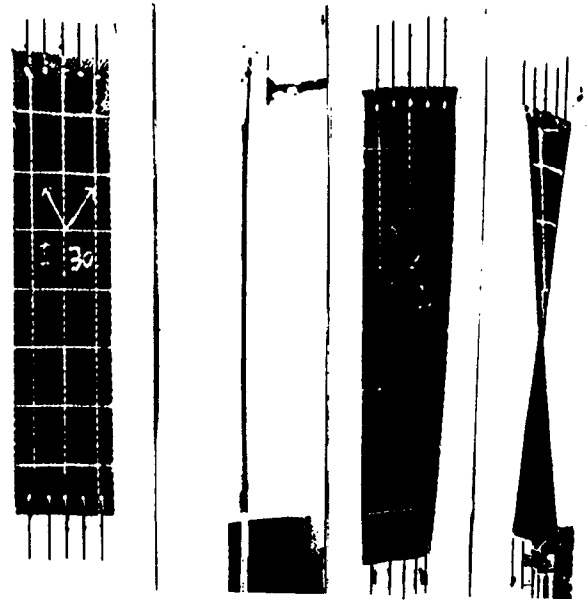

a Unloaded b Loaded with N_x

Figure 4-9 Twisting of a Two-Layered Antisymmetric Laminate under Tension *(After Ashton, Halpin, and Petit [4-3])*

4.2.4 Summary

Classical lamination theory consists of a comprehensive set of deformation hypotheses leading to the force-strain-curvature and moment-strain-curvature relations of Equations (4.22) and (4.23) shown in Figure 4-10 where the physical significances of the A_{ij}, B_{ij}, and D_{ij} are labeled. There, A_{16} and A_{26} represent shear-extension coupling at the laminate level analogous to that found for a single lamina in Chapter Two. Of course, the B_{ij} represent coupling between bending and extension, a phenomenon not found at the lamina level. Finally, D_{16} and D_{26} represent bend-twist coupling. Bend-twist coupling is illustrated by bending a fiber-reinforced rubber beam that has unidirectional nylon fibers at some angle to the spanwise direction in the horizontal plane as in Figure 4-11b. There, the beam not only bends in the spanwise direction, but it also twists about its spanwise axis as outlined with white ink on the black rubber body of the beam such that two diagonally opposite corners of the beam actually lift off the supports. If the same beam is rotated 90° about its spanwise axis (so the fibers are at some angle to the spanwise axis in the *vertical* plane) and bent as in Figure 4-11a, then no twisting occurs! A plate with fibers at an angle to the spanwise direction behaves in a similar manner as shown in Figure 4-12.

SHEAR-EXTENSION COUPLING

BENDING-EXTENSION COUPLING

$$\begin{Bmatrix} N_x \\ N_y \\ N_{xy} \end{Bmatrix} = \begin{bmatrix} A_{11} & A_{12} & A_{16} \\ A_{12} & A_{22} & A_{26} \\ A_{16} & A_{26} & A_{66} \end{bmatrix} \begin{Bmatrix} \epsilon_x^0 \\ \epsilon_y^0 \\ \gamma_{xy}^0 \end{Bmatrix} + \begin{bmatrix} B_{11} & B_{12} & B_{16} \\ B_{12} & B_{22} & B_{26} \\ B_{16} & B_{26} & B_{66} \end{bmatrix} \begin{Bmatrix} \kappa_x \\ \kappa_y \\ \kappa_{xy} \end{Bmatrix}$$

$$\begin{Bmatrix} M_x \\ M_y \\ M_{xy} \end{Bmatrix} = \begin{bmatrix} B_{11} & B_{12} & B_{16} \\ B_{12} & B_{22} & B_{26} \\ B_{16} & B_{26} & B_{66} \end{bmatrix} \begin{Bmatrix} \epsilon_x^0 \\ \epsilon_y^0 \\ \gamma_{xy}^0 \end{Bmatrix} + \begin{bmatrix} D_{11} & D_{12} & D_{16} \\ D_{12} & D_{22} & D_{26} \\ D_{16} & D_{26} & D_{66} \end{bmatrix} \begin{Bmatrix} \kappa_x \\ \kappa_y \\ \kappa_{xy} \end{Bmatrix}$$

BENDING-EXTENSION COUPLING

BEND-TWIST COUPLING

Figure 4-10 Physical Significance of Stiffness Terms in Force and Moment Resultants

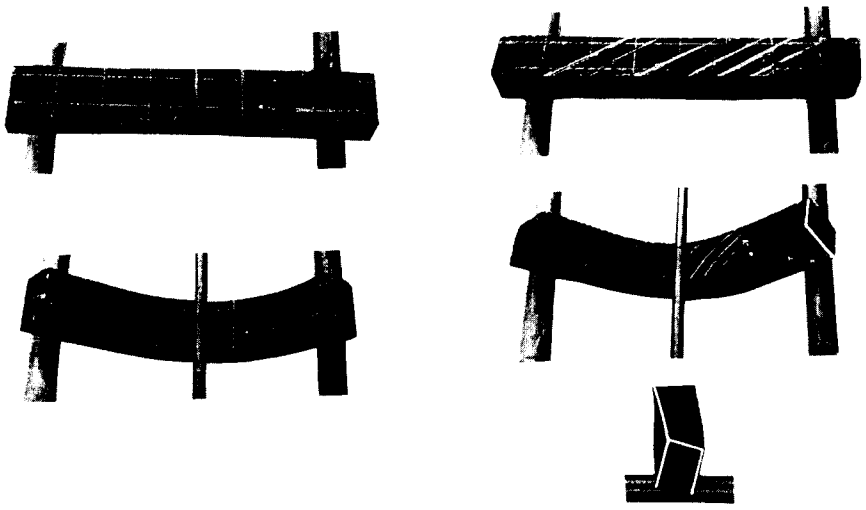

Figure 4-11 Effect of Bend-Twist Coupling on Beam Bending *(After Ashton, Halpin, and Petit [4-3])*

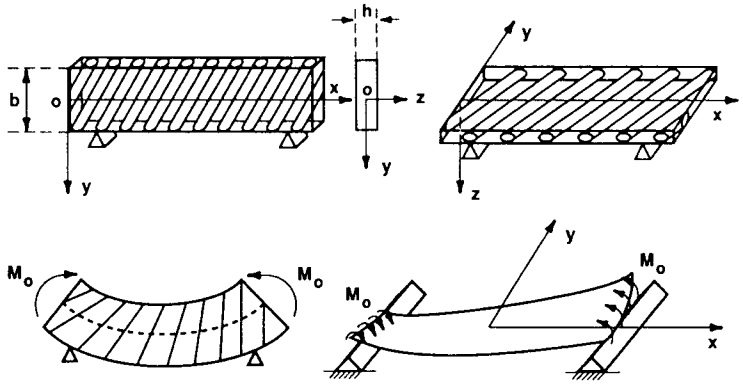

Figure 4-12 Effect of Bend-Twist Coupling on Plate Bending *(After Ashton, Halpin, and Petit [4-3])*

The behaviors studied so far include isotropic materials, orthotropic materials (sometimes called specially orthotropic if loaded in principal material directions), generally orthotropic materials (merely an orthotropic material loaded in non-principal material directions), and laminates. Each of the configurations is shown in Figure 4-13 along with deformation response to axial loading. Note that shear-extension coupling does not occur for orthotropic materials loaded in principal material directions, but does occur if the loading is not in those directions. Finally, a laminate can twist when pulled in the axial direction. Also shown in Figure 4-13 is the number of independent elastic constants for each material class (two for isotropic materials and four for orthotropic materials). Note especially that a laminate has a maximum of 18 stiffnesses (six each of A_{ij}, B_{ij}, and D_{ij}). The number of elastic constants for a laminate is a maximum of four per layer, but if the laminate is made of the same material in each layer, then the laminate has only four elastic constants.

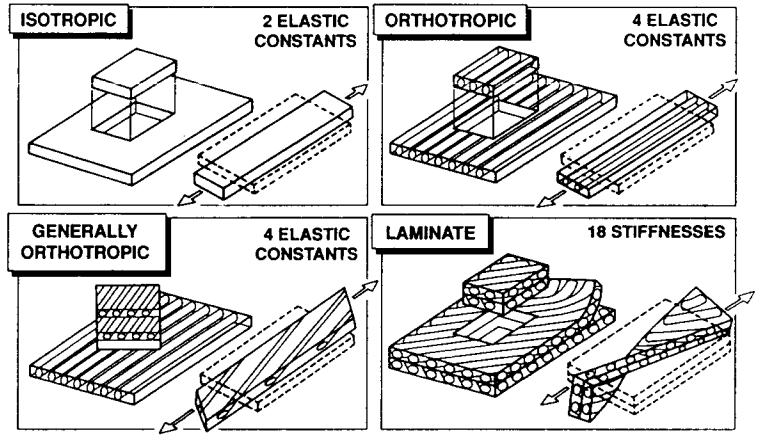

Figure 4-13 Material Forms *(After Ashton, Halpin, and Petit [4-3])*

Some engineers have tried to characterize laminates with effective laminate stiffnesses, E_x, E_y, ν_{xy}, and G_{xy}, and indeed such properties can be determined for a laminate by the usual measurements. However, it is crucial to recognize that with an effective laminate stiffness approach

- shear-extension coupling is ignored
- all bending response is ignored (including, of course, bend-twist coupling)
- coupling between bending and extension is ignored (many laminates are symmetric, but many others are not)

We must conclude that *a laminate is not a material, but instead is a structural element with essential features of both material properties and geometry that cannot be ignored.* Thus, an effective laminate stiffness approach is fatally flawed in most practical applications (although not for a laminate that is symmetric about the middle surface and subjected only to extensional loading). Accordingly, *we must characterize laminates with the essential extension, bending-extension coupling, and bending stiffnesses of Equation (4.24).*

In conclusion, classical lamination theory enables us to calculate forces and moments if we know the strains and curvatures of the middle surface (or vice versa). Then, we can calculate the laminae stresses in laminate coordinates. Next, we can transform the laminae stresses from laminate coordinates to lamina principal material directions. Finally, we would expect to apply a failure criterion to each lamina in its own principal material directions. This process seems straightforward in principle, but the force-strain-curvature and moment-strain-curvature relations in Equations (4.22) and (4.23) are difficult to completely understand. Thus, we attempt some simplifications in the next section in order to enhance our understanding of classical lamination theory.

Problem Set 4.2

4.2.1 Verify for a single layer of isotropic material with material properties E and ν and thickness t that the extensional and bending stiffnesses are

$$A_{11} = A_{22} = \frac{E\,t}{1-\nu^2} \qquad D_{11} = D_{22} = \frac{E\,t^3}{12(1-\nu^2)}$$

which are commonly called B and D, respectively, in ordinary isotropic plate theory. What are the bending-extension coupling stiffnesses?

4.2.2 Derive the summation expressions for extensional, bending-extension coupling, and bending stiffnesses for laminates with constant properties in each orthotropic lamina; that is, derive Equation (4.24) from Equations (4.20) and (4.21).

4.2.3 Show that the stiffnesses in Equation (4.24) can be written as

$$A_{ij} = \sum_{k=1}^{N} (\bar{Q}_{ij})_k\, t_k \qquad B_{ij} = \sum_{k=1}^{N} (\bar{Q}_{ij})_k\, t_k\, \bar{z}_k \qquad D_{ij} = \sum_{k=1}^{N} (\bar{Q}_{ij})_k \left[t_k\, \bar{z}_k^2 + \frac{t_k^3}{12} \right]$$

wherein t_k is the thickness and $\bar{z}_k$ is the distance to the centroid of the k^{th} orthotropic layer. What is the physical meaning of the coefficients of $(\bar{Q}_{ij})_k$ in each of the foregoing expressions?

4.2.4 Determine the extensional, bending-extension coupling, and bending stiffnesses of an equal-thickness bimetallic strip as shown in Figure 1-3 (a beam made of two different isotropic materials with E_1, ν_1, α_1, E_2, ν_2, and α_2). Use the middle surface of the beam as the reference surface.

4.2.5 Demonstrate that the force per unit width on a two-layered laminate with orthotropic laminae of equal thickness oriented at $+\alpha$ and $-\alpha$ to the applied force is

$$N_x = A_{11}\varepsilon_x^o + A_{12}\varepsilon_y^o + B_{16}\kappa_{xy}$$

What are A_{11}, A_{12}, and B_{16} in terms of the transformed reduced stiffnesses, $(\bar{Q}_{ij})_{+\alpha}$, of a lamina and the lamina thickness, t?

4.2.6 Do all parts of Problem 4.2.5 for moment per unit width, M_x.

4.3 SPECIAL CASES OF LAMINATE STIFFNESSES

This section is devoted to those special cases of laminates for which the stiffnesses take on certain simplified values as opposed to the general form in Equation (4.24). The general force-moment-strain-curvature relations in Equations (4.22) and (4.23) are far too comprehensive to easily understand. Thus, we build up our understanding of laminate behavior from the simplest cases to more complicated cases. Some of the cases are almost trivial, others are more specialized, some do not occur often in practice, but the point is that *all* are contributions to the understanding of the concept of laminate stiffnesses. Many of the cases result from the common practice of constructing laminates from laminae that have the same material properties and thickness, but have different orientations of the principal material directions relative to one another and relative to the laminate axes. Other more general cases are examined as well.

Stiffnesses for single-layered configurations are treated first to provide a baseline for subsequent discussion. Such stiffnesses should be recognizable in terms of concepts previously encountered by the reader in his study of plates and shells. Next, laminates that are symmetric about their middle surface are discussed and classified. Then, laminates with laminae that are antisymmetrically arranged about their middle surface are described. Finally, laminates with complete lack of middle-surface symmetry, i.e., unsymmetric laminates, are discussed. For all laminates, the question of laminae thicknesses arises. Regular laminates have equal-thickness laminae, and irregular laminates have non-equal-thickness laminae.

4.3.1 Single-Layered Configurations

The special single-layered configurations treated in this section are isotropic, specially orthotropic, generally orthotropic, and anisotropic. The generally orthotropic configuration cannot, of course, be distinguished from an anisotropic layer from the analysis point of view, but does have only the four independent material properties of an orthotropic material.

Single Isotropic Layer

For a single isotropic layer with material properties, E and ν, and thickness, t, the laminate stiffnesses of Equation (4.24) reduce to

$$A_{11} = \frac{Et}{1-\nu^2} = A \qquad D_{11} = \frac{Et^3}{12(1-\nu^2)} = D$$
$$A_{12} = \nu A \qquad D_{12} = \nu D$$
$$A_{22} = A \qquad B_{ij} = 0 \qquad D_{22} = D \qquad (4.26)$$
$$A_{16} = 0 \qquad D_{16} = 0$$
$$A_{26} = 0 \qquad D_{26} = 0$$
$$A_{66} = \frac{Et}{2(1+\nu)} = \frac{1-\nu}{2}A \qquad D_{66} = \frac{Et^3}{24(1+\nu)} = \frac{1-\nu}{2}D$$

whereupon the resultant forces depend only on the in-plane strains of the laminate middle surface, and the resultant moments depend only on the curvatures of the middle surface:

$$\begin{bmatrix} N_x \\ N_y \\ N_{xy} \end{bmatrix} = \begin{bmatrix} A & \nu A & 0 \\ \nu A & A & 0 \\ 0 & 0 & \frac{1-\nu}{2}A \end{bmatrix} \begin{bmatrix} \varepsilon_x^\circ \\ \varepsilon_y^\circ \\ \gamma_{xy}^\circ \end{bmatrix} \qquad (4.27)$$

$$\begin{bmatrix} M_x \\ M_y \\ M_{xy} \end{bmatrix} = \begin{bmatrix} D & \nu D & 0 \\ \nu D & D & 0 \\ 0 & 0 & \frac{1-\nu}{2}D \end{bmatrix} \begin{bmatrix} \kappa_x \\ \kappa_y \\ \kappa_{xy} \end{bmatrix} \qquad (4.28)$$

Thus, there is no coupling between bending and extension of a single isotropic layer. Also note that

$$D = \frac{At^2}{12} \qquad (4.29)$$

Single Specially Orthotropic Layer

For a single specially orthotropic layer of thickness, t, and lamina stiffnesses, Q_{ij}, given in Equation (2.61), the laminate stiffnesses are

$$A_{11} = Q_{11}t \qquad D_{11} = \frac{Q_{11}t^3}{12}$$
$$A_{12} = Q_{12}t \qquad D_{12} = \frac{Q_{12}t^3}{12}$$
$$A_{22} = Q_{22}t \qquad B_{ij} = 0 \qquad D_{22} = \frac{Q_{22}t^3}{12} \qquad (4.30)$$
$$A_{16} = 0 \qquad D_{16} = 0$$
$$A_{26} = 0 \qquad D_{26} = 0$$
$$A_{66} = Q_{66}t \qquad D_{66} = \frac{Q_{66}t^3}{12}$$

whereupon, as with a single isotropic layer, the resultant forces depend only on the in-plane strains, and the resultant moments depend only on the curvatures:

$$\begin{bmatrix} N_x \\ N_y \\ N_{xy} \end{bmatrix} = \begin{bmatrix} A_{11} & A_{12} & 0 \\ A_{12} & A_{22} & 0 \\ 0 & 0 & A_{66} \end{bmatrix} \begin{bmatrix} \varepsilon_x^\circ \\ \varepsilon_y^\circ \\ \gamma_{xy}^\circ \end{bmatrix} \qquad (4.31)$$

$$\begin{bmatrix} M_x \\ M_y \\ M_{xy} \end{bmatrix} = \begin{bmatrix} D_{11} & D_{12} & 0 \\ D_{12} & D_{22} & 0 \\ 0 & 0 & D_{66} \end{bmatrix} \begin{bmatrix} \kappa_x \\ \kappa_y \\ \kappa_{xy} \end{bmatrix} \qquad (4.32)$$

Single Generally Orthotropic Layer

For a single generally orthotropic layer of thickness, t, and lamina stiffnesses, $\overline{Q}_{ij}$, given in Equation (2.80), the laminate stiffnesses are

$$A_{ij} = \overline{Q}_{ij}t \qquad B_{ij} = 0 \qquad D_{ij} = \frac{\overline{Q}_{ij}t^3}{12} \qquad (4.33)$$

Again, there is no coupling between bending and extension, so the force and moment resultants are

$$\begin{bmatrix} N_x \\ N_y \\ N_{xy} \end{bmatrix} = \begin{bmatrix} A_{11} & A_{12} & A_{16} \\ A_{12} & A_{22} & A_{26} \\ A_{16} & A_{26} & A_{66} \end{bmatrix} \begin{bmatrix} \varepsilon_x^\circ \\ \varepsilon_y^\circ \\ \gamma_{xy}^\circ \end{bmatrix} \qquad (4.34)$$

$$\begin{bmatrix} M_x \\ M_y \\ M_{xy} \end{bmatrix} = \begin{bmatrix} D_{11} & D_{12} & D_{16} \\ D_{12} & D_{22} & D_{26} \\ D_{16} & D_{26} & D_{66} \end{bmatrix} \begin{bmatrix} \kappa_x \\ \kappa_y \\ \kappa_{xy} \end{bmatrix} \qquad (4.35)$$

Note, in contrast to both an isotropic layer and a specially orthotropic layer, that extensional forces depend on shearing strain as well as on extensional strain. Also, the resultant shearing force, N_{xy}, depends on the extensional strains, ε_x° and ε_y°, as well as on the shear strain, γ_{xy}°. Similarly, the moment resultants all depend on both the bending curvatures, κ_x and κ_y, and on the twist curvature, κ_{xy}.

Single Anisotropic Layer

The only difference in appearance between a single generally orthotropic layer and an anisotropic layer is that the latter has lamina

stiffnesses, Q_{ij}, defined implicitly in Equation (2.84) whereas the generally orthotropic layer has stiffnesses, $\bar{Q}_{ij}$, defined in Equation (2.80). The laminate stiffnesses are

$$A_{ij} = Q_{ij}\, t \qquad B_{ij} = 0 \qquad D_{ij} = \frac{Q_{ij}\, t^3}{12} \tag{4.36}$$

and the force and moment resultants are Equations (4.34) and (4.35).

4.3.2 Symmetric Laminates

For laminates that are symmetric in *both geometry and material properties* about the middle surface, the general stiffness equations, Equation (4.24), simplify considerably. That symmetry has the form such that for each pair of equal-thickness laminae: (1) both laminae are of the same material properties and principal material direction orientations, i.e., both laminae have the same $(\bar{Q}_{ij})_k$; and (2) if one lamina is a certain distance above the middle surface, then the other lamina is the same distance *below* the middle surface. A single layer that straddles the middle surface can be considered a pair of half-thickness laminae that satisfies the symmetry requirement (note that such a lamina is inherently symmetric about the middle surface).

Because of the symmetry of the $(\bar{Q}_{ij})_k$ and the thicknesses t_k, all the bending-extension coupling stiffnesses, that is, the B_{ij}, can be shown to be zero. The elimination of coupling between bending and extension has two important practical ramifications. First, such laminates are usually much easier to analyze than laminates with bending-extension coupling. Second, symmetric laminates do not have a tendency to bend or twist from the inevitable thermally induced contractions that occur during cooling following the curing process. For example, an unsymmetric cross-ply laminate that was laid up from individual layers on a flat steel plate and enclosed top and bottom with flat steel plates during curing in a hot press is shown in Figure 4-14 after being removed from the plates and the hot press. What a shock to see such a highly curved laminate come out of the curing process after you put in a set of flat laminae between flat steel plates in a flat hot press! Consequently, symmetric laminates are commonly used unless special circumstances require an unsymmetric laminate. For example, part of the function of a laminate might be to serve as a heat shield, but the heat comes from only one side; thus, an unsymmetric laminate must be used (or will result anyway!) The force and moment resultants for a symmetric laminate are

$$\begin{bmatrix} N_x \\ N_y \\ N_{xy} \end{bmatrix} = \begin{bmatrix} A_{11} & A_{12} & A_{16} \\ A_{12} & A_{22} & A_{26} \\ A_{16} & A_{26} & A_{66} \end{bmatrix} \begin{bmatrix} \varepsilon_x^o \\ \varepsilon_y^o \\ \gamma_{xy}^o \end{bmatrix} \tag{4.37}$$

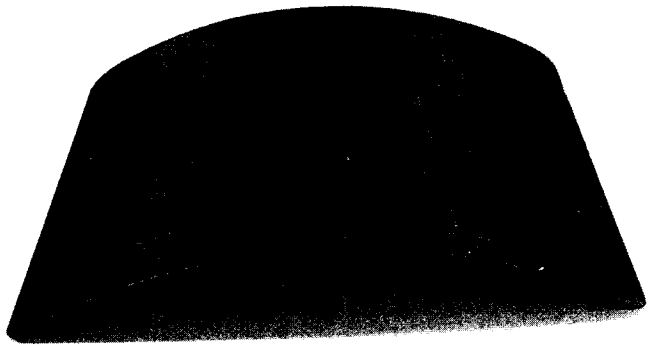

Figure 4-14 An Unsymmetric Laminate after Curing

$$\begin{bmatrix} M_x \\ M_y \\ M_{xy} \end{bmatrix} = \begin{bmatrix} D_{11} & D_{12} & D_{16} \\ D_{12} & D_{22} & D_{26} \\ D_{16} & D_{26} & D_{66} \end{bmatrix} \begin{bmatrix} \kappa_x \\ \kappa_y \\ \kappa_{xy} \end{bmatrix} \tag{4.38}$$

Special cases of symmetric laminates will be described in the following subsections. In each case, the A_{ij} and D_{ij} in Equations (4.37) and (4.38) take on different values, and some will even vanish.

Note that even a laminate that is made symmetrically about the middle surface can have coupling between bending and extension! If the laminae have temperature-dependent material properties and a thermal gradient through the thickness is applied (recall the heat shield example in the beginning paragraph of this subsection), then the premises on which Equations (4.20) and (4.21) are based are no longer applicable. The stiffnesses are far more complicated than in Equation (4.24). The temperature gradient actually changes the material properties and, hence, destroys the original laminate symmetry.

Symmetric Laminates with Multiple Isotropic Layers

If multiple isotropic layers of various thicknesses are arranged symmetrically about a middle surface from both a geometric and a material property standpoint, then the resulting laminate does not exhibit coupling between bending and extension. A simple example of a symmetric laminate with three isotropic layers is shown in Figure 4-15. There, the two types of symmetry, material property and geometric, are quite evident. A more complicated example of a symmetric laminate with six isotropic layers of different elastic properties and thicknesses is given in Table 4-1. There also, the geometric and material property symmetry are both obvious. Note that layers 3 and 4 in Table 4-1 could together be regarded as a single layer of thickness 6t without changing the stiffness characteristics.

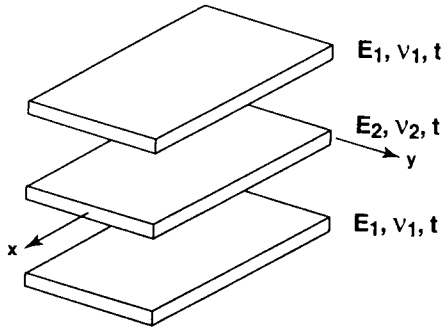

Figure 4-15 Unbonded View of a Three-Layered Symmetric Laminate with Isotropic Layers

Table 4-1 Symmetric Laminate with Six Multiple Isotropic Layers

Layer	Material Properties	Layer Thickness
1	E_1, ν_1	t
2	E_2, ν_2	2t
3	E_3, ν_3	3t
4	E_3, ν_3	3t
5	E_2, ν_2	2t
6	E_1, ν_1	t

The extensional and bending stiffnesses for the general case are calculated from Equation (4.24) wherein for the k^{th} layer

$$(\bar{Q}_{11})_k = (\bar{Q}_{22})_k = \frac{E_k}{1-\nu_k^2} \qquad (\bar{Q}_{16})_k = (\bar{Q}_{26})_k = 0$$
$$(\bar{Q}_{12})_k = \frac{\nu_k E_k}{1-\nu_k^2} \qquad (\bar{Q}_{66})_k = \frac{E_k}{2(1-\nu_k)} \qquad (4.39)$$

The force and moment resultants take the simplified form

$$\begin{bmatrix} N_x \\ N_y \\ N_{xy} \end{bmatrix} = \begin{bmatrix} A_{11} & A_{12} & 0 \\ A_{12} & A_{22} & 0 \\ 0 & 0 & A_{66} \end{bmatrix} \begin{bmatrix} \varepsilon_x^\circ \\ \varepsilon_y^\circ \\ \gamma_{xy}^\circ \end{bmatrix} \qquad (4.40)$$

$$\begin{bmatrix} M_x \\ M_y \\ M_{xy} \end{bmatrix} = \begin{bmatrix} D_{11} & D_{12} & 0 \\ D_{12} & D_{22} & 0 \\ 0 & 0 & D_{66} \end{bmatrix} \begin{bmatrix} \kappa_x \\ \kappa_y \\ \kappa_{xy} \end{bmatrix} \qquad (4.41)$$

wherein, for isotropic layers, $A_{11} = A_{22}$ and $D_{11} = D_{22}$ because of the first condition of Equation (4.39). The specific form of the A_{ij} and D_{ij} can be somewhat involved, as can easily be verified by examining some simple examples.

Symmetric Laminates with Multiple Specially Orthotropic Layers

Because of the analytical complications involving the stiffnesses A_{16}, A_{26}, D_{16}, and D_{26}, a laminate is sometimes desired that does not have these stiffnesses. Laminates can be made with orthotropic layers that have principal material directions aligned with the laminate axes. If the thicknesses, locations, and material properties of the laminae are symmetric about the middle surface of the laminate, there is no coupling between bending and extension. A general example is shown in Table 4-2. Note that the material property symmetry requires equal $[\bar{Q}_{ij}]_k$ of the two layers that are placed at the same distance above and below the middle surface. Thus, both the orthotropic material properties, $[Q_{ij}]_k$, of the layers *and* the angle of the principal material directions to the laminate axes (i.e., the orientation of each layer) must be identical.

The extensional and bending stiffnesses are calculated from Equation (4.24) wherein for the k^{th} layer

$$(\bar{Q}_{11})_k = \frac{E_1^k}{1-\nu_{12}^k\nu_{21}^k} \qquad (\bar{Q}_{12})_k = \frac{\nu_{12}^k E_1^k}{1-\nu_{12}^k\nu_{21}^k} \qquad (\bar{Q}_{22})_k = \frac{E_2^k}{1-\nu_{12}^k\nu_{21}^k}$$
$$(\bar{Q}_{16})_k = 0 \qquad (\bar{Q}_{26})_k = 0 \qquad (\bar{Q}_{66})_k = G_{12}^k \qquad (4.42)$$

Because $(\bar{Q}_{16})_k$ and $(\bar{Q}_{26})_k$ are zero, the stiffnesses A_{16}, A_{26}, D_{16}, and D_{26} vanish. Also, the bending-extension coupling stiffnesses B_{ij} are zero because of laminate symmetry. This type of laminate could therefore be called a specially orthotropic laminate in analogy to a specially orthotropic lamina (but really a laminate should not be called by a material property characterization name because laminates are not materials, but instead are structural elements). The force and moment resultants take the form of Equations (4.40) and (4.41), respectively, except that $A_{11} \neq A_{22}$ and $D_{11} \neq D_{22}$.

Table 4-2 Symmetric Laminate with Five Specially Orthotropic Layers

Layer	Material Properties				Orientation	Thickness
	Q_{11}	Q_{12}	Q_{22}	Q_{66}		
1	F_1	F_2	F_3	F_4	0°	t
2	G_1	G_2	G_3	G_4	90°	2t
3	H_1	H_2	H_3	H_4	90°	4t
4	G_1	G_2	G_3	G_4	90°	2t
5	F_1	F_2	F_3	F_4	0°	t

A very common special case of symmetric laminates with multiple specially orthotropic layers occurs when the laminae are all of the same thickness and material properties, but have their major principal material

directions alternating at 0° and 90° to the laminate axes, for example, 0°/90°/0°. Such laminates are called *regular symmetric cross-ply laminates* (*regular* because the laminae thicknesses are the same and *cross-ply* because the fibers in adjacent layers are at 90° to one another). A simple example of a regular symmetric cross-ply laminate with three layers of equal thickness and properties is shown in Figure 4-16. The fiber directions of each lamina are schematically indicated by the use of light lines in Figure 4-16. The laminate must have an odd number of layers to satisfy the symmetry requirement by which coupling between bending and extension is eliminated. Cross-ply laminates with an even number of layers are obviously not symmetric and will be discussed in Section 4.3.3. The less-common case of cross-ply laminates that have odd-numbered layers with equal thicknesses and even-numbered layers with thicknesses equal to each other but not to that of the odd-numbered layers will be discussed in Section 4.4, Theoretical versus Measured Laminate Stiffnesses.

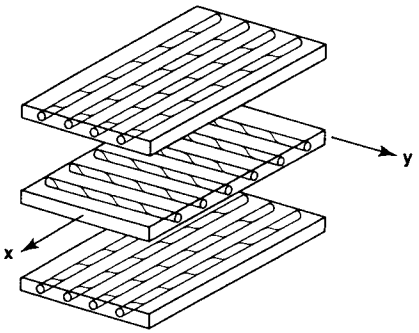

Figure 4-16 Unbonded View of a Three-Layered Regular Symmetric Cross-Ply Laminate

The logic to establish the various stiffnesses will be traced to illustrate the general procedures. First, consider the extensional stiffnesses

$$A_{ij} = \sum_{k=1}^{N} (\bar{Q}_{ij})_k (z_k - z_{k-1}) \tag{4.43}$$

The A_{ij} are the sum of the product of the individual laminae $\bar{Q}_{ij}$ and the laminae thicknesses. Thus, the only ways to obtain a zero individual A_{ij} are for all $\bar{Q}_{ij}$ to be zero or for some $\bar{Q}_{ij}$ to be negative and some positive so that their products with their respective thicknesses sum to zero. From the expressions for the transformed lamina stiffnesses, $\bar{Q}_{ij}$, in Equation (2.80), apparently $\bar{Q}_{11}$, $\bar{Q}_{12}$, $\bar{Q}_{22}$, and $\bar{Q}_{66}$ are positive-definite because all trigonometric functions appear to even powers. Thus, A_{11}, A_{12}, A_{22}, and A_{66} are positive-definite because the thicknesses are, of course, always positive. However, $\bar{Q}_{16}$ and $\bar{Q}_{26}$ are zero for lamina orientations of 0° and 90° to the laminate axes. Thus, A_{16} and A_{26} are zero for laminates of orthotropic laminae oriented at either 0° or 90° to the laminate axes.

Second, consider the bending-extension coupling stiffnesses

$$B_{ij} = \frac{1}{2} \sum_{k=1}^{N} (\bar{Q}_{ij})_k (z_k^2 - z_{k-1}^2) \tag{4.44}$$

If the cross-ply laminate is symmetric about the middle surface in both material properties and geometry, then the B_{ij} all vanish as is easily shown.

Finally, consider the bending stiffnesses

$$D_{ij} = \frac{1}{3} \sum_{k=1}^{N} (\bar{Q}_{ij})_k (z_k^3 - z_{k-1}^3) \tag{4.45}$$

The various D_{ij} are sums of the product of the individual laminae $\bar{Q}_{ij}$ and the term $(z_k^3 - z_{k-1}^3)$. Because $\bar{Q}_{11}$, $\bar{Q}_{12}$, $\bar{Q}_{22}$, and $\bar{Q}_{66}$ are positive-definite and the geometric term is positive-definite, then D_{11}, D_{12}, D_{22}, and D_{66} are positive-definite. Also, $\bar{Q}_{16}$ and $\bar{Q}_{26}$ are zero for lamina principal material property orientations of 0° and 90° to the laminate coordinate axes. Thus, D_{16} and D_{26} are zero.

Symmetric Laminates with Multiple Generally Orthotropic Layers

A laminate of multiple generally orthotropic layers that are symmetrically arranged about the middle surface exhibits no coupling between bending and extension; that is, the B_{ij} are zero. Therefore, the force and moment resultants are represented by Equations (4.37) and (4.38), respectively. There, all the A_{ij} and D_{ij} are required because of coupling between normal forces and shearing strain, shearing force and normal strains, normal moments and twist, and twisting moment and normal curvatures. Such coupling is evidenced by the A_{16}, A_{26}, D_{16}, and D_{26} stiffnesses.

Bend-twist coupling stiffnesses are the mechanism for control of forward-swept wings on the X-29A in Figure 1-37. Forward-swept wings are subjected to aerodynamic forces that tend to twist the wing about an axis that is along the wing and off perpendicular to the fuselage by the angle of the wing sweep, e.g., M_y in Figure 7-10. Aerodynamic divergence (gross wing flapping that in the limit tears the wing off) is the possible result. A composite laminate with laminae at various angles to the wing axis has D_{16} and D_{26} that cause the wing to twist in the opposite sense to the aerodynamic wing-twisting effect seen in Figure 4-17. Countering the wing-twisting effect on a metal wing causes large weight and cost penalties because the only way to create a structural D_{16} and D_{26} for metal wings requires many stiffeners at an angle to the wing axis. In contrast, the laminated composite wing might require a few extra layers of material, but no stiffeners, so both the weight and cost penalties are small to achieve the aircraft performance advantages of a forward-swept wing (e.g., improved agility and improved high angle-of-attack flying qualities). In fact, a forward-swept wing can be smaller in size, weight, and cost than the usual rearward-swept wing. Concepts of what has become known as aeroelastic tailoring of composite structures are reviewed by Hertz, Shirk, Ricketts, and Weisshaar [4-4].

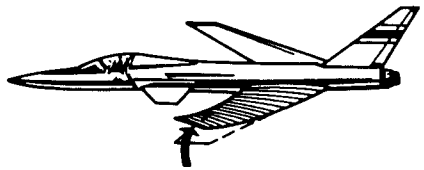

METAL WING BENDS AND TWISTS UNDER AERODYNAMIC LOADS

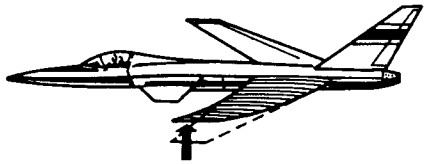

COMPOSITE WING BENDS, BUT DOES NOT TWIST

Figure 4-17 Response of Forward-Swept Wings

A special subclass of this class of symmetric laminates is the *regular symmetric angle-ply laminate* (*angle-ply* because the adjacent laminae are at $+\alpha$ and $-\alpha$ to axial direction of the laminate). Such laminates have orthotropic laminae of equal thicknesses. The adjacent laminae have opposite signs of the angle of orientation of the principal material properties with respect to the laminate axes, for example, $[+\alpha/-\alpha/+\alpha]$. Thus, for symmetry, there must be an odd number of layers. A simple example of a three-layered regular symmetric angle-ply laminate is shown in Figure 4-18. A more complicated example of a symmetric laminate with generally orthotropic layers is given in Table 4-3. Note that the laminae orthotropic material properties, orientations, and thicknesses are all symmetric about the middle surface.

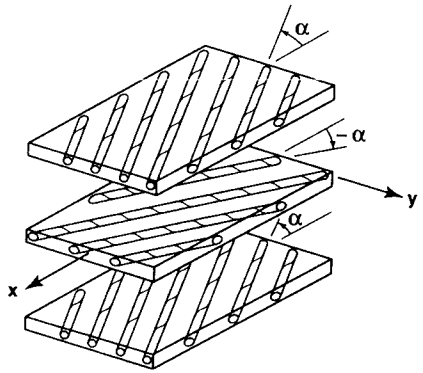

Figure 4-18 Unbonded View of a Three-Layered Regular Symmetric Angle-Ply Laminate

Table 4-3 Symmetric Laminate with Five Generally Orthotropic Layers

Layer	Material Properties				Orientation	Thickness
	Q_{11}	Q_{12}	Q_{22}	Q_{66}		
1	F_1	F_2	F_3	F_4	+30°	t
2	G_1	G_2	G_3	G_4	−60°	3t
3	H_1	H_2	H_3	H_4	+10°	5t
4	G_1	G_2	G_3	G_4	−60°	3t
5	F_1	F_2	F_3	F_4	+30°	t

The aforementioned coupling that involves A_{16}, A_{26}, D_{16}, and D_{26} takes on a special form for symmetric angle-ply laminates. Those stiffnesses can be shown to be largest when $N = 3$ (the lowest N for which this class of laminates exists) and decrease in proportion to 1/N as N increases (see Section 4.4.4). Actually, in the expressions for the extensional and bending stiffnesses A_{16} and D_{16},

$$A_{16} = \sum_{k=1}^{N} (\bar{Q}_{16})_k (z_k - z_{k-1}) \tag{4.46}$$

$$D_{16} = \frac{1}{3} \sum_{k=1}^{N} (\bar{Q}_{16})_k (z_k^3 - z_{k-1}^3) \tag{4.47}$$

Obviously, A_{16} and D_{16} are sums of terms of alternating signs because

$$(\bar{Q}_{16})_{+\alpha} = -(\bar{Q}_{16})_{-\alpha} \tag{4.48}$$

Thus, for many-layered symmetric angle-ply laminates, the values of A_{16}, A_{26}, D_{16}, and D_{26} can be quite small when compared to the other A_{ij} and D_{ij}, respectively.

When the always-present advantage of zero B_{ij} because of symmetry is considered in addition to the low A_{16}, A_{26}, D_{16}, and D_{26}, many-layered symmetric angle-ply laminates can offer significant, practically advantageous simplifications over some more general laminates. In addition, symmetric angle-ply laminates offer more shear stiffness than do the simpler cross-ply laminates, so are used more often. However, knowledge of the effect of A_{16}, A_{26}, D_{16}, and D_{16} on the individual class of problems being considered by an analyst or designer is essential because even a small A_{16} or D_{16} might cause significantly different response results from cases in which those stiffnesses are exactly zero. Only in the situation where A_{16}, A_{26}, D_{16}, and D_{26} are exactly zero can they be ignored without further thought or analysis.

Symmetric Laminates with Multiple Anisotropic Layers

The general case of a laminate with multiple anisotropic layers symmetrically disposed about the middle surface does not have any stiffness simplifications other than the elimination of the B_{ij} by virtue of symmetry. The A_{16}, A_{26}, D_{16}, and D_{26} stiffnesses all exist and do not necessarily go to zero as the number of layers is increased. That is, the A_{16} stiffness, for example, is derived from the Q_{ij} matrix in Equation (2.84) for an anisotropic lamina which, of course, has more independent

material properties than an orthotropic lamina. Thus, many of the stiffness simplifications possible for other laminates cannot be achieved for this class.

4.3.3 Antisymmetric Laminates

Symmetry of a laminate about the middle surface is often desirable to avoid coupling between bending and extension. However, many physical applications of laminated composite materials require unsymmetric laminates to achieve design requirements. For example, some form of coupling is necessary to make jet turbine fan blades with pretwist without using a complex mold. As a further example, if the shear stiffness of a laminate made of laminae with unidirectional fibers must be increased, one way to achieve this requirement is to position layers at some angle to the laminate axes. To stay within weight and cost requirements, an even number of such layers might be necessary at orientations that alternate from layer to layer, e.g., $[+\alpha/-\alpha/+\alpha/-\alpha]$. Therefore, symmetry about the middle surface is destroyed, and the behavioral characteristics of the laminate can be substantially changed from the symmetric case. Although the example laminate is not symmetric, it is antisymmetric about the middle surface, and certain stiffness simplifications are possible.

Antisymmetry of a laminate requires (1) symmetry about the middle surface of geometry (i.e., consider a pair of equal-thickness laminae, one some distance above the middle surface and the other *the same distance below the middle surface*), but (2) some kind of a 'reversal' or mirror image of the material properties $[\bar{Q}_{ij}]_k$. In fact, the orthotropic material properties $[Q_{ij}]_k$ are symmetric, but the orientations of the laminae principal material directions are not symmetric about the middle surface. Those orientations are reversed from 0° to 90° (or vice versa) or from $+\alpha$ to $-\alpha$ (a mirror image about the laminate x-axis). Because the $[\bar{Q}_{ij}]_k$ are not symmetric, bending-extension coupling exists.

Antisymmetric laminates must have an even number of layers if adjacent laminae also have alternating signs of the principal material property directions with respect to the laminate axes. If adjacent laminae do not have alternating signs, then the number of layers need not be even.

The stiffnesses of an antisymmetric laminate of anisotropic laminae do not simplify from those presented in Equations (4.22) and (4.23). However, as a consequence of antisymmetry of material properties of generally orthotropic laminae,[2] but symmetry of their thicknesses, the shear-extension coupling stiffness A_{16},

$$A_{16} = \sum_{k=1}^{N} (\bar{Q}_{16})_k (z_k - z_{k-1}) \qquad (4.49)$$

[2]Because of the existance of bending-extension coupling, the terminology 'generally orthotropic' and 'specially orthotropic' have meaning only with reference to an individual layer and not to a laminate.

is easily seen to be zero because

$$(\bar{Q}_{16})_{+\alpha} = -(\bar{Q}_{16})_{-\alpha} \qquad (4.50)$$

and layers symmetric about the middle surface have equal thickness and hence the same value of the geometric term multiplying $(\bar{Q}_{16})_k$. Similarly, A_{26} is zero as is the bend-twist coupling stiffness D_{16}.

$$D_{16} = \frac{1}{3} \sum_{k=1}^{N} (\bar{Q}_{16})_k (z_k^3 - z_{k-1}^3) \qquad (4.51)$$

because again Equation (4.50) holds, and the geometric term multiplying $(\bar{Q}_{16})_k$ is the same for two layers symmetric about the middle surface. The preceding reasoning applies also for D_{26}.

The bending-extension coupling stiffnesses, B_{ij}, vary for different classes of antisymmetric laminates of generally orthotropic laminae, and, in fact, no general representation exists other than in the following force and moment resultants:

$$\begin{bmatrix} N_x \\ N_y \\ N_{xy} \end{bmatrix} = \begin{bmatrix} A_{11} & A_{12} & 0 \\ A_{12} & A_{22} & 0 \\ 0 & 0 & A_{66} \end{bmatrix} \begin{bmatrix} \varepsilon_x^\circ \\ \varepsilon_y^\circ \\ \gamma_{xy}^\circ \end{bmatrix} + \begin{bmatrix} B_{11} & B_{12} & B_{16} \\ B_{12} & B_{22} & B_{26} \\ B_{16} & B_{26} & B_{66} \end{bmatrix} \begin{bmatrix} \kappa_x \\ \kappa_y \\ \kappa_{xy} \end{bmatrix} \qquad (4.52)$$

$$\begin{bmatrix} M_x \\ M_y \\ M_{xy} \end{bmatrix} = \begin{bmatrix} B_{11} & B_{12} & B_{16} \\ B_{12} & B_{22} & B_{26} \\ B_{16} & B_{26} & B_{66} \end{bmatrix} \begin{bmatrix} \varepsilon_x^\circ \\ \varepsilon_y^\circ \\ \gamma_{xy}^\circ \end{bmatrix} + \begin{bmatrix} D_{11} & D_{12} & 0 \\ D_{12} & D_{22} & 0 \\ 0 & 0 & D_{66} \end{bmatrix} \begin{bmatrix} \kappa_x \\ \kappa_y \\ \kappa_{xy} \end{bmatrix} \qquad (4.53)$$

The purpose of the remainder of this section is to discuss two important classes of antisymmetric laminates, the antisymmetric cross-ply laminate and the antisymmetric angle-ply laminate. Neither laminate is used much in practice, but both add to our understanding of laminates.

Antisymmetric Cross-Ply Laminates

An antisymmetric cross-ply laminate consists of an even number of orthotropic laminae laid on each other with principal material directions alternating at 0° and 90° to the laminate axes as in the simple example of Figure 4-19. A more complicated example is given in Table 4-4 (where the adjacent layers do not always have the sequence 0°, then 90°, then 0°, etc.). Such laminates do not have A_{16}, A_{26}, D_{16}, and D_{26}, but do have bending-extension coupling. We will show later that the coupling is such that the force and moment resultants are

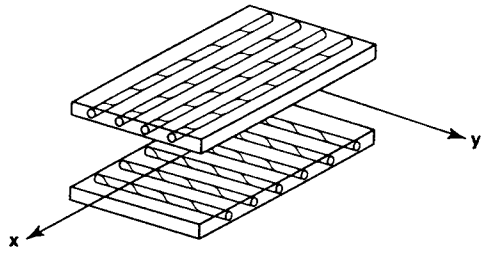

Figure 4-19 Unbonded View of a Two-Layered Regular Antisymmetric Cross-Ply Laminate

Table 4-4 Antisymmetric Laminate with Six Specially Orthotropic Layers

Layer	Material Properties				Orientation	Thickness
	Q_{11}	Q_{12}	Q_{22}	Q_{66}		
1	F_1	F_2	F_3	F_4	0°	t
2	G_1	G_2	G_3	G_4	90°	3t
3	H_1	H_2	H_3	H_4	90°	2t
4	H_1	H_2	H_3	H_4	0°	2t
5	G_1	G_2	G_3	G_4	0°	3t
6	F_1	F_2	F_3	F_4	90°	t

$$\begin{bmatrix} N_x \\ N_y \\ N_{xy} \end{bmatrix} = \begin{bmatrix} A_{11} & A_{12} & 0 \\ A_{12} & A_{22} & 0 \\ 0 & 0 & A_{66} \end{bmatrix} \begin{bmatrix} \varepsilon_x^\circ \\ \varepsilon_y^\circ \\ \gamma_{xy}^\circ \end{bmatrix} + \begin{bmatrix} B_{11} & 0 & 0 \\ 0 & -B_{11} & 0 \\ 0 & 0 & 0 \end{bmatrix} \begin{bmatrix} \kappa_x \\ \kappa_y \\ \kappa_{xy} \end{bmatrix} \tag{4.54}$$

$$\begin{bmatrix} M_x \\ M_y \\ M_{xy} \end{bmatrix} = \begin{bmatrix} B_{11} & 0 & 0 \\ 0 & -B_{11} & 0 \\ 0 & 0 & 0 \end{bmatrix} \begin{bmatrix} \varepsilon_x^\circ \\ \varepsilon_y^\circ \\ \gamma_{xy}^\circ \end{bmatrix} + \begin{bmatrix} D_{11} & D_{12} & 0 \\ D_{12} & D_{22} & 0 \\ 0 & 0 & D_{66} \end{bmatrix} \begin{bmatrix} \kappa_x \\ \kappa_y \\ \kappa_{xy} \end{bmatrix} \tag{4.55}$$

A *regular antisymmetric cross-ply laminate* is defined to have laminae all of equal thickness and is common because of simplicity of fabrication. As the number of layers increases, the bending-extension coupling stiffness B_{11} can be shown to approach zero.

Antisymmetric Angle-Ply Laminates

An antisymmetric angle-ply laminate has laminae oriented at $+\alpha$ degrees to the laminate coordinate axes on one side of the middle surface and corresponding equal-thickness laminae oriented at $-\alpha$ degrees on the other side at the same distance from the middle surface. A simple example of an antisymmetric angle-ply laminate is shown in Figure 4-20. A more complicated example with mixed materials and lamination angles is given in Table 4-5.

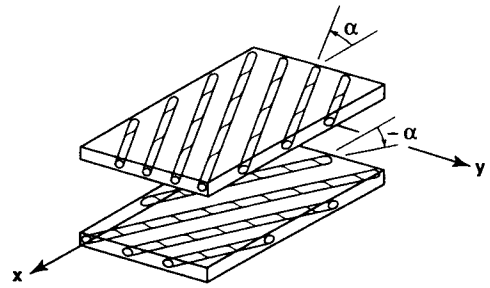

Figure 4-20 Unbonded View of a Two-Layered Regular Antisymmetric Angle-Ply Laminate

Table 4-5 Six-Layered Antisymmetric Angle-Ply Laminate

Layer	Material Properties				Orientation	Thickness
	Q_{11}	Q_{12}	Q_{22}	Q_{66}		
1	F_1	F_2	F_3	F_4	–45°	t
2	G_1	G_2	G_3	G_4	+30°	2t
3	H_1	H_2	H_3	H_4	0°	3t
4	H_1	H_2	H_3	H_4	0°	3t
5	G_1	G_2	G_3	G_4	–30°	2t
6	F_1	F_2	F_3	F_4	+45°	t

A *regular antisymmetric angle-ply laminate* has laminae all of the same material and thickness for ease of fabrication. This class of laminates can be further restricted to have a single value of α as opposed to the several orientations, materials, and thicknesses in Table 4-5.

The force and moment resultants for an antisymmetric angle-ply laminate are

$$\begin{bmatrix} N_x \\ N_y \\ N_{xy} \end{bmatrix} = \begin{bmatrix} A_{11} & A_{12} & 0 \\ A_{12} & A_{22} & 0 \\ 0 & 0 & A_{66} \end{bmatrix} \begin{bmatrix} \varepsilon_x^\circ \\ \varepsilon_y^\circ \\ \gamma_{xy}^\circ \end{bmatrix} + \begin{bmatrix} 0 & 0 & B_{16} \\ 0 & 0 & B_{26} \\ B_{16} & B_{26} & 0 \end{bmatrix} \begin{bmatrix} \kappa_x \\ \kappa_y \\ \kappa_{xy} \end{bmatrix} \tag{4.56}$$

$$\begin{bmatrix} M_x \\ M_y \\ M_{xy} \end{bmatrix} = \begin{bmatrix} 0 & 0 & B_{16} \\ 0 & 0 & B_{26} \\ B_{16} & B_{26} & 0 \end{bmatrix} \begin{bmatrix} \varepsilon_x^\circ \\ \varepsilon_y^\circ \\ \gamma_{xy}^\circ \end{bmatrix} + \begin{bmatrix} D_{11} & D_{12} & 0 \\ D_{12} & D_{22} & 0 \\ 0 & 0 & D_{66} \end{bmatrix} \begin{bmatrix} \kappa_x \\ \kappa_y \\ \kappa_{xy} \end{bmatrix} \tag{4.57}$$

The bending-extension coupling stiffnesses B_{16} and B_{26} can be shown to go to zero as the number of layers in the laminate increases for a fixed laminate thickness.

4.3.4 Unsymmetric Laminates

Unsymmetric or nonsymmetric or asymmetric laminates are the most general class of laminate. Lack of symmetry can occur by design as in deliberately constructing a laminate that is not symmetric about the middle surface. Or, a symmetric laminate could be built but subjected in service to heating from one side so that the resulting thermal gradient acting on the temperature-dependent material properties renders the laminate unsymmetric. We will briefly address unsymmetric laminates with multiple isotropic, specially orthotropic, generally orthotropic, and anisotropic layers.

For the general case of multiple isotropic layers of thickness t_k and material properties E_k and ν_k, the extensional, bending-extension coupling, and bending stiffnesses are given by Equation (4.24) wherein

$$(\bar{Q}_{11})_k = (\bar{Q}_{22})_k = \frac{E_k}{1-\nu_k^2} \qquad (\bar{Q}_{16})_k = (\bar{Q}_{26})_k = 0$$
$$(\bar{Q}_{12})_k = \frac{\nu_k E_k}{1-\nu_k^2} \qquad (\bar{Q}_{66})_k = \frac{E_k}{2(1+\nu_k)} \tag{4.58}$$

No special reduction of the stiffnesses is possible when t_k is arbitrary. That is, coupling between bending and extension can be obtained by unsymmetric arrangement about the middle surface of isotropic layers with different material properties and possibly (but not necessarily) different thicknesses. Thus, coupling between bending and extension is *not* a result of material orthotropy but rather of laminate heterogeneity; that is, a combination of *both* geometric and material properties. The force and moment resultants are

$$\begin{bmatrix} N_x \\ N_y \\ N_{xy} \end{bmatrix} = \begin{bmatrix} A_{11} & A_{12} & 0 \\ A_{12} & A_{11} & 0 \\ 0 & 0 & A_{66} \end{bmatrix} \begin{bmatrix} \varepsilon_x^o \\ \varepsilon_y^o \\ \gamma_{xy}^o \end{bmatrix} + \begin{bmatrix} B_{11} & B_{12} & 0 \\ B_{12} & B_{11} & 0 \\ 0 & 0 & B_{66} \end{bmatrix} \begin{bmatrix} \kappa_x \\ \kappa_y \\ \kappa_{xy} \end{bmatrix} \tag{4.59}$$

$$\begin{bmatrix} M_x \\ M_y \\ M_{xy} \end{bmatrix} = \begin{bmatrix} B_{11} & B_{12} & 0 \\ B_{12} & B_{11} & 0 \\ 0 & 0 & B_{66} \end{bmatrix} \begin{bmatrix} \varepsilon_x^o \\ \varepsilon_y^o \\ \gamma_{xy}^o \end{bmatrix} + \begin{bmatrix} D_{11} & D_{12} & 0 \\ D_{12} & D_{11} & 0 \\ 0 & 0 & D_{66} \end{bmatrix} \begin{bmatrix} \kappa_x \\ \kappa_y \\ \kappa_{xy} \end{bmatrix} \tag{4.60}$$

Unsymmetric laminates with multiple specially orthotropic layers can be shown to have the force and moment resultants in Equations (4.59) and (4.60) but with different A_{22}, B_{22}, and D_{22} from A_{11}, B_{11}, and D_{11}, respectively. That is, there are no shear-extension coupling terms nor any bend-twist coupling terms, so the solution of problems with this kind of lamination is about as easy as with isotropic layers.

Unsymmetric laminates with multiple generally orthotropic layers or with multiple anisotropic layers have force and moment resultants no simpler than Equations (4.22) and (4.23). All stiffnesses are present. Hence, configurations with either of those two laminae are much more difficult to analyze than configurations with either multiple isotropic layers or multiple specially orthotropic layers.

4.3.5 Common Laminate Definitions

First, we need a common, unambiguous manner of writing how a laminate is specified to be laid-up, i.e., stacking-sequence notation. Then, quasi-isotropic, balanced, and hybrid laminates are defined.

Stacking-Sequence Notation

The manner of describing a laminate by use of individual layer thicknesses, principal material property orientations, and overall stacking sequence could be quite involved. However, fortunately, all pertinent parameters are represented in a simple, concise fashion by use of the following stacking-sequence terminology. For regular (equal-thickness layers) laminates, a listing of the layers and their orientations suffices, for example, [0°/90°/45°]. Note that only the principal material direction orientations need be given. Many different laminates could be made with the same layers, for example, [90°/0°/45°]. For irregular (layers do not have the same thickness) laminates, a notation of layer thicknesses must be appended to the previous notation, for example, $[0^\circ_t/90^\circ_{2t}/45^\circ_{3t}]$ or [0°@t/90°@2t/45°@3t]. Finally, for symmetric laminates, the simplest representation of, for example, the laminate [0°/90°/45°/45°/90°/0°] is $[0°/90°/45°]_{symmetric}$ or $[0°/90°/45°]_{sym}$ or $[0°/90°/45°]_S$. If multiple laminae occur at the same angle, then subscripts are used to designate the number of such multiple layers, e.g., $[0°/0°/0°/90°/90°] = [0^\circ_3/90^\circ_2]$. If sequences of laminae are repeated, then those sequences are grouped with a subscript to indicate the number of sequence repetitions, e.g., $[0°/90°/45°/0°/90°/45°] = [0°/90°/45°]_2$. If one layer is equally split by the middle surface, then a bar is put over the split layer, e.g., $[0°/90°/0°] = [0°/\overline{90°}]_S$. Finally, if all the laminae are specified in the stacking sequence shown and no implications of symmetry, repeated sequences, etc., are desired nor can any ambiguity be tolerated, then a subscript T is used to indicate complete or total specification for emphasis, e.g., $[0°/90°/45°/-45°/0°/90°]_T$, i.e., no symmetry or repeated sequence is desired. This notation will be used throughout the remainder of the book and is used widely in composite structures practice.

Quasi-Isotropic Laminates

The term *quasi-isotropic laminate* is used to describe laminates that have isotropic *extensional* stiffnesses (the same in all directions in the plane of the laminate). As background to the definition, recall that the term *isotropy* is a material property whereas laminate stiffnesses are a function of both material properties and *geometry*. Note also that the prefix *quasi* means 'in a sense or manner'. Thus, a quasi-isotropic laminate must mean a laminate that, in some sense, appears isotropic, but is not actually isotropic in all senses. In this case, a quasi-isotropic

laminate is taken to mean equal extensional stiffnesses in all in-plane directions of the laminate, i.e.,

$$\bar{A}_{ij} = A_{ij} \quad A_{11} = A_{22} \quad A_{12} = \nu A_{11} \quad A_{66} = \frac{1-\nu}{2} A_{11} \quad A_{16} = A_{26} = 0 \quad (4.61)$$

where the overbar is used to designate a transformed property as with the Q_{ij} and $\bar{Q}_{ij}$ and ν is the apparent Poisson's ratio of the laminate defined only for extensional properties. Moreover, all layers are of the same material and of equal thickness. (Another possible definition of a quasi-isotropic laminate is one that has equal bending stiffnesses in all in-plane directions.) The simplest example of a quasi-isotropic laminate is a three-layer laminate [–60°/0°/60°]. The next simplest example is a four-layer laminate [0°/–45°/45°/90°]. Those laminates are depicted in Figure 4-21 wherein the notation $\pi/3$ and $\pi/4$ is used. Those names, $\pi/3$ and $\pi/4$, result from the facts that (1) the angle between layers in 60° and 45°, respectively, and (2) 60° and 45° are $\pi/3$ and $\pi/4$, respectively, in SI units. As the number of layers increases, the angle between the adjacent laminae decreases such that $\Delta\theta = 180°/N$ where N is the number of layers. Although the A_{ij} are identical in all directions, the B_{ij} and D_{ij} depend on the orientation of the coordinate axes of the laminate. Thus, a quasi-isotropic laminate can have bending-extension coupling as well as a varying bending response as the laminate is rotated in plane.

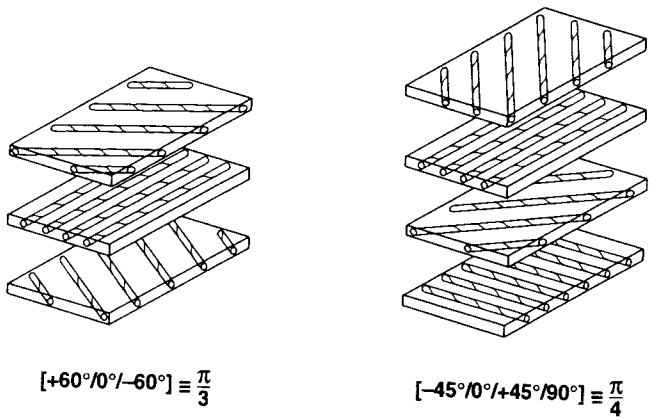

Figure 4-21 Unbonded View of Simple Quasi-Isotropic Laminates

Balanced Laminates

Although the word 'balanced' is ambiguous and not definitive, the common meaning for a *balanced laminate* is a laminate in which all equal-thickness laminae at angles θ other than 0° and 90° to the reference axis occur only in $\pm\theta$ pairs. The individual $+\theta$ and $-\theta$ layers are not necessarily adjacent to each other. Note also that balanced laminates are required to be symmetric about the laminate middle surface, so there must be two $+\theta$ laminae and two $-\theta$ laminae for each $\pm\theta$ pair. The behavioral characteristics of a balanced laminate are that shear-extension coupling does not exist, nor does bending-extension coupling exist. However, bend-twist coupling does exist.

Hybrid Laminates

A *hybrid laminate* is a mixture of two or more material systems to form a laminate. For example, graphite-epoxy laminae are used with Kevlar-49®-epoxy laminae to create wing-to-body fairings for the Boeing 757 and 767. Note that the two epoxies must be cure-compatible in order to achieve a functioning laminate. Thus, different fiber systems are often mixed in hybrid laminates, but not many different matrix systems can be used. An example of a graphite-epoxy laminate surrounded by layers of boron-epoxy could be written as $[0^\circ_B/\pm45^\circ_{Gr}/90^\circ_{Gr}]_S$. Note that this laminate is *not* quasi-isotropic because the laminae, although of the correct angular orientation for a $\pi/4$ laminate, are of different material systems.

4.3.6 Summary Remarks

Single-layer 'laminates' (of course, such configurations are *not* laminates, but laminate stiffnesses must reduce to individual layer stiffnesses) with a reference surface at the middle surface do not exhibit coupling between bending and extension. With any other reference surface, there is indeed such coupling. Multilayered laminates, in general, develop coupling between bending and extension. The coupling is influenced by the geometrical as well as by the material property characteristics of laminates. There are, however, combinations of the geometrical and material property characteristics for which there is no coupling between bending and extension. Those special cases have been reviewed in this section along with other special cases. All the special cases should be well understood in order to appreciate more complex laminates. Note from the collection of special cases that the elastic symmetry of the laminae (whether isotropic, orthotropic, etc.) is not necessarily maintained in the laminate. The symmetry can be increased, decreased, or remain the same. Moreover, the symmetries of the three stiffness matrices, A, B, and D, need not be the same. Unavoidable geometrical factors enter the stiffness calculations.

The basic concept of coupling between bending and extension must be understood because there are many applications of composite materials where neglect of coupling can be catastrophic. This coupling is the key to the correct analysis of eccentrically stiffened plates and shells. For example, Card and Jones [4-5] showed that if longitudinal stiffeners are placed on the outside of an axially loaded circular cylindrical shell, the buckling load is twice the value when the same stiffeners are on the inside of the shell. Previously, the bending-extension coupling between the stiffeners and the shell had been ignored! Similarly significant differences will be shown in Chapter 5 for laminated plates.

Problem Set 4.3

4.3.1 Prove that the bending-extension coupling stiffnesses, B_{ij}, are zero for laminates that are symmetric in both material properties and geometry about the middle surface.

4.3.2 Consider two laminae with principal material directions at $+\alpha$ and $-\alpha$ with respect to a reference axis. Prove that for orthotropic materials

$$(\bar{Q}_{16})_{+\alpha} = -(\bar{Q}_{16})_{-\alpha}$$

Discuss whether this relation is valid for anisotropic materials. That is, demonstrate whether a $\pm\alpha$ angle-ply laminate of the same anisotropic laminae that are symmetric geometrically is antisymmetric or not. The transformation equations for anisotropic materials are given in Section 2.7.

4.3.3 Quasi-isotropic laminates do not behave like isotropic homogeneous materials. Discuss why not, and describe how they do behave. Why is a two-ply laminate with a [0°/90°] stacking sequence and equal-thickness layers not a quasi-isotropic laminate? Determine whether the extensional stiffnesses are the same irrespective of the laminate axes for the two-ply and three-ply cases. Hint: use the invariant properties in Equation (2.93).

4.3.4 Show that B_{16} and B_{26} for an antisymmetric angle-ply laminate with equal-thickness layers of the same material approach zero as the even number of (equal-thickness) layers increases if the total laminate thickness is held constant. What happens if equal-thickness layers are added so the total laminate thickness increases? In both cases, develop equations for B_{16} and B_{26} that you can study, modify, and use to determine your answers.

4.3.5 Show that $A_{16} = A_{26} = D_{16} = D_{26} = 0$ for regular antisymmetric laminates wherein each equal-thickness layer is made of the same material.

4.3.6 Start with the general expression for the force per unit width, N_x, in terms of the middle-surface strains and curvatures to derive the specific expression for N_x for a two-layered, equal-thickness [0°/90°] laminate. Your final expression must be in terms of Q_{ij} and t, the laminate thickness. What is such a laminate called? What deformation characteristics does this laminate exhibit when subjected to N_x, i.e., what does this laminate do?

4.3.7 Do all parts of Problem 4.3.6 for moment per unit width, M_x.

4.3.8 A laminate consists of equal-thickness fiber-reinforced laminae with 40% of the unidirectional laminae in the x-direction, 30% at +45° to the x-direction, and the remaining 30% at -45° to the x-direction. What is the minimum number of layers to achieve precisely the given percentages? How many layers are required to avoid coupling between bending and extension, if indeed that is possible? How many layers are required to make this laminate macroscopically orthotropic (i.e., behave as a single orthotropic layer)? Or is it ever macroscopically orthotropic? Discuss! In each case, state the stacking sequence of the laminate.

4.4 THEORETICAL VERSUS MEASURED LAMINATE STIFFNESSES

In preceding sections, laminate stiffnesses were predicted on the basis of combination of lamina stiffnesses in accordance with classical lamination theory. However, the actual, practical realization of those laminate stiffnesses remains to be demonstrated. The purpose of this section is to compare predicted laminate stiffnesses with measured laminate stiffnesses to determine the validity of classical lamination theory. Results for two types of laminates, cross-ply and angle-ply laminates, are presented.

4.4.1 Inversion of Stiffness Equations

Before the predicted stiffnesses are compared with measured stiffnesses, however, a slight reinterpretation of laminate stiffnesses is

required. Ordinarily, the resultant forces and moments are written in terms of the middle-surface extensional strains and curvatures as

$$\begin{bmatrix} N \\ \hline M \end{bmatrix} = \left[\begin{array}{c|c} A & B \\ \hline B & D \end{array}\right] \begin{bmatrix} \varepsilon^\circ \\ \hline \kappa \end{bmatrix} \tag{4.62}$$

However, in most experiments, the loads are applied, and the resulting deformations are measured, i.e., the deformations are the dependent variables, not the loads. Thus, the expressions for the middle-surface extensional strains and curvatures in terms of the force and moment resultants would be convenient.

The first step in the derivation of the inverse of Equation (4.62) is to write it in the form

$$N = A\varepsilon^\circ + B\kappa \tag{4.63}$$

$$M = B\varepsilon^\circ + D\kappa \tag{4.64}$$

and solve Equation (4.63) for ε°:

$$\varepsilon^\circ = A^{-1}N - A^{-1}B\kappa \tag{4.65}$$

whereupon Equation (4.64) becomes

$$M = BA^{-1}N + (-BA^{-1}B + D)\kappa \tag{4.66}$$

Equations (4.65) and (4.66) can be written as

$$\begin{bmatrix} \varepsilon^\circ \\ \hline M \end{bmatrix} = \left[\begin{array}{c|c} A^{-1} & -A^{-1}B \\ \hline BA^{-1} & D - BA^{-1}B \end{array}\right] \begin{bmatrix} N \\ \hline \kappa \end{bmatrix} \tag{4.67}$$

or

$$\varepsilon^\circ = A^*N + B^*\kappa \tag{4.68}$$

$$M = H^*N + D^*\kappa \tag{4.69}$$

where B^* is not equal to H^*. Now solve Equation (4.69) for κ:

$$\kappa = D^{*-1}M - D^{*-1}H^*N \tag{4.70}$$

and substitute in Equation (4.68) to get

$$\varepsilon^\circ = B^*D^{*-1}M + (A^* - B^*D^{*-1}H^*)N \tag{4.71}$$

Thus,

$$\begin{bmatrix} \varepsilon^\circ \\ \hline \kappa \end{bmatrix} = \left[\begin{array}{c|c} A^* - B^*D^{*-1}H^* & B^*D^{*-1} \\ \hline -D^{*-1}H^* & D^{*-1} \end{array}\right] \begin{bmatrix} N \\ \hline M \end{bmatrix} \tag{4.72}$$

or

$$\begin{bmatrix} \varepsilon^\circ \\ \hline \kappa \end{bmatrix} = \left[\begin{array}{c|c} A' & B' \\ \hline H' & D' \end{array}\right] \begin{bmatrix} N \\ \hline M \end{bmatrix} \tag{4.73}$$

wherein H' can be shown to be equal to $(B')^T$ by virtue of the symmetry of the A, B, and D matrices and the definitions of the A', B', D', A*, B*,

nd D* matrices. Of course, H' must equal $(B')^T$ because the matrix of e coefficients in Equation (4.62) is symmetric, so its inverse, the matrix coefficients in Equation (4.73), must also be symmetric. Demonration that the predicted values of A', B', and D' agree with measured alues is therefore fully equivalent to verification of the prediction techques for A, B, and D.

4.2 Special Cross-Ply Laminate Stiffnesses

A cross-ply laminate in this section has N unidirectionally reinforced rthotropic) layers of the same material with principal material directions ternatingly oriented at 0° and 90° to the laminate coordinate axes. The er direction of odd-numbered layers is the x-direction of the laminate. he fiber direction of even-numbered layers is then the y-direction of the minate. Consider the special case of odd-numbered layers with equal ickness and even-numbered layers also with equal thickness, but not ecessarily the same thickness as that of the odd-numbered layers. ote that we have imposed very special requirements on how the fiber ientations change from layer to layer and on the thicknesses of the vers to define a special subclass of cross-ply laminates. Thus, these minates are termed 'special' cross-ply laminates and will be explored this subsection. More general cross-ply laminates have no such conions on fiber orientation and laminae thicknesses. For example, a eneral) cross-ply laminate could be described with the specification @t/90°@2t/90°@2t/0°@t] wherein the fiber orientations do *not* alterte and the thicknesses of the odd- or even-numbered layers are *not* e same; however, this laminate is clearly a symmetric cross-ply lamite.

For the special cross-ply laminates, two geometrical parameters e important: N, the total number of layers, and M, the ratio of the total ckness of odd-numbered layers to the total thickness of evenmbered layers (called the cross-ply ratio). Thus,

$$M = \frac{\sum_{k=\text{odd}} t_k}{\sum_{k=\text{even}} t_k} \tag{4.74}$$

r example, if a five-layered laminate has a stacking sequence of $/90^\circ_{2t}/0^\circ_t/90^\circ_{2t}/0^\circ_t]$, then

$$M = \frac{t+t+t}{2t+2t} = \frac{3}{4} \tag{4.75}$$

te that the cross-ply ratio, M, has specific meaning only when the ers have alternating 0° and 90° orientations. If the middle layer of the egoing example were two layers of 0° orientation with each layer being thick, then M is easily shown to be one. However, then the layers uld not have alternating orientation nor would odd-numbered layers ve the same thickness. Thus, more general cross-ply laminates can be described by use of the cross-ply ratio, M.

The laminate stiffnesses,

$$A_{ij} = \sum_{k=1}^{N} (\bar{Q}_{ij})_k (z_k - z_{k-1})$$

$$B_{ij} = \frac{1}{2} \sum_{k=1}^{N} (\bar{Q}_{ij})_k (z_k^2 - z_{k-1}^2) \tag{4.76}$$

$$D_{ij} = \frac{1}{3} \sum_{k=1}^{N} (\bar{Q}_{ij})_k (z_k^3 - z_{k-1}^3)$$

can be expressed in terms of M and N for laminates with an odd or even number of layers. In addition, F, the ratio of principal lamina stiffnesses,

$$F = \frac{Q_{22}}{Q_{11}} = \frac{E_2}{E_1} \tag{4.77}$$

is used where F is the inverse of the usual modulus ratio E_1/E_2. Tsai [4-6] displayed the following stiffnesses for laminates with t = laminate thickness.

Special Cross-Ply Laminates with N Odd (Symmetric)

$$A_{11} = \frac{1}{1+M}(M+F)Q_{11}t$$

$$A_{12} = Q_{12}t$$

$$A_{22} = \frac{1}{1+M}(1+MF)Q_{11}t = \frac{1+MF}{M+F}A_{11} \tag{4.78}$$

$$A_{16} = A_{26} = 0$$

$$A_{66} = Q_{66}t$$

$$B_{ij} = 0 \tag{4.79}$$

$$D_{11} = \frac{[(F-1)P+1]Q_{11}t^3}{12} = [(F-1)P+1]\frac{1+M}{M+F}\frac{A_{11}t^2}{12}$$

$$D_{12} = \frac{Q_{12}t^3}{12}$$

$$D_{22} = \frac{[(1-F)P+F]Q_{11}t^3}{12} = [(1-F)P+F]\frac{1+M}{M+F}\frac{A_{11}t^2}{12} \tag{4.80}$$

$$D_{16} = D_{26} = 0$$

$$D_{66} = \frac{Q_{66}t^3}{12}$$

where

$$P = \frac{1}{(1+M)^3} + \frac{M(N-3)[M(N-1)+2(N+1)]}{(N^2-1)(1+M)^3} \tag{4.81}$$

Special Cross-Ply Laminates with N Even (Antisymmetric)

$$A_{11} = \frac{1}{1+M}(M+F)Q_{11}t$$

$$A_{12} = Q_{12}t$$

$$A_{22} = \frac{1}{1+M}(1+MF)Q_{11}t = \frac{1+MF}{M+F}A_{11} \qquad (4.82)$$

$$A_{16} = A_{26} = 0$$

$$A_{66} = Q_{66}t$$

$$B_{11} = \frac{M(F-1)}{N(1+M)^2}Q_{11}t^2 = \frac{M(F-1)}{N(1+M)(M+F)}A_{11}t$$

$$B_{22} = -B_{11} \qquad (4.83)$$

$$B_{12} = B_{16} = B_{26} = B_{66} = 0$$

$$D_{11} = \frac{[(F-1)R+1]Q_{11}t^3}{12} = [(F-1)R+1]\frac{1+M}{M+F}\frac{A_{11}t^2}{12}$$

$$D_{12} = \frac{Q_{12}t^3}{12}$$

$$D_{22} = \frac{[(1-F)R+F]Q_{11}t^3}{12} = [(1-F)R+F]\frac{1+M}{M+F}\frac{A_{11}t^2}{12} \qquad (4.84)$$

$$D_{16} = D_{26} = 0$$

$$D_{66} = \frac{Q_{66}t^3}{12}$$

where

$$R = \frac{1}{1+M} + \frac{8M(M-1)}{N^2(1+M)^3} \qquad (4.85)$$

Observations on Special Cross-Ply Laminates

The special cross-ply laminate stiffnesses are given for symmetric laminates in Equations (4.78) through (4.80) and for antisymmetric laminates in Equations (4.82) through (4.84). The extensional, bending-extension coupling, and bending stiffnesses are discussed separately in the following paragraphs.

For both odd- and even-layered special cross-ply laminates, the extensional stiffnesses, A_{ij}, are independent of N, the number of layers (although the N individual lamina thicknesses can be summed to get the total laminate thickness t, so N is implicit in Equations (4.78) and (4.82)). However, A_{11} and A_{22} depend on M, the cross-ply ratio, and on F, the lamina stiffness ratio, as shown in Figures 4-22 and 4-23. For a typical glass-fiber-reinforced lamina, F = .3, so A_{11} varies from $.65Q_{11}t$ to $.93Q_{11}t$ as M changes from 1 to 10. Similarly, A_{22} varies from A_{11} to $.38A_{11}$ over the same range of M. The stiffnesses A_{12} and A_{66} are independent of M and F. The remaining stiffnesses A_{16} and A_{26} are zero for all cross-ply laminates.

Only special cross-ply laminates with an even number of layers have bending-extension coupling because the B_{ij} are all zero for a special cross-ply laminate with an odd number of layers. The bending-extension coupling stiffnesses B_{11} and B_{22} are plotted as a function of the cross-ply ratio, M, in Figure 4-24. The number of layers, N, appears in the numerator of the ordinate in Figure 4-24. Thus, the value of B_{11} obviously decreases as N increases because NB_{11} is constant for a fixed cross-ply ratio. Because N must be even to get any coupling, N = 2 corresponds to the largest coupling between bending and extension. One physical interpretation of the bending-extension coupling stiffness B_{11} is that it is a measure of the location of the neutral (stress-free) axis relative to the laminate middle surface. As a matter of fact, the ordinate in Figure 4-24 is the fraction of the total laminate thickness, T, that the neutral axis is shifted from the middle surface. The shifting, like B_{11}, is inversely proportional to N, so the neutral-axis shift gets smaller as the number of layers increases. Note that there is a different neutral axis in the x-direction than in the y-direction, i.e., there is *no neutral surface.*

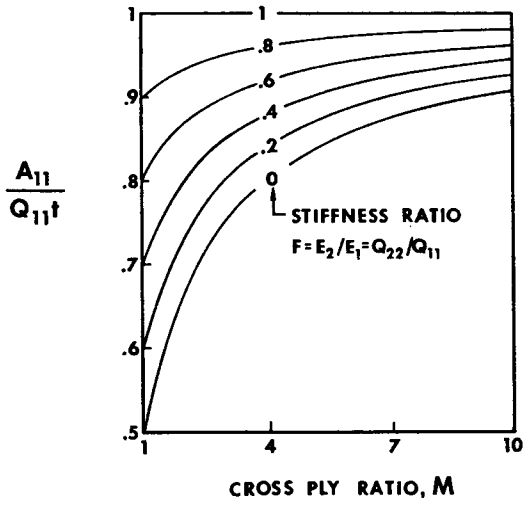

Figure 4-22 Extensional Stiffness, A_{11}, versus Cross-Ply Ratio, M *(After Tsai [4-6])*

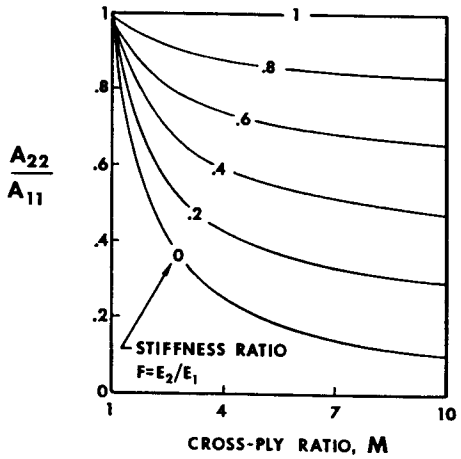

Figure 4-23 Extensional Stiffness, A_{22}, versus Cross-Ply Ratio, M *(After Tsai [4-6])*

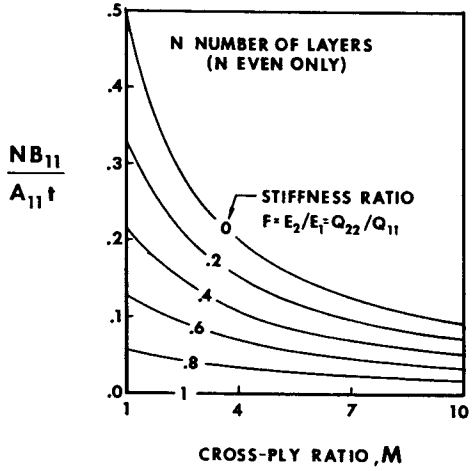

Figure 4-24 Bending-Extension Coupling Stiffness, B_{11}, versus Cross-Ply Ratio, M *(After Tsai [4-6])*

The bending stiffnesses, D_{ij}, are complicated functions of the number of layers, N, the cross-ply ratio, M, and the lamina stiffness ratio, F. Normalized values of D_{11} and D_{22} are shown in Figures 4-25 and 4-26 for several values of F and N as a function of M. Extreme values of D_{11} and D_{22} occur when $N=2$ and $N=3$ with values for all other N falling in between. The value of D_{11} approaches $A_{11}t^2/12$ and D_{22} approaches $A_{22}t^2/12$ as (1) M gets large, (2) N gets large, or (3) F approaches one. Thus, with certain types of laminate layups, the stiffnesses can approach those for a homogeneous plate- or shell-like element.

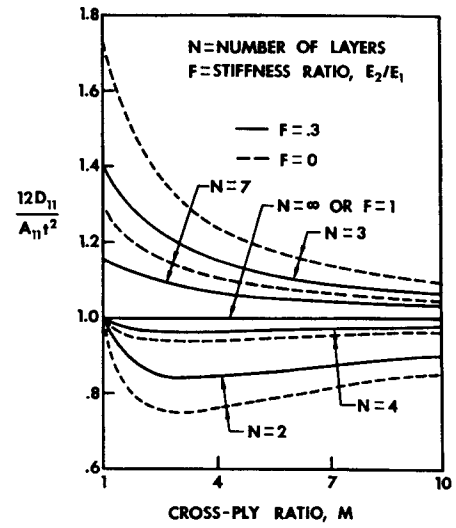

Figure 4-25 Bending Stiffness, D_{11}, versus Cross-Ply Ratio, M *(After Tsai [4-6])*

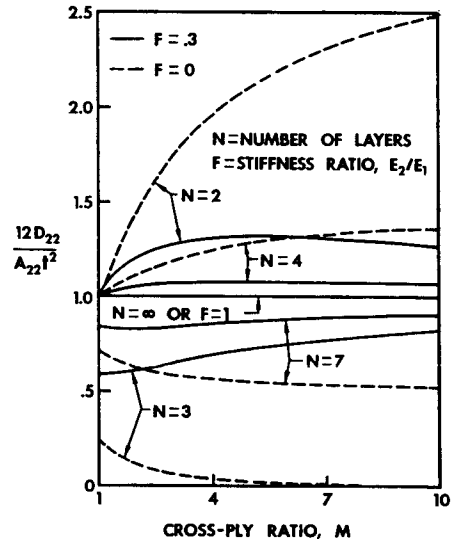

Figure 4-26 Bending Stiffness, D_{22}, versus Cross-Ply Ratio, M *(After Tsai [4-6])*

4.4.3 Theoretical and Measured Cross-Ply Laminate Stiffnesses

Two- and three-layered special cross-ply laminates were shown to have extrema of behavior in the preceding section. Thus, comparisons between theoretical and measured stiffnesses for such laminates should

be quite revealing. Any agreement for those cases would imply equal or better agreement for special cross-ply laminates with more than three layers.

The individual laminae used by Tsai [4-6] consist of unidirectional glass fibers in a resin matrix (U.S. Polymeric Co. E-787-NUF) with moduli given in Table 2-3. A series of special cross-ply laminates was constructed with M = 1,2,3,10 for two-layered laminates and M = 1,2,5,10 for three-layered laminates. The laminates were subjected to axial loads and bending moments whereupon surface strains were measured. Accordingly, the stiffness relations as strains and curvatures in terms of forces and moments, that is,

$$\begin{bmatrix} \varepsilon \\ \kappa \end{bmatrix} = \begin{bmatrix} A' & B' \\ B'^{T} & D' \end{bmatrix} \begin{bmatrix} N \\ M \end{bmatrix} \tag{4.86}$$

are natural to use. That is, theoretical values of A', B', and D' will be compared with measured values. Verification of one set of stiffnesses implies verification of the other set because the two sets, A, B, and D and A', B', and D', are inverses of one another as *sets* (that is, $A \neq A'^{-1}$, etc.).

The experiments were performed on two sets of beams with the beam axis at 0° and 90°, respectively, to the fiber direction of the odd-numbered layers. The beams were 1-in (25.4-mm) wide, .12-in (3-mm) thick, and of 6-in (152-mm) span. Strain rosettes were located on the upper and lower beam surfaces so that the middle-surface strains and curvatures can be calculated from simultaneous solution of

$$\begin{aligned} \varepsilon_i^{\circ} + \frac{t}{2}\kappa_i &= \varepsilon_i^{\text{upper}} \\ \varepsilon_i^{\circ} - \frac{t}{2}\kappa_i &= \varepsilon_i^{\text{lower}} \end{aligned} \qquad i = 1, 2, 6 \tag{4.87}$$

where t is the beam thickness.

The stiffnesses A'_{11}, $A'_{12} = A'_{12}$, B'_{11}, and B'_{12} were measured after application of pure uniaxial tension, N_1, to a 0° beam; the stiffnesses B'_{11}, $B'_{21} = B'_{12}$, D'_{11}, and $D'_{21} = D'_{12}$, after application of pure bending moment, M_1, to a 0° beam. The stiffnesses $A'_{12} = A'_{21}$, A'_{22}, $B'_{21} = B'_{12}$, B'_{22}, $D'_{12} = D'_{21}$, and D'_{22} were measured on a 90° beam. Pure twisting on a 0° square plate was used to measure D_{66}. That is, two upward and two downward forces were applied at the four corners of a plate as in Figure 4-27 whereupon

$$D_{66} = \frac{PL^2}{4w_c} \tag{4.88}$$

where w_c is the corner deflection. The in-plane shear stiffness, A_{66}, was not measured.

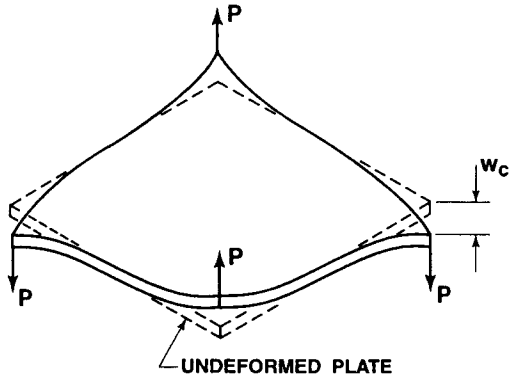

Figure 4-27 Twisting of a Square Plate

The measured stiffnesses for two- and three-layered special cross-ply laminates are shown with symbols in Figure 4-28, and the theoretical results are shown with solid lines. In all cases, the load was kept so low that no strain exceeded 500μ. Thus, the behavior was linear and elastic. The agreement between theory and experiment is quite good. Both the qualitative and the quantitative aspects of the theory are verified. Thus, the capability to predict cross-ply laminate stiffnesses exists and is quite accurate.

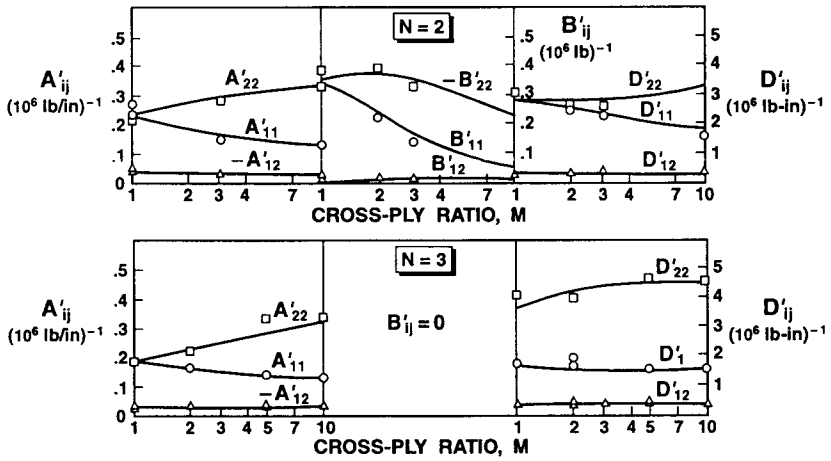

Figure 4-28a Theoretical and Measured Special Cross-Ply Laminate Stiffnesses (U. S. Standard Units) *(After Tsai [4-6])*

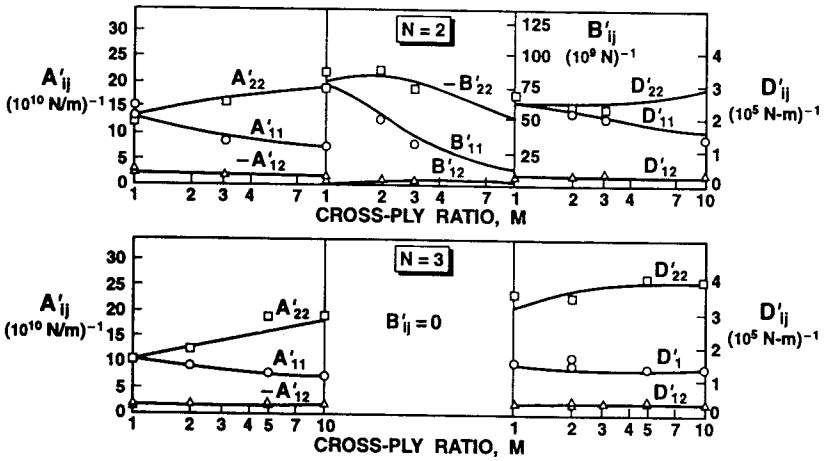

Figure 4-28b Theoretical and Measured Special Cross-Ply Laminate Stiffnesses (SI Units) *(After Tsai [4-6])*

4.4.4 Special Angle-Ply Laminate Stiffnesses

An angle-ply laminate in this section has N unidirectionally reinforced (orthotropic) layers of the same material with principal material directions alternatingly oriented at $+\alpha$ and $-\alpha$ to the laminate x-axis. The odd-numbered layers are at $-\alpha$, and the even-numbered layers are at $+\alpha$. Consider the special, but practical, case where all layers have the same thickness, that is, regular angle-ply laminates. Because of the special requirements on how the fiber orientations change from layer to layer and the equal thicknesses of each layer, these laminates are termed 'special' angle-ply laminates and will be explored in this subsection. More general angle-ply laminates have no such conditions on fiber orientation or laminae thicknesses. For example, an angle-ply laminate could be $[45°@t/60°@2t/60°@2t/45°@t]_S$ wherein the fiber orientations do *not* alternate and the laminae thicknesses are *not* the same; however, this laminate is clearly a symmetric angle-ply laminate.

The laminate behavior of these special angle-ply laminates can be described with the number of layers, N, the laminae orientation, α, and the laminae stiffnesses, Q_{ij}, in addition to the total laminate thickness, t. The laminate stiffnesses,

$$A_{ij} = \sum_{k=1}^{N} (\bar{Q}_{ij})_k (z_k - z_{k-1})$$

$$B_{ij} = \frac{1}{2} \sum_{k=1}^{N} (\bar{Q}_{ij})_k (z_k^2 - z_{k-1}^2) \qquad (4.89)$$

$$D_{ij} = \frac{1}{3} \sum_{k=1}^{N} (\bar{Q}_{ij})_k (z_k^3 - z_{k-1}^3)$$

can be expressed in terms of N, $\bar{Q}_{ij}$ (in which α is accounted for), and t for laminates with an even number of layers and with an odd number of layers. In both cases, $\bar{Q}_{ij}$ is calculated for $-\alpha$ and

$$\begin{aligned} \bar{Q}_{11+\alpha} &= \bar{Q}_{11-\alpha} & \bar{Q}_{66+\alpha} &= \bar{Q}_{66-\alpha} \\ \bar{Q}_{12+\alpha} &= \bar{Q}_{12-\alpha} & \bar{Q}_{16+\alpha} &= -\bar{Q}_{16-\alpha} \\ \bar{Q}_{22+\alpha} &= \bar{Q}_{22-\alpha} & \bar{Q}_{26+\alpha} &= -\bar{Q}_{26-\alpha} \end{aligned} \qquad (4.90)$$

as can be verified by substitution in Equation (2.80). Tsai [4-6] displayed the following stiffnesses:

Special Angle-Ply Laminates with N Odd (Symmetric)

$$A_{11}, A_{12}, A_{22}, A_{66} = (\bar{Q}_{11}, \bar{Q}_{12}, \bar{Q}_{22}, \bar{Q}_{66})t$$
$$A_{16}, A_{26} = (\bar{Q}_{16}, \bar{Q}_{26}) \frac{t}{N} \qquad (4.91)$$

$$B_{ij} = 0 \qquad (4.92)$$

$$D_{11}, D_{12}, D_{22}, D_{66} = (\bar{Q}_{11}, \bar{Q}_{12}, \bar{Q}_{22}, \bar{Q}_{66}) \frac{t^3}{12}$$
$$D_{16}, D_{26} = (\bar{Q}_{16}, \bar{Q}_{26}) \frac{t^3}{12} \left[\frac{3N^2 - 2}{N^3} \right] \qquad (4.93)$$

Special Angle-Ply Laminates with N Even (Antisymmetric)

$$A_{11}, A_{12}, A_{22}, A_{66} = (\bar{Q}_{11}, \bar{Q}_{12}, \bar{Q}_{22}, \bar{Q}_{66})t$$
$$A_{16}, A_{26} = 0 \qquad (4.94)$$
$$B_{11}, B_{12}, B_{22}, B_{66} = 0$$

$$B_{16}, B_{26} = -(\bar{Q}_{16}, \bar{Q}_{26}) \frac{t^2}{2N} \qquad (4.95)$$

$$D_{11}, D_{12}, D_{22}, D_{66} = (\bar{Q}_{11}, \bar{Q}_{12}, \bar{Q}_{22}, \bar{Q}_{66}) \frac{t^3}{12}$$
$$D_{16}, D_{26} = 0 \qquad (4.96)$$

Observations on Special Angle-Ply Laminates

The extensional stiffnesses, A_{ij}, are shown in Figure 4-29 as a function of the lamination angle. The terms A_{11}, A_{12}, A_{22}, and A_{66} are independent of the number of layers, N. However, A_{16} and A_{26} depend on N. When N is odd, they are inversely proportional to N. When N is even, they are zero. Thus, the biggest values of A_{16} and A_{26} occur when N = 3.

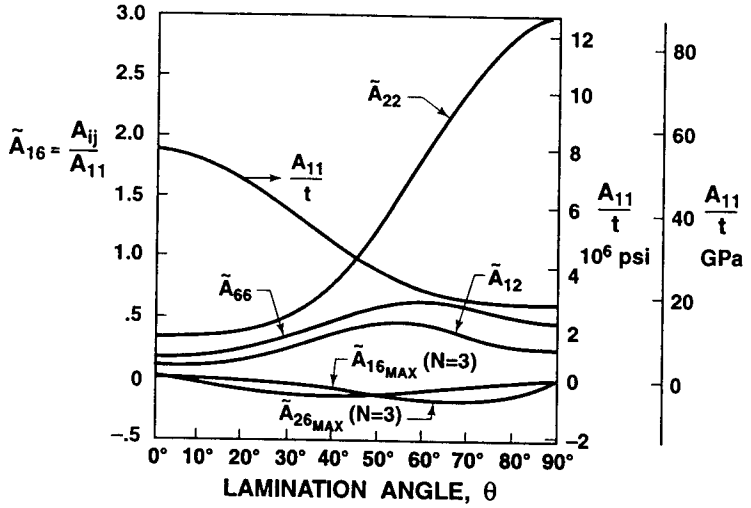

Figure 4-29 Normalized Extensional Stiffnesses for a Glass-Epoxy Angle-Ply Laminate *(After Tsai [4-6])*

The bending-extension coupling stiffnesses, B_{ij}, are zero for an odd number of layers, but can be large for an even number of layers. The values of $B_{16}/(tA_{11})$ are shown as a function of lamination angle in Figure 4-30. Because B_{16} is inversely proportional to N, the largest value of B_{16} occurs when N = 2. The quantity plotted can be shown to be

$$\frac{B_{16}}{tA_{11}} = \frac{M_{xy}}{tN_x} \tag{4.97}$$

that is, the ratio of twisting moment to axial extensional force for pure extension, ε_x°. Similarly,

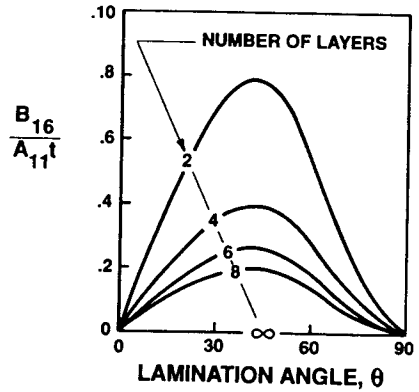

Figure 4-30 Bending-Extension Coupling Stiffness B_{16} for a Glass-Epoxy Angle-Ply Laminate *(After Tsai [4-6])*

$$\frac{B_{26}}{tA_{22}} = \frac{M_{xy}}{tN_y} \tag{4.98}$$

From Figure 4-30, bending-extension coupling is largest when θ = 45° and N = 2.

The bending stiffnesses include the bend-twist coupling terms D_{16} and D_{26} when N is odd, but $D_{16} = D_{26} = 0$ for N even. Because, by virtue of Equation (4.93), D_{16} and D_{26} are inversely proportional to N, then their maximum value occurs when N = 3. Also, D_{16} and D_{26} achieve a maximum for a lamination angle of 45° as shown in Figure 4-31. In simple bending, the twisting moment induced by the presence of D_{16} and D_{26} is 30% of the applied bending moment. This coupling does *not* decrease rapidly as N increases. Thus, approximate solutions in which bend-twist coupling is ignored are not likely to be accurate.

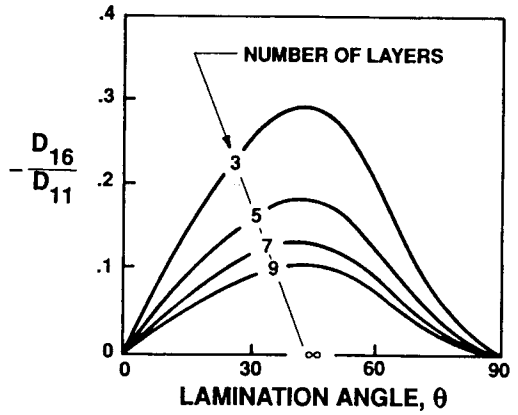

Figure 4-31 Bend-Twist Coupling Stiffness D_{16} for a Glass-Epoxy Angle-Ply Laminate *(After Tsai [4-6])*

4.4.5 Theoretical and Measured Angle-Ply Laminate Stiffnesses

The measurement procedures chosen to compare theory and experiment are the same as those in Section 4.4.3 for special cross-ply laminates. A two-layered special angle-ply laminate has the largest B_{16} and B_{26}. A three-layered laminate has the largest A_{16}, A_{26}, D_{16}, and D_{26}. The experiments were conducted on beams with angle-ply layers at $\pm\alpha$ to the beam axis. Note that only half as many specimens are required as for special cross-ply laminates because, for example, A_{11} and A_{22} are mirror images of one another about θ = 45°. Because coupling between extensional forces and shearing deformations exists as well as between bending moments and twisting deformations, a complex strain state was anticipated. Thus, three-element strain rosettes were placed on the top and bottom beam surfaces. The shearing strain, γ_{xy}, is then calculated from

$$\gamma_{xy}^{upper} = 2\,\varepsilon_{45°}^{upper} - (\varepsilon_x^{upper} + \varepsilon_y^{upper})$$
$$\gamma_{xy}^{lower} = 2\,\varepsilon_{45°}^{lower} - (\varepsilon_x^{lower} + \varepsilon_y^{lower}) \qquad (4.99)$$

where $\varepsilon_{45°}$ is the third strain (at 45° to the x and y axes) in the strain rosette. The middle surface strains and curvatures are calculated from Equation (4.87).

The theoretical and measured stiffnesses are shown in Figure 4-32. As with cross-ply laminates, very good agreement was obtained. Thus, the predictions of laminate stiffnesses are quite accurate.

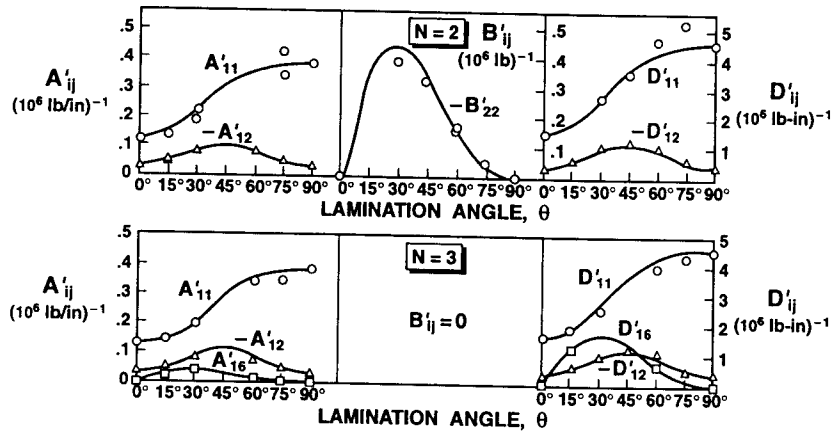

Figure 4-32a Theoretical and Measured Special Angle-Ply Laminate Stiffnesses (U. S. Standard Units) *(After Tsai [4-6])*

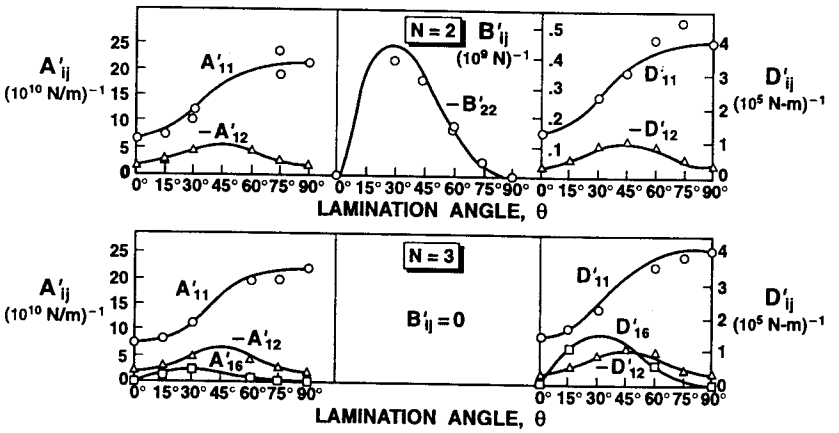

Figure 4-32b Theoretical and Measured Special Angle-Ply Laminate Stiffnesses (SI Units) *(After Tsai [4-6])*

4.4.6 Summary Remarks

Measured special cross-ply and angle-ply laminate stiffnesses were compared with theoretical stiffnesses from classical lamination theory. Both symmetric and antisymmetric laminates were treated. The number of layers in each laminate correspond to predictions of the largest coupling stiffnesses A_{16}, A_{26}, B_{ij}, D_{16}, and D_{26} where these stiffnesses existed. Thus, the comparisons between theory and experiment were for worst-case conditions. Accordingly, the good agreement obtained lends high confidence to theoretical predictions of stiffnesses for less severe conditions of coupling and for more general laminates.

Problem Set 4.4

4.4.1 Derive the extensional stiffnesses for regular symmetric special cross-ply laminates, that is, derive Equation (4.78) for the special case in which $t_{odd} = t_{even} = t/N$.
4.4.2 Derive the bending stiffnesses for regular symmetric special cross-ply laminates, that is, derive Equation (4.80) for the special case in which $t_{odd} = t_{even} = t/N$.
4.4.3 Derive the extensional stiffnesses for regular antisymmetric special cross-ply laminates, that is, derive Equation (4.82) for the special case in which $t_{odd} = t_{even} = t/N$ (for which also M = 1).
4.4.4 Derive the bending-extension coupling stiffnesses for regular special antisymmetric cross-ply laminates, that is, derive Equation (4.83) for the special case in which $t_{odd} = t_{even} = t/N$ (for which also M = 1).
4.4.5 Derive the bending stiffnesses for regular antisymmetric special cross-ply laminates, that is, derive Equation (4.84) for the special case in which $t_{odd} = t_{even} = t/N$ (for which also M = 1).
4.4.6 Derive the stiffnesses for symmetric special angle-ply laminates in Equations (4.91)-(4.93).
4.4.7 Derive the stiffnesses for antisymmetric special angle-ply laminates in Equations (4.94) - (4.96).
4.4.8 Derive Equations (4.97) and (4.98).

4.5 STRENGTH OF LAMINATES

4.5.1 Introduction

Metal plates under in-plane tensile loading can exhibit either brittle or ductile behavior to failure as in Figure 4-33. There, a metal plate under in-plane compressive loading can buckle and yet carry an even higher load than the buckling load, although at the expense of much-increased deflection per unit of additional load applied. Neither the buckling load nor the yield load represents the maximum load-carrying capacity of the structural element. However, exceeding the buckling load (operating in the postbuckling regime) or the yield load is not always permissible in usual operating conditions.

Laminated composite plates under in-plane tensile loading exhibit deformation response that is both like a ductile metal plate under tension and like a metal plate that buckles. That is, a composite plate exhibits progressive failure on a layer-by-layer basis as in Figure 4-34. Of course, a composite plate in compression buckles in a manner similar to that of a metal plate except that the various failures in the compressive loading version of Figure 4-34 could be lamina failures or the various plate buckling events (more than one buckling load occurs).

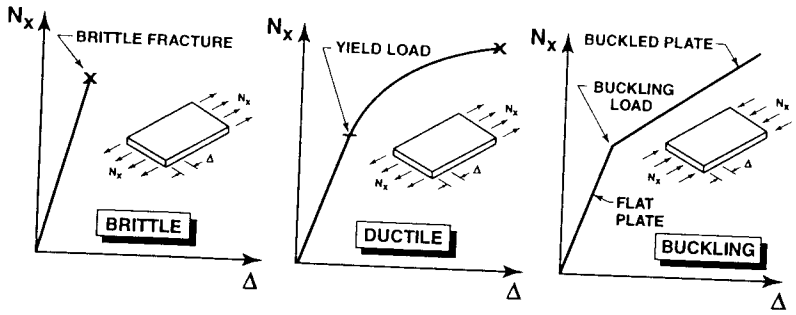

Figure 4-33 Load-Deflection Behavior of Metal Plates

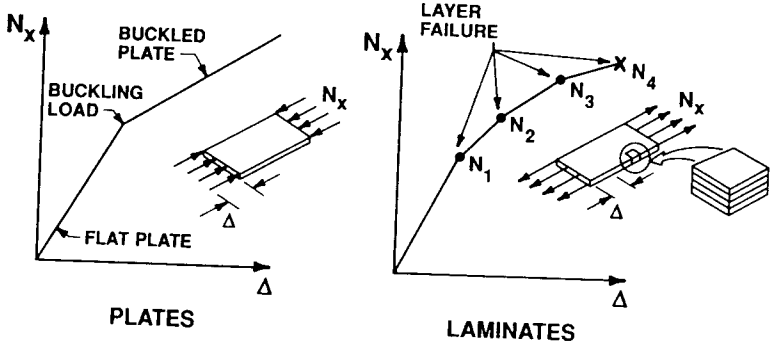

Figure 4-34 Analogy between Buckled Plate and Laminate Load-Deformation Behavior

For laminate strength, just as for laminate stiffness, the basic building block is the lamina with its inherent characteristics. The objective of this section is to present a methodology for predicting laminate strength based on the strengths and interactions of its laminae. Fundamental to such a methodology is the knowledge of the stress state in each lamina, based on concepts developed earlier in this book. However, because of the heterogeneous and orthotropic or perhaps even anisotropic nature of composite materials, failure modes occur that require new analysis quite unlike those for isotropic homogeneous materials. In particular, for a laminated composite material, failure of one layer does not necessarily imply failure of the entire laminate; the laminate might, in fact, be capable of sustaining higher loads despite a significant change (decrease) in stiffness. An analogy to this phenomenon is the ability of a plate loaded in in-plane compression to carry loads higher than the buckling load, but at an increase in the amount of deformation per unit of load (a decreased stiffness) as shown in Figure 4-34.

Because of the various characteristics of composite laminates, it is difficult to determine a strength criterion in which all failure modes and their interactions are properly accounted for. Moreover, the verification of a proposed strength criterion is greatly complicated by scatter in measured strengths caused by inconsistent processing techniques (that

are mainly unavoidable) and sometimes inappropriate and misleading experimental techniques. Nevertheless, a continuing effort must be made to define strength criteria that enable the accurate prediction of composite laminate strengths. Strength criteria are essential so a designer can predict the capability of a structural element under a complex loading state. Such criteria must be verified by comparison with measured strengths; subsequently, judgment must be made as to whether the criteria adequately represent the physical phenomena given the inherent experimental difficulties of measuring the phenomena.

All strength criteria for composite laminates depend on the strengths in the laminae principal material directions, which likely do not coincide with laminae principal stress directions. Therefore, the strength of each lamina in a laminate must be assessed in a coordinate system that is likely different from those of its neighboring laminae. This coordinate mismatch is but one of the complications that characterizes even a macroscopic strength criterion for laminates. The main factors or elements that are peculiar to laminate strength analysis are shown in several categories in Figure 4-35. There, the *cure and use conditions* affect the *state of the material* that is used in the laminate. For example, the difference between the stress-free, elevated-temperature, curing temperature and the service temperature causes thermal or residual stresses. Similarly, the difference between curing moisture content and service moisture content causes moisture stresses as does the difference between moisture contents at any two different times. Moisture diffuses throughout epoxy matrix materials at a far slower rate (months) than temperature (minutes). In some cases, the history of environmental effects such as temperature and moisture must be considered.

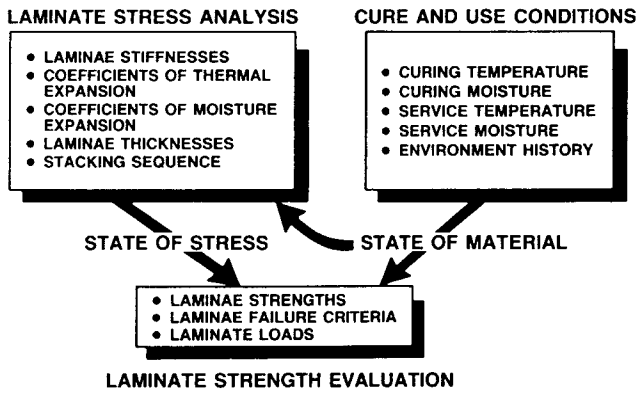

Figure 4-35 Laminate Strength-Analysis Elements

The *laminate stress-analysis* elements are affected by the *state of the material* and, in turn, determine the *state of stress.* For example, the laminate stiffnesses are usually a function of temperature and can be a function of moisture, too. The laminae hygrothermomechanical properties, thicknesses, and orientations are important in determining the directional characteristics of laminate strength. The stacking sequence

affects the bending and bending-extension coupling stiffnesses and hence the strengths of the laminate.

Finally, both the *state of the material* and the *state of stress* affect the laminate strength evaluation. That is, the actual temperature and moisture conditions influence the laminae strengths. Taken together with the laminae stresses, the laminae strengths and the laminate loads lead to an evaluation of the laminate capabilities.

A laminate can be subjected to thermal, moisture, and mechanical loads with the objective of surviving those loads. A method of strength analysis is required to determine either (1) the maximum loads a given laminate can withstand or (2) the laminate characteristics necessary to withstand a given load. The maximum loads problem is, of course, an analysis situation, and the laminate characteristics problem is a design situation that will be discussed in Chapter 7.

4.5.2 Laminate Strength-Analysis Procedure

The analysis of stresses in the laminae of a laminate is a straightforward, but sometimes tedious, task. The reader is presumed to be familiar with the basic lamination principles that were discussed earlier in this chapter. There, the stresses were seen to be a linear function of the applied loads if the laminae exhibit linear elastic behavior. Thus, a single stress analysis suffices to determine the stress field that causes failure of an individual lamina. That is, if all laminae stresses are known, then the stresses in each lamina can be compared with the lamina failure criterion and uniformly scaled upward to determine the load at which failure occurs.

The overall procedure of laminate-strength analysis, which simultaneously results in the laminate load-deformation behavior, is shown schematically in Figure 4-36. There, *load* is taken to mean both forces and moments; similarly, *deformations* are meant to include both strains and curvatures. The analysis is composed of two different approaches that depend on whether any laminae have failed.

If no laminae have failed, the load must be determined at which the first lamina fails (so-called *first-ply failure*), that is, violates the lamina failure criterion. In the process of this determination, the laminae stresses must be found as a function of the unknown magnitude of loads first in the laminate coordinates and then in the principal material directions. The proportions of load (i.e., the ratios of N_x to N_y, M_x to M_y, etc.) are, of course, specified at the beginning of the analysis. The load parameter is increased until some individual lamina fails. The properties of the failed lamina are then degraded in one of two ways: (1) totally to zero if the fibers in the lamina fail or (2) to fiber-direction properties if the failure is by cracking parallel to the fibers (matrix failure). Actually, because of the matrix manipulations involved in the analysis, the failed lamina properties must not be zero, but rather effectively zero values in order to avoid a singular matrix that could not be inverted in the structural analysis problem. The laminate strains are calculated from the known load and the stiffnesses prior to failure of a lamina. The laminate deformations just after failure of a lamina are discussed later.

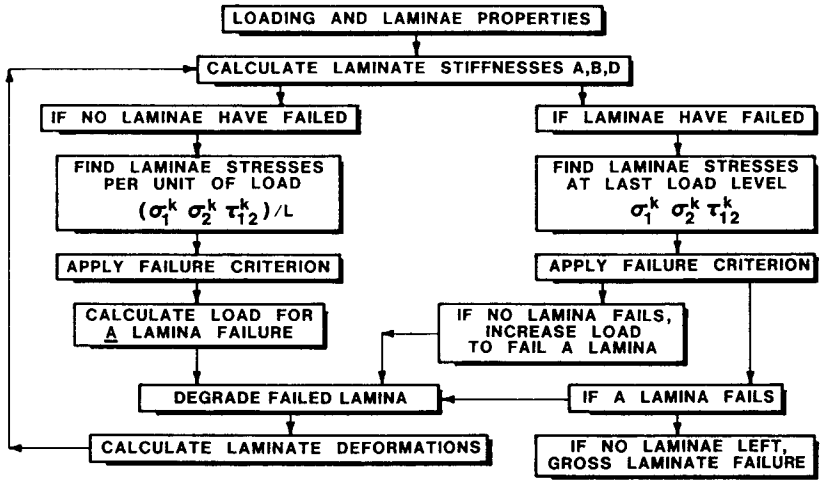

Figure 4-36 Analysis of Laminate Strength and Load-Deformation Behavior

If one or more laminae have now failed, new laminate extensional, bending-extension coupling, and bending stiffnesses are calculated. Laminae stresses are recalculated to determine their distribution after a lamina has failed (the stresses in the remaining laminae must increase to maintain equilibrium). Then we must verify that the remaining laminae, at their increased stress levels, do not fail at the same load that caused failure of the lamina in the preceding cycle through the analysis. That is, can the laminae stresses be successfully redistributed among the unfailed layers? If no more laminae fail, then the load can be increased until another lamina fails, and the cycle is repeated. In each cycle, the increased stresses caused by failure of a lamina must be verified not to cause an instantaneously progressive failure, that is, where the laminae all successively fail at the same load. When such a multiple failure occurs, the laminate is said to have suffered gross failure.

Note that the lamina failure criterion was not mentioned explicitly in the discussion of Figure 4-36. The entire *procedure* for strength analysis is independent of the actual lamina failure criterion, but the *results* of the procedure, the maximum loads and deformations, do depend on the specific lamina failure criterion. Also, the load-deformation behavior is piecewise linear because of the restriction to linear elastic behavior of each lamina. The laminate behavior would be piecewise nonlinear if the laminae behaved in a nonlinear elastic manner. At any rate, the overall behavior of the laminate is nonlinear if one or more laminae fail prior to gross failure of the laminate. In Section 2.9, the Tsai-Hill lamina failure criterion was determined to be the best practical representation of failure

of an E-glass-epoxy lamina under biaxial stress conditions. Thus, the Tsai-Hill criterion will be used in subsequent strength predictions in this section. However, one of the other criteria might be more suitable for materials other an E-glass-epoxy.

4.5.3 Thermal and Mechanical Stress Analysis

Mechanical stress analysis, treated earlier in this chapter, does not suffice for analysis of laminates that have been cured at temperatures different from the design operating temperature. In such cases, thermal stresses arise and must be accounted for. The concepts of mechanical stress analysis will be reiterated in this section along with the necessary modifications for thermal stress analysis.

The three-dimensional thermoelastic anisotropic strain-stress relations are

$$\varepsilon_i = S_{ij}\sigma_j + \alpha_i \Delta T \qquad i, j = 1, 2, \ldots, 6 \tag{4.100}$$

wherein the total strains, ε_i, are the sum of the mechanical strains, $S_{ij}\sigma_j$, and the six free thermal strains, $\alpha_i \Delta T$, for a temperature change ΔT. The three-dimensional stress-strain relations are obtained by inversion:

$$\sigma_i = C_{ij}(\varepsilon_i - \alpha_j \Delta T) \qquad i, j = 1, 2, \ldots, 6 \tag{4.101}$$

In both Equations (4.100) and (4.101), the six α_i are the coefficients of thermal deformation (expansion or contraction and distortion, i.e., shear), and ΔT is the temperature difference. In Equation (4.101), the terms $C_{ij}\alpha_j \Delta T$ are the thermal stresses if the total strain is zero.

For plane stress on an orthotropic lamina in principal material coordinates,

$$\begin{bmatrix} \sigma_1 \\ \sigma_2 \\ \tau_{12} \end{bmatrix} = \begin{bmatrix} Q_{11} & Q_{12} & 0 \\ Q_{12} & Q_{22} & 0 \\ 0 & 0 & Q_{66} \end{bmatrix} \begin{bmatrix} \varepsilon_1 - \alpha_1 \Delta T \\ \varepsilon_2 - \alpha_2 \Delta T \\ \gamma_{12} \end{bmatrix} \tag{4.102}$$

Note that the coefficients of thermal expansion affect only extensional strains, not the shearing strain.

The stresses in laminate coordinates for the k^{th} layer are obtained by transformation of coordinates in the manner of Section 2.6 as

$$\begin{bmatrix} \sigma_x \\ \sigma_y \\ \tau_{xy} \end{bmatrix}_k = \begin{bmatrix} \overline{Q}_{11} & \overline{Q}_{12} & \overline{Q}_{16} \\ \overline{Q}_{12} & \overline{Q}_{22} & \overline{Q}_{26} \\ \overline{Q}_{16} & \overline{Q}_{26} & \overline{Q}_{66} \end{bmatrix}_k \begin{bmatrix} \varepsilon_x - \alpha_x \Delta T \\ \varepsilon_y - \alpha_y \Delta T \\ \gamma_{xy} - \alpha_{xy} \Delta T \end{bmatrix}_k \tag{4.103}$$

wherein the appearance of α_{xy} signifies an apparent coefficient of thermal shear or distortion as in the right-hand side of Figure 4-37.

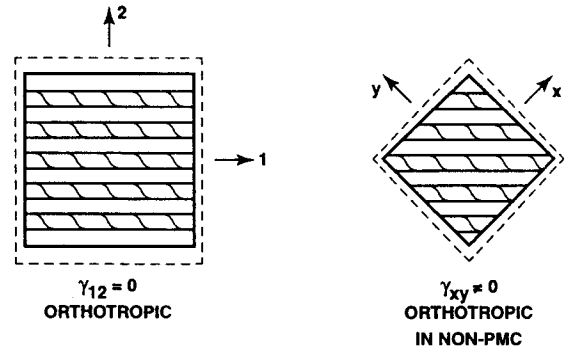

Figure 4-37 Thermal Expansion and Distortion of an Orthotropic Lamina

When the linear variation of strain through the thickness, Equation (4.13), is substituted in Equation (4.103) and the resulting expressions for the layer stresses are integrated through the thickness, the force resultants are

$$\begin{bmatrix} N_x \\ N_y \\ N_{xy} \end{bmatrix} = \begin{bmatrix} A_{11} & A_{12} & A_{16} \\ A_{12} & A_{22} & A_{26} \\ A_{16} & A_{26} & A_{66} \end{bmatrix} \begin{bmatrix} \varepsilon_x^o \\ \varepsilon_y^o \\ \gamma_{xy}^o \end{bmatrix} + \begin{bmatrix} B_{11} & B_{12} & B_{16} \\ B_{12} & B_{22} & B_{26} \\ B_{16} & B_{26} & B_{66} \end{bmatrix} \begin{bmatrix} \kappa_x \\ \kappa_y \\ \kappa_{xy} \end{bmatrix} - \begin{bmatrix} N_x^T \\ N_y^T \\ N_{xy}^T \end{bmatrix} \tag{4.104}$$

in which the A_{ij} and B_{ij} are the usual extensional and bending-extension coupling stiffnesses defined in Equation (4.24) and the thermal forces are

$$\begin{bmatrix} N_x^T \\ N_y^T \\ N_{xy}^T \end{bmatrix} = \int \begin{bmatrix} \overline{Q}_{11} & \overline{Q}_{12} & \overline{Q}_{16} \\ \overline{Q}_{12} & \overline{Q}_{22} & \overline{Q}_{26} \\ \overline{Q}_{16} & \overline{Q}_{26} & \overline{Q}_{66} \end{bmatrix}_k \begin{bmatrix} \alpha_x \\ \alpha_y \\ \alpha_{xy} \end{bmatrix}_k \Delta T \, dz \tag{4.105}$$

Note that the so-called thermal forces, N^T, are true thermal forces only when the total strains and curvatures are perfectly restrained, that is, zero.

In a similar manner, the moment resultants are obtained by integrating the moment of the stresses through the thickness:

$$\begin{bmatrix} M_x \\ M_y \\ M_{xy} \end{bmatrix} = \begin{bmatrix} B_{11} & B_{12} & B_{16} \\ B_{12} & B_{22} & B_{26} \\ B_{16} & B_{26} & B_{66} \end{bmatrix} \begin{bmatrix} \varepsilon_x^o \\ \varepsilon_y^o \\ \gamma_{xy}^o \end{bmatrix} + \begin{bmatrix} D_{11} & D_{12} & D_{16} \\ D_{12} & D_{22} & D_{26} \\ D_{16} & D_{26} & D_{66} \end{bmatrix} \begin{bmatrix} \kappa_x \\ \kappa_y \\ \kappa_{xy} \end{bmatrix} - \begin{bmatrix} M_x^T \\ M_y^T \\ M_{xy}^T \end{bmatrix} \tag{4.106}$$

in which the D_{ij} are the usual bending stiffnesses defined in Equation (4.24) and the thermal moments are

$$\begin{bmatrix} M_x^T \\ M_y^T \\ M_{xy}^T \end{bmatrix} = \int \begin{bmatrix} \bar{Q}_{11} & \bar{Q}_{12} & \bar{Q}_{16} \\ \bar{Q}_{12} & \bar{Q}_{22} & \bar{Q}_{26} \\ \bar{Q}_{16} & \bar{Q}_{26} & \bar{Q}_{66} \end{bmatrix}_k \begin{bmatrix} \alpha_x \\ \alpha_y \\ \alpha_{xy} \end{bmatrix}_k \Delta T \, z \, dz \tag{4.107}$$

Actually, only in the restricted case of perfect constraint are the N^T and M^T thermal forces and moments, respectively. However, the force and moment resultants can be rearranged to read

$$\begin{bmatrix} \bar{N}_x \\ \bar{N}_y \\ \bar{N}_{xy} \end{bmatrix} = \begin{bmatrix} N_x + N_x^T \\ N_y + N_y^T \\ N_{xy} + N_{xy}^T \end{bmatrix} = \begin{bmatrix} A_{11} & A_{12} & A_{16} \\ A_{12} & A_{22} & A_{26} \\ A_{16} & A_{26} & A_{66} \end{bmatrix} \begin{bmatrix} \varepsilon_x^\circ \\ \varepsilon_y^\circ \\ \gamma_{xy}^\circ \end{bmatrix} + \begin{bmatrix} B_{11} & B_{12} & B_{16} \\ B_{12} & B_{22} & B_{26} \\ B_{16} & B_{26} & B_{66} \end{bmatrix} \begin{bmatrix} \kappa_x \\ \kappa_y \\ \kappa_{xy} \end{bmatrix} \tag{4.108}$$

$$\begin{bmatrix} \bar{M}_x \\ \bar{M}_y \\ \bar{M}_{xy} \end{bmatrix} = \begin{bmatrix} M_x + M_x^T \\ M_y + M_y^T \\ M_{xy} + M_{xy}^T \end{bmatrix} = \begin{bmatrix} B_{11} & B_{12} & B_{16} \\ B_{12} & B_{22} & B_{26} \\ B_{16} & B_{26} & B_{66} \end{bmatrix} \begin{bmatrix} \varepsilon_x^\circ \\ \varepsilon_y^\circ \\ \gamma_{xy}^\circ \end{bmatrix} + \begin{bmatrix} D_{11} & D_{12} & D_{16} \\ D_{12} & D_{22} & D_{26} \\ D_{16} & D_{26} & D_{66} \end{bmatrix} \begin{bmatrix} \kappa_x \\ \kappa_y \\ \kappa_{xy} \end{bmatrix} \tag{4.109}$$

In the form of Equations (4.108) and (4.109), the thermal portion of thermal and mechanical stress problems can be treated as equivalent mechanical loads defined by N^T and M^T in Equations (4.105) and (4.107), respectively, in addition to the mechanical loads, N and M.

The fictitious forces and moments, $\bar{N}$ and $\bar{M}$, are subject to the same rules as N and M for problems of mechanical loading only. For example, Equations (4.108) and (4.109) can be written as

$$\begin{bmatrix} \bar{N} \\ \hline \bar{M} \end{bmatrix} = \left[\begin{array}{c|c} A & B \\ \hline B & D \end{array}\right] \begin{bmatrix} \varepsilon^\circ \\ \hline \kappa \end{bmatrix} \tag{4.110}$$

in analogy to Equation (4.62). Also, upon inversion of Equation (4.110),

$$\begin{bmatrix} \varepsilon^\circ \\ \hline \kappa \end{bmatrix} = \left[\begin{array}{c|c} A' & B' \\ \hline H' & D' \end{array}\right] \begin{bmatrix} \bar{N} \\ \hline \bar{M} \end{bmatrix} \tag{4.111}$$

in analogy to Equation (4.73). Thus, a highly advantageous formulation has been achieved.

Upon normal solution of mechanical loading, or mechanical and thermal loading, problems, the stresses in the laminae can be determined from Equation (4.102). The laminae stresses are used in the lamina failure criterion to determine the laminate stiffness up to the maximum load the laminate can take. Obviously, classical lamination theory including thermal effects is essential to the correct description of laminate behavior because of heterogeneity and the curing process for fabricating laminates. Interactions between laminae are developed as a result of the manner in which the laminae are placed in the laminate and cured. These interactions will be described and discussed in examples of cross-ply and angle-ply laminates.

4.5.4 Hygroscopic Stress Analysis

Hygroscopic (moisture) effects arise for polymer materials such as some epoxies that absorb moisture chemically after curing and therefore expand. These effects are directly analogous to thermal effects and are characterized by coefficients of moisture expansion β_1 and β_2 in principal material coordinates in direct analogy to α_1 and α_2 for coefficients of thermal expansion. All calculations for thermal effects with the α_i can be replaced by or supplemented with analogous terms for moisture expansion.

The time scale is quite different for diffusion or spreading of thermal effects as opposed to moisture effects. Thermally induced changes in deformations and stresses are usually rapid (within at most moments) because thermal diffusion is fairly rapid. In contrast, hygroscopic effects are quite slow because they depend on moisture diffusion in the material, a very slow process (weeks to months to even years to achieve uniform saturation). Shen and Springer showed that the usual thermal versus moisture diffusion values for materials lead to the conclusion that the temperature inside a surface-heated body approaches equilibrium (thermal soak) about 10^6 times faster than the moisture content approaches saturation [4-7]. For example, a .50-in (12.5-mm) thick T300-1034 graphite-epoxy laminate exposed to 90% humidity air at 170°F (77°C) takes about 15 seconds to reach thermal equilibrium, but about 13 years to reach moisture saturation [4-7]! The coefficient of moisture diffusion changes very little with moisture content but changes rapidly with temperature [4-7].

Calculation of the effects of both thermal and moisture processes depends on knowledge of the temperature field and the moisture field, respectively, in the structure being considered. Thermal problems involving temperature gradients are not uncommon (the structure might be heated from one side, and the heat is nonuniformly distributed prior to the thermal-soak condition). Moisture problems involving complex moisture distributions in the laminate such as in Figure 4-38 are the 'usual' problem. A form of the curves in Figure 4-38 were obtained by Pipes, Vinson, and Chou for various values of Dt (D is the diffusion coefficient and t is the time with D constant over the range of temperature and moisture considered) [4-8]. The present curves were obtained from those of Pipes, Vinson, and Chou by using the approximate value of $D = 2 \times 10^{-6}$ in^2/hr obtained from the work of Browning, Husman, and

Whitney [4-9] to get a time value for each curve. Note in Figure 4-38 that the moisture content changes continuously through the laminate thickness. That is, nothing special happens at lamina boundaries because the moisture diffusion occurs through the matrix phase of the composite material and is thus unaffected by fiber orientation in each lamina. The moisture through-the-thickness profiles for a T300-5208 $[0/+45/-45]_S$ laminate are shown for 5, 25, 50, and 250 hr, where the latter curve nearly represents moisture saturation (after 1 1/2 weeks). Obviously, moisture diffusion is quite slow, but also the moisture content is quite variable through the thickness. Naturally, with such a nonlinear time-dependent moisture distribution, the solution for stresses is complicated [4-8]. For moisture-saturated laminates, the solution is no more complex than the thermal effects found in the following subsections.

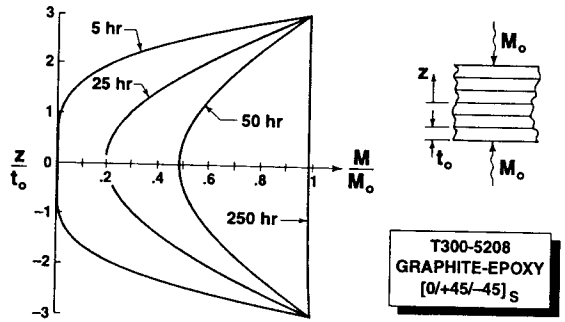

Figure 4-38 Possible Moisture Profiles through the Laminate Thickness *(Adapted from Pipes, Vinson, and Chou [4-8])*

4.5.5 Strength of Cross-Ply Laminates

The procedure of laminate strength analysis outlined in Section 4.5.2, with the Tsai-Hill lamina failure criterion will be illustrated for cross-ply laminates that have been cured at a temperature above their service or operating temperature in the manner of Tsai [4-10]. Thus, the thermal effects discussed in Section 4.5.3 must be considered as well. For cross-ply laminates, the transformations of lamina properties are trivial, so the laminate strength-analysis procedure is readily interpreted.

The particular cross-ply laminate to be examined [4-10] has three layers, so is symmetric about its middle surface. Thus, no coupling exists between bending and extension. Under the condition $N_x = N$ and all other loads and moments are zero, the stresses in the (symmetric) outer layers are identical. One outer layer is called the 1-layer and has fibers in the x-direction (see Figure 4-39). The inner layer is called the 2-layer and has fibers in the y-direction. The other outer layer is the 3-layer, but because of symmetry there is no need to refer to it. The cross-ply ratio, M, is .2, so the thickness of the inner layer is ten times that of each of the outer layers (actually, the inner 'layer' is ten like-oriented laminae). Each lamina is .005 in (.1270 mm) thick, so the total laminate thickness is .060 in (1.524 mm).

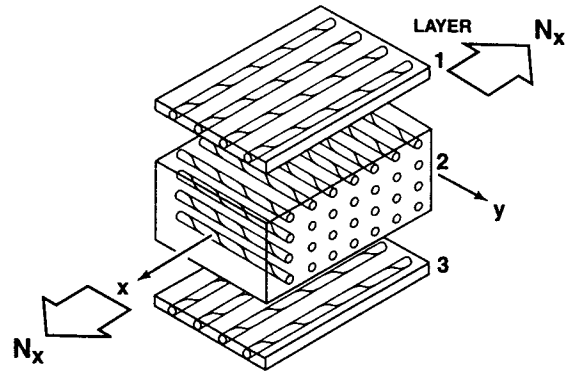

Figure 4-39 Unbonded View of a Three-Layered M = .2 Cross-Ply Laminate under Tensile Loading

The properties of the example E-glass-epoxy lamina are

$$\begin{aligned} E_1 &= 7.8\times10^6 \text{ psi } (53.78 \text{ GPa}) & X_t &= X_c = 150 \text{ ksi } (1035 \text{ MPa}) \\ E_2 &= 2.6\times10^6 \text{ psi } (17.93 \text{ GPa}) & Y_t &= 4 \text{ ksi } (27.6 \text{ MPa}) \\ \nu_{12} &= .25 & Y_c &= 20 \text{ ksi } (138 \text{ MPa}) \\ G_{12} &= 1.25\times10^6 \text{ psi } (8.62 \text{ GPa}) & S &= 6 \text{ ksi } (41.4 \text{ MPa}) \\ \alpha_1 &= 3.5\times10^{-6}/°\text{F } (6.3\times10^{-6}/°\text{C}) & \alpha_2 &= 11.4\times10^{-6}/°\text{F } (20.52\times10^{-6}/°\text{C}) \end{aligned} \tag{4.112}$$

where the number of significant figures for the SI units exceeds reasonable engineering practice in order to accurately convert U.S. Standard results to SI results throughout this example. The highest modulus is in the fiber direction, and the highest coefficient of thermal expansion is in the direction perpendicular to the fibers. Moreover, all stiffnesses are regarded as the same in tension as in compression, although the strengths perpendicular to the fibers are different.

Pre-failure Deformation

Prior to any failure, the lamina reduced stiffnesses are

$$\begin{aligned} Q_{11}^{(1)} &= Q_{22}^{(2)} = 7.9660\times10^6 \text{ psi } (54.92 \text{ GPa}) \\ Q_{12}^{(1)} &= Q_{12}^{(2)} = .6638\times10^6 \text{ psi } (4.578 \text{ GPa}) \\ Q_{22}^{(1)} &= Q_{11}^{(2)} = 2.6550\times10^6 \text{ psi } (18.31 \text{ GPa}) \\ Q_{66}^{(1)} &= Q_{66}^{(2)} = 1.250\times10^6 \text{ psi } (8.620 \text{ GPa}) \\ Q_{16}^{(1)} &= Q_{16}^{(2)} = Q_{26}^{(1)} = Q_{26}^{(2)} = 0 \end{aligned} \tag{4.113}$$

and the apparent coefficients of thermal expansion are

$$\begin{aligned}
\alpha_x^{(1)} &= \alpha_y^{(2)} = 3.5\times10^{-6}/°F \ (6.3\times10^{-6}/°C)\\
\alpha_y^{(1)} &= \alpha_x^{(2)} = 11.4\times10^{-6}/°F \ (20.52\times10^{-6}/°C)\\
\alpha_{xy}^{(1)} &= \alpha_{xy}^{(2)} = 0
\end{aligned} \tag{4.114}$$

The laminate extensional stiffnesses are

$$\begin{aligned}
A_{11} &= .21243\times10^{6} \text{ lb/in } (.037207 \text{ GN/m})\\
A_{12} &= .03983\times10^{6} \text{ lb/in } (.0069767 \text{ GN/m})\\
A_{22} &= .42485\times10^{6} \text{ lb/in } (.074405 \text{ GN/m})\\
A_{66} &= .07500\times10^{6} \text{ lb/in } (.013137 \text{ GN/m})
\end{aligned} \tag{4.115}$$

The inverse extensional stiffnesses are

$$\begin{aligned}
A'_{11} &= 4.7918\times10^{-6}/(\text{lb/in}) \ [.27358\times10^{-7}/(\text{N/m})]\\
A'_{12} &= -.44923\times10^{-6}/(\text{lb/in}) \ [-.025653\times10^{-7}/(\text{N/m})]\\
A'_{22} &= 2.3959\times10^{-6}/(\text{lb/in}) \ [.13680\times10^{-7}/(\text{N/m})]\\
A'_{66} &= 13.333\times10^{-6}/(\text{lb/in}) \ [.76122\times10^{-7}/(\text{N/m})]
\end{aligned} \tag{4.116}$$

Thus, all numbers are in hand for calculation of the stresses in the example cross-ply laminate.

Consider a constant temperature of the laminate different from, and relative to, its stress-free curing temperature. Then, the thermal forces are, from Equation (4.105),

$$\begin{aligned}
N_x^T &= 33.1\,t\,\Delta T \text{ psi/°F } (.41049\,t\,\Delta T \text{ MPa/°C})\\
N_y^T &= 35.0\,t\,\Delta T \text{ psi/°F } (.43407\,t\,\Delta T \text{ MPa/°C})\\
N_{xy}^T &= 0
\end{aligned} \tag{4.117}$$

and the thermal moments, from Equation (4.107), are zero.

By means of rather involved successive substitutions of Equation (4.108) in (4.111), in (4.13), and finally in (4.103), the stresses in the inner and outer layers can be shown to be

$$\begin{aligned}
\sigma_x^{(1)} &= 2.27\frac{N_x}{t} + 35.5\Delta T \text{ psi/°F } \left[2.27\frac{N_x}{t} + .4409\Delta T \text{ MPa/°C}\right]\\
\sigma_y^{(1)} &= .12\frac{N_x}{t} - 16.0\Delta T \text{ psi/°F } \left[.12\frac{N_x}{t} - .1977\Delta T \text{ MPa/°C}\right]\\
\tau_{xy}^{(1)} &= 0
\end{aligned} \tag{4.118}$$

$$\begin{aligned}
\sigma_x^{(2)} &= .75\frac{N_x}{t} - 7.1\Delta T \text{ psi/°F } \left[.75\frac{N_x}{t} - .08819\Delta T \text{ MPa/°C}\right]\\
\sigma_y^{(2)} &= -.024\frac{N_x}{t} + 3.2\Delta T \text{ psi/°F } \left[-.024\frac{N_x}{t} + .03954\Delta T \text{ MPa/°C}\right]\\
\tau_{xy}^{(2)} &= 0
\end{aligned} \tag{4.119}$$

The stresses have now been determined as a linear function of the applied loads, N_x and ΔT. Note that the laminae stresses have been expressed as a function of the average laminate stress, N_x/t. The laminate stresses are different from one another because of different fiber orientation in each lamina. One plot of a hypothetical laminate stress distribution is shown in Figure 4-5. A simpler plot for a three-layered regular cross-ply laminate under N_x is shown in Figure 4-40. There, it is obvious that the laminae stresses must be quite different from one another. The concept of an average laminate stress has some merit as an indicator of normalized laminate load. However, be very careful in interpreting the average laminate stress because it is merely a calculated norm, and, as is apparent in Figure 4-40, *the average laminate stress need not exist in any layer!* Nevertheless, the average laminate stress is used in this analysis and the following analysis for angle-ply laminates.

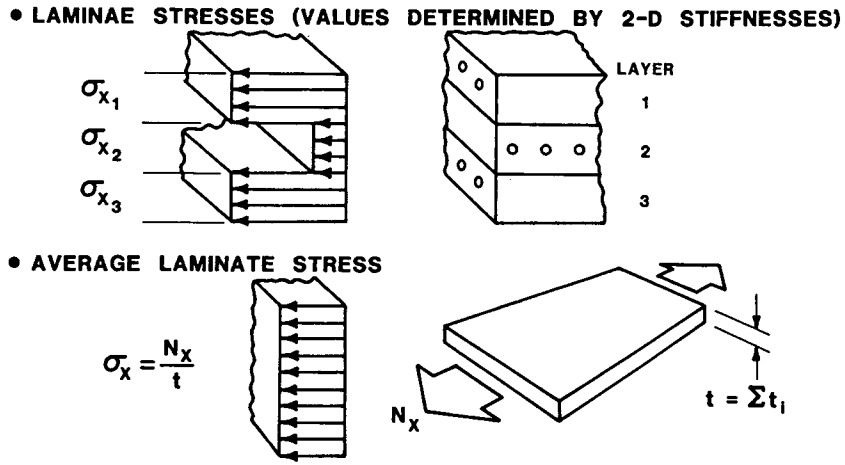

Figure 4-40 Average Laminate Stress

Application of the Lamina Failure Criterion

The failure criterion must be applied to determine the maximum values of N_x and ΔT that can be sustained without failure of any layer. Actually, the failure criterion is applied to each layer separately. For the special orientation of cross-ply laminates, the Tsai-Hill failure criterion for each layer can be expressed as

$$\left[\frac{\sigma_x}{X}\right]^2 - \frac{\sigma_x\sigma_y}{X^2} + \left[\frac{\sigma_y}{Y}\right]^2 + \left[\frac{\tau_{xy}}{S}\right]^2 = 1 \qquad (4.120)$$

In the outer layer, because $\tau_{xy} = 0$, the criterion simplifies to

$$\sigma_x^2 - \sigma_x\sigma_y + \left[\frac{X}{Y}\right]^2 \sigma_y^2 = X^2 \qquad (4.121)$$

from which, upon substitution of the stresses, results a quadratic equation with solution

$$\frac{N_x}{t} = 110\Delta T \text{ psi/°F} + [57.5Y^2 - 3000\Delta T^2(\text{psi/°F})^2]^{1/2}$$
$$= 1.365\Delta T \text{ MPa/°C} + [57.5Y^2 - .4621\Delta T^2(\text{MPa/°C})^2]^{1/2} \qquad (4.122)$$

If the curing temperature is 270°F (132°C) and the laminate operates at 70°F (21°C) (room temperature), $\Delta T = -200$°F (-111°C), so

$$\frac{N_x}{t} = 6300 \text{ psi } (43.37 \text{ MPa}) \qquad (4.123)$$

Alternatively, if the laminate is cured at room temperature, $\Delta T = 0$, so

$$\frac{N_x}{t} = 30{,}400 \text{ psi } (209.3 \text{ MPa}) \qquad (4.124)$$

In the inner layer, a similar set of steps yields

$$\frac{N_x}{t} \cong 9.6\Delta T \text{ psi/°F} + 5320 \text{ psi } (.1191\Delta T \text{ MPa/°C} + 36.68 \text{ MPa}) \qquad (4.125)$$

so if the laminate is cured at 270°F (132°C) and used at 70°F (21°C),

$$\frac{N_x}{t} = 3400 \text{ psi } (23.44 \text{ MPa}) \qquad (4.126)$$

or if cured and used at 70°F (21°C),

$$\frac{N_x}{t} = 5320 \text{ psi } (36.68 \text{ MPa}) \qquad (4.127)$$

Obviously, if the laminate is cured at 270°F (132°C), the inner layer will fail first by cracking in the y-direction because of the large $\sigma_x^{(2)}$ reaching Y_t. Why are there cracks between *all* the indicated fibers in the middle (90°) layer in Figure 4-41? The applied or induced stress level has reached the inherent strength of the middle layer, so we would expect the middle layer to break in one place if it were only a single lamina subjected to the failure stress as in Chapter 2. However, the middle layer is surrounded by and bonded to, top and bottom, two load-carrying layers. Those two layers impose stress (and strain) in the x-direction on the middle layer at all points in the middle layer along its length in the x-direction. Thus, if one break occurs, then other positions in the middle layer will still be subjected to the failure stress (or strain) and must also fail. Those additional failures will continue until all x-direction positions are broken so that no load is carried in the x-direction in the middle layer.

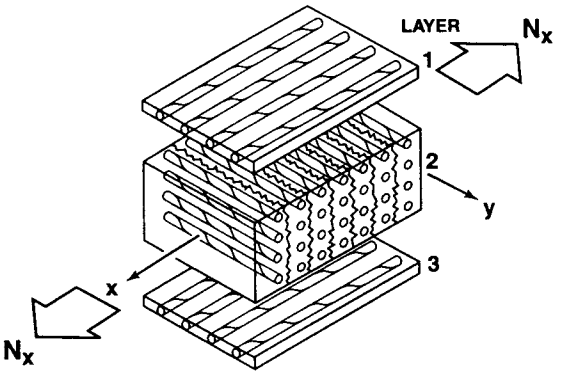

Figure 4-41 Unbonded View of a Three-Layered Cross-Ply Laminate with a Cracked Middle Layer

Actually, the inner layer fails for both example curing temperatures, although the outer layer would fail first if the curing temperature were high enough. On the other hand, if the curing temperature were lowered, the laminate would exhibit higher strength. The values of N_x/t for the two curing conditions are the values at failure of the inner layer. Those values correspond to the point labeled N_1 in Figure 4-34, that is, the so-called 'knee' of the load-deformation diagram. Up to the load corresponding to the knee, the load-deformation diagram is linear and all layers are intact. The axial strain at the knee is

$$\varepsilon_x^o = A'_{11}N_x = .098\% \qquad (4.128)$$

if the residual strains are ignored, that is, ε_x^o is measured from zero load which is not the stress-free state.

Behavior after the First Layer Fails

After a layer fails, the behavior of the laminate depends on how the mechanical and thermal interactions between layers uncouple. Actually, failure of a layer might not mean that it can no longer carry load. In the present example of a cross-ply laminate, the inner layer with fibers at 90° to the x-axis has 'failed', but, because of the orientation of the fibers (perpendicular to the main failure-causing stress), the failure should be only a series of cracks *parallel* to the fibers. Thus, stress can still be carried by the inner layer in the fiber direction (y-direction).

The degraded laminate then has stiffnesses based on the original properties of the outer layer and the following properties of the inner layer

$$Q_{11}^{(2)} = 0 \qquad Q_{22}^{(2)} = 7.9660 \times 10^6 \text{ psi } (54.92 \text{ GPa})$$
$$Q_{12}^{(2)} = 0 \qquad Q_{66}^{(2)} = 0 \qquad (4.129)$$

where the zeros are actually a very small number in order to avoid numerical difficulties in a computer analysis. The inverse extensional stiffness matrix of the laminate then has the values

$$A'_{11} = .7542 \times 10^{-6}/(\text{t psi}) \quad [109.4 \times 10^{-6}/(\text{t MPa})]$$
$$A'_{12} = -.01178 \times 10^{-6}/(\text{t psi}) \quad [1.7 \times 10^{-6}/(\text{t MPa})] \qquad (4.130)$$
$$A'_{22} = .1414 \times 10^{-6}/(\text{t psi}) \quad [20.5 \times 10^{-6}/(\text{t MPa})]$$

Note that A'_{22} is about the same as in the undegraded state.
The resulting stresses are

$$\sigma_x^{(1)} = 6.00 \frac{N_x}{t}$$
$$\sigma_y^{(1)} = .47 \frac{N_x}{t} - 19.3\Delta T \text{ psi/°F} \quad \left[.47 \frac{N_x}{t} - .23953\Delta T \text{ MPa/°C}\right] \qquad (4.131)$$
$$\tau_{xy}^{(1)} = 0$$
$$\sigma_x^{(2)} = 0$$
$$\sigma_y^{(2)} = -.09 \frac{N_x}{t} + 3.9\Delta T \text{ psi/°F} \quad \left[-.09 \frac{N_x}{t} + .04840\Delta T \text{ MPa/°C}\right] \qquad (4.132)$$
$$\tau_{xy}^{(2)} = 0$$

Obviously, there is no thermal coupling in the x-direction, but the thermal coupling in the y-direction has increased from the undegraded state [compare Equations (4.118) and (4.119) with Equations (4.131) and (4.132)]. The thermal coupling is so strong under the condition $N_x/t = 3400$ psi (23.44 MPa) and $\Delta T = -200$°F (−111°C) that the outer layers fail by developing multiple cracks parallel to the fibers as in Figure 4-42. This contention can be verified by substituting the resulting stresses in the failure criterion for the outer layer. Thus, as is indicated to be possible in the strength-analysis procedure of the right side of Figure 4-36, more than one lamina fails simultaneously, that is, at the same load.

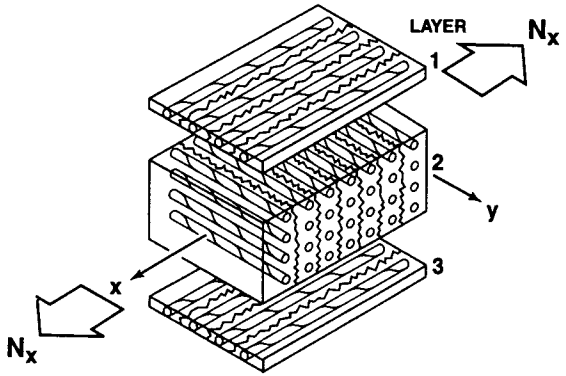

Figure 4-42 Unbonded View of a Three-Layered Cross-Ply Laminate with All Layers Degraded (Cracked)

Behavior after Degradation

The laminate is now degraded to the point where the outer layers carry stress only in the x-direction and the inner layers can carry stress only in the y-direction. In both cases, the stress is parallel to the fibers. Thus, the laminate is completely decoupled, both thermally and mechanically. The only nonzero reduced stiffnesses are

$$Q_{11}^{(1)} = Q_{22}^{(2)} = 7.9660 \times 10^6 \text{ psi (54.92 GPa)} \qquad (4.133)$$

and the associated laminate inverse extensional stiffnesses are

$$A'_{11} = .7532 \times 10^{-6}/(\text{t psi}) \quad [.010925/(\text{t GPa})]$$
$$A'_{12} = 0 \qquad (4.134)$$
$$A'_{22} = .1506 \times 10^{-6}/(\text{t psi}) \quad [.002185/(\text{t GPa})]$$

Accordingly, the only lamina stress that develops is

$$\sigma_x^{(1)} = 6.00 \frac{N_x}{t} \qquad (4.135)$$

and the resulting laminate extensional stiffness in the x-direction above the 'knee' of the load-deformation curve is

$$\frac{N_x/t}{\varepsilon_x^o} = \frac{1}{A'_{11}t} = 1.3 \times 10^6 \text{ psi (8.96 GPa)} \qquad (4.136)$$

which is about one-third the undegraded stiffness.

Maximum Laminate Load

The stage is now set to determine the largest load the laminate can carry. Only the outer layers resist the load N_x after the 'knee' of the load-deformation curve. There, the stress in the outer layers is, from Equation (4.118),

$$\sigma_x^{(1)} = 618 \text{ psi (4.26 MPa)} \qquad (4.137)$$

The largest possible value of σ_x under uniaxial conditions is 150 ksi (1035 MPa). Thus, the outer layer can be stressed about an additional 149.4 ksi (1030.7 MPa). The corresponding change in the force resultant is obtained from Equation (4.135) as

$$\frac{\Delta N_x}{t} = \frac{\Delta\sigma_x^{(1)}}{6.00} = 149{,}400 \text{ psi}/6 = 24{,}900 \text{ psi (171.8 MPa)} \qquad (4.138)$$

When this change in force resultant is added to the force resultant at the 'knee', the largest laminate average stress is determined to be

$$\frac{N_x}{t} = 3400 \text{ psi} + 24{,}900 \text{ psi} = 28{,}300 \text{ psi (194.5 MPa)} \qquad (4.139)$$

which is reasonably close to the measured maximum load in Figure 4-43. Note that a 'knee' is observed in the experiments. Also, the results of another theory called Netting Analysis are shown in Figure 4-43; obviously, that theory is incorrect for fiber-reinforced materials. Netting analysis is premised on all load being carried in the fibers, so is more appropriate for woven fabrics because they have no matrix to carry loads.

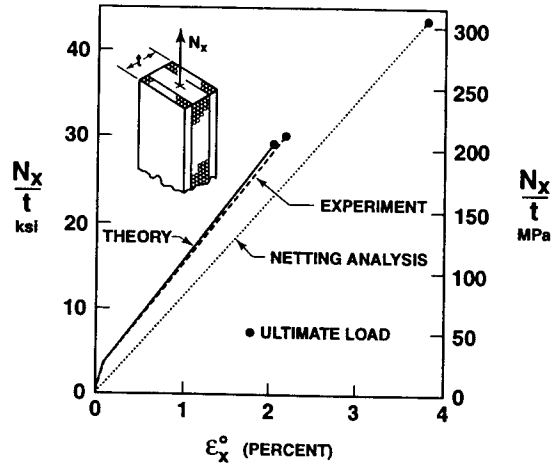

Figure 4-43 Strength of a Cross-Ply Laminate with M = .2 *(After Tsai [4-10])*

Strength and Stiffness for Other Cross-Ply Ratios

Theoretical and measured strengths and stiffnesses of three-layer cross-ply laminates with cross-ply ratios ranging from .2 to 4 are shown in Figure 4-44. The scatter in the data is partially due to the difficulty of making good tensile specimens; the characteristic dog-bone shape is formed by routing that often damages the 90° layer.

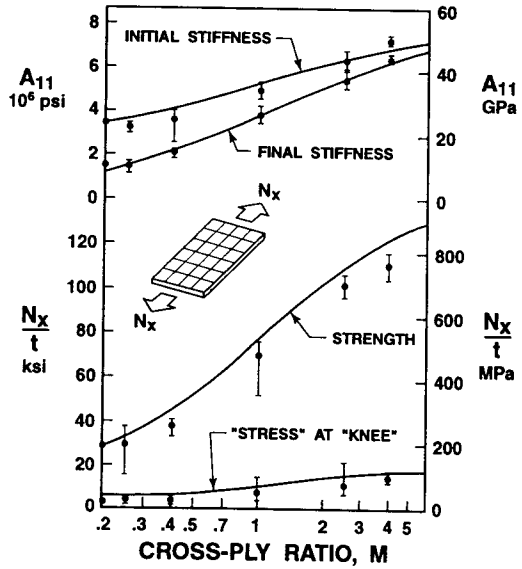

Figure 4-44 Strength of Cross-Ply Laminates
(After Tsai, Adams, and Doner [4-11])

The predicted strengths in Figure 4-44 are generally somewhat above the measured values. The predicted and observed stiffnesses, both initial (below the knee) and final, are in very good agreement. Thus, the stiffness aspects of classical lamination theory, as well as the present strength-analysis procedure, are verified.

4.5.6 Strength of Angle-Ply Laminates

Angle-ply laminates have more complicated stiffness matrices than cross-ply laminates because nontrivial coordinate transformations are involved. However, the behavior of simple angle-ply laminates (only one angle, i.e., $\pm\alpha$) will be shown to be simpler than that of cross-ply laminates because no 'knee' results in the load-deformation diagram under uniaxial loading. Other than the preceding two differences, analysis of angle-ply laminates is conceptually the same as that of cross-ply laminates.

The example considered to illustrate the strength-analysis procedure is a three-layered laminate with a [+15°/−15°/+15°] stacking sequence [4-10]. The laminae are the same E-glass-epoxy as in the cross-ply laminate example with thickness .005 in (.1270 mm), so that the total laminate thickness is .015 in (.381 mm). In laminate coordinates, the transformed reduced stiffnesses are

$$\begin{aligned}
\bar{Q}_{11}^{(1)} &= \bar{Q}_{11}^{(2)} = 7.342\times10^6 \text{ psi } (50.68 \text{ GPa})\\
\bar{Q}_{12}^{(1)} &= \bar{Q}_{12}^{(2)} = .932\times10^6 \text{ psi } (6.428 \text{ GPa})\\
\bar{Q}_{22}^{(1)} &= \bar{Q}_{22}^{(2)} = 2.743\times10^6 \text{ psi } (18.91 \text{ GPa})\\
\bar{Q}_{16}^{(1)} &= -\bar{Q}_{16}^{(2)} = -1.129\times10^6 \text{ psi } (-7.781 \text{ GPa})\\
\bar{Q}_{26}^{(1)} &= -\bar{Q}_{26}^{(2)} = -.199\times10^6 \text{ psi } (-1.372 \text{ GPa})\\
\bar{Q}_{66}^{(1)} &= \bar{Q}_{66}^{(2)} = 1.518\times10^6 \text{ psi } (10.47 \text{ GPa})
\end{aligned} \tag{4.140}$$

and the apparent coefficients of thermal expansion are

$$\begin{aligned}
\alpha_x^{(1)} &= \alpha_y^{(2)} = 4.029\times10^{-6}/°\text{F } (7.253\times10^{-6}/°\text{C})\\
\alpha_y^{(1)} &= \alpha_x^{(2)} = 10.871\times10^{-6}/°\text{F } (19.57\times10^{-6}/°\text{C})\\
\alpha_{xy}^{(1)} &= -\alpha_{xy}^{(2)} = 1.975\times10^{-6}/°\text{F } (3.555\times10^{-6}/°\text{C})
\end{aligned} \tag{4.141}$$

The inverse extensional stiffness matrix can be shown to be

$$A' = \begin{bmatrix} 9.603 & -3.210 & 2.239 \\ & 25.41 & .3148 \\ \text{(symmetric)} & & 44.48 \end{bmatrix} \times 10^{-6}/(\text{lb/in}) \tag{4.142}$$

or

$$A' = \begin{bmatrix} .05483 & -.01832 & .01278 \\ & .1450 & .001797 \\ \text{(symmetric)} & & .2539 \end{bmatrix} \times 10^{-6}/(\text{N/m}) \qquad (4.142)$$

For a constant lamination temperature,

$$\begin{aligned} N_x^T &= 37.5\, t\, \Delta T \text{ psi/°F} \quad (.4655\, t\, \Delta T \text{ MPa/°C}) \\ N_y^T &= 33.2\, t\, \Delta T \text{ psi/°F} \quad (.4118\, t\, \Delta T \text{ MPa/°C}) \\ N_{xy}^T &= -1.24\, t\, \Delta T \text{ psi/°F} \quad (.01535\, t\, \Delta T \text{ MPa/°C}) \end{aligned} \qquad (4.143)$$

and the thermal moments are zero. When the laminate is subjected to N_x only, the stresses are

$$\begin{aligned} \sigma_x^{(1)} &= .97\frac{N_x}{t} - .44\Delta T \text{ psi/°F} \quad \left[.97\frac{N_x}{t} - .00551\Delta T \text{ MPa/°C}\right] \\ \sigma_y^{(1)} &= -.005\frac{N_x}{t} - .08\Delta T \text{ psi/°F} \quad \left[-.005\frac{N_x}{t} - .00097\Delta T \text{ MPa/°C}\right] \\ \tau_{xy}^{(1)} &= -.10\frac{N_x}{t} - 1.79\Delta T \text{ psi/°F} \quad \left[-.10\frac{N_x}{t} - .0222\Delta T \text{ MPa/°C}\right] \end{aligned} \qquad (4.144)$$

$$\begin{aligned} \sigma_x^{(2)} &= 1.05\frac{N_x}{t} + .89\Delta T \text{ psi/°F} \quad \left[1.05\frac{N_x}{t} - .0110\Delta T \text{ MPa/°C}\right] \\ \sigma_y^{(2)} &= .01\frac{N_x}{t} + .16\Delta T \text{ psi/°F} \quad \left[.01\frac{N_x}{t} - .00194\Delta T \text{ MPa/°C}\right] \\ \tau_{xy}^{(2)} &= .20\frac{N_x}{t} + 3.58\Delta T \text{ psi/°F} \quad \left[.20\frac{N_x}{t} - .0445\Delta T \text{ MPa/°C}\right] \end{aligned} \qquad (4.145)$$

Note that the stresses σ_y are very small in comparison to the shearing stresses. Thus, the Tsai-Hill lamina failure criterion can be simplified for this lamina to

$$K_1\sigma_x^2 + K_2\sigma_x\tau_{xy} + K_3\tau_{xy}^2 = X^2 \qquad (4.146)$$

in which

$$\begin{aligned} K_1 &= \cos^4\theta + 624\cos^2\theta\sin^2\theta + 1406\sin^4\theta \\ K_2 &= -(1244\cos^3\theta\sin\theta + 4386\cos\theta\sin^3\theta) \\ K_3 &= 625\cos^4\theta + 4382\cos^2\theta\sin^2\theta + 625\sin^4\theta \end{aligned} \qquad (4.147)$$

The values of K_i for $\theta = -15°$ are

$$K_1 = 46.20 \qquad K_2 = 363.91 \qquad K_3 = 821.00 \qquad (4.148)$$

and for $\theta = +15°$ are

$$K_1 = 46.20 \qquad K_2 = -363.91 \qquad K_3 = 821.00 \qquad (4.149)$$

Thus, in the outer layer, the largest average laminate stress is

$$\frac{N_x}{t} = 11.14\Delta T \text{ psi/°F} + 37{,}400 \text{ psi} \quad (.1383\Delta T \text{ MPa/°C} + 257.9 \text{ MPa}) \qquad (4.150)$$

so if the laminate is cured at 270°F (132°C) and used at 70°F (21°C)

$$\frac{N_x}{t} = 35{,}170 \text{ psi} \quad (242.5 \text{ MPa}) \qquad (4.151)$$

Similarly, in the inner layer,

$$\frac{N_x}{t} = 52{,}600 \text{ psi} \quad (362.7 \text{ MPa}) \qquad (4.152)$$

so the outer layer fails first and fails by fiber fracture, so no load or stress in any direction can be carried by the outer layer. Recall that actually there are two symmetric outer layers, so both fail totally and simultaneously. Because the remaining inner layer cannot, by itself, withstand the laminate average stress of 35,170 psi (242.5 MPa), the inner layer fails immediately after the outer layers. Therefore, the maximum laminate average stress is

$$\frac{N_x}{t} = 35{,}170 \text{ psi} \quad (242.5 \text{ MPa}) \qquad (4.153)$$

and there is, as claimed, no knee in the load-deformation behavior.

For other angle-ply lamination angles, similar predicted strengths were obtained and are shown along with experimental results in Figure 4-45. The agreement between prediction and measurement is quite good. As further substantiation of the stiffness-prediction techniques in Section 4.4, theoretical and measured stiffnesses are plotted in Figure 4-45 and are also seen to be in very good agreement. However, for lamination angles around 45°, the deformations at failure are, in general, several times the predicted deformations because of nonlinear stress-strain behavior. The nonlinear behavior is not unexpected because the large shearing stresses that are developed tend to deform the (nonlinear) matrix of the fiber-reinforced composite material more than they deform the fibers. Another interesting observation involves a comparison of the present angle-ply laminate data with the data for a unidirectional lamina at various orientations given in Figure 2-25 in Section 2.9. For angles larger than 0° but less than 45°, the angle-ply has up to about 50% higher strength than the unidirectional lamina. However, above 45°, the unidirectional lamina exhibits higher strength. These differences result from mechanical and thermal interactions between layers that do not occur in a lamina.

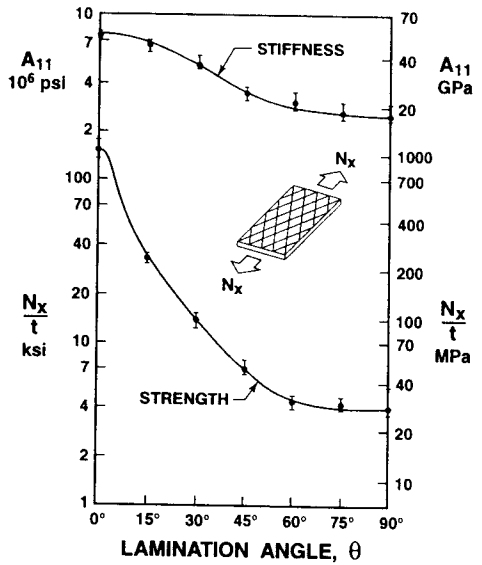

Figure 4-45 Strength of Angle-Ply Laminates *(After Tsai [4-10])*

4.5.7 Summary Remarks

The strength of special classes of laminated fiber-reinforced composite materials has been analyzed on the basis of several hypotheses:

- Linear elastic behavior to failure occurs for individual laminae.
- The Kirchhoff hypothesis of linear strain variation through the laminate thickness applies (prior to degradation, if any; after degradation, linear only through the thickness of each lamina).
- Strengths and stiffnesses of the laminae are the same in tension as in compression.
- The Tsai-Hill criterion governs failure of a lamina (the strength-analysis procedure could, of course, involve another criterion).
- Failure of a lamina might mean, for example, only lack of stiffness and strength perpendicular to the fibers with no degradation of lamina capability in the fiber direction.

For cross-ply laminates, a 'knee' in the load-deformation curve occurs after the mechanical and thermal interactions between layers uncouple because of failure (which might be only degradation, not necessarily fracture) of a lamina. The mechanical interactions are caused by Poisson effects and/or shear-extension coupling. The thermal interactions are caused by different coefficients of thermal expansion in different layers because of different angular orientations of the layers (even though the orthotropic materials in each lamina are the same). The interactions are disrupted if the layers in a laminate separate.

For angle-ply laminates, no such 'knee' or change in slope occurs in the load-deformation behavior. Simultaneous failure (fracture) of all layers occurs.

For two- and three-layered cross-ply and angle-ply laminates of E-glass-epoxy, Tsai [4-10] tabulates all the stiffnesses, inverse stiffnesses, thermal forces and moments, etc. Results are obtained for various cross-ply ratios and lamination angles, as appropriate, from a short computer program that could be used for other materials.

In the strength-analysis procedure discussed in this section, no account was taken of the possible increase in deflection that occurs when a layer fails. That is, if the laminate is simplistically represented by a set of springs in parallel (one spring represents one lamina) as in Figure 4-46, then, when one spring breaks, the remaining springs must each have a higher load and hence a higher deflection. Accordingly, a horizontal jump (in strain or deflection) occurs in the load-deflection behavior of the laminate as depicted schematically in Figure 4-46. Such a stepwise load-deflection behavior has not been observed in experiments nor has it been analyzed, to the author's knowledge. The parallel-springs model for laminate failure in Figure 4-46 is far too simple to represent all pertinent events and conditions. For example, the loading conditions are not properly modeled in Figure 4-46. Loading in a loading frame could be either constant (prescribed) load or constant (prescribed) displacement on the loading head. Constant load would produce behavior in Figure 4-46, but constant displacement (such as in a screw-type loading frame) would produce a vertical jump (constant displacement) in the load-deformation behavior as in Figure 4-47. There, the postfailure loading slopes are identical, but the curves are offset from one another. In fact, the failures between fibers probably do not occur at precisely the same load. Thus, the actual load-deformation curve might be a series of small events (shifts down or to the right) spread over some range of load that merely tends to change the curve gradually. Available plots of measured load-deformation behavior do not resolve this question. Actual behavior in a real structure is probably neither prescribed load nor prescribed displacement, but something in between.

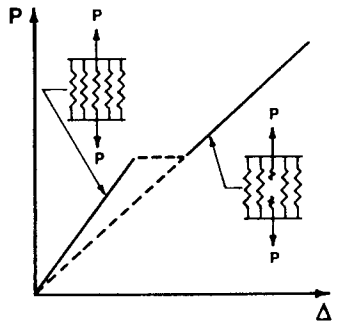

Figure 4-46 Spring Analogy for Laminate Load-Deflection Behavior

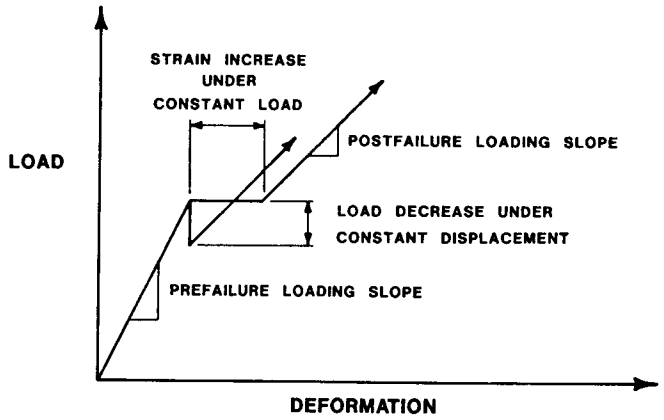

Figure 4-47 Behavior upon First-Layer Failure

Problem Set 4.5

4.5.1 Derive the thermoelastic stress-strain relations for an orthotropic lamina under plane stress, Equation (4.102), from the anisotropic thermoelastic stress-strain relations in three dimensions, Equation (4.101) [or from Equation (4.100)].

4.5.2 Derive expressions for α_x, α_y, and α_{xy} in Equation (4.103) as a function of α_1, α_2, and θ. Verify that α_{xy} vanishes for isotropic materials. What is α_{xy} for a bidirectional woven lamina with equal numbers of fibers in each directions?

4.5.3 Verify that the thermal forces N_x^T, N_y^T, and N_{xy}^T for a three-layered cross-ply laminate with $M = .2$ are given by Equation (4.117).

4.5.4 Verify that the stress $\sigma_x^{(1)}$ for a three-layered cross-ply laminate with $M = .2$ is given by Equation (4.118).

4.5.5 Verify that the lamina mechanical and thermal stresses in Equations (4.118) and (4.119) for a three-layered cross-ply laminate with $M = .2$ satisfy the laminate equilibrium conditions.

4.6 INTERLAMINAR STRESSES

In classical lamination theory, no account is taken of stresses such as σ_z, τ_{zx}, and τ_{zy} which are shown on an element of an angle-ply laminate loaded with N_x in Figure 4-48. These stresses are called interlaminar stresses and exist on surfaces between adjacent layers although they exist within the layers but are usually largest at the layer interfaces. Thus, in CLT, only the stresses in the plane of the laminate, σ_x, σ_y, and τ_{xy}, are considered; that is, a plane-stress state is assumed to exist. Accordingly, classical lamination theory does not include some of the stresses that actually cause failure of a composite laminate. High interlaminar stresses are the basis for one of the failure mechanisms uniquely characteristic of composite laminates, namely, free-edge delamination and subsequent delamination growth as in Figure 4-49. There, the laminae could come apart in the z-direction as shown. They could also merely experience a crack between them and slide along the crack in either the x- or y-directions. See Section 6.5 for discussion of the opening, parallel-shear, and forward-shear modes of crack extension.

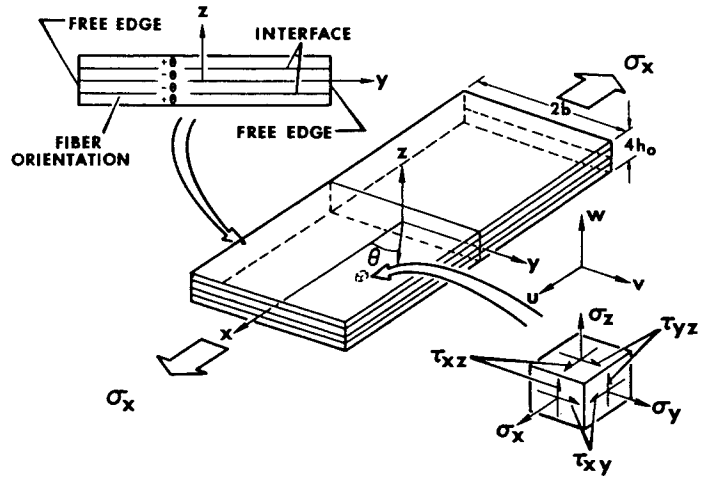

Figure 4-48 Symmetric Angle-Ply Laminate Geometry and Stresses *(After Pipes and Pagano [4-12])*

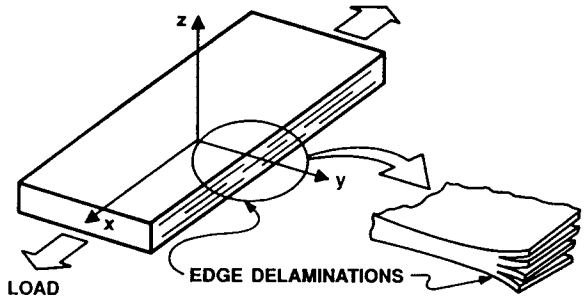

Figure 4-49 Free-Edge Delamination

Moreover, classical lamination theory often implies values of σ_y and τ_{xy} where they cannot possibly exist, namely at the edge of a laminate. Physical grounds will be used to establish that:

- At the free edges of a laminate (sides of a laminate or holes), the interlaminar shearing stresses and/or interlaminar normal stress are very high (perhaps even singular) and would therefore cause the debonding that has been observed in such regions.
- Layer stacking-sequence changes produce differences in tensile strength of a laminate even though the orientations of each layer do not change (in classical lamination theory, such changes have no effect on the extensional stiffnesses). Failures caused by interlaminar shear stresses, τ_{zx} and τ_{zy}, and/or interlaminar normal stress, σ_z, changes near the laminate boundaries are believed to provide the answer to such strength differences.

In this section, first, the interlaminar stress in the simple case of the free edges of an angle-ply laminate will be identified. Then, the concept of interlaminar stresses will be described with an elasticity approach. Next, experimental verification of the theory is offered. Then, a cross-ply laminate will be analyzed, followed by a mixed-angle laminate. Finally, the interaction of interlaminar stresses and stacking sequence and their influence on laminate strength will be examined along with some suggestions for how to suppress free-edge delamination.

4.6.1 Classical Lamination Theory

Consider an angle-ply laminate composed of orthotropic laminae that are symmetrically arranged about the middle surface as shown in Figure 4-48. Because of the symmetry of both material properties and geometry, there is no coupling between bending and extension. That is, the laminate in Figure 4-48 can be subjected to N_x and will only extend in the x-direction and contract in the y- and z-directions, but will not bend.

The analysis of such a laminate by use of classical lamination theory revolves about the stress-strain relations of an individual orthotropic lamina under a state of plane stress in principal material directions

$$\begin{bmatrix}\sigma_1\\ \sigma_2\\ \tau_{12}\end{bmatrix}_k = \begin{bmatrix}Q_{11} & Q_{12} & 0\\ Q_{12} & Q_{22} & 0\\ 0 & 0 & Q_{66}\end{bmatrix}_k \begin{bmatrix}\varepsilon_1^\circ\\ \varepsilon_2^\circ\\ \gamma_{12}^\circ\end{bmatrix} \tag{4.154}$$

which can be transformed to the laminate axes by use of Equation (2.85):

$$\begin{bmatrix}\sigma_x\\ \sigma_y\\ \tau_{xy}\end{bmatrix}_k = \begin{bmatrix}\overline{Q}_{11} & \overline{Q}_{12} & \overline{Q}_{16}\\ \overline{Q}_{12} & \overline{Q}_{22} & \overline{Q}_{26}\\ \overline{Q}_{16} & \overline{Q}_{26} & \overline{Q}_{66}\end{bmatrix}_k \begin{bmatrix}\varepsilon_x^\circ\\ \varepsilon_y^\circ\\ \gamma_{xy}^\circ\end{bmatrix} \tag{4.155}$$

The extensional stiffnesses of the laminate are then

$$A_{ij} = \sum_{k=1}^{N} (\overline{Q}_{ij})_k (z_k - z_{k-1}) \tag{4.156}$$

and the force-strain relations are

$$\begin{bmatrix}N_x\\ 0\\ 0\end{bmatrix} = \begin{bmatrix}A_{11} & A_{12} & 0\\ A_{12} & A_{22} & 0\\ 0 & 0 & A_{66}\end{bmatrix} \begin{bmatrix}\varepsilon_x^\circ\\ \varepsilon_y^\circ\\ \gamma_{xy}^\circ\end{bmatrix} \tag{4.157}$$

The membrane strain state is

$$\varepsilon_x^\circ = \frac{A_{22}N_x}{A_{11}A_{22} - A_{12}^2} \qquad \varepsilon_y^\circ = \frac{-A_{12}N_x}{A_{11}A_{22} - A_{12}^2} \tag{4.158}$$

There is no overall shearing (γ_{xy}°) of the laminate. However, there is shearing strain in the principal material coordinates of each lamina in addition to normal strains as is proved by use of Equation (2.75):

$$\begin{bmatrix}\varepsilon_1\\ \varepsilon_2\\ \gamma_{12}\end{bmatrix}_k = \begin{bmatrix}\cos^2\theta - \dfrac{A_{12}}{A_{22}}\sin^2\theta\\ \sin^2\theta - \dfrac{A_{12}}{A_{22}}\cos^2\theta\\ -2\cos\theta\sin\theta\left[1 + \dfrac{A_{12}}{A_{22}}\right]\end{bmatrix}_k \frac{A_{22}N_x}{A_{11}A_{22} - A_{12}^2} \tag{4.159}$$

We examine a buildup of two laminae to construct a two-layered angle-ply laminate in order to study the stress implications of classical lamination theory. First, we subject two unbonded laminae with fibers at $+\alpha$ and $-\alpha$, respectively, to the same σ_x. The two separate laminae must deform into two oppositely oriented parallelograms as shown in Figure 4-50. To prepare those two laminae to be bonded to form a laminate (without shear deformation), equal and opposite shear stresses, τ_{xy}, must be applied to the laminae to return them to rectangular shape to form a deformation-compatible laminate. The two laminae, shown in pictorial view in Figure 4-50, have shearing stresses along the free edges! Those shearing stresses, although in equilibrium for the laminate as a whole, simply cannot exist on any free edge. Thus, classical lamination theory (CLT) has an inherent contradiction of obvious stress boundary conditions on each layer.

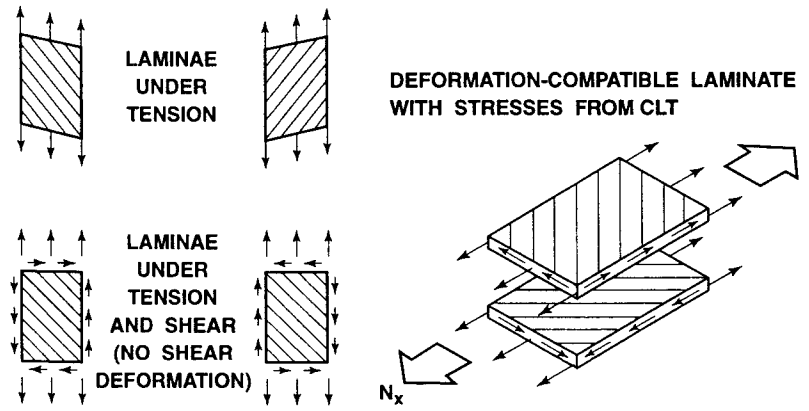

Figure 4-50 CLT Approach to Analysis of a Two-Layered Angle-Ply Laminate

Alternatively, consider the free-body diagram of half of the top layer of the four-layered angle-ply laminate in Figure 4-51. There, the left-hand side in the x-z plane is far from a free edge, so can have τ_{xy} as predicted with classical lamination theory. In contrast, at the free edge, as in Figure 4-51, τ_{xy} cannot exist on face ABCD. That is, ABCD must be stress-free because it is a free edge. Moreover, τ_{xy} on the front and back faces must go to zero at AB and CD. To achieve force equilibrium in the x-direction, we must identify a stress that could replace the action of the stress τ_{xy} that cannot exist on face ABCD. The only possible such stress is τ_{xz} that must exist on the bottom of the top-layer free-body diagram. For moment equilibrium about a vertical axis, τ_{xz} must be quite high because it exists only near the free edge. Although we know the stress (τ_{xz}) we are looking for and that it is high, we cannot determine how high without appealing to elasticity theory in the next subsection.

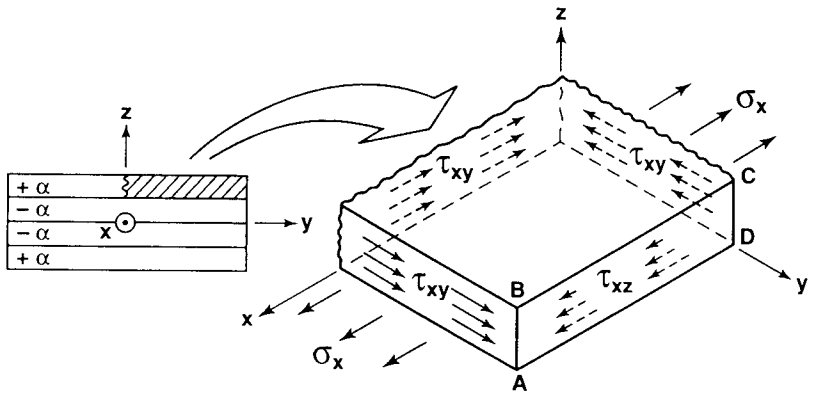

Figure 4-51 Free-Body Diagram for an Angle-Ply Laminate

4.6.2 Elasticity Formulation

Rather than a plane-stress state, a three-dimensional stress state is considered in the elasticity approach of Pipes and Pagano [4-12] to the problem of Section 4.6.1. The stress-strain relations for each orthotropic layer in principal material directions are

$$\begin{bmatrix}\sigma_1\\ \sigma_2\\ \sigma_3\\ \tau_{23}\\ \tau_{31}\\ \tau_{12}\end{bmatrix} = \begin{bmatrix} C_{11} & C_{12} & C_{13} & 0 & 0 & 0\\ C_{12} & C_{22} & C_{23} & 0 & 0 & 0\\ C_{13} & C_{23} & C_{33} & 0 & 0 & 0\\ 0 & 0 & 0 & C_{44} & 0 & 0\\ 0 & 0 & 0 & 0 & C_{55} & 0\\ 0 & 0 & 0 & 0 & 0 & C_{66}\end{bmatrix}\begin{bmatrix}\varepsilon_1\\ \varepsilon_2\\ \varepsilon_3\\ \gamma_{23}\\ \gamma_{31}\\ \gamma_{12}\end{bmatrix} \tag{4.160}$$

and can, upon transformation of coordinates in the 1-2 plane, be expressed in laminate coordinates as

$$\begin{bmatrix}\sigma_x\\ \sigma_y\\ \sigma_z\\ \tau_{yz}\\ \tau_{zx}\\ \tau_{xy}\end{bmatrix} = \begin{bmatrix} \overline{C}_{11} & \overline{C}_{12} & \overline{C}_{13} & 0 & 0 & \overline{C}_{16}\\ \overline{C}_{12} & \overline{C}_{22} & \overline{C}_{23} & 0 & 0 & \overline{C}_{26}\\ \overline{C}_{13} & \overline{C}_{23} & \overline{C}_{33} & 0 & 0 & \overline{C}_{36}\\ 0 & 0 & 0 & \overline{C}_{44} & \overline{C}_{45} & 0\\ 0 & 0 & 0 & \overline{C}_{45} & \overline{C}_{55} & 0\\ \overline{C}_{16} & \overline{C}_{26} & \overline{C}_{36} & 0 & 0 & \overline{C}_{66}\end{bmatrix}\begin{bmatrix}\varepsilon_x\\ \varepsilon_y\\ \varepsilon_z\\ \gamma_{yz}\\ \gamma_{zx}\\ \gamma_{xy}\end{bmatrix} \tag{4.161}$$

The strain-displacement relations are

$$\begin{aligned} \varepsilon_x &= u_{,x} & \varepsilon_y &= v_{,y} & \varepsilon_z &= w_{,z}\\ \gamma_{yz} &= v_{,z} + w_{,y} & \gamma_{zx} &= w_{,x} + u_{,z} & \gamma_{xy} &= u_{,y} + v_{,x} \end{aligned} \tag{4.162}$$

where a comma denotes partial differentiation of the principal symbol with respect to the subscript.

If the laminate is subjected to uniform axial extension on the ends x = constant, then all stresses are independent of x. The stress-displacement relations are obtained by substituting the strain-displacement relations, Equation (4.162), in the stress-strain relations, Equation (4.161). Next, the stress-displacement relations can be integrated under the condition that all stresses are functions of y and z only to obtain, after imposing symmetry and antisymmetry conditions, the form of the displacement field for the present problem:

$$u = Kx + U(y,z) \qquad v = V(y,z) \qquad w = W(y,z) \tag{4.163}$$

The stress-equilibrium equations then reduce to

$$\begin{aligned} \tau_{xy,y} + \tau_{zx,z} &= 0\\ \sigma_{y,y} + \tau_{yz,z} &= 0\\ \tau_{yz,y} + \sigma_{z,z} &= 0 \end{aligned} \tag{4.164}$$

Upon substitution of the displacement field, Equation (4.163), in the stress-displacement relations and subsequently in the stress-equilibrium differential equations, Equation (4.164), the displacement-equilibrium equations are, for each layer,

$$\begin{aligned} &\overline{C}_{66}U_{,yy} + \overline{C}_{55}U_{,zz} + \overline{C}_{26}V_{,yy} + \overline{C}_{45}V_{,zz} + (\overline{C}_{36} + \overline{C}_{45})W_{,yz} = 0\\ &\overline{C}_{26}U_{,yy} + \overline{C}_{45}U_{,zz} + \overline{C}_{22}V_{,yy} + \overline{C}_{44}V_{,zz} + (\overline{C}_{23} + \overline{C}_{44})W_{,yz} = 0\\ &(\overline{C}_{45} + \overline{C}_{36})U_{,yz} + (\overline{C}_{44} + \overline{C}_{23})V_{,yz} + \overline{C}_{44}W_{,yy} + \overline{C}_{33}W_{,zz} = 0 \end{aligned} \tag{4.165}$$

These coupled second-order partial differential equations do not have a closed-form solution. Accordingly, the approximate numerical technique of finite differences is employed. First, however, the boundary conditions must be prescribed in order to complete the formulation of the problem. Symmetry of the laminate about several planes permits reduction of the region of consideration to a quarter of the laminate cross section in the y-z plane at any value of x as shown in Figure 4-52. There, along the stress-free upper surface,

$$\tau_{xz} = 0 \qquad \sigma_z = 0 \qquad \tau_{yz} = 0 \tag{4.166}$$

along the stress-free outer edge,

$$\tau_{xy} = 0 \qquad \sigma_y = 0 \qquad \tau_{yz} = 0 \tag{4.167}$$

along the middle surface, $z = 0$, because U and V must be symmetric and W antisymmetric,

$$U_{,z}(y,0) = 0 \qquad V_{,z}(y,0) = 0 \qquad W(y,0) = 0 \tag{4.168}$$

and along the line $y = 0$, because U and V must be antisymmetric and W symmetric,

$$U(0,z) = 0 \qquad V(0,z) = 0 \qquad W_{,y}(0,z) = 0 \tag{4.169}$$

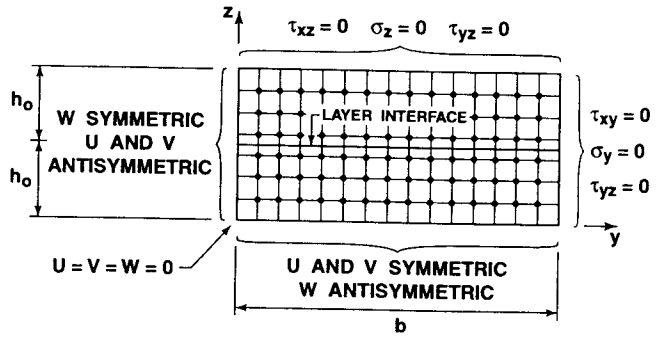

Figure 4-52 Finite Difference Representation and Boundary Conditions *(After Pipes and Pagano [4-12])*

At the corner (b, $2h_o$) of the region, five stress conditions apparently govern the behavior. However, the problem would be overspecified if all five conditions were imposed at the same time. Rather, three are specified and, subsequently, the remaining two are seen to be automatically satisfied thereby acting as a built-in verification of the numerical results. Numerical experimentation revealed that the choice of the three conditions is immaterial; the remaining two are always satisfied.

The numerical solution, as mentioned earlier, was obtained by the finite difference method. The two regions (layers) indicated in Figure 4-52 are represented with a series of regularly spaced material points

as shown. At each point, the differential equations are approximated by finite difference operators (central difference operators inside the region with forward and backward difference operators being used at the boundaries). At the interface between layers, the continuity conditions for U, V, W, σ_z, τ_{xz}, and τ_{yz} are approximately satisfied by locating material points symmetrically about the interface.

The resulting finite difference equations constitute a set of nonhomogeneous linear algebraic equations. Because there are three dependent variables, the number of equations in the set is three times the number of material points. Obviously, if a large number of points is required to accurately represent the continuous elastic body, a computer is essential.

4.6.3 Elasticity Solution Results

For a high-modulus graphite-epoxy composite material[3] with

$$E_1 = 20.0 \times 10^6 \text{ psi (138 GPa)} \quad G_{12} = G_{23} = G_{31} = .85 \times 10^6 \text{ psi (5.9 GPa)}$$
$$E_2 = E_3 = 2.1 \times 10^6 \text{ psi (14.5 GPa)} \quad \nu_{12} = \nu_{23} = \nu_{31} = .21 \tag{4.170}$$

in a laminate with $b = 8h_o$ (width is four times the thickness), distributions of the stresses σ_x, τ_{xy}, and τ_{xz} at the interface between layers ($z = h_o$) are shown in Figure 4-53. There, the stresses predicted with classical lamination theory are obtained in the central portion of the cross section. However, as the free edge is approached, σ_x decreases, τ_{xy} goes to zero, and, most significantly, τ_{xz} increases from zero to infinity (a singularity exists at $y = \pm b$). By use of other laminate geometries, the width of the region in which the stresses differ from those of classical lamination theory has been shown to be about the thickness of the laminate, $4h_o$. Thus, the deviation from classical lamination theory can be regarded as a boundary layer or edge effect. One laminate thickness away from the edge, classical lamination theory is expected to be valid.

The interlaminar shear stress, τ_{xz}, has a distribution through half the cross-section thickness shown as several profiles at various distances from the middle of the laminate in Figure 4-54. Stress values that have been extrapolated from the numerical data at material points are shown with dashed lines. The value of τ_{xz} is zero at the upper surface of the laminate and at the middle surface. The maximum value for any profile always occurs at the interface between the top two layers. The largest value of τ_{xz} occurs, of course, at the intersection of the free edge with the interface between layers and appears to be a singularity, although such a contention cannot be proved by use of a numerical technique.

[3]Note that these example material properties are not realistic (i.e., not physically possible) because the reciprocal relation is not satisfied for ν_{23} or ν_{31} and because G_{23} must be less than G_{12} and G_{31}.

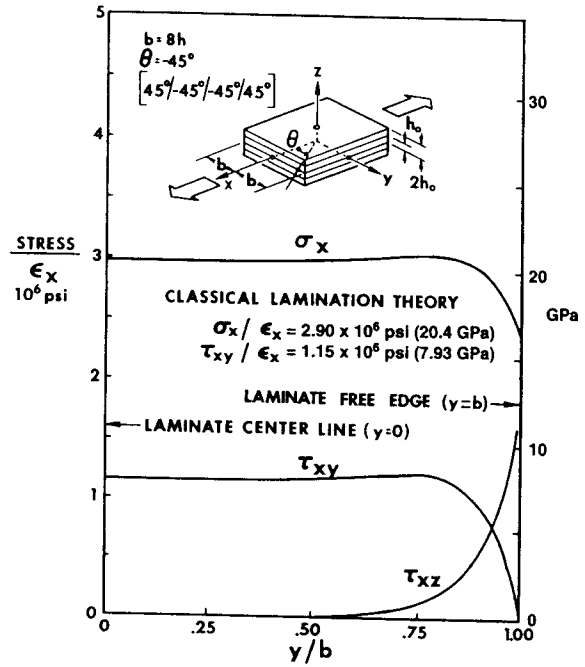

Figure 4-53 Stresses at the Interface *(After Pipes and Pagano [4-12])*

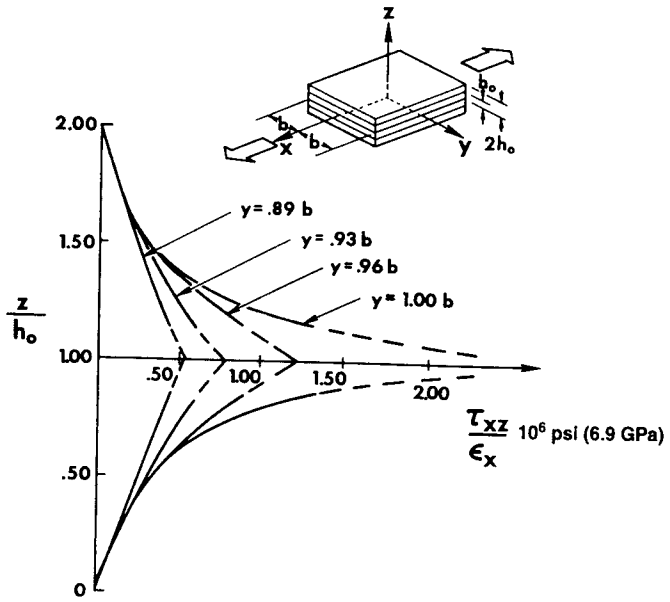

Figure 4-54 Interlaminar Shear Stress Distribution through the Laminate Thickness *(After Pipes and Pagano [4-12])*

4.6.4 Experimental Confirmation of Interlaminar Stresses

Pipes and Daniel [4-13] performed experiments to confirm Pipes and Pagano's solution for interlaminar stresses. They used the Moiré technique to examine the surface displacements of the symmetric angle-ply laminate under axial extension of Section 4.6.1. The Moiré technique depends on an optical phenomenon of fringes caused by displacement of two sets of arrays of lines relative to one another (see Post, Han, and Ifju [4-14]). One array is placed on the deformable specimen and the other nearby as a fixed reference. A laser beam is directed on the two arrays to produce the fringes. A fringe is the locus of points with the same component of displacement normal to the direction of the array lines. The number of fringes is proportional to the surface displacement. That one array is on the *surface* of the specimen is evidence that only surface displacements can be measured (we cannot put an array *below* the surface and also *see* it!). These fringes can be crudely observed in principle by putting two pieces of screen-door wire close to one another, shining a flashlight through the parallel screens, and slightly moving one screen, but keeping the other screen fixed in space.

At various load levels on long, flat graphite-epoxy specimens, Moiré fringes were photographed on the top surface of the upper angle-ply lamina. That lamina is one lamina thickness away from the interlaminar plane where both laminae must be a rectangle. The farther away from that interlaminar plane, the more the top lamina tends to deform into a parallelogram, as typified by the left half of Figure 4-55. On the right half of Figure 4-55 is shown a schematic representation of the S-shaped Moiré fringes. The axial displacements determined by a more accurate Moiré fringe analysis are shown along with the elasticity solution of Pipes and Pagano in Figure 4-56. If an orthotropic lamina is loaded off-axis with a tensile stress, then shear-extension coupling exists, leading to an originally rectangular shape both elongating and shearing into a parallelogram. That shape is the natural shape toward which even a lamina in a laminate is tending as we observe the behavior as we go away from the interface between the two top layers ($\pm\alpha$ layers that must be a rectangle at their interface). Thus, a line drawn horizontally across the specimen in Figure 4-55 before loading tends to deform into a diagonal line indicating shear deformation. However, the influence in the top layer of the shear stress τ_{xz}, which is high at the free edge and quickly decreases in the direction away from the edge and in the direction toward the top surface, is to deform the diagonal line more at the free edge than as the middle of the laminate is approached. Thus, the predicted surface deformation is the somewhat S-shaped divergence from a straight line. That predicted divergence is plotted with the measured deformation in Figure 4-56 where we see excellent agreement. Thus, the physical existence of interlaminar stresses has been clearly demonstrated.

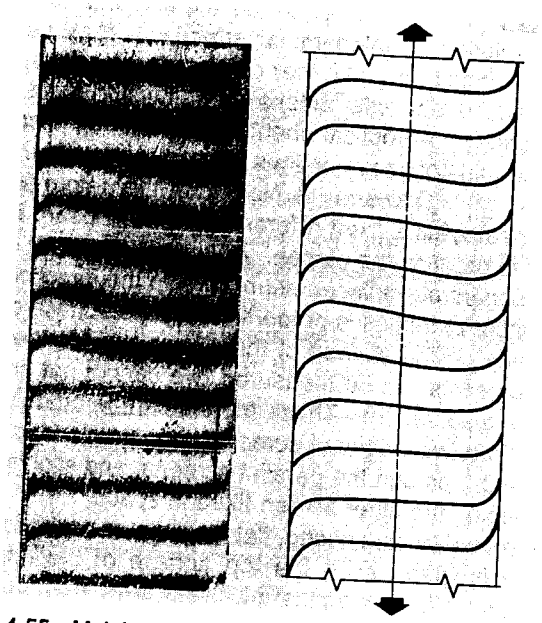

Figure 4-55 Moiré Fringe Pattern *(After Pipes and Daniel [4-13])*

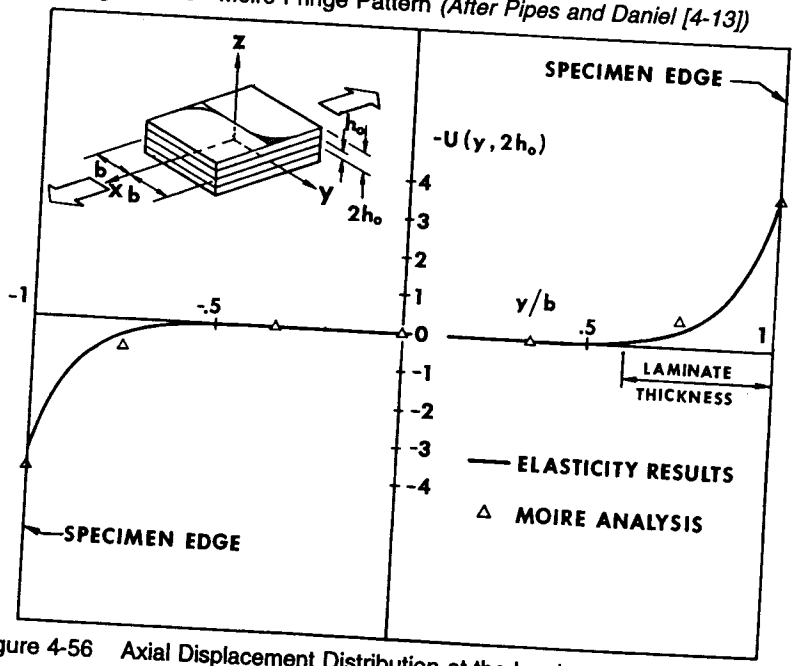

Figure 4-56 Axial Displacement Distribution at the Laminate Surface, $z = 2h_o$ *(After Pipes and Daniel [4-13])*

4.6.5 Interlaminar Stresses in Cross-Ply Laminates

Consider the free-body diagram of half of the top layer of a $[90°/0°]_S$ cross-ply laminate in Figure 4-57. There, σ_y, which we showed in Section 4.1 must exist from classical lamination theory (because of a mismatch in moduli and Poisson's ratios between the 0° and 90° layers in laminate coordinates), can exist on the left-hand side of the free body. However, the free-body diagram has free edge ABCD as its right boundary, so σ_y cannot exist on ABCD. To satisfy force equilibrium in the y-direction, the only stress with a component in the y-direction is τ_{yz}. Moreover, τ_{yz} must exist on the bottom of the top layer near the free edge (because τ_{xy} can exist on the left-hand side of any free-body diagram of part of the right half of the top layer). For moment equilibrium about the x-axis, a couple with clockwise orientation must be provided to equilibrate the moment of σ_y on the left-hand face. The only stress that can provide such a moment is σ_z. However, σ_z is subject to the z-direction force-equilibrium requirement of no force resultant. A distribution of σ_z that satisfies those two requirements is hypothesized by Pagano and Pipes to be as shown in Figure 4-58 [4-15]. Note that σ_z goes to zero in the region where classical lamination theory applies and perhaps to infinity at the free edge. High tensile values of σ_z would obviously cause free-edge delamination as could high values of τ_{yz}.

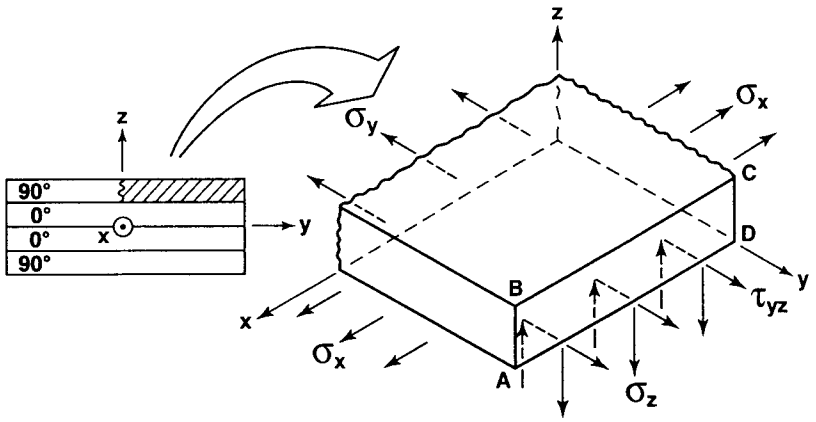

Figure 4-57 Free-Body Diagram for Cross-Ply Laminate

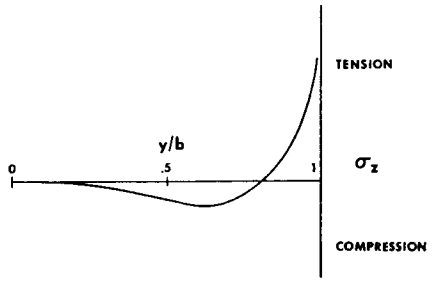

Figure 4-58 Interlaminar Normal Stress *(After Pagano and Pipes [4-15])*

4.6.6 Implications of Interlaminar Stresses

The existence of interlaminar stresses means that laminated composite materials can delaminate near free edges whether they be at the edge of a plate, around a hole, or at the ends of a tubular configuration used to obtain material properties. In all cases, delamination could cause premature failure so must be considered in specimen design because otherwise the specimen does not represent the true physical situation.

That the interlaminar stresses are affected by the laminate stacking sequence (arrangement of laminae, e.g., $[+45/-45/+15/-15]_S$ versus $[+15/-15/+45/-45]_S$) is significant to design analysts. Pagano and Pipes [4-15] hypothesized that the interlaminar normal stress, σ_z, can be changed from tension to compression by changing the stacking sequence. Their work was motivated by observations of Foye and Baker [4-16] of fatigue strengths differing by about 25,000 psi (173 MPa) for $[\pm 15°/\pm 45°]_S$ angle-ply laminates when the positions of the $\pm 15°$ laminae and the $\pm 45°$ laminae were reversed. Other data on static strength reveal qualitatively similar differences. However, classical lamination theory extensional stiffnesses and stresses are entirely unaffected by stacking sequence (bending stresses are excluded from the discussion because there is no coupling between bending and extension because middle-surface symmetry exists). Foye and Baker observed progressive delamination as the failure mode in fatigue. The contention of Pagano and Pipes that the interlaminar normal stress, σ_z, is responsible for delamination seems quite reasonable because of the following analysis.

Consider the free-body diagram of a symmetric eight-layered laminate cross section in Figure 4-59. The laminate is subjected to load in the x-direction as in Figure 4-48. In the free-body diagram, a tensile σ_y in the 15° layer implies a tensile σ_z at the free edge; the converse holds for a compressive σ_y. The interlaminar normal stress, σ_z, is hypothesized by Pagano and Pipes to exhibit the distribution shown in Figure 4-58 [4-15]. Note that σ_z goes to zero in the region where classical lamination theory applies and perhaps to infinity at the free edge. The distribution of σ_z is, of course, self-equilibrating. If the 45° layers were placed on the outside of the laminate, a compressive σ_y would be predicted with classical lamination theory; thus, σ_z would be compressive and the laminate would not tend to delaminate.

Accordingly, Pagano and Pipes reasoned that σ_z is distributed through the thickness as shown in Figure 4-60 for two stacking sequences, $[15°/-15°/45°/-45°]_S$ and $[15°/45°/-45°/-15°]_S$ [4-15]. Obviously, the latter sequence should have a greater strength than the former sequence because of less tendency to delaminate. The sequence $[45°/-45°/15°/-15°]_S$ should, by similar reasoning, lead to compressive stresses that are the mirror images of the tensile stresses of the $[15°/-15°/45°/-45°]_S$ laminate and be much stronger. The interlaminar shear stresses in the two cases can be shown to be essentially the same if not identical. Thus, the only logical conclusion to be drawn is that the interlaminar normal stress, σ_z, must be the key to the success of this type of laminate.

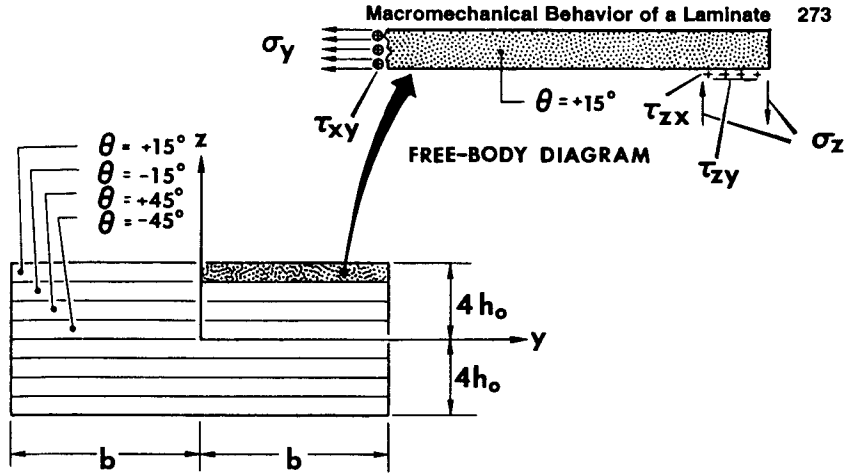

Figure 4-59 Mixed-Angle-Ply Laminate Free-Body Diagram *(After Pagano and Pipes [4-15])*

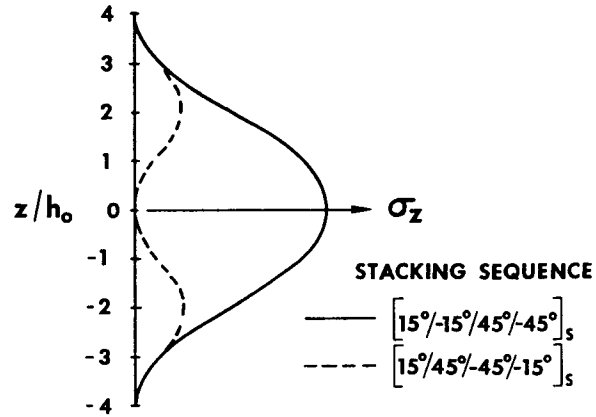

Figure 4-60 Distribution of Interlaminar Normal Stress in Boundary-Layer Region vs. z *(After Pagano and Pipes [4-15])*

In summary, three classes of interlaminar stress problems exist:

(1) $[\pm\theta]$ laminates exhibit only shear-extension coupling (no Poisson mismatch between layers), so τ_{xz} is the only nonzero interlaminar stress.
(2) $[0°/90°]$ laminates exhibit only a Poisson mismatch between layers (no shear-extension coupling), so τ_{yz} and σ_z are the only nonzero interlaminar stresses.
(3) combinations of the above, for example, $[\pm\theta_1/\pm\theta_2]$ laminates, exhibit both shear-extension coupling and Poisson mismatch between layers, so have τ_{xz}, τ_{yz}, and σ_z interlaminar stresses.

The significance of interlaminar stresses relative to laminate stiffness, strength, and life is determined by Classical Lamination Theory, i.e., CLT stresses are accurate over most of the laminate except in a very narrow boundary layer near the free edges. Thus, laminate stiffnesses are affected by global, not local, stresses, so laminate stiffnesses are essentially unaffected by interlaminar stresses. On the other hand, the details of locally high stresses dominate the failure process whereas lower global stresses are unimportant. Thus, laminate strength and life are dominated by interlaminar stresses.

4.6.7 Free-Edge Delamination-Suppression Concepts

Passive free-edge delamination-suppression concepts are essentially laminate stacking-sequence changes. The laminate stacking sequence can sometimes be rearranged to reduce the delaminating effect of interlaminar stresses. For example, laminae of like orientation angle (whether $+\theta$ or $-\theta$) should be separated and dispersed, i.e., use $[15/45/-45/-15]_S$, not $[45/-45/15/-15]_S$. In general, avoid thick or effectively thick laminae, i.e., use $[45/-45/45/-45]_S$, not $[45_2/-45_2]_S$. Note if laminae are interchanged in the stacking sequence that the A_{ij} are unaffected whereas the D_{ij} are highly affected.

Active delamination-suppression concepts include edge reinforcement and edge modification. Edge reinforcement is a strengthening of the free edge such as edge caps, stitching, or interleaved adhesive layers as in Figure 4-61. Edge caps and stitching are capable of resisting both interlaminar normal and shear stresses. In contrast, interleaved adhesive layers cannot resist interlaminar normal stress any better than an unreinforced laminate, but do resist interlaminar shear stresses better.

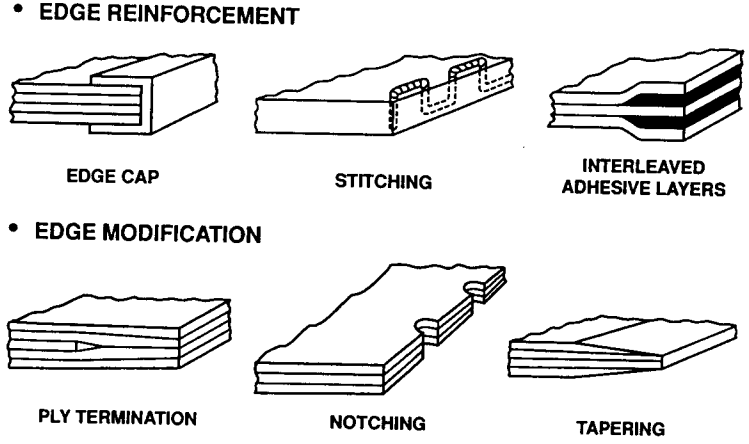

Figure 4-61 Free-Edge Delamination-Suppression Concepts

Edge modification is a change in the nature of the free edge that does not involve reinforcement with examples of ply termination, notching, and tapering also shown in Figure 4-61. Ply termination is a way of changing from a stacking sequence that would perform poorly at the free edge to a stacking sequence that is not highly affected by interlaminar stresses. Notching, although not an obvious aid, nevertheless 'confuses' the stress field near the free edge enough to reduce the delamination effect. Finally, tapering is a method of gradually changing from an unfavorable laminate to a favorable laminate as the free edge is approached. An overview of the effectiveness of these delamination-suppression concepts is given by Jones [4-17].

Problem Set 4.6

4.6.1 Demonstrate that use of classical lamination theory leads to

$$\frac{\sigma_x}{\varepsilon_x} = 2.96 \times 10^6 \text{ psi (20.4 GPa)} \qquad \frac{\tau_{xy}}{\varepsilon_x} = 1.15 \times 10^6 \text{ psi (7.93 GPa)}$$

as stresses in each layer of the four-layered graphite-epoxy angle-ply laminate discussed in Section 4.6.3. Disregard the sign of τ_{xy}. What is σ_y?

4.6.2 Obtain the displacements

$$u = -(C_1 z + C_2)y + (C_4 y + C_5 z + C_6)x + U(y,z)$$

$$v = (C_1 z + C_2)x - \frac{C_4 x^2}{2} + V(y,z)$$

$$w = -C_1 xy + C_7 x - \frac{C_5 x^2}{2} + C_8 + W(y,z)$$

by integration of the stress-displacement relations when the stresses are functions of y and z only. These displacements result before the various symmetry conditions are applied to obtain Equation (4.163). (Hint: see Timoshenko and Goodier [4-18]).

REFERENCES

4-1 K. S. Pister and S. B. Dong, Elastic Bending of Layered Plates, *Journal of the Engineering Mechanics Division*, ASCE, October 1959, pp. 1–10.

4-2 E. Reissner and Y. Stavsky, Bending and Stretching of Certain Types of Heterogeneous Aeolotropic Elastic Plates, *Journal of Applied Mechanics*, September 1961, pp. 402–408.

4-3 J. E. Ashton, J. C. Halpin, and P. H. Petit, *Primer on Composite Materials: Analysis*, Technomic, Westport, Connecticut, 1969. See also J. C. Halpin, *Revised Primer on Composite Materials: Analysis*, Technomic, Lancaster, Pennsylvania, 1984.

4-4 Terrence J. Hertz, Michael H. Shirk, Rodney H. Ricketts, and Terrence A. Weisshaar, On the Track of Practical Forward-Swept Wings, *Aeronautics & Astronautics*, American Institute for Aeronautics and Astronautics, Washington, January 1982, pp. 40–52.

4-5 Michael F. Card and Robert M. Jones, *Experimental and Theoretical Results for Buckling of Eccentrically Stiffened Cylinders*, NASA TN D-3639, October 1966.

4-6 Stephen W. Tsai, *Structural Behavior of Composite Materials*, NASA CR-71, July 1964.

4-7 Chi-Hung Shen and George S. Springer, Moisture Absorption and Desorption of Composite Materials, *Journal of Composite Materials*, January 1976, pp. 2–20.

4-8 R. Byron Pipes, Jack R. Vinson, and Tsu-Wei Chou, On the Hygrothermal Response of Laminated Composite Systems, *Journal of Composite Materials*, April 1976, pp. 129–148.

4-9 C. E. Browning, G. E. Husman, and J. M. Whitney, Moisture Effects in Epoxy Matrix Composites, In *Composite Materials: Testing and Design (Fourth Conference)*, J.

G. Davis, Jr. (Chairman), Valley Forge, Pennsylvania, 3–4 May 1976, ASTM STP 617, American Society for Testing and Materials, 1977, pp. 481–496.

4-10 Stephen W. Tsai, *Strength Characteristics of Composite Materials*, NASA CR-224, April 1965.

4-11 Stephen W. Tsai, Donald F. Adams, and Douglas R. Doner, *Analysis of Composite Structures*, NASA CR-620, November 1966.

4-12 R. Byron Pipes and N. J. Pagano, Interlaminar Stresses in Composite Laminates Under Uniform Axial Extension, *Journal of Composite Materials*, October 1970, pp. 538–548.

4-13 R. Byron Pipes and I. M. Daniel, Moiré Analysis of the Interlaminar Shear Edge Effect in Laminated Composites, *Journal of Composite Materials*, April 1971, pp. 255–259.

4-14 Daniel Post, Bongtae Han, and Peter Ifju, *High Sensitivity Moiré: Experimental Analysis for Mechanics and Materials*, Springer-Verlag, New York, 1994.

4-15 N. J. Pagano and R. Byron Pipes, The Influence of Stacking Sequence on Laminate Strength, *Journal of Composite Materials*, January 1971, pp. 50–57.

4-16 R. L. Foye and D. J. Baker, Design of Orthotropic Laminates, *AIAA/ASME 11th Structures, Structural Dynamics, and Materials Conference*, Denver, Colorado, 22–24 April 1970 (presentation only — no paper).

4-17 Robert M. Jones, Delamination-Suppression Concepts for Composite Laminate Free Edges, *Composite Design, Manufacture, and Application, Proceedings of the Eighth International Conference on Composite Materials*, Stephen W. Tsai and George S. Springer (editors), Honolulu, Hawaii, 15–19 July 1991, Society for the Advancement of Material and Process Engineering, Covina, California, 1991, pp. 28-M-1 to 28-M-10.

4-18 S. P. Timoshenko and J. N. Goodier, *Theory of Elasticity*, 3rd edition, McGraw-Hill, New York, 1970, pp. 240 and 280.

Chapter 5

BENDING, BUCKLING, AND VIBRATION OF LAMINATED PLATES

5.1 INTRODUCTION

Laminated plates are one of the simplest and most widespread practical applications of composite laminates. Laminated beams are, of course, simpler. However, such essentially one-dimensional structural elements do not display well the unique two-dimensional capabilities and characteristics of composite laminates.

The objective in this chapter is to demonstrate the effect of the various coupling stiffnesses (A_{16}, A_{26}, B_{ij}, D_{16}, and D_{26}) on the bending, buckling, and vibration behavior of laminated plates. That is, the basic question of laminated plate analysis is: what is the response of laminated plates to bending, buckling, and vibration as in Figure 5-1? The study of these effects is the logical culmination of a course on the mechanics of fiber-reinforced composite materials. The objective does not include a complete study of laminated plate theory. Instead, some of the important laminated plate theory results are examined so that the physical significance of the effects of the stiffnesses are appreciated. The theory of laminated plates with associated solution techniques is a very suitable topic for further study. A more complete cataloging and classification of laminated plate problems is found in books by Whitney [5-1], Vinson and Sierakowski [5-2], Vasiliev [5-3], and Reddy [5-4].

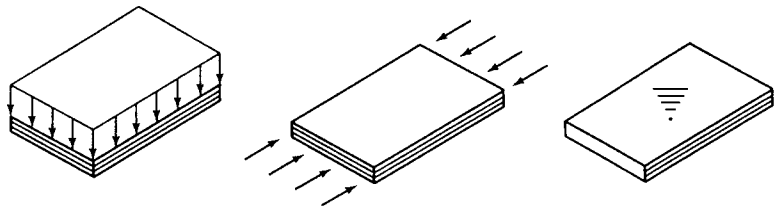

Figure 5-1 Basic Questions of Laminated Plate Analysis

The theoretical considerations underlying the basic theory of laminated plates are discussed in Section 5.2. Then, the differential equations and associated boundary conditions governing the bending, buckling, and vibration behavior of laminated plates are displayed along with a brief discussion of possible solution techniques. Next, solutions for the various laminate configurations described in Section 4.3 are displayed in Sections 5.3 through 5.5 for bending, buckling, and vibration problems.

A simply supported rectangular plate is used consistently in all sections to illustrate the kinds of results that can be obtained, i.e., the influence of the various stiffnesses on laminated plate behavior. In addition, only the simplest types of loading will be studied in order to avoid the solution difficulties inherent to complex loadings. Accordingly, in the interest of simplicity, just the bare thread of laminated plate results will be displayed.

Specially orthotropic plates, i.e., plates with multiple specially orthotropic layers that are symmetric about the plate middle surface have, as has already been noted in Section 4.3, force and moment resultants in which there is no bending-extension coupling nor any shear-extension or bend-twist coupling, that is,

$$\begin{bmatrix} N_x \\ N_y \\ N_{xy} \end{bmatrix} = \begin{bmatrix} A_{11} & A_{12} & 0 \\ A_{12} & A_{22} & 0 \\ 0 & 0 & A_{66} \end{bmatrix} \begin{bmatrix} \varepsilon_x^o \\ \varepsilon_y^o \\ \gamma_{xy}^o \end{bmatrix} \tag{5.1}$$

$$\begin{bmatrix} M_x \\ M_y \\ M_{xy} \end{bmatrix} = \begin{bmatrix} D_{11} & D_{12} & 0 \\ D_{12} & D_{22} & 0 \\ 0 & 0 & D_{66} \end{bmatrix} \begin{bmatrix} \kappa_x \\ \kappa_y \\ \kappa_{xy} \end{bmatrix} \tag{5.2}$$

For plate problems, whether the specially orthotropic laminate has a single layer or multiple layers is essentially immaterial; the laminate need only be characterized by D_{11}, D_{12}, D_{22}, and D_{66} in Equation (5.2). That is, because there is no bending-extension coupling, the force-strain relations, Equation (5.1), are not used in plate analysis for transverse loading causing only bending. However, note that force-strain relations are needed in shell analysis because of the differences between deformation characteristics of plates as opposed to shells.

Often, because specially orthotropic laminates are virtually as easy to analyze as isotropic plates, other laminates are regarded as, or approximated with, specially orthotropic laminates. This approximation will be studied by comparison of results for each type of laminate with and without the various stiffnesses that distinguish it from a specially orthotropic laminate. Specifically, the importance of the bend-twist coupling terms D_{16} and D_{26} will be examined for symmetric angle-ply laminates. Then, bending-extension coupling will be analyzed for antisymmetric cross-ply and angle-ply laminates and compared with the specially orthotropic approximation in which the B_{ij} are ignored. These comparisons will be made successively for bending, buckling, and vibration of simply supported plates in Section 5.3, 5.4, and 5.5, respectively. Finally, the engineering significance of the various coupling stiffnesses is summarized in Section 5.6.

5.2 GOVERNING EQUATIONS FOR BENDING, BUCKLING, AND VIBRATION OF LAMINATED PLATES

5.2.1 Basic Restrictions, Assumptions, and Consequences

Most of the restrictions and assumptions on which laminated plate theory is based have been utilized in Chapter 4. However, for completeness, they will be reiterated here in a slightly different manner. The seemingly dual terminology of restrictions and assumptions is used because the terms have fundamentally different meanings. *Restrictions* are limitations on the use of the theory that are *obviously* either satisfied or they are not. Thus, restrictions are concerned with the *known*. For example, a theory for square plates does not apply to round plates. *Assumptions* are limitations on the theory that have a nature of uncertainty to them. That is, assumptions are concerned with the *unknown*. For example, stresses perpendicular to the surface of a plate are commonly assumed to be small enough to be regarded as zero, or assumed to be zero; however, we do not know for certain just how small the stresses are unless we appeal to a more accurate theory. Also, displacements might be assumed to be small to enable certain approximations. However, whether the displacements actually are small can be determined only when the final results are known. In summary, the difference between restrictions and assumptions is that restrictions involve the *known* and assumptions involve the *unknown* (about which we wish to speculate). Thus, we certainly do not 'assume a rectangular plate', but instead we 'restrict our attention to rectangular plates'. The following restrictions and assumptions provide further opportunity to clarify the difference between the two classifications, but mainly to build a firm foundation for the study of laminated plate theory. Recall from Chapter 3 that assumptions in engineering must be justified, i.e., we must know *why* we believe the assumption to be true from a physical standpoint.

The geometry, forces, and moments for a plate are shown in Figures 5-2, 5-3, and 5-4, respectively. Note in Figure 5-2 that the plate aspect ratio, a/b, is merely a common way of quantitatively describing the shape of a rectangular plate. Recall that N_x, N_y, N_{xy} and M_x, M_y, M_{xy} are the forces and moments per unit width of the plate. New are the Kirchhoff shear forces K_x and K_y in Figure 5-3 as well as the distributed transverse loading, p(x,y). Recall that the laminate geometry is defined in Figure 4-8.

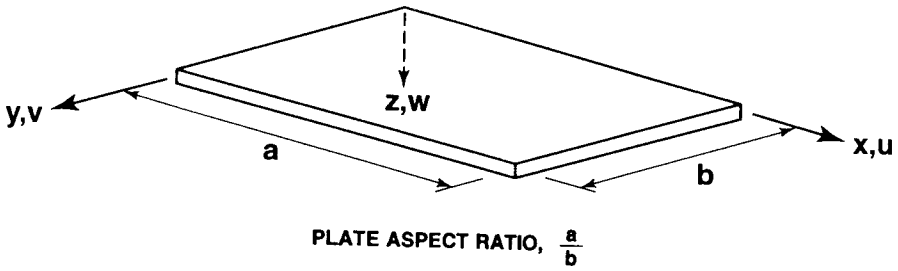

Figure 5-2 Plate Geometry and Displacements

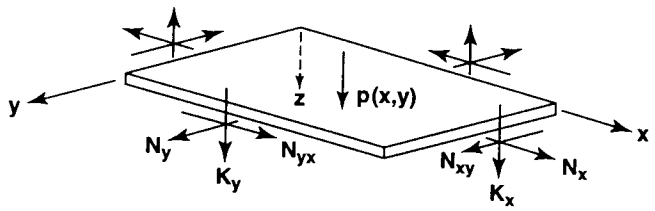

Figure 5-3 Plate Forces

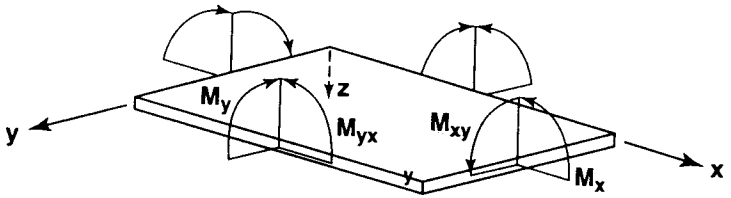

Figure 5-4 Plate Moments

Restrictions

- Each layer is orthotropic (but the principal material directions of each layer need not be aligned with the plate axes), linear elastic, and of constant thickness (so the entire plate is of constant thickness).
- The plate thickness is very small compared to its length and width (such a configuration is commonly called a thin plate, although the name *plate* itself implies such a geometry).
- No body forces exist.

Assumptions

- Stresses acting in the x-y plane (the plane of the plate) dominate the plate behavior. Then, σ_z, τ_{xz}, and τ_{yz} are assumed to be zero such that an approximate state of *plane stress* is said to exist (wherein only σ_x, σ_y, and τ_{xy} are considered).

- The *Kirchhoff hypothesis* of negligible transverse shear strains, γ_{xz} and γ_{yz}, and negligible transverse normal strain, ε_z, constitutes a statement of nondeformable normals to the middle surface although there is an inherent, but commonly ignored, conflict with the assumption of zero transverse normal stress, σ_z. (This hypothesis is relaxed in Section 6.6.)
- Displacements u, v, and w are small compared to the plate thickness (generally, although not necessarily, indicative of small-deflection theory).
- Strains, ε_x, ε_y, and γ_{xy}, are small compared to unity (small-strain theory).
- Rotatory inertia terms are negligible.

Consequences

- If transverse shear strains are ignored or are assumed to be zero, then transverse shear stresses are also zero throughout the plate by virtue of the stress-strain relations. On the other hand, even if nothing is said about the transverse shear strains, we still know that the transverse shear stresses are zero on both the upper and lower plate surfaces if there is no shear loading. Commonly, in classical plate theory, the transverse shear strains are regarded as zero, yet transverse shear stresses are calculated from equilibrium considerations. Such procedures will be ignored in this book for the sake of simplicity in presenting only a demonstration of the effect of the various coupling stiffnesses.
- By virtue of the Kirchhoff hypothesis, the remaining strains, ε_x, ε_y, and γ_{xy}, as well as the displacements, u and v, are a linear function of the transverse coordinate z. Moreover, the stresses are accordingly a linear, but discontinuous, function of the transverse coordinate z. Both of these results are shown schematically in Figure 5-5.
- As the restriction to thin plates is relaxed, i.e., as the plate becomes thicker, the assumption of plane stress, $\sigma_z = \tau_{xz} = \tau_{yz} = 0$, becomes less accurate.

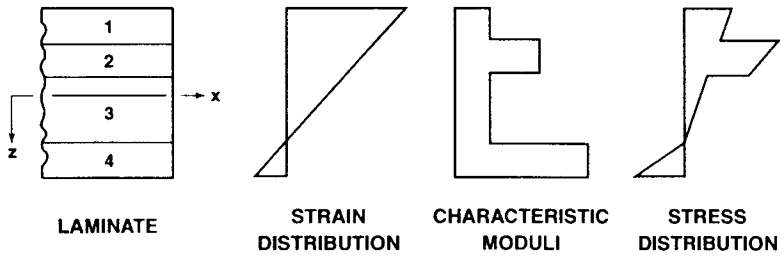

Figure 5-5 Stress and Strain Distribution through the Laminate Thickness

Note that no assumptions involve fiber-reinforced composite materials explicitly. Instead, only the restriction to orthotropic materials at various orientations is significant because we treat the macroscopic behavior of an individual orthotropic (easily extended to anisotropic) lamina. Therefore, what follows is essentially a classical plate theory for laminated materials. Actually, interlaminar stresses cannot be entirely disregarded in laminated plates, but this refinement will not be treated in this book other than what was studied in Section 4.6. Transverse shear effects away from the edges will be addressed briefly in Section 6.6.

5.2.2 Equilibrium Equations for Laminated Plates

The equilibrium differential equations in terms of the force and moment resultants derived in Chapter 4 and the transverse loading p(x,y) are

$$N_{x,x} + N_{xy,y} = 0 \tag{5.3}$$

$$N_{xy,x} + N_{y,y} = 0 \tag{5.4}$$

$$M_{x,xx} + 2M_{xy,xy} + M_{y,yy} = -p \tag{5.5}$$

where a comma denotes differentiation of the principal symbol with respect to the subscript that follows the comma. In this form, the equilibrium equations are merely those of classical plate theory as derived from the equilibrium of a differential element in Appendix D. When the stipulation of a laminated plate is introduced by the explicit use of the force and moment resultants in Equations (4.22) and (4.23) and the strain and change of curvature definitions in Equations (4.14) and (4.15), then the equilibrium equations, Equations (5.3) to (5.5), become (upon dropping the zero subscript used to denote middle-surface displacements)

$$\begin{aligned} &A_{11}u_{,xx} + 2A_{16}u_{,xy} + A_{66}u_{,yy} + A_{16}v_{,xx} + (A_{12} + A_{66})v_{,xy} + A_{26}v_{,yy} \\ &\quad - B_{11}w_{,xxx} - 3B_{16}w_{,xxy} - (B_{12} + 2B_{66})w_{,xyy} - B_{26}w_{,yyy} = 0 \end{aligned} \tag{5.6}$$

$$\begin{aligned} &A_{16}u_{,xx} + (A_{12} + A_{66})u_{,xy} + A_{26}u_{,yy} + A_{66}v_{,xx} + 2A_{26}v_{,xy} + A_{22}v_{,yy} \\ &\quad - B_{16}w_{,xxx} - (B_{12} + 2B_{66})w_{,xxy} - 3B_{26}w_{,xyy} - B_{22}w_{,yyy} = 0 \end{aligned} \tag{5.7}$$

$$\begin{aligned} &D_{11}w_{,xxxx} + 4D_{16}w_{,xxxy} + 2(D_{12} + 2D_{66})w_{,xxyy} + 4D_{26}w_{,xyyy} + D_{22}w_{,yyyy} \\ &\quad - B_{11}u_{,xxx} - 3B_{16}u_{,xxy} - (B_{12} + 2B_{66})u_{,xyy} - B_{26}u_{,yyy} \\ &\quad - B_{16}v_{,xxx} - (B_{12} + 2B_{66})v_{,xxy} - 3B_{26}v_{,xyy} - B_{22}v_{,yyy} = p \end{aligned} \tag{5.8}$$

Obvious and sometimes drastic simplifications occur when the laminate is symmetric about the middle surface ($B_{ij} = 0$), specially orthotropic (all the terms with 16 and 26 subscripts vanish in addition to the B_{ij}), homogeneous ($B_{ij} = 0$ and $D_{ij} = A_{ij}t^2/12$), or isotropic. In all those cases, Equations (5.6) and (5.7) are coupled to each other, but uncoupled from Equation (5.8). That is, Equation (5.8) contains derivatives of the transverse displacement w only, and Equations (5.6) and (5.7) contain both u and v but not w. Accordingly, only Equation (5.8) must be solved to determine the transverse deflections of a plate with the aforementioned

simplifications; the in-plane displacements can be found from the solution of Equations (5.6) and (5.7). The more general case of unsymmetrical laminates requires the simultaneous solution of the three coupled equations, Equations (5.6)–(5.8) for the transverse and in-plane displacements.

Boundary conditions used to be thought of as a choice between simply supported, clamped, or free edges if all classes of elastically restrained edges are neglected. The real situation for laminated plates is more complex than for isotropic plates because now there are actually *four* types of boundary conditions that can be called simply supported edges. These more complicated boundary conditions arise because now we must consider u, v, and w instead of just w alone. Similarly, there are four kinds of clamped edges. These boundary conditions can be concisely described as a displacement or derivative of a displacement or, alternatively, a force or moment is equal to some prescribed value (often zero) denoted by an overbar at the edge:

$$\begin{aligned} u_n &= \bar{u}_n \quad \text{or} \quad N_n = \bar{N}_n \\ u_t &= \bar{u}_t \quad \text{or} \quad N_{nt} = \bar{N}_{nt} \\ w_{,n} &= \bar{w}_{,n} \quad \text{or} \quad M_n = \bar{M}_n \\ w &= \bar{w} \quad \text{or} \quad M_{nt,t} + Q_n = \bar{K}_n \end{aligned} \tag{5.9}$$

in n and t coordinates where n is the direction normal to the edge and t is the direction tangent to the edge as in Figure 5-6. Also, Q_n is the shear force and K_n is the well-known Kirchhoff force of classical plate theory (see Timoshenko and Woinowsky-Krieger [5-5]). For example, on the edge x = 0 in Figures 5-2 and 5-3,

$$u = 0 \quad \text{or} \quad N_x = 0 \tag{5.10}$$

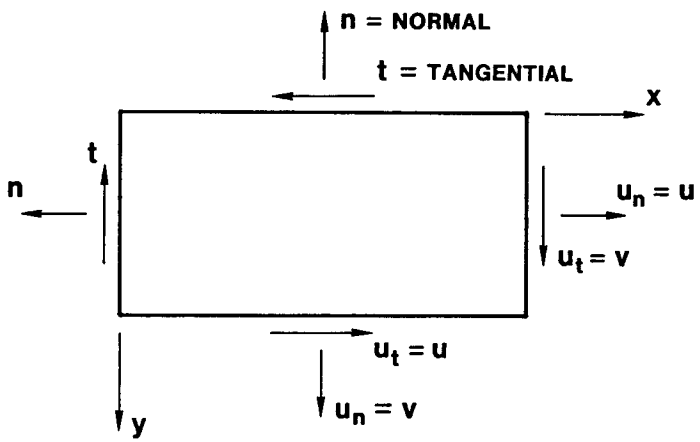

Figure 5-6 Boundary Condition Notation

The eight possible types of simply supported (prefix S) and clamped (prefix C) edge boundary conditions [combinations of the conditions in Equation (5.9)] are commonly classified as (see Almroth [5-6]):

$$
\begin{aligned}
&\text{S1:}\quad w=0 \quad M_n=0 \quad u_n=\bar{u}_n \quad u_t=\bar{u}_t\\
&\text{S2:}\quad w=0 \quad M_n=0 \quad N_n=\bar{N}_n \quad u_t=\bar{u}_t\\
&\text{S3:}\quad w=0 \quad M_n=0 \quad u_n=\bar{u}_n \quad N_{nt}=\bar{N}_{nt}\\
&\text{S4:}\quad w=0 \quad M_n=0 \quad N_n=\bar{N}_n \quad N_{nt}=\bar{N}_{nt}
\end{aligned}
\tag{5.11}
$$

$$
\begin{aligned}
&\text{C1:}\quad w=0 \quad w_{,n}=0 \quad u_n=\bar{u}_n \quad u_t=\bar{u}_t\\
&\text{C2:}\quad w=0 \quad w_{,n}=0 \quad N_n=\bar{N}_n \quad u_t=\bar{u}_t\\
&\text{C3:}\quad w=0 \quad w_{,n}=0 \quad u_n=\bar{u}_n \quad N_{nt}=\bar{N}_{nt}\\
&\text{C4:}\quad w=0 \quad w_{,n}=0 \quad N_n=\bar{N}_n \quad N_{nt}=\bar{N}_{nt}
\end{aligned}
\tag{5.12}
$$

whereupon a rectangular plate can be characterized as having any one of the eight conditions in Equations (5.11) and (5.12) on each of its four edges. The range of possibilities is, therefore, quite large (twelve possible conditions on each of the four edges if the free-edge conditions are included). The simplest cases to analyze naturally involve like types of boundary conditions on opposite, if not all, edges. The emphasis in this book is on plates with four simply supported edges, so cases are chosen from those in Equation (5.11). Note that simply supported edges have no rotational restraint, but when this simplified terminology of simply supported edges is used, the specific in-plane conditions are not determined. Obviously, the totality of boundary conditions including in-plane conditions must be specified by stating, for example, that a solution is obtained for S1 boundary conditions.

To better appreciate the four possible simply supported edge boundary conditions, consider the support system for the edge of a plate illustrated in Figure 5-7 in near-physical terms with mechanisms that the reader can easily understand. Note that the support mechanisms depicted are only for understanding how the various supports *could* work. Only the reader can decide what support conditions are applicable to a specific structure of interest. For a simply supported plate edge, the principal support mechanism in Figure 5-7 is a triangular prism with a circular-cross-section prismatic protrudance on top as a realistic mechanism for the usual so-called knife-edge support for free rotation, i.e., $M_x = 0$. The end view of the triangular prism looks similar to the usual beam support, but with more realistic mechanisms that permit the motion required. For a plate, the protrudance is a bearing that permits (limited) rotation about the y-axis through the center of the protrudance which is located at the middle surface of the plate (but not precisely at the edge of the plate). The protrudance fits in a cavity in the plate such that rotation around the y-axis is possible, but motion transverse to the plate surface is prevented ($w = 0$) and translation along the y-axis of the circular prism is not permitted. The four manners of supporting the triangular prism are:

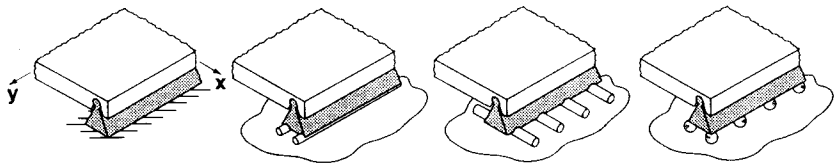

(S1)	(S2)	(S3)	(S4)
$w = 0$	$w = 0$	$w = 0$	$w = 0$
$M_x = 0$	$M_x = 0$	$M_x = 0$	$M_x = 0$
$u = 0$	$N_x = 0$	$u = 0$	$N_x = 0$
$v = 0$	$v = 0$	$N_{xy} = 0$	$N_{xy} = 0$

Figure 5-7 Simply Supported Edge Boundary Conditions

(1) For the S1 condition, the triangular prism is fastened to a horizontal surface such that the prism cannot translate in either the x- or y-directions. Thus, $u = 0$ and $v = 0$. Hence, forces N_x and N_{xy} must exist.
(2) For the S2 condition, the triangular prism is supported on partially embedded y-direction roller bearings that permit translation in the x-direction, but none in the y-direction. Thus, $u \neq 0$ and $v = 0$. Hence, force N_x must be zero, but N_{xy} must exist.
(3) For the S3 condition, the triangular prism is supported on partially embedded x-direction roller bearings that permit translation in the y-direction, but none in the x-direction. Thus, $u = 0$ and $v \neq 0$. Hence, force N_x must exist, but N_{xy} must be zero.
(4) For the S4 condition, the triangular prism is supported on partially embedded spherical bearings that permit translation in any direction in the x-y plane. Thus, $u \neq 0$ and $v \neq 0$, so both forces N_x and N_{xy} must be zero.

For a clamped plate edge, the principal support mechanism is a boxy mass that restrains rotation about the edge of the plate ($w_{,x} = 0$) and motion transverse to the plate surface ($w = 0$). The four ways of supporting the boxy mass are analogous to the four ways for a simply supported edge and are shown in Appendix D.

5.2.3 Buckling Equations for Laminated Plates

A plate buckles when the in-plane compressive load gets so large that the originally flat equilibrium state is no longer stable, and the plate deflects into a nonflat (wavy) configuration. The load at which the departure from the flat state takes place is called the buckling load. The flat equilibrium state has only in-plane forces and undergoes only ex-

tension, compression, and shear. Thus, the flat equilibrium state is often called the membrane prebuckled state and consists of only in-plane deformations. More comprehensively, the load at which the plate deformed configuration *suddenly* changes into a *different configuration* is called the buckling load. Note that with bending-extension coupling, an originally flat plate (when without load) under axial in-plane compression *bends* at all loads prior to bifurcation buckling.[1] Thus, a membrane (flat and uniformly stressed) prebuckled state is not actually possible. However, a first-order approximation to the bifurcation buckling load is made by ignoring the prebuckling out-of-plane deflections. Jones and Hennemann studied this approximation for laminated shells and found that the bifurcation buckling loads for a shell with bending-extension coupling induced prebuckling deformations are as much as 15% lower than a shell with such prebuckling deformations ignored [5-7].

Analysis of plates buckling under in-plane loading involves solution of an eigenvalue problem as opposed to the boundary value problem of equilibrium analysis. The distinctions between boundary value problems and eigenvalue problems are too involved to treat here. Instead, the buckling differential equations governing the buckling behavior from a membrane prebuckled state (prebuckling out-of-plane deformations are ignored) are

$$\delta N_{x,x} + \delta N_{xy,y} = 0 \tag{5.13}$$

$$\delta N_{xy,x} + \delta N_{y,y} = 0 \tag{5.14}$$

$$\delta M_{x,xx} + 2\delta M_{xy,xy} + \delta M_{y,yy} + \bar{N}_x \delta w_{,xx} + 2\bar{N}_{xy} \delta w_{,xy} + \bar{N}_y \delta w_{,yy} = 0 \tag{5.15}$$

where δ denotes a variation of the principal symbol from its value in the prebuckled equilibrium state. Thus, the terms δN_x, ... δM_x, ... are variations of forces and moments, respectively, from their values in a membrane prebuckling equilibrium state. The terms δw and, by implication, δu and δv are variations in displacement from the same flat prebuckled state. In appearance, the buckling differential equations *resemble* the equilibrium differential equations except for the all-important variational notation and the fact that the right-hand sides of the buckling differential equations are zero. Note that if the prebuckling state is a membrane, then $\delta w = w$ because there is no prebuckling out-of-plane displacement. Also note that the applied in-plane loads $\bar{N}_x$, $\bar{N}_y$, and $\bar{N}_{xy}$ enter the mathematical formulation of the eigenvalue problem as coefficients of the curvatures rather than as 'loads' on the right-hand side of the equilibrium equation. The essence of the eigenvalue problem is to determine the smallest applied loads, $\bar{N}_x$, etc., that cause buckling. An important consequence of this type of problem is that the magnitude of the deformations after buckling cannot be determined without resort to large-deflection analysis; i.e., the deformations are indeterminate when only Equations (5.13) to (5.15) are considered.

[1] Bifurcation buckling occurs at the load at which the load path forks into two load paths, the new one stable and the other, the continuation of the old path, unstable, irrespective of the type of deformation path prior to buckling (linear or nonlinear).

The variations in force and moment resultants are

$$\begin{bmatrix} \delta N_x \\ \delta N_y \\ \delta N_{xy} \end{bmatrix} = \begin{bmatrix} A_{11} & A_{12} & A_{16} \\ A_{12} & A_{22} & A_{26} \\ A_{16} & A_{26} & A_{66} \end{bmatrix} \begin{bmatrix} \delta\varepsilon_x^\circ \\ \delta\varepsilon_y^\circ \\ \delta\gamma_{xy}^\circ \end{bmatrix} + \begin{bmatrix} B_{11} & B_{12} & B_{16} \\ B_{12} & B_{22} & B_{26} \\ B_{16} & B_{26} & B_{66} \end{bmatrix} \begin{bmatrix} \delta\kappa_x \\ \delta\kappa_y \\ \delta\kappa_{xy} \end{bmatrix} \tag{5.16}$$

$$\begin{bmatrix} \delta M_x \\ \delta M_y \\ \delta M_{xy} \end{bmatrix} = \begin{bmatrix} B_{11} & B_{12} & B_{16} \\ B_{12} & B_{22} & B_{26} \\ B_{16} & B_{26} & B_{66} \end{bmatrix} \begin{bmatrix} \delta\varepsilon_x^\circ \\ \delta\varepsilon_y^\circ \\ \delta\gamma_{xy}^\circ \end{bmatrix} + \begin{bmatrix} D_{11} & D_{12} & D_{16} \\ D_{12} & D_{22} & D_{26} \\ D_{16} & D_{26} & D_{66} \end{bmatrix} \begin{bmatrix} \delta\kappa_x \\ \delta\kappa_y \\ \delta\kappa_{xy} \end{bmatrix} \tag{5.17}$$

where the variations in in-plane strains and changes in curvature are related to the variations in displacements by

$$\delta\varepsilon_x^\circ = \delta u_{,x} \qquad \delta\varepsilon_y^\circ = \delta v_{,y} \qquad \delta\gamma_{xy}^\circ = \delta u_{,y} + \delta v_{,x} \tag{5.18}$$

$$\delta\kappa_x = -\delta w_{,xx} \qquad \delta\kappa_y = -\delta w_{,yy} \qquad \delta\kappa_{xy} = -2\delta w_{,xy} \tag{5.19}$$

The buckling differential equations can be expressed in terms of the variations in displacements by substituting the variations in in-plane strains and curvatures, Equations (5.18) and (5.19), in the variations in force and moment resultants, Equations (5.16) and (5.17), and subsequently in the buckling differential equations in terms of the variations of forces, moments, and displacements during buckling, i.e., Equations (5.13) to (5.15). The resulting equations take a form similar to the corresponding equilibrium equations, Equations (5.6) to (5.8). Just as for equilibrium problems, buckling of generally laminated plates has bending-extension coupling. However, some special laminates exhibit no bending-extension coupling; hence, their buckling loads are obtained by solution of only Equation (5.15) or its variation of deflections equivalent.

The boundary conditions for buckling problems are applied only to the buckling deformations because the prebuckling deformations are assumed to be a membrane state (even if bending-extension coupling does exist). One of the distinguishing features of an eigenvalue problem is that all the boundary conditions are homogeneous, i.e., zero. Thus, during buckling, the simply supported edge boundary conditions are

$$\begin{aligned}
&\text{S1:} \quad \delta w = 0 \quad \delta M_n = 0 \quad \delta u_n = 0 \quad \delta u_t = 0 \\
&\text{S2:} \quad \delta w = 0 \quad \delta M_n = 0 \quad \delta N_n = 0 \quad \delta u_t = 0 \\
&\text{S3:} \quad \delta w = 0 \quad \delta M_n = 0 \quad \delta u_n = 0 \quad \delta N_{nt} = 0 \\
&\text{S4:} \quad \delta w = 0 \quad \delta M_n = 0 \quad \delta N_n = 0 \quad \delta N_{nt} = 0
\end{aligned} \tag{5.20}$$

$$\begin{aligned}
&\text{C1:}\quad \delta w = 0 \quad \delta w_{,n} = 0 \quad \delta u_n = 0 \quad \delta u_t = 0\\
&\text{C2:}\quad \delta w = 0 \quad \delta w_{,n} = 0 \quad \delta N_n = 0 \quad \delta u_t = 0\\
&\text{C3:}\quad \delta w = 0 \quad \delta w_{,n} = 0 \quad \delta u_n = 0 \quad \delta N_{nt} = 0\\
&\text{C4:}\quad \delta w = 0 \quad \delta w_{,n} = 0 \quad \delta N_n = 0 \quad \delta N_{nt} = 0
\end{aligned} \tag{5.21}$$

The boundary conditions could be different for each edge of a plate, so the number of combinations of possible boundary conditions is quite large as it was with equilibrium problems.

5.2.4 Vibration Equations for Laminated Plates

As with plate buckling, plate vibration, or oscillation about a state of static equilibrium, is an eigenvalue problem. The objective of the analysis is to determine the natural frequencies and the mode shapes in which laminated plates vibrate. The magnitude of the deformations in a particular mode, however, is indeterminate because vibration is an eigenvalue problem. The governing vibration differential equations are obtained from the buckling differential equations by adding an acceleration term to the right-hand side of Equation (5.15) and reinterpreting all variations to occur during vibration about an equilibrium state (no difficulty is presented because the variations during buckling are also from the equilibrium state):

$$\delta N_{x,x} + \delta N_{xy,y} = 0 \tag{5.22}$$

$$\delta N_{xy,x} + \delta N_{y,y} = 0 \tag{5.23}$$

$$\delta M_{x,xx} + 2\delta M_{xy,xy} + \delta M_{y,yy} + \bar{N}_x \delta w_{,xx} + 2\bar{N}_{xy}\delta w_{,xy} + \bar{N}_y \delta w_{,yy} = \rho \delta w_{,tt} \tag{5.24}$$

where ρ is the mass per unit area of the plate.

The variations in forces and moments during vibration are given by Equations (5.16) and (5.17). The membrane prestress state (equilibrium stress state) is specified by $\bar{N}_x$, $\bar{N}_y$, and $\bar{N}_{xy}$.

As with both the plate bending and buckling problems, plate vibrations include bending-extension coupling when the plate is unsymmetrically laminated. For symmetrically laminated plates, the coupling vanishes, and the vibration problem reduces to solution of Equation (5.24) alone because rotatory inertia terms are ignored. Irrespective of the lamination characteristics, the boundary conditions are the same as for the buckling problem. Alternatively, both the buckling and vibration problems can be formulated as a vibration problem with buckling loads being determined when the vibration frequency is equated to zero.

5.2.5 Solution Techniques

Many techniques exist for solution of the equilibrium, buckling, and vibration problems formulated in the preceding subsections. The techniques range from fortuitous exact solutions that are obtained essentially by 'observation' through numerical approximations such as finite element and finite difference approaches to the various approximate energy methods such as those of Rayleigh-Ritz and Galerkin. Because the objective here is to demonstrate the importance of the various coupling stiffnesses, only those solution techniques necessary for fruitful illustrations are used.

A prominent part of many of the techniques is separation of variables. In that method, the deflection variables, or the variation in deflection variables, are arbitrarily separated into functions of plate coordinate x alone times functions of y alone. Wang [5-8] determined that separation of variables leads to exact solutions for some classes of plate problems, but does not for others, i.e., the deflections are not always separable. A specific example of an approximate use of separation of variables due to Ashton [5-9] will be discussed in Section 5.3.2. Other exact uses of the method abound throughout Section 5.3 through 5.5.

Problem Set 5.2

5.2.1 Derive Equations (5.6)–(5.8).
5.2.2 Derive the analogy of Equations (5.6)–(5.8) for the buckling differential equations, Equations (5.13)–(5.15).
5.2.3 Derive the analogy of Equations (5.6)–(5.8) for the vibration differential equations, Equations (5.22)–(5.24).

5.3 DEFLECTION OF SIMPLY SUPPORTED LAMINATED PLATES UNDER DISTRIBUTED TRANSVERSE LOAD

Consider the general class of laminated rectangular plates that are simply supported along edges x = 0, x = a, y = 0, and y = b and subjected to a distributed transverse load, p(x,y), in Figure 5-8. The transverse load can be expanded in a double Fourier sine series:

$$p(x,y) = \sum_{m=1}^{\infty}\sum_{n=1}^{\infty} p_{mn} \sin\frac{m\pi x}{a} \sin\frac{n\pi y}{b} \tag{5.25}$$

Many different types of transverse loading can easily be represented by Equation (5.25). For example, a uniform load, p_0, is given by

$$p(x,y) = \sum_{m=1,3,\ldots}^{\infty}\sum_{n=1,3,\ldots}^{\infty} \frac{16p_o}{\pi^2}\frac{1}{mn} \sin\frac{m\pi x}{a} \sin\frac{n\pi y}{b} \tag{5.26}$$

See Timoshenko and Woinowsky-Krieger [5-5] for other examples.

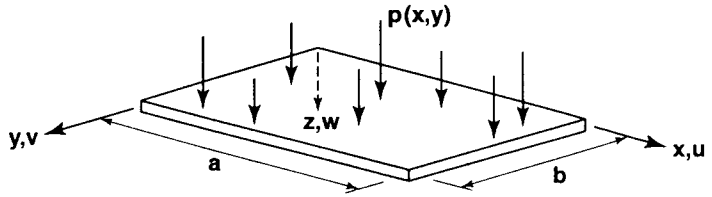

Figure 5-8 Simply Supported Laminated Rectangular Plate under Distributed Transverse Load, p(x,y)

Some of the various types of lamination possible, specially orthotropic, symmetric angle-ply, antisymmetric cross-ply, and antisymmetric angle-ply, will be analyzed for the loading given in Equation (5.25). The results will be compared with each other to determine the influence of the bend-twist-coupling stiffnesses (D_{16} and D_{26}) and the bending-extension coupling stiffnesses (B_{ij}). All the plate edges are simply supported; however, as has been observed in Section 5.2, such a specification is still ambiguous. Thus, pay special attention to the precise formulation for the boundary conditions in each of the cases discussed.

5.3.1 Specially Orthotropic Laminated Plates

A specially orthotropic laminate has either a single layer of a specially orthotropic material or multiple specially orthotropic layers that are symmetrically arranged about the laminate middle surface. In both cases, the laminate stiffnesses consist solely of A_{11}, A_{12}, A_{22}, A_{66}, D_{11}, D_{12}, D_{22}, and D_{66}. That is, neither shear-extension or bend-twist coupling nor bending-extension coupling exists. Thus, for plate problems, the transverse deflections are described by only one differential equation of equilibrium:

$$D_{11}w_{,xxxx} + 2(D_{12} + 2D_{66})w_{,xxyy} + D_{22}w_{,yyyy} = p(x,y) \tag{5.27}$$

subject to the simply supported edge boundary conditions that for this laminate are

$$\begin{aligned} x = 0, a: \quad & w = 0 \quad M_x = -D_{11}w_{,xx} - D_{12}w_{,yy} = 0 \\ y = 0, b: \quad & w = 0 \quad M_y = -D_{12}w_{,xx} - D_{22}w_{,yy} = 0 \end{aligned} \tag{5.28}$$

Note that because the in-plane deformations, u and v, are not present in the differential equation, the simply supported edge boundary condition takes on an especially simple form as compared to Equation (5.11).

If the transverse loading is represented by the Fourier sine series in Equation (5.25), the solution to this fourth-order partial differential equation and subject to its associated boundary conditions is remarkably simple. As with isotropic plates, the solution can easily be verified to be

$$w = \sum_{m=1}^{\infty} \sum_{n=1}^{\infty} a_{mn} \sin \frac{m\pi x}{a} \sin \frac{n\pi y}{b} \tag{5.29}$$

That is, Equation (5.29) satisfies the differential equation, Equation (5.27), and the boundary conditions, Equation (5.28), so is the exact solution if

$$a_{mn} = \frac{\dfrac{p_{mn}}{\pi^4}}{D_{11}\left[\dfrac{m}{a}\right]^4 + 2(D_{12} + 2D_{66})\left[\dfrac{m}{a}\right]^2\left[\dfrac{n}{b}\right]^2 + D_{22}\left[\dfrac{n}{b}\right]^4} \tag{5.30}$$

For a uniform transverse load, the solution is easily shown to be

$$w = \frac{16p_o}{\pi^4} \sum_{m=1,3,5,\ldots}^{\infty} \sum_{n=1,3,5,\ldots}^{\infty} \times \times \frac{\dfrac{1}{mn} \sin \dfrac{m\pi x}{a} \sin \dfrac{n\pi y}{b}}{D_{11}\left[\dfrac{m}{a}\right]^4 + 2(D_{12} + 2D_{66})\left[\dfrac{m}{a}\right]^2\left[\dfrac{n}{b}\right]^2 + D_{22}\left[\dfrac{n}{b}\right]^4} \tag{5.31}$$

Once the deflections are known, the stresses are straightforwardly obtained by substitution in the stress-strain relations, Equation (4.16), after the strains are found from Equation (4.12). Note that the solution in Equation (5.31) is expressed in terms of only the laminate stiffnesses D_{11}, D_{12}, D_{22}, and D_{66}. This solution will not be plotted here, but will be used as a baseline solution in the following subsections and plotted there in comparison with more complicated results.

5.3.2 Symmetric Angle-Ply Laminated Plates

Symmetric angle-ply laminates were described in Section 4.3.2 and found to be characterized by a full matrix of extensional stiffnesses as well as bending stiffnesses (but of course no bending-extension coupling stiffnesses because of middle-surface symmetry). The new facet of this type of laminate as opposed to specially orthotropic laminates is the appearance of the bend-twist coupling stiffnesses D_{16} and D_{26} (the shear-extension coupling stiffnesses A_{16} and A_{26} do not affect the transverse deflection w when the laminate is symmetric). The governing differential equation of equilibrium is

$$\begin{aligned} D_{11}w_{,xxxx} + 4D_{16}w_{,xxxy} + 2(D_{12} + 2D_{66})w_{,xxyy} \\ + 4D_{26}w_{,xyyy} + D_{22}w_{,yyyy} = p(x,y) \end{aligned} \tag{5.32}$$

subject to the simply supported edge boundary conditions

$$\begin{aligned} x = 0, a: \quad & w = 0 \quad M_x = -D_{11}w_{,xx} - D_{12}w_{,yy} - 2D_{16}w_{,xy} = 0 \\ y = 0, b: \quad & w = 0 \quad M_y = -D_{12}w_{,xx} - D_{22}w_{,yy} - 2D_{26}w_{,xy} = 0 \end{aligned} \tag{5.33}$$

Note the presence of the bend-twist coupling stiffnesses in the boundary conditions as well as in the differential equation. As with the specially orthotropic laminated plate, the simply supported edge boundary condition cannot be further distinguished by the character of the in-plane boundary conditions on u and v because the latter do not appear in any plate problem for a symmetric laminate.

The solution to the governing differential equation, Equation (5.32), is not as simple as for specially orthotropic laminated plates because of the presence of D_{16} and D_{26}. The Fourier expansion of the deflection w, Equation (5.29), is an example of separation of variables. However, because of the terms involving D_{16} and D_{26}, the expansion does not satisfy the governing differential equation because the variables are not separable. Moreover, the deflection expansion also does not satisfy the boundary conditions, Equation (5.33), again because of the terms involving D_{16} and D_{26}.

Ashton solved this problem approximately by recognizing that the differential equation, Equation (5.32), is but one result of the equilibrium requirement of making the total potential energy of the mechanical system stationary relative to the independent variable w [5-9]. An alternative method is to express the total potential energy in terms of the deflections and their derivatives. Specifically, Ashton approximated the deflection by the Fourier expansion in Equation (5.29) and substituted it in the expression for the total potential energy, V:

$$V = \frac{1}{2}\iint [D_{11}(w_{,xx})^2 + 2D_{12}w_{,xx}w_{,yy} + D_{22}(w_{,yy})^2 + 4D_{66}(w_{,xy})^2 + 4D_{16}w_{,xx}w_{,xy} + 4D_{26}w_{,yy}w_{,xy} - 2pw]dxdy \tag{5.34}$$

where the term involving pw is the potential energy of the external forces (negative of the work done), namely the transverse load p, and the remainder of V is the internal strain energy of the plate. The energy for an unsymmetrically laminated plate is displayed by Whitney [5-1]. Basic energy principles and their application to applied mechanics, particularly structural mechanics, are discussed in the classical book by Langhaar [5-10].

If enough terms are taken in the deflection expansion, the approximate energy converges to the exact energy as long as the geometric boundary conditions ($w = 0$ and $w_{,x} = 0$) are satisfied even if the natural boundary conditions ($M_n = \bar{M}_n$ and $N_n = \bar{N}_n$) are not satisfied. This method is the well-known Rayleigh-Ritz method when the energy is made stationary relative to the coefficients of the deflection expansion according to the principle of stationary potential energy. The resulting equations are a set of simultaneous linear algebraic equations that can be solved numerically with the aid of a digital computer. Note that, for the simply supported edge boundary conditions, only one geometric boundary condition, $w = 0$, exists. Also, only one natural boundary condition, $M_n = 0$, exists. The double sine series deflection function, Equation (5.29), satisfies the geometric boundary condition, but not the natural boundary condition. Thus, Equation (5.29) is an acceptable deflection approximation for the Rayleigh-Ritz method. However, the convergence of the method is slow because the natural boundary condition is not satisfied exactly.

Ashton used 49 terms (up through $m = 7$ and $n = 7$) in the deflection approximation, Equation (5.29), to obtain for a uniformly loaded square plate with stiffnesses $D_{22}/D_{11} = 1$, $(D_{12} + 2D_{66})/D_{11} = 1.5$, and $D_{16}/D_{11} = D_{26}/D_{11} = -.5$ a maximum deflection (at the plate center) [5-9] of

$$w_{max} = .00425\frac{a^4 p}{D_{11}} \tag{5.35}$$

However, if D_{16} and D_{26} are ignored, that is, the symmetric angle-ply laminate is approximated as a specially orthotropic laminate with $D_{22}/D_{11} = 1$, $(D_{12} + 2D_{66})/D_{11} = 1.5$, and $D_{16} = D_{26} = 0$, then the maximum deflection is

$$w_{max} = .00324\frac{a^4 p}{D_{11}} \tag{5.36}$$

Thus, the error from ignoring the bend-twist coupling terms is about 24%, certainly not a negligible error. Hence, the specially orthotropic laminated plate is an unacceptable approximation to a symmetric angle-ply laminated plate. Recognize, however, that Ashton's Rayleigh-Ritz results are also approximate because only a finite number of terms were used in the deflection approximation. Thus, a comparison of his results with an exact solution would lend more confidence to the rejection of the specially orthotropic laminated plate approximation.

Ashton observed that skew (parallelogram-shaped) isotropic plates under uniform distributed load $\bar{p}_o$ as shown in the orthogonal X-Y coordinates in Figure 5-9 are governed by the equilibrium differential equation

$$w_{,xxxx} - 4\cos\theta\, w_{,xxxy} + 2(1 + 2\cos^2\theta)w_{,xxyy} - 4\cos\theta\, w_{,xyyy} + w_{,yyyy} = \frac{\bar{p}_o \sin^4\theta}{D} \tag{5.37}$$

with simply supported edge boundary conditions [5-11]

$$\begin{aligned} x = 0, a: \quad & w = 0 \quad w_{,xx} - 2\cos\theta\, w_{,xy} = 0 \\ y = 0, b: \quad & w = 0 \quad w_{,yy} - 2\cos\theta\, w_{,xy} = 0 \end{aligned} \tag{5.38}$$

The essence of Ashton's contribution is that he identified the skew plate stiffnesses as being a transformation of the symmetric angle-ply stiffnesses or, more generally, the anisotropic bending stiffnesses, that is,

$$\begin{aligned} & D_{22} = D_{11} = D & & \frac{D_{12} + 2D_{66}}{D_{11}} = (1 + 2\cos^2\theta) \\ & \frac{D_{16}}{D_{11}} = \frac{D_{26}}{D_{11}} = -\cos\theta & & p = \bar{p}\sin^4\theta \end{aligned} \tag{5.39}$$

The stiffnesses in Equation (5.39) are equivalent to the stiffnesses of an equivalent orthotropic material with principal material axes of orthotropy at 45° to the plate sides. The orthotropic bending stiffnesses of the equivalent material can be shown to be

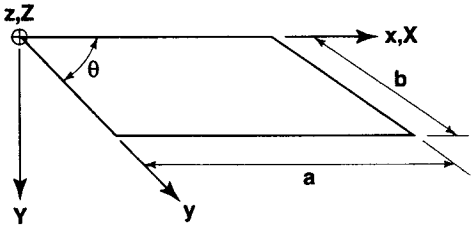

Figure 5-9 Skew Plate Geometry

$$D'_{11} = D(1 + 2\cos\theta + \cos^2\theta)$$
$$D'_{22} = D(1 - 2\cos\theta + \cos^2\theta) \qquad (5.40)$$
$$D'_{12} + 2D'_{66} = D\sin^2\theta$$

where, of course, D'_{16} and D'_{26} are zero because they are in principal material directions for an orthotropic material. Values of D'_{ij} and D_{ij} are given in Table 5-1 for several values of the equivalent skew angle θ. From Equation (5.40), as θ gets smaller, D'_{11} gets larger, D'_{22} gets smaller, and, most importantly, D_{16} gets larger, that is, the plate becomes more anisotropic.

Because exact solutions for skew isotropic plates are readily available, Ashton was able to get some exact solutions for anisotropic rectangular plates by the special identification process outlined in the preceding paragraph. Specifically, values for the center deflection of a uniformly loaded square plate are shown in Table 5-2. There, the exact solution is shown along with the Rayleigh-Ritz solution and the specially orthotropic solution. For the case already discussed where $D_{22}/D_{11} = 1$, $(D_{12} + 2D_{66})/D_{11} = 1.5$, and $D_{16}/D_{11} = D_{26}/D_{11} = -.5$, the exact solution is

$$w_{max} = .00452\frac{a^4 p}{D_{11}} \qquad (5.41)$$

Thus, the Rayleigh-Ritz solution is 6% in error, whereas the specially orthotropic solution is 28% in error.

Table 5-1 Equivalent Bending Stiffness Ratios *(After Ashton [5-11])*

Equivalent Skew Angle θ	$\frac{D'_{22}}{D'_{11}}$	$\frac{D'_{12}+2D'_{66}}{D'_{11}}$	$\frac{D'_{16}}{D'_{11}}$	$\frac{D_{22}}{D_{11}}$	$\frac{D_{12}+2D_{66}}{D_{11}}$	$\frac{D_{16}}{D_{11}}$
90°	1.000	1.000	0.	1.	1.000	0.
80°	.495	.702	0.	1.	1.061	−.174
63°	.141	.376	0.	1.	1.412	−.454
60°	.111	.333	0.	1.	1.500	−.500
54°	.0675	.260	0.	1.	1.690	−.587

Table 5-2 Maximum Deflection Coefficients, K, for Exact, Specially Orthotropic, and Rayleigh-Ritz Solutions*

Equivalent Skew Angle θ	Exact Solution K	Specially Orthotropic Solution K	Rayleigh-Ritz Solution K
90°	.00406	.00406	.00406
80°	.00411	.00394	.00408
63°	.00444	.00336	.00422
60°	.00452	.00324	.00425
54°	.00476	.00301	.00430

*After Ashton [5-11]

The deflection results for the three approaches are plotted in Figure 5-10 as a function of the ratio of the principal stiffnesses, D'_{11}/D'_{22}, which gets large as θ decreases. Thus, the larger the D_{16} and D_{26}, the smaller θ becomes and hence the more inaccurate both the Rayleigh-Ritz approach and the specially orthotropic approximation become.

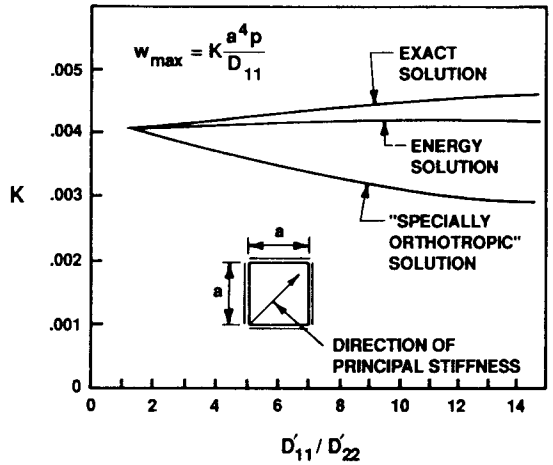

Figure 5-10 Transverse Deflection Coefficient versus Principal Stiffness Ratio *(After Ashton [5-11])*

5.3.3 Antisymmetric Cross-Ply Laminated Plates

Antisymmetric cross-ply laminates were described in Section 4.3.3 and found to have extensional stiffnesses A_{11}, A_{12}, $A_{22} = A_{11}$, and A_{66}; bending-extension coupling stiffnesses B_{11} and $B_{22} = -B_{11}$; and bending stiffnesses D_{11}, D_{12}, $D_{22} = D_{11}$, and D_{66}. The new terms here in comparison to a specially orthotropic laminate are B_{11} and B_{22}. Because of this coupling, the three equilibrium differential equations are coupled:

$$A_{11}u_{,xx} + A_{66}u_{,yy} + (A_{12} + A_{66})v_{,xy} - B_{11}w_{,xxx} = 0 \qquad (5.42)$$
$$(A_{12} + A_{66})u_{,xy} + A_{66}v_{,xx} + A_{11}v_{,yy} + B_{11}w_{,yyy} = 0 \qquad (5.43)$$
$$D_{11}(w_{,xxxx} + w_{,yyyy}) + 2(D_{12} + 2D_{66})w_{,xxyy} - B_{11}(u_{,xxx} - v_{,yyy}) = p \qquad (5.44)$$

Whitney and Leissa solved this problem for the simply supported edge boundary condition S2:

$$x = 0, a: \quad w = 0 \quad M_x = B_{11}u_{,x} - D_{11}w_{,xx} - D_{12}w_{,yy} = 0 \qquad (5.45)$$
$$v = 0 \quad N_x = A_{11}u_{,x} + A_{12}v_{,y} - B_{11}w_{,xx} = 0 \qquad (5.46)$$
$$y = 0, b: \quad w = 0 \quad M_y = -B_{11}v_{,y} - D_{12}w_{,xx} - D_{11}w_{,yy} = 0 \qquad (5.47)$$
$$u = 0 \quad N_y = A_{12}u_{,x} + A_{11}v_{,y} + B_{11}w_{,yy} = 0 \qquad (5.48)$$

and observed that the deflections

$$u = \sum_{m=1}^{\infty}\sum_{n=1}^{\infty} A_{mn} \cos\frac{m\pi x}{a} \sin\frac{n\pi y}{b}$$

$$v = \sum_{m=1}^{\infty}\sum_{n=1}^{\infty} B_{mn} \sin\frac{m\pi x}{a} \cos\frac{n\pi y}{b} \qquad (5.49)$$

$$w = \sum_{m=1}^{\infty}\sum_{n=1}^{\infty} C_{mn} \sin\frac{m\pi x}{a} \sin\frac{n\pi y}{b}$$

satisfy the three governing differential equations and the boundary conditions if the transverse loading is represented by the Fourier sine series in Equation (5.25), so are the exact solution (the form of which need not be repeated here) [5-12].

If the transverse load is but one term of the Fourier series, that is,

$$p = p_{mn} \sin\frac{m\pi x}{a} \sin\frac{n\pi y}{b} \qquad (5.50)$$

as for $m = 1$ and $n = 1$ in Figure 5-11, then fortunately the governing differential equations and boundary conditions can be solved exactly. The A_{mn}, B_{mn}, and C_{mn} in Equations (5.49) can be expressed in terms of p_{mn} and the laminate stiffnesses in analogy to Equation (5.30). Then, for an arbitrary transverse loading described with a Fourier series, we merely sum the contributions from the deflection solution for each term of the series.

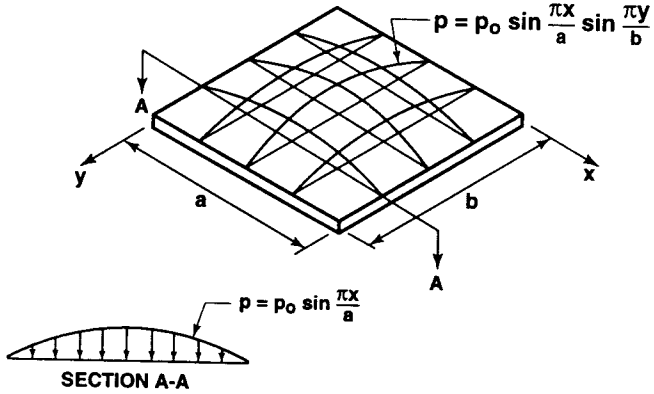

Figure 5-11 Sinusoidal Plate Transverse Loading

We want to study the effect of the number of layers on laminate performance. The fair comparison is to keep the total laminate thickness constant to consider only equal-weight laminates. Then, we vary the number of layers by dividing the laminate into more and more layers. That is, we construct the sequence of antisymmetric cross-ply laminates with an increasing number of layers but of constant thickness as in Figure 5-12.

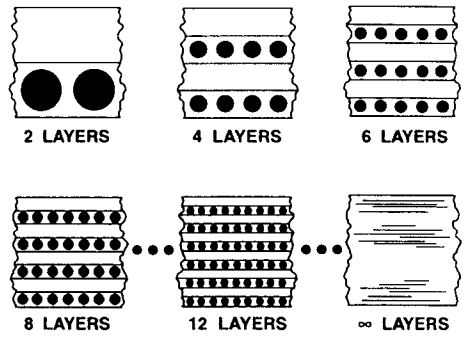

Figure 5-12 Antisymmetric Cross-Ply Laminate Example

The normalized maximum deflection of a rectangular antisymmetric cross-ply laminated graphite-epoxy plate subjected to the sinusodial transverse loading of Figure 5-11 [m=1 and n=1 in Equation (5.50)] is plotted in Figure 5-13 for 2, 4, 6, and an infinite number of layers. The infinite-number-of-layers case corresponds to the specially orthotropic plate solution in which bending-extension coupling is ignored. For a two-layered plate, neglect of bending-extension coupling results in an underprediction of the deflection by 64%; that is, the actual deflection is nearly three times the specially orthotropic plate approximation! The effect of bending-extension coupling on the deflections obviously dies out quite rapidly as the number of layers increases, irrespective of the plate aspect ratio, a/b. That is, the specially orthotropic plate solution is rapidly approached. However, only when there are more than six layers can coupling be ignored without significant error.

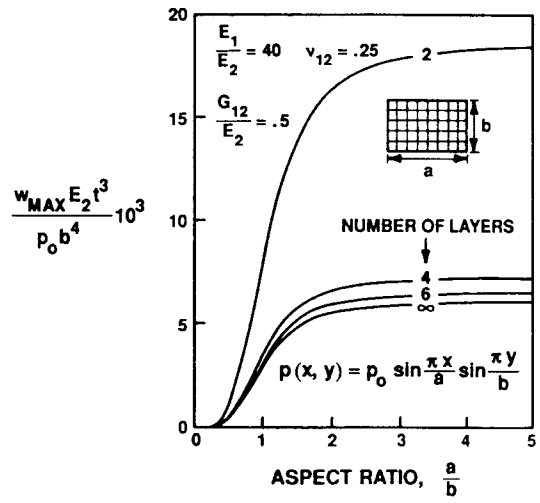

Figure 5-13 Deflection of an Antisymmetric Cross-Ply Laminated Plate under Sinusoidal Transverse Load

For various laminated composite materials, the effect of bending-extension coupling on plate deflections depends essentially on the orthotropic modulus ratio, E_1/E_2. Values of G_{12}/E_2 and ν_{12} are fixed in this example because the influence of their variation on the deflections is very small compared to that of E_1/E_2. At $E_1/E_2 = 1$ in Figure 5-14, the effect of bending-extension coupling is nonexistent, as it must be. As E_1/E_2 increases, the effect of bending-extension coupling increases. Thus, the deflections in a two-layered boron-epoxy plate ($E_1/E_2 = 10$) are not as much larger than the specially orthotropic plate approximation as in a two-layered graphite-epoxy plate ($E_1/E_2 = 40$).

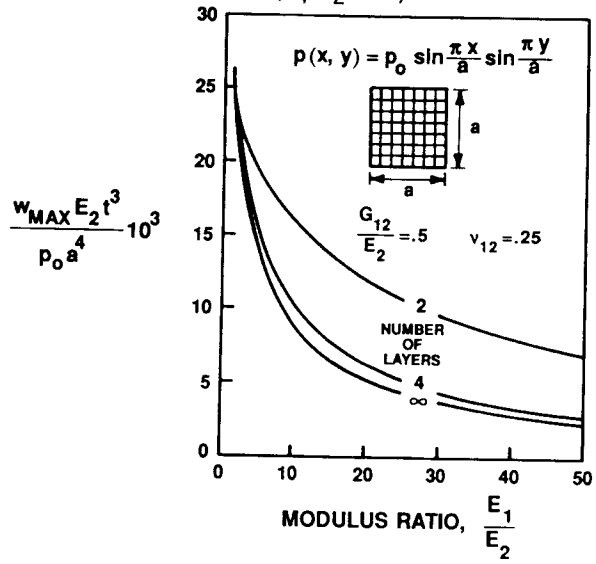

Figure 5-14 Deflection of a Square Antisymmetric Cross-Ply Laminated Plate under Sinusoidal Transverse Load
(After Whitney and Leissa [5-12])

5.3.4 Antisymmetric Angle-Ply Laminated Plates

Antisymmetric angle-ply laminates were described in Section 4.3.3 and found to have extensional stiffnesses A_{11}, A_{12}, A_{22}, and A_{66}; bending-extension coupling stiffnesses B_{16} and B_{26}; and bending stiffnesses D_{11}, D_{12}, D_{22}, and D_{66}. Thus, this laminate exhibits a different type of bending-extension coupling than does the antisymmetric cross-ply laminate. The coupled governing differential equations of equilibrium are

$$A_{11}u_{,xx} + A_{66}u_{,yy} + (A_{12} + A_{66})v_{,xy} - 3B_{16}w_{,xxy} - B_{26}w_{,yyy} = 0 \quad (5.51)$$

$$(A_{12} + A_{66})u_{,xy} + A_{66}v_{,xx} + A_{22}v_{,yy} - B_{16}w_{,xxx} - 3B_{26}w_{,xyy} = 0 \quad (5.52)$$

$$D_{11}w_{,xxxx} + 2(D_{12} + 2D_{66})w_{,xxyy} + D_{22}w_{,yyyy} - B_{16}(3u_{,xxy} - v_{,xxx}) - B_{26}(u_{,yyy} + 3v_{,xyy}) = p \quad (5.53)$$

Whitney solved the problem for simply supported edge boundary condition S3 [5-13 and 5-14] (recall that S2 was used for antisymmetric cross-ply laminated plates in Section 5.3.3):

$$x = 0, a: \quad w = 0 \quad M_x = B_{16}(u_{,y} + v_{,x}) - D_{11}w_{,xx} - D_{12}w_{,yy} = 0 \quad (5.54)$$

$$u = 0 \quad N_{xy} = A_{66}(u_{,y} + v_{,x}) - B_{16}w_{,xx} - B_{26}w_{,yy} = 0 \quad (5.55)$$

$$y = 0, b: \quad w = 0 \quad M_y = B_{26}(u_{,y} + v_{,x}) - D_{12}w_{,xx} - D_{22}w_{,yy} = 0 \quad (5.56)$$

$$v = 0 \quad N_{xy} = A_{66}(u_{,y} + v_{,x}) - B_{16}w_{,xx} - B_{26}w_{,yy} = 0 \quad (5.57)$$

He then observed that the deflections

$$u = \sum_{m=1}^{\infty}\sum_{n=1}^{\infty} A_{mn} \sin\frac{m\pi x}{a}\cos\frac{n\pi y}{b}$$

$$v = \sum_{m=1}^{\infty}\sum_{n=1}^{\infty} B_{mn} \cos\frac{m\pi x}{a}\sin\frac{n\pi y}{b} \quad (5.58)$$

$$w = \sum_{m=1}^{\infty}\sum_{n=1}^{\infty} C_{mn} \sin\frac{m\pi x}{a}\sin\frac{n\pi y}{b}$$

identically satisfy the governing differential equations and boundary conditions if the transverse loading is represented by the Fourier sine series in Equation (5.25), so are the exact solution. Thus, the A_{mn}, B_{mn}, and C_{mn} in Equation (5.58) can be expressed in terms of p_{mn} and the laminate stiffnesses in analogy to Equation (5.30). Then, for an arbitrary transverse loading described with a Fourier sine series, we merely sum the contributions from the deflection solution for each term of the series.

To study the effect of number of layers on laminate performance, we construct a sequence of equal-weight (constant thickness) angle-ply laminates with an increasing number of layers as in Figure 5-15.

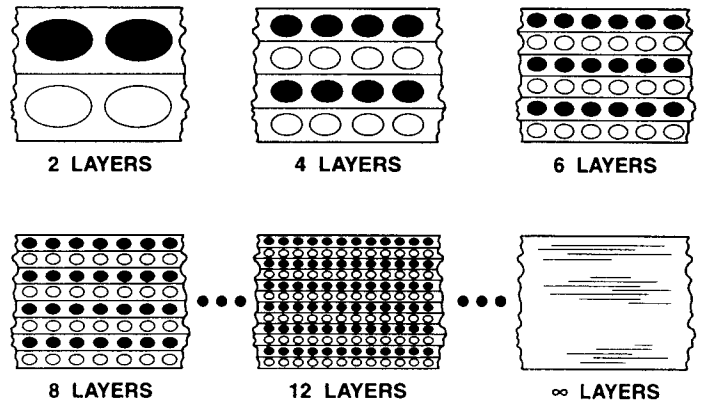

Figure 5-15 Antisymmetric Angle-Ply Laminate Example

Maximum deflection results for a graphite-epoxy laminate for which

$$\frac{E_1}{E_2} = 40 \qquad \frac{G_{12}}{E_2} = .5 \qquad \nu_{12} = .25 \tag{5.59}$$

are shown in Figure 5-16 as a function of angle-ply angle for the sinusoidal transverse loading

$$p = p_o \sin\frac{\pi x}{a} \sin\frac{\pi y}{a} \tag{5.60}$$

The deflection behavior is symmetric about $\theta = 45°$, i.e., the maximum deflection for $\theta = 30°$ is the same as the result for $\theta = 60°$, etc. Clearly, bending-extension coupling is quite significant for two-layered laminates, but rapidly decreases as the number of layers increases. The bending-extension coupling effect has nearly vanished if the laminate has eight or ten layers. For a fixed laminate thickness, the bending-extension coupling stiffnesses

$$(B_{16}, B_{26}) = (Q_{16}, Q_{26})\frac{t^2}{2N} \tag{5.61}$$

obviously decrease as N increases, so the source of the change in the influence of bending-extension coupling is clear.

Results for a square plate under sinusoidal transverse load with a variable modulus ratio, E_1/E_2, and a $\pm 45°$ lamination angle are shown in Figure 5-17. There, the effect of bending-extension coupling on deflections is significant for all modulus ratios except those quite close to $E_1/E_2 = 1$.

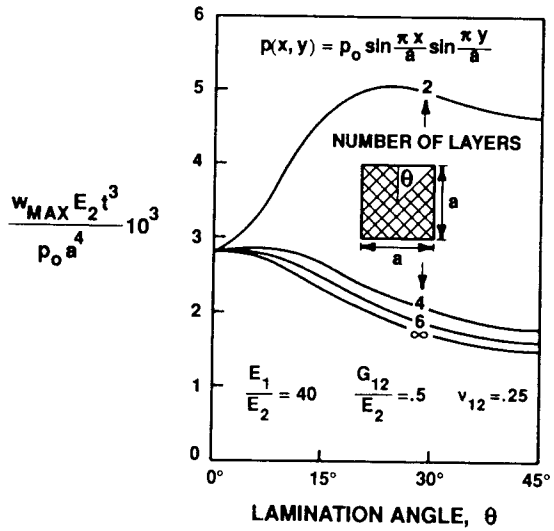

Figure 5-16 Deflection of a Square Antisymmetric Angle-Ply Laminated Plate under Sinusoidal Transverse Load

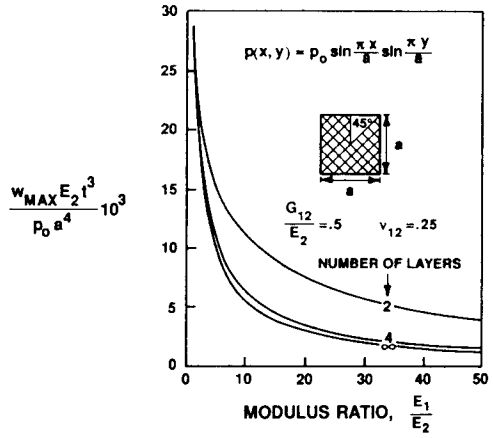

Figure 5-17 Deflection of a Square Antisymmetric Angle-Ply Laminated Plate under Sinusoidal Transverse Load

Problem Set 5.3

5.3.1 Derive Equation (5.30).
5.3.2 Verify Equation (5.31).
5.3.3 Obtain the coefficients A_{mn}, B_{mn}, and C_{mn} in Equation (5.49).
5.3.4 How do A_{11}, A_{22}, D_{11}, and D_{22} change as the number of laminae increases for the example antisymmetric cross-ply laminates in Figure 5-12?
5.3.5 Obtain the coefficients A_{mn}, B_{mn}, and C_{mn} in Equation (5.58).
5.3.6 How do A_{11}, A_{22}, D_{11}, and D_{22} change as the number of laminae increases for the example antisymmetric angle-ply laminates in Figure 5-15?

5.4 BUCKLING OF SIMPLY SUPPORTED LAMINATED PLATES UNDER IN-PLANE LOAD

Consider the general class of laminated rectangular plates that are simply supported along edges $x = 0$, $x = a$, $y = 0$, and $y = b$ and subjected to uniform in-plane force in the x-direction as in Figure 5-18. Other more complicated loads and boundary conditions could be treated. However, the importance of the various stiffnesses in buckling problems is well-illustrated with this simple loading. More comprehensive treatment of plate buckling in general is given by Timoshenko and Gere [5-15] and of laminated plate buckling in particular is given by Whitney [5-1].

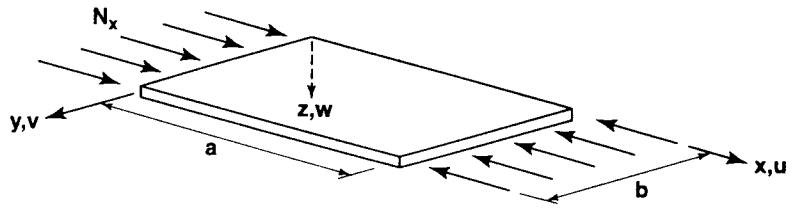

Figure 5-18 Simply Supported Laminated Rectangular Plate under Uniform Uniaxial In-Plane Compression

When columns buckle, a lateral deformation develops along the column length, as is well known. When plates buckle, the deformation transverse to the plane of the plate has a two-dimensional wavy nature. Moreover, that two-dimensional nature has multiple sine waves in the load direction, as shown for the example of two buckle waves in Figure 5-19. Generally, if the plate is very long in the load direction, many sine waves develop. Note that the nodal line in Figure 5-19 does not move during buckling.

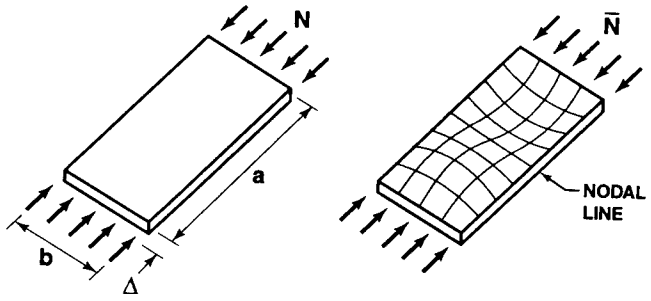

Figure 5-19 Typical Simply Supported Plate Buckling Mode

The load-deformation behavior of plates is more complicated than that of columns. First, as load increases, the plate simply shortens in the load direction while remaining flat. Then, the plate buckles at $\bar{N}$ where the deformation path bifurcates (takes one of two paths) from the flat shape to the buckled shape in Figure 5-20. After buckling, the plate can actually support increased load over the buckling load, but at decreased stiffness as in Figure 5-20. In contrast, columns cannot support any load higher than the buckling load. Thus, the two structural elements have a very different meaning for their buckling loads; one (the column) is the maximum load, the other (the plate) is only an interruption in the load-deformation behavior (a change in slope called a knee).

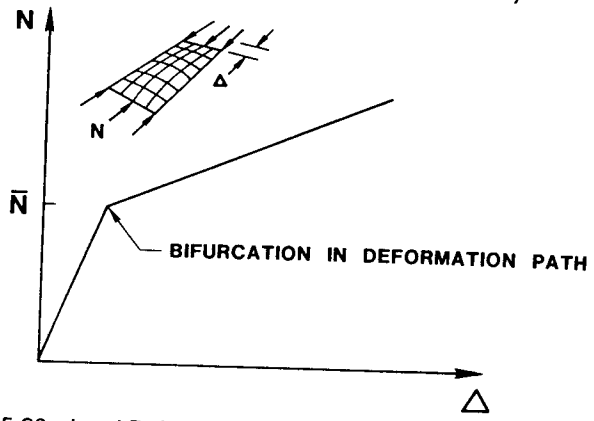

Figure 5-20 Load-Deformation Behavior for an In-Plane Loaded Plate

This knee in the load-deformation curve for a plate occurs only for a plate that is perfectly flat before loading. For plates with increasing magnitudes of initial imperfections, the knee is rounded over, and the load-deformation curve decreases as in Figure 5-21.

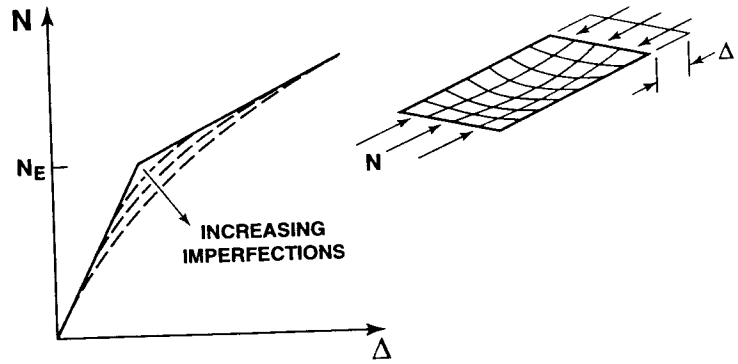

Figure 5-21 Buckling of Plates with Increasing Initial Imperfections

The buckling load will be determined for plates with various laminations: specially orthotropic, symmetric angle-ply, antisymmetric cross-ply, and antisymmetric angle-ply. The results for the different lamination types will be compared to find the influence of bend-twist coupling and bending-extension coupling. As with the deflection problems in Section 5.3, different simply supported edge boundary conditions will be used in the several problems addressed for convenience of illustration.

5.4.1 Specially Orthotropic Laminated Plates

A specially orthotropic laminate has either a single layer of a specially orthotropic material or multiple specially orthotropic layers that are symmetrically arranged about the laminate middle surface (to form a symmetric cross-ply laminate). In both cases, the laminate stiffnesses consist solely of A_{11}, A_{12}, A_{22}, A_{66}, D_{11}, D_{12}, D_{22}, and D_{66}. That is, neither shear-extension or bend-twist coupling nor bending-extension coupling exists. Then, for plate problems, the buckling loads are determined from only one buckling differential equation:

$$D_{11}\delta w_{,xxxx} + 2(D_{12} + 2D_{66})\delta w_{,xxyy} + D_{22}\delta w_{,yyyy} + \bar{N}_x \delta w_{,xx} = 0 \qquad (5.62)$$

subject to the simply supported edge boundary conditions

$$\begin{aligned} x = 0, a: \quad & \delta w = 0 \quad \delta M_x = -D_{11}\delta w_{,xx} - D_{12}\delta w_{,yy} = 0 \\ y = 0, b: \quad & \delta w = 0 \quad \delta M_y = -D_{12}\delta w_{,xx} - D_{22}\delta w_{,yy} = 0 \end{aligned} \qquad (5.63)$$

Note that because of the absence of the variations in in-plane displacements, δu and δv, the boundary conditions are much simpler than the general case in Equation (5.20).

The solution to this fourth-order partial differential equation and associated homogeneous boundary conditions is just as simple as the analogous deflection problem in Section 5.3.1. The boundary conditions are satisfied by the variation in lateral displacement (for plates, δw actually is the physical buckle displacement because $w = 0$ in the membrane prebuckling state; however, δu and δv are variations from a nontrivial equilibrium state. Hence, we retain the more rigorous variational notation consistently):

$$\delta w = A_{mn} \sin \frac{m\pi x}{a} \sin \frac{n\pi y}{b} \tag{5.64}$$

where m and n are the number of buckle half wavelengths in the x- and y-directions, respectively. In addition, the governing differential equation is satisfied by Equation (5.64) if

$$\bar{N}_x = \pi^2 \left[D_{11} \left[\frac{m}{a} \right]^2 + 2(D_{12} + 2D_{66}) \left[\frac{n}{b} \right]^2 + D_{22} \left[\frac{n}{b} \right]^4 \left[\frac{a}{m} \right]^2 \right] \tag{5.65}$$

The smallest value of $\bar{N}_x$ obviously occurs when $n = 1$, so the buckling load expression further reduces to

$$\bar{N}_x = \pi^2 \left[D_{11} \left[\frac{m}{a} \right]^2 + 2(D_{12} + 2D_{66}) \frac{1}{b^2} + D_{22} \left[\frac{1}{b^4} \right] \left[\frac{a}{m} \right]^2 \right] \tag{5.66}$$

The smallest value of $\bar{N}_x$ for various m is not obvious, but varies for different values of the stiffnesses and the plate aspect ratio, a/b.

For example, if $D_{11}/D_{22} = 10$ and $(D_{12} + 2D_{66})/D_{22} = 1$ (representative values for boron-epoxy, then Equation (5.66) becomes

$$\bar{N}_x = \pi^2 D_{22} \left[10 \left[\frac{m}{a} \right]^2 + \frac{2}{b^2} + \left[\frac{a}{m} \right]^2 \frac{1}{b^4} \right] \tag{5.67}$$

which is plotted in Figure 5-22 versus the plate aspect ratio. There, for small plate aspect ratios (that is, $a/b < 2.5$), the plate buckles into a single half-wave in the x-direction. For example, the buckling load of a square plate is

$$\bar{N}_x = \frac{13\pi^2 D_{22}}{b^2} \tag{5.68}$$

As the plate aspect ratio increases, the plate buckles into more and more buckle half-waves in the x-direction and has an $\bar{N}_x$ versus a/b curve that gets even flatter and, in fact, approaches

$$\bar{N}_x = \frac{8.32456\pi^2 D_{22}}{b^2} \tag{5.69}$$

For other materials, other families of curves such as in Figure 5-22 are obtained with correspondingly different buckling loads and different points of change from one buckling mode to another.

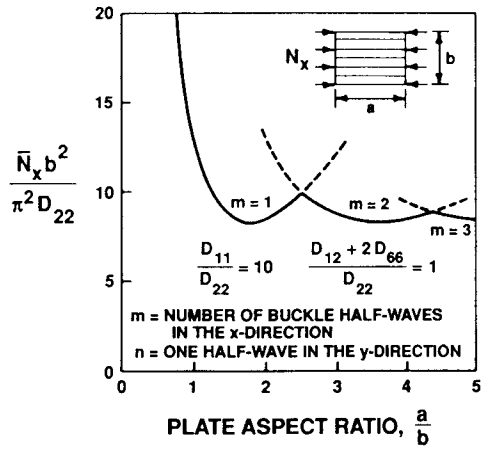

Figure 5-22 Buckling of Rectangular Specially Orthotropic Laminated Plates under Uniform Compression, N_x

We are now prepared to address the question posed in Figure 5-23. Consider two rectangular plates that are simply supported on all four edges, of the same thickness, and made of the same fiber-reinforced material. One plate consists of all unidirectional material with fibers in the load direction. The other plate has the same layers, but alternately arranged in the form of a symmetric cross-ply laminate. Many might think or expect that the plate with the most fibers in the load direction would have the highest buckling load. However, that position is based on the premise that the buckling load depends primarily on the bending resistance in the load direction. However, *the plate buckling load is a function of all four bending stiffnesses* D_{11}, D_{12}, D_{22}, and D_{66}, as is clear from Equation (5.66). Thus, it should not be surprising that the cross-ply plate has a higher buckling load than the unidirectionally reinforced plate. In fact, the support on all four edges of a plate signifies that a plate cannot simply deform as a wide column (as a plate supported on only the two loaded edges would be). The behavior of a wide column would, of course, be dominated by the bending stiffness in the direction of the load.

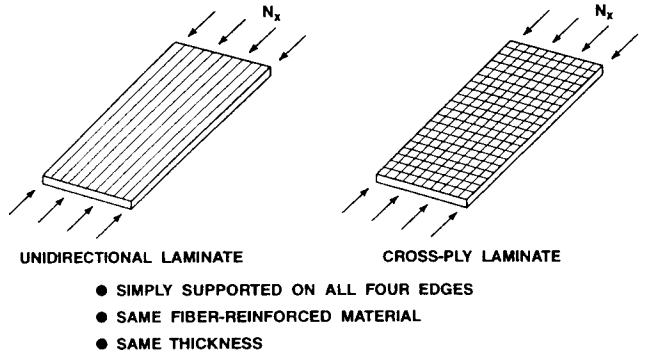

Figure 5-23 Which Plate Has the Highest Buckling Load?

5.4.2 Symmetric Angle-Ply Laminated Plates

Symmetric angle-ply laminates were found in Section 4.3.2 to be characterized by a full matrix of extensional stiffnesses as well as bending stiffnesses, but not to have bending-extension coupling. The principal difference between these laminates and specially orthotropic laminates is the introduction here of the bend-twist coupling stiffnesses D_{16} and D_{26} (the shear-extension coupling stiffnesses A_{16} and A_{26} are immaterial for buckling of a symmetrically laminated plate because the three governing differential equations are uncoupled). Accordingly, the governing buckling differential equation is

$$D_{11}\delta w_{,xxxx} + 4D_{16}\delta w_{,xxxy} + 2(D_{12} + 2D_{66})\delta w_{,xxyy} + 4D_{26}\delta w_{,xyyy} + D_{22}\delta w_{,yyyy} + \bar{N}_x\delta w_{,xx} = 0 \tag{5.70}$$

subject to the simply supported edge boundary conditions

$$\begin{aligned} x = 0, a: \quad & \delta w = 0 \quad \delta M_x = -D_{11}\delta w_{,xx} - D_{12}\delta w_{,yy} - 2D_{16}\delta w_{,xy} = 0 \\ y = 0, b: \quad & \delta w = 0 \quad \delta M_y = -D_{12}\delta w_{,xx} - D_{22}\delta w_{,yy} - 2D_{26}\delta w_{,xy} = 0 \end{aligned} \tag{5.71}$$

The presence of D_{16} and D_{26} in the governing differential equation and boundary conditions makes a closed-form solution impossible. That is, in analogy to bending of symmetric angle-ply laminated plates, the variation in lateral displacement, δw, cannot be separated into a function of x alone times a function of y alone such as in Equation (5.64). However, again in analogy to bending of symmetrically laminated angle-ply plates, an approximate Rayleigh-Ritz solution was obtained by Ashton and Waddoups [5-16] (or equivalently a Galerkin solution as presented by Chamis [5-17]) by substituting the variation in lateral displacement expression

$$\delta w = \sum_{m=1}^{\infty}\sum_{n=1}^{\infty} A_{mn} \sin\frac{m\pi x}{a} \sin\frac{n\pi y}{b} \tag{5.72}$$

in the expression for the second variation of the total potential energy and subsequently making it stationary relative to the A_{mn}. Note that Equation (5.72) satisfies the geometric boundary conditions of the problem ($\delta w = 0$ on all edges), but not the natural boundary conditions ($\delta M_n = 0$ on all edges) or the differential equations, so the results probably converge slowly toward the actual solution.

The actual solution procedure is only incidental to the present objectives, so we are satisfied to report the results for several laminates of boron-epoxy with $E_1/E_2 = 10$, $G_{12}/E_2 = .3$, and $\nu_{12} = .3$. Normalized buckling loads for three laminates, 20 layers at $+\theta$, 20 layers alternating at $\pm\theta$, and the specially orthotropic approximation, are plotted in Figure 5-24. The Rayleigh-Ritz curves are for 49 terms ($m = 7$ and $n = 7$). Experimental results by Mandell [5-18] are also shown in Figure 5-24; obviously, the agreement between theory and experiment is very satisfactory. Apparently, bend-twist coupling is just as important for buckling problems as it is for bending problems. The principal influence

of bend-twist coupling is to lower the buckling load from what would be obtained with the specially orthotropic approximation. Thus, the specially orthotropic approximation is unconservative in design applications. To the author's knowledge, no skew plate analogy results exist for plate buckling in contrast to the bending problem.

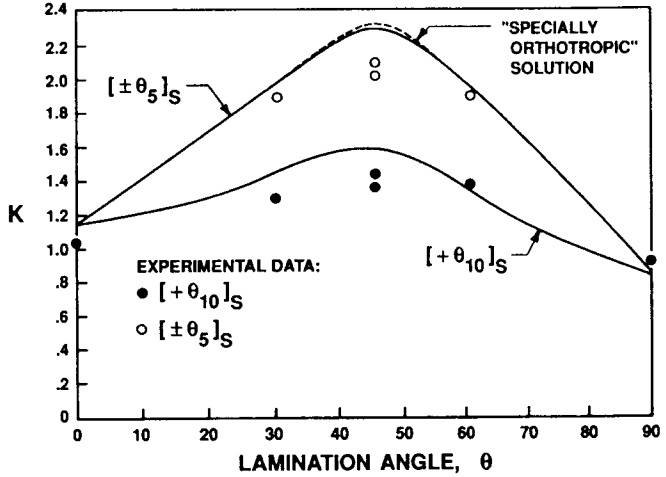

Figure 5-24 Buckling Loads for Rectangular Symmetric Angle-Ply Plates under Uniform Compression, N_x *(After Whitney [5-1])*

5.4.3 Antisymmetric Cross-Ply Laminated Plates

Antisymmetric cross-ply laminates were found in Section 4.3.3 to have extensional stiffnesses A_{11}, A_{12}, $A_{22} = A_{11}$, and A_{66}; bending-extension coupling stiffnesses B_{11} and $B_{22} = -B_{11}$; and bending stiffnesses D_{11}, D_{12}, $D_{22} = D_{11}$, and D_{66}. The new terms here in comparison to a specially orthotropic laminate are B_{11} and B_{22}. Because of this bending-extension coupling, the three buckling differential equations are coupled:

$$A_{11}\delta u_{,xx} + A_{66}\delta u_{,yy} + (A_{12} + A_{66})\delta v_{,xy} - B_{11}\delta w_{,xxx} = 0 \tag{5.73}$$

$$(A_{12} + A_{66})\delta u_{,xy} + A_{66}\delta v_{,xx} + A_{11}\delta v_{,yy} + B_{11}\delta w_{,yyy} = 0 \tag{5.74}$$

$$D_{11}(\delta w_{,xxxx} + \delta w_{,yyyy}) + 2(D_{12} + 2D_{66})\delta w_{,xxyy} - B_{11}(\delta u_{,xxx} - \delta v_{,yyy}) + \bar{N}_x\delta w_{,xx} = 0 \tag{5.75}$$

Jones solved the problem for simply supported edge boundary condition S2 [5-19]:

$$x = 0, a: \quad \delta w = 0 \quad \delta M_x = B_{11}\delta u_{,x} - D_{11}\delta w_{,xx} - D_{12}\delta w_{,yy} = 0 \tag{5.76}$$

$$\delta v = 0 \quad \delta N_x = A_{11}\delta u_{,x} + A_{12}\delta v_{,y} - B_{11}\delta w_{,xx} = 0 \tag{5.77}$$

$$y = 0, b: \quad \delta w = 0 \quad \delta M_y = -B_{11}\delta v_{,y} - D_{12}\delta w_{,xx} - D_{11}\delta w_{,yy} = 0 \tag{5.78}$$

$$\delta u = 0 \quad \delta N_y = A_{12}\delta u_{,x} + A_{11}\delta v_{,y} + B_{11}\delta w_{,yy} = 0 \tag{5.79}$$

and verified that the variations in deflections

$$\delta u = \bar{u}\cos\frac{m\pi x}{a}\sin\frac{n\pi y}{b}$$
$$\delta v = \bar{v}\sin\frac{m\pi x}{a}\cos\frac{n\pi y}{b} \qquad (5.80)$$
$$\delta w = \bar{w}\sin\frac{m\pi x}{a}\sin\frac{n\pi y}{b}$$

satisfy both the boundary conditions and the governing differential equations exactly if the buckling load is

$$\bar{N}_x = \left[\frac{a}{m\pi}\right]^2\left[T_{33} + \frac{2T_{12}T_{23}T_{13} - T_{22}T_{13}^2 - T_{11}T_{23}^2}{T_{11}T_{22} - T_{12}^2}\right] \qquad (5.81)$$

where

$$T_{11} = A_{11}\left[\frac{m\pi}{a}\right]^2 + A_{66}\left[\frac{n\pi}{b}\right]^2$$
$$T_{12} = (A_{12} + A_{66})\left[\frac{m\pi}{a}\right]\left[\frac{n\pi}{b}\right]$$
$$T_{13} = -B_{11}\left[\frac{m\pi}{a}\right]^3$$
$$T_{22} = A_{11}\left[\frac{n\pi}{b}\right]^2 + A_{66}\left[\frac{m\pi}{a}\right]^2 \qquad (5.82)$$
$$T_{23} = B_{11}\left[\frac{n\pi}{b}\right]^3$$
$$T_{33} = D_{11}\left[\left[\frac{m\pi}{a}\right]^4 + \left[\frac{n\pi}{b}\right]^4\right] + 2(D_{12} + 2D_{66})\left[\frac{m\pi}{a}\right]^2\left[\frac{n\pi}{b}\right]^2$$

Note that if B_{11} is zero, then T_{13} and T_{23} are also zero, so Equation (5.81) reduces to the specially orthotropic plate solution, Equation (5.65), if $D_{11} = D_{22}$. Because T_{11}, T_{12}, and T_{22} are functions of both m and n, no simple conclusion can be drawn about the value of n at buckling as could be done for specially orthotropic laminated plates where n was determined to be one. Instead, Equation (5.81) is a complicated function of both m and n. At this point, recall the discussion in Section 3.5.3 about the difference between finding a minimum of a function of discrete variables versus a function of continuous variables. We have already seen that plates buckle with a small number of buckles. Consequently, the lowest buckling load must be found in Equation (5.81) by a searching procedure due to Jones involving *integer* values of m and n [5-20] and *not* by equating to zero the first partial derivatives of $\bar{N}_x$ with respect to m and n.

One of the major complications in the plate buckling solution is the need to investigate the influence of buckle mode shape on the buckling load itself. That is, the plate buckling load in Equation (5.81) is a function

of the buckling mode shape parameters m and n as well as the laminated plate stiffnesses. In contrast, the column buckling load can, of course, be expressed in terms of the buckle mode shape parameter m, i.e.,

$$P = m^2\pi^2\frac{EI}{L^2} \qquad (5.83)$$

However, because we are usually interested only in the lowest buckling load for a column, m is always one. For plates, both m and n enter the buckling equation as well as the plate aspect ratio, a/b, so the lowest buckling load does not typically occur for m = 1 and n = 1. Thus, we must find the absolute minimum of the values of the buckling load, $\bar{N}_x$, or more generally, λ, for a wide range of m and n values.

First, the relative minima of λ for a series of fixed values of m are found by varying n over a prescribed range, as in Figure 5-25a. The absolute minima of the λ for each value of m are then compared to find the absolute minimum λ for all m and n in Figure 5-25b. The aforementioned procedure of searching for an absolute minimum λ for discrete values of m and n is necessary because of the possibility of more than one relative minimum for plates as in Figure 5-25b. In such cases, the ordinary procedures of determining a stationary value of λ by differentiating λ with respect to m and n and equating the results to zero are both totally inadequate and misleading. Those procedures depend on the buckling load being a continuous function of m and n, and obviously that function is not continuous. Moreover, more than one minimum of λ could occur.

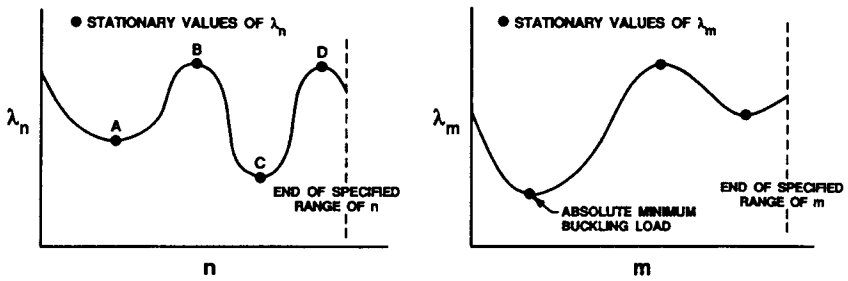

a Values of λ for Each Value of n when m is Fixed

b Absolute Minimum Values of λ_n for Each Value of m

Figure 5-25 Determination of the Absolute Minimum Buckling Load

The sign of the second derivative of λ with respect to m and n must be examined in order to determine whether a minimum, maximum, or inflection point is obtained by the stationary value procedure that many erroneously call 'minimization.' Actually, the determination of such de-

rivatives and the associated logic for selection of the absolute minimum would result in noninteger values of m and n that are physically unrealistic and indeed impossible. Moreover, that inappropriate procedure would take about the same computational effort as the present more-suitable procedure.

The present search procedure obviates the need for determining any derivatives of λ, but is subject to the limitation that a sufficiently wide range of values of m and n must be prescribed before starting the solution. Otherwise, the absolute minimum λ can be missed, i.e., the prescribed range of values of m and n must include the values for the true absolute minimum and cannot be truncated below that range without overestimating the buckling load. Two factors ease the difficulty in deciding on the range of values of m and n to be investigated: (1) practical experience and (2) behavior such as a decreasing λ as the end of a range of n (or m) is approached as in Figure 5-25a is noted by the computer program developed by Jones [5-21]. A message is printed that the range of n (or m) should be increased to see if a lower λ is found. Such a procedure is obviously not infallible. For example, if the range of n investigated stopped after C but before D in Figure 5-25a, no message would be printed, whereas the minimum after D could be lower than the minimum at C. Practical experience with this computational aid should lead to reasonable assurance that no relative minimum that might be the absolute minimum is missed.

As for the deflection problem in Section 5.3.3, the effect of the number of layers on the buckling load is found by dividing a constant-thickness, equal-weight cross-ply laminate into more and more laminae as in Figure 5-12. Results for graphite-epoxy antisymmetric cross-ply laminated plates for which $E_1/E_2 = 40$, $G_{12}/E_2 = .5$, and $\nu_{12} = .25$ are shown in Figure 5-26. There, the buckling load is normalized with respect to the plate width b and plate stiffness D_{22} for various rectangular plate aspect ratios and for various numbers of layers. The solution for an infinite number of layers (a specially orthotropic laminated plate) is shown as a limiting case of no bending-extension coupling. The coupling is extremely significant for a small number of layers. For two layers at a plate aspect ratio of one, the overestimate of buckling resistance is 183% if the orthotropic approximation is made. From another point of view, the actual resistance is 65% less than calculated by use of the specially orthotropic approximation. For four layers, the analogous numbers are 19% overestimate and 16% reduction, respectively. For six layers, the numbers drop to 8% overestimate and 7% reduction, respectively. Obviously, the effect of bending-extension coupling dies out very rapidly as the number of layers increases for an antisymmetric laminate. However, for fewer than six layers, the effect cannot be ignored.

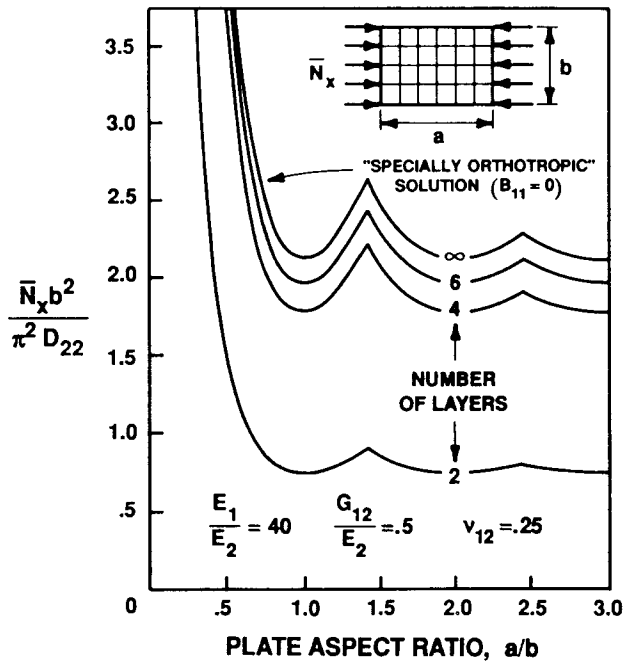

Figure 5-26 Buckling Loads for Antisymmetric Cross-Ply Laminated Plates under Uniform Uniaxial Compression N_x *(After Jones [5-19])*

When other composite materials are considered, the effect of bending-extension coupling on the buckling load depends essentially on the orthotropic modulus ratio, E_1/E_2, as shown in Figure 5-27. There, the buckling load is normalized by the buckling load of a specially orthotropic square plate ($B_{11} = 0$). Values of G_{12}/E_2 and ν_{12} are fixed because they do not vary significantly and their influence on the buckling load is small compared to that of E_1/E_2. As the modulus ratio decreases from the graphite-epoxy value of 40, the influence of bending-extension coupling decreases slowly. As noted previously, the reduction in buckling load of a square two-layered graphite-epoxy plate from the specially orthotropic plate is about 65%. For a square boron-epoxy plate, the reduction is about 43%. From the design-analysis point of view, the specially orthotropic plate solution is too high by 183% for a graphite-epoxy plate and by 74% for an analogous boron-epoxy plate. Obviously, bending-extension coupling is extremely important when the plate has only two layers. However, the influence of coupling dies out quite rapidly as the number of layers increases. For example, the reduction in buckling load for a six-layered graphite-epoxy plate is only about 7% and about 5% for a boron-epoxy plate.

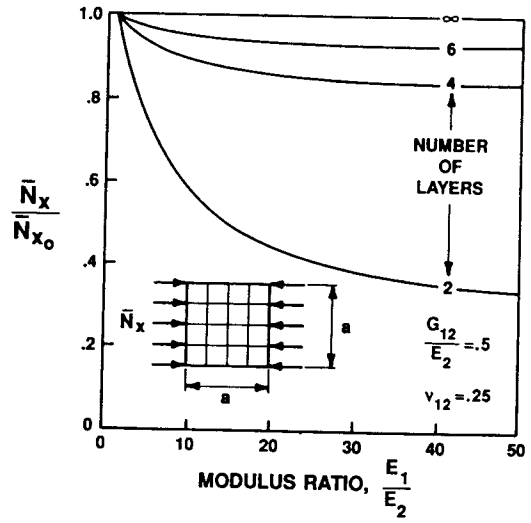

Figure 5-27 Relative Uniaxial Buckling Loads of Square Antisymmetric Cross-Ply Laminated Plates *(After Jones [5-19])*

5.4.4 Antisymmetric Angle-Ply Laminated Plates

Antisymmetric angle-ply laminates were found in Section 4.3.3 to have extensional stiffnesses A_{11}, A_{12}, A_{22}, and A_{66}; bending-extension coupling stiffnesses B_{16} and B_{26}; and bending stiffnesses D_{11}, D_{12}, D_{22}, and D_{66}. Thus, this type of laminate exhibits a very different kind of bending-extension coupling than does the antisymmetric cross-ply laminate examined in Section 5.4.3. The coupled buckling differential equations are

$$A_{11}\delta u_{,xx} + A_{66}\delta u_{,yy} + (A_{12} + A_{66})\delta v_{,xy} - 3B_{16}\delta w_{,xxy} - B_{26}\delta w_{,yyy} = 0 \quad (5.84)$$

$$(A_{12} + A_{66})\delta u_{,xy} + A_{66}\delta v_{,xx} + A_{22}\delta v_{,yy} - B_{16}\delta w_{,xxx} - 3B_{26}\delta w_{,xyy} = 0 \quad (5.85)$$

$$D_{11}w_{,xxxx} + 2(D_{12} + 2D_{66})\delta w_{,xxyy} + D_{22}\delta w_{,yyyy} - B_{16}(3\delta u_{,xxy} + \delta v_{,xxx}) - B_{26}(\delta u_{,yyy} + 3\delta v_{,xyy}) + \bar{N}_x\delta w_{,xx} = 0 \quad (5.86)$$

Whitney solved the problem for simply supported edge boundary condition S3 [5-13 and 5-14] (note that this boundary condition differs significantly from the S2 condition used for buckling of antisymmetric cross-ply laminated plates in Section 5.4.3)):

$$x = 0, a: \quad \delta w = 0 \quad \delta M_x = B_{16}(\delta v_{,x} + \delta u_{,y}) - D_{11}\delta w_{,xx} - D_{12}\delta w_{,yy} = 0 \quad (5.87)$$

$$\delta u = 0 \quad \delta N_{xy} = A_{66}(\delta v_{,x} + \delta u_{,y}) - B_{16}\delta w_{,xx} - B_{26}\delta w_{,yy} = 0 \quad (5.88)$$

$$y = 0, b: \quad \delta w = 0 \quad \delta M_y = B_{26}(\delta v_{,x} + \delta u_{,y}) - D_{12}\delta w_{,xx} - D_{22}\delta w_{,yy} = 0 \quad (5.89)$$

$$\delta v = 0 \quad \delta N_{xy} = A_{66}(\delta v_{,x} + \delta u_{,y}) - B_{16}\delta w_{,xx} - B_{26}\delta w_{,yy} = 0 \quad (5.90)$$

He then observed that the variations in displacement

$$\delta u = \bar{u}\sin\frac{m\pi x}{a}\cos\frac{n\pi y}{b}$$
$$\delta v = \bar{v}\cos\frac{m\pi x}{a}\sin\frac{n\pi y}{b} \quad (5.91)$$
$$\delta w = \bar{w}\sin\frac{m\pi x}{a}\sin\frac{n\pi y}{b}$$

satisfy the boundary conditions and also satisfy the governing differential equations exactly if the buckling load is

$$\bar{N}_x = \left[\frac{a}{m\pi}\right]^2\left[T_{33} + \frac{2T_{12}T_{23}T_{13} - T_{22}T_{13}^2 - T_{11}T_{23}^2}{T_{11}T_{22} - T_{12}^2}\right] \quad (5.92)$$

where

$$T_{11} = A_{11}\left[\frac{m\pi}{a}\right]^2 + A_{66}\left[\frac{n\pi}{b}\right]^2$$
$$T_{12} = (A_{12} + A_{66})\left[\frac{m\pi}{a}\right]\left[\frac{n\pi}{b}\right]$$
$$T_{13} = -\left[3B_{16}\left[\frac{m\pi}{a}\right]^2 + B_{26}\left[\frac{n\pi}{b}\right]^2\right]\left[\frac{n\pi}{b}\right]$$
$$T_{22} = A_{22}\left[\frac{n\pi}{b}\right]^2 + A_{66}\left[\frac{m\pi}{a}\right]^2 \quad (5.93)$$
$$T_{23} = -\left[B_{16}\left[\frac{m\pi}{a}\right]^2 + 3B_{26}\left[\frac{n\pi}{b}\right]^2\right]\left[\frac{m\pi}{a}\right]$$
$$T_{33} = D_{11}\left[\frac{m\pi}{a}\right]^4 + 2(D_{12} + 2D_{66})\left[\frac{m\pi}{a}\right]^2\left[\frac{n\pi}{b}\right]^2 + D_{22}\left[\frac{n\pi}{b}\right]^4$$

Note that if B_{16} and B_{26} are zero, then T_{13} and T_{23} are also zero, so Equation (5.92) reduces to the specially orthotropic plate solution, Equation (5.65). The character of Equation (5.92) is the same as that of Equation (5.81) for antisymmetric cross-ply laminated plates, so the remarks on finding the buckling load in Section 5.4.3 are equally applicable here.

As for the deflection problem in Section 5.3.4, the effect of the number of layers on the buckling load is found by dividing a constant-thickness, equal-weight angle-ply laminate into more and more laminae as in Figure 5-15. Numerical results for graphite-epoxy composite material with $E_1/E_2 = 40$, $G_{12}/E_2 = .5$, and $\nu_{12} = .25$ in square plates are shown in Figure 5-28. The influence of bending-extension coupling is to reduce the buckling load for two-layered plates from the many layered result (which is the specially orthotropic plate solution of Section 5.4.1). At 45°, the reduction is by about a factor of 2/3; perhaps more significant is the fact that use of the specially orthotropic approximation leads to a predicted buckling load that is three times the actual buckling load! Obviously, the specially orthotropic approximation is highly unconservative

for antisymmetric angle-ply laminates with less than six layers. For six layers, the error in the buckling load is about 7%. Thus, the bending-extension coupling effect dies out rapidly as the number of layers increases. This conclusion is valid for other materials as represented in Figure 5-29 in the manner of Section 5.4.3.

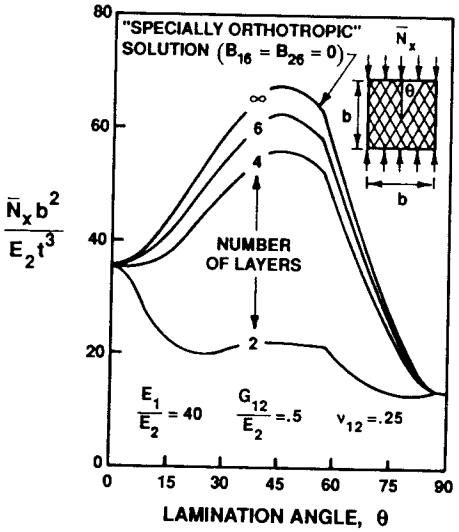

Figure 5-28 Buckling of Square Antisymmetric Angle-Ply Laminated Plates under Uniform Uniaxial Compression, N_x
(After Jones, Morgan, and Whitney [5-22])

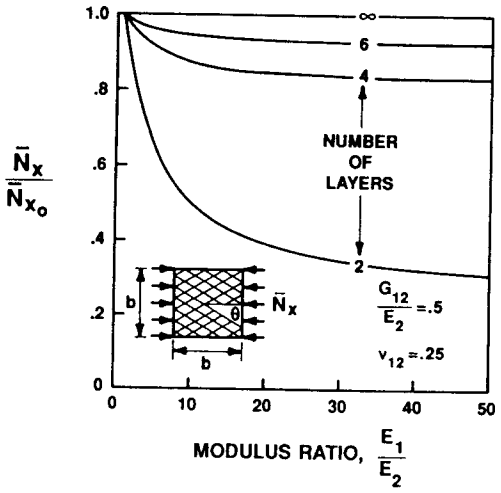

Figure 5-29 Relative Uniaxial Buckling Loads of Square Antisymmetric Angle-Ply Laminated Plates

Problem Set 5.4

5.4.1 Derive Equation (5.65).

5.4.2 Consider a symmetric cross-ply laminated plate and a unidirectionally reinforced plate as in Figure 5-23. Both plates have three graphite-epoxy layers each of thickness t, simple supports on all four edges, and N_x applied. Demonstrate that the bending stiffnesses have the inequalities: $D_{11UD} > D_{22UD}$ (UD = unidirectional), $D_{11UD} > D_{11CP}$ (CP = cross-ply), and $D_{22CP} > D_{22UD}$. Express all laminate bending stiffnesses in terms of that of a single 0° layer, i.e., $E_1 t^3/12(1 - \nu_{12}\nu_{21})$. Use these stiffness results to calculate the buckling load in Equation (5.66) to explore the importance of D_{22} (as well as D_{12} and D_{66}) in the calculation for a/b = 2 and m = 1. Describe the importance of the second two terms in Equation (5.66) as (1) a/b increases and (2) m increases. What happens to m as a/b increases?

5.4.3 Derive Equation (5.81). Hint: for a set of homogeneous equations to have a non-trivial solution, the determinant of the coefficients must be zero.

5.4.4 Derive Equation (5.92). See hint in Problem 5.4.2.

5.5 VIBRATION OF SIMPLY SUPPORTED LAMINATED PLATES

Consider the general class of laminated rectangular plates that are simply supported along edges x = 0, x = a, y = 0, and y = b as shown in Figure 5-30. The nature of the free (not forced) vibrations of such a structural configuration about an equilibrium state will be addressed in this section according to the governing differential equations and boundary conditions discussed in Section 5.2. Other more complicated boundary conditions and the effect of an equilibrium stress state could be considered. However, in consonance with the restricted objectives of this book, those topics are left for further study. A more comprehensive treatment of laminated plate vibrations is provided by Whitney [5-1].

The free vibration frequencies and mode shapes will be determined for plates with various laminations: specially orthotropic, symmetric angle-ply, antisymmetric cross-ply, and antisymmetric angle-ply. The results for the different types of lamination will be compared to determine the influence of bend-twist coupling and bending-extension coupling on the vibration behavior. As with the deflection problems in Section 5.3 and the buckling problems in Section 5.4, different simply supported edge boundary conditions will be used in the several problems presented.

5.5.1 Specially Orthotropic Laminated Plates

A specially orthotropic laminate has either a single layer of a specially orthotropic material or multiple specially orthotropic layers that are symmetrically arranged about the laminate middle surface. In both

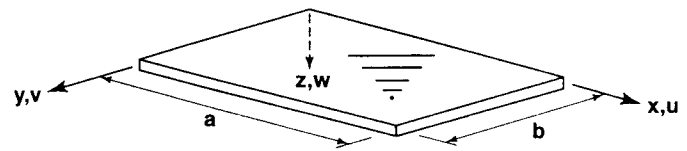

Figure 5-30 Vibration of a Simply Supported Laminated Rectangular Plate

cases, the laminate stiffnesses consist solely of A_{11}, A_{12}, A_{22}, A_{66}, D_{11}, D_{12}, D_{22}, and D_{66}. That is, neither shear-extension or bend-twist coupling nor bending-extension coupling exists. Then, for plate problems, the vibration frequencies and mode shapes are determined from solution of a single vibration differential equation

$$D_{11}\delta w_{,xxxx} + 2(D_{12} + 2D_{66})\delta w_{,xxyy} + D_{22}\delta w_{,yyyy} + \rho\delta w_{,tt} = 0 \qquad (5.94)$$

subject to the simply supported edge boundary conditions

$$\begin{aligned} x = 0, a: \quad & \delta w = 0 \quad \delta M_x = -D_{11}\delta w_{,xx} - D_{12}\delta w_{,yy} = 0 \\ y = 0, b: \quad & \delta w = 0 \quad \delta M_y = -D_{12}\delta w_{,xx} - D_{22}\delta w_{,yy} = 0 \end{aligned} \qquad (5.95)$$

The free vibration of an elastic continuum is harmonic in time, so Whitney chose a harmonic solution

$$\delta w(x,y,t) = (A\cos\omega t + B\sin\omega t)\delta w(x,y) \qquad (5.96)$$

and observed that the problem has now been separated into time and spatial variations [5-1]. The resulting differential equation and boundary conditions are satisfied with the spatial variation of lateral displacement

$$\delta w(x,y) = \sin\frac{m\pi x}{a}\sin\frac{n\pi y}{b} \qquad (5.97)$$

if the frequency is

$$\omega^2 = \frac{\pi^4}{\rho}\left[D_{11}\left[\frac{m}{a}\right]^4 + 2(D_{12} + 2D_{66})\left[\frac{m}{a}\right]^2\left[\frac{n}{b}\right]^2 + D_{22}\left[\frac{n}{b}\right]^4\right] \qquad (5.98)$$

where the various natural frequencies, ω, correspond to different mode shapes (different values of m and n in Equation (5.97), so accordingly different shapes of w). The fundamental natural frequency (lowest frequency) is obviously obtained when m and n are both one.

For a specially orthotropic square boron-epoxy plate with stiffness ratios $D_{11}/D_{22} = 10$ and $(D_{12} + 2D_{66}) = 1$, the four lowest frequencies are displayed in Table 5-3 along with the four lowest frequencies of an isotropic plate. There, the factor k is defined as

$$\omega = \frac{k\pi^2}{b^2}\sqrt{\frac{D_{22}}{\rho}} \qquad (5.99)$$

Table 5-3 Normalized Vibration Frequencies for Specially Orthotropic and Isotropic Simply Supported Square Plates

Mode	Specially Orthotropic			Isotropic		
	m	n	k	m	n	k
1st	1	1	3.60555	1	1	2
2nd	1	2	5.84095	1	2	5
3rd	1	3	10.44031	2	1	5
4th	2	1	13	2	2	8

where for an isotropic plate $D_{22} = D$. The corresponding mode shapes are shown in Figure 5-31, where the nodal lines (lines of zero deflection with time) are indicated with dashed lines. The significant observation is that *the specially orthotropic plate has a different set of four lowest frequencies than does the isotropic plate.* That is, a directional preference is exhibited by the specially orthotropic plate as evidenced by the m = 1, n = 3 mode having a lower frequency than the m = 2, n = 1 mode. In contrast, the isotropic plate has the same frequency for both the m = 2, n = 1 mode and the m = 1, n = 2 mode. Similar information could be developed for all the examples that follow. However, we will concentrate on the fundamental natural frequency to simplify the discussion.

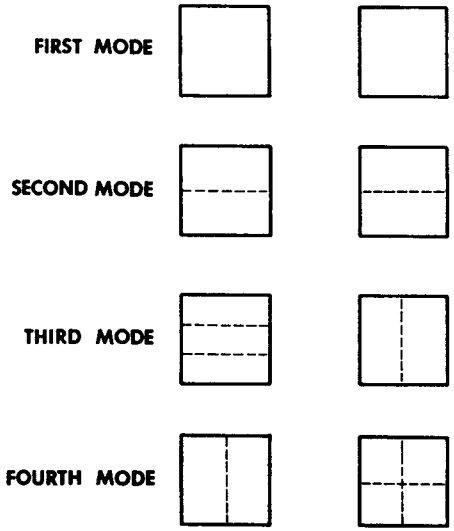

Figure 5-31 Vibration Mode Shapes for Simply Supported Square Specially Orthotropic and Isotropic Plates

5.5.2 Symmetric Angle-Ply Laminated Plates

Symmetric angle-ply laminates were found in Section 4.3.2 to be characterized by a full matrix of extensional stiffnesses as well as bending stiffnesses, but to have no bending-extension coupling. The principal difference between these laminates and specially orthotropic laminates is the introduction here of the bend-twist coupling stiffnesses D_{16} and D_{26} (the shear-extension coupling stiffnesses A_{16} and A_{26} are immaterial for transverse vibration of a symmetrically laminated plate because the governing differential equations are uncoupled). Accordingly, the governing vibration differential equation is

$$\begin{aligned} D_{11}\delta w_{,xxxx} + 4D_{16}\delta w_{,xxxy} + 2(D_{12} + 2D_{66})\delta w_{,xxyy} \\ + 4D_{26}\delta w_{,xyyy} + D_{22}\delta w_{,yyyy} + \rho\delta w_{,tt} = 0 \end{aligned} \qquad (5.100)$$

subject to the simply supported edge boundary conditions at all time

$$\begin{aligned} x = 0, a: \quad & \delta w = 0 \quad \delta M_x = -D_{11}\delta w_{,xx} - D_{12}\delta w_{,yy} - 2D_{16}\delta w_{,xy} = 0 \\ y = 0, b: \quad & \delta w = 0 \quad \delta M_y = -D_{12}\delta w_{,xx} - D_{22}\delta w_{,yy} - 2D_{26}\delta w_{,xy} = 0 \end{aligned} \tag{5.101}$$

The presence of D_{16} and D_{26} in the governing differential equation and the boundary conditions renders a closed-form solution impossible. That is, in analogy to both bending and buckling of a symmetric angle-ply (or anisotropic) plate, the variation in lateral displacement, δw, cannot be separated into a function of x alone times a function of y alone. Again, however, the Rayleigh-Ritz approach is quite useful. The expression

$$\delta w = \sum_{m=1}^{\infty}\sum_{n=1}^{\infty} A_{mn} \sin\frac{m\pi x}{a} \sin\frac{n\pi y}{b} \tag{5.102}$$

satisfies the geometric boundary conditions ($w = 0$ on all edges), but not the natural boundary conditions ($M_n = 0$ on all edges) or the governing differential equation. Therefore, the use of Equation (5.102) in the appropriate energy expression might result in rather slow convergence toward the exact solution. No numerical results for this laminate class are known to the author.

5.5.3 Antisymmetric Cross-Ply Laminated Plates

Antisymmetric cross-ply laminates were found in Section 4.3.3 to have extensional stiffnesses A_{11}, A_{12}, $A_{22} = A_{11}$, and A_{66}, bending-extension coupling stiffnesses B_{11} and $B_{22} = -B_{11}$, and bending stiffnesses D_{11}, D_{12}, $D_{22} = D_{11}$, and D_{66}. The new terms here in comparison to a specially orthotropic laminate are B_{11} and B_{22}. Because of this bending-extension coupling, the three vibration differential equations are coupled:

$$A_{11}\delta u_{,xx} + A_{66}\delta u_{,yy} + (A_{12} + A_{66})\delta v_{,xy} - B_{11}\delta w_{,xxx} = 0 \tag{5.103}$$

$$(A_{12} + A_{66})\delta u_{,xy} + A_{66}\delta v_{,xx} + A_{11}\delta v_{,yy} + B_{11}\delta w_{,yyy} = 0 \tag{5.104}$$

$$\begin{aligned} D_{11}(w_{,xxxx} + \delta w_{,yyyy}) + 2(D_{12} + 2D_{66})\delta w_{,xxyy} \\ - B_{11}(\delta u_{,xxx} - \delta v_{,yyy}) + \rho\delta w_{,tt} = 0 \end{aligned} \tag{5.105}$$

Whitney observed that the variations in displacement

$$\begin{aligned} \delta u(x,y,t) &= \bar{u}\cos\frac{m\pi x}{a}\sin\frac{n\pi y}{b}e^{i\omega t} \\ \delta v(x,y,t) &= \bar{v}\sin\frac{m\pi x}{a}\cos\frac{n\pi y}{b}e^{i\omega t} \\ \delta w(x,y,t) &= \bar{w}\sin\frac{m\pi x}{a}\sin\frac{n\pi y}{b}e^{i\omega t} \end{aligned} \tag{5.106}$$

satisfy simply supported edge boundary condition S2 at all time

$$\begin{aligned} x = 0, a: \quad & \delta w = 0 \quad \delta M_x = B_{11}\delta u_{,x} - D_{11}\delta w_{,xx} - D_{12}\delta w_{,yy} = 0 \\ & \delta v = 0 \quad \delta N_x = A_{11}\delta u_{,x} + A_{12}\delta v_{,y} - B_{11}\delta w_{,xx} = 0 \end{aligned} \tag{5.107}$$

$$\begin{aligned} y = 0, b: \quad & \delta w = 0 \quad \delta M_y = -B_{11}\delta v_{,y} - D_{12}\delta w_{,xx} - D_{11}\delta w_{,yy} = 0 \\ & \delta u = 0 \quad \delta N_y = A_{12}\delta u_{,x} + A_{11}\delta v_{,y} + B_{11}\delta w_{,yy} = 0 \end{aligned} \tag{5.108}$$

and the governing differential equations if frequency is

$$\omega^2 = \frac{\pi^4}{\rho}\left[T_{33} + \frac{2T_{12}T_{23}T_{13} - T_{22}T_{13}^2 - T_{11}T_{23}^2}{T_{11}T_{22} - T_{12}^2}\right] \tag{5.109}$$

where the T_{ij} are defined in Equation (5.82) [5-12 and 5-13]. Note that if $B_{11} = 0$, then T_{13} and T_{23} are also zero, so Equation (5.109) reduces to the specially orthotropic plate solution, Equation (5.98), if $D_{11} = D_{22}$. Because T_{11}, T_{12}, and T_{22} are functions of both m and n and appear in the denominator of Equation (5.109), no simple conclusion can be drawn about the values of m and n for the lowest frequency. Instead, Equation (5.109) must be treated as a function of the discrete variables m and n and minimized accordingly. As a matter of fact, for the results presented in the numerical example, the fundamental frequency does correspond to both m and n are one. Caution is urged against a general conclusion for the mode shape of the fundamental frequency.

As for the deflection problem in Section 5.3.3, the effect of the number of layers on the vibrations is found by dividing a constant-thickness, equal-weight cross-ply laminate into more and more laminae as in Figure 5-12. Numerical results from Equation (5.109) are presented in Figure 5-32 for graphite-epoxy composite materials with $E_1/E_2 = 40$, $G_{12}/E_2 = .5$, and $\nu_{12} = .25$. The effect of bending-extension coupling is to lower the vibration frequencies. For example, the fundamental frequency of a square plate is reduced by about 40% from the specially orthotropic plate solution to the exact solution for a two-layered plate.[2] More importantly, the specially orthotropic plate approximation is too high by 60%! As the number of layers increases, the effect of bending-extension coupling decreases. For example, a six-layered plate has a fundamental frequency only 5% smaller than the specially orthotropic plate approximation. Nevertheless, it is readily apparent that bending-extension coupling must be considered in laminated plate vibrations. This conclusion is reinforced by observation of the vibration results for other composite materials in Figure 5-33.

[2]Note that the vibration frequency reductions are far less than the buckling load reductions. That this conclusion must be reached is clear from the fact that Equation (5.109) involves the *square* of the natural frequency, whereas Equation (5.81) involves the buckling load to the first power. Thus, the square root of the differences represented by the right-hand sides of Equations (5.81) and (5.109) is smaller than the differences themselves.

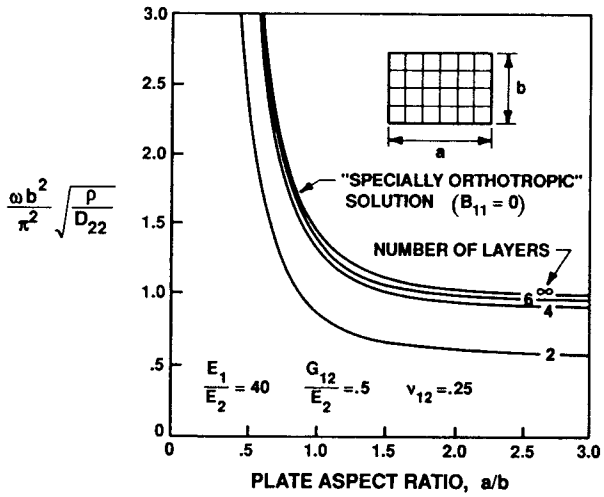

Figure 5-32 Fundamental Natural Vibration Frequencies for Rectangular Antisymmetric Cross-Ply Laminated Plates *(After Jones [5-19])*

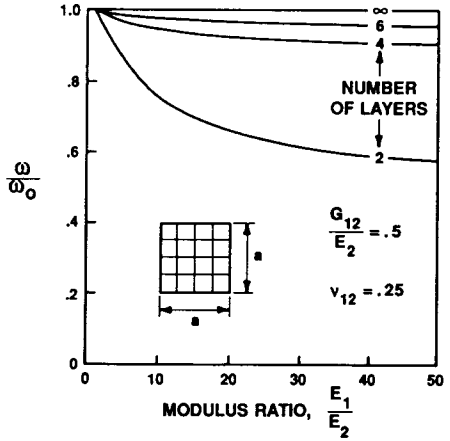

Figure 5-33 Relative Fundamental Natural Vibration Frequencies of Square Antisymmetric Cross-Ply Laminated Plates *(After Jones [5-19])*

5.5.4 Antisymmetric Angle-Ply Laminated Plates

Antisymmetric angle-ply laminates were found in Section 4.3.3 to have extensional stiffnesses A_{11}, A_{12}, A_{22}, and A_{66}; bending-extension coupling stiffnesses B_{16} and B_{26}; and bending stiffnesses D_{11}, D_{12}, D_{22}, and D_{66}. Thus, this laminate exhibits a different kind of bending-extension coupling than the antisymmetric cross-ply laminate discussed in Section 5.5.3. The coupled vibration differential equations are

$$A_{11}\delta u_{,xx} + A_{66}\delta u_{,yy} + (A_{12} + A_{66})\delta v_{,xy} - 3B_{16}\delta w_{,xxy} - B_{26}\delta w_{,yyy} = 0 \quad (5.110)$$

$$(A_{12} + A_{66})\delta u_{,xy} + A_{66}\delta v_{,xx} + A_{22}\delta v_{,yy} - B_{16}\delta w_{,xxx} - 3B_{26}\delta w_{,xyy} = 0 \quad (5.111)$$

$$D_{11}\delta w_{,xxxx} + 2(D_{12} + 2D_{66})\delta w_{,xxyy} + D_{22}\delta w_{,yyyy} - B_{16}(3\delta u_{,xxy} + \delta v_{,xxx}) - B_{26}(\delta u_{,yyy} + 3\delta v_{,xyy}) + \rho\delta w_{,tt} = 0 \quad (5.112)$$

Whitney used the variations in displacements

$$\delta u(x,y,t) = \bar{u}\sin\frac{m\pi x}{a}\cos\frac{n\pi y}{b}e^{i\omega t}$$
$$\delta v(x,y,t) = \bar{v}\cos\frac{m\pi x}{a}\sin\frac{n\pi y}{b}e^{i\omega t} \quad (5.113)$$
$$\delta w(x,y,t) = \bar{w}\sin\frac{m\pi x}{a}\sin\frac{n\pi y}{b}e^{i\omega t}$$

that satisfy the simply supported edge boundary condition S3:

$$x = 0, a: \quad \begin{matrix} \delta w = 0 & \delta M_x = B_{16}(\delta v_{,x} + \delta u_{,y}) - D_{11}\delta w_{,xx} - D_{12}\delta w_{,yy} = 0 \\ \delta u = 0 & \delta N_{xy} = A_{66}(\delta v_{,x} + \delta u_{,y}) - B_{16}\delta w_{,xx} - B_{26}\delta w_{,yy} = 0 \end{matrix} \quad (5.114)$$

$$y = 0, b: \quad \begin{matrix} \delta w = 0 & \delta M_y = B_{26}(\delta v_{,x} + \delta u_{,y}) - D_{12}\delta w_{,xx} - D_{22}\delta w_{,yy} = 0 \\ \delta v = 0 & \delta N_{xy} = A_{66}(\delta v_{,x} + \delta u_{,y}) - B_{16}\delta w_{,xx} - B_{16}\delta w_{,yy} = 0 \end{matrix} \quad (5.115)$$

at all time and the governing differential equations if the frequency is

$$\omega^2 = \frac{\pi^4}{\rho}\left[T_{33} + \frac{2T_{12}T_{23}T_{13} - T_{22}T_{13}^2 - T_{11}T_{23}^2}{T_{11}T_{22} - T_{12}^2}\right] \quad (5.116)$$

where the T_{ij} are defined in Equation (5.93) [5-12 and 5-13]. Note that if B_{16} and B_{26} are zero, then T_{13} and T_{23} are also zero, so Equation (5.116) reduces to the specially orthotropic plate solution, Equation (5.65). The character of Equation (5.116) is the same as that of Equations (5.81), (5.92), and (5.109), so the remarks in Section 5.4.3 are equally valid here.

As for the deflection problem in Section 5.3.4, the effect of the number of layers on the vibrations is found by dividing a constant-thickness, equal-weight angle-ply laminate into more and more laminae as in Figure 5-15. Numerical results for graphite-epoxy composite materials with $E_1/E_2 = 40$, $G_{12}/E_2 = .5$, and $\nu_{12} = .25$ are given as a function of lamination angle in Figure 5-34. As with B_{11} in Section 5.5.3, the effect of the bending-extension coupling stiffnesses B_{16} and B_{26} is to lower the fundamental vibration frequencies. For example, the fundamental natural frequency of a square plate with $\theta = 45°$ and two layers is about 40% less than the specially orthotropic plate solution which is valid when the number of layers is infinite. Put another way, the specially orthotropic plate solution is too high by about 80%! Again, as the number of layers increases, the bending-extension coupling decreases rapidly. For a six-layered plate, the difference between the specially orthotropic plate solution and the exact solution is about 4%. Obviously, bending-extension coupling can be quite important for antisymmetrically laminated plates.

This conclusion is unchanged when other composite materials are considered as in Figure 5-35.

Problem Set 5.5

5.5.1 Derive Equation (5.98).
5.5.2 Derive Equation (5.109). See hint in Problem 5.4.2.
5.5.3 Derive Equation (5.116). See hint in Problem 5.4.2.

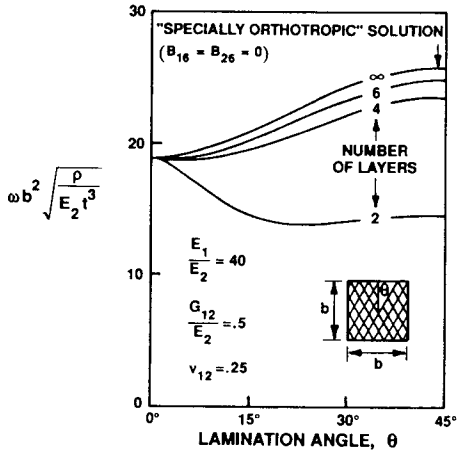

Figure 5-34 Fundamental Natural Vibration Frequencies for Square Antisymmetric Angle-Ply Laminated Plates *(After Jones, Morgan, and Whitney [5-22])*

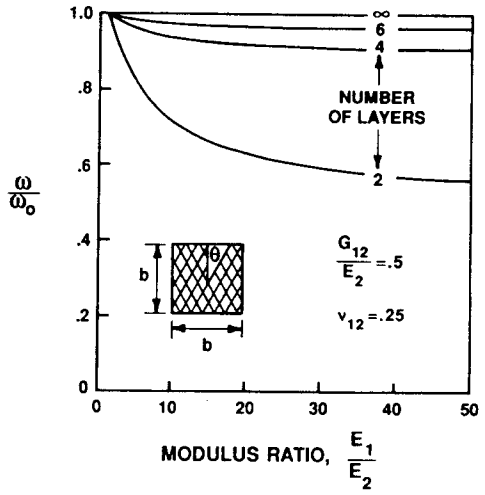

Figure 5-35 Relative Fundamental Natural Vibration Frequencies of Square Antisymmetric Angle-Ply Laminated Plates

5.6 SUMMARY REMARKS ON EFFECTS OF STIFFNESSES

The presence of bending-extension coupling in a laminated plate generally increases deflections. Hence, coupling decreases the effective bending stiffnesses of a laminate. At the same time, this coupling reduces buckling loads and vibration frequencies significantly as would be expected for plates with effectively lower bending stiffnesses.

Similarly, for laminated plates with bend-twist coupling, the deflections are increased, the buckling loads decreased, and the vibration frequencies decreased. In both cases of bending-extension coupling and bend-twist coupling, the effect on deflections, buckling loads, and vibration frequencies for a fixed-thickness antisymmetric or symmetric laminate, respectively, dies out rapidly as the number of layers increases. For more general laminates, specific investigation is required. That is, *there is simply no guarantee or even any reason to expect that conclusions reached for many layered antisymmetric laminated plates have any validity whatsoever for more general unsymmetrically laminated plates.*

A somewhat more general class of laminates, unsymmetric cross-ply laminates, was discussed by Jones [5-19] as well as Jones and Morgan [5-23]. All geometric and material property symmetry requirements of the preceding sections are relaxed. Still, the restriction to cross-ply laminates (of arbitrary layer thickness and 0° and 90° stacking sequence) enables a simple exact solution to be obtained. However, because of the infinite complexity of this class of laminates, general results are impossible. Instead, consider the cross sections of the contrived, but representative unsymmetric laminate example in Figure 5-36. There, the fibers in the second layer from the bottom are always oriented at 90°, and the fibers in all other layers are oriented at 0° to the plate x-axis. Thus, for a constant-thickness laminate, the 90° layer gets thinner and moves toward the bottom of the laminate as the number of layers increases. This example is probably never encountered in engineering practice, but it is a simple, straightforward example of unsymmetric laminates that is amenable to comprehensive parametric study. The results obtained will serve as a very simple proof by contradiction that the structural effects of bending-extension coupling do not necessarily die out rapidly as the number of layers increases (contrary to the

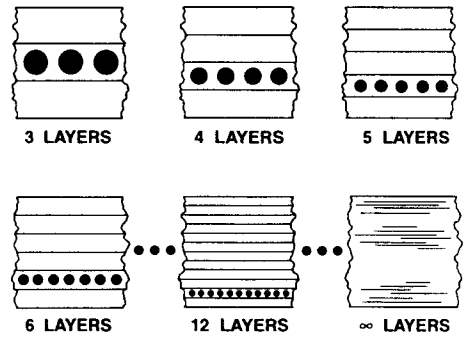

Figure 5-36 Unsymmetric Cross-Ply Laminate Example *(After Jones [5-19])*

results for antisymmetric cross-ply and angle-ply laminated plates). The applicable theory is already available in Sections 5.3–5.5.

Normalized maximum deflections (at the center) for graphite-epoxy unsymmetrically cross-ply laminated rectangular plates with uniform transverse loading are shown in Figure 5-37. The results are obtained by summing exact deflection solutions, Equation (5.49), for each component of the Fourier sine series expansion for a uniform transverse load, Equation (5.26). The plate aspect ratio is 3, a value for which the results are the most strikingly different from the baseline results of a laminate with all 0° layers in the x-direction (in which a = 3b) and the unsymmetric laminate with bending-extension coupling ignored ($B_{ij} = 0$): hence, an orthotropic laminate or a specially orthotropic laminate. The unsymmetric laminate is stiffer than the all-0°-layer laminate (i.e., less center deflection occurs for the unsymmetric laminate) and more flexible than the orthotropic laminate.

We will see that the unsymmetric laminate has more bending stiffness in the y-direction than the all-0°-layer laminate and almost as much bending stiffness in the x-direction. Thus, the center deflection of the unsymmetrically laminated plate *should* exceed that of the all-0°-layer laminated plate. However, we are already aware that bending-extension coupling increases deflections, so the center deflection of the unsymmetric laminate *should* exceed that of the orthotropic laminated plate.

The real point of this example is that the deflection effects just discussed are very significant for numbers of layers that, in our studies of antisymmetric laminates earlier in this chapter, we concluded that bending-extension coupling had disappeared! Here, the exact solution exceeds the orthotropic solution by 165% at 6 layers, 165% at 10 layers, 90% at 20 layers, and 30% at 50 layers. Even at 100 layers, the discrepancy is still 11%. These differences are well within the consideration

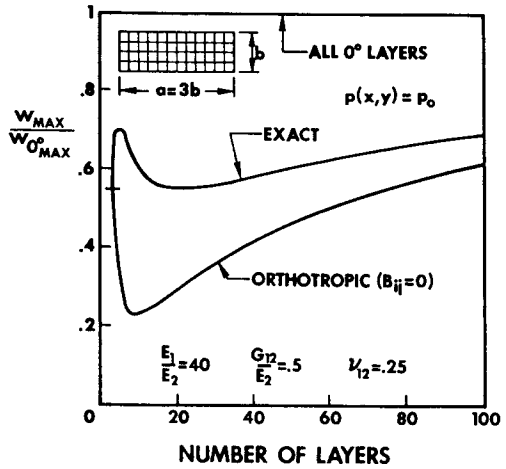

Figure 5-37 Deflection under Uniform Transverse Loading of Unsymmetric Cross-Ply Laminated Graphite-Epoxy Plates *(After Jones and Morgan [5-23])*

of usual engineering design practice. These discrepancies exist for many more layers than bending-extension coupling was believed to be important. That belief (by some, not all) was established on the basis of extrapolating antisymmetric cross-ply and antisymmetric angle-ply results like those in Sections 5.2 through 5.4. Obviously, such extrapolation is invalid. However, truly no one had any better basis except to remain skeptical and try to find out what actually happens for unsymmetric laminates.

As an aid to understanding the deflection behavior in Figure 5-36, the normalized extensional, bending-extension coupling, and bending stiffnesses are plotted versus the number of layers in Figure 5-38. The stiffnesses in the x-direction (with which most fibers are aligned), $\bar{A}_{11}$ and $\bar{D}_{11}$, are nearly independent of the number of layers. However, the 90° layer causes the stiffnesses in the y-direction, $\bar{A}_{22}$ and $\bar{D}_{22}$, to deviate by up to an order of magnitude from the values for the all-0°-layer laminate (which are the same as for an infinite number of layers). These discrepancies die out very, very slowly as the number of layers increases. Moreover, the normalized stiffness for bending-extension coupling, which can be shown to be

$$\frac{B_{11}}{Q_{11}t^2} = \frac{1}{2N^2}\left[1 - \frac{E_2}{E_1}\right](N-3) \tag{5.117}$$

(where N is the number of layers) and which appears in Equation (5.81) and thereby enables stiffnesses A_{22} and D_{22} to influence the buckling load, also dies out very slowly. The maximum bending-extension coupling occurs for this unsymmetric laminate at N = 6. Do not attempt to compare the magnitudes of, for example, the terms $\bar{D}_{22}$ and $B_{11}/(Q_{11}t^2)$

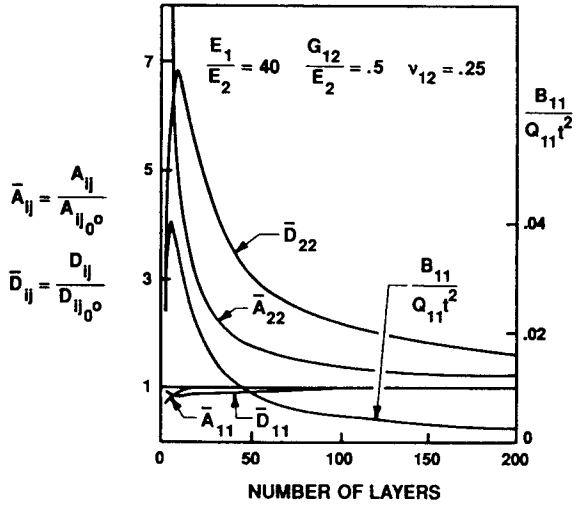

Figure 5-38 Normalized Stiffnesses of Example Unsymmetric Cross-Ply Graphite-Epoxy Laminate *(After Jones [5-19])*

quantitatively. They do not have the same base for normalization (B_{11} cannot be normalized relative to its value for an all-0°-layer laminate because in that case its value is zero). Thus, the effect of a single unsymmetrically placed 90° layer on the deflection dies out very slowly as the number of layers increases.

Normalized buckling loads for graphite-epoxy unsymmetric cross-ply laminated rectangular plates are shown in Figure 5-39. The plate aspect ratio is 2, a value for which the results are the most strikingly different from baseline results. One of the baseline comparison values is the buckling load for a laminate with all 0° layers. The other comparison case is an unsymmetric laminate for which bending-extension coupling is ignored ($B_{ij} = 0$). Results for the actual unsymmetric laminate, for which coupling is considered, are labeled exact solution. The actual laminate has, not surprisingly, less buckling resistance than a laminate with $B_{ij} = 0$. On the other hand, the actual laminate has more buckling resistance than a laminate with all 0° layers. This curious result is a consequence of the relative values of the bending stiffnesses in the x- and y-directions as well as the plate aspect ratio. As will be seen subsequently, D_{11} is decreased somewhat by the presence of a 90° layer, but simultaneously D_{22} is increased by factors of up to an order of magnitude. The influence of D_{22} is most easily examined for a three-layered plate that is, of course, symmetric. Thus, the exact solution corresponds to the specially orthotropic solution ($B_{ij} = 0$); for example, see the horizontal mark at three layers in Figure 5-39 where the two curves coincide. At that point, the specially orthotropic solution for a plate with an aspect ratio of 2 which buckles into the m = 1, n = 1 mode is

$$\bar{N}_x L^2 = \pi^2 \left[\frac{D_{11}}{4} + 2(D_{12} + 2D_{66}) + 4D_{22} \right] \qquad (5.118)$$

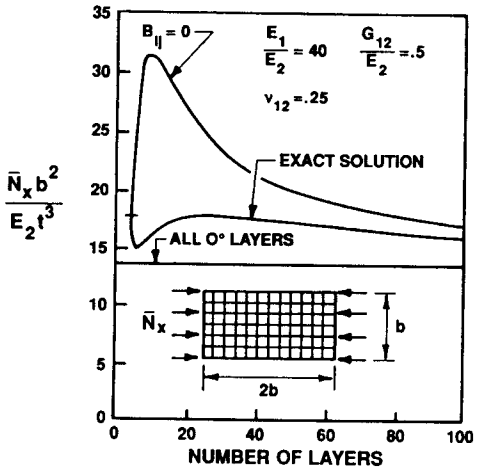

Figure 5-39 Uniaxial Buckling Loads of Graphite-Epoxy Unsymmetric Cross-Ply Laminated Rectangular Plates *(After Jones [5-19])*

which is readily obtained from Equation (5.81). The term in Equation (5.118) involving D_{11} decreases by less than 4% when the actual laminate is considered as opposed to the all-0°-layer laminate. The net result is a normalized buckling load that is 33% bigger for the actual laminate than for the all-0°-layer laminate.

The differences between the exact, specially orthotropic, and all-0°-layer predictions in Figure 5-39 range from 48% less than the specially orthotropic solution at 6 layers to 18% less at 40 layers to 6% less at 100 layers. In addition, the exact results range from about 30% more than the all-0°-layer laminate results at 30 layers to about 18% more at 100 layers. Again, such differences are well within the consideration of usual engineering design practice.

Normalized fundamental natural frequencies for the example unsymmetrical cross-ply laminated graphite-epoxy plates are shown in Figure 5-40. The vibration results are analogous to the buckling results in the same manner as explained for antisymmetric laminates, namely, lesser differences for vibration frequencies because of the square-root factor.

The approximation of a general laminate by a specially orthotropic laminate can result in errors as big as a factor of 3. Thus, use of the specially orthotropic approximation must be carefully proven to be justified for each case under consideration. Always remember that the specially orthotropic approximation yields *unconservative* results. Thus, the only general rule is that bending-extension coupling and bend-twist coupling should be included in every analysis of laminated plates unless such coupling is proven to be insignificant for the specific laminated plate under consideration.

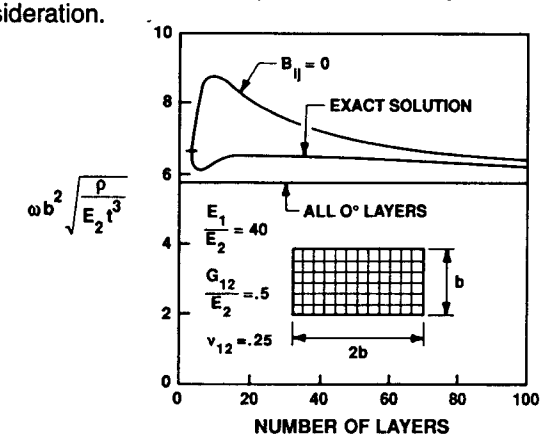

Figure 5-40 Fundamental Natural Vibration Frequencies of Rectangular Unsymmetric Cross-Ply Graphite-Epoxy Plates *(After Jones [5-19])*

More Accurate Approach to Bend-Twist Coupling

The effects of the bend-twist coupling stiffnesses on deflections, buckling loads, and vibration frequencies of laminated plates can be as-

sessed more accurately than in this book by use of a procedure due to Whitney [5-24]. He uses a double Fourier series expansion of the unknown displacement to satisfy the natural boundary conditions and thereby speed convergence to precise results. Note that the Rayleigh-Ritz method described here does not satisfy the natural boundary conditions and therefore convergence is very slow and sometimes not to the correct solution. As an example, consider a simply supported square graphite-epoxy plate ($E_1/E_2 = 25$, $\nu_{12} = .25$, and $Q_{66}/Q_{22} = .5$) with principal material directions at 45° to the plate sides. When the plate is subjected to biaxial in-plane compression, $\bar{N}_x = \bar{N}_y$, the buckling loads are given in Table 5-4 for Whitney's approach and the Rayleigh-Ritz approach due to Ashton [5-25]. Obviously, Whitney's results converge rapidly although there is some oscillation. In contrast, the Rayleigh-Ritz results converge (?) slowly and to an incorrect value. Ashton showed that the rate of convergence of a Rayleigh-Ritz method for simply supported anisotropic plates depends on the orthotropy ratio, E_1/E_2, when the natural boundary conditions are not satisfied [5-26]. Thus, his results in Table 5-4 are to be expected.

Table 5-4 Buckling under Biaxial Compression of Simply Supported Square Graphite-Epoxy Anisotropic Plates* *(After Whitney [5-24])*

Number of Terms in Series m = n	$\bar{N}b^2/Q_{22}t^3$	
	Whitney's Fourier Analysis	Ashton's Rayleigh-Ritz Analysis
1	6.763	21.438
3	8.115	13.013
5	8.318	11.565
7	8.418	11.060
9	8.481	-
11	8.521	-
13	8.556	-

*$Q_{11}/Q_{22} = 25$, $Q_{12}/Q_{22} = .25$, $Q_{66}/Q_{22} = .5$ with principal material directions at 45° to plate sides

Reduced Bending Stiffness Approach

In their pioneering paper on laminated plates, Reissner and Stavsky investigated an approximate approach (in addition to their exact approach) to calculate deflections and stresses for antisymmetric angle-ply laminated plates [5-27]. Much later, Ashton extended their approach to structural response of more general unsymmetrically laminated plates and called it the 'reduced stiffness matrix' method [5-28]. The attraction of what is now called the Reduced Bending Stiffness (RBS) method is that an unsymmetrically laminated plate can be treated as an orthotropic plate using only a modified D matrix in the solution, i.e.,

$$D^* = D - BA^{-1}B \tag{5.119}$$

or, at worst, an anisotropic plate if the D^* matrix is full. Thus, analyses in which only bending stiffnesses occur can be used to treat unsymmetric

laminates that actually have all three stiffness matrices by replacing the various elements of the D matrix with the corresponding elements of the D^* matrix. Note that physically this substitution makes sense, i.e., a lower D^* than D would lead to higher deflections and lower buckling loads and vibration frequencies, as we know happens when bending-extension coupling exists. However, the term $BA^{-1}A$ must be proven positive for D^* to be less than D (and it has not been proven for other than antisymmetric cross-ply and angle-ply laminated plates). In the one-dimensional case of cylindrical bending of a plate examined in Section 6.5, the exact coefficient on the deflection is shown to be

$$D_{11}^* = D_{11} - \frac{B_{11}^2}{A_{11}} \tag{5.120}$$

which is the one-dimensional equivalent of Equation (5.119) and, indeed, $D^* < D$. Ashton obtained reasonably accurate approximations to Whitney's results for antisymmetric cross-ply and angle-ply laminated plates under uniform and sinusoidal transverse loading [5-14]. A disadvantage of the RBS approximation is that in-plane boundary conditions are not included so there is no distinction between the four simply supported edge boundary conditions in Equation (5.11) nor between the four clamped edge boundary conditions in Equation (5.12). Thus, it is not surprising that Whitney found significant differences between various clamped edge solutions and the RBS approximation for bending, buckling, and vibration of antisymmetric cross-ply and angle-ply laminated plates [5-29]. Ewing, Hinger, and Leissa found excellent agreement (error ≤ .25%) for bending, buckling, and vibration of antisymmetric cross-ply plates with S2 boundary conditions [5-30]. However, they found far less favorable results for antisymmetric angle-ply plates with S3 boundary conditions (up to 28% overestimate in maximum deflection, 22% underestimate in buckling loads, and 12% underestimate in vibration frequencies in the worst-case situation of two-layered square plates with $\theta = \pm 10°$). Unfortunately, the quality of the approximation has not been determined for truly unsymmetric laminates, such as the unsymmetric cross-ply at the beginning of Section 5.6 or more practically applicable laminates.

REFERENCES

5-1 James M. Whitney, *Structural Analysis of Laminated Anisotropic Plates*, Technomic, Lancaster, Pennsylvania, 1987. See also J. E. Ashton and J. M. Whitney, *Theory of Laminated Plates*, Technomic, Westport, Connecticut, 1970.

5-2 J. R. Vinson and R. L. Sierakowski, *The Behavior of Structures Composed of Composite Materials*, Martinus Nijhoff, Dordrecht, The Netherlands, 1986.

5-3 Valery V. Vasiliev [Robert M. Jones (English Edition Editor)], *Mechanics of Composite Structures*, Taylor & Francis, Washington, 1993.

5-4 J. N. Reddy, *Mechanics of Laminated Composite Plates: Theory and Analysis*, CRC Press, Boca Raton, Florida, 1997.

5-5 S. P. Timoshenko and S. Woinowsky-Krieger, *Theory of Plates and Shells*, McGraw-Hill, New York, 1959.

5-6 B. O. Almroth, Influence of Edge Conditions on the Stability of Axially Compressed Cylindrical Shells, *AIAA Journal*, January 1966, pp. 134–140.

5-7 Robert M. Jones and Jose C. F. Hennemann, Effect of Prebuckling Deformations on Buckling of Laminated Composite Circular Cylindrical Shells, *AIAA Journal*, January 1980, pp. 110–115.

5-8 James Ting-shun Wang, On the Solution of Plates of Composite Materials, *Journal of Composite Materials*, July 1969, pp. 590–592.

5-9 J. E. Ashton, *Anisotropic Plate Analysis*, General Dynamics Research and Engineering Report, FZM-4899, 12 October 1967.

5-10 Henry L. Langhaar, *Energy Methods in Applied Mechanics*, John Wiley, New York, 1962 (also Krieger, Malabar, Florida, 1982).

5-11 J. E. Ashton, An Analogy for Certain Anisotropic Plates, *Journal of Composite Materials*, April 1969, pp. 355–358.

5-12 J. M. Whitney and A. W. Leissa, Analysis of Heterogeneous Anisotropic Plates, *Journal of Applied Mechanics*, June 1969, pp. 261–266.

5-13 James Martin Whitney, *A Study of the Effects of Coupling Between Bending and Stretching on the Mechanical Behavior of Layered Anisotropic Composite Materials*, Ph.D thesis, Department of Engineering Mechanics, The Ohio State University, Columbus, Ohio, 1968. (Available from University Microfilms, Inc., Ann Arbor, Michigan, as no. 69-5000.)

5-14 J. M. Whitney, Bending-Extension Coupling in Laminated Plates Under Transverse Loading, *Journal of Composite Materials*, January 1969, pp. 20–28.

5-15 Stephen P. Timoshenko and James M. Gere, *Theory of Elastic Stability*, McGraw-Hill, New York, 1961.

5-16 J. E. Ashton and M. E. Waddoups, Analysis of Anisotropic Plates, *Journal of Composite Materials*, January 1969, pp. 148–165.

5-17 C. C. Chamis, *Thermostructural Response, Structural and Material Optimization of Particulate Composite Plates*, Case Western Reserve University, Report No. SMSMDD 21, Cleveland, Ohio, 1968.

5-18 J. F. Mandell, *Experimental Investigation of the Buckling of Anisotropic Fiber Reinforced Plastic Plates*, Air Force Materials Laboratory Technical Report AFML-TR-68-281, October 1968.

5-19 Robert M. Jones, Buckling and Vibration of Rectangular Unsymmetrically Laminated Cross-Ply Plates, *AIAA Journal*, December 1973, pp. 1626–1632.

5-20 Robert M. Jones, Plastic Buckling of Eccentrically Stiffened Multilayered Circular Cylindrical Shells, *AIAA Journal*, February 1970, pp. 262–270.

5-21 Robert M. Jones, *Plastic Buckling of Eccentrically Stiffened Circular Cylindrical Shells*, Aerospace Corporation Report No. TR-0158(S3816-72)-1, San Bernardino, California, December 1967. See also *AIAA Journal*, June 1967, pp. 1147–1152.

5-22 Robert M. Jones, Harold S. Morgan, and James M. Whitney, Buckling and Vibration of Antisymmetrically Laminated Angle-Ply Rectangular Plates, *Journal of Applied Mechanics*, December 1973, pp. 1143–1144.

5-23 Robert M. Jones and Harold S. Morgan, Deflection of Unsymmetrically Laminated Cross-Ply Rectangular Plates, *Proceedings of the 12th Annual Meeting of the Society of Engineering Science*, 20–22 October 1975, Austin, Texas, pp. 155–167.

5-24 J. M. Whitney, *On the Analysis of Anisotropic Rectangular Plates*, Air Force Materials Laboratory Technical Report AFML-TR-72-76, August 1972.

5-25 J. E. Ashton, Clamped Skew Plates of Orthotropic Material Under Transverse Load, in *Developments in Mechanics*, Vol. 5, The Iowa State University Press, Ames, Iowa, 1969, pp. 297–306.

5-26 J. E. Ashton, Anisotropic Plate Analysis—Boundary Conditions, *Journal of Composite Materials*, April 1970, pp. 162–171.

5-27 E. Reissner and Y. Stavsky, Bending and Stretching of Certain Types of Heterogeneous Aeolotropic Elastic Plates, *Journal of Applied Mechanics*, September 1961, pp. 402–408.

5-28 J. E. Ashton, Approximate Solutions for Unsymmetrically Laminated Plates, *Journal of Composite Materials*, January 1969, pp. 189–191.

5-29 J. M. Whitney, The Effect of Boundary Conditions on the Response of Laminated Composites, *Journal of Composite Materials*, April 1970, pp. 192–203.

5-30 M. S. Ewing, R. J. Hinger, and A. W. Leissa, On the Validity of the Reduced Bending Stiffness Method for Laminated Composite Plate Analysis, *Composite Structures*, Volume 9, 1988, pp. 301–317.

Chapter 6

OTHER ANALYSIS AND BEHAVIOR TOPICS

6.1 INTRODUCTION

The objective of this chapter is to address introductory sketches of some fundamental behavior issues that affect the performance of composite materials and structures. The basic questions are, given the mechanics of the problem (primarily the state of stress) and the materials basis of the problem (essentially the state of the material): (1) what are the stiffnesses, (2) what are the strengths, and (3) what is the life of the composite material or structure as influenced by the behavioral or environmental issues in Figure 6-1?

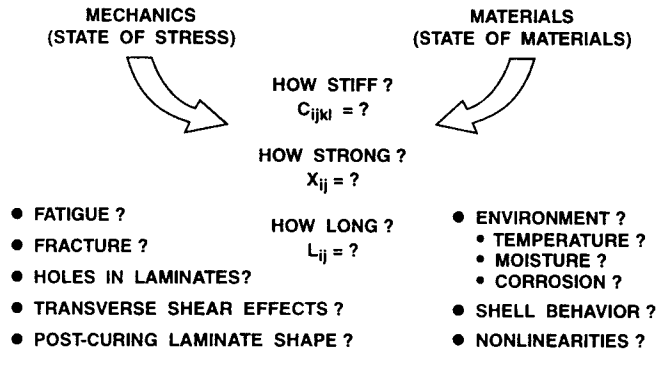

Figure 6-1 Basic Questions in Composite Materials and Structures

6.2 REVIEW OF CHAPTERS 1 THROUGH 5

The basic nature of composite materials was introduced in Chapter 1. An overall classification scheme was presented, and the mechanical behavior aspects of composite materials that differ from those of conventional materials were described in a qualitative fashion. The book was then restricted to laminated fiber-reinforced composite materials. The basic definitions and how such materials are made were then treated. Finally, the current and potential advantages of composite materials were discussed along with some case histories that clearly reveal how composite materials are used in structures.

The macromechanical behavior of a lamina was quantitatively described in Chapter 2. The basic three-dimensional stress-strain relations for elastic anisotropic and orthotropic materials were examined. Subsequently, those relations were specialized for the plane-stress state normally found in a lamina. The plane-stress relations were then transformed in the plane of the lamina to enable treatment of composite laminates with different laminae at various angles. The various fundamental strengths of a lamina were identified, discussed, and subsequently used in biaxial strength criteria to predict the off-axis strength of a lamina.

The micromechanical behavior of a lamina was treated in Chapter 3. Both a mechanics of materials and an elasticity approach were used to predict the fundamental lamina stiffnesses that were compared to measured stiffnesses. Mechanics of materials approaches were used to predict some of the fundamental strengths of a lamina.

A collection of the basic building block, a lamina, was bonded together to form a laminate in Chapter 4. The behavior restrictions were covered in the section on classical lamination theory. Special cases of laminates were discussed to learn about laminate characteristics and behavior. Predicted and measured laminate stiffnesses were favorably compared to give credence to classical lamination theory. Then, the strength of laminates was discussed and found to be reasonably predictable. Finally, interlaminar stresses were analyzed because of their apparent strong influence on laminate strength (and life).

The influence of composite laminate characteristics on analysis of bending, buckling, and vibration of plates was examined in Chapter 5. First, the governing differential equations were introduced. Then, each of the basic structural problems was analyzed for orthotropic, anisotropic, antisymmetric cross-ply, and antisymmetric angle-ply laminated, simply supported, rectangular plates. Thus, the effects of bend-twist coupling and bending-extension coupling on structural response were evaluated with special attention paid to general laminates in which these effects could be important.

Obviously, the foregoing description of problems in the mechanics of composite materials is incomplete. Some topics do not fit well within the logical framework just described. Other topics are too advanced for an introductory book, even at the graduate level. Thus, the rest of this chapter is devoted to a brief discussion of some basic lamina and laminate analysis and behavior characteristics that are not included in preceding chapters.

6.3 FATIGUE

Fatigue of a structural element may be a significant design parameter in some applications. The aircraft crashes caused by fatigue failures are well known. Thus, the obvious question is: how do composite materials fatigue characteristics compare to those of conventional metals? The answer is, in brief, much better! The material or internal damping in composite materials is high, yet the fatigue characteristics are quite good. One of the main reasons for this fortunate circumstance is schematically depicted in Figure 6-2 [6-1]. There, the initial imperfections in composite materials such as broken fibers, delamination, matrix cracking, fiber-matrix debonding, voids, etc., can be much larger than corresponding imperfections in conventional metals such as cracks. In contrast, the initial imperfection in a metal is simply a small crack. However, the growth of damage in a metal is typically much more abrupt, as evidenced by Figure 6-2, and hence potentially more dangerous than in a composite material.

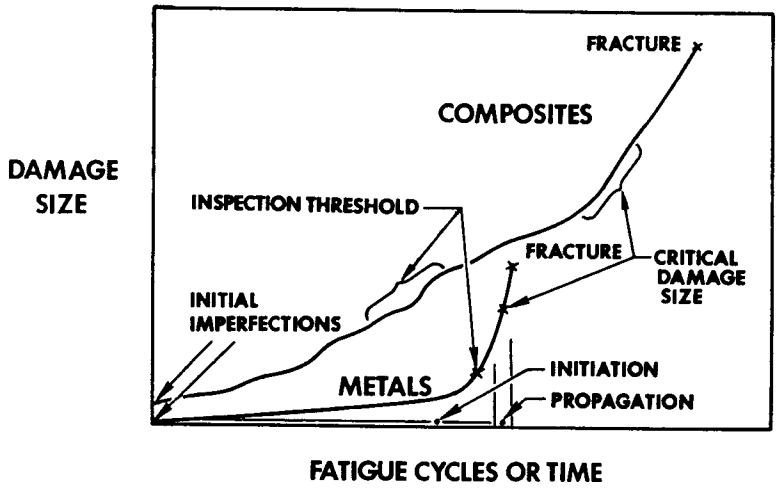

Figure 6-2 Fatigue Damage Behavior of Composite Materials and Metals *(After Salkind [6-1])*

Composite materials undergo a variety of different damage modes during fatigue as in Figure 6-3. There, stage 1 is characterized by matrix cracking and fiber breaking. Stage 2 consists of coupling of cracks with interfacial debonding in addition to fiber breaking. Stage 3 includes delamination as well as fiber breaking. Stage 4 has delamination growth along with localized fiber breaking. Stage 5 is gross fracture of the entire material. This figure is the basis for the approach to damage mechanics used by Reifsnider, Henneke, Stinchcomb, and Duke [6-2].

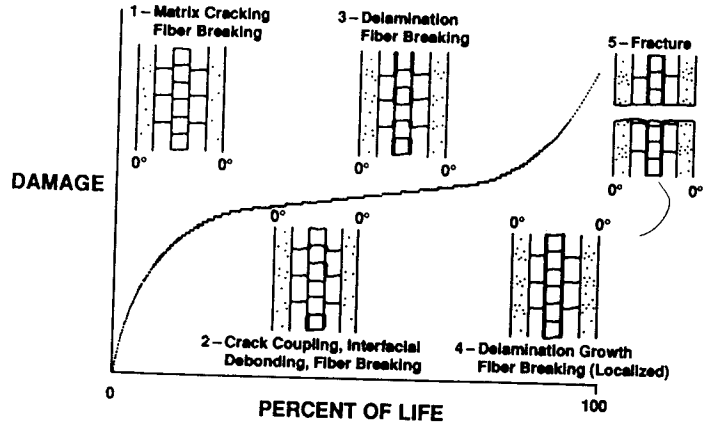

Figure 6-3 Damage Modes during Fatigue Life
(After Reifsnider, Henneke, Stinchcomb, and Duke [6-2])

Because of the many types of damage and damage growth in composite materials, the initial state of the material is difficult, if not impossible, to characterize. Moreover, it is much more difficult to formulate a boundary-value problem to describe crack propagation in composite materials than in metals.

Typical S-N (stress versus number of cycles) curves for various metals and composite materials are shown in Figure 6-4 [6-3]. The boron-epoxy composite material curve is much flatter than the aluminum curve as well as being flatter than the curves for any of the metals shown. The susceptibility of composite materials to effects of stress concentrations such as those caused by notches, holes, etc., is much less than for metals. Thus, the initial advantage of higher strength of boron-epoxy

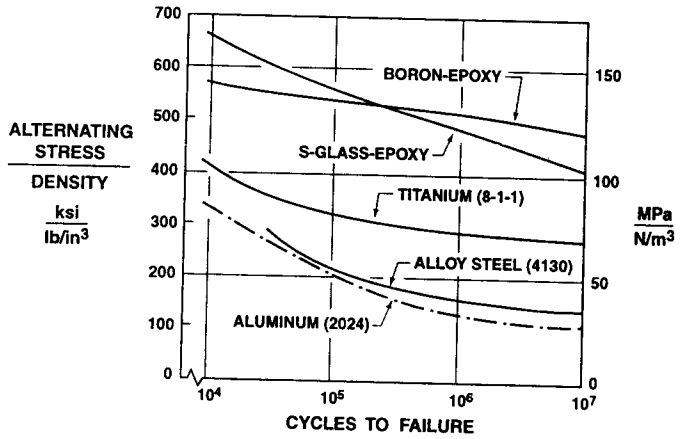

Figure 6-4 Typical Tension-Tension Fatigue Data *(After Pinckney [6-3])*

over aluminum in Figure 6-4 actually *increases* under fatigue conditions. This advantage of increased life as well as increased specific strength and stiffness over conventional metals is one of the principal reasons for the rapidly expanding use of composite materials. Salkind [6-4] reviewed fatigue characteristics of composite materials. Eisenmann, Kaminski, Reed, and Wilkins [6-5] used fatigue characteristics as a basis for a composite materials reliability procedure. Talreja characterizes the fatigue process, fatigue damage characterization, and fatigue reliability in a monograph on his work [6-6].

Fatigue has a strong effect on the stiffness of a composite material in addition to the strength effect just discussed. A typical metal such as steel is qualitatively contrasted with a composite material such as graphite-epoxy on the basis of measured stiffness versus life in Figure 6-5. There, the metal typically retains most of its stiffness until a high percentage of its life is gone, and then the stiffness drops precipitously. In contrast, a composite material is more likely to lose stiffness gradually and significantly over its lifetime. Two implications of Figure 6-5 are clear. First, composite materials typically have longer fatigue lives than metals. Second, composite materials give a warning that the material is losing life in the sense that significantly lower stiffness is perceived. However, metals give virtually no warning that their life is over. These two characteristics can be used to advantage in two quite different structural applications, cables and springs.

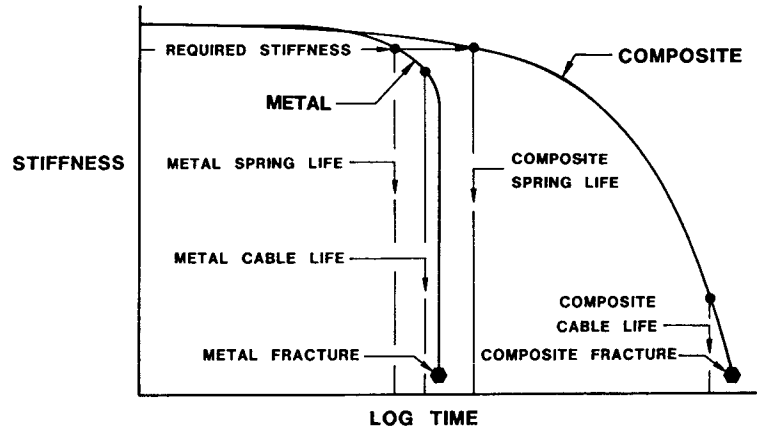

Figure 6-5 Metal versus Composite Material Stiffness Behavior in Fatigue
(After Salkind [6-4])

For cables such as in elevators or cranes, the service life might be based on 95% of the fatigue life of the material. In such circumstances, a composite cable would clearly last far longer than a metal cable. Moreover, the composite cable length, if measured, would be found to be longer than originally as time passes (an elevator would have to be periodically adjusted to stop precisely at each floor). Such measurements when recorded would be an evidential record of the cable per-

formance and a sign of what is to come. Metal cables have no such sign. Exceeding the service life by 5% would obviously result in cable breakage for both materials.

For springs such as in cars or trucks, the service life would probably be based on a certain minimum level of stiffness. Otherwise, springs that are too flexible would permit the vehicle to sag so low that some parts of the vehicle might drag on the highway or otherwise not perform correctly. We can tell from Figure 6-5 that composite spring life significantly exceeds metal spring life. That result is a quantifiable economic advantage for composite springs. A perhaps more important advantage of composite springs over metal springs is that if composite springs are used beyond their service life based on required minimum stiffness, they will not fail by breaking, whereas metal springs will break without warning. Composite springs will give clear warning by deforming excessively far before they fail by breaking! Thus, composite springs have a built-in stiffness reserve along with an automatic warning of impending difficulty.

6.4 HOLES IN LAMINATES

Laminates, as any structure, must have holes to serve various purposes. An obvious purpose is to accommodate a bolt. Another purpose is to provide access from one side of the laminate to the other. The analysis of the stresses around holes is quite difficult.

One of the first solutions to the problem of stresses around an elliptical hole in an infinite anisotropic plate was given by Lekhnitskii [6-7]. A more recent and comprehensive summary of the problem and many others is Savin's monograph [6-8]. Numerous results by Lekhnitskii are shown in his books [6-9 and 6-10]. Two special cases are of particular interest.

First, stress is applied in one of the principal material directions on an orthotropic plate as in Figure 6-6. There, Greszczuk [6-11] plotted the circumferential stress around the hole for an isotropic material and several unidirectional composite materials. Observe that the usual isotropic material stress concentration factor is 3; that is, $\sigma_{\theta_1}/\sigma_1 = 3$ at $\theta = 90°$. For composite materials, the stress concentration factor is much higher (4 for glass-epoxy, about 6 for boron-epoxy, and about 9 for graphite-epoxy). Moreover, the circumferential stress at $\theta = 0°$ is reduced for composite materials relative to isotropic materials. Because the material properties are isotropic, the key factor in failure of isotropic plates with holes is the magnitude of the stress concentration factor from which the maximum (failure) stress is obtained. However, for orthotropic materials, a combined stress failure criterion instead of a maximum stress failure criterion must be used as noted in Section 2.9. Also, many isotropic engineering materials such as steel or aluminum are ductile enough to yield to accommodate stress concentrations locally in the vicinity of a stress concentration. However, most composite materials are considerably less ductile than isotropic metals. Thus, composite materials have the dual disadvantage of higher stress concentrations and less ability to yield than isotropic metals. Accordingly, stress concentration factors alone, as in

Figure 6-6, are insufficient for failure prediction of orthotropic (and anisotropic) plates. Moreover, if the plates are laminated, the comparison of stress states with failure stress states must be done on a layer-by-layer basis.

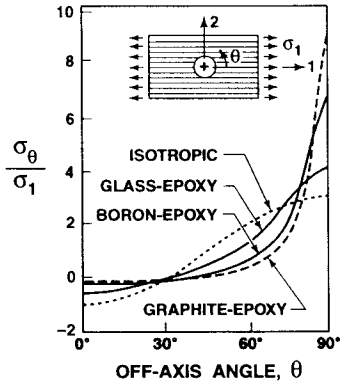

Figure 6-6 Effect of Material Properties on Circumferential Stress σ_θ at the Edge of a Circular Hole in an Orthotropic Plate under σ_1 *(After Greszczuk [6-11])*

The second special case is an orthotropic lamina loaded at angle α to the fiber direction. Such a situation is effectively an anisotropic lamina under load. Stress concentration factors for boron-epoxy were obtained by Greszczuk [6-11] in Figure 6-7. There, the circumferential stress around the edge of the circular hole is plotted versus angular position around the hole. The circumferential stress is normalized by σ_α, the applied stress. The results for $\alpha = 0°$ are, of course, identical to those in Figure 6-6. As α approaches 90°, the peak stress concentration factor decreases and shifts location around the hole. However, as shown, the combined stress state at failure, upon application of a failure criterion, always occurs near $\theta = 90°$. Thus, the analysis of failure due to stress concentrations around holes in a lamina is quite involved.

The next obvious step is to extend the analysis to a laminate. Greszczuk considered a symmetric cross-ply laminate that is subjected to tension in a fiber direction [6-11]. The resulting stress concentration is shown in Figure 6-8. As before, the circumferential stress is normalized by the applied stress. However, the circumferential stress is not a maximum lamina stress but a gross stress on the entire laminate; that is, it is actually N_θ/t, where N_θ is a circumferential force per unit width and t is the laminate thickness. The stresses in each lamina are then found by use of the concepts in Section 4.2, classical lamination theory. Failure is determined by application of a biaxial strength criterion to *each* layer. Thus, the effect of holes on laminate behavior is much more complex than on lamina or plate behavior. The interlaminar stresses studied in Section 4.6 are ignored. Accordingly, the predicted stresses are not accurate within about one laminate thickness from the edge.

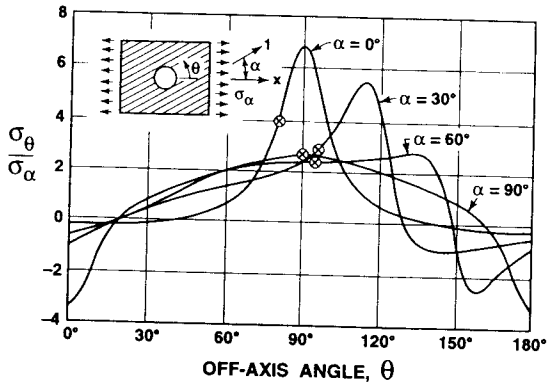

Figure 6-7 Stress Concentration at the Edge of a Circular Hole in a Generally Orthotropic Plate Subjected to Stress at Angle α to the Principal Material Direction *(After Greszczuk [6-11])*

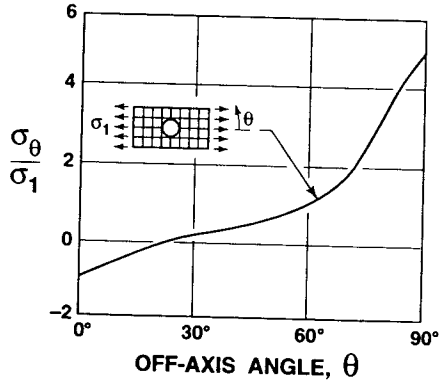

Figure 6-8 Stress Concentration at the Edge of a Circular Hole in a Cross-Ply Laminate *(After Greszczuk [6-11])*

The overall stress concentration effect around holes in composite laminates can be reduced in two different manners that are unique to composite materials and have no analog in metal structures practice. The first way is called the Stiffening Strip Concept that consists of placing strips of a stiffer composite material in a region away from the hole to attract load (away from the hole boundary), as in Figure 6-9. There, we know where the load will be taken in the laminate. In contrast, in the second way, the Softening Strip Concept, a strip of composite material that is less stiff (softer) is placed right beside each hole to slough the load that would ordinarily be concentrated near the hole to some other region of the laminate. However, we do not know where that load will be carried, just where it will *not* be carried. Both concepts are commonly used in design practice.

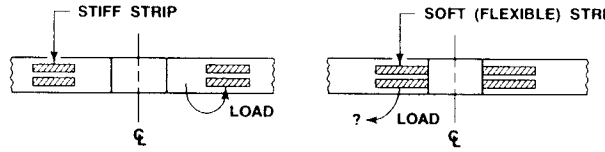

a Stiffening Strip b Softening Strip

Figure 6-9 Concepts for Stress Concentration Reduction around Holes

6.5 FRACTURE MECHANICS

The strength of any material is inherently related to the flaws that are always present. Specifically, the strengths of composite materials are governed by their flaw-initiated characteristics. Thus, the mechanics of fracture including crack propagation or extension are of extreme importance in the design analysis of composite structures. Fracture mechanics criteria are now a part of every metal airplane design. This step was made by the Air Force as a result of fracture and fatigue problems on F-111, C5-A, Electra, etc. The prospect for composite materials applications in the near future is that they, too, will have fracture mechanics design criteria imposed.

The fracture process generally takes place in three stages. First, a microcrack is initiated (or a preexisting flaw or imperfection can be present). Second, the microcrack grows in a stable fashion and might link with other microcracks to attain macrocrack size. Third, the macrocrack propagates in an unstable fashion at a critical stress level. These three stages are found and clearly defined only in ductile materials. Some of the stages, for example, stage two, are not found in brittle materials. A prominent characteristic of composite materials is their high resistance to crack propagation because of the matrix ductility and the crack-stopping ability of fibers at the fiber-matrix interface.

Fracture is caused by higher stresses around flaws or cracks than in the surrounding material. However, fracture mechanics is much more than the study of stress concentration factors. Such factors are useful in determining the influence of relatively large holes in bodies (see Section 6.3, Holes in Laminates), but are not particularly helpful when the body has sharp notches or crack-like flaws. For composite materials, fracture has a new dimension as opposed to homogeneous isotropic materials because of the presence of two or more constituents. Fracture can be a fracture of the individual constituents or a separation of the interface between the constituents.

The discussion of fracture mechanics will be divided in two parts. First, basic principles of fracture mechanics will be described. Second, the application of fracture mechanics concepts to composite materials will be discussed. In both parts, the basic approach is that of Wu [6-12].

6.5.1 Basic Principles of Fracture Mechanics

The acknowledged father of fracture mechanics is A. A. Griffith [6-13]. His principal contribution is an analysis of crack stability based on energy equilibrium. If a crack is in equilibrium, the decrease of strain energy U must be equal to the increase of surface energy S due to crack extension, that is,

$$\frac{\partial U}{\partial a} = \frac{\partial S}{\partial a} \tag{6.1}$$

where a is the crack length. The strain-energy-release rate, $\partial U/\partial a$, is actually the crack-extension force. Prior to Griffith's approach, the application of classical elasticity concepts led to infinite stresses at the crack tip.

Irwin [6-14] extended Griffith's theory to elastic-plastic materials and pointed out the three kinematically admissible crack-extension modes shown in Figure 6-10. These modes, opening, forward-shear, and parallel-shear, can be summed to obtain any crack.

Attention will be restricted to the strain-energy-release rate for the opening mode. This mode occurs for the plate with a centrally located crack of length 2a under load P in Figure 6-11.

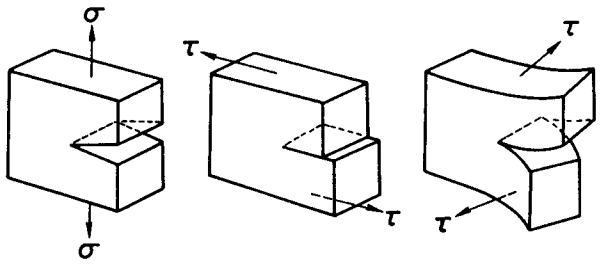

a Opening Mode b Forward-Shear Mode c Parallel-Shear Mode

Figure 6-10 Crack-Extension Modes

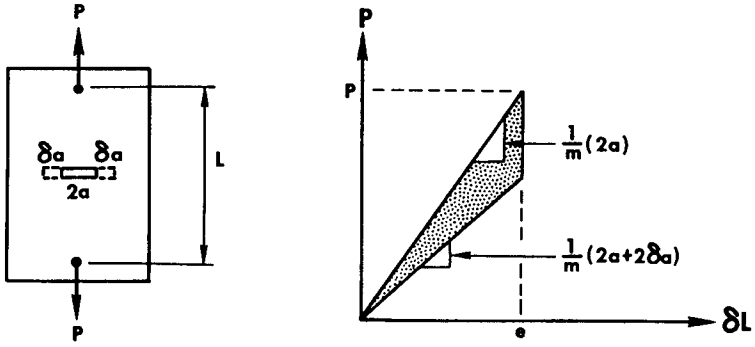

Figure 6-11 Cracked Plate and Load-Deformation Diagram *(After Wu [6-12])*

The strain energy in the plate is

$$U = \frac{1}{2} Pe \tag{6.2}$$

where e is the elongation between loading points separated by distance L. The spring constant of the plate is

$$\frac{1}{m} = \frac{P}{e} \tag{6.3}$$

The strain-energy-release rate due to crack extension $2\delta a$ is the shaded area in Figure 6-11 if the loading-frame head does not move during crack extension, that is,

$$\frac{\partial e}{\partial a} = 0 \tag{6.4}$$

From Equation (6.2),

$$\frac{\partial U}{\partial a} = \frac{1}{2} e \frac{\partial P}{\partial a} + \frac{1}{2} P \frac{\partial e}{\partial a} \tag{6.5}$$

but, because of Equation (6.4),

$$\frac{\partial U}{\partial a} = \frac{1}{2} e \frac{\partial P}{\partial a} \tag{6.6}$$

Then, from Equation (6.3),

$$\frac{\partial P}{\partial a} = \frac{1}{m} \frac{\partial e}{\partial a} + e \frac{\partial}{\partial a}\left[\frac{1}{m}\right] = -\frac{P}{m} \frac{\partial m}{\partial a} \tag{6.7}$$

so that

$$\frac{\partial U}{\partial a} = -\frac{P^2}{m} \frac{\partial m}{\partial a} \tag{6.8}$$

Irwin [6-14] calls the strain-energy-release rate G, so

$$G = \frac{P^2}{m} \frac{\partial m}{\partial a} \tag{6.9}$$

which can be measured because P and m can be measured. The same value of G results if the load is held constant during crack extension.

The strain-energy-release rate was expressed in terms of stresses around a crack tip by Irwin. He considered a crack under a plane stress loading of σ^∞, a symmetric stress relative to the crack, and τ^∞ a skew-symmetric stress relative to the crack in Figure 6-12. The stresses have a superscript $^\infty$ because they are applied an infinite distance from the crack. The stress distribution very near the crack can be shown by use of classical elasticity theory to be, for example,

$$\sigma_x = \frac{\sigma^\infty \sqrt{a}}{\sqrt{2r}} \cos\frac{\theta}{2}\left[1 - \sin\frac{\theta}{2}\sin\frac{3\theta}{2}\right] - \frac{\tau^\infty \sqrt{a}}{\sqrt{2r}} \sin\frac{\theta}{2}\left[2 + \cos\frac{\theta}{2}\cos\frac{3\theta}{2}\right] \tag{6.10}$$

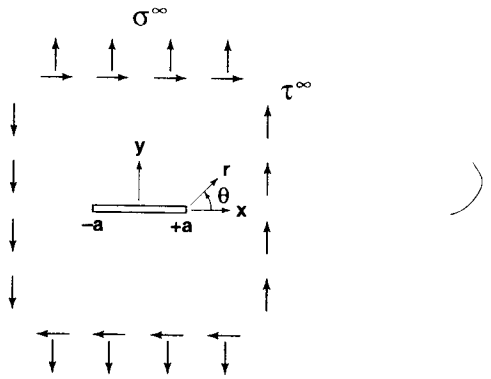

Figure 6-12 Cracked Plate with Symmetric and Skew-Symmetric Stresses at Infinity

The stress singularity for this and the other stress components σ_y and τ_{xy} is of order $1/\sqrt{r}$. Moreover, the terms $\sigma^\infty\sqrt{a}$ and $\tau^\infty\sqrt{a}$ are called symmetric and skew-symmetric stress-intensity factors:

$$k_1 = \sigma^\infty\sqrt{a}$$
$$k_2 = \tau^\infty\sqrt{a} \qquad (6.11)$$

The symmetric stress-intensity factor k_1 is associated with the opening mode of crack extension in Figure 6-10. The skew-symmetric stress-intensity factor k_2 is associated with the forward-shear mode. These plane-stress-intensity factors must be supplemented by another stress-intensity factor to describe the parallel-shear mode. The stress-intensity factors depend on the applied loads, body geometry, and crack geometry. For plane loads, the stress distribution around the crack tip can always be separated into symmetric and skew-symmetric distributions.

The stress-intensity factors are quite different from stress concentration factors. For the same circular hole, the stress concentration factor is 3 under uniaxial tension, 2 under biaxial tension, and 4 under pure shear. Thus, the stress concentration factor, which is a single scalar parameter, cannot characterize the stress state, a second-order tensor. However, the stress-intensity factor exists in all stress components, so is a useful concept in stress-type fracture processes. For example,

$$G = \frac{\pi k_1^2}{E} \qquad (6.12)$$

for an opening-mode crack that extends parallel to itself. Other such relations can be obtained for plane strain and the other crack modes. The point is that the stress-intensity factors appear in the strain-energy-release rate.

6.5.2 Application of Fracture Mechanics to Composite Materials

Composite materials have many distinctive characteristics relative to isotropic materials that render application of linear elastic fracture mechanics difficult. The anisotropy and heterogeneity, both from the standpoint of the fibers versus the matrix, and from the standpoint of multiple laminae of different orientations, are the principal problems. The extension to homogeneous anisotropic materials should be straightforward because none of the basic principles used in fracture mechanics is then changed. Thus, the approximation of composite materials by homogeneous anisotropic materials is often made. Then, stress-intensity factors for anisotropic materials are calculated by use of complex variable mapping techniques.

Wu [6-12] derives the stress distribution around a crack tip in an anisotropic material. He finds the intensities of the stresses σ_x, σ_y, and τ_{xy} are controlled not only by the parameters $\sigma^\infty\sqrt{a}$ and $\tau^\infty\sqrt{a}$ but also by functions of the anisotropic material properties and the orientation of the crack relative to the principal material directions. A simplification occurs when the crack maintains a constant orientation relative to the principal material directions (a likely circumstance if the flaws or possible paths of crack extension are, for example, all parallel to the fibers in a unidirectional lamina). However, unless the material is orthotropic and the crack is parallel to a principal material direction, the opening mode has both symmetric and skew-symmetric stresses in the stress distribution around the crack tip.

Wu [6-12] performed a series of experiments to determine the applicability of linear elastic fracture mechanics to composite materials. He subjected unidirectionally reinforced fiberglass-epoxy plates with centrally located cracks in the fiber direction to tension, pure shear, and combined tension and shear as in Figure 6-13. He recorded the critical load and crack length at incipient rapid crack extension and noted that the cracks propagated colinear with the original crack. Moreover, the symmetric loads led to the crack-opening mode, and the skew-symmetric loads led to the forward-shear or sliding mode. This distinction is clearer than for isotropic materials! For load path 1, the stress-intensity factors are

$$k_1 = \sigma^\infty\sqrt{a}$$
$$k_2 = 0 \qquad (6.13)$$

and the critical stress-intensity factors are

$$k_{1_c} = \sigma_c^\infty\sqrt{a_c}$$
$$k_{2_c} = 0 \qquad (6.14)$$

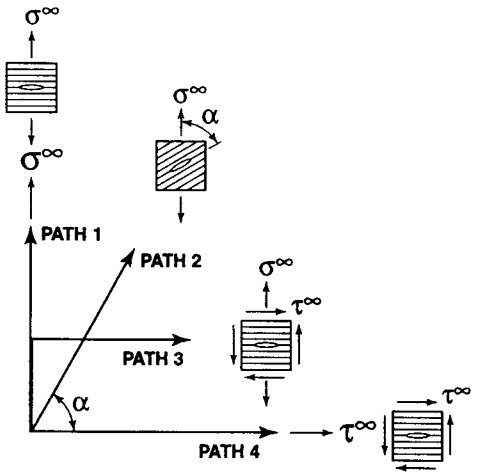

Figure 6-13 Wu's Load Paths and Crack Orientations *(After Wu [6-12])*

where σ_c^∞ is the critical stress and a_c the critical crack length at incipient rapid crack propagation. If k_{1_c} is truly a material constant, as we would hope it is, then the experimental data on a plot of $\log \sigma_c^\infty$ versus $\log a_c$ should be a straight line with slope – 1/2 because Equation (6.14) can be written

$$\log k_{1_c} = \log \sigma_c^\infty + \frac{1}{2} \log a_c \qquad (6.15)$$

Indeed, the slope of Figure 6-14 is actually –.49, so the theory is apparently applicable to an orthotropic lamina with cracks in the fiber direction. The contention is further substantiated by tests for the other loading paths shown in Figure 6-13.

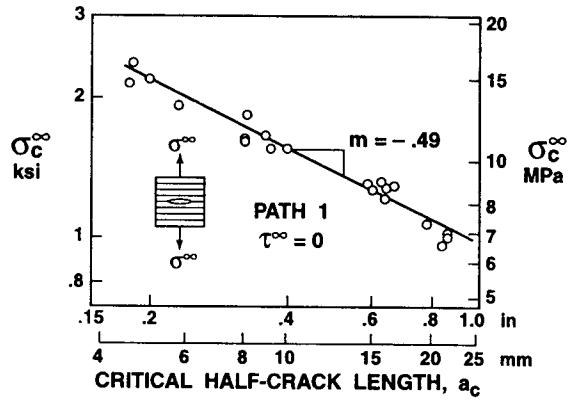

Figure 6-14 Cracked Unidirectionally Reinforced Plate under Tension Perpendicular to Fibers *(After Wu [6-12])*

Other researchers have substantially advanced the state of the art of fracture mechanics applied to composite materials. Tetelman [6-15] and Corten [6-16] discuss fracture mechanics from the point of view of micromechanics. Sih and Chen [6-17] treat the mixed-mode fracture problem for noncollinear crack propagation. Waddoups, Eisenmann, and Kaminski [6-18] and Konish, Swedlow, and Cruse [6-19] extend the concepts of fracture mechanics to laminates. Impact resistance of unidirectional composites is discussed by Chamis, Hanson, and Serafini [6-20]. They use strain energy and fracture strength concepts along with micromechanics to assess impact resistance in longitudinal, transverse, and shear modes.

All efforts to predict crack growth and fatigue in a composite laminate are affected by the unique and complex manner in which cracks can grow in a laminate. Cracks tend to grow in the matrix parallel to the fibers. Thus, if a crack is cut parallel to the fibers, as in Figure 6-15a, it will grow in a direction parallel to itself, i.e., in a *self-similar* manner. However, if a crack is cut at some angle to the fibers, then the crack will still grow parallel to the fibers and not parallel to itself, i.e., *non-self-similar* crack growth as in Figure 6-15b. Then, because a composite laminate has many layers at various orientations, a crack cut in a laminate results in crack growth that is locally sometimes self-similar and sometimes not. Globally, crack growth is non-self-similar, so predicting the effects of many kinds of damage growth is very difficult, if not impossible.

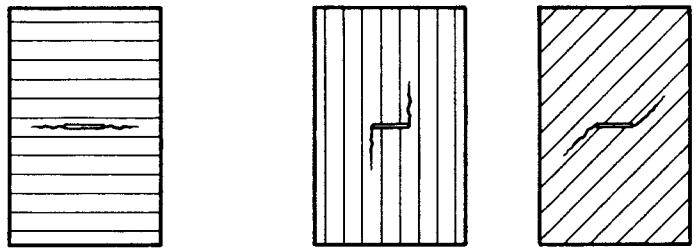

a Self-Similar Crack Growth b Non-Self-Similar Crack Growth

Figure 6-15 Composite Laminate Crack Growth

6.6 TRANSVERSE SHEAR EFFECTS

Composite materials typically have a low matrix Young's modulus in comparison to the fiber modulus and even in comparison to the overall laminae moduli. Because the matrix material is the bonding agent between laminae, the shearing effect on the entire laminate is built up by summation of the contributions of each interlaminar zone of matrix material. This summation effect cannot be ignored because laminates can have 100 or more layers! The point is that the composite material shear moduli G_{xz} and G_{yz} are much lower relative to the direct modulus E_x than for isotropic materials. Thus, the effect of transverse shearing stresses,

τ_{xz} and τ_{yz}, can be more important for laminated composite plates and shells than for isotropic plates and shells.

Study of transverse shearing stress effects is divided in two parts. First, some exact elasticity solutions for composite laminates in cylindrical bending are examined. These solutions are limited in their applicability to practical problems but are extremely useful as checkpoints for more broadly applicable approximate theories. Second, various approximations for treatment of transverse shearing stresses in plate theory are discussed.

6.6.1 Exact Solutions for Cylindrical Bending

Pagano studied cylindrical bending of symmetric cross-ply laminated composite plates [6-21]. Each layer is orthotropic and has principal material directions aligned with the plate axes. The plate is infinitely long in the y-direction (see Figure 6-16). When subjected to a transverse load, p(x), that is, p is independent of y, the plate deforms into a cylinder:

$$u = u(x) \qquad v = 0 \qquad w = w(x) \tag{6.16}$$

Thus, the plate is in a state of generalized plane strain in the x-z plane.

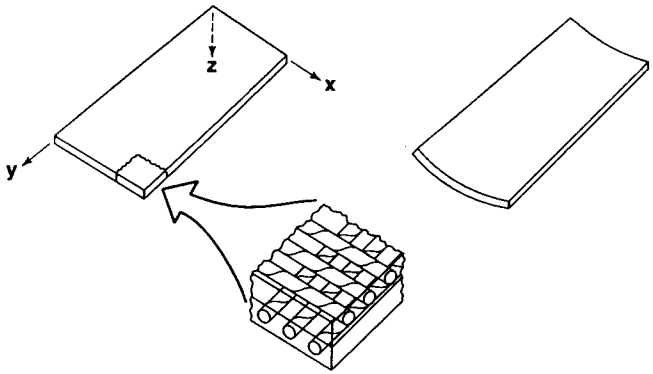

Figure 6-16 Cylindrical Bending of an Infinitely Long Cross-Ply Strip

Pagano's exact solution for the stresses and displacements is too complex to present here. The corresponding classical lamination theory result stems from the equilibrium equations, Equations (5.6) to (5.8), which simplify to

$$\begin{aligned} A_{11}u_{,xx} - B_{11}w_{,xxx} &= 0 \\ D_{11}w_{,xxxx} - B_{11}u_{,xxx} &= p \end{aligned} \tag{6.17}$$

when the orthotropy and Equation (6.16) are accounted for. These equilibrium equations can be uncoupled by differentiating the first equation to get

$$u_{,xxx} = \frac{B_{11}}{A_{11}} w_{,xxxx} \tag{6.18}$$

and substituting it in the second equation to yield

$$w_{,xxxx} = \frac{A_{11}}{D} p \tag{6.19}$$

where

$$D = A_{11}D_{11} - B_{11}^2 \tag{6.20}$$

when $p = p_o \sin \frac{n\pi x}{L}$, the solutions to Equations (6.18) and (6.19) are

$$u = \frac{B_{11}p_o}{D}\left[\frac{L}{n\pi}\right]^3 \cos\frac{n\pi x}{L} \qquad w = \frac{A_{11}p_o}{D}\left[\frac{L}{n\pi}\right]^4 \sin\frac{n\pi x}{L} \tag{6.21}$$

whereupon the only strain is

$$\varepsilon_x = u_{,x} - zw_{,xx} = \left[\frac{A_{11}z - B_{11}}{D}\right]\left[\frac{L}{n\pi}\right]^2 p_o \sin\frac{n\pi x}{L} \tag{6.22}$$

The stresses in each layer are

$$\begin{aligned} \sigma_{x_k} &= \frac{p_o Q_{11}^k (A_{11}z - B_{11})}{D}\left[\frac{L}{n\pi}\right]^2 \sin\frac{n\pi x}{L} \\ \sigma_{y_k} &= \frac{p_o Q_{12}^k (A_{11}z - B_{11})}{D}\left[\frac{L}{n\pi}\right]^2 \sin\frac{n\pi x}{L} \end{aligned} \tag{6.23}$$

Even though in classical lamination theory by virtue of the Kirchhoff hypothesis we assume the stresses τ_{xz} and σ_z are zero, we can still obtain these stresses approximately by integration of the stress equilibrium equations

$$\tau_{xz,z} = -\sigma_{x,x} \qquad \sigma_{z,z} = -\tau_{xz,x} \tag{6.24}$$

to obtain

$$\begin{aligned} \tau_{xz}^k &= -\frac{p_o Q_{11}^k}{D}\left[\frac{L}{n\pi}\right]\left[\frac{A_{11}}{2}z^2 - B_{11}z + H_k\right]\cos\frac{n\pi x}{L} \\ \sigma_z^k &= -\frac{p_o Q_{11}^k}{D}\left[\frac{A_{11}}{6}z^3 - \frac{B_{11}}{2}z^2 + H_k z + L_k\right]\sin\frac{n\pi x}{L} \end{aligned} \tag{6.25}$$

where the constants H_k and L_k are determined from the surface and interlaminar boundary conditions on the stresses.

Pagano presented numerical results for several laminates made of a high-modulus graphite-epoxy composite material with

$$E_1 = 25 \times 10^6 \text{ psi (172 GPa)} \qquad E_2 = 1 \times 10^6 \text{ psi (6.90 GPa)}$$

$$G_{12} = .5 \times 10^6 \text{ psi (3.45 GPa)} \qquad G_{23} = .2 \times 10^6 \text{ psi (1.38 GPa)}$$

$$\nu_{12} = \nu_{23} = .25$$

and loading $p = p_o \sin(\pi x/L)$ on a symmetric three-layer laminate [6-21]. First, the normalized transverse deflection w is plotted versus the span-to-thickness ratio, $S = L/t$, in Figure 6-17. The deviation of the actual elasticity solution from the approximate classical lamination theory solution is quite substantial at low span-to-thickness ratios. Even at $S = 20$, where classical plate theory is accurate for isotropic materials, the deviation is about 20%.

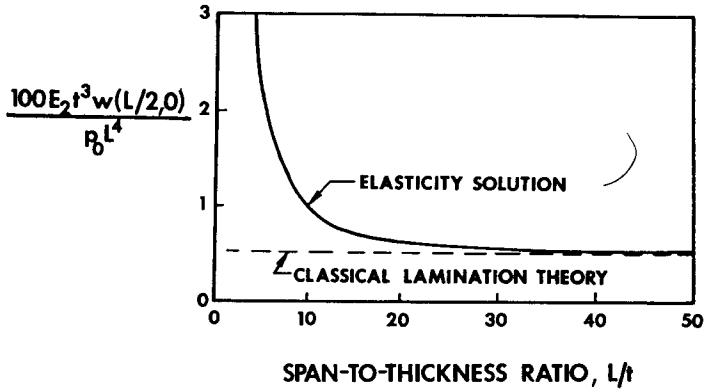

Figure 6-17 Normalized Deflection versus Span-to-Thickness Ratio *(After Pagano [6-21])*

For normal stress σ_x, the deviation of the classical lamination theory solution from the exact elasticity solution is quite drastic for S = 4, but not particularly large for S = 10 in Figures 6-18a and 6-18b, respectively. For transverse shearing stress τ_{xz}, the differences between classical lamination theory and the exact solution are not large for S = 4 and are fairly small for S = 10 in Figures 6-19a and b, respectively. The in-plane displacement u varies almost linearly in each layer, but is certainly not linear through the laminate thickness when S = 4 in Figure 6-19a. When S = 10, the deviation from linearity through the laminate thickness is not great in Figure 6-19b. Thus, the Kirchhoff hypothesis of nondeformable normals is not appropriate for low values of S. Lastly, the elasticity solution for the distribution of σ_z through the laminate thickness is not shown, but is very close to the distribution obtained from classical lamination theory by integrating $\tau_{xz,z}$ from Equation (6.24).

Obviously, the classical lamination theory stresses in Pagano's example converge to the exact solution much more rapidly than do the displacements as the span-to-thickness ratio increases. The stress errors are on the order of 10% or less for S as low as 20. The displacements are severely underestimated for S between 4 and 30, which are common values for laboratory characterization specimens. Thus, a practical means of accounting for transverse shearing deformations is required. That objective is attacked in the next section.

First, other work on the exact solutions to special problems will be reviewed. Pagano extended his theory to plates [6-22]; that is, his strip was of finite length. Then, he included the effect of in-plane shear-extension coupling in order to treat angle-ply laminates [6-23]. Pagano and Wang extended the orthotropic laminate solution to more general loadings [6-24]. Finally, Pagano and Hatfield examined laminated plates with many layers [6-25].

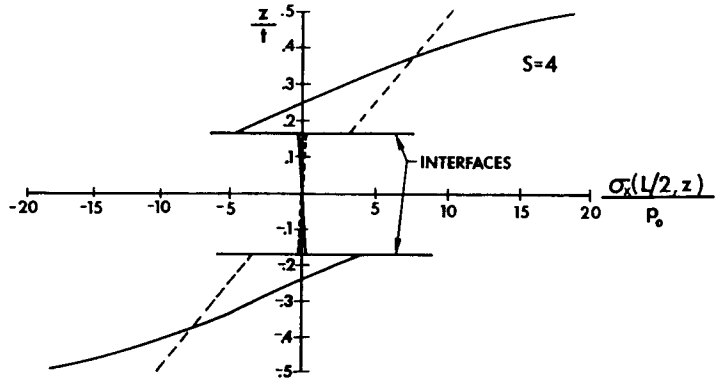

Figure 6-18a Variation of σ_x through the Thickness for S = 4 *(After Pagano [6-21])*

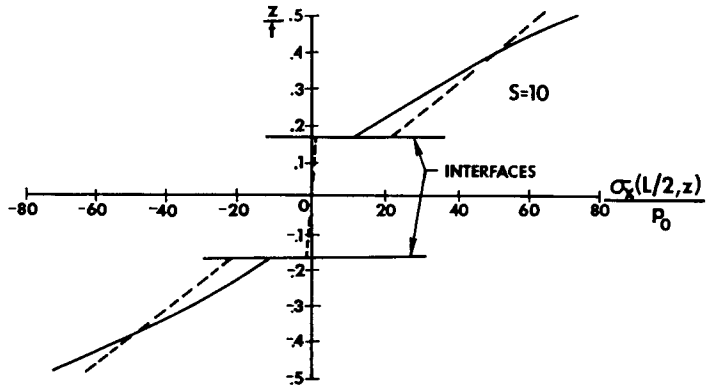

Figure 6-18b Variation of σ_x through the Thickness for S = 10 *(After Pagano [6-21])*

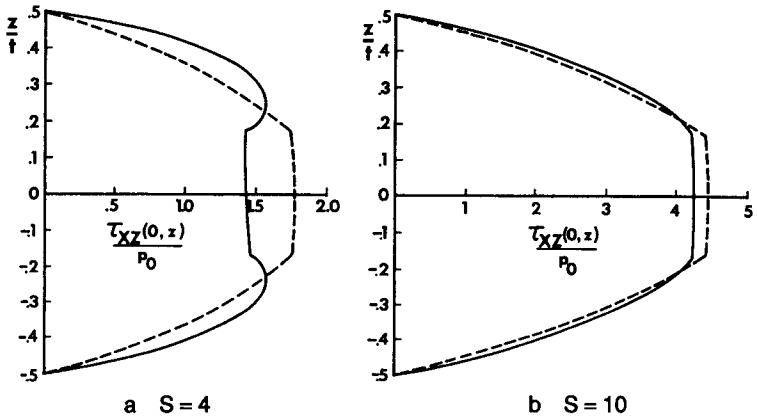

a S = 4 b S = 10

Figure 6-19 Variation of τ_{xz} through the Thickness *(After Pagano [6-21])*

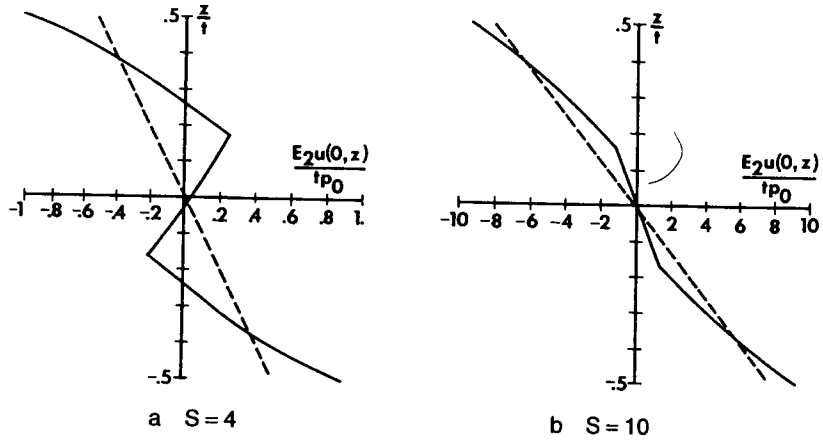

Figure 6-20 Variation of u through the Thickness *(After Pagano [6-21])*

6.6.2 Approximate Treatment of Transverse Shear Effects

The preceding subsection was devoted to a comparison of a special exact elasticity solution with classical lamination theory results. The importance of transverse shear effects was clearly demonstrated. However, that demonstration was for a special problem of rather narrow interest. The objective of this subsection is to display approaches and results for the approximate consideration of transverse shear effects for general laminated plates.

The treatment of transverse shear stress effects in plates made of isotropic materials stems from the classical papers by Reissner [6-26] and Mindlin [6-27]. Extension of Reissner's theory to plates made of orthotropic materials is due to Girkmann and Beer [6-28]. Ambartsumyan [6-29] treated symmetrically laminated plates with orthotropic laminae having their principal material directions aligned with the plate axes. Whitney [6-30] extended Ambartsumyan's analysis to symmetrically laminated plates with orthotropic laminae of arbitrary orientation.

The basic approaches as summarized by Ashton and Whitney [6-31] will now be discussed. First, a symmetric laminate with orthotropic laminae having principal material directions aligned with the plate axes will be treated. The transverse normal strain can be found from the orthotropic stress-strain relations, Equation (2.15), as

$$\varepsilon_z = \frac{1}{C_{33}}(\sigma_z - C_{13}\varepsilon_x - C_{23}\varepsilon_y) \tag{6.26}$$

which can be used to eliminate ε_z from the stress-strain relations for the k^{th} layer, leaving

$$\begin{bmatrix}\sigma_x\\ \sigma_y\\ \tau_{yz}\\ \tau_{xz}\\ \tau_{xy}\end{bmatrix}_k = \begin{bmatrix}Q_{11} & Q_{12} & 0 & 0 & 0\\ Q_{12} & Q_{22} & 0 & 0 & 0\\ 0 & 0 & Q_{44} & 0 & 0\\ 0 & 0 & 0 & Q_{55} & 0\\ 0 & 0 & 0 & 0 & Q_{66}\end{bmatrix}_k \begin{bmatrix}\varepsilon_x\\ \varepsilon_y\\ \gamma_{yz}\\ \gamma_{xz}\\ \gamma_{xy}\end{bmatrix}_k \tag{6.27}$$

where, if σ_z is neglected as in classical lamination theory,

$$Q_{ij} = \begin{cases} C_{ij} - \dfrac{C_{i3}C_{j3}}{C_{33}}, & \text{if } i,j = 1, 2\\ C_{ij}, & \text{if } i,j = 4, 5, 6\end{cases} \tag{6.28}$$

The transverse shearing stress distribution is then approximated by

$$\begin{aligned}\tau_{xz}^k &= \left[Q_{55}^k f(z) + a_{55}^k\right]\Phi_x(x,y)\\ \tau_{yz}^k &= \left[Q_{44}^k f(z) + a_{44}^k\right]\Phi_y(x,y)\end{aligned} \tag{6.29}$$

where $f(z) = f(-z)$ because of laminate symmetry. Also, a_{44}^k and a_{55}^k are determined from the equilibrium conditions that the shearing stresses vanish at the top and bottom surfaces of the plate $[f(t/2) = f(-t/2) = 0]$ and are continuous at layer interfaces. The shearing strains are obtained from the stress-strain relation as

$$\begin{aligned}\gamma_{xz}^k &= \left[f(z) + \frac{a_{55}^k}{Q_{55}^k}\right]\Phi_x\\ \gamma_{yz}^k &= \left[f(z) + \frac{a_{44}^k}{Q_{44}^k}\right]\Phi_y\end{aligned} \tag{6.30}$$

Then, integration of the strain-displacement relation, Equation (2.2), with respect to z (with w assumed to be independent of z) yields

$$\begin{aligned}u^k &= -zw_{,x} + \left[J(z) + g_1^k(z)\right]\Phi_x\\ v^k &= -zw_{,y} + \left[J(z) + g_2^k(z)\right]\Phi_y\end{aligned} \tag{6.31}$$

where

$$J(z) = \int f(z)dz \qquad g_1^k(z) = \frac{a_{55}^k}{Q_{55}^k}z + b_1^k \qquad g_2^k(z) = \frac{a_{44}^k}{Q_{44}^k}z + b_2^k \tag{6.32}$$

The constants b_1^k and b_2^k are found from continuity conditions for u and v at layer interfaces and the symmetry condition that u and v vanish at the laminate middle surface. Obviously, because of the presence of Φ_x and Φ_y, u and v are not linear functions of z as in classical lamination theory.

The moment relations are obtained from integration of the stress-strain relations, Equation (6.27), after the strain-displacement relations, Equation (6.22), and the displacement relations, Equation (6.31), are substituted:

$$\begin{aligned} M_x &= -D_{11}w_{,xx} - D_{12}w_{,yy} + (F_{11} + H_{111})\Phi_{x,x} + (F_{12} + H_{122})\Phi_{y,y} \\ M_y &= -D_{12}w_{,xx} - D_{22}w_{,yy} + (F_{12} + H_{121})\Phi_{x,x} + (F_{22} + H_{222})\Phi_{y,y} \\ M_{xy} &= -2D_{66}w_{,xy} + (F_{66} + H_{661})\Phi_{x,y} + (F_{66} + H_{662})\Phi_{y,x} \end{aligned} \tag{6.33}$$

where the D_{ij} are the usual bending stiffnesses and

$$\begin{aligned} F_{ij} &= \int_{-t/2}^{t/2} Q_{ij}^k z J(z)\,dz \qquad i,j = 1, 2, 6 \\ H_{ijl} &= \int_{-t/2}^{t/2} Q_{ij}^k z g_l^k(z)\,dz \qquad l = 1, 2 \end{aligned} \tag{6.34}$$

The shear resultants are

$$Q_x = \int_{-t/2}^{t/2} \tau_{xz}^k dz = K_{55}\Phi_x \qquad Q_y = \int_{-t/2}^{t/2} \tau_{yz}^k dz = K_{44}\Phi_y \tag{6.35}$$

where

$$K_{ii} = \int_{-t/2}^{t/2} \left[Q_{ii}^k f(z) + a_{ii}^k \right] dz \qquad i = 4,5 \tag{6.36}$$

The large-deflection equilibrium equations are

$$\begin{aligned} &M_{x,x} + M_{xy,y} - Q_x = 0 \\ &M_{xy,x} + M_{y,y} - Q_y = 0 \\ &Q_{x,x} + Q_{y,y} + p + N_x w_{,xx} + 2N_{xy} w_{,xy} + N_y w_{,yy} = 0 \end{aligned} \tag{6.37}$$

or, in terms of the present variables,

$$\begin{aligned} &D_{11}w_{,xxx} + (D_{12} + 2D_{66})w_{,xyy} - (F_{11} + H_{111})\Phi_{x,xx} - (F_{66} + H_{661})\Phi_{x,yy} \\ &\quad - (F_{12} + F_{66} + H_{122} + H_{662})\Phi_{y,xy} + K_{55}\Phi_x = 0 \\ &(D_{12} + 2D_{66})w_{,xxy} + D_{22}w_{,yyy} + (F_{12} + F_{66} + H_{121} + H_{661})\Phi_{x,xy} \\ &\quad + (F_{66} + H_{662})\Phi_{y,xx} + (F_{22} + H_{222})\Phi_{y,yy} + K_{44}\Phi_y = 0 \\ &K_{55}\Phi_{x,x} + K_{44}\Phi_{y,y} + p + N_x w_{,xx} + 2N_{xy} w_{,xy} + N_y w_{,yy} = 0 \end{aligned} \tag{6.38}$$

The boundary conditions for these equilibrium equations are more complicated than for classical lamination theory. However, they are more logical because the Kirchhoff shear force or free-edge condition, in which

a combination of shearing force and twisting moment (derivative) appears, is replaced by that force and moment themselves. In summary, the new boundary conditions along each edge are

$$Q_n = 0 \text{ or } w = 0 \qquad M_n = 0 \text{ or } w_{,n} = 0 \qquad M_{nt} = 0 \text{ or } u_{t,z}\big|_{z=0} = 0 \tag{6.39}$$

where n and t are directions normal to and along the edge, respectively.

For a simply supported laminated rectangular plate subjected to the distributed transverse load

$$p = p_o \sin\frac{m\pi x}{a} \sin\frac{n\pi y}{b} \tag{6.40}$$

the displacement and rotations

$$\begin{aligned} w &= A \sin\frac{m\pi x}{a} \sin\frac{n\pi y}{b} \\ \Phi_x &= B \cos\frac{m\pi x}{a} \sin\frac{n\pi y}{b} \\ \Phi_y &= C \sin\frac{m\pi x}{a} \cos\frac{n\pi y}{b} \end{aligned} \tag{6.41}$$

exactly satisfy the boundary conditions

$$\begin{aligned} M_x = v_{,z}\big|_{z=0} = w = 0 \quad &\text{on} \quad x = 0,a \\ M_y = u_{,z}\big|_{z=0} = w = 0 \quad &\text{on} \quad y = 0,b \end{aligned} \tag{6.42}$$

The shearing stresses are assumed on the basis of elasticity results [6-21] to vary approximately as a segment of a parabola in each layer, that is,

$$f(z) = 1 - 4\left[\frac{z}{t}\right]^2 \tag{6.43}$$

Then, the overall problem is determinate and reduces to the solution of the following set of simultaneous algebraic equations for A, B, and C:

$$\begin{aligned} &\left[D_{11}m^2 + (D_{12} + 2D_{66})n^2R^2\right]\left[\frac{m\pi}{a}\right]A \\ &\quad - \left[(F_{11} + H_{111})m^2 + (F_{66} + H_{661})n^2R^2 + \frac{K_{55}R^2S^2}{\pi^2}\right]B \\ &\quad - (F_{12} + F_{66} + H_{122} + H_{662})mnRC = 0 \\ &\left[(D_{12} + 2D_{66})m^2 + D_{22}n^2R^2\right]\left[\frac{n\pi R}{a}\right]A - (F_{121} + F_{66} + H_{121} + H_{661})mnRB \\ &\quad - \left[(F_{66} + H_{662})m^2 + (F_{22} + H_{222})n^2R^2 + \frac{K_{44}R^2S^2}{\pi^2}\right]C = 0 \\ &K_{55}mB + K_{44}nRC = \frac{p_o a}{\pi} \end{aligned} \tag{6.44}$$

in which $R = a/b$ and $S = a/t$.

Whitney solved Equations (6.44) for a square four-layered symmetric cross-ply [0°/90°/90°/0°] laminated graphite-epoxy plate under the transverse load $p = p_o \sin(\pi x/a) \sin(\pi y/a)$ [6-30]. The material properties are typical of a high-modulus graphite-epoxy:

$$\frac{E_1}{E_2} = 40 \qquad \frac{G_{12}}{E_2} = .6 \qquad \frac{G_{13}}{E_2} = .5 \qquad \nu_{12} = .25$$

The results shown in Figure 6-21 for the present shear-deformation approach versus classical lamination theory are quite similar qualitatively to the comparison between the exact cylindrical bending solution and classical lamination theory in Figure 6-17.

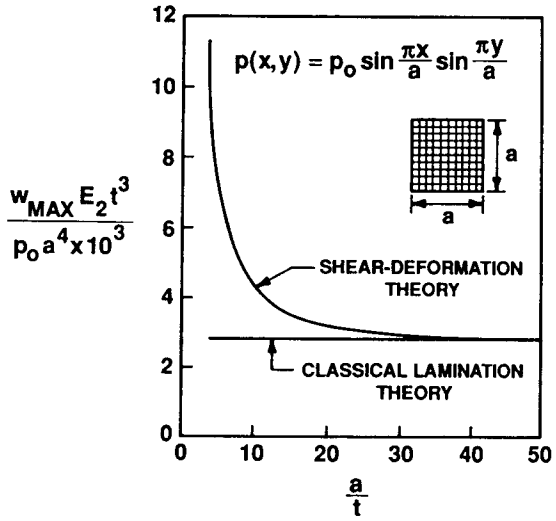

Figure 6-21 Deflection under $p_o \sin(\pi x/a) \sin(\pi y/a)$ of a Square Four-Layer Symmetric Cross-Ply Graphite-Epoxy Plate *(After Whitney [6-30])*

A more direct comparison of Whitney's shear-deformation solution for deflection of an antisymmetric cross-ply infinite strip [6-30] with the elasticity solution and the classical lamination theory solution is shown in Figure 6-22. Obviously, Whitney's shear-deformation theory solution is quite good for prediction of deflections. However, Whitney's shearing stress distribution through the thickness at the edge of the infinite strip in Figure 6-23 does not agree well with the elasticity solution. If, instead of an equation analogous to Equation (6.43), the shearing stresses are calculated from the stresses σ_x, σ_y, and τ_{xy} by the elasticity equations, then the better agreement in Figure 6-23 between the modified shear-deformation theory and the elasticity solution is obtained.

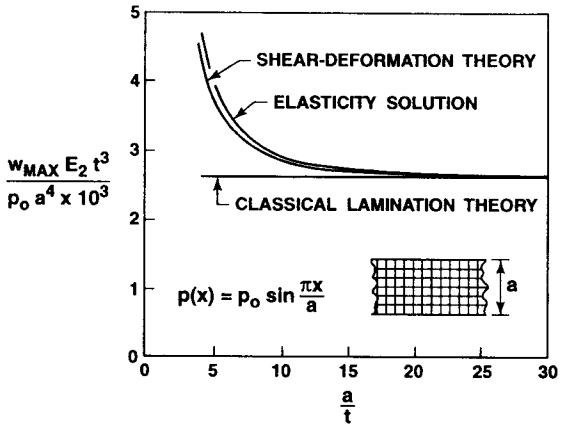

Figure 6-22 Deflection of an Infinite Two-Layer Cross-Ply Graphite-Epoxy Strip under $p_o \sin(\pi x/a)$ *(After Whitney [6-30])*

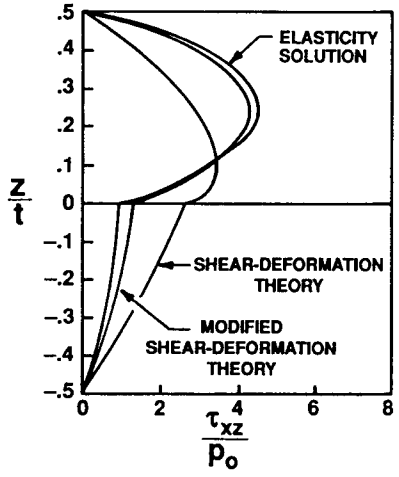

Figure 6-23 Transverse Shear Stress Distribution along the Edges of an Infinite Two-Layer Graphite-Epoxy Strip under $p_o \sin(\pi x/a)$ with $a/t = 4$ *(After Ashton and Whitney [6-31])*

Whitney and Pagano [6-32] extended Yang, Norris, and Stavsky's work [6-33] to the treatment of coupling between bending and extension. Whitney uses a higher order stress theory to obtain improved predictions of σ_x, σ_y, and τ_{xy} and displacements at low width-to-thickness ratios [6-34]. Reissner used his variational theorem to derive a consistent set of equations for inclusion of transverse shearing deformation effects in symmetrically laminated plates [6-35]. Finally, Ambartsumyan extended his treatment of transverse shearing deformation effects from plates to shells [6-36].

6.7 POSTCURING SHAPES OF UNSYMMETRIC LAMINATES

How do unsymmetric laminates deform during cooldown after curing? Note that we address merely laminates, not plates because there is no mechanical loading nor any support at the laminate edges. The motivation for such a question is that unsymmetric laminates deform in unusual ways relative to symmetric laminates, as seen for a variety of unsymmetric graphite-epoxy laminates in Figure 6-24. Those unusual ways are often regarded as undesirable, but, in fact, they could be quite useful and even desirable in certain structural applications. That is, sometimes we might need a laminate that has a certain curvature or twist rather than a flat laminate. Thus, we must investigate the possible shapes of cured unsymmetric laminates.

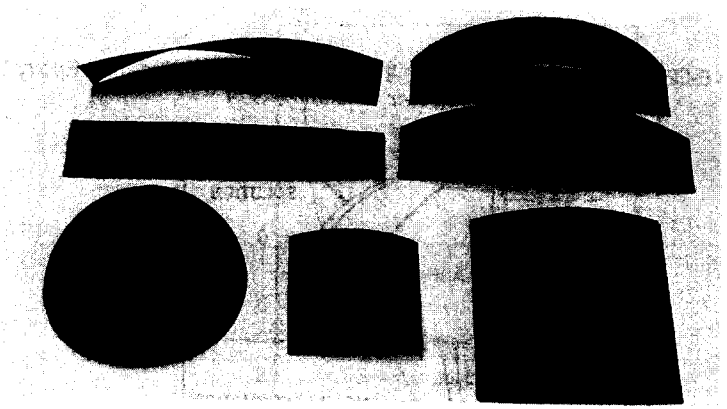

Figure 6-24 Postcuring Shapes of Various Unsymmetric Laminates *(After Hyer [6-37])*

If an unsymmetric laminate is held flat, e.g., in a press, during the curing process (the usual situation), its shape is flat at the highest curing temperature as in Figure 6-25a. However, when the press force is removed after curing is done, an unsymmetric laminate is compelled to take on shapes other than flat because of the significant thermal forces and moments that develop during cooldown from the highest curing temperature (because of different thermal stresses in each layer caused by different thermal contractions).

The first observation is that the cured shape of an unsymmetric cross-ply laminate is often cylindrical, whereas we would predict it to be a saddle shape (hyperbolic paraboloid) from classical lamination theory (the curvatures can be shown to be $\kappa_x = -\kappa_y$ or $-\kappa_x = \kappa_y$). A thick laminate (length and width not large compared to the thickness) will leave the curing process with the saddle shape in Figure 6-25b. Note that curvature is defined in this section without the negative signs of Equation (4.15). Also, the deflection is measured positive upward in Figure 6-25 (instead of positive downward as in Chapter 4). A thin laminate (length and width large compared to the thickness) will have a circular cylindrical

shape as in Figures 6-25c and 6-25d. If you try to force the circular cylindrical laminate to be flat, then a very audible snap-through buckling will occur from the configuration with ($+\kappa_x$, $\kappa_y = 0$) to a configuration with ($\kappa_x = 0$, $-\kappa_y$) or vice versa.

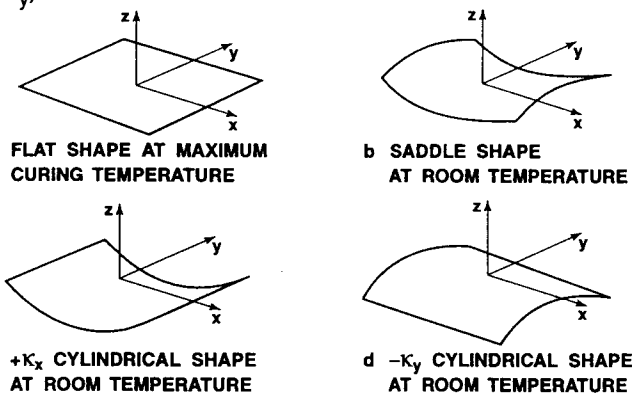

Figure 6-25 Unsymmetric Cross-Ply Laminate Shapes *(After Hyer [6-38])*

Hyer shows the conditions under which the cylindrical shape must exist and when the saddle shape must exist [6-38]. He approximates the transverse deflection of an unsymmetric cross-ply laminate as

$$w(x,y) = \frac{1}{2}(ax^2 + by^2) \tag{6.45}$$

with corresponding approximate in-plane displacements

$$u^o(x,y) = cx - \frac{a^2x^3}{6} - \frac{abxy^2}{4}$$
$$v^o(x,y) = dy - \frac{b^2y^3}{6} - \frac{abx^2y}{4} \tag{6.46}$$

in which the second and third terms in each equation are for large deformations. These deformations are an approximation to the large-deflection values that would exist for such laminates. Hyer uses these deformations with their implied strains to formulate the total potential energy of a laminate. He solves the resulting equations numerically to find the equilibrium states and their stability or instability for square T300-5208 graphite-epoxy laminates with properties:

$$E_1 = 26.2 \times 10^6 \text{ psi } (181 \text{ GPa}) \qquad E_2 = 1.49 \times 10^6 \text{ psi } (10.3 \text{ GPa})$$
$$\nu_{12} = .28 \qquad G_{12} = 1.04 \times 10^6 \text{ psi } (7.2 \text{ GPa})$$
$$\alpha_1 = -.059 \times 10^{-6}/°\text{F } (-.106 \times 10^{-6}/°\text{C})$$
$$\alpha_2 = 14.2 \times 10^{-6}/°\text{F } (25.6 \times 10^{-6}/°\text{C})$$

The laminates were cured at 350°F (177°C) and then cooled to room temperature of 70°F (21°C).

Hyer's results for various square laminate side lengths (length = width) for a $[0_2/90_2]_T$ laminate are shown in Figure 6-26. Three important cases exist:

(1) If the side lengths are zero, i.e., for a very thick laminate, then a saddle shape exists at point S (saddle) with $\kappa_x = a$ and $\kappa_y = -b$, where a = b. As the side lengths increase, i.e., as the laminate becomes thinner, the saddle shape still exists, but the curvature decreases in amplitude, i.e., the saddle gets more shallow.

(2) If the side lengths are small enough, i.e., if the laminate is thick enough, then only a saddle shape exists, as seen in Figure 6-26 as segment ST with equal and opposite curvatures that decrease in magnitude as the side length increases.

(3) At a critical length that depends on relative laminate thickness, the deformation solution *trifurcates* at point T, i.e., above the critical length, three possible room-temperature shapes exist: (1) a saddle shape, (2) a cylindrical shape with $\kappa_x = +\kappa$ and $\kappa_y = 0$, and (3) a cylindrical shape with $\kappa_x = 0$ and $\kappa_y = -\kappa$. For this $[0_2/90_2]_T$ laminate, the critical length is 35 mm.

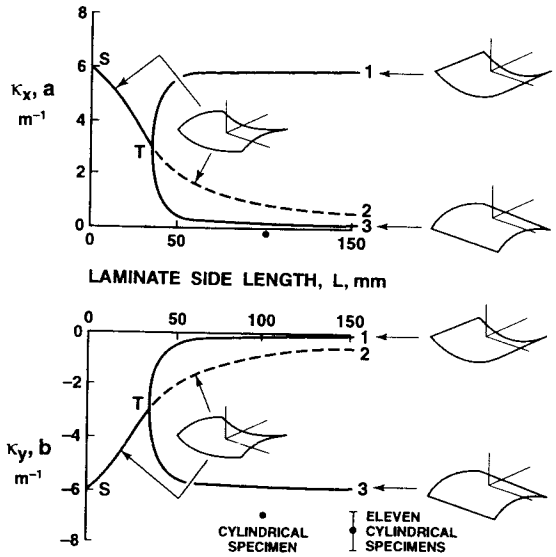

Figure 6-26 Room Temperature Shapes of Square Graphite-Epoxy Laminates *(After Hyer [6-38])*

The three branches of the equilibrium configurations after point T are labeled T1, T2, and T3 in Figure 6-26. Branch T2 is a continuation of the saddle shape of solution ST, but this branch is unstable, so the other branches are the real, physical solution because they are stable. Branch T1 has a larger κ_x than κ_y. If L is about 50% bigger than the critical L, the laminate of branch T1 has a large κ_x and nearly zero κ_y, so the shape is approximately cylindrical. In contrast, branch T3 has a cylindrical shape with a large κ_y and nearly zero κ_x if the laminate length is about 50% greater than the critical L. In fact, a laminate can be made to snap-through from branch T1 to branch T3 simply by applying a small amount of bending moment in the large-curvature direction, i.e., apply $-M_x$ to the $+\kappa_x$ cylindrical shape (with your fingers!). The converse is true for snap-through from branch T3 to branch T1.

Measured curvatures for a 100-mm laminate (a single closed circle on each curve) and eleven 150-mm laminates (a closed circle for the mean with a range for all other values shown) are shown in Figure 6-26. The quantitative comparison is only fair as might be expected for an approximate approach. However, the qualitative agreement as to mode of deformation is correct.

For a thicker laminate than in Figure 6-26, the critical length is longer and the curvatures are smaller. For example, for a $[0_4/90_4]_T$ laminate, the critical L is 71 mm. Moreover, what was a circular cylindrical specimen at 50 mm for a $[0_2/90_2]_T$ laminate becomes a saddle-shaped specimen [6-38].

A workable theory behind why unsymmetric cross-ply laminates deform as they do has been developed by Hyer (who has extended these papers). Thus, a reasonable understanding of the deformation mechanics exists and can be used to design laminates with specified curvatures.

6.8 ENVIRONMENTAL EFFECTS

Composite materials must survive in the environment to which they are subjected at least as well as the conventional materials they replace. Some of the harmful environments encountered include exposure to humidity, water immersion, salt spray, jet fuel, hydraulic fluid, stack gas (includes sulfur dioxide), fire, lightning, and gunfire as well as the combined effects of the space environment.

Humidity or water immersion can lead to degraded stiffnesses and strengths as shown by Fried [6-39]. However, after dehydration, the original properties are recovered. Some of the same but irreversible effects are found for salt spray (although it is somewhat corrosive), jet fuel, hydraulic fluid, and stack gas. Fire is, of course, an extreme environment, and its damage is obvious. Aircraft are subjected to lightning strikes, so must be protected and certainly not built of materials that are particularly susceptible to lightning damage. Lightning tests were performed on aluminum, fiberglass, boron-epoxy, and graphite-epoxy. The aluminum sustained little damage; the fiberglass had minor surface marks; the boron-epoxy had some cracks and bubble delaminations; and the graphite-epoxy had the resin stripped and a hole burned in another place. This range of effects is triggered by the inherent electrical conductivity of each material ranging from high to low. Surface coatings such as aluminum foil or embedded wire grids could reduce these effects substantially by increasing electrical conductivity.

Tsai listed and quantitatively discussed specific degradation mechanisms for environmental exposure [6-40]:

"A. Loss of strength of the reinforcing fibers by a stress-corrosion mechanism.
B. Degradation of the fiber-matrix interface resulting in loss of adhesion and interfacial bond strength.
C. Permeability of the matrix material to corrosive agents such as water vapor which affects both A and B above.
D. Normal viscoelastic dependence of matrix modulus and strength on time and temperature.
E. Combined action of temperature and moisture accelerated degradation."

A series of papers on environmental effects work prior to 1988 was collected by Springer and published in three volumes [6-41].

Elevated moisture and temperature effects on epoxy-matrix materials and on epoxy-matrix composite materials were addressed by Browning, Husman, and Whitney [6-42]. Moisture absorption for many, but not all epoxies causes swelling, plasticization, and decrease in glass-transition temperature. Plasticization is the increase in spacing between molecules so molecular mobility increases, and is a reversible process (hence, moisture causes reduced brittleness at room temperature). Fiber-matrix interface damage is only partially reversible by removal of moisture by 'bake-out' procedures. The glass-transition temperature, T_g, is the temperature at which a polymer changes from a hard, glassy solid to a soft, rubbery solid with associated decreases in stiffness and strength. Actually, this transition takes place not at a specific temperature, but over a temperature range. Such physical changes for the matrix of a polymer-matrix composite material cause the matrix-dominated properties to be most affected (degraded) and the fiber-dominated properties to be least affected. Browning, Husman, and Whitney present absorbed moisture profiles through the thickness of AS-3501-5 graphite-epoxy composite laminates with associated mechanical properties as a function of moisture and temperature.

For laminated plate deflections, buckling, and vibrations, Whitney and Ashton studied the effects of environmental factors that cause expansional strains [6-43]. Such factors include temperature rise and matrix swelling due to water vapor or sudden expansion of absorbed gases. Temperature rises and matrix expansion can cause degradation of material properties. However, Whitney and Ashton held the material properties constant and treated only the effects of temperature and swelling on structural response. Both phenomena cause buckling; thus, buckling caused by thermal expansion was assessed directly. They also analyzed the effect of matrix swelling on vibration frequencies and bending deflections. A limiting case of the vibration problem is buckling caused by matrix swelling. Swelling resulted in reduced buckling loads and vibration frequencies and increased bending deflections. These effects are all significant enough to warrant attention in composite structures design-analysis.

Galvanic corrosion is most commonly found for composite materials as the interaction of graphite in graphite-epoxy with aluminum (or other less noble metals such as steel, magnesium, and even cadmium-plated steels) in the presence of most electrolytes (sodium chloride, etc.) in moisture. The aluminum corrodes rather quickly (the graphite is unaffected), so aluminum fasteners in a graphite-epoxy structure would soon fail. To avoid galvanic corrosion, the simplest, but not always most practical solution is to not use graphite and aluminum in the same structure. If both graphite and aluminum are needed, then all direct contact must be avoided (including any path through salt water!). Contact can be avoided by placing intervening nonconductive layers between the graphite and aluminum. Moreover, mechanical fasteners must be titanium and perhaps stainless steel, both of which are more expensive than aluminum or cadmium-plated steel fasteners. The F-16 horizontal stabilizer is an example of a mixed graphite-epoxy and aluminum structure. The upper and lower graphite-epoxy skins are separated from a full-depth corrugated aluminum truss core by multiple layers: anodizing on the aluminum, epoxy primer, liquid skrim (chopped glass in epoxy), sealant, and finally glass-epoxy cloth is in contact with the graphite-epoxy skin. The assembly is then put together with corrosion-resistant steel fasteners dipped in a sealant.

Composite materials in space, such as in orbiting space stations, are subject to an environment of hard vacuum, thermal cycling because of passing in and out of the sun's rays, as well as ultraviolet, electron, and proton radiation. The effects of those environmental factors include: (1) vacuum causes outgassing and migration of low-molecular-weight components from matrix materials such as polymers, (2) thermal cycling can cause significant dimensional changes in such dimension-sensitive instruments as space telescopes, and (3) radiation causes damage because of competing effects of polymer chain-cutting and enhanced cross-linking. The latter effects change the melting point, hardness, strength, and stiffness as well as the dimensional stability of polymers.

6.9 SHELLS

Work on analysis of the common structural shell element made of composite materials is very extensive. Contributions will be mentioned that parallel the developments in Chapter 5 on plates. Some of the first analyses of laminated shells are by Dong, Pister, and Taylor [6-44] and the monograph by Ambartsumyan [6-36]. Further efforts include the buckling work on laminated shells by Cheng and Ho [6-45] and on eccentrically stiffened laminated shells by Jones [6-46].

Classical solutions to laminated shell buckling and vibration problems in the manner of Chapter 5 were obtained by Jones and Morgan [6-47]. Their results are presented as normalized buckling loads or fundamental natural frequency versus the Batdorf shell curvature parameter. They showed that, for antisymmetrically laminated cross-ply shells as for plates, the effect of coupling between bending and extension on buckling loads and vibration frequencies dies out rapidly as the number of layers

increases. However, for unsymmetrically laminated cross-ply shells, the effect of coupling dies out very, very slowly. Thus, analyses of all unsymmetrically laminated plates and shells should include the effects of coupling between bending and extension. Otherwise, serious overestimates of buckling loads and vibration frequencies can be obtained. Similarly, serious underestimates of plate and shell deflections, and hence stresses, can occur if coupling between bending and extension is ignored.

6.10 MISCELLANEOUS TOPICS

Some basic lamina and laminate behavioral characteristics were deliberately overlooked in the preceding discussion. Among them are plastic or nonlinear deformations, viscoelastic behavior, and wave propagation.

Shear-stress–shear-strain curves typical of fiber-reinforced epoxy resins are quite nonlinear, but all other stress-strain curves are essentially linear. Hahn and Tsai [6-48] analyzed lamina behavior with this nonlinear deformation behavior. Hahn [6-49] extended the analysis to laminate behavior. Inelastic effects in micromechanics analyses were examined by Adams [6-50]. Jones and Morgan [6-51] developed an approach to treat nonlinearities in all stress-strain curves for a lamina of a metal-matrix or carbon-carbon composite material. Morgan and Jones extended the lamina analysis to laminate deformation analysis [6-52] and then to buckling of laminated plates [6-53].

Viscoelastic characteristics of composite materials usually result from a viscoelastic-matrix material such as epoxy resin. General stress analysis of viscoelastic composites was discussed by Schapery [6-54]. An important application to laminated plates was made by Sims [6-55].

Wave propagation in an inhomogeneous anisotropic material such as a fiber-reinforced composite material is a very complex subject. However, its study is motivated by many important applications such as the use of fiber-reinforced composites in reentry vehicle nosetips, heatshields, and other protective systems. Chou [6-56] gives an introduction to analysis of wave propagation in composite materials. Others have applied wave propagation theory to shell stress problems.

REFERENCES

6-1 M. J. Salkind, VTOL Aircraft, in *Applications of Composite Materials*, Michael J. Salkind and Geoffry S. Hollister (Editors), ASTM STP 524, American Society for Testing and Materials, 1973, pp. 76–107 (reprinted with permission).

6-2 K. L. Reifsnider, E. G. Henneke, W. W. Stinchcomb, and J. C. Duke, Damage Mechanics and NDE of Composite Laminates, in *Mechanics of Composite Materials - Recent Advances*, Proceedings of the IUTAM Symposium on Mechanics of Composite Materials, Zvi Hashin and Carl T. Herakovich (Editors), Blacksburg, Virginia, 16–19 August 1982, Pergamon Press, New York, 1983, pp. 399–420.

6-3 R. L. Pinckney, Helicopter Rotor Blades, in *Applications of Composite Materials*, Michael J. Salkind and Geoffry S. Hollister (Editors), ASTM STP 524, American Society for Testing and Materials, 1973, pp. 108–133 (reprinted with permission).

6-4 M. J. Salkind, Fatigue of Composites, in *Composite Materials: Testing and Design (Second Conference)*, H. T. Corten (Chairman), Anaheim, California, 20–22 April 1971, ASTM STP 497, American Society for Testing and Materials, 1972, pp. 143–169.

6-5 J. R. Eisenmann, B. E. Kaminski, D. L. Reed, and D. J. Wilkins, Toward Reliable Composites: An Examination of Design Methodology, *Journal of Composite Materials*, July 1972, pp. 143–169.

6-6 Ramesh Talreja, *Fatigue of Composite Materials*, Technomic, Lancaster, Pennsylvania, 1987.

6-7 S. G. Lekhnitskii, Stresses in Infinite Anisotropic Plate Weakened by Elliptical Hole, *DAN SSSR*, Vol. 4, No. 3, 1936.

6-8 G. N. Savin, *Stress Distribution Around Holes*, Naukova Dumka Press, Kiev, 1968. Also NASA TT F-601, November 1970.

6-9 S. G. Lekhnitskii, *Theory of Elasticity of an Anisotropic Elastic Body*, Government Publishing House for Technical-Theoretical Works, Moscow and Leningrad, 1950. Also P. Fern (Translator), Holden-Day, San Francisco, 1963.

6-10 S. G. Lekhnitskii, *Anisotropic Plates*, S. W. Tsai and T. Cheron (Translators), Gordon and Breach, New York, 1968.

6-11 L. B. Greszczuk, Stress Concentrations and Failure Criteria for Orthotropic and Anisotropic Plates with Circular Openings, in *Composite Materials: Testing and Design (Second Conference)*, H. T. Corten (Chairman), Anaheim, California, 20–22 April 1971, ASTM STP 497, American Society for Testing and Materials, 1972, pp. 363–381 (reprinted with permission).

6-12 Edward M. Wu, Fracture Mechanics of Anisotropic Plates, in *Composite Materials Workshop*, S. W. Tsai, J. C. Halpin, and Nicholas J. Pagano (Editors), St. Louis, Missouri, 13–21 July 1967, Technomic, Westport, Connecticut, 1968, pp. 20–43.

6-13 A. A. Griffith, The Phenomena of Rupture and Flow in Solids, *Philosophical Transactions of the Royal Society*, Vol. 221A, October 1920, pp. 163–198.

6-14 G. R. Irwin, Fracture, in *Handbuch der Physik*, Vol. V, Springer, New York, 1958.

6-15 A. S. Tetelman, Fracture Processes in Fiber Composite Materials, in *Composite Materials: Testing and Design*, Steven Yurenka (Chairman), New Orleans, Louisiana, 11–13 February 1969, ASTM STP 460, American Society for Testing and Materials, 1969, pp. 473–502.

6-16 Herbert T. Corten, Micromechanics and Fracture Behavior of Composites, in *Modern Composite Materials*, Lawrence J. Broutman and Richard H. Krock (Editors), Addison-Wesley, New York, 1967, pp. 27–105.

6-17 G. C. Sih and E. P. Chen, Fracture Analysis of Unidirectional Composites, *Journal of Composite Materials*, April 1973, pp. 230–244.

6-18 M. E. Waddoups, J. R. Eisenmann, and B. E. Kaminski, Macroscopic Fracture Mechanics of Advanced Composite Materials, *Journal of Composite Materials*, October 1971, pp. 446–454.

6-19 H. J. Konish, Jr., J. L. Swedlow, and T. A. Cruse, Experimental Investigation of Fracture in an Advanced Fiber Composite, *Journal of Composite Materials*, January 1972, pp. 114–124.

6-20 C. C. Chamis, M. P. Hanson, and T. T. Serafini, Impact Resistance of Unidirectional Fiber Composites, in *Composite Materials: Testing and Design (Second Conference)*, H. T. Corten (Chairman), Anaheim, California, 20–22 April 1971, ASTM STP 497, American Society for Testing and Materials, 1972, pp. 324–349.

6-21 N. J. Pagano, Exact Solutions for Composite Laminates in Cylindrical Bending, *Journal of Composite Materials*, July 1969, pp. 398–411.

6-22 N. J. Pagano, Exact Solutions for Rectangular Bidirectional Composites and Sandwich Plates, *Journal of Composite Materials*, January 1970, pp. 20–34.

6-23 N. J. Pagano, Influence of Shear Coupling in Cylindrical Bending of Anisotropic Laminates, *Journal of Composite Materials*, July 1970, pp. 330–343.

6-24 N. J. Pagano and A. S. D. Wang, Further Study of Composite Laminates Under Cylindrical Bending, *Journal of Composite Materials*, October 1971, pp. 521–528.

6-25 N. J. Pagano and Sharon J. Hatfield, Elastic Behavior of Multilayered Bidirectional Composites, *AIAA Journal*, July 1972, pp. 931–933.

6-26 Eric Reissner, The Effect of Transverse Shear Deformation on the Bending of Elastic Plates, *Journal of Applied Mechanics*, June 1945, pp. A-69–77.

6-27 R. D. Mindlin, Influence of Rotatory Inertia and Shear on Flexural Motions of Isotropic, Elastic Plates, *Journal of Applied Mechanics*, March 1951, pp. 31–38.

6-28 K. Girkmann and R. Beer, Application of Eric Reissner's Refined Plate Theory to Orthotropic Plates, *Osterr. Ingenieur-Archiv.*, Vol. 12, 1958, pp. 101–110. Robert M. Jones (Translator), Department of Theoretical and Applied Mechanics, University of Illinois, Urbana, 1962.

6-29 S. A. Ambartsumyan, *Theory of Anisotropic Plates*, J. E. Ashton (Editor), T. Cheron (Translator), Technomic, Stamford, Connecticut, 1970. (Russian publication date unspecified.)

6-30 J. M. Whitney, The Effect of Transverse Shear Deformation on the Bending of Laminated Plates, *Journal of Composite Materials*, July 1969, pp. 534–547.

6-31 J. E. Ashton and J. M. Whitney, *Theory of Laminated Plates*, Technomic, Westport, Connecticut, 1970, Chapter VII.

6-32 J. M. Whitney and N. J. Pagano, Shear Deformation in Heterogeneous Anisotropic Plates, *Journal of Applied Mechanics*, December 1970, pp. 1031–1036.

6-33 P. Constance Yang, Charles H. Norris, and Yehuda Stavsky, Elastic Wave Propagation in Heterogeneous Plates, *International Journal of Solids and Structures*, October 1966, pp. 665–684.

6-34 James M. Whitney, Stress Analysis of Thick Laminated Composite and Sandwich Plates, *Journal of Composite Materials*, October 1972, pp. 426–440.

6-35 E. Reissner, A Consistent Treatment of Transverse Shear Deformations in Laminated Anisotropic Plates, *AIAA Journal*, May 1972, pp. 716–718.

6-36 S. A. Ambartsumyan, *Theory of Anisotropic Shells*, State Publishing House for Physical and Mathematical Literature, Moscow, 1961. Also NASA TT F-118, May 1964.

6-37 Michael W. Hyer, Some Observations on the Cured Shape of Thin Unsymmetric Laminates, *Journal of Composite Materials*, March 1981, pp. 175–194.

6-38 Michael W. Hyer, Calculations of the Room-Temperature Shapes of Unsymmetric Laminates, *Journal of Composite Materials*, July 1981, pp. 296–310.

6-39 N. Fried, Degradation of Composite Materials: The Effect of Water on Glass-Reinforced Plastic, in *Mechanics of Composite Materials, Proceedings of the 5th Symposium on Naval Structural Mechanics*, Philadelphia, Pennsylvania, 8–10 May 1967, F. W. Wendt, H. Liebowitz, and N. Perrone (Editors), Pergamon, New York, 1970, pp. 813–837.

6-40 Stephen W. Tsai, Environmental Factors in the Design of Composite Materials, in *Mechanics of Composite Materials, Proceedings of the 5th Symposium on Naval Structural Mechanics*, Philadelphia, Pennsylvania, 8–10 May 1967, F. W. Wendt, H. Liebowitz, and N. Perrone (Editors), Pergamon, New York, 1970, pp. 749–767.

6-41 George S. Springer (Editor), *Environmental Effects on Composite Materials*, Volume 1, 1981, Volume 2, 1984, Volume 3, 1988, Technomic, Lancaster, Pennsylvania.

6-42 C. E. Browning, G. E. Husman, and J. M. Whitney, Moisture Effects in Epoxy Matrix Composites, in *Composite Materials: Testing and Design (Fourth Conference)*, J. G. Davis, Jr. (Chairman), Valley Forge, Pennsylvania, 3–4 May 1976, ASTM STP 617, American Society for Testing and Materials, 1977, pp. 481–496.

6-43 J. M. Whitney and J. E. Ashton, Effect of Environment on the Elastic Response of Layered Composite Plates, *AIAA Journal*, September 1971, pp. 1708–1713.

6-44 S. B. Dong, K. S. Pister, and R. L. Taylor, On the Theory of Laminated Anisotropic Shells and Plates, *Journal of Aerospace Sciences*, August 1962, pp. 969–975.

6-45 S. Cheng and B. P. C. Ho, Stability of Heterogeneous Aeolotropic Cylindrical Shells under Combined Loading, *AIAA Journal*, April 1963, pp. 892–898.

6-46 Robert M. Jones, Buckling of Circular Cylindrical Shells with Multiple Orthotropic Layers and Eccentric Stiffeners, *AIAA Journal*, December 1968, pp. 2301–2305. Errata, October 1969, p. 2048.

6-47 Robert M. Jones and Harold S. Morgan, Buckling and Vibration of Cross-Ply Laminated Circular Cylindrical Shells, *AIAA Journal*, May 1975, pp. 664–671.

6-48 Hong T. Hahn and Stephen W. Tsai, Nonlinear Elastic Behavior of Unidirectional Composite Laminae, *Journal of Composite Materials*, January 1973, pp. 102–118.

6-49 Hong T. Hahn, Nonlinear Behavior of Laminated Composites, *Journal of Composite Materials*, April 1973, pp. 257–271.

6-50 Donald F. Adams, Inelastic Analysis of a Unidirectional Composite Subjected to Transverse Normal Loading, *Journal of Composite Materials*, July 1970, pp. 310–328.

6-51 Robert M. Jones and Harold S. Morgan, Analysis of Nonlinear Stress-Strain Behavior of Fiber-Reinforced Composite Materials, *AIAA Journal*, December 1977, pp. 1669–1676.

6-52 Harold S. Morgan and Robert M. Jones, Analysis of Nonlinear Stress-Strain Behavior of Laminated Fiber-Reinforced Composite Materials, *Proceedings of the 1978 International Conference on Composite Materials*, Bryan R. Noton, Robert A. Signorelli, Kenneth N. Street, and Leslie N. Phillips (Editors), Toronto, Canada, 16–20 April 1978, American Institute of Mining, Metallurgical and Petroleum Engineers, New York, 1978, pp. 337–352.

6-53 Harold S. Morgan and Robert M. Jones, Buckling of Rectangular Cross-Ply Laminated Plates with Nonlinear Stress-Strain Behavior, *Journal of Applied Mechanics*, September 1979, pp. 637–643.

6-54 R. A. Schapery, Stress Analysis of Viscoelastic Composite Materials, in *Composite Materials Workshop*, S. W. Tsai, J. C. Halpin, and Nicholas J. Pagano (Editors), St. Louis, Missouri, 13–21 July 1967, Technomic, Westport, Connecticut, 1968, pp. 153–192. Also *Journal of Composite Materials*, July 1967, pp. 228–267.

6-55 David Ford Sims, *Viscoelastic Creep and Relaxation Behavior of Laminated Composite Plates*, Ph.D. dissertation, Department of Mechanical Engineering and Solid Mechanics Center, Institute of Technology, Southern Methodist University, Dallas, Texas, 1972. (Also available from Xerox University Microfilms as Order 72-27,298.)

6-56 Pei Chi Chou, Introduction to Wave Propagation in Composite Materials, in *Composite Materials Workshop*, S. W. Tsai, J. C. Halpin, and Nicholas H. Pagano (Editors), St. Louis, Missouri, 13–21 July 1967, Technomic, Westport, Connecticut, 1968, pp. 193–216.

Chapter 7

INTRODUCTION TO DESIGN OF COMPOSITE STRUCTURES

In this chapter, we begin the study of design of composite structures. First, the basic structural design process is reviewed. Then, the important topics of materials selection, configuration selection, and joints are addressed in their special composites materials and structures context. Next, design requirements are posed along with design failure criteria. Then, we introduce laminate design and optimization. Finally, a simplified design philosophy is presented. All these topics are part of the basic questions of laminated plate design as expressed in Figure 7-1, as well as part of the larger picture of composite structures design.

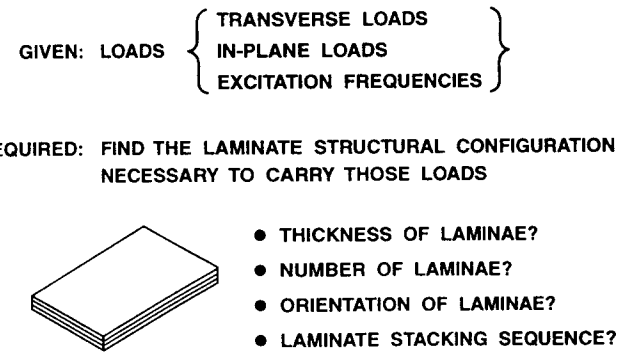

Figure 7-1 Basic Questions of Laminated Plate Design

7.1 INTRODUCTION

7.1.1 Objectives

The objectives of this chapter are listed in Figure 7-2. Each objective will be described in the following subsections.

- REVIEW THE STRUCTURAL DESIGN PROCESS
- LEARN THE NEW AND DIFFERENT USES OF COMPOSITE MATERIALS
- BECOME ACQUAINTED WITH MANUFACTURING PROCESSES
- BE ABLE TO RATIONALLY COMPARE ONE MATERIAL TO OTHERS
- KNOW THE ALTERNATIVE STRUCTURAL CONFIGURATIONS
- BE FAMILIAR WITH VARIOUS JOINT CONCEPTS
- UNDERSTAND DESIGN REQUIREMENTS AND FAILURE CRITERIA
- DETERMINE THE IMPORTANCE OF OPTIMIZATION CONCEPTS
- ESTABLISH A DESIGN PHILOSOPHY FOR COMPOSITE STRUCTURES

Figure 7-2 Objectives of the Introduction to Design Chapter

7.1.2 Introduction to Structural Design

We review the basic processes involved in structural design. You might not have background in structural design as a logic process, so some of the main aspects will be briefly described. That process is essentially independent of the material used (unless you focus on small details of the process). The structural design process is addressed in Section 7.2, which is a review of the basic design concepts that must be considered throughout the chapter. Pertinent design terms and procedures in the structural design process must be carefully defined.

7.1.3 New Uses of Composite Materials

You should learn and digest the very new and different characteristics of composite materials as actually used in structures as compared to what you are familiar with in metal structures. You must know the reasons why composite materials are used.

We all hear that composite materials are very expensive, but you have seen in Chapter 1 that, one, material cost is coming down, and, two, *composite structures can be less expensive to manufacture than metal structures.* An effective structure can be created with an even more-expensive raw material than metals by using less-expensive manufacturing processes. The bottom line is that the initial cost of the structure can in some cases be lower for a composite material than for a metal. Generally, the life-cycle cost of a composite structure is lower than that of a metal structure.

7.1.4 Manufacturing Processes

You should become acquainted with the various manufacturing processes for composite structures. That large body of processes for composite structures is very different from what most engineers are familiar with for metals. Manufacturing is one of the significant areas where composite materials hold tremendous advantages over metals. Manufacturing processes were addressed in Chapter 1 and will not be treated further here. Effective manufacturing is the key to cost competitiveness for a composite structure and, hence, the key to the success of a composite structure. Thus, the many alternative manufacturing processes unique to composite materials and structures must be explored within the design process itself.

7.1.5 Material Selection

You should be able to rationally compare one material to another material to select the best material for the structure you are designing. That comparison and selection activity is a very involved process because individual materials have their unique physical characteristics with virtues as well as faults. You try to find a material with a package of the best virtues with the least faults for your particular application. Your application is different from someone else's, so you will look for a material with a different package of characteristics than someone else. With composite materials, we have the inherent ability to construct many different combinations of materials. More than the ability is the fact that we actually have many different composite materials in practice that constitute many different members of a family of, for example, graphite-epoxies. Each member of the graphite-epoxy family has its own virtues for certain applications and would not be used for others. You must pick the right graphite-epoxy for the functional demands of your particular application. That material selection process is one of the keys to the success of any structural design. Section 7.3 is on materials selection where we will examine different materials as well as different forms of materials, and determine where and how they can be useful.

7.1.6 Configuration Selection

You should appreciate some of the various structural configurations or shapes that can be achieved with composite materials that are difficult, if not impossible, to achieve with metals. A broad, new dimension of flexibility exists with composite materials in structural configurations in general, and in stiffener configurations in particular, as compared to metals. Some configurations can be achieved very naturally with composite materials but simply cannot be done with metals. In Section 7.4, we address concepts in the process of selection of the appropriate structural configuration or shape to meet the design requirements. Among other things, we will examine how composite stiffeners can be made to be significantly more effective than metal stiffeners.

7.1.7 Joints

You should be familiar with some of the various concepts for how to analyze and design a joint between members of composite structures or between a composite structural element and a metallic structural ele-

ment. Transmitting loads between structural elements is a key problem area in the design process. We will consider joints, both bolted and bonded, in Section 7.5. Some of the difficulties in making a joint of composite materials will be examined as well as some of the successes that have been achieved.

7.1.8 Design Requirements

You should understand what design requirements are and what failure criteria mean in terms of design requirements. Satisfaction of a failure criterion for a structure does not necessarily mean that the structure has broken into two or more pieces. Failure in the context of a design simply means that object cannot perform its assigned function. That function could involve a deflection constraint instead of a stress constraint. Perhaps we are designing a piece of rotating machinery with an arm that cannot deflect downward too much or else the arm runs into another piece of the machine and jams the entire machine. Then, obviously, deflection is the governing design failure criterion, and our design's capability must be judged against that particular criterion. Many other examples exist to demonstrate how designs are measured in terms of their functional effectiveness.

In Section 7.6, we will discuss design failure criteria and how design requirements relate to an assessment of whether the design at hand satisfies those requirements. Many analysis results must be obtained before we can judge whether a design satisfies the pertinent design failure criteria. For example, a deflection-limiting condition was mentioned earlier for a particular piece of rotating machinery. We have analyzed for that circumstance what the deflections will be. Very obviously, we also must make certain that the part in question does not fail before that limiting deflection has been reached where failure means breaking into two parts, i.e., fracture. Therefore, we must look at the fracture requirements as well as the stiffness requirements. If the structure is a piece of rotating equipment, we usually have fatigue requirements as well. Thus, a multiplicity of conditions must be examined, and the totality of all those conditions is the set of design failure criteria that must be satisfied.

7.1.9 Optimization

You should determine the importance of various optimization concepts in design of composite structures. Actually, *the structural design process is optimization,* i.e., you are always seeking the *best* design where 'best' is measured in a variety of ways depending on the application. We must deal with many design variables such as plate thickness, stiffener spacing, etc. Thus, to believe that optimization concepts are the ideal approach to structural design is very tempting. It would be nice if we could say that mathematical optimization is a practical way for us to design a large structure right now, because that's what we would like very much to do. However, some practical limitations on optimization do exist that involve computer size, speed, and cost, as well as an ability to treat all the design variables.

We will consider optimization concepts in Section 7.7 to try to understand how we can take the many design variables that exist for a composite structure and try to answer the fundamental question in design: *what is the combination of the design variables that leads to the best composite structure?* The process flows from the design variables to 'a' structure via crude design and then to the 'best' structure via optimization techniques as in Figure 7-3. Some designers stop with 'a' structure having achieved their (limited) goals. However, optimization techniques enable us to go far beyond merely 'a' design, which is presumably inefficient, to a design which is optimum in some sense or senses. That second step is far more complex and rewarding than the trial and error techniques of the past. In fact, that second step is firmly based on mechanistic relationships between properties and performance that are used in contemporary design sensitivity studies.

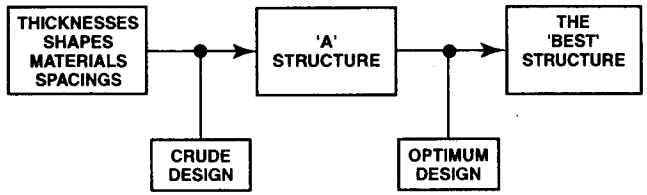

Figure 7-3 How to Get the 'Best' Structure

The 'best' structure could be interpreted in various ways. For airplanes, typically the most-desired situation is lowest weight. If the driving issue is performance, as in a military fighter, then the 'best' situation might be both highest performance and some combination of weight and cost. For commercial transport planes, the 'best' structure might be some combination of performance and cost. Thus, the question of how we optimize depends on what kind of structure we are building as well as on the overall optimization requirements. In the optimization concepts area in Section 7.7, we will examine a few techniques that are used, as well as some of the problems that are encountered for composite structures.

7.1.10 Design Philosophy

The final area of concern is to develop a practical design philosophy for composite structures. Is there a philosophy that will enable us to account for and accommodate all the essential behavioral characteristics of composite materials? Can we do it without getting bogged down in overly complicated issues?

Section 7.8 is on design philosophy for composite structures to explore some relatively simple and practical approaches to achieve an

effective composite design without stumbling over many problem areas. Those problem areas include micromechanics, optimization, nonlinear characteristics, free-edge effects, and all those behavioral aspects that you have heard of that could be significant problems with composite structures. The basic question is: how can we get around all those problems and design a composite structure that does all that we want it to do, yet suffers none of those problems?

7.1.11 Summary

Each of the preceding topics is addressed in the following sections of this chapter. Remember, this is only a brief introduction to the amazing and complex area of design of composite structures. Thus, detail must be kept subservient to the overall concepts.

7.2 INTRODUCTION TO STRUCTURAL DESIGN

7.2.1 Introduction

The general structural design process, irrespective of material used, is described as an introductory exercise in preparation for design with composite materials as in the outline in Figure 7-4. Then, design objectives and design drivers are defined to aid in the development of a design methodology. Next, the three basic design-analysis stages are described. The importance of testing parts of the structure at each stage of design is emphasized because the design process is not just a paper exercise, but must have practical applicability, and therefore must be validated.

- **WHAT IS DESIGN?**
- **ELEMENTS OF DESIGN**
- **STEPS IN THE STRUCTURAL DESIGN PROCESS**
- **DESIGN OBJECTIVES AND DESIGN DRIVERS**
- **DESIGN-ANALYSIS STAGES**

Figure 7-4 Outline of Structural Design

7.2.2 What is Design?

Let's begin with an introduction to the area of design of structures. We will first contrast analysis, with which you are presumably quite familiar, and design. Analysis is viewed in Figure 7-5 in this manner: *analysis is the determination of the behavior that a specific structural configuration exhibits under specific loads.* That is, what load does the structure take? Or, how much does the structure deflect at a certain crucial point? Analysis is a one-way street. We start with a specific structure, and ask: how good is this structure, how much stress can it take, or how much overall load can it take without violating any stress

limitations, deflection limitations, or any other performance limitations? What is the load at which the structure buckles? What are its vibration frequencies? Thus, *analysis is an overall assessment of the response and capabilities of the structure.* We start with one structural configuration and uniquely determine all the pertinent response characteristics. This process is generally a collection of either boundary-value problems or eigenvalue problems. Thus, analysis is a *deterministic* approach to solving a very narrow set of problems. We think of analysis as a very broad process of various features, but, relative to design, analysis is actually a quite narrow and restricted process.

- **ANALYSIS**

  THE DETERMINATION OF THE BEHAVIORAL RESPONSE EXHIBITED BY A PARTICULAR STRUCTURAL CONFIGURATION UNDER SPECIFIC LOADS (WHAT LOAD DOES THE STRUCTURE TAKE?)

- **DESIGN**

  THE PROCESS OF ALTERING DIMENSIONS, SHAPES, AND MATERIALS TO FIND THE BEST (OPTIMUM) STRUCTURAL CONFIGURATION TO CARRY SPECIFIC LOADS AND PERFORM SPECIFIC TASKS (WHAT IS THE 'BEST' STRUCTURE TO TAKE THE LOAD?)

Figure 7-5 Analysis versus Design

Many analysts tend to believe that design is merely a sequence of analyses. They also tend to think that finite element analysis is the foremost design tool in the world. Some people know me best as a finite element specialist, and yes, I did imply that finite elements are not the 'be all and end all'! Certainly finite element analysis is an indispensable *part* of most design practice for complicated structures. However, *the driving soul behind design is the* ***logic*** *for how to change the design variables in the configuration to meet the design requirements.*

In contrast to analysis, *design is the process of altering all the dimensions, the shapes, and perhaps the materials that are involved in a structural configuration to enable that configuration to carry specific loads, perform specific tasks, cost the least, weigh the least, or satisfy some other criterion for 'goodness'.* That is, we turn the problem around from analysis in one respect. We are saying: we do not know the structural configuration, but we know only the loads. What structure will carry these loads? *This problem does not have a unique answer!* We can find many different structures that will carry the desired loading. The process of design is trying to determine, under the constraints or guidelines for the particular object we want to design, what is the *best structure* to carry those loads. Therefore, *design is not a deterministic process.* Instead, design is an iterative procedure of selecting a configuration and seeing how close its capabilities are to satisfying the design requirements, and then making changes that we hope will lead toward satisfaction of all the design requirements. Typically included in the design process is a state-

ment that cost must be as low as possible and that weight must be as low as possible, if in fact those factors are considerations.

The key to a rational design process is establishing a set of mechanistic relationships that relate the configuration to its performance. Use of those mechanistic relationships is what distinguishes the structural designer from a dress designer.

Philosophically, *design is much more than just the inverse of analysis.* Analysis versus design is not a mathematical inverse problem. We have changed from a deterministic analysis problem to a nondeterministic design problem. The design problem has many decisions that must be made, and those decisions make design very complicated as well as nondeterministic. Moreover, the end result of the design process is not a unique solution to the design specifications! That is, many possible configurations might meet the design performance requirements. The question then becomes: which of the possible configurations is the 'best'?

As an example of the contrast between analysis and design, consider the column buckling problem. To analyze the buckling resistance of a simply supported, axially loaded column, we use the Euler-Bernoulli equation,

$$P = \frac{\pi^2 EI}{L^2} \tag{7.1}$$

usually derived in basic mechanics of materials, where P is the buckling load, E is the modulus of elasticity of the material, I is the moment of inertia of the column cross section, and L is the unsupported length of the column. A typical analysis problem consists of finding the buckling load for a specific column. Hence, E, I, and L are known, so the problem obviously is deterministic. That is, all the variables on the right-hand side of the single governing equation are known, so the equation can readily be evaluated.

In contrast to the analysis problem, suppose we must design a column to resist buckling under a prescribed load. Therefore, we seek the column properties E, I, and L knowing only the buckling load P, i.e., the load that must be carried without buckling. However, we have three unknowns, one known, and only one governing equation, so the problem obviously is not deterministic. Even if we know the column length as in a typical column design problem, we still do not have a tractable problem. We make the problem tractable by selecting the column from a specified set of possible materials, say steel, concrete, wood, or aluminum for an ordinary building column. That is, if we know L and E for a desired load P, we can solve for I from Equation (7.1):

$$I = \frac{PL^2}{\pi^2 E} \tag{7.2}$$

However, four different moments of inertia for each of the four different materials (hence different moduli of elasticity) are obtained from Equation (7.2). Moreover, *knowing the moment of inertia of a column does not tell us the shape or dimensions of a column!* We usually select a column

that has a moment of inertia at least as great as that determined from Equation (7.2). However, that selection process usually results in considering quite a few columns that meet the design requirements. Thus, we must exercise some other criterion besides buckling in order to select the actual column. That is, many columns can have the same required moment of inertia, so how do we decide which column is 'best'? Perhaps cost is an appropriate basis on which to compare the various columns, so we would select the material and cross section that correspond to the least-cost column. Or, perhaps weight is the design driver, so we would select the least-weight column. At any rate, the complexity of the design problem as opposed to the analysis problem is suitably illustrated in this example as summarized in Figure 7-6.

- **BUCKLING LOAD <u>ANALYSIS</u>**

$$P = \pi^2 \frac{EI}{L^2} \quad E, I, L \rightarrow P$$

- **<u>DESIGN</u> AGAINST BUCKLING**
  - **P DESIRED $\not\rightarrow$ E, I, L**
  - **IF L KNOWN, P, L $\not\rightarrow$ E, I**
  - **IF L KNOWN AND MATERIAL SELECTED, P, L, E $\rightarrow$ I**
  - **OR IF L KNOWN AND MATERIAL SELECTED FROM STEEL, CONCRETE, WOOD, AND ALUMINUM,**

$$P, L, E_S, E_C, E_W, E_A \not\rightarrow I_S, I_C, I_W, I_A$$

Figure 7-6 Buckling Design versus Analysis Example

An even more difficult problem occurs if the bar is not prismatic, i.e., if the moment of inertia is not constant along the length. We must then solve for I(x) where x is the axial coordinate of the bar. This optimization of cross-section distribution has been addressed only for problems with fixed E and L, not the general column design problem.

The term *trade-off* arises frequently in discussions of the design process. When conflicting objectives are encountered, some compromise must be achieved between the conflicts. To trade-off means to exchange (or trade) one achievement for another. For example, aircraft weight increases can be accommodated by shortening the range, decreasing the payload, increasing the fuel consumption, or some combination of all three possibilities. The appropriate trade-off of these consequences can be arrived at only by examining the requirements for successful operation of the aircraft and deciding what combination of factors is the most meaningful. Trade-offs are confined to the nonunique design process because of the existence of many possible solutions to the design problem. Trade-offs do not exist in analysis because there we deal with an already-defined configuration, so no changes are even possible.

7.2.3 Elements of Design

Let's investigate the fundamental elements of design. Some elements you will surely recognize, but others might not be so familiar. Still, in order to start out properly, let's begin with the basics so you understand the terms and the concepts addressed in this chapter. The following paragraphs are an explanation of the design elements displayed in Figure 7-7.

- **ANALYSIS POSSIBILITIES**
  IF WE CAN'T ANALYZE IT, WE CAN'T DESIGN IT
- **MANUFACTURING ALTERNATIVES**
  IF WE CAN'T MAKE IT, THE 'DESIGN' IS WASTED
- **MATERIALS SELECTION**
  DID WE CHOOSE THE 'BEST' MATERIAL?
- **CONFIGURATION SELECTION**
  WHAT ALTERNATIVE CONFIGURATIONS WOULD BE BETTER?
- **JOINING TECHNIQUES**
  WE MUST BE ABLE TO PUT IT TOGETHER
- **OPTIMIZATION**
  DO WE HAVE THE 'BEST' DESIGN?

Figure 7-7 Elements of Design

As the first element, we must determine whether we can analyze the object. We must consider and evaluate the analysis possibilities because *if we cannot analyze the object, then we cannot possibly design it in a rational way.* If design means putting together a collection of parts that we are certain will do the job, then, admittedly, analysis is not essential. Presumably, we are trying to rationally design something where we ask: what size and shape must each part be in order to do its job in the overall structure? Answering that fundamental question requires us to be able to perform a collection of definitive analyses to evaluate the capability of each part of the structure as well as that of the overall structure. Accordingly, analysis in the form of mechanistic relations is absolutely essential.

The second major element of design is the collection of manufacturing alternatives because *if we cannot make the object, then the design is virtually useless.* We might seemingly have a nice idea for a structure, but if nobody can build the structure, then the idea is a waste of time.

Next, the material selection element: *did we choose the 'best' possible material for each part of the structure?* For the overall structure, the question is more general: did we choose the right set of materials to be able to make the structure in the 'best' possible way?

Configuration selection is: *have we found among all the alternative configurations the one that 'best' satisfies our objectives?* Is there something about a composite structure that involves different freedoms than we customarily consider for metals? Will those new freedoms enable us to select the 'best' possible configuration for our particular structure?

Joining techniques is the next element of design. *It does no good whatsoever to have a collection of structural elements that cannot be fastened together.* Thus, joining techniques are fundamental to our appreciation of how to design an entire structure. Without them, the structure has no meaning, but is just a collection of pieces that do not work together. Some areas in joining techniques bear some similarities to those for metal structures, although there are some very significant differences.

The next element of optimization is really the fundamental question in design. To many people, *design is optimization.* How successfully we are able to optimize a structure depends upon the number of design variables and the mathematical techniques available to perform that optimization. However, optimization means we must consider all the many design variables and find the 'best', i.e., the optimum, combination of values of design variables. Stating that objective or goal is easy. Our inability to actually accomplish that goal is related to limitations on our computational and theoretical techniques as well as to lack of effective strategies for optimization. When we try to automate the design procedure, we find that we must, in some respects, simulate the complex workings of the human mind. We often think of design as a task that we can do in our heads, and, in fact, with simple designs that is exactly what we do. However, for a composite structure with all of its design variables (many more than for a metal structure), a very wide range of actions must be taken that, right now, our computer technology does not permit us to take. We cannot, at present, totally automate the design of a Boeing 747 jumbo jet. However, we can make progress here and there toward that goal. We can do certain pieces of the overall project. But if you have ever seen a drawing of the structural framework in a Boeing 747, you would very easily recognize that the number of decisions that must be made is extremely high and hence would involve an enormously complex automated design procedure. Note that I addressed the use of finite elements in design, not analysis! The Boeing 747 was *analyzed* with the finite element method (which was largely developed by Boeing personnel in the 1950s).

The acceptability of a design in an optimization procedure depends on the nature of the behavior aspect that we want to optimize (often called the *merit function*) in the vicinity of the optimum. For example, if weight is the merit function, then we want to find the least-weight structure that will fulfill the design requirements. To simplify the example, we consider a structure with only a single design variable, x. If the optimum weight is very different from the surrounding weights in design space as in Figure 7-8, then only the optimum design is acceptable. That is, a big weight penalty exists for small variations of the design variable away from the optimum value. However, if the optimum weight is only slightly lower than the weight of many designs adjacent in design space as in Figure 7-9, then many acceptable designs exist. That is, a very small weight

penalty exists for rather sizeable variations of the design variable away from the optimum value. Achieving the optimum design in the latter case might not be very worthwhile. That is, the payoff in weight saved by using the optimum design might not be worth the cost of finding the optimum design in this case. That situation would surely exist if some part of the Boeing 747 had an optimization curve like Figure 7-9. In that example, the cost of finding the optimum design would be many times higher than simply finding a design somewhere in the broad more or less trough-like region. Sensitivity studies for various design variables must be performed to determine whether a design is strongly affected by a particular variable as in Figure 7-8 or weakly affected by another variable as in Figure 7-9. The strength of the effect depends on whether the derivative dW/dx in Figures 7-8 and 7-9 is high or low near the optimum design.

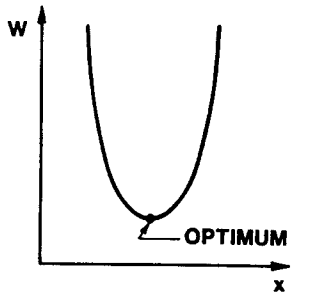

ONLY THE OPTIMUM DESIGN IS ACCEPTABLE

Figure 7-8 Narrow Optimum Design

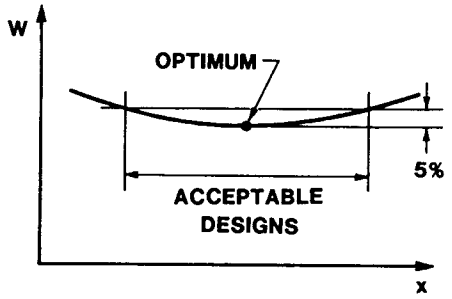

MANY DESIGNS ARE NEARLY OPTIMUM

Figure 7-9 Wide Optimum Design

Each design is actually a function of many design variables, e.g., lamina orientations, stiffener spacings, stiffener web heights, etc. The dependence of the merit function on a single design variable at a time is depicted in Figures 7-8 and 7-9 instead of a difficult-to-visualize function of many variables that cannot be depicted in three dimensions. Some design variables are strong design drivers as in Figure 7-8, whereas other design drivers are weak design drivers as in Figure 7-9. Thus, the notion of strong design drivers being associated with critical derivatives in different directions in design space must be considered. One of the main problems in design is determining which variables are strong drivers, which variables are weak drivers, and which variables do not matter in the specific design being considered. That is, what are the critical derivatives for the design?

One of the key elements in laminated composite structures design is the ability to *tailor* a laminate to suit the job at hand. Tailoring consists of the following steps. We want to design the constituents of the laminate, and those constituents include the basic building blocks of the individual laminae and as well how they are oriented within the laminate. We design those constituents to just barely meet (with an appropriate factor of safety) the specific requirements for, say, strength and stiffness,

although there could be many other design factors as well. Therefore, at the very least, we must evaluate elements of strength and stiffness. One of the elements is how big can the load be, and that is a problem which we have previously addressed for a metal structure. We size the structure to take a certain magnitude of load. Now we are able to include with a composite laminate a very different characteristic, namely the *direction* from which the load comes.

We could in fact prejudice a metal structure to be able to take higher loads from one direction than from another by using stiffeners. But, for the basic metallic monocoque plate structural element used for example in an aircraft wing, the same capabilities for carrying load exist in all directions of that wing skin. The metal wing's load-carrying capabilities are prejudiced by putting stiffeners in various directions. Then, the wing is able to resist a different bending moment M_x along the axis of the wing in Figure 7-10 than twisting moment M_y about the axis of the wing. We make those changes in capability by using different stiffeners in different directions with a metal structure.

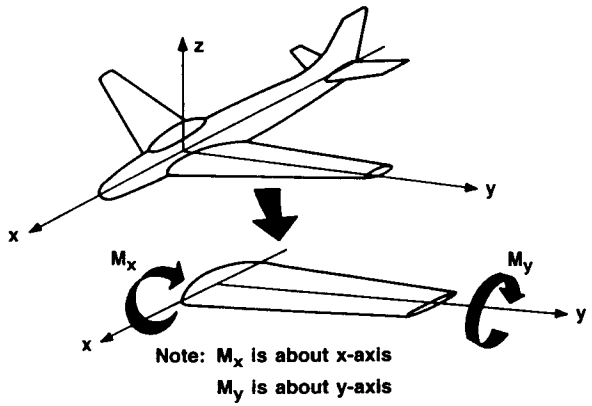

Figure 7-10 Aircraft Wing Loadings

In contrast, for composite structures, we have two methods of achieving different load-carrying capabilities in different directions. One method is at the laminate level where *the laminate's capabilities can be directionally prejudiced without changing its thickness simply by changing the laminate stacking sequence.* Changing the stacking sequence of a composite laminate has no analog for a metal structure. The other method of achieving different load-carrying capability in different directions for a composite structure is that we can, of course, use stiffeners just as we do for metallic structures. However, with composite structures we can go one step further than for a metallic structure in the sense that we can have much more efficient stiffeners. If the stiffeners are made of composite materials, then we can make them of different kinds of composite materials in different regions of the stiffeners. We can take advantage of the best possible performance of a very high-modulus fiber by putting it in the flange of an I-section and letting the web be a less-

capable material because the web is not where most of the structural action takes place. If we can transfer the shear loading to that web, we have done the job we must do. Often that shear loading can be transmitted with a glass-epoxy web, whereas the flange might be graphite-epoxy or boron-epoxy. Thus, we can tailor portions of the structural elements as well as the overall laminate to take directionally different loads in a composite structure.

7.2.4 Steps in the Structural Design Process

In structural design, we start with a set of design requirements in order to define our objectives. The design requirements are merely a statement of what we want the structure to do. That overly simplistic definition will be expanded upon throughout the book, especially in Section 7.2.5 and in Section 7.6. With that objective in mind, we will now examine the steps we must take to attack the objective.

The structural design process is depicted by means of a schematic flow chart in Figure 7-11. That is, the flow chart is not a precisely defined computer program flow chart, but is instead a flow chart of ideas, concepts, and procedures. We start presumably knowing the loads that must be carried and what materials might possibly be considered for our design. Through some process, we then choose an initial configuration for our structure. That configuration might be very crude, but constitutes a start to the *necessarily iterative design process*. At this point, we might have a significant problem because if our structure is an airplane, we do not know the precise aerodynamic loads without knowing the actual structural configuration. Thus, sometimes there is a lot of interplay between choosing the initial configuration and determining the loads used in design. Accordingly, the design process is often not as simple as portrayed here. However, once we have the initial configuration, some knowledge of the loads, and some idea of what materials we might like to use, then we can begin the actual structural design process.

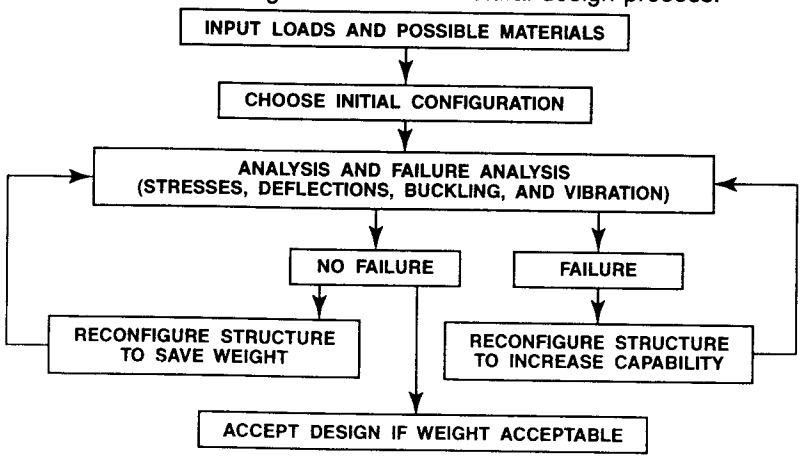

Figure 7-11 The Structural Design Process

7.2.4.1 Structural Analysis

We go next to the analysis and failure analysis block in Figure 7-11. That is, we consider the initial configuration with a particular material or materials. Then, for the prescribed loads, we perform a set of structural analyses to get the various structural response parameters like stresses, displacements, buckling loads, natural frequencies, etc. Those analyses are all deterministic processes. That is, within the limits of accuracy of the available analysis techniques, we are able to predict a specific set of responses for a particular structural configuration. We must know how a particular structural configuration behaves so we can compare the actual behavior with the desired behavior, i.e., with the design requirements.

7.2.4.2 Elements of Analysis in Design

Let's examine the elements of analysis that occur in the overall design process. The objective of analysis is to determine the pertinent structural response parameters in Figure 7-12. Then, we must assess various modes of failure, and the failure modes will be described by relating them to the structural response characteristics. Stiffness, for example, is related to the common requirement that we cannot have too much deflection in various critical parts of the structure. Buckling will occur if the load is so high that this structure cannot actually carry the desired level of load without the added deflections and decreased stiffness that constitute the structural response behavior typical of a buckled structure. We must be able to predict the vibration modes and frequencies so that we know how to avoid resonance or, alternatively, what the dynamic response will be. We must evaluate the strength by predicting various stresses in preparation for comparing them to appropriate failure criteria. Those stresses include membrane stresses, bending stresses, stresses between layers, stresses around holes and cutouts, stresses around defects, etc. Moreover, we must be able to analyze joints so we are assured that loads can be transmitted between structural elements.

- **DETERMINE PERTINENT STRUCTURAL RESPONSE PARAMETERS**
  - **DEFLECTIONS**
  - **BUCKLING LOADS**
  - **VIBRATION FREQUENCIES**
  - **STRESSES**
    - **FULL-FIELD STRESSES**
    - **STRESSES AROUND CUTOUTS**
    - **STRESSES AROUND DEFECTS**

Figure 7-12 Elements of Analysis in Design

7.2.4.3 Failure Analysis

Next, we perform a failure analysis in which the various structural response parameters just obtained are compared with their allowable or required values as in Figure 7-13 to determine whether the current design is satisfactory. If all response parameters are in acceptable ranges, then that fact is acknowledged on the left-hand side of Figure 7-11 by exiting the failure analysis box to a box labeled 'no failure'. If the current design does not violate any of the design requirements, then that fact signifies there is no failure. However, just because there is no failure does not mean we have the best structure or even an acceptable structure. If weight is the driving factor in the structural design, for example, then the structure must have the least weight. Then, if there has been no failure, we can conclude that the structure is overdesigned to some degree. We will, of course, include in all failure analyses appropriate factors of safety. Factors of safety must be applied against too much stress, against too much deflection, against approaching a buckling load, against approaching a natural frequency to avoid resonance, etc.

- **ARE THE STRUCTURAL RESPONSE PARAMETERS WITHIN DESIGN BOUNDS?**
  - **DEFLECTIONS TOO HIGH?**
  - **BUCKLING LOADS TOO CLOSE?**
  - **VIBRATION FREQUENCIES NEAR RESONANCE?**
  - **STRESSES TOO HIGH? LESS THAN STRENGTH?**
    - **FULL-FIELD STRESSES**
    - **STRESSES AROUND CUTOUTS**
    - **STRESSES AROUND DEFECTS**

Figure 7-13 Failure Analysis in Design

Those factors of safety for various types of failure can be very different from one another depending on whether we are designing against a catastrophic failure event or against a benign failure event. Obviously, factors of safety against catastrophic failure events must be considerably higher that those against benign failure events. For example, the factor of safety against buckling of a column must be higher than the factor of safety against buckling of a plate. The reason for that relationship is the basic physical response characteristic that a column cannot carry any higher load than the buckling load (see Section 5.4). In contrast, a plate can carry considerably more load after buckling, but does so with a reduced stiffness. Thus, column buckling is a much more limiting and drastic event than is plate buckling. That nature of failure is accordingly reflected in the value of the factor of safety, i.e., how far away we must stay from that event. Also, factors of safety for a manned structure are higher than for an unmanned structure.

In practice, factors of safety are, for various reasons, different for composite structures than for metal structures. A factor of safety is usually a legislated number that is arrived at 'in committee' by evaluation of the various consequences of a specific kind of failure in a particular

type of structure. Such a committee can have representatives from engineering societies, industry associations, governments, and universities. A different factor of safety might result for the load-carrying capacity of a fastener in a composite bolted joint than for a metal bolted joint because of issues such as the following. With a composite bolted joint, bearing capability is typically lower than for metals. Also, at a hole, a higher stress concentration factor exists for a composite material than for a metal. If the metal were aluminum, certain yielding capabilities exist around that stress concentration area that do not exist with a more brittle (i.e., nonyielding) composite material. Thus, a factor of safety for a fastener in a metal joint is quite different than that for a composite material joint because of the many factors that affect the level of stress versus the potential failure. Other examples of a similar nature exist because of the unique behavioral characteristics of composite materials as compared to metals. We must evaluate the failure of composite materials in a different manner than we do metals, so different factors of safety are appropriate.

Finally, *failure analysis* is the process of comparing actual performance with the desired performance. Thus, failure analysis is a nontrivial part of the structural design process. Facets of failure analysis including what failure means for a structure are addressed in Section 7.6 on Design Requirements and Design Failure Criteria.

7.2.4.4 Structural Reconfiguration

Reconfiguration of a structure simply means to change some or all of the design variables such as thicknesses, fiber directions, stiffener sizes, etc. to achieve a more suitable structure than the current configuration. Note that the term 'more suitable' has two possible meanings. If the structure has too little capability relative to the loads and conditions we place on it, then the structure is underdesigned, and we must reconfigure the structure to *increase* its capability. However, if the structure has too much capability, then it is overdesigned, and we must reconfigure the structure to actually *decrease* its capability. Both alternatives will be discussed. Recognize that *structural reconfiguration is the very heart of structural design.*

Suppose we perform the failure evaluation for the structural configuration and find some kind of a failure, i.e., a violation of one or more of the design requirements. Thus, the structure is underdesigned, so its capacity must be increased. Accordingly, we must move to the next box labeled *reconfigure the structure to increase capability.* The word *capability* is used here in a very broad sense. Increasing the capability could actually mean increasing the stiffness to change the deflection conditions. That is, increasing capability could mean decreasing deflections if that was the violated design requirement. Increasing capability could also mean increasing buckling loads or increasing vibration frequencies. That is, somehow we must *reconfigure the structure to increase the basic structural capabilities.* Under some circumstances, we might actually want to decrease the stiffness to avoid an exciting frequency driving the structure into resonance.

If the current design in the iterative design process depicted in Figure 7-11 did not fail, then the structure is overdesigned. Accordingly, we must change the structure, i.e., reconfigure the structure, so that it will carry the same load but at a lower weight. And at that lower weight we must reevaluate the structural performance. Thus, we must go through some process to *reconfigure the structure to save weight.* After reconfiguration, we proceed back up on the flow chart in Figure 7-11 to the analysis and failure analysis box because we now have a new configuration to evaluate. We must go through the process all over again of determining the structural response parameters and comparing them with their allowable values.

With the newly reconfigured structure, we go back to the analysis and failure analysis block in Figure 7-11 and evaluate the new configuration. We keep cycling around the diagram (figuratively speaking) between failures and no failures until the design is refined to the point where it has the least weight and satisfies all the design functional requirements, i.e., does not fail in any of the possible ways. Those conditions are what is meant by the design not violating any of the design requirements in general. Then, we would accept that design if the weight is acceptable. Perhaps, from other analyses, we have determined that the airplane being designed cannot weigh more than a certain amount. Otherwise, for various propulsion requirements, we cannot make the plane travel at the required speed or have the required range and so on (those issues are design requirements, too). After all the design requirements are satisfied and the weight is as small as possible, then the design is declared to be satisfactory. The same kind of overall design process can be performed with a governing parameter other than weight. The other design parameter could be cost, or it could be various performance-related objectives, or some combination thereof.

We have examined one view of structural design, and we will focus our attention later on in Section 7.4 how to reconfigure a composite structure as opposed to a metal structure. That reconfiguration process will be our principal interest. In this section, we simply address the basic structural design process irrespective of the materials used.

7.2.4.5 Iterative Nature of Structural Design

The characteristic iterative nature of the structural design process is illustrated along with the obvious analysis content of design in Figure 7-14, which is a simplification of the more comprehensive Figure 7-11. In the simplified design-analysis iterations, we have three kinds of analysis: loads, stress and displacement, plus failure. When a specific configuration does not satisfy the design requirements imposed in the failure analysis, the design must be modified. Those modifications typically consist of either (1) geometrical parameters such as thicknesses or stiffener spacings or (2) material properties such as substituting a different material or (3) both geometrical parameters and material properties. The modifications and analysis are repeated in the design process in an *iterative* fashion until all the design requirements are satisfied.

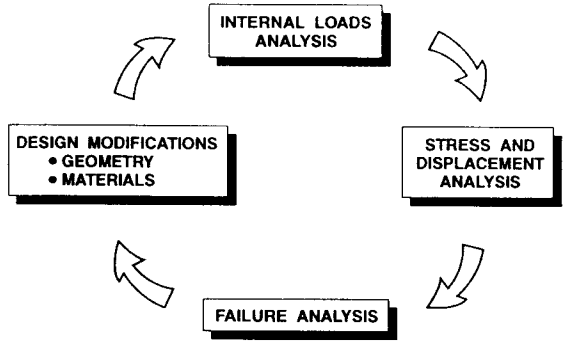

Figure 7-14 Simplified Design-Analysis Iterations

7.2.5 Design Objectives and Design Drivers

A *design objective* is a statement of what we want the structure to do and/or to be. The three principal design objectives are expressed in terms of function, cost, and weight. *Function* is the set of performance requirements or design requirements that the structure must meet or be able to do. *Cost* is the life-cycle cost of the structure, i.e., the initial purchase price plus the operating and maintenance costs over the life of the structure less any scrap value at the end of the structure's life as defined in Section 1.3.2. *Weight* is obviously the structural weight and might or might not be important. For aircraft, low weight is obviously crucial. For spacecraft, low weight is all-important. For buildings, weight is not usually a significant factor. Note that function often has many objectives, whereas cost and weight are each single objectives.

The structure can be optimized, i.e., designed, for any one, two, or all three design objectives. That is, the design objectives might be to have the lowest weight aircraft for a specified set of functions that must be performed. Or, the highest speed aircraft might be the most important objective with cost being allowed to rise in order to achieve the desired speed. Perhaps the cost might be minimized with certain compromises made for performance or weight. At any rate, every design must be measured against fundamental design objectives expressed in terms of function, cost, and weight.

A *design driver* is a design variable that, when changed, strongly influences the performance of the design as in Figure 7-8. A design driver can also be a design condition that strongly influences which design variables govern the design. One of the early objectives in the design process is to identify the design drivers and concentrate on manipulating them as opposed to changing variables that do not strongly influence the design. Thus, for aircraft, we would make many decisions based on how we can get each part of the structural job done with the least amount of weight because of its strong influence on range, econ-

omy, and performance. Similarly, spacecraft have a least-weight objective because of the design driver of high cost to boost the spacecraft into space. Accordingly, it is not at all surprising that we use high-stiffness–low-weight materials such as composite materials to achieve the design objective of least weight. Cars are also weight-sensitive, in general, but some parts are especially sensitive to strength and stiffness. Trusses are stiffness-sensitive because of the tendency of compression members to buckle.

A specific example of strong and weak design drivers is developed by examining the bending resistance of the stiffened panel in Figure 7-15. There, the stiffener web height is a strong influence on the panel bending resistance because the stiffener moment of inertia is strongly affected and, in turn, has a large influence on the bending resistance. (Refer to the discussion of the second moment of the area of a stiffener in Section 7.4.2.) However, stiffener web thickness is not a strong design driver because web thickness has little influence on bending resistance. We conclude through similar reasoning that flange thickness, flange width, and stiffener spacing are strong design drivers in Figure 7-15 and that skin thickness is a weak design driver. We must be conscious of the type of design drivers at each of the three stages of design-analysis.

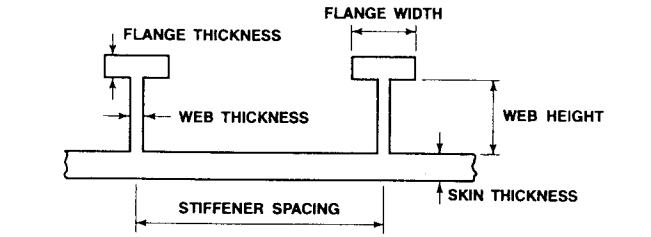

Figure 7-15 Anatomy of a Stiffened Panel

7.2.6 Design-Analysis Stages

The term *design-analysis* is used to emphasize the essential, but not dominant, role of analysis in the overall structural design process. Analysis plays no role whatsoever in dress design (with the possible exception of the now-classical analysis of a strapless evening gown). However, *engineering design of a structure must involve analysis in the form of mechanistic relationships.* Those mechanistic relationships must be used to quantitatively determine how to create the structural capabilities and then to match them to the structural requirements. The distinction between design and design-analysis is perhaps not quite so important for metal structures as for composite structures. For metal structures, designers can rely to a large extent on rules of thumb. Often, such designers were not educated as engineers, but were trained 'on the (drawing) boards'. However, composite structures designers do not have such simple and convenient rules of thumb because the configuration and behavior of composite structures are far more complex than those of metal structures. And, those behavioral complications and configurational options require the designer to use mechanistic relationships to provide the rationale to size the various parts of the structure. The word design *should* bring to mind the picture of an engineer putting to use the mechanistic relationships along with ingenuity to design a structure. However, the usual concept is more on the order of imagining a designer who is not necessarily an engineer using only a collection of rules of thumb to create a design. Accordingly, the essential role of analysis in the structural design process is emphasized in this book by using the term *design-analysis.*

The design-analysis stages that we address here are surely both logical and familiar: preliminary design-analysis, intermediate design-analysis, and final design-analysis as indicated in Figure 7-16. The differences between the three stages will now be defined. They are nearly self-explanatory, but let's examine the specific meanings.

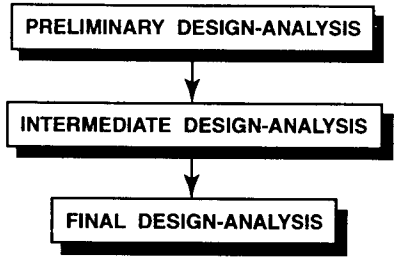

Figure 7-16 Design-Analysis Stages

7.2.6.1 Preliminary Design-Analysis

At the **preliminary design-analysis** stage of a structure, we make an initial attempt, i.e., take some kind of a first cut or approximation, at achieving a structural configuration to help define the *weight.* We also take a first cut at satisfying the various system requirements which relate to *function*, as suggested in Figure 7-17. And we also consider at this stage some kind of a first cut at determining the manufacturing feasibility, which has a big impact on what the structure will *cost.* Because we are dealing with a relatively simple structure at this stage, we must have an easy-to-use computer program for analysis. For some structures, perhaps only a one-dimensional treatment of the structural configuration is needed, e.g., a beam model.

- FIRST CUT AT STRUCTURAL CONFIGURATION (WEIGHT)
  - IDENTIFY DESIGN DRIVERS
  - PERHAPS USE ONE-DIMENSIONAL ANALYSIS
- FIRST CUT AT SYSTEM REQUIREMENTS (FUNCTION)
- FIRST CUT AT MANUFACTURING (COST)
- USE A SIMPLE COMPUTER PROGRAM

Figure 7-17 Preliminary Design-Analysis

7.2.6.2 Intermediate Design-Analysis

The **intermediate design-analysis** stage is sometimes called trade studies. The actual terminology depends on the industry or company where you work. Basically, we address analysis of the various design concepts that we are considering for use in our structure in a more sophisticated manner than was done at the preliminary design-analysis stage. Typically, at this stage, as in Figure 7-18, we would use a more sophisticated and capable analysis computer program than in the preliminary design-analysis stage. In the process of using this sort of program and evaluating the various design concepts, we determine the impact of all of those competing concepts on the three fundamental objectives of weight, cost, and function for our design. At this stage, we would expect to fabricate and test some simple models of the critical components in this structure to make sure that the design calculations are realistic instead of strictly a paper exercise that might not lead to an effective structure.

- MORE SOPHISTICATED ANALYSIS OF COMPETING DESIGN CONCEPTS
  - EXERCISE DESIGN DRIVERS
  - PERHAPS USE TWO-DIMENSIONAL ANALYSIS
- ASSESS IMPACT OF ALL CONCEPTS ON WEIGHT, COST, AND FUNCTION
- USE AN INTERMEDIATE-LEVEL COMPUTER PROGRAM
- FABRICATE AND TEST SIMPLE MODELS OF CRITICAL COMPONENTS

Figure 7-18 Intermediate Design-Analysis

7.2.6.3 Final Design-Analysis

In the last stage of **final design-analysis**, which is sometimes called detailed design, we must study all the final details of the shape, the joints, perhaps cutouts and stiffeners, especially stiffeners around cutouts and so on, and all the system interactions in a very sophisticated model of the structure as listed in Figure 7-19. A sophisticated model is necessary to incorporate those kinds of details. Typically, we would use a super-sophisticated general-purpose computer program such as NASTRAN. In this final design-analysis stage, we must assess the impact of all the details of the competing structural concepts on the weight, cost, and function of the structure that we are trying to design. Naturally, we will have only one structural concept to address at this design-analysis stage because we will have eliminated all of the other concepts in earlier design-analysis stages.

- STUDY FINAL DETAILS OF JOINTS, CUTOUTS, STIFFENERS, AND SYSTEM INTERACTIONS IN A SOPHISTICATED MODEL
  - REFINE DESIGN DRIVERS
  - PERHAPS USE THREE-DIMENSIONAL ANALYSIS
- USE A SUPER-SOPHISTICATED COMPUTER PROGRAM SUCH AS NASTRAN
- ASSESS IMPACT OF ALL DETAILS ON WEIGHT, COST, AND FUNCTION
- FABRICATE AND TEST GOOD SIMULATIONS OF CRITICAL COMPONENTS

Figure 7-19 Final Design-Analysis

At this stage, we typically fabricate and test some good simulations of critical components of the structure. These tests are not necessarily subscale tests, although we could still have some of them, but we probably go all the way up to full-scale tests. When do we regard the structure as having been designed? The structure is designed when we can demonstrate that it meets all the design requirements, and, more often than not, that demonstration takes a full-scale structural test, as well as many time-consuming flight tests for an aircraft.

7.2.7 Summary

In this section, the structural design process was briefly described with emphasis on analysis, failure analysis, and structural reconfiguration. The three fundamental design-analysis stages, preliminary, intermediate, and final, were defined and illustrated. At each stage of design-analysis, testing representative components of the structure or subassembly of the structure is essential in order to be reasonably assured that nothing has gone wrong or has been overlooked in the design process.

7.3 MATERIALS SELECTION

7.3.1 Introduction

The fundamental objective in this section is to describe the factors and procedures to select the right material for a specific structural application. The 'right stuff' for a material, as for a fighter pilot or an astronaut, is a complex combination of characteristics. To select the proper material requires being able to characterize and evaluate various composite materials (or metals!) and to compare their attractive characteristics with the behavioral features required for a particular structure. Finally, a materials selection example of a space truss design problem will be addressed.

7.3.2 Materials Selection Factors

The discussion of materials selection factors is naturally divided into three parts: (1) overall factors pertinent to selection of the composite material itself, (2) factors governing the selection of the fibers, and (3) factors essential to selection of the matrix system. Those three types of selection trade-offs will be described, followed by summary remarks on the process of selecting a suitable composite material.

The materials selection factors that might be considered are fairly obvious and are displayed in Figure 7-20. These factors are actually the same ones that would be used when choosing a composite material as opposed to a metal.

- STRENGTH
- STIFFNESS
- FATIGUE LIFE
- DENSITY
- TOUGHNESS
- COST
- TEMPERATURE DEPENDENCE
- THERMAL EXPANSION
- WEAR RESISTANCE
- CORROSION RESISTANCE
- CONDUCTIVITY
  - ELECTRICAL
  - THERMAL
- INSULATION
  - ACOUSTICAL
  - THERMAL

Figure 7-20 Materials Selection Factors

The factors that might be generally considered first and foremost are stiffness and strength for structural applications. Much of the developmental and applications work for composite materials has been focused on weight-sensitive structures such as aircraft. There, the high strength-to-weight and high stiffness-to-weight characteristics of composite materials are the primary design drivers. However, for many applications, other factors or drivers are more important than stiffness and strength.

The toughness of a material is a design driver in many structures subjected to impact loading. For those materials that must function under a wide range of temperatures, the temperature dependence of the various material properties is often of primary concern. Other structures are subjected to wear or corrosion, so the resistance of a material to those attacks is an important part of the material choice. Thermal and electrical conductivity can be design drivers for some applications, so materials with 'proper' ranges of behavior for those factors must be chosen. Similarly, the acoustical and thermal insulation characteristics of materials often dictate the choice of materials.

For a space structure of any kind, the main concern will probably be with the coefficients of thermal expansion and the various stiffnesses. Most readers are probably aware from various Space Shuttle problems that the Shuttle gets heated more on one side than the other if it does not keep turning around relative to the sun. During one mission, the payload-bay doors were opened, but could not be closed again. The television commentator said that the doors had expanded and were warped so much that they would not fit back into the opening to be locked

shut. However, door expansion was not the problem at all because the graphite-epoxy cloth in the doors has, at worst, coefficients of thermal expansion in various directions that more or less match the surrounding metallic structure. Actually, the *underside* of the Shuttle had been overexposed to the Sun and therefore expanded to cause the Shuttle to bend into a banana shape. Thus, the opening into which the graphite-epoxy doors must fit was made smaller. The only way that problem can be solved is by rotisarizing the Space Shuttle, and that is just what NASA did. The astronauts rolled the Shuttle over to keep the lower body away from the sun for a while, and then they could shut the doors.

For a space telescope, the pointing accuracy required is quite high and can be thought of in the following manner. If the telescope is in New York and pointed at San Francisco, the accuracy with which it must be pointed is within the diameter of an orange nearly three thousand miles away! Thus, not much deformation of the telescope or its supporting structure can be tolerated. The overall objective is to be able to point the telescope within that accuracy, and we must then do what is necessary in order to achieve that required accuracy. In the scope of a project like the Hubble Space Telescope with the overall project cost exceeding $1 billion, there is considerable latitude to find materials that will do the job. If there is a job to be done, then the material must be found that will do it. Cost is therefore not the most pressing issue. *Function* is the most pressing issue!

Other examples exist where different factors on the list of material selection factors in Figure 7-20 are the design drivers. However, at the time of the initial applications of advanced composite materials, the main issues were simply strength and stiffness. Perhaps a fatigue-life issue could be more important in some applications. Some applications are made despite some disadvantages for composite materials in some of these material selection factors. For example, the electrical conductivity of graphite-epoxy is not sufficient when designing an aircraft subject to a lightning strike (as are all aircraft). All parts of an aircraft must be able to dissipate the electrical charges of lightning strikes. Thus, some supplementary material or electrically conductive material systems must be added to the graphite-epoxy in order to provide the aircraft with appropriate lightning-resistant characteristics.

7.3.3 Fiber Selection Factors

Fibers are often regarded as the dominant constituents in a fiber-reinforced composite material. However, simple micromechanics analysis described in Section 7.3.5, Importance of Constituents, leads to the conclusion that fibers dominate only the fiber-direction modulus of a unidirectionally reinforced lamina. Of course, lamina properties in that direction have the potential to contribute the most to the strength and stiffness of a laminate. Thus, the fibers do play the dominant role in a *properly designed* laminate. Such a laminate must have fibers oriented in the various directions necessary to resist all possible loads.

Fiber selection is usually based primarily on the required strength or stiffness. That selection process is relatively straightforward, but other

selection factors such as those listed in Figure 7-20 require more consideration. In space structures that must be dimensionally stable, e.g., telescopes or antennae, carbon fibers have a negative coefficient of thermal expansion that can be used to offset the usually positive value for matrix materials, resulting in an extremely attractive near-zero coefficient of thermal expansion structural material. In all applications, a fiber-matrix bond is essential, so a fiber surface treatment or coating often must be used.

7.3.4 Matrix Selection Factors

The selection of a suitable matrix for a composite material involves many factors, and is especially important because the matrix is usually the weak and flexible link in all properties of a two-phase composite material. The matrix selection factors include ability of the matrix to wet the fiber (which affects the fiber-matrix interface strength), ease of processing, resulting laminate quality, and the temperature limit to which the matrix can be subjected. Other performance-related factors include strain-to-failure, environmental resistance, density, and cost.

Those basic matrix selection factors are used as bases for comparing the four principal types of matrix materials, namely polymers, metals, carbons, and ceramics, listed in Table 7-1. Obviously, no single matrix material is best for all selection factors. However, if high temperatures and other extreme environmental conditions are not an issue, polymer-matrix materials are the most suitable constituents, and that is why so many current applications involve polymer matrices. In fact, those applications are the easiest and most straightforward for composite materials. Ceramic-matrix or carbon-matrix materials must be used in high-temperature applications or under severe environmental conditions. Metal-matrix materials are generally more suitable than polymers for moderately high-temperature applications or for modest environmental conditions other than elevated temperature.

Historically, polymer-matrix composite materials such as boron-epoxy and graphite-epoxy first found favor in applications, followed by metal-matrix materials such as boron-aluminum. Ceramic-matrix and carbon-matrix materials are still under development at this writing, but carbon-matrix materials have been applied in the relatively limited areas of reentry vehicle nosetips, rocket nozzles, and the Space Shuttle since the early 1970s.

Table 7-1 Matrix Selection Factors

SELECTION FACTOR	RANKING OF MATRIX MATERIALS POOR ← → GOOD			
FIBER WETTING	CERAMIC	METAL	CARBON	POLYMER
PROCESSING EASE	CERAMIC	METAL	CARBON	POLYMER
LAMINATE QUALITY	CERAMIC	CARBON	METAL	POLYMER
STRAIN-TO-FAILURE	CERAMIC	CARBON	METAL	POLYMER
ENVIRONMENTAL RESISTANCE	POLYMER	METAL	CARBON	CERAMIC
DENSITY	METAL	CERAMIC	CARBON	POLYMER
COST	METAL	CARBON	CERAMIC	POLYMER

Polymer-matrix materials include a wide range of specific materials. Perhaps the most commonly used polymer is epoxy. Other polymers include vinyl ester and polyester. Polymers can be either of the thermoset type, where cross-linking of polymer chains is irreversible, or of the thermoplastic type, where cross-linking does not take place but the matrix only hardens and can be softened and hardened repeatedly. For example, thermoplastics can be heated and reheated, as is essential to any injection-molding process. In contrast, thermosets do not melt upon reheating, so they cannot be injection molded. Polyimides have a higher temperature limit than epoxies (650°F versus 250°F or 350°F) (343°C versus 121°C or 177°C), but are much more brittle and considerably harder to process.

7.3.5 Importance of Constituents

The process of selecting the appropriate combination of fibers and matrix material for a particular application is rather involved. The imposed design requirements will aid in eliminating from consideration certain matrix materials or fibers or combinations thereof. However, some combinations of constituent materials are not so obviously evaluated.

A simplified performance index for stiffness is readily obtained from the essentials of micromechanics theory (see, for example, Chapter 3). The fundamental engineering constants for a unidirectionally reinforced lamina, E_1, E_2, ν_{12}, and G_{12}, are easily analyzed with simple back-of-the-envelope calculations that reveal which engineering constants are dominated by the fiber properties, which by the matrix properties, and which are not dominated by either fiber or matrix properties. Recall that the fiber-direction modulus, E_1, is fiber-dominated. Moreover, both the modulus transverse to the fibers, E_2, and the shear modulus, G_{12}, are matrix-dominated. Finally, the Poisson's ratio, ν_{12}, is neither fiber-dominated nor matrix-dominated. Accordingly, if for design purposes the matrix has been selected but the value of E_1 is insufficient, then another more-capable fiber system is necessary. However, if E_2 and/or G_{12} are insufficient, then selection of a different fiber system will do no practical good. The actual problem is the matrix system! The same arguments apply to variations in the relative percentages of fiber and matrix for a fixed material system.

The micromechanics analysis alluded to in the previous paragraph can also be applied to thermophysical properties such as thermal expansion, moisture expansion, thermal conductivity, etc. However, be aware that micromechanics analysis is generally much more valuable as a *qualitative* guide to the design of a material than it is to any *quantitative* considerations. That is, the accuracy of the micromechanical predictions of the matrix-dominated properties is quite low. Accordingly, reliable quantitative performance predictions are not possible. In other words, using constituent properties to predict the behavior of a composite material is not feasible at this time in the structural design environment. Micromechanics is best suited for understanding and designing the ma-

terial itself. Actual property measurements for a composite material cannot be avoided.

When some of the possible combinations of fibers and matrix systems are examined, a picture of the usefulness of composite materials begins to form. That usefulness is measured from only the standpoint of operating temperature range in Table 7-2. There, both with some thermoset-matrix materials as well as some thermoplastic-matrix materials, the matrix controls the operating temperature of the composite material. The only exceptions in Table 7-2 are the incompatibilities of phenolics and polyimides with Kevlar. The carbon-matrix system also controls the operating temperature and, because of processing reasons (both glass and Kevlar fibers would be melted at the processing temperatures of the carbon matrix), is compatible only with carbon fibers. That is, only carbon fibers can withstand the high temperatures required to create the carbon matrix around the fibers. An encyclopedia of composite materials will not be attempted. For such an objective, consult the excellent handbooks by Lubin [7-1] and Schwartz [7-2].

Table 7-2 Operating Temperatures of Some Composite Material Systems

Constituent Materials				Operating Temperature
	Fiber			
Matrix	Glass	Kevlar	Carbon	-70 RT 250 500 750 1000 2000°F
Thermosets				
Epoxy (250°F cure)*	ok	ok	ok	
Epoxy (350°F cure)**	ok	ok	ok	
Phenolics	ok	no	ok	
Bismaleimides	ok	ok	ok	
Polyimides	ok	no	ok	
Thermoplastics				
Polysulfone	ok	ok	ok	
Peek	ok	ok	ok	
Carbon	no	no	ok	
				-60 RT 200 400 600 1100°C

*(121°C cure) **(177°C cure)

7.3.6 Space Truss Material Selection Example

Let's design a space truss with the primary objective being selection of the proper material. The truss will be used to construct a space station or large antenna. Suppose a truss is being assembled from various kinds of struts stored in the Space Shuttle payload bay as in Figure 7-21. Those struts are conical and can be nested in one another, just as ice cream cones are nested in a store before they are used. The large ends of two of the struts are fastened together as in Figure 7-21. The small ends of the struts are fastened to joints. Collections of these nested half struts are stored in canisters on the Shuttle, and the joints are also stored in canisters. This space truss is very large in volume,

but low in weight, so it cannot be carried into space in a preassembled state. Thus, the truss must be assembled in space. The problem here is selecting the material out of which this truss will be made. The answer is given in Figure 7-21, namely that the columns are made of graphite-epoxy, but you probably suspected that solution. The question is: why? And which of several graphite-epoxies should be used?

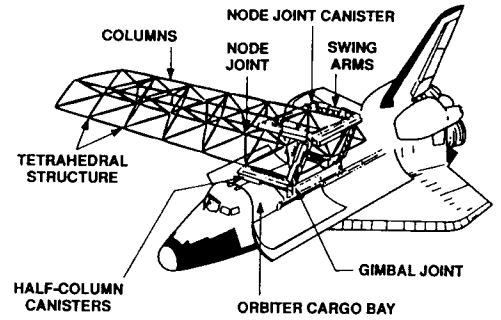

Figure 7-21 Space Shuttle with a Truss Being Erected

The problem must be simplified considerably to permit solution in the context of this book. Suppose an equilateral triangle is subjected to some loads in the vertical direction as in Figure 7-22. A load P of 100 lb (445 N) is applied to the top joint, and that load can go in either the downward or upward direction (in the diagram, not in space!). This truss must take its reversible load with, say, a factor of safety of two against whatever event would cause it to fail. What material, size, and weight of truss element would you select to satisfy the design requirements that include building the structure for the lowest cost?

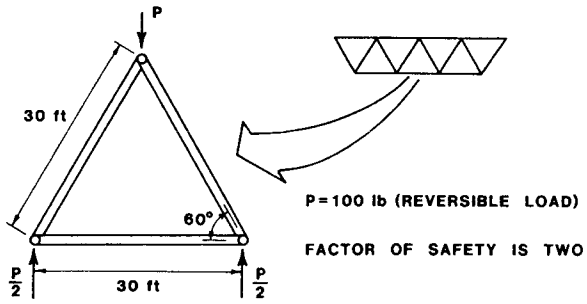

Figure 7-22 Space Truss Idealization

In order to evaluate one of the issues that is very pertinent to this material selection, the cost to get the truss elements up into space must be known. In 1985, a Shuttle flight cost $90 million. If the Shuttle is capable of carrying a payload of 60,000 lb (27,000 kg), then for every

pound taken up in the Shuttle, the transportation charges are $1500. That cost is quite a bit higher than the original projected cost of a Shuttle flight. That is, NASA used to think a flight would cost $15 million, and that would correspond to a transportation cost of several hundred dollars per pound ($700/kg). The reality is that even more than 1500 Dollars per pound ($3300/kg) is now required to get an object up into space. The boost cost is independent of the material involved. Thus, you are clearly motivated to select the least-dense material that will satisfy the functional requirements.

Other factors that enter into this material selection process include the cost to make parts with various materials. Consider four different candidate materials: an ordinary steel that as a raw material might cost perhaps a dollar per pound ($2/kg), aluminum that might cost $5 per pound ($11/kg), a high-strength graphite-epoxy AS-3501 that might cost about $20 per pound ($44/kg), and a high-stiffness graphite-epoxy GY-70-HYE1534 that costs $200 per pound ($440/kg) (GY-70 can no longer be purchased for that low a price). Also shown in Table 7-3 are various costs for fabrication and assembly. Both graphite-epoxies are lower in fabrication and assembly cost than steel and aluminum. Your eye is drawn to the highest cost: GY-70-HYE1534 costs $200 per pound ($440/kg)! Assembly cost includes assembly in space, assembly of fixtures at the ends of the graphite-epoxy columns that will permit locking one column into another and at the smaller end that permit locking a column into a joint. The numbers in the table are representative, but not necessarily accurate; however, they will suffice for this example.

Table 7-3 Fabrication and Assembly Costs

MATERIAL	MANUFACTURING PHASE					
	RAW MATERIAL		FABRICATION		ASSEMBLY	
STEEL	$1/lb	($2.2/kg)	$4/lb	($8.8/kg)	$3/lb	($6.6/kg)
ALUMINUM	$5/lb	($11/kg)	$4/lb	($8.8/kg)	$3/lb	($6.6/kg)
GRAPHITE-EPOXY GY-70-HYE1534	$200/lb	($440/kg)	$3/lb	($6.6/kg)	$2/lb	($4.4/kg)
GRAPHITE-EPOXY AS-3501	$20/lb	($44/kg)	$3/lb	($6.6/kg)	$2/lb	($4.4/kg)

The real question is: which of the graphite-epoxies should be used? Two cost factors exist: (1) the cost of the material itself and what is done with it in the way of manufacturing, fabrication, and subsequently its assembly and (2) the cost of boost into space. A set of properties including stiffnesses and strengths is listed in Table 7-4 along with coefficients of thermal expansion and densities for the various materials. Steel has the highest density, and GY-70-HYE1534 graphite-epoxy has the second lowest density. The high-strength graphite-epoxy has the lowest density. The highest strengths on an absolute basis exist for the high-strength graphite-epoxy with the highest strength in the fiber direction, but not perpendicular to the fiber direction. For stiffness, high-modulus graphite-epoxy has the highest absolute stiffness. Some highs and lows exist in properties and costs. What is the balance? What is important for this particular problem?

Table 7-4a Properties of Candidate Materials (U. S. Standard Units)

MATERIAL	STIFFNESS	STRENGTH	THERMAL EXPANSION 10^{-6}in/in/°F	DENSITY lb/in^3
STEEL	$E = 30 \times 10^6$ psi $\nu = .3$	$\sigma_{max} = 30$ ksi	$\alpha = 6.5$	.282
ALUMINUM	$E = 10 \times 10^6$ psi $\nu = .25$	$\sigma_{max} = 55$ ksi	$\alpha = 12$	.097
HIGH-MODULUS GRAPHITE-EPOXY (GY-70-HYE1534)	$E_1 = 42 \times 10^6$ psi $E_2 = 1 \times 10^6$ psi $\nu_{12} = .25$ $G_{12} = .7 \times 10^6$ psi	$X_t = 90$ ksi $X_c = 90$ ksi $Y_t = 2$ ksi $Y_c = 28$ ksi $S = 4$ ksi	$\alpha_1 = -.58$ $\alpha_2 = 16.5$	.061
HIGH-STRENGTH GRAPHITE-EPOXY (AS-3501)	$E_1 = 18.5 \times 10^6$ psi $E_2 = 1.6 \times 10^6$ psi $\nu_{12} = .25$ $G_{12} = .65 \times 10^6$ psi	$X_t = 169$ ksi $X_c = 162$ ksi $Y_t = 6$ ksi $Y_c = 25$ ksi $S = 7$ ksi	$\alpha_1 = .25$ $\alpha_2 = 15.2$	.055

Table 7-4b Properties of Candidate Materials (SI Units)

MATERIAL	STIFFNESS	STRENGTH	THERMAL EXPANSION 10^{-6}m/m/°C	DENSITY N/m^3
STEEL	$E = 207$ GPa $\nu = .3$	$\sigma_{max} = 207$ MPa	$\alpha = 3.6$	49.4
ALUMINUM	$E = 69$ GPa $\nu = .25$	$\sigma_{max} = 380$ MPa	$\alpha = 6.67$	17
HIGH-MODULUS GRAPHITE-EPOXY (GY-70-HYE1534)	$E_1 = 290$ GPa $E_2 = 6.9$ GPa $\nu_{12} = .25$ $G_{12} = 4.8$ GPa	$X_t = 621$ MPa $X_c = 621$ MPa $Y_t = 13.8$ MPa $Y_c = 193$ MPa $S = 27.6$ MPa	$\alpha_1 = -.32$ $\alpha_2 = 9.17$	10.7
HIGH-STRENGTH GRAPHITE-EPOXY (AS-3501)	$E_1 = 128$ GPa $E_2 = 11$ GPa $\nu_{12} = .25$ $G_{12} = 4.5$ GPa	$X_t = 1170$ MPa $X_c = 1120$ MPa $Y_t = 41$ MPa $Y_c = 170$ MPa $S = 48$ MPa	$\alpha_1 = .14$ $\alpha_2 = 8.44$	9.63

What is important for this space truss problem depends on which of the various technical issues influence the design. Is stiffness an issue? Is strength an issue? If so, why? Is buckling an issue? Can fatigue be a problem? Or corrosion? Thermal expansion or joints? Those factors are listed in Figure 7-23.

- STIFFNESS
- STRENGTH
- BUCKLING
- FATIGUE
- CORROSION
- THERMAL EXPANSION
- JOINTS

Figure 7-23 Possible Pertinent Technical Factors

The problem statement is that you are asked to compare the use of four different materials for this space truss by using a simplified method for how the struts themselves might be made. The problem is enormously simplified compared to the overall problem seen in Figure 7-21. The present columns are required to be of the same diameter throughout their length. There is no concern about connecting them at the middle of the strut or about how they are connected to each other at the joints. Examine the basic structural design—see if you can determine which of the materials does the best job, and why, relative to the possible pertinent technical issues listed in Figure 7-23.

There are at least two ways to make the struts. They could be solid members, or they could be hollow members. You could well imagine that, under certain circumstances, solid members would be perhaps preferable to hollow members, and for other reasons just the opposite would be true. It is up to you to figure out which of those two choices is best for this application. Look at both choices, or you can, alternatively, give a compelling argument as to which configuration, solid cross section, or hollow cross section, you use, with an emphasis on *why*. Then, you will not have to do the other calculations.

You must consider the technical factors in Figure 7-23 and figure out which one(s) governs for this particular kind of problem. You can probably imagine that fatigue and corrosion might not be issues because you were not given any data on those situations. And joints have been ignored, so you suspect they are not an issue. Thus, the critical issue must lie elsewhere on that list of technical issues.

Degradation of materials in space has not yet been considered. Not enough is known about that effect yet, so it cannot be considered in this design problem. If you are faced with designing something and you don't know the effects of the environment, then perhaps you would have to recommend that the design is premised on there being no degradation. In fact, if there were any degradation, then the design would have to be strengthened or stiffened in some fashion to account for the degradation. Or perhaps degradation would dictate use of a different material. Thus, all of those factors are issues for which you don't know the answer. However, you must at least put some disclaimers on the design. That is, state that there are certain risks involved with using the design in the way you have described it because the influence of certain factors on the performance of the structure that you designed is not known.

You are to address several questions. Basic questions such as: given the parameters, which of those four materials leads to the most *cost-effective* design? Which leads to the *least-weight* solution for this problem? And then consider another problem: suppose you had to make an emergency trip with the Shuttle to take a certain number of trusses into orbit. Suppose you had to get 5000 truss bays, those three units shown in Figure 7-22, up on one Shuttle flight. Moreover, suppose, for example, that either the frames were available made from the material that you select or they could be made in two days with people working day and night. Which of the materials would you choose under that circumstance? The third question is: suppose the space truss is either a buckling-critical design or a strength-critical design—which one is it? If you say it is stiffness-critical instead of strength-critical, then what if it were actually strength-critical? Which material would you choose under those circumstances? And finally the last question is one that does not relate directly to those evaluations but to the other kind of issue which is why you were given the thermal-expansion data. The space truss is not permitted to change size as it passes in and out of the sun. In effect, zero thermal expansion is desired, or zero thermal contraction. Both expansion and contraction are bad because they cause change in dimensions. Under those circumstances, which material of the four would you use, and in what general way would you use it to accomplish those objectives? That is, describe a concept, but calculations are not required.

To solve this problem, you will appeal to relatively simple equations. Nothing is complicated in the overall problem as simplified herein. Think about what you are doing, and make sure that you are taking into consideration all the pertinent factors. You will need no more than a programmable calculator to evaluate the expressions repetitively for the different materials. A spreadsheet or a brief computer program might be more convenient. In order to find a truss that meets the requirements of certain size, you will have to state how big a diameter the rod must have if it is solid. Or its outer diameter, inner diameter, and thickness if the strut has a hollow cross section. Then, based on those dimensions and the densities, you can determine how much the truss weighs, and that is how you get to the issue of cost in orbit. Money must be spent for every pound sent up into orbit, so you must know the weight. That is an inescapable problem in this particular kind of design circumstance. Other issues in materials selection involve what you can do with the material, which often depends on *how* it was made to begin with, especially with composite materials.

The following hints and reminders might be helpful. For a column that is simply supported (pinned) at both ends, the Euler-Bernoulli buckling equation is

$$P = \pi^2 \frac{EI}{L^2} \tag{7.3}$$

Moreover, the moment of inertia of a solid circular cross section is

$$I_{solid} = \frac{\pi d^4}{64} \tag{7.4}$$

where d is the diameter. Finally, the moment of inertia of a thin hollow circular cross section can be approximated with

$$I_{hollow} = \frac{\pi d^3 t}{8} \tag{7.5}$$

where t is the thickness of the tube.

This space truss is seemingly an unusual example, but space is now a part of our everyday lives. Thus, there are many space examples in which you must expect to use composite materials because they are the least-expensive design solution. The raw material cost is not even close to the bottom-line cost. The raw material cost has something to do with the bottom line, but the ordering of material choices that you get based on raw material cost does not mean anything in comparison to the ordering of the actual bottom-line costs.

7.3.7 Summary

Familiarity with an enormous amount of detailed information about a wide variety of materials is essential to be able to rationally select suitable materials for a specific application. Remember, even a metal might be the correct material to use!

7.4 CONFIGURATION SELECTION

7.4.1 Introduction

Configuration selection is the process of choosing the proper combination of structural elements that make up the structure being designed. Those structural elements could be the usual beams, plates, and shells or more complex structural elements such as stiffened shells with a honeycomb core. The more unusual aspects of composite structures include the details and the breadth of stiffener types as well as various reinforcements around cutouts and holes, etc. The global configuration elements of plates and shells are the easy part of the design problem. The more difficult part is designing the local details so that the global elements have the opportunity to do their job. Configuration selection must be done in close conjunction with materials selection as well as selection of a suitable manufacturing process. We will primarily address stiffened structures, a topic that contributes to the objective of being able to rationally select the specific configuration for a structure. In this section, some of the differences between metal and composite structures are revealed.

7.4.2 Stiffened Structures

We usually must go beyond the simple concept of a monocoque or single-thickness skin for whatever structure we design. That is, we must usually consider the bending stiffness, and, to achieve structural efficiency, we often must stiffen a structure in some manner. We will first address the terminology of stiffening and how it is used. Then, we will consider the types of stiffeners that could be used. Next, an important issue that arises in the design of stiffeners is whether the stiffener has an open- or a closed-cross section. Then, we will address some of the

stiffener design parameters and some design considerations for stiffeners. Finally, we will examine a new concept for stiffening composite structures, namely orthogrid.

Certain terms are commonly used to describe stiffened aerospace structures. The relatively common eccentrically stiffened circular cylindrical shell configuration is used as an example for discussion purposes. A panel is the unstiffened flat or curved sheet between stiffeners. For example, a panel occupies the space a by b in the shell in Figure 7-24. Stiffeners have different names depending on their direction and often on the type of structure (e.g., aircraft versus ships). Rings are circumferential stiffeners as shown on the inside of the shell in Figure 7-24. The ring stiffeners could be on the outside of the shell, unless not permitted for aerodynamic or hydrodynamic reasons. Rings are sometimes called frames or ribs. Stringers are axial stiffeners as shown on the outside of the shell in Figure 7-24. Of course, the stringers could be placed on the inside of the shell. Stringers are also known as longerons or spars in the aircraft industry. Often, both rings and stringers are placed on the same side of the shell, resulting in intersecting stiffeners. For example, in aircraft, submarine, and missile fuselage applications, all stiffeners must be placed on the inside to maintain an aerodynamically or hydrodynamically clean exterior. Then, quite often the rings are continuous, and the stringers are only long enough to fit between rings.

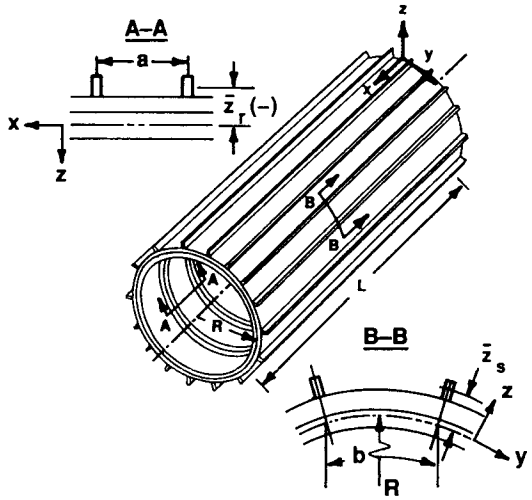

Figure 7-24 Eccentrically Stiffened Circular Cylindrical Shell

7.4.2.1 Advantages of Composite Materials in Stiffened Structures

Many metal stiffener shapes are rather regular and usually have constant thickness unless they are machined (which adds enormously to the cost). However, with composite materials, such regularity is not necessary. In fact, individual stiffener elements can be tailored with

composite materials to a more nearly optimum effectiveness than with metals. Accordingly, different stiffener elements have both different thicknesses and different materials in different regions as in Figure 7-25. That is, with metals, the stiffener wall *must* have both constant thickness and uniform material unless expensive machining is to be done and/or stiffener elements of different materials are mechanically fastened. In contrast, with composite materials, the stiffener wall *can* have different thicknesses and different laminate layups with more or less no essential change, including cost, in the manufacturing process. That is, different thicknesses and different layups are a natural feature of composite structures fabrication.

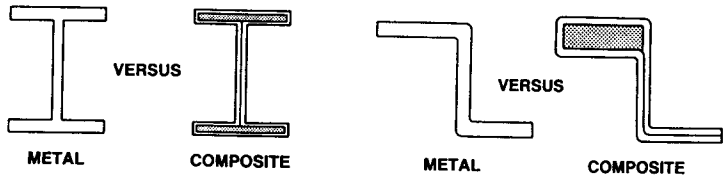

Figure 7-25 Shapes of Metal versus Composite Stiffeners

Further contrast between metal and composite stiffeners is revealed when we examine the objectives and characteristics of stiffener design. For a metal stiffener of uniform or even nonuniform thickness, we attempt to maximize the moment of inertia of the stiffener in order to maximize the bending stiffness of the stiffener. Those two factors are proportional to one another when we realize that the bending stiffness of metal stiffeners about the middle surface of the plate or shell to which they are attached is

$$EI = E\iint y^2 dx\, dy \tag{7.6}$$

and that, because of a uniform (homogeneous) material throughout the metal stiffener, the modulus of elasticity can be brought outside the integral. Of course, the integral in Equation (7.6) reduces to the familiar parallel-axis theorem result:

$$I_{\text{middle surface}} = I_c + Ad^2 \tag{7.7}$$

where I_c is the second moment of the area about the stiffener centroidal axis parallel to the panel middle surface; A is the stiffener area; and d is the distance between the middle surface and the stiffener centroid. Thus, the bending stiffness can be increased by making the stiffener taller without increasing A, but increasing I_c and d.

In contrast, because of the spatially variable (inhomogeneous) nature of material in a composite stiffener, the bending stiffness cannot be separated into a material factor times a geometric term as in Equation (7.6). Instead, the composite stiffener bending stiffness is

$$EI = \iint E(x,y)\, y^2 dx\, dy \tag{7.8}$$

where the heterogeneous nature of the material distribution, E(x,y), cannot be taken outside the integral. That is, the geometric character of the bending stiffness cannot be separated from the material character. Thus, *proper* design of a stiffener *does not necessarily involve maximizing the moment of inertia of the stiffener.* In fact, the moment of inertia no longer has meaning by itself when we shift from metal to composite stiffeners. We must tailor the stiffener components to achieve a maximum combination property (bending stiffness) EI in the sense of an integral.

For distributions of laminae such as in Figure 7-26, the moment of inertia itself is of no consequence. We must put materials with high E as far away from the plate or shell bending axis as possible so that they have the greatest effect or do the most good (i.e., make the largest contribution to the bending stiffness). We tailor the stiffener components in fiber direction, area, and position of area to achieve the necessary high bending stiffness. Thus, laminae are placed with fibers in the axial direction of the stiffener in the top of the hat section in Figure 7-26 to maximize their contribution to the bending stiffness. Other laminae are placed with fibers at ±45° in the web to carry the shear stresses from the top of the hat section to the underlying panel. Those ±45° laminae do not make a large contribution to the bending stiffness for two reasons: (1) they have a low E in the axial direction of the stiffener, and (2) they have a small area not very far from the bottom of the stiffener.

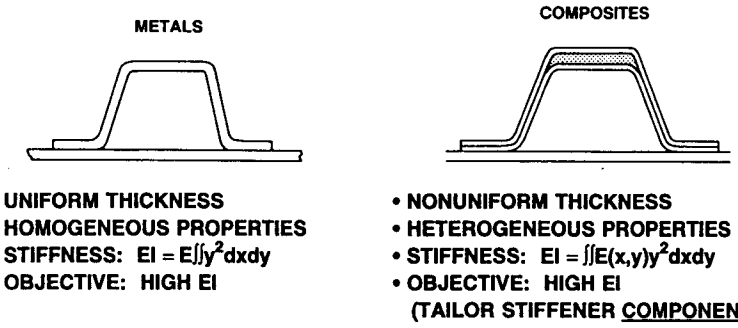

Figure 7-26 Metal Versus Composite Stiffener Characteristics

7.4.2.2 Types of Stiffeners

The rings and stringers can have a wide variety of cross-sectional shapes, some of which are shown in Figure 7-27. For metal stiffeners, some of the shapes are typically rolled sections that are then fastened to the panel, e.g., tee, I, z, hat, or channel shapes. Fastening could be mechanical, bonding, or welding. Other more unusual shapes or thickness distributions over the cross section are typically machined integrally with the panel from material that is at least as thick as the stiffener height plus the panel thickness, e.g., inverted tee, blade, or J shapes. That machining is either mechanical, i.e., chip producing, or chemical, known as chem milling. Both machining processes are quite expensive.

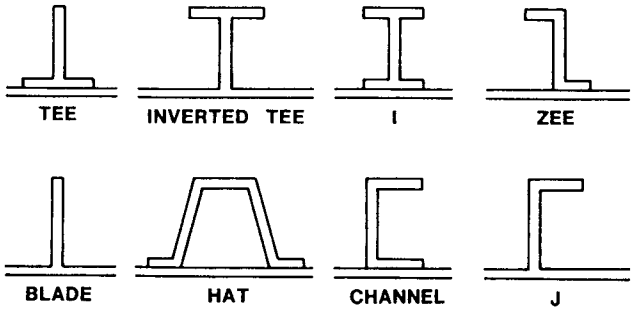

Figure 7-27 Nominal Stiffener Cross-Sectional Shapes

For composite stiffeners, all shapes are builtup from individual layers of material. Of course, some stiffener shapes can be produced by roll forming or pultrusion, for example, and then fastened to panels. Or, the stiffened panel could be made in a single operation involving the placement, usually by hand, of individual laminae of various dimensions in positions such that a builtup structure results. Stiffeners can be fastened to panels by bonding, stitching, or mechanical fastening.

Standard shapes for composite stiffeners are not likely to occur for most aerospace applications. There, the value and function of the structure warrant optimizing the stiffener design. In contrast, for more everyday applications such as scaffolding, stairways, and walkways in chemical plants, competitive pressures lead to a situation where compromises in stiffener efficiency are readily accepted (overdesign) in order to achieve lower cost than would be associated with optimum design.

The embedded stiffening strap is an interesting concept that is easy to apply with composite materials. The panel skin is made of material that, because it is made in layers, we are able to separate at the specific level where we would like to embed a stiffening strap as in Figure 7-28. More accurately, we simply stop laying up laminae on the panel long enough to lay down a strap, and then continue with the panel layup and drape material of the panel over the strap. In the process, we have embedded a strap in the panel. Then, we can put another stiffener on top of that strap if we choose. The strap could consist of all 0° fibers to get the maximum stiffening effect in one direction as opposed to the multidirectional stiffening effect of the surrounding laminate. The main purpose of the stiffening strap is to stiffen the underlying panel so the stiffener flange can more easily adhere to the deforming panel (which now has smaller deformations). The only difficulty with this stiffening concept is the possible presence of resin-rich areas near the ends of the embedded strap. Those resin-rich areas are weak and hence a possible origin of delamination.

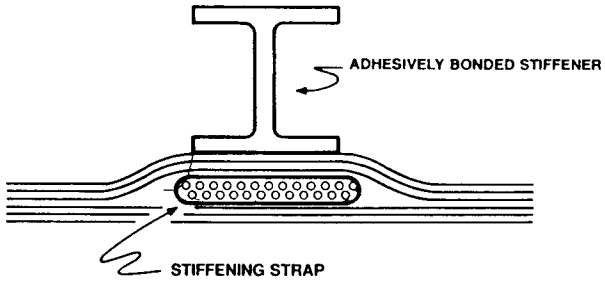

Figure 7-28 Embedded Stiffening Strap

Simply bonding a stiffener to a panel with adhesive is certainly a very feasible and natural procedure with typical composite structure construction. We have not discussed any procedure for joining parts except co-curing. Alternatively, to use film adhesive for bonding parts together, we simply cut a sheet or film of adhesive to the proper size, place it between the two parts that we wish to bond together, and then go through a cure cycle that causes the adhesive to adhere to both the stiffener and to the panel itself. We can also mechanically fasten any stiffener we like to a panel.

7.4.2.3 Open- versus Closed-Section Stiffeners

The open- versus closed-section stiffener issue essentially revolves around the question of the torsional stiffness of the stiffener. You might not think torsional stiffness is terribly important for a stiffener, but in fact it can be because the stiffener often twists as the stiffened panel buckles. In calculations to evaluate the buckling resistance of a stiffened skin panel, the torsional resistance of the stiffener exerts a significant influence. That is, the torsional stiffness aids the stiffened panel in resisting the buckling deformations that can be rather unusual. Those buckling deformations are not simply a pure bending; sometimes they are some sort of a twisting. And even if they are pure bending in one plane, if a stiffener crosses that plane at a certain angle, then we ask that stiffener to twist. Therefore, the stiffener twisting resistance is quite important in resisting those bending and buckling deformations. An open-section stiffener, by definition, does not have all parts of its periphery connected to one another. That is, for the sandwich-blade stiffener on the left in Figure 7-29, part of the blade sticks up in the air and the portion at the very top is not connected to the flanges on the side. Naturally, that kind of a structure has much lower torsional resistance than does the closed-section stiffener on the right in Figure 7-29, where all parts of the stiffener periphery are connected to one another. The flange on the left of the hat-section stiffener is certainly not connected to the flange on the right by means of the stiffener, but the flanges are connected by means of the panel, so effectively the section is closed.

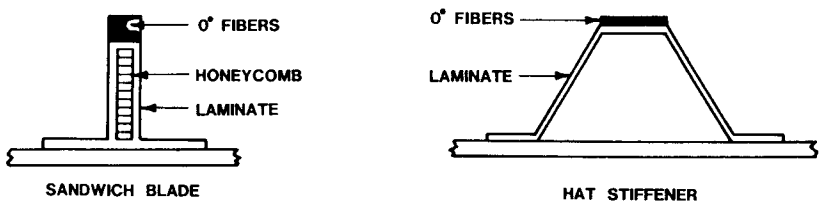

Figure 7-29 Open- versus Closed-Section Stiffeners

Let's contrast the sandwich-blade stiffener with the hat stiffener by addressing several performance issues. For example, from the standpoint of fabrication, it is relatively easy to make a sandwich-blade stiffener even though there is a honeycomb insert in the middle. This building up of the stiffener in the blade form is easy and natural when we make a composite stiffener, simply because we are already in the business of *building up* a geometric and/or material shape. Rather than applying layers of graphite-epoxy, instead put in some honeycomb. The hat-shaped stiffener is more difficult to make than the sandwich blade because of more complex geometry (and some internal support is required until the stiffener is cured).

From the standpoint of inspection to see if the stiffener is properly made, it is relatively easy to inspect the sandwich-blade stiffener, but the hat-shaped stiffener is difficult to inspect on the inside. We must get some kind of device to peer inside. If we were going to try to inspect from the outside, about all we can tell from ultrasonics is how well the flanges are bonded to the base of the panel. Typically, we must have some kind of a mold around the stiffener, and we must remove that mold. A mold is necessary so that during the cure process when the stiffener is under pressure it does not collapse. As a matter of fact, there might be instances in which, for the sake of simplified manufacturing process, we might want to leave a core or mold of some kind inside the stiffener simply because it is too difficult to get out. That situation is especially true for intersecting stiffeners at 90° or some other angle to one another where there is an intersection region where webs of one stiffener pass through and intersect webs of another stiffener. We do not have the freedom to cut the stiffener sides and remove whatever core exists inside to prevent the stiffener from collapsing during curing. If we do leave the core inside, we cannot inspect the stiffener from the inside. Thus, inspection is a much more involved operation for the hat-section stiffener than for the sandwich-blade stiffener.

The relative efficiency of the two stiffeners is compared principally on the basis of the torsional resistance. The reason for the lower efficiency rating of the sandwich-blade stiffener is its low torsional resistance (and the bending stiffness is not high) and for the high efficiency of the hat stiffener is its high torsional resistance because of the basic open- versus closed-section stiffener issue. Stiffener torsional resistance affects the buckling load of a stiffened panel or shell as shown by Card and Jones [7-3].

Suppose we want to analyze the stresses in the two stiffeners. The geometry of the sandwich-blade stiffener is actually more complicated and less amenable to analysis than is the hat-shaped stiffener. Issues that arise in the analysis to determine the influence of the various portions of the stiffeners include the in-plane shear stiffness. In the plane of the vertical blade is a certain amount of shear stiffness. That is, the shear stiffness is necessary to transfer load from the 0° fibers at the top of the stiffener down to the panel. In hat-shaped stiffeners, that shear stiffness is the only way that load is transferred from the 0° fibers at the top of the stiffener down to the panel. Thus, shear stiffness is the dominant issue in the design. And that is why we typically put ±45° fibers in the web of the hat-shaped stiffener.

Another issue that turns out to be very important for the sandwich-blade stiffener, but not at all important for the hat-shaped stiffener, is shear in the vertical web. Not shear in the plane of the web, but shear in the plane perpendicular to the web. This transverse shear stiffness turns out to dominate the behavior or be very important in the behavior of the sandwich blade, but simply is not addressed at all in the hat-shaped stiffener. You can imagine that the transverse shearing stiffness would be more important in the sandwich blade when you consider the observation that the sandwich blade is a thick element and the hat-shaped stiffener is a thin element. That is, bending and in-plane shear would dominate this response, whereas transverse shear, because the sandwich blade is thick, can very easily be an important factor in the sandwich blade. For both stiffeners, appropriate analyses and design rationale have been developed to be able to make an optimally shaped stiffener.

7.4.2.4 Stiffener Design

The stiffener design parameters that are of interest include some obvious factors and some less obvious ones as listed in Figure 7-30. The bending stiffness (not moment of inertia) of a stiffener is what we probably think of first as being the most important factor. Not only do we need to know the bending stiffnesses about each of the axes, but we probably need to know the polar bending stiffness in some analyses. The torsional stiffness for the stiffener, as already mentioned, is an important issue as well. That factor is the principal difference between the sandwich-blade stiffener and the hat-shaped stiffener that we just considered. To a lesser extent, the warping constant or the way the cross section warps out of its original plane when being twisted can be important for some stiffeners. Of course, we always want to address a stiffener not just as a complete stiffener, but as components of the elements that make it up, i.e., flanges, webs, and how they connect to one another. Thus, we want to know, in the context of the design of a composite stiffener, what are the stiffnesses of the individual laminates that make up each of those components of the stiffener. For a web-like object, we will be very interested in its in-plane shear stiffness as already pointed out. Moreover, the transverse shear stiffness of the web is important for honeycomb-stiffened webs.

- BENDING STIFFNESSES, $(EI)_x$,$(EI)_y$
- POLAR BENDING STIFFNESS, $(EI)_p$
- TORSIONAL STIFFNESS, $(GJ)_z$
- WARPING CONSTANT, Γ
- LAMINATE STIFFNESSES OF STIFFENER COMPONENTS
- IN-PLANE SHEAR STIFFNESS OF THE WEB
- TRANSVERSE SHEAR STIFFNESS OF THE WEB
- ECCENTRICITY, $\bar{z}$
- SPACING
- ORIENTATION
- MATERIALS

Figure 7-30 Stiffener Design Parameters

The importance of stiffener eccentricity is an issue that you might not be aware of. That eccentricity, $\bar{z}$, is simply the distance from the stiffener centroid to the reference surface of the panel to which the stiffener is attached as in Figure 7-24. For example, with an aircraft fuselage panel, we do not have total freedom to put the stiffeners on the inside or on the outside with equal favor. However, it can make a very big difference whether we put them on the inside or the outside in terms of, for example, the buckling resistance of that stiffened panel. Under some circumstances, merely changing the location of the stiffeners from the inside to the outside of a circular cylindrical shell can result in a factor of two or three difference in buckling load [7-3]! Obviously, any analysis in which that eccentricity is ignored could be seriously deficient. The same type of behavior exists for composite structures, as is very easy to understand. That stiffener eccentricity effect is inherently related to bending-extension coupling, not of lamina in a laminate, but of a stiffening element that is not unlike layers relative to other layers, or other elements. That coupling between bending and extension can be very important and must be considered in any stiffened structure analysis, except those that involve a flat plate, because there we cannot tell the difference whether the stiffener is on the top or on the bottom of the plate. Coupling between bending and extension will influence the behavior to some extent, but it will not matter whether the stiffeners are on the top or on the bottom of a flat laminate except to influence which way the panel bends under axial force.

Most of what has been described so far for stiffener design involves shape and size of the stiffener. Those issues involve selection of the type of stiffener, H-shaped cross section, blade, hat-shaped, etc. as well as the specific dimensions and material makeup of each stiffener element. Other obvious factors in the design of a stiffener include how far apart we space them, at what orientation we place them, and, perhaps most obviously in connection with what we addressed in Section 7.3, out of what material we make the elements. As you saw in some of the previous sketches for stiffeners, we are able with a composite stiffener to use different materials in different places very easily and to essentially optimize our materials usage so that the stiffening comes out to be as good as we can possibly make it.

Some of the design considerations for stiffeners include issues that relate to the sizing of a panel, and the panel can mean two issues. We can consider the planform area or the thickness of the panel. That is, we address three different dimensions: how thick, how long, and how wide? Those issues must generally be integrated in some fashion with the kinds of stiffeners that we deal with. For example, in order to take advantage of large stiffeners, we might require a thick panel. Otherwise, bulky stiffeners on a thin panel would simply overpower the panel. On the other hand, we might be able to have some very small stiffeners rather closely spaced on a thin panel. Thus, interaction of relative sizes of stiffeners and panels must be taken into account.

The unstiffened panel is generally designed by sizing the maximum in-plane dimensions of the panel and its minimum thickness to resist buckling. Then, the panel area dimensions can be reduced, and the thickness can be increased in the stiffened panel optimization process.

To decrease the thickness of a laminate, some of the laminae must be selectively stopped, dropped, or terminated. Moreover, the stopped laminae are covered with at least one continuous lamina as in Figure 7-31. There, resin-rich zones occur naturally in the vicinity of the ply drop. Such regions are also local stress-concentration sites. However, the tapered laminate creates a globally lessened stress concentration.

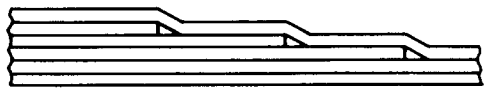

Figure 7-31 Ply Drops

In contrast to ply drops decreasing the laminate thickness, *padding up* is a local thickness increase created by adding layers (pads). Such added composite layers are typically compressed and molded into a different shape as in Figure 7-32. However, if the added layers are essentially rigid as a metal layer would be, then voids or resin-rich regions are created. Padding up is used to (a) provide a firmer foundation for applying stiffeners to panels, (b) increase the local bearing capacity, and (c) provide a stiffer and stronger attachment zone in Figure 7-33.

- COMPRESSES AND MOLDS IF A COMPOSITE LAYER

- ESSENTIALLY RIGID IF A METAL LAYER (LEAVES VOIDS OR RESIN-RICH AREAS)

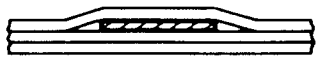

Figure 7-32 Padding Up

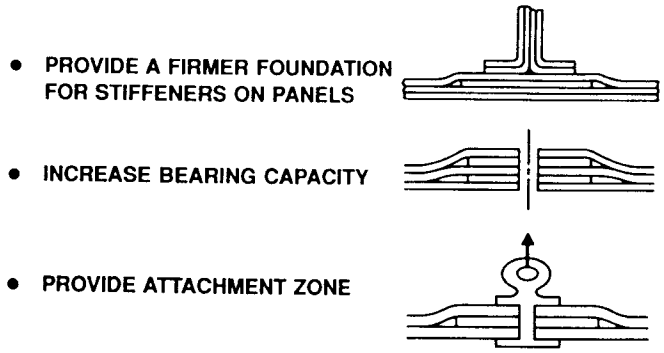

Figure 7-33 Padding Up Applications

7.4.2.5 Orthogrid

Orthogrid is an interesting stiffening concept that is a special modification of the stiffening concepts we have examined so far. This concept consists of building up an intersecting blade-type stiffener in a waffle-grid type of configuration. That is, the stiffened panel itself looks somewhat like a waffle perhaps with bigger spacing between the vertical blades, but the main idea is that we can actually construct the intersecting blade-type stiffeners in a very special automated way. For example, suppose we create the skin of the panel and then wind or wrap strips of unidirectional fibers preimpregnated with epoxy around the skin in certain trajectories so we build up in areas that can be geometrically called a blade stiffener. We do this building up in a criss-crossing fashion so that the various blades interlock. That is, alternating directions of fibers can be seen in Figure 7-34 so that the two intersecting blades are interlocked with one another just as if you can interlock your fingers with each another. Actually, the stiffeners are laminated bars built up with alternating layers of fiber-reinforced epoxy tape and then syntactic-resin tape. The fiber-epoxy strips are thinner and more dense than the syntactic-resin strips. The compressible syntactic-resin tape is used to vertically space the fiber layers so there is little build-up of overlapping layers at the stiffener intersections. The principal merit of this orthogrid approach is its automatic production via filament-winding or some variation thereof.

This structural configuration, orthogrid, has the potential for efficient manufacture of large fuselage panels, essentially one of the reasons that manufacturers are very interested in it. Stiffened structures are used when structures are heavily loaded in which case stiffened structures are more efficient than single-layer structures. Orthogrid structures are being considered for large transport aircraft that are built in more or less cylindrical segments, so that the filament-winding mandrel can be easily removed from the inside and reused.

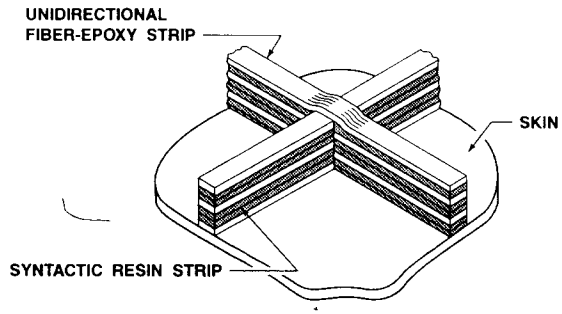

Figure 7-34 Orthogrid

As a structural concept, orthogrid is not new, but was used in the 1960s with metals (the Saturn 4B rocket stage that was made to carry astronauts to the moon had a waffle-like pattern). Metal orthogrid began with a thick sheet of aluminum that was milled between where stiffeners were desired down to the panel thickness so as to leave the stiffeners protruding. Chemical milling was found to be less expensive than simply brute-force machining all the interior material out of the structure. Orthogrid is just a modern way of achieving that same structural shape, and it is a less expensive way because we are building the composite structure up instead of tearing metal down. Chemical milling is a very expensive process, and obviously the process of simply brute-force machining all that material away is particularly expensive as well. The angle of intersection of each pair of stiffeners need not be 90°, i.e., the 'ortho' in orthogrid is too restrictive. In fact, if the angle between stiffeners is 60° so that the stiffeners form equilateral triangles, then the stiffening effect is essentially isotropic, so these stiffeners are called isogrid.

7.4.3 Configuration in Design Cost

Let's look at some of the cost drivers for a specific industry, namely the aerospace industry. First, let's lead up to that situation by looking at what happens with other industries. Generally, in any industry, we must consider the cost of energy, whatever material goes into the process we are dealing with, and the equipment necessary to process energy and material. Specifically, in the aerospace industry, metal-removal operations are strong cost drivers, and composite materials are just the opposite because with them there is virtually no such thing as material removal. High part count is also a big cost driver, and composite structures counter that problem by naturally and inexpensively combining segments of structures or structural elements. Fewer parts mean fewer fasteners, another very significant cost driver both in purchase price and installation cost (think of the cost of drilling thousands of carefully aligned holes in a structure!). Material utilization is another high cost driver, and composite materials are countering that in two different ways: (1) in terms of the types of efficient manufacturing operations of composites buildup

instead of metal removal and (2) in replacing some scarce strategic materials with other materials whose sources we control.

Specifically, within the aerospace industry, for aircraft, the airframe manufacture itself is one of the major cost drivers, using the factors already addressed. Let's look at the character of how we would build an aerospace vehicle. There is typically a lot of manpower dependence. The industry itself is cyclic because the demands ebb and flow. There is typically little automation simply because of relatively low production rates, and there are very few customers. But, despite all those characteristics, there is typically also a large capacity that is founded on many highly skilled personnel, and the orientation is much more high tech than that of most other industries. Without product excellence as a driving factor, the whole industry would be an unworkable mess.

Let's look at the nature of a configuration trade-off study by trying to apply some of those factors that we were just examining for an aircraft fuselage panel. Basically, our objective is to obtain the lowest-cost structural configuration that meets the design requirements expressed in terms of stiffness and strength, our old friends, as well as minimum weight. For high-speed aircraft, we need elevated-temperature performance. We need certain fatigue resistance. We do not want to spend a lot of money on maintenance. We would like the aircraft to be extremely crashworthy, corrosion resistant, damage tolerant, and, if a minor accident does happen, easy to repair.

Suppose then we start thinking about some different structural concepts as alternatives to the usual approaches. Let's look into those alternative concepts from the standpoint of what materials we use, what sizing there is of the skin panel, what shape of frames are needed, what spacing they might have, and ask the same kind of questions for the longitudinal stiffeners or stringers. How do we put all of this structure together? Do we bond everything, do we stitch it, or do we use mechanical fasteners? In general, what kind of manufacturing methods must we be concerned with? Given all of those factors, we are then charged with evaluating the cost of each of the alternative concepts from the standpoint of manufacturing, assembly, testing, inspection, kind of materials, and tooling expenses.

Consider a study of a fuselage panel for the F-16 reported by Noton [7-4]. The panel that is being addressed is located in the bottom of the fuselage as in Figure 7-35. The various candidate concepts would be an unstiffened skin (i.e., a monocoque fuselage), stringers only, one stringer and a variety of frames, three frames, some frames with cutouts in the web and stringer, and two frames of double curvature. Those are the kinds of trade-off configurations that we must examine. With composite materials, we have the additional complexity of asking how these structural elements are fastened to one another. Is there a special way that we might want to construct each of those stiffeners? Should we make them with some selective reinforcement in the flanges? Is that reinforcement worthwhile? If in fact selective reinforcement might be of lower cost in general, would it be of lower cost for this specific application? That is, is there enough in the context of this study to learn how

to provide those kinds of selective reinforcements and make that a cost-effective trade-off for this single fuselage panel? Or is that a trade-off that can be done only if we were going to redesign the whole aircraft? The situation might very well be the latter case, i.e., total redesign is the only situation in which selective reinforcement might work. Some pretty severe constraints exist if we are going to try to make some changes in a very restricted area on just one panel.

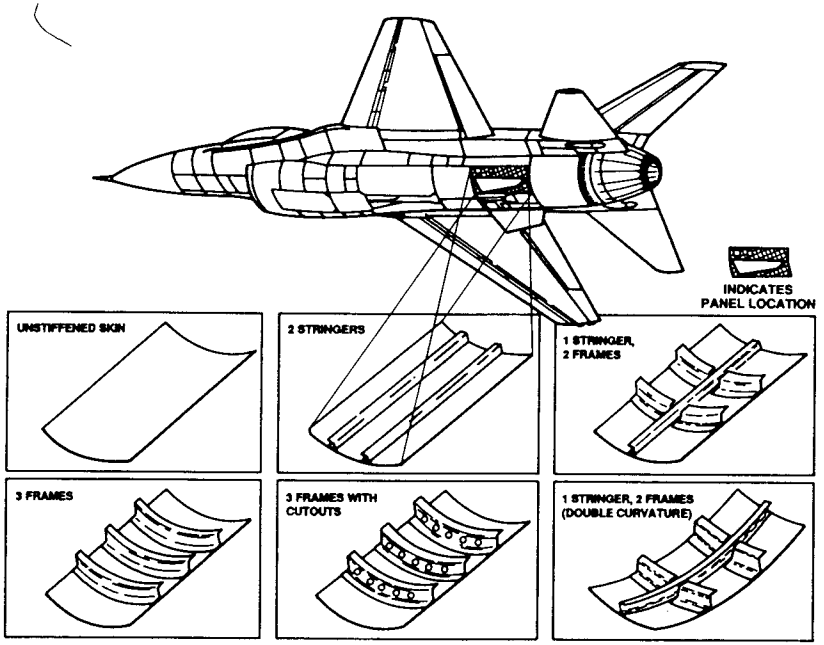

Figure 7-35 F-16 Fuselage Panel Trade-off Study

7.4.4 Configuration versus Structure Size

Large fuselage panels for aircraft, particularly large transport aircraft, must have a stiffened skin to enable them to carry very large bending loads. The point is that a large transport aircraft has a very heavy loading on the fuselage, much more so than a small business aircraft of six passengers or so. Thus, we will see drastically different fuselage configurations for the two sizes of aircraft. Small-diameter fuselage business aircraft will likely have honeycomb sandwich structures as fuselage because their cost is lower than a stiffened structure. And the higher the load that we want to achieve, the more likely it is that we will use a discretely stiffened structure as for large-fuselage-diameter transport aircraft.

Insofar as configurations go, we might see a Kevlar skin over a Nomex honeycomb core as the primary fuselage for a relatively small

aircraft, but not for any large aircraft. The relative cost of honeycomb-core construction and stiffened construction is plotted versus the fuselage diameter with an indication for relatively small-diameter fuselages in Figure 7-36 that the sandwich-core approach to a fuselage is probably a lower-cost option than using skins with various kinds of stiffeners on them. In contrast, for a very large-diameter fuselage, the skin-stringer configuration would be the least expensive of the two alternatives. And this is, simply put, the difference between small aircraft such as the Learfan and the Beech Starship and so on as opposed to larger aircraft such as the 747, 777, or C-5A. Thus, the approaches that we see used for small aircraft do not usually scale up to large aircraft. The configuration trade-off is totally different for large-diameter fuselage aircraft.

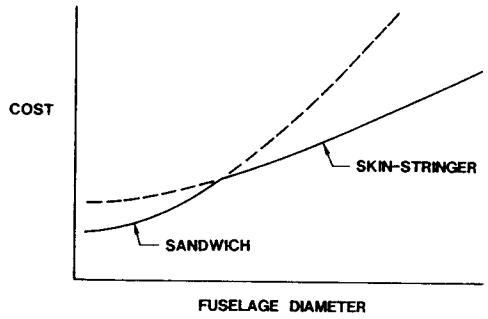

Figure 7-36 Configuration Trade-offs

7.4.5 Reconfiguration of Composite Structures

Recall from discussion of the structural design process in Section 7.2 that reconfiguration of the structure is an essential step. Reconfiguration occurs either to increase the capability or to decrease the weight because the structure has more than adequate capability. The term *capability* is meant to include margin of safety relative to fracture, adequate resistance to buckling, sufficient difference of excitation frequency from resonant frequencies, etc.

How specifically do we change or reconfigure a composite structure? First, with a laminate fiber-reinforced composite structure, *we will reorient the various layers.* That procedure will change the direction-dependent characteristics of strength and stiffness of the composite structure. Importantly, that *reorientation of laminae will not cause a weight penalty!* By simply changing the orientations of the layers, we have not added any material nor have we subtracted any, so there is no change in weight. No analogous design reconfiguration approach exists for a metal structure without changing its weight. There is nothing we can do for a metal structure aside from changing the materials such as changing to an aluminum-lithium alloy from aluminum. That material change will change the structure and its performance because of better weight efficiency. That material change is the only kind of situation that

is in any way analogous to reorienting composite laminae. That material substitution would be an obvious weight-saving approach. With composite structures, we are saying 'we're going to fix the material', and all we have to do is reorient the various layers to change the structural capabilities drastically.

A second major reconfiguration option is to *reorder the individual laminae or layers* within the laminate without changing their orientations. The resulting extensional stiffnesses are no different from before the reordering. However, the bending-extension coupling stiffnesses and, usually more importantly, the bending stiffnesses can be quite different. The major point is that *reordering the laminae does not change the laminate weight.* This design approach has no analog in metal structures design.

Another reconfiguration option is to *add layers to the laminate,* but then a weight penalty is involved. The analogy with a metal structure is obviously to make the metal thicker. However, a metal structure, if machined, has a much finer possible variation in thickness than a composite laminate. A laminate must have an integer number of layers unless you are willing to machine away part of the thickness of a layer. However, most manufacturers are not willing to risk degradation of fibers by machining a layer.

For a bending-dominated structure, we can add stiffeners that are, by definition, a weight-saving aid. Stiffeners do not, of course, offer any advantage in an extension-dominated structural element. Stiffeners allow us to prejudice the bending stiffness of the structure more in one direction, where the stiffeners go, than in the other directions. Or perhaps we can install stiffeners in two different directions (often, but not necessarily, perpendicular to one another). For both metal structures and composite structures, adding stiffeners saves weight as compared to a monocoque (unstiffened) structure. However, *composite stiffeners can be much more efficient than metal stiffeners, so stiffening can be even more of a weight-saving approach for composite structures than it is for metal structures.*

Next, we can, of course, make a material substitution. We can often substitute one specific graphite-epoxy for another member of the graphite-epoxy family. We can obviously substitute one metal for another metal. We can also substitute a composite material for a metal. All those approaches are taken in the interest of weight savings or cost savings, although the substitutions could also be made solely to achieve the required function of the structure.

Using a honeycomb laminate, i.e., having some kind of a lightweight core like the honeycomb in a bees' nest inside the outer layers of the laminate, is typically a way of increasing the bending stiffness of a structure with very little increase in weight. That is, we could use a very thick laminate, which is heavy, to do the job, or we could get the same bending stiffnesses with a laminate that has two sets of thin laminates, one at the top and one at the bottom, with a shear-deformable core bonded in the middle of the two laminates. Such a structural element has very high bending stiffness. The honeycomb-core laminate is, of

course, thicker, but lighter than the monocoque laminate with equal bending stiffness. We also can use honeycomb cores with metal structures, in which case we have actually created another form of composite structure! Honeycomb is often placed inside many aluminum structures, so that approach is quite common.

Let's review six different ways to reconfigure composite structures. Some have an analog with metal structures, and some do not. The first, layer reorientation in Figure 7-37, is unique to composite structures. Changing the order of the layers, like layer reorientation, is both unique to composite structures and offers a myriad of possibilities for controlling strength and stiffness. Because of the inherent higher stiffness-to-weight and strength-to-weight capabilities of a composite material, adding layers is a more efficient way of adding stiffness and strength than can be done with metals. We can do a better job of stiffening with composite structures than with metal structures. The material substitution process has far more possibilities with various composite materials than with metals. With honeycomb-core laminates, we can do a more efficient job with composite materials than we can with metals. Thus, reconfiguration of a structure has a new set of dimensions for a composite structure relative to a metal structure.

- **REORIENT LAYERS (NO WEIGHT PENALTY)**
- **REORDER LAYERS (NO WEIGHT PENALTY)**
- **ADD LAYERS (WEIGHT PENALTY)**
- **ADD STIFFENERS (SAVE WEIGHT)**
- **CHANGE MATERIAL (SAVE WEIGHT)**
- **USE HONEYCOMB-CORE LAMINATE (SAVE WEIGHT)**

Figure 7-37 Reconfiguration of Composite Structures

What kinds of configurations are possible for composite structures? The most obvious is that of a fiber-reinforced laminate. With a laminate, we can change laminae orientations, stacking sequence, and laminae materials to arrive at a suitable structure. We can stiffen the laminate, or we can put a sandwich core in the middle of those laminae. We can do all of those possibilities, but recognize that we will also have, in virtually any structure, some kind of hole or a cutout for some reason. Thus, we must have a procedure to place an appropriate amount of reinforcement around those cutouts so that load can be transferred around them. Without that reinforcement, the structure cannot do the job it is required to do. These various possible configurations are shown in Figure 7-38.

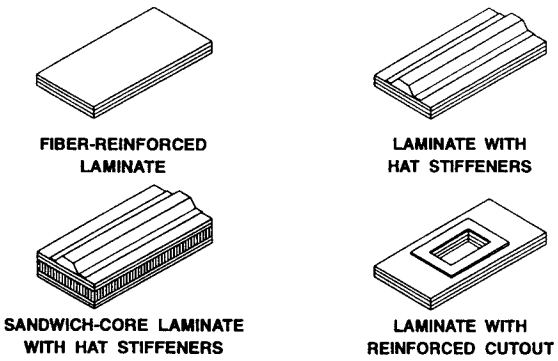

Figure 7-38 Possible Structural Configurations

7.4.6 Summary

Unique and unusual stiffening concepts can make composite structures far more effective and efficient than metal structures. We have introduced some of these stiffening concepts, but more are being developed. We should look forward to even more innovative unique-to-composites stiffening concepts in the future.

7.5 LAMINATE JOINTS

7.5.1 Introduction

High stiffnesses and strengths can be attained for composite laminates. However, these characteristics are quite different from those of ordinary materials to which we often need to fasten composite laminates. Often, the full strength and stiffness characteristics of the laminate cannot be transferred through the joint without a significant weight penalty. Thus, the topic of joints or other fastening devices is critical to the successful use of composite materials.

The purpose of this subsection is to familiarize the reader with some of the basic characteristics and problems of composite laminate joints. The specific design of a joint is much too complex for an introductory textbook such as this. The published state-of-the-art of laminate joint design is summarized in the *Structural Design Guide for Advanced Composite Applications* [7-5] and *Military Handbook 17A, Plastics for Aerospace Vehicles, Part 1, Reinforced Plastics* [7-6]. Further developments can be found in the technical literature and revisions of the two preceding references.

The two major classes of laminate joints are bonded joints as in Figure 7-39 and bolted joints as in Figure 7-40. Often, the two classes are combined, for example, as in the bonded-bolted joint of Figure 7-41. Joints involving composite materials are often bonded because of the natural presence of resin in the composite and are often also bolted for

reasons discussed later. Several characteristics of fiber-reinforced composite materials render them more susceptible to joint problems than conventional metals. These characteristics are weakness in in-plane shear, transverse tension, interlaminar shear, and bearing strength relative to the primary assets of a lamina, the strength and stiffness in the fiber direction.

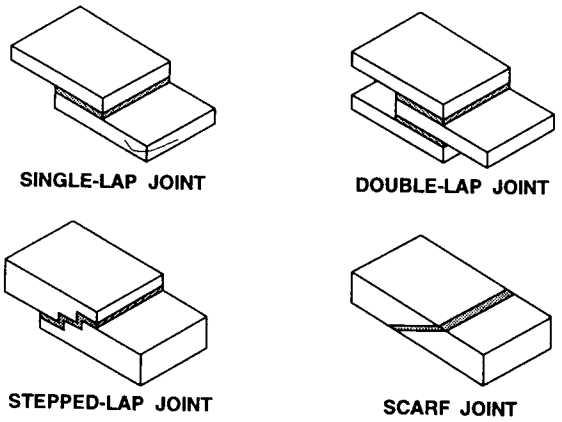

Figure 7-39 Bonded Joints

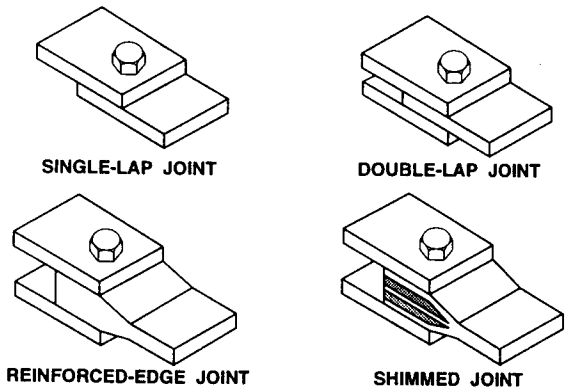

Figure 7-40 Bolted Joints

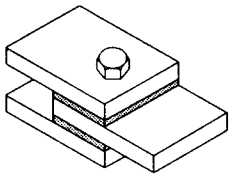

Figure 7-41 Bonded-Bolted Double-Lap Joint

7.5.2 Bonded Joints

Goland and Reissner studied the stresses in bonded single-lap joints for two important limiting cases: (1) a bond layer so thin that it has no contribution to the joint flexibility (inverse of stiffness), and (2) a bond layer so thick that it is the primary contributor to the joint flexibility [7-7] (this classic paper is referred to by nearly every researcher in bonded joints). They considered the shearing and normal stresses in the bond layer as well as those in the joined plates. For fiber-reinforced composite materials, the thick-bond-layer approach of Goland and Reissner is more appropriate than the thin-bond-layer approach because of the presence of epoxy resin in the composite material and the effective thickness of the bond relative to the joined pieces. They found, for equal-thickness isotropic plates, that the bond layer shear stress has nearly uniform distribution except for a large concentration near the end of the joint.[1] The bond stress perpendicular to the bond layer also has high values near the joint edge, although not nearly as high as the inflexible bond case. Berg analyzed a bonded double-lap joint and suggested interleaving the materials of a lap joint to reduce the high stresses that otherwise occur where layers meet [7-8].

The fundamental design problem in bonded joints is to get enough bond area in shear to carry the load through the joint. Bond area in tension is of little value because of the typically low strength of bonding materials compared to the far higher strength of the metals or composite materials being joined. The contrast between the two types of bonding area is shown in Figure 7-42. The extension of these concepts to many types of bonded joints is illustrated in Figure 7-43 along with their types of failure. There, an increase in adherend thickness does not always lead to a stronger joint!

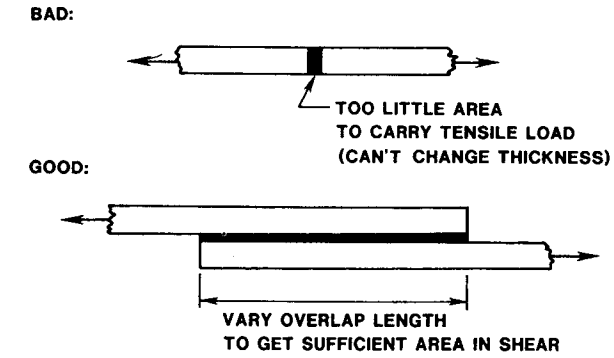

Figure 7-42 Good and Bad Load Transfer in Bonded Joints

[1]The geometry and material discontinuities at the ends of the bond material in the single-lap joint in Figure 7-42 naturally lead to high stresses. That is, the classical bi-material problem necessarily leads to singularities (infinite stresses) at the end of the interface between the materials in the usual elasticity approaches to the problem. Thus, we must always exercise considerable judgement when interpreting bonded-joint analysis results.

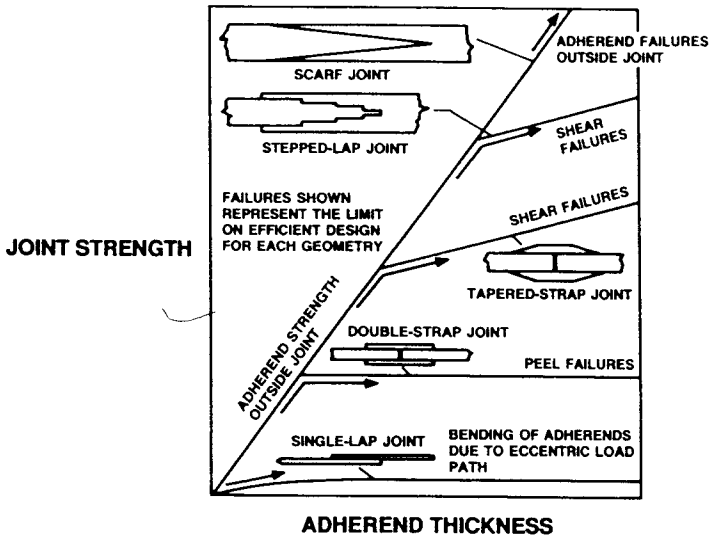

Figure 7-43 Types of Bonded Joints and Their Failures *(After Hart-Smith [7-9])*

7.5.3 Bolted Joints

The principal failure modes of bolted joints are (1) bearing failure of the material as in the elongated bolt hole of Figure 7-44, (2) tension failure of the material in the reduced cross section through the bolt hole, (3) shear-out or cleavage failure of the material (actually transverse tension failure of the material), and (4) bolt failures (mainly shear failures). Of course, combinations of these failures do occur.

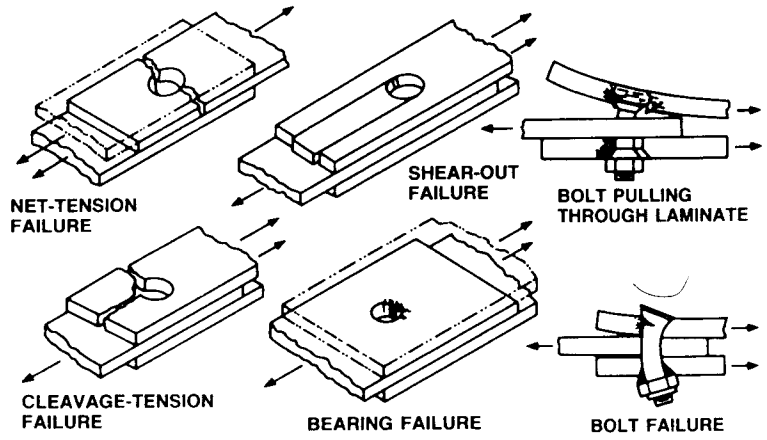

Figure 7-44 Bolted Joint Failures *(After Hart-Smith [7-10])*

One of the ways to increase the bearing strength of a joint is to use metal inserts as in the shimmed joint of Figure 7-40. Another way is to thicken a section of the composite laminate as in the reinforced-edge joint in Figure 7-40.

Net-tension failures can be avoided or delayed by increased joint flexibility to spread the load transfer over several lines of bolts. Composite materials are generally more brittle than conventional metals, so loads are not easily redistributed around a stress concentration such as a bolt hole. Simultaneously, shear-lag effects caused by discontinuous fibers lead to difficult design problems around bolt holes. A possible solution is to put a relatively ductile composite material such as S-glass-epoxy in a strip of several times the bolt diameter in line with the bolt rows. This approach is called the softening-strip concept, and was addressed in Section 6.4.

7.5.4 Bonded-Bolted Joints

Bonded-bolted joints generally have better performance than either bonded or bolted joints. The bonding results in reduction of the usual tendency of a bolted joint to shear out. The bolting decreases the likelihood of a bonded joint debonding in an interfacial shear mode. The usual mode of failure for a bonded-bolted joint is either a tension failure through a section including a fastener or an interlaminar shear failure in the composite material or a combination of both.

Bonded-bolted joints have good load distribution and are generally designed so that the bolts take all the load. Then, the bolts would take all the load after the bond breaks (because the bolts do not receive load until the bond slips). The bond provides a change in failure mode and a sizable margin against fatigue failure.

An example of a complex bonded-bolted joint used in the box beam of a folding aircraft wing is shown in Figure 7-45. There, a basic structure of graphite-epoxy and boron-epoxy layers over honeycomb is attached to an aluminum forging. The honeycomb is gradually replaced by graphite-epoxy as the joint is approached from the wing direction (the

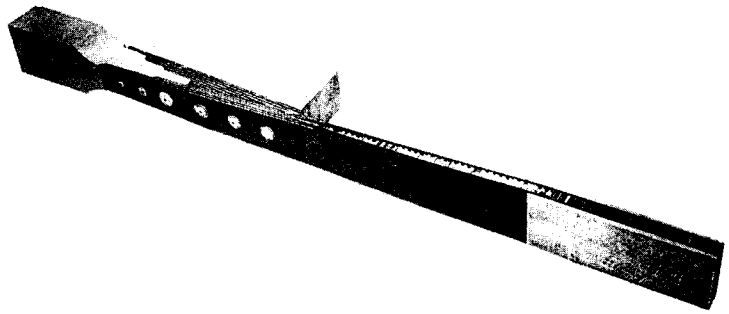

Figure 7-45 Complex Bonded-Bolted Joint *(Courtesy of Vought Systems Division, LTV Aerospace Corporation)*

right in Figure 7-45). Then, titanium sheaves are successively introduced to increase the bearing strength of the joint. Finally, the combined graphite-epoxy and titanium composite material is stair-stepped over the Christmas-tree-like aluminum forging. The titanium sheaves are bonded to the graphite-epoxy with a film adhesive. The graphite-epoxy is bonded to the aluminum forging with a paste adhesive. The entire joint is then bolted together.

7.5.5 Summary

Bolted, bonded, and bonded-bolted joints have barely been introduced. Further behavioral and design information is available in the book *Joining Fibre-Reinforced Plastics* edited by F. L. Mathews [7-11], which has chapters written by various authors including two chapters on design by L. J. Hart-Smith.

7.6 DESIGN REQUIREMENTS AND DESIGN FAILURE CRITERIA

7.6.1 Introduction

Establishing suitable design failure criteria is a difficult task, yet fundamental to the design process. The concept of design failure criteria is much more complicated and involved than just the issue of gross failure of a lamina or even gross failure of a laminate as treated in traditional composite materials analysis. Thus, the term *design failure criteria* does not mean the application of the Tsai-Hill failure criterion or the Hoffman failure criterion or anything like them for a single lamina. Establishing design failure criteria is a much more complicated issue than establishing lamina failure because we must ask *how* the *structure* itself fails. What does failure mean in the context of that specific design? Failure simply means that the structure cannot fulfill some design requirement(s). All failure really means then is that we have designed a structure or object to do a particular job, and that structure cannot do its job. Obviously, nothing was mentioned about the structure breaking or falling down. That is, failure means far more than just fracture.

7.6.2 Design Requirements

Design requirements are simply a collection of statements of what we ask the structure being designed to do. What is its required performance? Those requirements can be expressed in terms of structural response or, alternatively, in terms of system performance.

Consider an example involving several design requirements. For a beam overhead above a ceiling, the most important thing we want the beam to do is to hold up the ceiling so it does not fall on our heads. That requirement is a strength issue. We also do not want that ceiling beam to deflect very much, and deflection is a stiffness issue. One of the problems with a ceiling beam deflecting too much is if the ceiling is plaster, then the plaster will crack as in Figure 7-46, and that is obviously unsightly. If you were paying for a building, you certainly would not want

cracked plaster, so obviously a stiffness requirement exists. There is also a stiffness requirement because we do not want people who are in the building to perceive that the floor above them is sagging so much that they get scared. Thus, we are faced with two very clear issues, i.e., strength and stiffness. Another issue is that the ceiling beam must withstand whatever loads are imposed on it over the *lifetime* of the structure such as intermittent snow loads, a lot of walking around, or moving equipment around, or whatever. That collection of circumstances is a life issue. Thus, we have identified three different structural issues in the design of a ceiling beam, namely ***strength, stiffness,*** and *life.* Failure of the beam is not failure from the standpoint of simply breaking apart, although obviously that is the essence of the first issue, strength. After that simplistic concern, other significant issues must be addressed, namely stiffness and life, just to list two such issues.

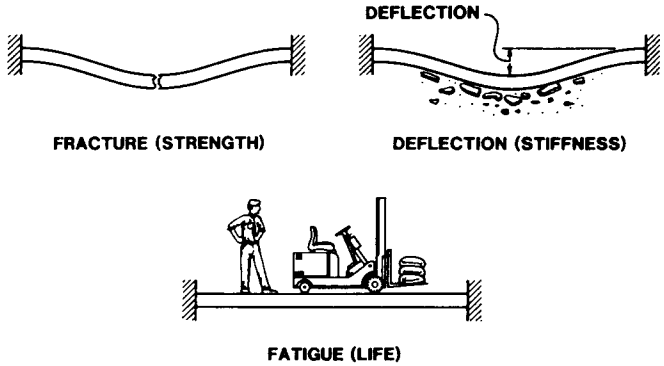

Figure 7-46 Ceiling Beam Design Requirements

We could go through that same kind of problem analysis for many different structures, and, in the process, design requirements could be expressed for each of them. The most common design requirements would be expressed in some manner in terms of strength, stiffness, and life, but there are many other issues as well. Whether the material will corrode, for example. Whether it will provide the proper insulation or just the opposite, sufficient conductivity, and so on. There are many, many different types of tasks that we ask a structure to perform.

Failure has many meanings or interpretations in the context of the structural design process. The main meaning is that failure is the inability of the structure to perform up to its design requirements. Those requirements can be expressed simplistically in terms of the following functional ways:

(1) strength — the material will have limits of stress or strain that cannot be exceeded without fracture
(2) stiffness — the structure will be designed to deform a specific amount or perhaps be limited to a specific deformation without vibrating excessively or buckling.

(3) life — the structure might have a specified life span
(4) energy — the structure might have to absorb specified amounts of energy and still remain functional
(5) weight — the structure might have to weigh less than a specified amount for the configuration to be a feasible design
(6) cost — the structure might have to cost less than a specified amount or else a configuration that works in every other respect must be redesigned
(7) manufacturing — if the structure cannot be built, then the configuration is unacceptable

If these or other specific design criteria cannot be met, then the design is a failure, and the structure must be redesigned to meet the requirements. Thus, design is an iterative process coupled with analysis and testing activities to assess the success or failure of a composite structure. All design activities must be accompanied by an evaluation program to assess each of the goals and the progress toward satisfaction of the goals. Accordingly, each of the goals or design criteria must be clearly definable and readily measurable, or else they are too vague to be of use in the design process.

7.6.3 Design Load Definitions

In aircraft, as well as spacecraft, certain design load definitions are common. *Design limit load* is the largest load on a structural element that is expected during normal service. Thus, design limit loading includes drastic maneuvers and high wing loadings that would be encountered, for example, in gusty winds during a severe Texas thunderstorm. Of course, most flights have loadings well under the design limit load. *Design ultimate load* is some factor greater than one times the limit load. That factor depends on the type of failure (benign or catastrophic), on the type of usage (man-rated or unmanned structures), and on whether actual structural loading tests are performed to verify the design. Obviously, the factor must be high for a structural element that fails catastrophically, is used for a man-rated structure, and is not load-tested prior to use. On the other hand, the factor could be low for a structural element that fails in a benign manner, is used on an unmanned structure, and is load-tested prior to use. Of course, neither set of circumstance constitutes responsible design! Because the multiplying factor is arbitrary, the actual failure load might well exceed the design ultimate load. Unfortunately, some engineers refer to the design ultimate load as the 'ultimate load'. Of course, the term *ultimate load* is properly used only for the load at which the structural element actually fails, i.e., receives its *ultimate* loading. These critical design loads are displayed in the context of a load-deflection curve in Figure 7-47. Note that first-ply failure might not be allowed below the design limit load. Moreover, the design limit load might be cyclically applied, which is all the more reason to avoid a first-ply failure in a cyclic-loading environment.

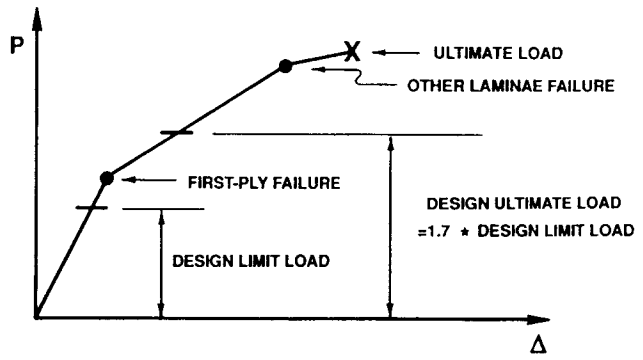

Figure 7-47 Critical Design Loads

7.6.4 Summary

We have considered example design requirements in general terms, and the main issue to emphasize is that *strength is not the sole concern.* There is much more to design requirements than simply whether the object is strong enough to avoid fracture. We must go far beyond that overly simplistic viewpoint to issues of stiffness, life, corrosion, permeability, etc.

The area of design failure criteria impacts, and is a quantitative measure of, the success of a design. Fundamentally, design failure criteria *are* the statement of the design requirements. The manner in which individual laminae as well as laminates fail is but a part of design failure criteria. Failure of laminae and laminates, as in Chapters 2 and 4, is a fundamental portion of all strength-related failure criteria, but those failures are also determining factors in stiffness-related failure criteria.

7.7 OPTIMIZATION CONCEPTS

7.7.1 Introduction

The fundamental objective in design is to achieve the *best* structural configuration that will do the job intended. The concept of 'best' implies that a measure of design quality is available. For example, in aircraft structures, the lowest-weight design often is regarded as the 'best' design because of positive implications for range, economy, and performance. For other structures, the least-cost design might be judged the 'best'. The answer to any design problem is not unique, so some means must be established to define and determine the 'best' configuration. The functional requirements of strength, stiffness, and life as discussed in Section 7.6 are the basis for defining the 'best' configuration. Optimization is the more or less mathematical procedure by which that 'best' configuration is obtained in a direct, rational way. In this section, we will first examine some fundamental concepts of optimization as in Figure 7-48. Next, we will address analysis and optimization for strength,

one of the five principal structural response areas of stiffness, strength, buckling, vibration, and life prediction. Analysis and optimization could be performed for other structural response phenomena if mechanistic relationships between those phenomena and structural configuration are available. Then, we will investigate invariant laminate concepts that could be used in design. Finally, we will consider several issues that are crucial to laminate design.

- **FUNDAMENTALS OF OPTIMIZATION**
- **ANALYSIS AND OPTIMIZATION**
- **INVARIANT LAMINATE CONCEPTS**
- **DESIGN OF LAMINATES**

Figure 7-48 Outline of Optimization Concepts

7.7.2 Fundamentals of Optimization

The criteria used for any type of an optimization scheme can be varied. The criteria depend on what is most important in your structure. Do you need a structure that must be of least weight? If that is your primary objective, then least weight is the characteristic of the structure for which you would optimize. Design of a weight-sensitive structure is probably the most common aerospace structural optimization problem. Cost is also an appropriate criterion for some optimization problems, whether cost be initial cost or life-cycle cost. Sometimes you want the longest range or the highest speed if you are designing a high-performance airplane. Or, another possibility is the longest life of a satellite. Those factors are all valid optimization criteria usually called *merit functions* or *objective functions.* Perhaps you would like to optimize for more than one merit function at the same time. You cannot expect both of two merit functions to necessarily be maximized (or minimized, if appropriate) in the absolute sense. However, two merit functions can be maximized in the sense that both can be forced to be an approximate optimum. When more than one merit function is addressed, a very difficult mathematical problem results.

7.7.2.1 Structural Optimization

Let's try to define in a practical sense the structural optimization problem. To do so, let's work our way through the complete definition by examining a sequence of useful lesser definitions.

First, we must realize that many variables exist in any structural design. We can make a list of structural variables such as sizes, lengths of objects, materials, laminae orientations, and so on. Those variables all have influence just as column length, moment of inertia, and Young's modulus influence column-buckling loads. The complete list of design variables will be called the vector $\bar{x}_i$, and that vector will have N components. That list constitutes the definition of the structural configuration.

Then, we ask: how does this structure behave? The structure deflects and has stresses, buckling loads, and vibration frequencies, and

these response characteristics are evaluations of the structural performance. That behavior can be represented by some other function, say C_{ij}, of the design variables, i.e., $C_{ij}(x_i)$. That symbolism or notation is really an equation that we write in some way, and it could be as simple as the Euler buckling-load equation for a column. The Euler buckling load then is the C_{ij} value. The Euler buckling-load equation has length, Young's modulus, and moment of inertia as the design variables.

Next, certain conditions or *constraints* must be placed on the problem. We ask, for example, that the strength of the object be greater than a certain amount of load because we want the object to carry that amount of load safely. Calling that minimum strength a constraint might be a different philosophy than you are used to. Let's just view the constraint as a *design requirement.* Go back to design failure criteria in Section 7.6 — certain design requirements exist and can be stated in the form of a mathematical constraint equation, e.g., $\sigma_{1_{max}} < X$, which is a statement that the maximum allowed fiber-direction stress must be lower than the strength in that direction. For example, the response must be greater than zero in a particular response mode. That is, the real load-carrying ability minus the desired load-carrying capability must be greater than zero. We can always work the equation into an inequality with zero on one side simply by subtracting a constant. That constant is the design load requirement including a factor of safety. Or, as another example, a certain frequency of excitation must exist for the object. We must make certain that all the natural frequencies are above (or below) that particular frequency so that resonance is avoided. Thus, we simply write a frequency evaluation equation, subtract from that frequency the frequency of driving, and say that that result must be greater (or less) than zero. Then, when the structure satisfies that constraint, the frequency requirement is satisfied, i.e., the structure will not resonate.

Finally, we must address some merit function, M, that is a function of the design variables, i.e., $M(x_i)$ If that merit function or objective function is the structural weight to be minimized, then the equation for the weight of the structure is some function of its design variables. All we must do is use all the dimensions to calculate the volumes of various parts of the structure and multiply by the appropriate densities to get the weight. We then minimize that weight. Or, we could address some merit function other than weight, e.g., the range of an airplane.

You have been presented with a collection of equations and definitions in the past few paragraphs. The way to put them all together is to simply say that the structural optimization problem is *the minimization of an inequality-constrained function of N design variables.* If I had started out with that statement as a sentence, you might have been unhappy because too many undefined terms are used. However, when we break down the sentence with the preceding definitions, a fairly straightforward explanation of a design optimization problem results. The design variables used to express the structure's weight can be put into another form with which we evaluate the behavior and compare it to the design requirements. Once we put all those steps together for the least-weight structure, we have the answer to our design problem.

Structural synthesis or optimization is a method of direct and rational solution of the problem just expressed, i.e., *the inequality-constrained minimization problem.* 'Direct rational solution' — that means mathematics. Design can be done in two different ways. One way in which design is approached is a rational fashion in which we have equations for the performance, we compare the actual performance with the requirements, and we make appropriate adjustments to the design until the performance meets the requirements. The other way to design is to put something on paper, i.e., select a trial design in some manner, and make certain evaluations to assess performance. If the structural configuration will do the job, i.e., meet the performance requirements, then that is our design. The latter approach is not optimization unless we iterate that design to try to answer the question: can we make some design variable changes that will lead us to a lower-weight structure, or higher-speed structure if speed is the issue, or whatever? But if we simply draw designs on paper and evaluate them, that is not a direct and rational solution. That approach is just trying many solutions and seeing if by chance one of them is better than any of the others. That approach does not satisfy any rational definition of design because only a deliberately restricted number of possible designs has been examined. Obviously, the real optimum design just might not be within that restricted number. However, precisely that approach is the most common in industry today.

Various rational approaches to design do exist. We can exercise what really amounts to a brute-force approach, which is not a particularly good approach, but there is a way of making that approach almost rational. That is, we can try all the possible solutions for certain problems. We can sometimes define all the solutions, and then pick the 'best' solution. Then, we know we have the optimum design because we have examined *all* possible designs. We will study an instance in which that brute-force approach is possible and even quite useful. Obviously, other instances exist in which we could not even imagine knowing all the solutions. For example, if we want to design a 150-passenger airplane to fly from New York to Los Angeles, then we must realize that an infinite number of solutions exists, and we cannot possibly try them all. But if we want a laminate that will carry a certain load, there is a finite number of solutions to that problem (if we ignore obviously inappropriate laminates such as all laminates thicker than necessary), and we actually can try them all. More rational optimization approaches involve more refined mathematical procedures, such as Monte Carlo techniques, dynamic programming, or nonlinear programming. Some very complicated issues arise with using those techniques for structures.

For structures, especially composite structures, the number of design variables is very large, and we must also perform a large number of response evaluations. Thus, we are automatically pushing very hard against our computer limitations. As a matter of fact, we exceed usual computer capabilities for all structural design problems that are really practical except for nonlinear programming. Monte Carlo and dynamic programming techniques are useful for some physical problems that have fewer design variables than are typical for structures. Thus, you might hear about those techniques being used in other engineering areas, but not in structures design.

The term *nonlinear* in *nonlinear programming* does not refer to a material or geometric nonlinearity but instead refers to the nonlinearity in the mathematical optimization problem itself. The first step in the optimization process involves answering questions such as: what is the buckling response, what is the vibration response, what is the deflection response, and what is the stress response? Requirements usually exist for every one of those response variables. Putting those response characteristics and constraints together leads to an equation set that is inherently nonlinear, irrespective of whether the material properties themselves are linear or nonlinear, and that nonlinear equation set is where the term *nonlinear programming* comes from.

How many organizations do what we could really call direct rational solution of the composite structure design problem? — very, very few. Perhaps only in some very restricted design areas do people feel that they can use a mathematically oriented optimization approach. That situation is unfortunate, but changing.

7.7.2.2 Mathematics of Optimization

Let us contrast two approaches to optimization. One approach is searching, and the other one is mathematical optimization.

Searching is an approach in which we either try all of the possible solutions or look at a few solutions and try to infer from them what we must do to obtain other, more appropriate solutions. As an example, suppose we are faced with an equation that we must solve, e.g., some function f(x) must be zero. We could plot discrete values of that function as in Figure 7-49. The values of the function are plotted as a sequence of dots, i.e., the function is evaluated at specific values of x. The objective is to find where that function is zero. You could look at Figure 7-49 and imagine connecting all the dots to see where the curve crosses the axis. There are three crossings, and that fact gives us some feeling for the solutions to the equation. That is, simply look at discrete values of x, find what f is, and then visually make a comparison with the desired zero value of the function and ask: what value, or values, of x correspond to a zero value of the function? Obviously, the objective function must be evaluated a large number of times in this search procedure.

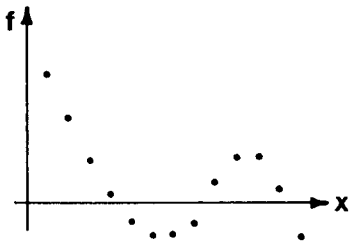

Figure 7-49 Search Procedure

Mathematical optimization, in contrast to searching, is a way of not even necessarily having to look at a collection of specific values of the function. We do not even need to plot the function, although for various reasons plotting the function is very desirable. You probably have used Newton's method to solve an equation such as $f(x) = 0$. The equation for Newton's method is fairly simple, and is related to the geometry of the curve. For some approximate solution x_i, we calculate a value of f which is not zero. We look at the slope of the curve in Figure 7-50 at that point (x_i) and project a line with the slope at x_i down to the horizontal axis. Where that line intersects the horizontal axis is the new approximation to the solution of the problem, i.e., the best estimate of the solution based on a linear extrapolation. That new approximation, x_{i+1}, is related to the old approximation by the geometry of the triangle in Figure 7-50, which involves the value of the function, its slope, and the base of the triangle. The slope (the function derivative) multiplied by the horizontal distance (the triangle base) is the vertical distance (the function value),

$$f'(x_i)(x_{i+1} - x_i) = f(x_i) \tag{7.9}$$

and that relation can be rearranged as

$$x_{i+1} = x_i + \frac{f(x_i)}{f'(x_i)} \tag{7.10}$$

Our next guess for the solution of the equation is x_{i+1}. The approximation process is repeated until the function is close enough to zero to satisfy us.

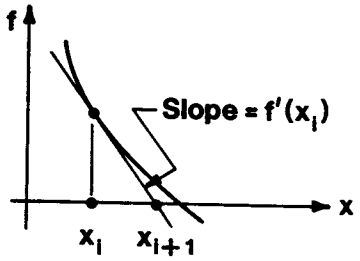

Figure 7-50 Mathematical Optimization

This mathematical optimization procedure is a rational process because the slope (or derivative) enables us to know *which way to go* and *how far to go.* In contrast, in the search procedure, we just arbitrarily choose some values of x at which to evaluate the function. Those arbitrary choices are much like what people do in most design situations. They are simply searching in a rather crude manner for the solution to the problem, and they will not achieve the solution precisely. With mathematical optimization, our hope is both to speed up that process and to get a more precisely optimum solution.

The mathematical procedure for a single merit function optimization for many design variables involves derivatives of the merit function with respect to each of the design variables (as a generalization to multiple

variables of the single-variable Newton's method just illustrated). Thus, the usual structural optimization procedure cannot be visualized in two or three dimensions, so typically conventional visualization concepts are not part of optimization. However, more recently developed visualization concepts might be quite useful. Mathematical optimization has been used for structural optimization starting with Schmit [7-12].

7.7.2.3 Optimization of a Composite Laminate

Let's consider one rather restricted structural optimization problem, that of a composite laminate. You have seen claimed as attractive advantages of composite structures the fact that we can orient the laminae in a laminate to our heart's content to try to get the most efficient structure. This characteristic is totally unlike what is possible with metal structures. This laminate orientation flexibility is certainly an advantage, but how do we use it?

Let's start by reviewing quantitatively the analysis and design process for metal plates. For an isotropic metal plate under extensional loading, N_x only, the load is related to the strains by

$$\begin{aligned} N_x &= \frac{E\,t}{(1-\nu^2)}(\varepsilon_x^\circ + \nu\varepsilon_y^\circ) \\ N_y &= \frac{E\,t}{(1-\nu^2)}(\varepsilon_y^\circ + \nu\varepsilon_x^\circ) = 0 \end{aligned} \tag{7.11}$$

Then, from the lateral force condition that $N_y = 0$,

$$\varepsilon_y^\circ = -\nu\varepsilon_x^\circ \tag{7.12}$$

the applied force becomes

$$N_x = E\,t\,\varepsilon_x^\circ \tag{7.13}$$

Thus, for a prescribed allowable strain, we can solve for the plate thickness necessary to avoid failure (without consideration of a factor of safety):

$$t_{required} = \frac{N_x}{E}\frac{1}{\varepsilon_{allowable}} \tag{7.14}$$

Note that different thicknesses result from Equation (7.14) for different materials with their characteristic values of E and $\varepsilon_{allowable}$. That is, the design problem has only one answer if the material is specified, but many answers exist if the material is not specified.

In a similar manner, if a bending moment, M_x only, is applied,

$$\begin{aligned} M_x &= \frac{E\,t^3}{12(1-\nu^2)}(\kappa_x + \nu\kappa_y) \\ M_y &= \frac{E\,t^3}{12(1-\nu^2)}(\kappa_y + \nu\kappa_x) = 0 \end{aligned} \tag{7.15}$$

Then, from the lateral moment condition ($M_y = 0$),

$$\kappa_y = -\nu\kappa_x \tag{7.16}$$

Thus, the applied moment becomes

$$M_x = \frac{E\,t^3}{12}\,\kappa_x \tag{7.17}$$

However, from the linear strain distribution through the plate thickness,

$$\varepsilon_x = \varepsilon_x^\circ + z\,\kappa_x \tag{7.18}$$

For pure bending ($\varepsilon_x^\circ = 0$), the largest strain is at $z = \pm t/2$, so

$$\kappa_{x_{max}} = \frac{2}{t}\,\varepsilon_{x_{max}} \tag{7.19}$$

Accordingly, the required thickness is

$$t_{required} = \left[\frac{6\,M_x}{E\,\varepsilon_{allowable}}\right]^{1/2} \tag{7.20}$$

Thus, for both extensional loading and pure bending of isotropic metal plates, the required thickness to support a specific loading can be determined directly by an inverse of the analysis equations, i.e., the design process is *deterministic*.

For a simple symmetric cross-ply laminated plate subjected to in-plane force N_x, the force-strain relations are

$$\begin{bmatrix} N_x \\ N_y \end{bmatrix} = \begin{bmatrix} A_{11} & A_{12} \\ A_{12} & A_{22} \end{bmatrix}\begin{bmatrix} \varepsilon_x^\circ \\ \varepsilon_y^\circ \end{bmatrix} = \begin{bmatrix} N_x \\ 0 \end{bmatrix} \tag{7.21}$$

From the lateral force condition ($N_y = 0$),

$$0 = A_{12}\varepsilon_x^\circ + A_{22}\varepsilon_y^\circ \tag{7.22}$$

or

$$\varepsilon_y^\circ = -\frac{A_{12}}{A_{22}}\,\varepsilon_x^\circ \tag{7.23}$$

Thus, the applied force becomes

$$N_x = \left(A_{11} - \frac{A_{12}^2}{A_{22}}\right)\varepsilon_x^\circ \tag{7.24}$$

However, recall that the extensional stiffnesses are

$$A_{ij} = \sum_{k=1}^{N} (\bar{Q}_{ij})_k t_k \tag{7.25}$$

where the $\bar{Q}_{ij}$ are known complicated functions of Q_{11}, Q_{12}, Q_{22}, Q_{66}, and α_k, the fiber orientation of the k^{th} layer, as well as the laminae thicknesses, t_k. Obviously, the Q_{11}, Q_{12}, and Q_{22} are known in terms of E_1, E_2, and ν_{12}. However, we cannot solve for the laminae thicknesses, number of layers, and laminae angles from a *single* (force-strain) equation. Thus, even the simplest laminate design problem is *indeterminate* or *nondeterministic*. That fact creates a particularly big problem when we would actually like to optimize the laminate design, and we have trouble determining a single laminate design, much less the best design.

For more general laminated fiber-reinforced composite plates, the relations between forces, moments, middle-surface strains, and middle-surface curvatures,

$$\begin{bmatrix} N_x \\ N_y \\ N_{xy} \\ M_x \\ M_y \\ M_{xy} \end{bmatrix} = \begin{bmatrix} A_{11} & A_{12} & A_{16} & B_{11} & B_{12} & B_{16} \\ A_{12} & A_{22} & A_{26} & B_{12} & B_{22} & B_{26} \\ A_{16} & A_{26} & A_{66} & B_{16} & B_{26} & B_{66} \\ B_{11} & B_{12} & B_{16} & D_{11} & D_{12} & D_{16} \\ B_{12} & B_{22} & B_{26} & D_{12} & D_{22} & D_{26} \\ B_{16} & B_{26} & B_{66} & D_{16} & D_{26} & D_{66} \end{bmatrix}\begin{bmatrix} \varepsilon_x \\ \varepsilon_y \\ \gamma_{xy} \\ \kappa_x \\ \kappa_y \\ \kappa_{xy} \end{bmatrix} \tag{7.26}$$

are such complicated functions of the number of layers and the stacking sequence that no direct solution exists in the same manner as for isotropic metal plates. That is, there are no solutions for the required thickness of a laminated plate that are analogous to Equations (7.14) and (7.20). The problem is that we seek more than one unknown, i.e., the thickness *and* the laminae orientations, but we have only one equation! Or, at most, six equations from Equation (7.26).

The solution to this laminate design problem with more design variables than loading parameters is nontrivial. Without a direct solution, we must appeal to an indirect solution approach. One such indirect approach is described in Section 7.7.2.4 on optimization methods. There, a brute-force, try-many-possible-combinations scheme is used to find a laminate that satisfies the design requirements. Another approach is Tsai's laminate-ranking procedure [7-13], which is not a true design approach, but instead is a sequence of evaluations of different predetermined laminates under specified loading with subsequent ordering of the chosen set of laminates with respect to their ability to bear the prescribed load. The best laminate is chosen from those examined, so the actual best laminate could be missed. However, Tsai's method has the advantage that searching can be limited to those laminates or laminate families that are of interest. For example, attention might be restricted to laminates for which fatigue data are available.

The fundamental laminate problem is: given the overall loading and a rough idea of the shape that we want, what is the optimum set of laminae orientations that constitute this laminate? Here, we must get quantitative and outline a specific approach to laminate design. First, we do not even know *how many* laminae we need! Our basic objective is that we want to carry a certain set of loads. The design process is not simply finding a thickness as with a metal plate, it is finding a thickness and *what goes into that thickness*, namely the number and orientation

of the laminae as in Figure 7-51. That basic process for composite laminates is much more complicated than that for metal structures where we must determine only one variable — the thickness.

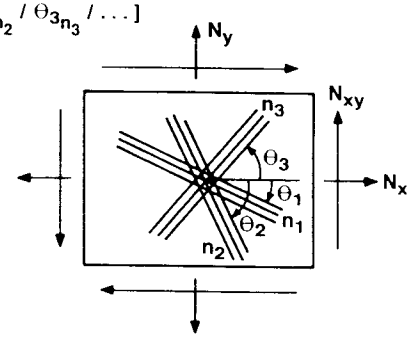

Figure 7-51 The Fundamental Laminate Design Problem

The evaluation of the load-carrying capacity of a specific laminate (including the load-deformation behavior) is a straightforward deterministic process and is described in Section 4.5. For example, a 20-layered laminate has a certain load-carrying capacity for one type of loading (and a different capacity for a different type of loading).

In contrast, the same specified load-carrying capacity can be achieved with perhaps a 20-, 30-, 40-, or 50-layered laminate or with many other laminates. All those laminates meet the load-carrying requirement, so *the process of laminate design is nondeterministic.* If each lamina is of the same material, then the laminate weight is directly proportional to the number of laminae. Obviously, then the 20-layered laminate weighs the least of the several just mentioned. When laminate weight is considered, we have a quantifiable means of distinguishing between the various possible answers to the laminate design question. That is, with a merit function such as weight, we can *rank* the laminates as to how well they satisfy the design requirements. Note that strength is *not* such a merit function because strength is a *constraint* on the laminate design problem, so it cannot possibly be a merit function also.

In general, we might like to consider all possible laminae orientations for the laminate, but that approach is rather tedious. That is, if we were to try to evaluate all the corresponding laminates, an infinite number of solutions is possible, so that approach is obviously not realistic. Considering a totally arbitrary set of orientations for most laminates is also unrealistic simply because for manufacturing reasons you do not want to specify that one layer must be at 67.3° and the next at 52.7°. Such refined specification of laminae angles cannot be easily achieved in manufacturing, nor is it necessary or desirable. A much more practical approach is to think in terms, at the most refined stage, of allowing the laminae to be oriented at various 5° increments. That restriction on laminae angular orientation drastically cuts down the number of possible laminates. That restriction, however, still leaves a very large number of possibilities for laminae orientation in a laminate as you will soon see.

An even more practical approach for various reasons is to restrict the acceptable laminae angles to certain combinations, such as 0° laminae, 90° laminae, and ±45° laminae. I am not suggesting that we build only quasi-isotropic laminates because I did not say that you must have the same number of 90° laminae as 0° laminae as +45° laminae as –45° laminae. Let the numbers of laminae, the proportions of those various types of layers, change. We are dealing with a family of 0°, 90°, and ±45° laminae. The design parameters that we then search for are the values of three parameters, L, M and N, the numbers of 0°, 90°, and ±45° laminae, respectively. We are searching for three numbers in this case (the number of layers in each respective angular orientation group), but we are searching for many more numbers if we drop back one stage and let the layers be oriented at 5° increments as possible orientations. The mathematical nature of the design optimization problem is changed very drastically when we cut down the number of design variables or restrict the possible values of the design variables. Those two approaches to laminate design will be contrasted in the next section.

7.7.2.4 Strength Optimization Programs

We will discuss, to various degrees and for various reasons, commonly used strength optimization programs such as RC7 and OPLAM. Each program has a particularly attractive feature in the design sense. Of course, new programs are always being developed, so this discussion is out-of-date even before publication. However, the discussion has some lasting general educational value.

The RC7 program was developed by Waddoups, McCullers, Olsen, and Ashton to address a configuration with at most 20 laminae in a laminate [7-14]. Each of the laminae can be oriented in increments of 5°. That simple laminate is the total configuration, i.e., no stiffeners or honeycomb core are considered. The only design condition that is evaluated is the laminate strength through the means of two alternative failure criteria for individual laminae: the Tsai-Hill failure criterion and the maximum strain failure criterion. The only kind of loading is uniform in-plane loading, i.e., no bending moments can be applied. Stiffness is not considered (although it could readily be evaluated), and thus there can be no evaluation of buckling or vibration capabilities. Thus, RC7 is a point-stress analysis embedded in a strength optimization program.

The method of optimization is a brute-force search technique. All the possible laminates that can be obtained by changing the individual laminae orientations by 5° increments are candidates for the optimization process. We consider RC7 because this program is widely used and because it is representative of the brute-force search technique. The basic question is: because we must carry a certain load, what laminate do we need? We have no idea how many layers are required, much less their orientation, but we must start someplace.

Start with a 'laminate' of only one layer, and place that unidirectional layer or lamina in various orientations at 5° increments. How many orientations are possible? Divide 180° by 5° to get 36 orientations (after a unidirectional lamina has been rotated more than 180°, previous orientations are simply repeated). That is, by the time we have reoriented the unidirectionally reinforced lamina around 180°, the fiber direction of the lamina is in the position where it started. For that single layer, we ask the question: which of those 36 possible orientations has the highest load-carrying capability? To answer that question requires a selection procedure among the various possible laminates to find which is the strongest. That process leads to some angle that we will call α_1. The pertinent design question now is: does the load-carrying capacity represented by one lamina with orientation α_1 meet the load-carrying requirements? If the 'laminate' does not have enough capability (as we surely must suspect), even though the lamina is in its best orientation, then we must add at least one more layer.

When we add the second layer, *we arbitrarily fix the orientation of the first layer at the previously determined* α_1 *to begin the procedure.* We now determine the orientation of the second layer to give the best (i.e., the strongest) response. Let the second layer float around in value at 5° increments in orientation with 36 possible choices until the combination of the new angle with the first layer being fixed in orientation gives the strongest laminate. The resulting laminate is not necessarily the best two-layered laminate. However, the point is that we are revealing the strategy for making changes in all the design variables. That strategy involves a brute-force search approach. We are not using a more direct mathematical optimization approach in which we somehow mathematically find the optimum number of laminae and their orientations. We are helped by a computer in performing many repetitive calculations, but we are overlaying those repetitive calculations with a rather simple strategy for keeping track of the orientations with which we deal. Now that we have examined those 36 possible orientations of layer two and found the strongest combination, we have effectively chosen another laminate that can be specified as $[\alpha_1/\alpha_2]$.

Now, *release the constraint of having the first layer still oriented at* α_1. That constraint must surely seem quite arbitrary and not at all physically reasonable. Also, we must admit that the second layer probably is not in its proper orientation either. Thus, we will allow the two laminae orientations to float from $[\alpha_1/\alpha_2]$ to something else. And we will call that procedure for changing the laminae *lamina reorientation.* There are two stages of lamina reorientation: (1) coarse reorientation and (2) fine reorientation.

In coarse laminae reorientation, we allow the laminae angles to change by 15° increments. That is, α_1 changes to $\alpha_1 + \Delta\alpha$, where $\Delta\alpha$ is 0°, ± 15°, or ± 30°. We will also change α_2 in the same manner. As all those changes are made, the laminate strength is simultaneously evaluated, and, of all those combinations, the laminate that is the strongest is the desired result. That laminate will be called $[\beta_1/\beta_2]$. To determine the new laminate took 5^2 choices. Coarse reorientation is performed a second time with 25 additional choices leading to the best laminate of those choices with specification $[\omega_1/\omega_2]$.

Next, address fine reorientation, where we reconsider the laminate defined as $[\omega_1/\omega_2]$, and let those two angles change by some amount $\Delta\omega$. In fine reorientation, $\Delta\omega$ is 5° increments over a range of 20°, so the angles are changed by 0°, ± 5°, ± 10°. These five $\Delta\omega$ choices per layer lead to another 25 combinations of laminae to examine. The laminate of those laminae that is the strongest is designated as $[\phi_1/\phi_2]$. Do the fine lamina reorientation again, and the result of those additional 25 calculations is the laminate $[\theta_1/\theta_2]$.

During all those laminate calculations, obviously many calculations were repeated. For example, when $\Delta\alpha$ was 0° for the first layer and 0° for the second layer, we already knew the answer, but we did the calculation over again anyway. If the calculation that we perform is very simple, then we would rather perform the calculation over again than to establish strategies for both remembering all the results that we previously calculated and recalling whether we had calculated them before. Our strength calculations turn out to be in that short and simple category. Individual calculations are simple, so it is much easier to recalculate them than to store and remember them. Providing the *storage capacity* for all previous calculations and the *logic* for deciding whether we had ever previously calculated the strength of a particular laminate requires significant additional computer program space and logic, hence time.

This brute-force search strategy is followed as more layers are added because we do not know how many layers we need for the prescribed load. If the load is very high, perhaps we will need 19 layers, and we will work our way up to that laminate by adding one layer at a time and finding the best laminate of that number of laminae.

The lamina coarse and fine reorientations are essential because the process of fixing the fiber direction of one lamina while varying the fiber direction of another lamina introduces an *artificial constraint* on the optimization problem. There is at least one laminate optimization problem for which we know the correct answer (i.e., the correct laminae orientations), and if we had not done the laminae reorientation, we would have gotten the wrong answer for that problem. The test problem for which we know the answer is equal biaxial loading. Loads are applied equally in the x-direction and the y-direction. If we ask for that loading to be carried by a single layer, we know the answer would be an orientation of either +45° or –45° as in Figure 7-52. If we add another layer to the first layer, but fix the orientation of the first layer, then the answer for the orientation of the second layer is either –45° or +45°, respectively. If we stop there, then we know we do not have the right laminate because the correct answer is a laminate with one set of fibers in the x-direction and one set of fibers in the y-direction. If you think about it, the coarse and fine reorientation allows the right answer to appear somewhere within the (large) number of cases we examine. That is, the number of cases is expanded by relaxing the artificial constraint of one or more fixed-direction laminae. We do not calculate the right answer directly, but instead we search in a restricted field. If the restricted field

in which we search does not include the right answer, then we get the answer that is best only in the restricted field, but not the best overall answer. Thus, removing that arbitrary restriction is the motivation for lamina reorientation. Whether two coarse or two fine reorientations are performed, or what angle change is chosen must be resolved by considering some specific laminate problems for which we know the answer. In the process, we must determine whether one approach leads to the answer more rapidly than does another approach and, moreover, that the correct answer is obtained to the equal-biaxial-loading problem (or some other problem for which the optimum solution is known).

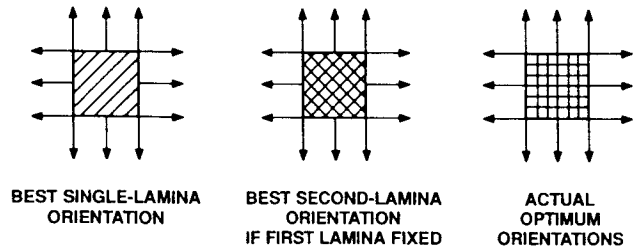

Figure 7-52 Equal Biaxial Loading

For the equal-biaxial-loading example, two coarse reorientations suffice to extend the search field from $\pm 45°$ to 0° and 90°. However, more complicated loadings than equal biaxial loading must be provided for. If, for example, instead of biaxial loading for which $N_x = N_y$, the loading were of the proportion $N_x = 1.1N_y$, then the 15° adjustments of coarse reorientation would obviously not suffice to calculate a laminate optimum to 5° laminae orientations. That is, coarse reorientation is not sensitive enough to enable optimization under general loading. Thus, some form of fine lamina reorientation is essential.

In the laminate selection process, the number of calculations is quite large. For only one layer, no reorientation is needed. We just have those 36 choices, so 36 total laminate strength calculations are made. For a two-layered laminate, two coarse reorientations of the laminae must be performed as well as two fine reorientations. Thus, 100 calculations are added to the 36 for originally orienting that second layer added to the 36 already done for the first lamina, so the total number of calculations for a two-layered laminate is 172 as in Table 7-5. By the time we get to four layers, more than 3000 calculations have been performed, but they are very simple calculations. Those 3244 calculations take about a minute on an IBM 360/65 computer, a very out-of-date mainframe computer. This laminate strength analysis is the kind of calculation that can easily be done now on a personal computer. For n layers, 5^n calculations are necessary. That number is big, so a 10-layered laminate requires a huge number of calculations. But, again, the calculations are trivial, so we do not actually need to calculate for a long time, even on a personal computer.

Table 7-5 Number of Calculations in RC7

NUMBER OF LAYERS	NUMBER OF REORIENTATIONS	TOTAL NUMBER OF CALCULATIONS	CUMULATIVE NUMBER OF CALCULATIONS
1	0	36	36
2	25 x 2 x 2	136	172
3	125 x 2 x 2	536	708
4	625 x 2 x 2	2536	3244
•	•	•	•
•	•	•	•
•	•	•	•
N	5^N x 2 x 2	BIG	BIGGER

One procedure that could be used to speed up the optimization process is to restrict attention to symmetric laminates. Symmetric laminates are often required in order to eliminate warping upon release from a mold after curing. And laminate symmetry is also often required to eliminate bending-extension coupling under mechanical loading (the curing-related coupling involves thermal loading). To retain laminate symmetry, nothing need be done, obviously, for a single layer. Moreover, two-layered laminates must have the same angle in both layers (effectively a single-layered laminate). Only for three-layered laminates do we begin to consider more usual laminates. For three layers, the two outer layers must have the same angle whereas the inner layer can be at any angle (unless shear-extension coupling and/or bend-twist coupling must be avoided). Note that the one-, two-, and three-layered laminates can have shear-extension coupling. For four layers, the two outer layers must have the same angle θ, and the two inner layers must have the same angle β to achieve symmetry (effectively a three-layered laminate with unequal-thickness layers). Moreover, θ must equal $-\beta$ to avoid shear-extension coupling. Perhaps we might be more interested in achieving laminate symmetry than in eliminating shear-extension coupling.

The next program to consider is OPLAM [7-15], which is for the optimization of a laminate. The program was developed by Hadcock et al. for the very special laminate configuration mentioned earlier with only 0°, $\pm 45°$, and 90° laminae, i.e., $[0°_L/90°_M/\pm 45°_N]$. However, different proportions of those laminae would exist than would be necessary to have a quasi-isotropic laminate. The design question is: what are L, M, and N, i.e., the number of 0°, $\pm 45°$, and 90° laminae, respectively? The $\pm 45°$ laminae must occur in pairs to avoid shear-extension coupling. No stiffeners or honeycomb core are addressed in this program. The laminate strength is evaluated with the Tsai-Hill failure criterion under conditions of only in-plane loads, so the analysis is for strictly a membrane stress state. Neither buckling loads nor vibration frequencies are calculated. The point in describing this program is that a *simplified design space* is addressed by not worrying about at what angle each lamina

might be placed, but just how many of these specified-angle laminae are necessary to provide the required load-carrying capability.

Knowledge of fatigue behavior is usually required for any laminate expected to be used in a structure. If the optimum laminate for a structure is quite different from any laminate for which fatigue information is available, then we *must* perform new fatigue tests. However, if the optimum laminate is a member of a family for which we have at least some scattered fatigue information, then we might not be required to obtain fatigue results for a new laminate being considered. For example, suppose we have fatigue information on some of the $[0^\circ_L/90^\circ_M/\pm 45^\circ_N]$ family where L = 7 and L = 11 with M and N the same as our optimum laminate. Moreover, suppose that the behavior of the L = 7 laminate is quite similar to that of the L = 11 laminate. Then, if our optimium laminate turns out to be L = 9, we might not expect to be required to run anything but nominal fatigue tests, if any at all. That is, we might be able to interpolate the already available information. However, if the behavior of the L = 7 laminate were quite different from that of the L = 11 laminate and one of the two laminates were not acceptable, then fatigue data are needed for the optimum laminate with L = 9. The same conclusion follows for L values quite different from L values for available fatigue data.

7.7.3 Invariant Laminate Stiffness Concepts

Invariant stiffness concepts as developed by Tsai and Pagano [7-16 and 7-17] can be used as an aid to understanding the stiffnesses of laminates of arbitrary orientation and how those stiffnesses can be varied. The concepts and their use are discussed in Sections 7.7.3.1 through 7.7.3.3.

7.7.3.1 Invariant Laminate Stiffnesses

The topic of invariant transformed reduced stiffnesses of orthotropic and anisotropic laminae was introduced in Section 2.7. There, the rearrangement of stiffness transformation equations by Tsai and Pagano [7-16 and 7-17] was shown to be quite advantageous. In particular, certain invariant components of the lamina stiffnesses become apparent and are helpful in determining how the lamina stiffnesses change with transformation to non-principal material directions that are essential for a laminate.

The invariant stiffness concepts for a lamina will now be extended to a laminate. All results in this and succeeding subsections on invariant laminate stiffnesses were obtained by Tsai and Pagano [7-16 and 7-17]. The laminate is composed of orthotropic laminae with arbitrary orientations and thicknesses. The stiffnesses of the laminate in the x-y plane can be written in the usual manner as

$$(A_{ij}, B_{ij}, D_{ij}) = \int \bar{Q}_{ij}(1, z, z^2)dz \qquad (7.27)$$

where the $\bar{Q}_{ij}$ are constant in each layer, but vary from layer to layer. The values of the $\bar{Q}_{ij}$ are given in Table 2-2 when U_6 and U_7 are zero. For example,

$$(A_{11}, B_{11}, D_{11}) = \int [U_1 + U_2 \cos 2\theta + U_3 \cos 4\theta](1, z, z^2)\, dz \qquad (7.28)$$

When all orthotropic laminae are of the same material, the constants U_1, U_2, and U_3 can be brought outside the integrals:

$$\begin{aligned}(A_{11}, B_{11}, D_{11}) = U_1\left[t, 0, \frac{t^3}{12}\right] + U_2\int \cos 2\theta\,(1, z, z^2)\, dz \\ + U_3\int \cos 4\theta\,(1, z, z^2)\, dz\end{aligned} \qquad (7.29)$$

The final result is given in Table 7-6 along with the values for all the stiffnesses. There, the $V_{i(A, B, D)}$ are

$$\begin{aligned}V_{0(A, B, D)} &= \left[t, 0, \frac{t^3}{12}\right] \\ V_{1(A, B, D)} &= \int \cos 2\theta\,(1, z, z^2)\, dz \\ V_{2(A, B, D)} &= \int \sin 2\theta\,(1, z, z^2)\, dz \\ V_{3(A, B, D)} &= \int \cos 4\theta\,(1, z, z^2)\, dz \\ V_{4(A, B, D)} &= \int \sin 4\theta\,(1, z, z^2)\, dz\end{aligned} \qquad (7.30)$$

Because each layer is macroscopically homogeneous in its own region of space, the integrals in Equation (7.30) further simplify to summations:

$$\begin{aligned}V_{iA} &= \sum_{k=1}^{N} W_k(z_{k+1} - z_k) \\ V_{iB} &= \frac{1}{2}\sum_{k=1}^{N} W_k(z_{k+1}^2 - z_k^2) \\ V_{iD} &= \frac{1}{3}\sum_{k=1}^{N} W_k(z_{k+1}^3 - z_k^3)\end{aligned} \qquad (7.31)$$

Table 7-6 Laminate Stiffnesses as a Function of Lamina Properties *(After Tsai and Pagano [7-17])*

Stiffnesses	$V_{0(A, B, D)}$	$V_{1(A, B, D)}$	$V_{2(A, B, D)}$	$V_{3(A, B, D)}$	$V_{4(A, B, D)}$
(A_{11}, B_{11}, D_{11})	U_1	U_2	0	U_3	0
(A_{22}, B_{22}, D_{22})	U_1	$-U_2$	0	U_3	0
(A_{12}, B_{12}, D_{12})	U_4	0	0	$-U_3$	0
(A_{66}, B_{66}, D_{66})	U_5	0	0	$-U_3$	0
$2(A_{16}, B_{16}, D_{16})$	0	0	$-U_2$	0	$-2U_3$
$2(A_{26}, B_{26}, D_{26})$	0	0	$-U_2$	0	$2U_3$

in which the z_i are defined in Figure 4-8, N is the number of layers, and

$$W_k = \begin{bmatrix} \cos 2\theta_k, & i = 1 \\ \sin 2\theta_k, & i = 2 \\ \cos 4\theta_k, & i = 3 \\ \sin 4\theta_k, & i = 4 \end{bmatrix} \tag{7.32}$$

wherein θ_k is the orientation of the 1-direction in the k^{th} lamina from the laminate x-axis. The stiffnesses in Table 7-6 are for a laminate with N layers of a single orthotropic material with various laminae principal material property orientations relative to the laminate axes.

The stiffnesses in Table 7-6 are *not* transformed stiffnesses in analogy to Table 2-2. That is, the x-axis of the laminate is fixed relative to the θ_k of each lamina. However, the transformed stiffnesses can be obtained by rotating the entire laminate through angle ϕ, that is, by substituting $(\theta - \phi)$ for θ in Equation (7.29). For example,

$$\bar{A}_{11} = U_1 t + U_2 \int \cos 2(\theta - \phi) dz + U_3 \int \cos 4(\theta - \phi) dz \tag{7.33}$$

Then, by use of the trigonometric identity for subtraction of two angles,

$$\cos(\alpha - \beta) = \cos\alpha \cos\beta + \sin\alpha \sin\beta \tag{7.34}$$

and the fact that ϕ, and hence its trigonometric functions, are independent of z, we see that

$$\bar{A}_{11} = U_1 t + U_2 V_{1A} \cos 2\phi + U_2 V_{2A} \sin 2\phi + U_3 V_{3A} \cos 4\phi + U_3 V_{4A} \sin 4\phi \tag{7.35}$$

where V_{iA} are defined in Equation (7.31). The transformed extensional stiffnesses, $\bar{A}_{ij}$, are given in Table 7-7. The transformed bending-extension coupling stiffnesses, $\bar{B}_{ij}$, and the transformed bending stiffnesses, $\bar{D}_{ij}$, have the same form as in Table 7-7 except the V_{iA} are replaced by V_{iB} and V_{iD}, respectively. The form of the transformation relations for the A_{ij}, B_{ij}, and D_{ij} in Table 7-7 is identical to that for the anisotropic Q_{ij} in Table 2-2. Exercises in which additional points are made about the invariants are given at the end of the subsection.

Table 7-7 Transformation Equations for A_{ij} *(After Tsai and Pagano [7-17])*

Transformed Extensional Stiffness	Constant	cos 2θ	sin 2θ	cos 4θ	sin 4θ
$\bar{A}_{11}$	U_1V_{0A}	U_2V_{1A}	U_2V_{2A}	U_3V_{3A}	U_3V_{4A}
$\bar{A}_{22}$	U_1V_{0A}	$-U_2V_{1A}$	$-U_2V_{2A}$	U_3V_{3A}	U_3V_{4A}
$\bar{A}_{12}$	U_4V_{0A}	0	0	$-U_3V_{3A}$	$-U_3V_{4A}$
$\bar{A}_{66}$	U_5V_{0A}	0	0	$-U_3V_{3A}$	$-U_3V_{4A}$
$2\bar{A}_{16}$	0	U_2V_{2A}	$-U_2V_{1A}$	$2U_3V_{4A}$	$-2U_3V_{3A}$
$2\bar{A}_{26}$	0	U_2V_{2A}	$-U_2V_{1A}$	$-2U_3V_{4A}$	$2U_3V_{3A}$

7.7.3.2 Special Results for Invariant Laminate Stiffnesses

Several special laminates will be examined to help understand the summations $\bar{V}_{i(A,B,D)}$ in Equation (7.31). Recall first from mathematics that

$$\int_{-z}^{+z} (\text{odd function})\, dz = 0 \qquad \int_{-z}^{+z} (\text{even function})\, dz = \text{finite} \tag{7.36}$$

where z is the coordinate perpendicular to the plane of the laminate (in the thickness direction). We will consider laminates with laminae orientations that are (1) odd functions of z, (2) even functions of z, (3) random functions of z, and (4) increments of π/N, where N is the number of equal-thickness layers. Examples of these laminates are shown in Figure 7-53.

First, for laminae orientations with θ_k that are an odd function of z, as illustrated with the 2-layer angle-ply laminate with $\pm\alpha$ orientation in Figure 7-53a, the following integrands in $V_{i(A,B,D)}$, Equation (7.30), are odd:

$$\cos p\theta\,(z) \qquad \sin p\theta\,(1, z^2)$$

and the following integrands are even:

$$\cos p\theta\,(1, z^2) \qquad \sin p\theta\,(z)$$

where p is 2 or 4. Thus, the following summations vanish:

$$V_{2A} = V_{4A} = V_{1B} = V_{3B} = V_{2D} = V_{4D} = 0 \tag{7.37}$$

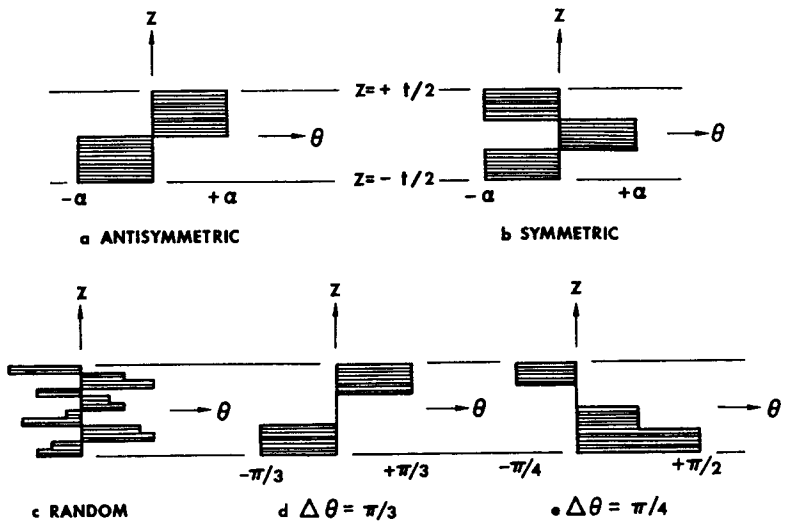

Figure 7-53 Laminate Examples *(After Tsai and Pagano [7-17])*

Accordingly, the following stiffnesses in Table 7-6 are zero:

$$A_{16} = A_{26} = B_{11} = B_{22} = B_{12} = B_{66} = D_{16} = D_{26} = 0 \qquad (7.38)$$

The extensional and bending stiffnesses are those of an orthotropic material, but the bending-extension coupling stiffnesses are not all zero (B_{16} and B_{26} remain).

Next, for laminae orientations with θ_k that are an even function of z (symmetric), as illustrated by the three-layered laminate in Figure 7-53b, the following integrands in $V_{i(A,B,D)}$, Equation (7.30), are odd:

$$\cos p\theta\,(z) \qquad \sin p\theta\,(z)$$

and the following integrands are even

$$\cos p\theta\,(1, z^2) \qquad \sin p\theta\,(1, z^2)$$

Thus, the following summations vanish:

$$V_{1B} = V_{2B} = V_{3B} = V_{4B} = 0 \qquad (7.39)$$

Accordingly, all the bending-extension coupling stiffnesses, B_{ij}, in Table 7-6 vanish. The A_{ij} and D_{ij} are those of an anisotropic material.

If the laminae orientation is a random function of z as in Figure 7-53c, define $\bar{V}_i$ as the spatial average of the individual $V_{i(A,B,D)}$ (they all will be treated alike):

$$\bar{V}_i = \frac{1}{\pi}\int_{-\pi/2}^{\pi/2} V_i\, d\theta = \frac{1}{\pi}\int_{-\pi/2}^{\pi/2}\int_{-t/2}^{t/2}\begin{bmatrix}\cos p\theta \\ \sin p\theta\end{bmatrix}(1, z, z^2)\, dz\, d\theta \qquad (7.40)$$

where p is even. Interchange the order of integration to get

$$\bar{V}_i = \frac{1}{\pi}\int_{-t/2}^{t/2}\int_{-\pi/2}^{\pi/2}\begin{bmatrix}\cos p\theta \\ \sin p\theta\end{bmatrix} d\theta\,(1, z, z^2)\, dz \qquad (7.41)$$

which is zero. When all the $V_{i(A,B,D)}$ are zero, only the constant terms remain in the stiffnesses. Moreover, the laminate is macroscopically isotropic because now

$$A_{11} = A_{22} = U_1 t \qquad A_{12} = U_4 t \qquad A_{66} = U_5 t \qquad A_{16} = A_{26} = 0$$
$$B_{ij} = 0 \qquad D_{ij} = \frac{A_{ij} t^2}{12} \qquad (7.42)$$

and $A_{11} - A_{12} = 2A_{66}$. Although the laminate is macroscopically isotropic, it is still inhomogeneous from layer to layer, so the stress distribution is discontinuous and different from that of a material that is isotropic.

For a laminate of N equal-thickness layers ($N > 2$) with orientation angles differing by π/N as in Figures 7-53d and 7-53e, the summation for V_{1A} is

$$V_{1A} = \left[\cos\frac{2\pi}{N} + \cos\frac{4\pi}{N} + \cdots + \cos 2\pi\right]\frac{t}{N} \qquad (7.43)$$

but

$$\cos x + \cos 2x + \cdots + \cos nx = \frac{\sin\left[n + \frac{1}{2}\right]x}{2\sin\frac{x}{2}} - \frac{1}{2} \qquad (7.44)$$

which for $x = 2\pi/N$ is zero. Also

$$V_{3A} = \left[\sin\frac{2\pi}{N} + \sin\frac{4\pi}{N} + \cdots + \sin 2\pi\right]\frac{t}{N} \qquad (7.45)$$

and

$$\sin x + \sin 2x + \cdots + \sin nx = \frac{\sin\frac{1+n}{2}x\,\sin\frac{n}{2}x}{\sin\frac{x}{2}} \qquad (7.46)$$

which for $x = 2\pi/N$ is zero. Similarly, $V_{2A} = 0$ because the expression in Equation (7.44) vanishes for $x = 4\pi/N$ and, as well, $V_{4A} = 0$. Thus, because the variable terms are zero, the A_{ij} are isotropic and are given in Equation (7.42). However, the B_{ij} are not zero, so the laminates in this class are not isotropic, but are called quasi-isotropic (see Section 4.3). This class of laminates occurs for laminate stacking sequences of $[0/\pm\pi/3]$, $[\pi/2/\pi/4/0/-\pi/4]$, etc. Other more complicated lamination sequences have isotropic B_{ij} or isotropic D_{ij}.

A final result of interest is the integral of the area under the transformed stiffness versus angle of rotation curve from $\phi = 0$ to $\phi = 2\pi$, that is, one complete revolution of the laminate:

$$\int_0^{2\pi} \bar{A}_{ij}\, d\phi \qquad (7.47)$$

The integral

$$\int_0^{2\pi}\begin{bmatrix}\cos p\phi \\ \sin p\phi\end{bmatrix} d\phi \qquad (7.48)$$

is zero when p is an integer, so only the constant terms contribute to Equation (7.33) which is then independent of ϕ. The average values of the integral are the isotropic A_{ij} in Equation (7.42) obtained for randomly oriented laminates and extensionally quasi-isotropic laminates. Those A_{ij} contain U_1, U_4, and U_5, but we showed in Problem 2.7.3 that U_4 is dependent on U_1 and U_5. Thus, U_1 and U_5 appear to be a measure of orthotropic laminates as well as of orthotropic materials. That is, because the integral of $\bar{A}_{ij}$ is constant irrespective of the lamination sequence of laminae orientations, there are constant measures of the laminate, namely U_1 and U_5, which are related to the area under the $\bar{A}_{ij}$ versus ϕ curve. Similarly, the area under the $\bar{B}_{ij}$ versus ϕ curve can be shown to be zero and that under the $\bar{D}_{ij}$ versus ϕ curve is constant. These results will be put to use in the next subsubsection.

7.7.3.3 Use of Invariant Laminate Stiffnesses in Design

Two simple invariants, U_1 and U_5, were shown in the previous subsubsection to be the basic indicators of average laminate stiffnesses. For isotropic materials, these invariants reduce to $U_1 = Q_{11}$ and $U_5 = Q_{66}$, the extensional stiffness and shear stiffness. Accordingly, Tsai and Pagano suggested the orthotopic invariants U_1 and U_5 be called the isotropic stiffness and isotropic shear rigidity, respectively [7-16 and 7-17]. They observed that these 'isotropic properties' are a realistic measure of the minimum stiffness capability of composite laminates. These isotropic properties can be compared directly to properties of isotropic materials as well as to properties of other orthotropic laminates. Obviously, the comparison criterion is more complex than for isotropic materials because now we have two measures, U_1 and U_5, instead of the usual isotropic stiffness U_1 or E. Comparison of values of U_1 alone is not fair because of the degrading influence of the usually low values of U_5 for composite materials.

The optimization or design of a laminate can be performed with the aid of the isotropic stiffnesses. Start with a laminate of unidirectional layers for which $A_{ij} = Q_{ij}t$. If some of the laminae orientations are changed from 0°, then the new values of A_{ij} will be given by the relations of Table 7-6. The actual $\bar{A}_{ij}$ will vary with rotation ϕ in accordance with Table 7-7. However, that variation is always about the isotropic values. For example, variation of $\bar{A}_{11}$ and $\bar{A}_{66}$ with ϕ for boron-epoxy (properties are given in Table 2-3) is shown in Figure 7-54. The unidirectional and isotropic laminate values are both shown in addition to results for two cross-ply and two angle-ply laminates. The areas under all curves in Figure 7-54 are obviously all the same. Thus, if the cross-ply laminate with $M = 1$ and the angle-ply laminate of the same thickness with $\alpha = 45°$ are combined, the resulting laminate is extensionally isotropic (this is the case of the four-layered quasi-isotropic laminate with difference in orientation of 45°). Note, however, even though $\bar{A}_{11}$ and $\bar{A}_{66}$ are constant irrespective of rotation, they are not related in the same manner as true isotropic material properties E and G.

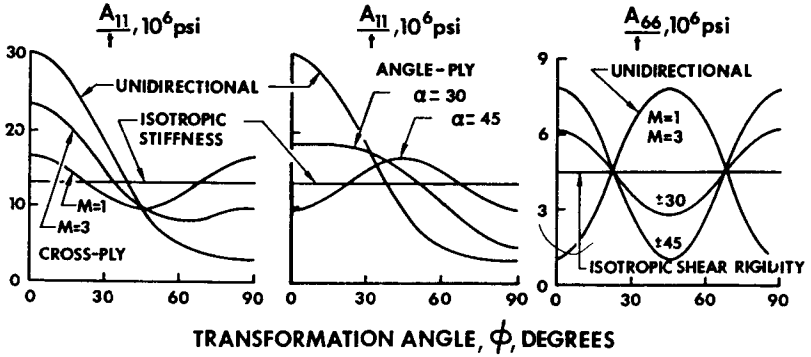

Figure 7-54 Transformed Laminate Stiffnesses *(After Tsai and Pagano [7-17])*

Tsai and Pagano further defined the isotropic stiffness and shear rigidity [7-16] to be

$$U_1 = \bar{E} \qquad U_5 = \bar{G} \tag{7.49}$$

and show for highly orthotropic composite materials such as boron-epoxy and graphite-epoxy that

$$\begin{aligned} \bar{E} &\cong \frac{3}{8}E_1 + \frac{5}{8}E_2 \\ \bar{G} &\cong \frac{1}{8}E_1 + \frac{1}{4}E_2 \end{aligned} \tag{7.50}$$

Thus, the usual emphasis on the value of E_1 is badly misplaced. Obviously, the value of E_2 enters the representative average properties quite strongly. These approximations are quite accurate as can be verified by simple calculations.

Problem Set 7.7.3

7.7.3.1 Show that $\bar{A}_{11} + \bar{A}_{22} + \bar{A}_{12}$ is invariant under rotation about the z-axis, that is, that

$$\bar{A}_{11} + \bar{A}_{22} + 2\bar{A}_{12} = A_{11} + A_{22} + 2A_{12}$$

irrespective of angle of rotation, ϕ. Also, relate this invariant to the reduced stiffness invariant $Q_{11} + Q_{22} + 2Q_{12}$.

7.7.3.2 Show that $A_{66} - A_{12}$ is invariant under rotation about the z-axis, that is, that

$$\bar{A}_{66} - \bar{A}_{12} = A_{66} - A_{12}$$

Also, relate this invariant to the reduced stiffness invariant $Q_{66} - Q_{12}$.

7.7.3.3 What is the value of the bending-extension coupling stiffness invariants $\bar{B}_{11} + \bar{B}_{22} + 2\bar{B}_{12}$ and $\bar{B}_{66} - \bar{B}_{12}$?

7.7.3.4 Relate the bending stiffness invariants $\bar{D}_{11} + \bar{D}_{22} + 2\bar{D}_{12}$ and $\bar{D}_{66} - \bar{D}_{12}$ to the reduced stiffness invariants and the extensional stiffness invariants.

7.7.4 Design of Laminates

The analytical tools to accomplish laminate design are at least twofold. First, the invariant laminate stiffness concepts developed by Tsai and Pagano [7-16 and 7-17] used to vary laminate stiffnesses. Second, structural optimization techniques as described by Schmit [7-12] can be used to provide a decision-making process for variation of laminate design parameters. This duo of techniques is particularly well suited to composite structures design because the simultaneous possibility and necessity to tailor the material to meet structural requirements exists to a degree not seen in isotropic materials.

The key to the design of efficient laminates is to resist both the *magnitude* and the *directional nature* of the loads without overdesign in either respect. That is, the laminate is tailored to *just meet* specific requirements. Structures made of isotropic materials are usually inefficient, i.e., overdesigned because excess strength and stiffness are inevitably available in some direction. By appropriate consideration of the loads and their directions, a laminate can be constructed of individual laminae

in such a manner as to just resist those loads and no more (with, of course, an appropriate factor of safety). For example, a cross-ply laminate can be used to resist loads in the principal directions 1 and 2 where N_1 and M_1 are resisted by A_{11}, A_{12}, D_{11}, and D_{12} and N_2 and M_2 are resisted by A_{12}, A_{22}, D_{12}, and D_{22} if the laminate is symmetric. In more complex situations where shearing forces and twisting moments are applied, angle-ply laminates might be required in order to obtain the necessary shearing and twisting stiffnesses. Other design factors become evident when the strength characteristics of laminates are considered.

Laminate design is a much more complex process than metal plate design. Under a specified loading for a metal plate, the only design variable is the thickness of the plate (unless the plate material is not specified). Even for a simple loading, laminate design involves finding the number of laminae and the orientations of each lamina (even if the material is specified). Thus, many more design variables must be determined for a laminate that for a plate. Moreover, laminate design involves issues of stiffness, strength, and energy absorption (the area under the load-deformation curve) as depicted implicitly in Figure 7-55 along with fatigue life that cannot be depicted. Also depicted is the potentially large number of failure events that occur during laminate loading and influence the suitability of a particular laminate for a specific set of design requirements.

In this section, a generic concept for laminate design will be outlined. That is, the general nature of laminate design and how to alter a laminate to better achieve the design objectives expressed in terms of stiffness, strength, energy absorption, and fatigue life will be addressed. The generic approach is based on obtaining a laminate with a load-deformation curve (or curves) to failure that satisfies the fundamental laminate design requirements expressed in terms of stiffness, strength, energy absorption, and fatigue life. This fourfold requirement is naturally far more complex than the situation for many laminates with simple design requirements. However, we will address this general case to achieve a completeness of overview of the laminate design process.

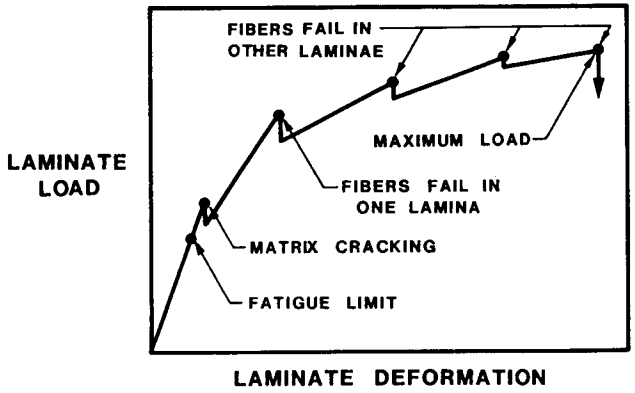

Figure 7-55 Events during Laminate Loading

The nature of laminate behavior can range from very brittle to very ductile. A typical brittle behavior to a particular uniaxial failure load is shown as curve A (laminate A) in Figure 7-56. More ductile behaviors in the sense of larger deformations (and strains) to failure are shown as laminates B, C, and D in Figure 7-56. There, the principal difference between the four behaviors to the same failure load is the amount of energy absorbed. In addition, the initial slope of each load-deflection curve varies. The combination of the highest initial slope and highest energy absorption is laminate B. Laminate C has a significant energy absorption but also a very low first-ply failure load. Thus, under fatigue loading, laminate C would not be a good choice because the operating load must likely be less than the relatively low first-ply failure load. The presence of these different laminate behaviors is an additional complication in design over and above the nature of metal structures. However, the different behaviors also present additional opportunity for latitude in design.

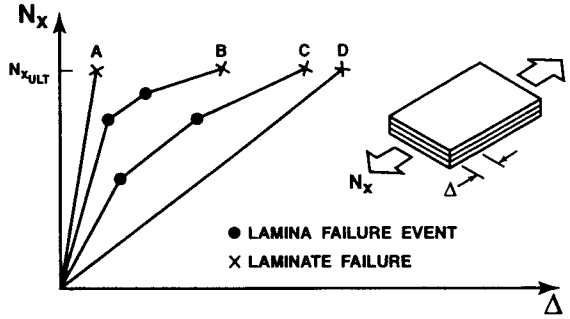

Figure 7-56 Possible Laminate Behaviors

The different laminate behaviors can be changed by changing the laminate stacking sequence. The aspects of behavior that are affected include stiffness, strength, energy absorption, and fatigue life. Discussion of these behavioral aspects is simplified by considering only a simple uniaxial loading N_x as in Figure 7-57 as opposed to a more general

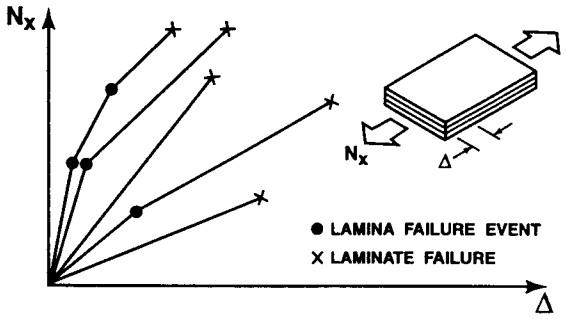

Figure 7-57 Effect of Changing Laminate Stacking Sequence

loading that includes all forces and moments. The stiffness is principally dependent on the stacking sequence, i.e., the individual laminae orientations, with some dependence on the number of layers. The strength is principally dependent on the number of layers, although the stacking sequence is also important. The energy absorption and fatigue life are dependent on both the stacking sequence and the number of laminae. Along with changing those variables, we can change the first-ply failure load.

The laminate design problem is to find a laminate that will meet the design performance goals expressed in terms of strength, stiffness, energy absorption, fatigue life, plus other structural response measures as in Figure 7-58. Those goals are attained by changing the stacking sequence and/or the number of layers to change the laminate behavior until the desired structural response is obtained.

OBJECTIVE: **FIND A LAMINATE THAT WILL MEET THE DESIGN PERFORMANCE GOALS EXPRESSED IN TERMS OF, E.G.,**

- **STRENGTH**
- **STIFFNESS**
- **ENERGY ABSORPTION**
- **FATIGUE LIFE**

APPROACH: **CHANGE THE STACKING SEQUENCE AND/OR THE THICKNESS TO CHANGE THE BEHAVIOR UNTIL THE DESIRED RESPONSE IS OBTAINED**

Figure 7-58 The Laminate Design Problem

That is, the fundamental laminate design problem can be expressed as: given the loading N_x, N_y, and N_{xy}, find the laminate stacking sequence in Figure 7-51. That is, what are the laminae orientations $\theta_1, \theta_2, \theta_3, \ldots$, and how many of each orientation are needed, i.e., what are $n_1, n_2, n_3, \ldots$?

From a practical standpoint, the layers that are added in the process of designing a laminate cannot have purely arbitrary fiber orientation. If the fiber orientations were unlimited, then the design process would sometimes lead to laminates quite unlike any previously built. Thus, the strength, and especially the fatigue life, would not be predictable or known with the necessary confidence. That is, considerable risk is involved in proposing a totally new laminate. Moreover, the cost of evaluating the strength and fatigue life for a new laminate is certainly not trivial. Thus, the addition of layers with often-used fiber orientations keeps design practice in the familiar territory of families of often-used laminates whose characteristics are relatively well-known so we can design with confidence and low cost in money and time.

The manner in which the laminate design is approached can be expressed in flow-chart form as in Figure 7-59. There, some initial laminate is arbitrarily selected to start the procedure. Then, the laminate load-deflection behavior is evaluated by use of the laminate strength analysis procedure described in Section 4.5. That evaluation is theoretical in nature. The next step is to evaluate the laminate fatigue life, and that evaluation can only be done experimentally, although progress is

being made with laminate life-prediction techniques. At this stage, we examine the strength, stiffness, fatigue life, and energy absorption of the candidate laminate. If they are either too high or too low, then we must change the stacking sequence and/or the number of layers until the response meets the required goals.

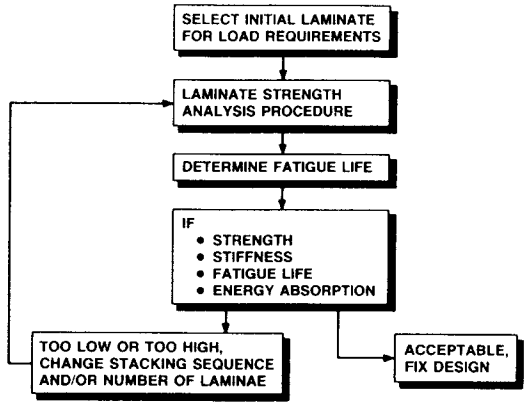

Figure 7-59 Laminate Design Procedure

Under the best of circumstances, the laminate at this iteration of the design process has known fatigue behavior. Under slightly less desirable circumstances, the laminate is close in stacking sequence to laminates with known fatigue behavior. Finally, under awkward, at best, circumstances, the laminate's fatigue behavior is totally unknown. In such a case, that laminate must either (1) be rejected from the design process as being an unknown entity or (2) have its fatigue behavior assessed. Obviously, the first choice is disappointing and the second choice is expensive and time-consuming, unlike the situation for the design of metal structures. The only helpful aspect is the fact that composite structures typically have longer fatigue lives than metal structures.

Let's consider an example to illustrate the foregoing concepts. Suppose the initial laminate choice is $[0°/90°_5]_s$ with the load-deflection behavior as in Figure 7-60. This laminate would appear to be obviously unsuited to the loading because most of the laminae have fibers in the wrong direction. However, we treat this example as being representative of the usual design circumstance in which each structural element is subjected to many different loadings. Some of those loadings are not critical or design-limiting for each structural element. That is, some loadings are easily accepted by the structural element. This laminate would obviously accept more load in the y-direction, but we investigate its capability in the x-direction. The 90° layers fail by cracking parallel to the fibers (perpendicular to the predominant loading). Simultaneously with, or immediately after, matrix cracking in the 90° layers, the 0° layers also fail by cracking parallel to the fibers, as shown by Tsai [7-18] and as summarized in Section 4.5. However, the 0° layers are still capable

of carrying significant load in the x-direction. In fact, the ultimate load is several times the first-ply failure load. Note that this laminate also is capable of carrying significant load in the y-direction, but that issue is not addressed.

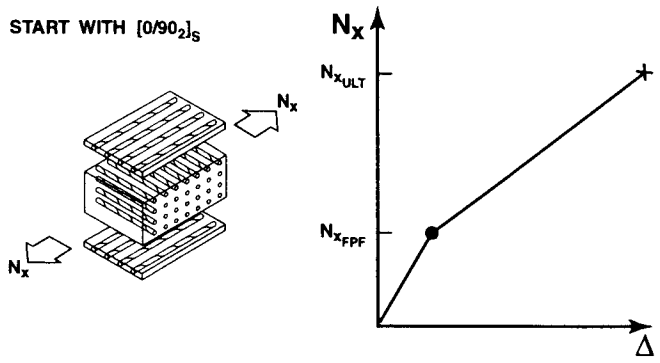

Figure 7-60 Initial Laminate Choice

Suppose we replace the 90° layers with ±α laminae in an attempt to increase the axial stiffness and to increase the first-ply failure load as in Figure 7-61. The load-deflection curve slope after first-ply failure also increases when ±α laminae replace the 90° layers. However, the energy absorption decreases with such a stacking sequence change. The associated fatigue lives are not known unless both laminates are made and subjected to fatigue loading.

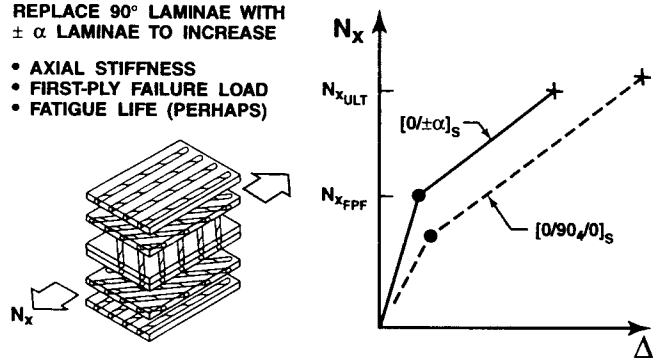

Figure 7-61 Second Laminate Choice

The general laminate design procedure is to continue to change the stacking sequence and/or the number of laminae to obtain required levels of strength, stiffness, fatigue life, and energy absorption. However, we must recognize that the design procedure has a very important limitation—the fatigue life can be determined only by measurement, not by prediction.

A possible adjunct to the laminate design procedure is a specific laminate failure criterion that is based on the maximum strain criterion. In such a criterion, all lamina failure modes are ignored except for fiber failure. That is, matrix cracking is regarded as unimportant. The criterion is exercised by finding the strains in the fiber directions of each layer. When these strains exceed the fiber failure strain in a particular type of layer, then that layer is deemed to have failed. Obviously, more laminae of that fiber orientation are needed to successfully resist the applied load. That is, this criterion allows us to preserve the identity of the failing lamina or laminae so that more laminae of that type (fiber orientation) can be added to the laminate to achieve a positive margin of safety.

The allowable stresses and/or strains in the design process are affected by many factors:

- stress concentrations due to holes
- hot, wet conditions
- notches
- free edges
- required factor of safety

That is, prudent structural design must address the 'what ifs'.

7.7.5 Summary

Some of the essential attributes of the laminate design process with optimization concepts were described in general terms. The process is indeterminate, unlike that for a metal plate. An iterative procedure must be used to guide a design toward satisfaction of the design requirements.

7.8 DESIGN-ANALYSIS PHILOSOPHY FOR COMPOSITE STRUCTURES

7.8.1 Introduction

We have seen in this and other books many complicated analysis methods as well as some involved design methods for composite structures. An immediate reaction might be that those analysis and design methods are overly involved and indeed intimidating. Some of the methods are so complicated, and there are so many behavioral aspects to take into consideration, that we have a difficult time trying to take account of all pertinent factors. We have, though, some very fundamental objectives in structural design. We know that we have some very attractive properties to deal with when we intend to use or consider composite materials for structural applications. We know that if we use those properties correctly, we can build structures which, with composite materials, have lower weight, or higher strength and stiffness, and generally higher performance indexes than with metals. We want to achieve those objectives, yet some significant problem areas or concerns exist. We will address those problem areas one-by-one and offer some recommendations for effective composite structures design. Much of the discussion in this section is patterned after the theme of a very insightful

and inspiring Structures Design Lecture by James E. Ashton at the 1975 AIAA/ASME/SAE Structures, Structural Dynamics, and Materials Conference [7-19].

7.8.2 Problem Areas

The problem areas in composite structures design are related to some of the following observations. One, the behavioral characteristics of composite materials are much more complicated than those of metals. Bending-extension coupling, shear-extension coupling, and bend-twist coupling are all responses that are typically not encountered in a metal structure but are in a composite structure, so you must know how to deal with them. However, that circumstance is a somewhat intimidating situation.

Some of the problem areas mentioned are sometimes overblown by many analysts. That is, they sometimes overemphasize the importance of a particular behavioral characteristic. That characteristic might be important only in one small regime of structural response, and you must know that limitation on the validity of the characteristic. The designer's job, on the other hand, is to either avoid all those problem areas or to in some way overcome them. The situation is somewhat like having a mountain in front of you, and you must get to the other side. You either climb over that mountain, in which case you definitely recognize that it is there and solve the problem, or go around it, in which case you have simply avoided the mountain. In both cases, you must recognize that the mountain exists in order to properly deal with it.

Given that we face some problem areas in the analysis and design of composite structures, we must either avoid them or deal with them directly. Otherwise, the structure is not going to do what we expect. If we do not recognize that bending-extension coupling is a possibility and we do not make certain we avoid it, then we could get a structure with significant bending-extension coupling response and have a wing that behaves entirely wrong for the proposed application.

A general observation about all the various problem areas we could think of is that they do not generally occur or govern all at the same time. In accordance with Murphy's law, if all factors would govern simultaneously, then we would be in bad shape. But they do not.

Let's consider a list of the specific problem areas. Bending-extension coupling was already mentioned. Also, anisotropy is a concern for a laminate, namely shear-extension coupling, and there is also bend-twist coupling. However, I would rather not call those laminate characteristics anisotropy because that word should be reserved for material behavior. Micromechanics can be used to predict the combined performance of the matrix and the fibers. The stress-strain behavior and even the structural behavior could in fact be nonlinear, in which case we must have some form of nonlinear analysis. Various optimization schemes exist as we just discussed in the preceding section. The laminate free-edge effect must be controlled in some laminates. Moreover, the importance of transverse shearing stresses in composite laminates arises at a much higher span-to-thickness ratio than for isotropic plates.

All these problem areas listed in Figure 7-62 are rather perplexing, and we must deal with them.

- **SHEAR-EXTENSION COUPLING AND BEND-TWIST COUPLING**
- **BENDING-EXTENSION COUPLING**
- **MICROMECHANICS**
- **NONLINEAR MATERIAL BEHAVIOR**
- **INTERLAMINAR STRESSES**
- **TRANSVERSE SHEAR STRESSES**
- **LAMINATE OPTIMIZATION**

Figure 7-62 Problem Areas in Analysis and Design

7.8.3 Design Philosophy

One way of perhaps beginning to cope with all those problems is to exercise a rather restrictive design philosophy in which only certain classes of laminates are allowed in design. That is, suppose we restrict the laminate stacking sequences to one of three different categories: $[\pm\theta]_S$, $[\pm\theta/0°]_S$, and $[\pm\theta/0°/90°]_S$. In all three cases, the value of θ ranges between 30° and 60°. What behavioral characteristics do those laminates exhibit? First, they are all symmetric, so we have immediately eliminated bending-extension coupling response. That response does not exist because we have 'designed it away'. Also, by virtue of the fact that we have the same number of $+\theta$ as $-\theta$ layers, no shear-extension coupling exists. That type of laminate we would characterize then as having extensional stiffnesses that are so-called orthotropic. I prefer to simply say that the A_{16} and A_{26} extensional stiffnesses are zero. However, that laminate specification does not mean that bend-twist coupling does not occur. In fact, bend-twist coupling does exist with the only question being the degree or strength of that coupling. That set of laminate specifications is one possible design philosophy. Let's examine the problem areas in composite structures in relationship to that proposed design philosophy.

7.8.4 'Anisotropic' Analysis

The first problem area of the so-called anisotropic analysis will be broken down into two subareas: shear-extension coupling and bend-twist coupling. We have already observed for the most complicated laminate in the design philosophy proposed earlier that the A_{16} and A_{26} stiffnesses are both zero. There is no shear-extension coupling in the context of that philosophy. However, in contemporary composite structures analyses, it is relatively easy to include the treatment of shear-extension coupling, so you should not be overwhelmed by that behavioral aspect or by the calculation of its influence.

Bend-twist coupling is a totally different animal. The governing stiffnesses, D_{16} and D_{26}, simply are never zero for any laminate that is more complicated than a cross-ply laminate. You cannot force those stiffnesses to go to zero unless you do something else to the laminate. You can make them go to zero if you let the laminate be unsymmetric, but that is robbing Peter to pay Paul. In fact, it is not very difficult in most contemporary analyses to include the influence of those bend-twist cou-

pling stiffnesses, so I urge you not to be afraid of them. Another observation is that if some $\pm\theta$ layers exist in a laminate and if the number of pairs of $\pm\theta$ layers is increased, then the bend-twist coupling stiffnesses will tend toward zero as that number of pairs increases. For a more or less general laminate, both the shear-extension coupling phenomenon and the bend-twist coupling phenomenon are negligibly small if a high enough number of those pairs of $+\theta$ and $-\theta$ layers exists in the laminate. That is a general observation, but you can find circumstances where that conclusion might not be true.

7.8.5 Bending-Extension Coupling

We would generally like to avoid bending-extension coupling response in most circumstances because if bending-extension coupling exists, then the laminate warps when it comes out of the hot press or autoclave or whatever curing device is being used. And that situation is generally not desirable. There are circumstances in which that kind of shape change is very desirable, but generally it is not. Grumman created a wing skin with curvature by using an unsymmetric laminate. The number of layers and their stacking sequence were carefully designed to obtain the correct curvature. The usual method of constructing curved wing panels is to drape uncured laminates that have been tape-laid on a flat-bed machine over curved forms for curing.

The effect of the specific values of the B_{ij} can be readily calculated for some simple laminates and can be calculated without significant difficulty for many more complex laminates. The influence of bending-extension coupling can be evaluated by use of the reduced bending stiffness approximation suggested by Ashton [7-20]. If you examine the matrix manipulations for the inversion of the force-strain-curvature and moment-strain-curvature relations (see Section 4.4), you will find a definition that relates to the reduced bending stiffness approximation. You will find that you could use as the bending stiffness of the entire structure,

$$\overline{D} = D - BA^{-1}B \tag{7.51}$$

The significance of the expression for reduced bending stiffness is that whatever bending stiffness exists is effectively smaller by virtue of the presence of the bending-extension coupling. In Equation (7.51), if the bending-extension coupling is zero, then there is no reduction of the effective bending stiffness. And that result can be interpreted very clearly. If bending-extension coupling exists, $BA^{-1}B$ is always positive, and therefore bending stiffness is reduced, you would expect larger bending deflections, lower buckling loads, and lower natural frequencies (see Chapter 5).

Even if you do not use the reduced bending stiffness approximation, there are other ways of evaluating the influence of the bending-extension coupling. They can be, and are, incorporated in many computer analyses. Therefore, bending-extension coupling, if present, should not be a serious stumbling block in a design-analysis situation. However, it is not common in many design situations simply because of the warping that would necessarily take place for a laminate after the curing process.

One overriding observation about bending-extension coupling is very important. Suppose you have a laminate that you could classify as a general laminate, i.e., it is not any one of the very special (and often impractical) laminates that you are accustomed to addressing, such as an antisymmetric cross-ply or an antisymmetric angle-ply laminate. If that laminate is asymmetric, which is implied in the word *general*, the number of layers does not matter — you *can* get a significant amount of bending-extension coupling. I am not saying you *will* get, but you *can* get. You simply cannot guarantee that you will have a small amount of bending-extension coupling simply by having a large number of layers. That coupling can, for any antisymmetric laminates, be shown to die out very rapidly. However, for more general laminates, that bending-extension coupling dies out very slowly (see [7-21] and [7-22] as well as Section 5.6), and therefore it is a factor to be concerned about if, in fact, you do have a general laminate.

7.8.6 Micromechanics

The next problem area of micromechanics is initially very attractive in some respects. We look to the fundamental definition of a composite material made up in this case of, say, a fiber and a matrix and attempt to actually design that material. Let us change the proportions of fibers and matrix so that we get the kind of material behavior characteristics we want. That objective is admirable, but achieving that objective in all cases is not entirely realistic.

The rule of mixtures is a very satisfactory approach to predicting the stiffness behavior of the composite material in the fiber direction. However, the analytical tools for prediction of the behavior transverse to the fiber direction simply do not work out well. The other analyses are not accurate enough to claim that micromechanics is a valid and effective design-analysis tool. Moreover, since the 1960s, we have changed from large-diameter, regular-array composite materials, such as boron-epoxy, when micromechanics was developed to small-diameter, irregular-array composite materials such as graphite-epoxy and Kevlar-epoxy. Thus, we simply cannot even begin to claim that the analyses that we formerly used for boron-epoxy, which were not very good then, are at all applicable to graphite-epoxy.

Not only are the micromechanical analyses not appropriate or effective, but, more importantly, we simply cannot afford to change the properties of a composite material for every structure we want to design. The principal reason for this statement is that we must have a fundamental material property data base on each of those composite materials if we expect to design structures with them. If we change the composite material just a small amount, then we must go through the whole range of characterization tests all over again as a function of sensitivity to moisture, temperature, fatigue, and so on. However, we simply cannot afford to characterize every possible combination of fiber and matrix. Therefore, we must have some restricted number of composite materials that we can afford to characterize, and that restricted number constitutes a set of more or less standard composite materials.

The basic idea of actually designing a material with micromechanics is nice, but the limitations of the analysis are so severe that it simply is not a practical tool, and most designers are really not forced to appeal to micromechanics anyway. You will not likely find anyone who will use micromechanical analysis to predict lamina properties, then use those lamina properties in the design, and finally build a structure based solely on that sequence of events. At some time in the design process, the predicted properties of a lamina *must* be compared with the *measured* properties to verify that those properties are actually achieved. That is, *the only rational basis for design is the real or actual material properties, not the predicted or imaginary properties.* You cannot put enough faith in the micromechanics analysis to give good, dependable results. Most structures designers probably do not design the materials anyway. They will consider certain more or less standard materials, and will pick from among them the best combination for their particular application. For one application, the selected material might be graphite-epoxy with a manufacturer-specified fiber-volume fraction. For another application, it might be Kevlar-epoxy with yet another fiber-volume fraction.

7.8.7 Nonlinear Behavior

Let's address the issue of nonlinear material behavior, i.e., nonlinear stress-strain behavior. Where does this nonlinear material behavior come from? Generally, any of the matrix-dominated properties will exhibit some degree of material nonlinearity because a matrix material is generally a plastic material, such as a resin or even a metal in a metal-matrix composite. For example, in a boron-aluminum composite material, recognize that the aluminum matrix is a metal with an inherently nonlinear stress-strain curve. Thus, the matrix-dominated properties, E_2 and G_{12}, generally have some level of nonlinear stress-strain curve.

On the other hand, for aircraft and spacecraft structures, real laminate behavior is pretty typically linear. Laminate behavior is reasonably linear even with some ±45° layers which you would expect to contribute their nonlinear shear deformation characteristic to the overall laminate and degrade its relative performance. If you go beyond the behavior of a laminate and look at a large structure, typically the load-response characteristics are linear. Even around a cutout, linear behavior exists. Beyond that apparent linear performance of many laminates, you might not like to operate in some kind of a nonlinear response regime. Certainly not when in a fatigue environment and probably not in a creep environment either would you like to operate in a nonlinear behavior range.

As a summary of nonlinear behavior, it appears possible to eliminate the nonlinear behavior, and at the same time, you typically do not want to operate in that nonlinear behavior regime anyway, so you are both able to, and want to, 'design out' nonlinear behavior. That observation is true generally in aircraft structures, but there are other structures, which are subjected to higher temperatures, for which you simply cannot avoid some of the nonlinear behavior aspects, so you must take them into account in any rational design analysis.

7.8.8 Interlaminar Stresses

The next problem area is interlaminar stresses or, actually, stresses near the free edge of a laminate. Early in the development of advanced composite materials, some people felt that a phenomenon called scissoring was the operative mechanism for failure near a free edge. That scissoring can be described on the basis of having two adjacent laminae of $+\theta$ and $-\theta$ orientation, respectively. If those two laminae are subjected independently to an in-plane tension load, they will distort into parallelograms of opposite orientation as in Figure 7-63. Now to prepare to bond those two laminae together, first apply a shear loading around the outsides of those parallelograms in opposite directions. That shear loading will bring the two oppositely oriented parallelograms back to the same size rectangles, so that there is no shear deformation. Suppose that, at this stage, those two rectangles look the same, and we bond them together as a laminate. We now have a laminate with two deformation-compatible laminae, and we have been able to predict the stresses in each of the laminae from classical lamination theory. However, as we look at that laminate in the lower right-hand corner of Figure 7-63, we see some stresses that are implied to be on the edges of that laminate which cannot possibly be there because those are unloaded edges. Therefore, a contradiction exists in the analysis. Basically, the physical accommodation of this deformation mechanism and the imposed boundary condition of no load leads us a stress state near the free edge which causes delamination. The problem is not the overall action like those layers trying to scissor into two oppositely oriented parallelograms. The response does not take place *between* the two layers as they try to move. Instead, the response takes place near the free edges in a very narrow boundary layer.

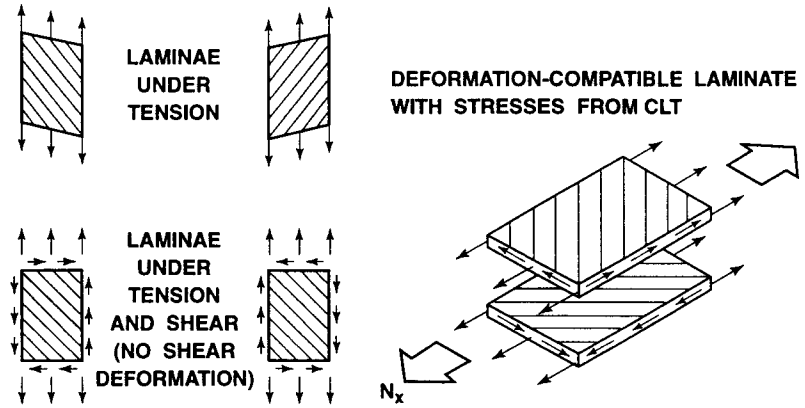

Figure 7-63 Laminate Free-Edge Stress State

Thus, we reject the mechanism of scissoring and try to look near the free edges in the boundary layer to evaluate the stresses. Then, in Section 4.6, we predict very large stresses that in practical situations cause premature static failure and adversely influence the fatigue life of a laminate as well. Our problem is the quantitative prediction of those

stresses. With linear analyses, Pipes and Pagano predicted the stresses to be singular, i.e., infinite at a point which in this case is at the intersection of the layer boundaries with the free edge [7-23]. The stresses cannot, in fact, be singular because the material will simply not support infinite stresses at loads that are infinitesimally small. Real material behavior is affected by local nonlinearities in the matrix material which are not reflected in a linear macroscopic analysis. Thus, the prediction of singular stresses is a basic contradiction, but, that situation aside, the real problem is to try to reduce those stresses in some way.

For a very thick laminate that has adjacent layers at the same orientation, such as a group of $+\theta$ layers in one stacking sequence, the interlaminar stresses build up to unacceptable values. If some $+\theta$ and $-\theta$ layers are alternated, those interlaminar stresses will not build up to as high a magnitude. Both of the laminates have large interlaminar stresses, but one profile of stresses looks better than the other. Thus, basically we will, in order to reduce some of those interlaminar stresses, alternate the various laminae and disperse them among one another so that like-angled laminae are not next to one another. That is, we try to avoid any thick laminae at all, or effectively thick laminae, because they generally cause free-edge stress problems as is discussed in Section 4.6 along with some other solutions to free-edge delamination.

7.8.9 Transverse Shearing Effects

The next problem area is transverse shearing effects. There are some distinct characteristics of composite materials that bear very strongly on this situation because for a composite material the transverse shearing stiffness, i.e., perpendicular to the plane of the fibers, is considerably less than the shear stiffness in the plane of the fibers. There is a shear stiffness for a composite material in a plane that involves one fiber direction. Shear involves two directions always, and one of the directions in the plane is a fiber direction. That shear stiffness is quite a bit bigger than the shear stiffness in a plane which is perpendicular to the axis of the fibers. The shear stiffness in a plane which is perpendicular to the axis of the fibers is matrix-dominated and hardly fiber-influenced. Therefore, that shear stiffness is much closer to that of the matrix material itself (a low value compared to the in-plane shear stiffness).

That low shear stiffness can influence the deformations of the material that we are idealizing as a continuum. Moreover, the shearing stiffness in any of the three principal material planes is considerably less than the fiber-direction Young's modulus. In most bending situations, we would tend to look at the fiber-direction Young's modulus if we didn't know any better and say that that is the governing factor. For a metal, there is only one Young's modulus, and the shearing modulus is approximately four-tenths of that modulus. For a composite material, the largest shearing modulus, which is in the plane of the fibers, is usually about an order of magnitude less than the value of the fiber-direction Young's modulus. That observation means that shear must play a different role, and in fact a more important role, in bending for composite materials than it does for a metal.

Because the shear stiffness is generally so much lower for composite materials than for metals, normals to the middle surface do not remain normal after deformation. That observation means that the fundamental analysis in the form of classical lamination theory, which parallels that of metals, is not as applicable to composite materials as it is to metals. The fundamental conclusion we reach is that the influence of transverse shear on deflections, for example, is important for composite plates that are much slimmer than metal plates. For example, a metal plate might require a span-to-thickness ratio of 10 or more before there is no concern about the influence of shear deformations. However, a composite laminate might require a span-to-thickness ratio of 30 or more before we can stop being concerned about transverse shear effects. That is, we are accustomed to thinking that an isotropic plate really must be very thick before we need ever worry about transverse shearing effects. We must change our way of thinking for composite materials because the geometric boundary between the span-to-thickness ratios for which shear deformations are important and not important has changed. That boundary has gone further out into the range where we would expect to find real structural designs.

The transverse shear problem exists, but what do we do about it? Some rather simple correction factors are available that can be used to adjust the stresses and the deflections obtained from a classical lamination theory analysis. Thus, you need not necessarily perform a precise analysis including transverse shearing effects for every composite laminate that you deal with. There is another issue: typically, a composite laminate is thinner than an equivalent metal element, and that means that you have automatically increased its span-to-thickness ratio. Thus, there is a natural tendency to drive actual composite laminates away from the region of importance of transverse shearing effects. Thus, although we hear about this problem, there are many instances in which we need not worry about it. Correction factors are available, as well as an analysis by Whitney and Pagano [7-24] (see also Chapter 6) for calculation of transverse shearing effects. Moreover, many contemporary composite laminate computer programs include the effect of transverse shear.

7.8.10 Laminate Optimization

For laminate optimization, which we examined in Section 7.7, we have some strong temptations. We could include many design variables. We could talk about which fibers we would deal with out of a collection of those offered by various manufacturers. In addition, we could consider which matrix materials, what percentage of fibers and matrix that we deal with, what orientation of each of the fiber directions, and the thicknesses of the various laminae. All of those various factors are potential design variables, and, in order to treat them, you must have a fairly complicated optimization scheme to be able to achieve the objective of actually tailoring a laminate for specific design requirements.

However, there are some significant problems with using an optimization scheme because you can end up with a design that simply is not practical to make. We might judge that a laminate would need a certain minimum number of layers for various reasons. One of those

reasons might be so that we keep the laminate symmetric. We cannot just simply say we are only going to use two layers, and one is a 0° and the other is a 90° layer, because the resulting laminate is not symmetric. We might then have to increase that laminate in thickness by one layer in order to get away from the asymmetry problem. That situation is quite different from that of a metal. There, typically, a minimum thickness exists for a metal layer, i.e., a minimum amount that can be machined or chem-milled. We will use only the minimum thickness that is available, and if the optimum design turns out to be thinner than that minimum thickness, then we reject the optimum and drop back to the one that is a little thicker because it is easier to make and more suitable in practice.

Various metallic materials are available in specified thicknesses, and composite laminae are available in specified thicknesses. A prepregger is not going to change his whole way of doing business just because you want a layer that is three-quarters as thick as the one which he is accustomed to producing. That change would cost a lot of money. Nor will a prepregger change the volume fraction of fibers just to suit you, unless you have a tremendously big order. Thus, some standardized available elements must be used in any optimization scheme, and that defeats some of the purpose of the optimization. Or at least it somewhat restricts the answers that can be obtained from the optimization scheme.

Probably the most important aspect that leads to the conclusion that the so-called optimum laminate cannot always be used is that, whatever laminate you come up with, you must have some kind of behavior data based on it. Otherwise, people will not let you use it in design for various safety and experience reasons. You must be able to demonstrate that you know the strength and fatigue behavior of the laminate that you want to use in a design. If the optimum laminate turns out to be one that is very different from anything that has ever been produced, then you must embark upon a fairly expensive property-characterization program to qualify that laminate for use in a composite structure. The idea of tailoring the various design variables so that the laminate turns out to be the very best is a nice idea, and it can be beneficial within limits. However, those limits must be dictated to us by the practicality of the various reasons just mentioned.

7.8.11 Summary

As a summary to the design philosophy section, some comments are in order. The properties of composite materials are, in general, enough better than those of an isotropic metal that, if you put your mind to it, you can save weight. If you are creative enough, you can do it. You can make it work. The behavioral aspects of composite materials are indeed more complicated than those of isotropic metals, but they can be modeled in relatively simple ways. That modeling requires some fundamental understanding of the mechanics involved. It is not always necessary to go through some kind of a sophisticated analysis that might involve transverse shear. Instead, you might look at some guidelines for where transverse shear could be important, and if it is not important in your particular application, skip that step. The point is that you must investigate whether a potential problem area is important in order to have a responsible design.

In the design of a composite structure, the job of an analyst is to identify and understand what problem areas might possibly arise (not that they necessarily will, but that they might possibly arise) and to be able to deal with them. Sometimes analysts are more than self-serving in that they try to justify their own work. If they were, for example, working on transverse shear or coupling between bending and extension, they might show you all the cases where those effects are important behavioral phenomena. You must ask the question in a design: is that phenomenon important in my particular design? That is, *you must identify the design drivers for your design.*

A designer, in contrast to an analyst, has one responsibility, and that is to create a structure that meets the design requirements. In doing so, the designer must make certain that all the possible problem areas are either avoided, which is like walking around a mountain, or he must go climb the mountain and deal with each of those problems directly, i.e., take them into account. In order to use either approach, the designer must know quite a bit about the behavior of composite materials and structures. He must know the significance of each of those problem areas, so that he can recognize whether they are, or are not, important in his design. Unless the designer knows the essential behavioral characteristics of a composite material or structure, he cannot possibly design an adequate composite material or structure, but he can design a dangerous one very easily.

7.9 SUMMARY

Two keys to the future use of composite materials are (1) achieving lower raw material cost and (2) developing innovative fabrication techniques that are uniquely suited to the characteristics of composite materials. This duality of approaches is leading to considerable success with composite structures right now, but they also hold the key to the even wider use of composite materials in the future. Let's address the two keys individually.

First, achieving lower raw material cost than at present is always an important economic factor. When the price for one material comes down relative to another, the point at which we trade-off between the two materials changes because cost is a factor in most designs. That statement is not meant to imply that engineers are not concerned about cost in some designs, but we must emphasize that some particular structures have functional requirements as the most important issue. Can they or can they not do the job? Cost is not the primary issue in that case. We would naturally like to have a less-expensive Space Shuttle, but can we do the job that the Space Shuttle is now doing with a lower-cost structure? We could use less-expensive materials, but would they be able to hold up, would they survive reentry, and would the astronauts be able to survive? If the astronauts would not be able to survive, then clearly you would acknowledge that we must pay the added cost to get the job done, i.e., to ensure their safety.

Suppose we change our attention from structures in which the driver is functional consideration alone to something like an automobile where cost is also extremely important. We can get the functional job done with other materials, like steel and aluminum and fiberglass in certain places and unreinforced plastic in others. Then, the question becomes: can we make a material substitution that will enable us to compete with the cost of these other materials to do a job that with all the other materials we cannot accomplish? That is a different kind of question, and then cost becomes an extremely important driver. And, as cost of advanced composite structures goes down, we can expect to see more and more utilization of advanced composite materials.

The second key element of innovative fabrication concepts is extremely important for composite structures because composite materials have unique capabilities of being formed into various parts. One fundamental aspect of those unique characteristics is that with a composite material we tend to build up the structure, actually build up the structural material, in layers as opposed to metal structure fabrication where we often take a big chunk of material and cut it down to the size and shape of the structure as in Figure 7-64. Thus, we are going in two fundamentally opposite directions when we consider metals versus composite materials. Machining away vast portions of a metallic block to achieve a smaller part that is useful or forging a metallic block into some desired shape are both very expensive and time-consuming processes. In contrast, with composite materials, we can build up the same shape with both less usage of materials, in terms of weight or volume, and less manufacturing operations like machining.

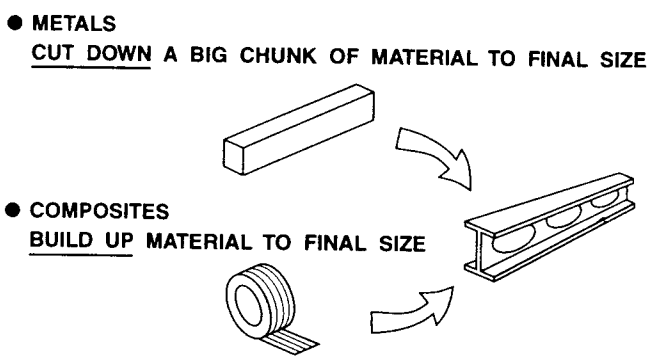

Figure 7-64 Fundamental Fabrication Difference between Composite and Metal Structures

Composite structures fabrication requires levels and types of expertise for layup and curing that are not typically found in metals fabrication industries. Therefore, a composite structure is more of a specialist-produced structure than is a metallic structure. Layup is a totally different process that is absolutely foreign to metals production technologists. We must somehow get those people into the mainstream of composite structures manufacturing before we will see widespread composite structures production.

This process of conversion from a metals production environment to a composite materials production environment is much more involved than just laminate layup and curing. Issues of inspection arise to make certain that the composite product is put together properly. Some of those inspection techniques are much more complicated than they were for a metallic structure. Truly, the picture is not totally rosy for composite materials. It would be quite unrealistic to say: (1) there are no problems and (2) composite materials are absolutely the best way to go.

Composite materials are now used primarily in so-called high-tech areas. Then, in regard to keys to the future of composites, when will we go beyond high-tech applications and go to low-tech applications? When will we build a composite washing machine? Maybe never; perhaps a favorable manufacturing trade-off will never be there; it certainly is not there right now. The key as to whether consumer products will be made of composite materials relates to manufacturing technologies. More and more people will manufacture composite structures simply because they are able to, for their particular structure, put together all the operations that must be performed for a composite structure, which may in fact not have any analog for a metal structure.

When the manufacturing folks can put all those operations together, they will be in the composite structures business, and that will be a dramatically expanding situation for a long time to come. We have already seen it in aircraft and spacecraft. We see it developing now for ships and submarines. We have seen it in golf clubs and tennis rackets. Competitive sports are a very special situation: a golfer typically wants to have an edge either on his previous scores or on his competitors, and he will pay quite a price to gain that edge. That a composite tennis racket might cost twice as much as a wooden tennis racket is not a concern. Golfers or tennis players would gladly pay twice as much for their golf clubs or their tennis rackets if in fact they thought they would get that edge over their competitor that they felt that they needed to have.

We just cannot expect situations like golf clubs and tennis rackets for all consumer products because all products do not have those same built-in characteristics of the competitive edge. When we consider a car, we must be realistic and acknowledge that the car must have a price low enough for people to afford. Think back to the days of Henry Ford: he made a car that could be sold for about $250, so that everyone could afford to have one. This affordability was the real beauty of his mass-production techniques. Everyone could afford to have a car, and then almost everyone did have one. In contrast, before Henry Ford, only the rich could afford an automobile. As soon as we get to the trade-off where composite materials will effectively compete in the automotive market place, we will see tremendously broader applications, but there are problems along the way. The manufacturing cost must be improved in order for those applications to ever come about.

REFERENCES

7-1 George Lubin (Editor), *Handbook of Composites*, Van Nostrand Reinhold, New York, 1982.

7-2 Mel M. Schwartz (Editor), *Composite Materials Handbook*, McGraw-Hill, New York, 1984.

7-3 Michael F. Card and Robert M. Jones, *Experimental and Theoretical Results for Buckling of Eccentrically Stiffened Cylinders*, NASA Technical Note TN D-3639, October 1966.

7-4 Bryan R. Noton, Integrated Computer-Aided Manufacturing Cost/Design Guides for Airframes and Electronics, Battelle's Columbus Laboratories, Columbus, Ohio, undated.

7-5 *DoD-NASA Advanced Composites Design Guide*, Air Force Wright Aeronautical Laboratories, Wright-Patterson AFB, Ohio, July 1983.

7-6 *Plastics for Aerospace Vehicles, Part 1, Reinforced Plastics*, Military Handbook MILHDBK-17A, January 1971.

7-7 M. Goland and E. Reissner, The Stresses in Cemented Joints, *Journal of Applied Mechanics*, March 1944, pp. A-17–A-27.

7-8 K. R. Berg, Problems in the Design of Joints and Attachments, in *Mechanics of Composite Materials, Proceedings of the 5th Symposium on Naval Structural Mechanics*, F. W. Wendt, H. Liebowitz, and N. Perrone (Editors), Philadelphia, Pennsylvania, 8–10 May 1967, Pergamon, New York, 1970, pp. 457–479.

7-9 L. J. Hart-Smith, Design of Adhesively Bonded Joints, in *Joining Fibre-Reinforced Plastics*, F. L. Mathews (Editor), Elsevier Applied Science, London and New York, 1987, pp. 271–311.

7-10 L. J. Hart-Smith, Design and Empirical Analysis of Bolted or Riveted Joints, in *Joining Fibre-Reinforced Plastics*, F. L. Mathews (Editor), Elsevier Applied Science, London and New York, 1987, pp. 227–269.

7-11 F. L. Mathews (Editor), *Joining Fibre-Reinforced Plastics*, Elsevier Applied Science, London and New York, 1987.

7-12 Lucien A. Schmit, The Structural Synthesis Concept and Its Potential Role in Design with Composites, in *Mechanics of Composite Materials, Proceedings of the 5th Symposium on Naval Structural Mechanics*, F. W. Wendt, H. Liebowitz, and N. Perrone (Editors), Philadelphia, Pennsylvania, 8–10 May 1967, Pergamon, New York, 1970, pp. 553–582.

7-13 Stephen W. Tsai, *Composites Design 1986*, Think Composites, Dayton, Ohio, 1986.

7-14 M. E. Waddoups, L. A. McCullers, F. O. Olsen, and J. E. Ashton, Structural Synthesis of Anisotropic Plates, presented at the AIAA/ASME 11th Structures, Structural Dynamics, and Materials Conference, Denver, Colorado, April 1970. (not in the Proceedings)

7-15 R. N. Hadcock, et al., *Preliminary Analysis and Optimization Methods*, Grumman Aerospace Corp., Contract F33615-68-C-1301, Air Force Materials Laboratory, Wright-Patterson AFB, Ohio, August 1968.

7-16 Stephen W. Tsai and Nicholas J. Pagano, Invariant Properties of Composite Materials, in *Composite Materials Workshop*, S. W. Tsai, J. C. Halpin, and Nicholas J. Pagano (Editors), St. Louis, Missouri, 13–21 July 1967, Technomic, Stamford, Connecticut, 1968, pp. 233–253.

7-17 Stephen W. Tsai and Nicholas J. Pagano, Invariant Properties of Composite Materials, AFML-TR-67-379, March 1968.

7-18 Stephen W. Tsai, *Strength Characteristics of Composite Materials*, NASA CR-224, April 1965.

7-19 James E. Ashton, Analysis and Design Methods for Composite Structures: ... Overly Intimidating!, Structures, Structural Dynamics, and Materials Lecture, AIAA/ASME/SAE 16th Structures, Structural Dynamics, and Materials Conference, Denver, Colorado, 27–29 May 1975. (not in the Proceedings).

7-20 J. E. Ashton, Approximate Solutions for Unsymmetrically Laminated Plates, *Journal of Composite Materials*, January 1969, pp. 189–191.

7-21 Robert M. Jones, Buckling and Vibration of Unsymmetrically Laminated Cross-Ply Rectangular Plates, *AIAA Journal*, December 1973, pp. 1626–1632.

7-22 Robert M. Jones and Harold S. Morgan, Deflection of Unsymmetrically Laminated Cross-Ply Rectangular Plates, in *Proceedings of the 12th Annual Meeting of the Society of Engineering Science*, 20–22 October 1975, Austin, Texas, pp. 155–167.

7-23 R. Byron Pipes and N. J. Pagano, Interlaminar Stresses in Composite Laminates Under Uniform Axial Extension, *Journal of Composite Materials*, October 1970, pp. 538–548.

7-24 James M. Whitney and Nicholas Pagano, Shear Deformation in Heterogeneous Anisotropic Plates, *Journal of Applied Mechanics*, December 1970, pp. 1031–1036.

Appendix A

MATRICES AND TENSORS

Matrix and tensor notation is useful when dealing with systems of equations. Matrix theory is a straightforward set of operations for linear algebra and is covered in Section A.1. Tensor notation, treated in Section A.2, is a classification scheme in which the complexity ranges upward from scalars (zero-order tensors) and vectors (first-order tensors) through second-order tensors and beyond.

The mathematical operations in the study of mechanics of composite materials are strongly dependent on use of matrix theory. Tensor theory is often a convenient tool, although such formal notation can be avoided without great loss. However, some of the properties of composite materials are more readily apparent and appreciated if the reader is conversant with tensor theory.

A.1 MATRIX ALGEBRA

A.1.1 Matrix Definitions

A *matrix* is a rectangular array of elements. The array has m rows and n columns and is called a rectangular matrix of order (m,n). If m = n, the array is called a *square matrix* of order n. The elements of an array [A] are called A_{ij}, that is, the element in the i^{th} row and j^{th} column of [A]. Thus, a matrix is an array:

$$[A] = \begin{bmatrix} A_{11} & A_{12} & \cdots & A_{1n} \\ A_{21} & A_{22} & \cdots & A_{2n} \\ \cdot & \cdot & & \cdot \\ \cdot & \cdot & & \cdot \\ \cdot & \cdot & & \cdot \\ A_{m1} & A_{m2} & \cdots & A_{mn} \end{bmatrix} \tag{A.1}$$

Two arrays [A] and [B] are equal only if they have the same number of rows and columns and all their corresponding elements are equal, that is,

$$A_{ij} = B_{ij} \qquad i = 1,m \qquad j = 1,n \tag{A.2}$$

A *row matrix* consists of a single row and has order (1,n):

$$[A] = [A_1 A_2 \ldots A_n] \tag{A.3}$$

A *column matrix* has a single column and has order (n,1):

$$[A] = \{A\} = \begin{bmatrix} A_1 \\ A_2 \\ \vdots \\ A_n \end{bmatrix} \tag{A.4}$$

where the braces are ordinarily used to distinguish a column matrix from a general matrix (although not in this book).

The *transpose* of a matrix is denoted by a superscript T:

$$[A]^T = \begin{bmatrix} A_{11} & A_{21} & \cdots & A_{m1} \\ A_{12} & A_{22} & \cdots & A_{m2} \\ \vdots & \vdots & & \vdots \\ A_{1n} & A_{2n} & \cdots & A_{mn} \end{bmatrix} \tag{A.5}$$

and is obtained by interchanging rows and columns of Equation (A.1).

For a square matrix, the *principal or main diagonal* goes from the upper left-hand corner to the lower right-hand corner of the matrix. Thus, the principal diagonal has elements A_{ii}. A *symmetric (square) matrix* has elements that are symmetric about the principal diagonal, that is

$$A_{ij} = A_{ji} \tag{A.6}$$

Another way of saying the same thing is $[A] = [A]^T$.

A *diagonal matrix* is a square matrix with zero elements everywhere except on the principal diagonal (that is, all off-diagonal elements are zero):

$$\begin{bmatrix} A_{11} & 0 & \ldots & 0 \\ 0 & A_{22} & \ldots & 0 \\ \vdots & \vdots & & \vdots \\ 0 & 0 & \ldots & A_{mn} \end{bmatrix} \tag{A.7}$$

If all the elements along the principal diagonal of a diagonal matrix are equal, the matrix is called a *scalar matrix*. One important scalar matrix has all ones on the principal diagonal and is called the *identity or unit matrix*:

$$[I] = \begin{bmatrix} 1 & 0 & \ldots & 0 \\ 0 & 1 & \ldots & 0 \\ \vdots & \vdots & & \vdots \\ 0 & 0 & \ldots & 1 \end{bmatrix} \tag{A.8}$$

The *determinant* of a square matrix of order two is called a determinant of order two and is defined as

$$D = \begin{vmatrix} A_{11} & A_{12} \\ A_{21} & A_{22} \end{vmatrix} = A_{11}A_{22} - A_{12}A_{21} \tag{A.9}$$

whereas for a determinant of order three,

$$D = \begin{vmatrix} A_{11} & A_{12} & A_{13} \\ A_{21} & A_{22} & A_{23} \\ A_{31} & A_{32} & A_{33} \end{vmatrix} = A_{11}\begin{vmatrix} A_{22} & A_{23} \\ A_{32} & A_{33} \end{vmatrix} - A_{12}\begin{vmatrix} A_{21} & A_{23} \\ A_{31} & A_{33} \end{vmatrix} + A_{13}\begin{vmatrix} A_{21} & A_{22} \\ A_{31} & A_{32} \end{vmatrix} \tag{A.10}$$

and, by mathematical induction, for a determinant of order n, if M_{1i} is the determinant of order n – 1 formed by deleting the first row and i^{th} column of D,

$$D = \begin{vmatrix} A_{11} & A_{12} & \cdots & A_{1n} \\ A_{21} & A_{22} & \cdots & A_{2n} \\ \vdots & \vdots & & \vdots \\ A_{n1} & A_{n2} & \cdots & A_{nn} \end{vmatrix} = A_{11}M_{11} - A_{12}M_{12} + \cdots + (-1)^{1+n}A_{1n}M_{1n} \tag{A.11}$$

That is, a determinant of order n is obviously defined in terms of determinants of order n – 1. In Equation (A.11), the determinant M_{1i} is called the *minor* of element A_{1i}, and the quantity $(-1)^{1+i}M_{1i}$ is called the *cofactor* of A_{1i}, i.e.,

$$a_{ij} = (-1)^{i+j}M_{ij} \tag{A.12}$$

A determinant can be evaluated by expansion along any row or column, i.e.,

$$D = \sum_{i=1}^{n} A_{ij}a_{ij} = \sum_{j=1}^{n} A_{ij}a_{ij} \tag{A.13}$$

where the free index is not summed.

Some elementary properties of determinants include:

(a) If each element in a row or column is multiplied by k, the determinant is multiplied by k.
(b) If two rows or two columns are proportional, the determinant is zero.

(c) If two rows or two columns are interchanged, the determinant changes sign.
(d) If rows and columns are interchanged, the determinant is not changed.

The *cofactor matrix* of a square matrix is the matrix of cofactors of each element, i.e.,

$$a = \begin{bmatrix} a_{11} & a_{12} & \cdots & a_{1n} \\ a_{21} & a_{22} & \cdots & a_{2n} \\ \cdot & \cdot & & \cdot \\ \cdot & \cdot & & \cdot \\ \cdot & \cdot & & \cdot \\ a_{n1} & a_{n2} & \cdots & a_{nn} \end{bmatrix} \tag{A.14}$$

A.1.2 Matrix Operations

Addition

Two matrices, [A] and [B], can be added only if they have the same number of rows and columns, respectively. Then, the sum [C] is obtained by adding the corresponding elements of [A] and [B]:

$$C_{ij} = A_{ij} + B_{ij} \tag{A.15}$$

For example,

$$\begin{bmatrix} C_{11} & C_{12} \\ C_{21} & C_{22} \end{bmatrix} = \begin{bmatrix} A_{11} & A_{12} \\ A_{21} & A_{22} \end{bmatrix} + \begin{bmatrix} B_{11} & B_{12} \\ B_{21} & B_{22} \end{bmatrix} = \begin{bmatrix} A_{11}+B_{11} & A_{12}+B_{12} \\ A_{21}+B_{21} & A_{22}+B_{22} \end{bmatrix} \tag{A.16}$$

Obviously, addition is both commutative, that is,

$$[A] + [B] = [B] + [A] \tag{A.17}$$

and associative, that is,

$$[[A] + [B]] + [C] = [A] + [[B] + [C]] \tag{A.18}$$

Subtraction

The difference of two matrices is obtained by subtraction of the corresponding elements of [A] and [B]:

$$C_{ij} = A_{ij} - B_{ij} \tag{A.19}$$

and is subject to the requirement that the number of rows and columns be the same for [A] and [B]. Subtraction is neither commutative nor associative.

Multiplication

The simplest form of matrix multiplication is the product of a scalar, s, and a matrix, [A], wherein all elements of [A] are multiplied by s:

$$s\,[A] = s\begin{bmatrix} A_{11} & A_{12} \\ A_{21} & A_{22} \end{bmatrix} = \begin{bmatrix} sA_{11} & sA_{12} \\ sA_{21} & sA_{22} \end{bmatrix} \tag{A.20}$$

The product, [A][B], of two matrices is defined only when the number of rows in [B] equals the number of columns in [A]. Here, [B] is said to be premultiplied by [A] or, alternatively, [A] is said to be postmultiplied by [B]. The product, [A][B], is obtained by first multiplying each element of the i^{th} row of [A] by the corresponding element of the j^{th} column of [B] and then adding those results:

$$[C] = [A][B] = [A_{ik}B_{kj}] \tag{A.21}$$

where the summation on k goes from 1 to the number of columns in [A]. For example,

$$\begin{bmatrix} A_{11} & A_{12} & A_{13} \\ A_{21} & A_{22} & A_{23} \\ A_{31} & A_{32} & A_{33} \end{bmatrix} \begin{bmatrix} B_{11} \\ B_{21} \\ B_{31} \end{bmatrix} = \begin{bmatrix} A_{11}B_{11}+A_{12}B_{21}+A_{13}B_{31} \\ A_{21}B_{11}+A_{22}B_{21}+A_{23}B_{31} \\ A_{31}B_{11}+A_{32}B_{21}+A_{33}B_{31} \end{bmatrix} = \begin{bmatrix} C_{11} \\ C_{21} \\ C_{31} \end{bmatrix} \tag{A.22}$$

For a more complicated [B] matrix that has, say, n columns whereas [A] has m rows (remember [A] must have p columns and [B] must have p rows), the [C] matrix will have m rows and n columns. That is, the multiplication in Equations (A.21) and (A.22) is repeated as many times as there are columns in [B]. Note that, although the product [A][B] can be found as in Equation (A.21), the product [B][A] is not simultaneously defined unless [B] and [A] have the same number of rows and columns. Thus, [A] cannot be premultiplied by [B] if [A][B] is defined unless [B] and [A] are square. Moreover, even if both [A][B] and [B][A] are defined, there is no guarantee that [A][B] = [B][A]. That is, matrix multiplication is not necessarily commutative.

Inversion

The *inverse* of a square matrix is denoted by a superscript –1 and is defined as

$$[A]^{-1} = \frac{[a]^T}{|A|} \tag{A.23}$$

(the transpose of the cofactor matrix is called the *adjoint matrix*) and has the property

$$[A][A]^{-1} = [A]^{-1}[A] = [I] \tag{A.24}$$

The determinant of [A] in Equation (A.23) cannot vanish; otherwise Equation (A.23) is not defined and [A] is said to be a *singular matrix.*

Solution of Linear Equations

The principal use of the inverse matrix is in solution of linear equations or the application of transformations. If

$$\{Y\} = [A]\{X\} \tag{A.25}$$

where {Y} and {X} are column matrices, then

$$[A]^{-1}\{Y\} = [A]^{-1}[A]\{X\} = \{X\} \tag{A.26}$$

The foregoing result along with Equation (A.23) is known as Cramer's rule. If {Y} in Equation (A.25) is zero, then the system of equations

$$[A]\{X\} = 0 \tag{A.27}$$

is said to be *homogeneous*. If matrix [A] is nonsingular (so its inverse $[A]^{-1}$ exists), then

$$\{X\} = [A]^{-1}\{0\} = \{0\} \tag{A.28}$$

This solution for {X} in which all the unknowns are zero is called the *trivial solution*. A nontrivial solution to Equation (A.27) exists, therefore, only when matrix [A] is singular, that is, when $|A| = 0$.

Miscellaneous

Some other matrix operations of interest include

$$\left[[A]^{-1}\right]^{T} = \left[[A]^{T}\right]^{-1} \tag{A.29}$$

that is, the transpose of the inverse of a matrix is equal to the inverse of the transpose. Also,

$$([A][B][C])^{T} = [C]^{T}[B]^{T}[A]^{T} \tag{A.30}$$

$$([A][B][C])^{-1} = [C]^{-1}[B]^{-1}[A]^{-1} \tag{A.31}$$

which are known as the *reversal laws* of transposition and inversion, respectively.

A.2 TENSORS

Vectors are commonly used for description of many physical quantities such as force, displacement, velocity, etc. However, vectors alone are not sufficient to represent all physical quantities of interest. For example, stress, strain, and the stress-strain laws cannot be represented by vectors, but can be represented with tensors. Tensors are an especially useful generalization of vectors. The key feature of tensors is that they *transform*, on rotation of coordinates, in special manners. Tsai [A-1] gives a complete treatment of the tensor theory useful in composite materials analysis. What follows are the essential fundamentals.

Cartesian tensors, i.e., tensors in a Cartesian coordinate system, will be discussed. Three independent quantities are required to describe the position of a point in Cartesian coordinates. This set of quantities is x_i where x_i is (x_1, x_2, x_3). The index i in x_i has values 1, 2, and 3 because of the three coordinates in three-dimensional space. The indices i and j in a_{ij} mean, therefore, that a_{ij} has nine components. Similarly, b_{ijk} has 27 components, c_{ijkl} has 81 components, etc. The indices are part of what is called *index notation*. The number of subscripts on the symbol denotes the *order* of the tensor. For example, a is a zero-order tensor

(a scalar), a_i a first-order tensor (vector), a_{ij} a second-order tensor, a_{ijkl} a fourth-order tensor, etc. The number of components, N, necessary for description of a tensor of order k in n-dimensional space is

$$N = n^{k} \tag{A.32}$$

The range convention and the summation convention will be used. The *range convention* is any subscript that appears only once on one side of an expression takes on values 1, 2, and 3. The *summation convention* is any subscript that appears twice on one side of an expression is summed from 1 to 3. The repeated index is called the *dummy index*.

A.2.1 Transformation of Coordinates

Consider the behavior of various tensors under the transformation of coordinates in Figure A-1 where a rotation about the z-axis is made. That is, the x, y, z coordinates are transformed to the x', y', z' coordinates where the z-direction coincides with the z'-direction. The *direction cosines* for this transformation are

$$[\alpha_{ij}] = [T] = \begin{bmatrix} \cos\theta & \sin\theta & 0 \\ -\sin\theta & \cos\theta & 0 \\ 0 & 0 & 1 \end{bmatrix} \tag{A.33}$$

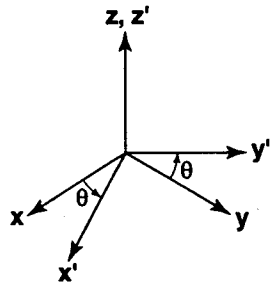

Figure A-1 Rotation of Coordinates in x-y Plane

where α_{ij} is the cosine of the angle between the i^{th} direction in the x', y', z' systems and the j^{th} direction in the x, y, z system, that is, for all transformations (not just the foregoing special rotation),

$$\alpha_{ij} = \cos(x_j', x_j) \tag{A.34}$$

Thus, the transformation of coordinates can be written in index notation as

$$x_i' = \alpha_{ij}x_j \tag{A.35}$$

or

$$\begin{aligned} x_1' &= \alpha_{11}x_1 + \alpha_{12}x_2 + \alpha_{13}x_3 \\ x_2' &= \alpha_{21}x_1 + \alpha_{22}x_2 + \alpha_{23}x_3 \\ x_3' &= \alpha_{31}x_1 + \alpha_{32}x_2 + \alpha_{33}x_3 \end{aligned} \tag{A.36}$$

or in matrix form as

$$\begin{bmatrix} x_1' \\ x_2' \\ x_3' \end{bmatrix} = \begin{bmatrix} \alpha_{11} & \alpha_{12} & \alpha_{13} \\ \alpha_{21} & \alpha_{22} & \alpha_{23} \\ \alpha_{31} & \alpha_{32} & \alpha_{33} \end{bmatrix} \begin{bmatrix} x_1 \\ x_2 \\ x_3 \end{bmatrix} \tag{A.37}$$

This type of transformation will be used to assist in the definition of various orders of tensors. Each tensor will be defined on the basis of the type of transformation it satisfies. Tensors transform according to the relations

$$x'_{ij\ldots kl} = \alpha_{im}\alpha_{jn}\cdots\alpha_{ko}\alpha_{lp}x_{mn\ldots op} \tag{A.38}$$

A.2.2 Definition of Various Tensor Orders

A *scalar* is a tensor of order zero and has $3^0 = 1$ component. Because it has only magnitude and not direction, no transformation relations are needed. Examples of scalars include speed (but not velocity), work, and energy.

A *vector* is a tensor of first order and has $3^1 = 3$ components. Vectors transform according to

$$A_i' = \alpha_{ij}A_j \tag{A.39}$$

where A_i' is the transformed vector, α_{ij} the direction cosines of the transformation, and A_j the original vector. Examples of vectors include displacements, coordinates, velocity, forces, and moments.

A *tensor of second order* has $3^2 = 9$ components and transforms as

$$A_{ij}' = \alpha_{ik}\alpha_{jl}A_{kl} \tag{A.40}$$

Stress and strain are both second-order tensors.

A *tensor of fourth order* has $3^4 = 81$ components and transforms as

$$A_{ijkl}' = \alpha_{im}\alpha_{jn}\alpha_{ko}\alpha_{lp}A_{mnop} \tag{A.41}$$

The stiffness and compliances in stress-strain and strain-stress relations are fourth-order tensors because they relate two second-order tensors:

$$\sigma_{ij} = C_{ijkl}\,\varepsilon_{kl} \tag{A.42}$$

$$\varepsilon_{ij} = S_{ijkl}\,\sigma_{kl} \tag{A.43}$$

A.2.3 Contracted Notation

Contracted notation is a rearrangement of terms such that the number of indices is reduced although their range increases. For second-order tensors, the number of indices is reduced from 2 to 1 and the range increased from 3 to 9. The stresses and strains, for example, are contracted as in Table A-1. Similarly, the fourth-order tensors for stiffnesses and compliances in Equations (A.42) and (A.43) have 2 instead of 4 free indices with a new range of 9. The number of components remains $81 (3^4 = 9^2)$.

Table A-1 Tensor versus Contracted Notation for Stresses and Strains

Stresses		Strains	
Tensor Notation	Contracted Notation	Tensor Notation	Contracted Notation
σ_{11}	σ_1	ε_{11}	ε_1
σ_{22}	σ_2	ε_{22}	ε_2
σ_{33}	σ_3	ε_{33}	ε_3
$\sigma_{23} = \tau_{32}$	σ_4	$2\varepsilon_{23} = \gamma_{23}$	ε_4
$\sigma_{31} = \tau_{31}$	σ_5	$2\varepsilon_{31} = \gamma_{31}$	ε_5
$\sigma_{12} = \tau_{12}$	σ_6	$2\varepsilon_{12} = \gamma_{12}$	ε_6
$\sigma_{32} = \tau_{32}$	σ_7	$2\varepsilon_{32} = \gamma_{32}$	ε_7
$\sigma_{13} = \tau_{13}$	σ_8	$2\varepsilon_{13} = \gamma_{13}$	ε_8
$\sigma_{21} = \tau_{21}$	σ_9	$2\varepsilon_{21} = \gamma_{21}$	ε_9

In contracted notation, the stress-strain and strain-stress relations, Equations (A.42) and (A.43), are written as

$$\sigma_i = C_{ij}\varepsilon_j \tag{A.44}$$

$$\varepsilon_i = S_{ij}\sigma_j \tag{A.45}$$

Obviously, the number of free indices no longer denotes the order of the tensor. Also, the range on the indices no longer denotes the number of spatial dimensions. If the stress and strain tensors are symmetric (they are if no body couples act on an element), then

$$\sigma_{ij} = \sigma_{ji} \qquad \varepsilon_{ij} = \varepsilon_{ji} \tag{A.46}$$

and, therefore, the number of independent stresses and strains is reduced to six each as in Table 2-1. This type of symmetry leads to a reduction of the number of independent components of C_{ij} and S_{ij} from 81 to 36 in 3-space. The C_{ij} and S_{ij} can further be shown to be symmetric (see Section 2.2), that is,

$$C_{ij} = C_{ji} \qquad S_{ij} = S_{ji} \tag{A.47}$$

whereupon the number of independent components of C_{ij} and S_{ij} is further reduced from 36 to 21 in 3-space. The stiffness matrix is then (the compliance matrix is similar)

$$C_{ij} = [C] = \begin{bmatrix} C_{11} & C_{12} & C_{13} & C_{14} & C_{15} & C_{16} \\ C_{12} & C_{22} & C_{23} & C_{24} & C_{25} & C_{26} \\ C_{13} & C_{23} & C_{33} & C_{34} & C_{35} & C_{36} \\ C_{14} & C_{24} & C_{34} & C_{44} & C_{45} & C_{46} \\ C_{15} & C_{25} & C_{35} & C_{45} & C_{55} & C_{56} \\ C_{16} & C_{26} & C_{36} & C_{46} & C_{56} & C_{66} \end{bmatrix} \tag{A.48}$$

wherein the relation of a component of C_{ij} to that of C_{ijkl} is rather complex.

A.2.4 Matrix Form of Tensor Transformations

Tensors can easily be written in matrix form. For example, a vector a_i can be represented with a column matrix:

$$a_i = [A] = \begin{bmatrix} A_1 \\ A_2 \\ A_3 \end{bmatrix} \tag{A.49}$$

or a row matrix

$$a_i = [A] = [A_1 \quad A_2 \quad A_3] \tag{A.50}$$

Also, a second-order tensor can be written

$$a_{ij} = [A] = \begin{bmatrix} A_{11} & A_{12} & A_{13} \\ A_{21} & A_{22} & A_{23} \\ A_{31} & A_{32} & A_{33} \end{bmatrix} \tag{A.51}$$

or in contracted notation as a column (or row) matrix:

$$a_i = [A] = \begin{bmatrix} A_1 \\ A_2 \\ A_3 \\ A_4 \\ A_5 \\ A_6 \\ A_7 \\ A_8 \\ A_9 \end{bmatrix} \tag{A.52}$$

A fourth-order tensor can be written as a 9×9 array in analogy to Equation (A.51) but, by use of contracted notation, is sometimes drastically simplified to a 6×6 symmetric array.

The stress-strain relations in this book are typically expressed in matrix form by use of contracted notation. Both the stresses and strains as well as the stress-strain relations must be transformed. First, the stresses transform for a rotation about the z-axis as in Figure A-1 according to

$$\{\sigma'\} = [T]\{\sigma\} \tag{A.53}$$

or

$$\begin{bmatrix} \sigma_1' \\ \sigma_2' \\ \sigma_3' \\ \sigma_4' \\ \sigma_5' \\ \sigma_6' \end{bmatrix} = \begin{bmatrix} \cos^2\theta & \sin^2\theta & 0 & 0 & 0 & 2\cos\theta\sin\theta \\ \sin^2\theta & \cos^2\theta & 0 & 0 & 0 & -2\cos\theta\sin\theta \\ 0 & 0 & 1 & 0 & 0 & 0 \\ 0 & 0 & 0 & \cos\theta & -\sin\theta & 0 \\ 0 & 0 & 0 & \sin\theta & \cos\theta & 0 \\ -\cos\theta\sin\theta & \cos\theta\sin\theta & 0 & 0 & 0 & \cos^2\theta - \sin^2\theta \end{bmatrix} \begin{bmatrix} \sigma_1 \\ \sigma_2 \\ \sigma_3 \\ \sigma_4 \\ \sigma_5 \\ \sigma_6 \end{bmatrix} \tag{A.54}$$

In two dimensions, this rotation simplifies to

$$\begin{bmatrix} \sigma_1' \\ \sigma_2' \\ \tau_{12}' \end{bmatrix} = \begin{bmatrix} \cos^2\theta & \sin^2\theta & 2\cos\theta\sin\theta \\ \sin^2\theta & \cos^2\theta & -2\cos\theta\sin\theta \\ -\cos\theta\sin\theta & \cos\theta\sin\theta & \cos^2\theta - \sin^2\theta \end{bmatrix} \begin{bmatrix} \sigma_1 \\ \sigma_2 \\ \tau_{12} \end{bmatrix} \tag{A.55}$$

which in graphical form is the well-known Mohr's circle. The strains transform in a similar manner as shown in Section 2.6 for a case of plane stress. The stiffness and compliance transformations are very complex even for a simple rotation about an axis as in Equation (A.33). The complete expressions are given by Tsai [A-1]. For plane stress states, the transformations of the reduced stiffnesses are given in Section 2.6.

REFERENCE

A-1 Stephen W. Tsai, *Mechanics of Composite Materials, Part II, Theoretical Aspects*, Air Force Materials Laboratory Technical Report, AFML-TR-66-149, November 1966.

Appendix B

MAXIMA AND MINIMA OF FUNCTIONS OF A SINGLE VARIABLE

Most engineering students are well aware that the first derivative of a continuous function is zero at a maximum or minimum of the function. Fewer recall that the sign of the second derivative signifies whether the stationary value determined by a zero first derivative is a maximum or a minimum. Even fewer are aware of what to do if the second derivative happens to be zero. Thus, this appendix is presented to put finding relative maxima and minima of a function on a firm foundation.

Consider a function V of a single variable x, V(x), for which a stationary value occurs at $x = x_1$, i.e.,

$$\left.\frac{dV}{dx}\right|_{x=x_1} = 0 \qquad \text{(B.1)}$$

Such a stationary value of V can be a relative maximum, a relative minimum, a neutral point, or an inflection point as shown in Figure B-1. There, Equation (B.1) is satisfied at points 1, 2, 3, 4, and 5. By inspection, the function V(x) has a relative minimum at points 1 and 4, a relative maximum at point 3, and an inflection point at point 2. Also shown in Figure B-1 at position 5 is a succession of neutral points for which all derivatives of V(x) vanish. A simple physical example of such stationary values is a bead on a wire shaped as in Figure B-1. That is, a minimum of V(x) (the total potential energy of the bead) corresponds to stable equilibrium, a maximum or inflection point to unstable equilibrium, and a neutral point to neutral equilibrium.

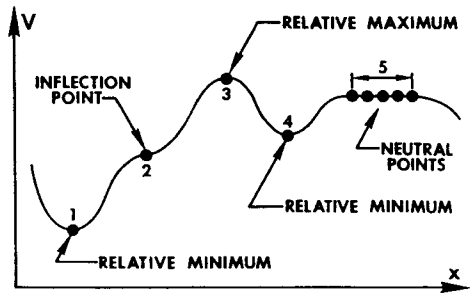

Figure B-1 Stationary Values of V(x)

To determine the specific character of a stationary point, first expand V(x) in a Taylor series about the stationary point $x = x_1$:

$$V(x_1 + h) = V(x_1) + h\left.\frac{dV}{dx}\right|_{x=x_1} + \frac{h^2}{2!}\left.\frac{d^2V}{dx^2}\right|_{x=x_1} + \frac{h^3}{3!}\left.\frac{d^3V}{dx^3}\right|_{x=x_1} + \cdots \quad \text{(B.2)}$$

where h is the expansion parameter about x_1, as shown in Figure B-2.

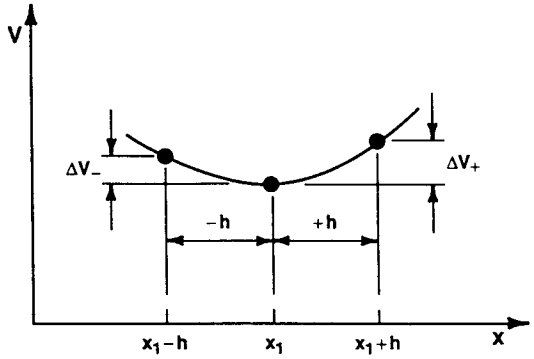

Figure B-2 Taylor Series Expansion of V(x) about $x = x_1$

Then, the change in V, ΔV, is

$$\Delta V = h\left.\frac{dV}{dx}\right|_{x=x_1} + \frac{h^2}{2!}\left.\frac{d^2V}{dx^2}\right|_{x=x_1} + \frac{h^3}{3!}\left.\frac{d^3V}{dx^3}\right|_{x=x_1} + \cdots \quad \text{(B.3)}$$

However, in accordance with the definition of a stationary point, Equation (B.1), the first term in Equation (B.3) for ΔV vanishes irrespective of the value or size of h so that

$$\Delta V = \frac{h^2}{2!}\left.\frac{d^2V}{dx^2}\right|_{x=x_1} + \frac{h^3}{3!}\left.\frac{d^3V}{dx^3}\right|_{x=x_1} + \frac{h^4}{4!}\left.\frac{d^4V}{dx^4}\right|_{x=x_1} + \cdots \quad \text{(B.4)}$$

The character of ΔV will determine the type of stationary value at $x = x_1$. Specifically, the dominant term in the Taylor series for ΔV must be examined in order to determine whether ΔV is always positive (a relative minimum), always negative (a relative maximum), sometimes negative and sometimes positive (an inflection point), or always zero (a neutral point). For ΔV to be positive, the leading term in the Taylor series, Equation (B.4), which is by inspection the largest term because h is a very small number, must be positive, i.e.,

$$\left.\frac{h^2}{2!}\frac{d^2V}{dx^2}\right|_{x=x_1} > 0 \quad \text{(B.5)}$$

But, even though h can have positive or negative values, because h is squared,

$$\left.\frac{d^2V}{dx^2}\right|_{x=x_1} > 0 \quad \text{(B.6)}$$

is sufficient for a minimum of V(x) at $x = x_1$. Similar reasoning leads to

$$\left.\frac{d^2V}{dx^2}\right|_{x=x_1} < 0 \quad \text{(B.7)}$$

as sufficient for a maximum of V(x) at $x = x_1$. However, if

$$\left.\frac{d^2V}{dx^2}\right|_{x=x_1} = 0 \quad \text{(B.8)}$$

then the second-derivative term in the Taylor series is no longer the dominant term.

Accordingly, the next term in the Taylor series

$$\left.\frac{h^3}{3!}\frac{d^3V}{dx^3}\right|_{x=x_1} \quad \text{(B.9)}$$

must be examined. Obviously, because h can have positive or negative values and is cubed, the term in Equation (B.9) can be positive or negative irrespective of the (nonzero) value of the third derivative. Thus, a nonzero third derivative of V(x) at $x = x_1$ corresponds to an inflection point of V(x) because ΔV can be either positive or negative.

If the term involving the third derivative, Equation (B.9) in the Taylor series, is zero, then the next higher term

$$\left.\frac{h^4}{4!}\frac{d^4V}{dx^4}\right|_{x=x_1} \quad \text{(B.10)}$$

is the dominant term. Of course, the second derivative must also be zero in order for us to need to consider the third-derivative term at all. Obviously, the conclusions reached for the second-derivative term are also valid for the fourth-derivative term, Equation (B.10).

Thus, by mathematical induction, the rules for determining the character of a stationary value of V(x) at $x = x_1$ are

(1) If the first nonzero derivative evaluated at $x = x_1$ is even and greater than zero, then $V(x_1)$ is a relative minimum.
(2) If the first nonzero derivative evaluated at $x = x_1$ is even and less than zero, then $V(x_1)$ is a relative maximum.
(3) If the first nonzero derivative evaluated at $x = x_1$ is odd, then $V(x_1)$ is an inflection point.
(4) If all derivatives are zero, then $V(x_1)$ is a neutral point.

These rules are schematically depicted in Figure B-3.

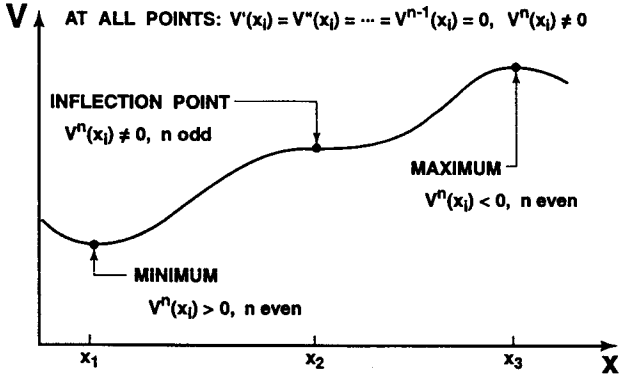

Figure B-3 Maxima, Minima, and Inflection Points of a Function of a Single Variable

The following simple examples are useful aids to understanding the foregoing rules.

(1) $V = x^2$ (plotted in Figure B-4)

$V_{,} = 2x$

$V_{,} = 0$ at $x = 0$

$V_{,,}\big|_{x=0} = 2$

$\therefore$ V(0) is a relative minimum

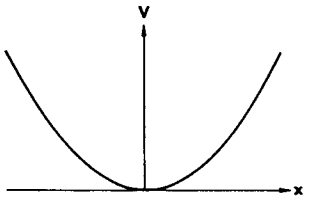

Figure B-4 $V = x^2$

(2) $V = x^3$ (plotted in Figure B-5)

$V_{,} = 3x^2$

$V_{,} = 0$ at $x = 0$

$V_{,,}\big|_{x=0} = 6x\big|_{x=0} = 0$

$V_{,,,}\big|_{x=0} = 6$

$\therefore$ V(0) is an inflection point

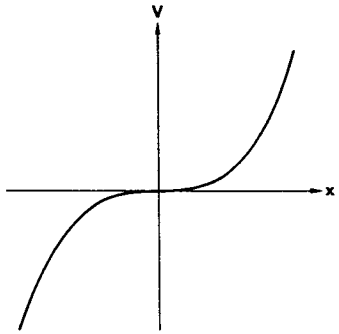

Figure B-5 $V = x^3$

(3) $V = x^4$ (plotted in Figure B-6)

$V_{,} = 4x^3$

$V_{,} = 0$ at $x = 0$

$V_{,,}\big|_{x=0} = 12x^2\big|_{x=0} = 0$

$V_{,,,}\big|_{x=0} = 24x\big|_{x=0} = 0$

$V^{A}_{,,,,}\big|_{x=0} = 24$

$\therefore$ V(0) is a minimum

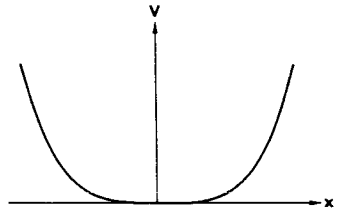

Figure B-6 $V = x^4$

(4) $V = x^{10}$ (Plotted in Figure B-7)

$V_{,} = 10x^9$

$V_{,} = 0$ at $x = 0$

By mathematical induction,

$V_{,,}\big|_{x=0} = 0$

$\vdots$

$V^{IX}\big|_{x=0} = 0$

$V^{X}\big|_{x=0} = 10!$

$\therefore$ V(0) is a minimum

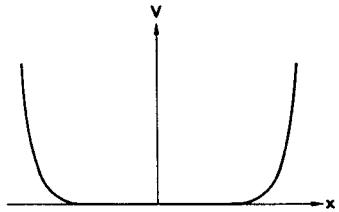

Figure B-7 $V = x^{10}$

If V is a function of more than one variable, then more complex criteria for determining maxima and minima are obtained. Generally, but not always, the second partial derivatives of the function with respect to all its variables are sufficient to determine the character of a stationary value of V. For such functions, the theory of quadratic forms as described by Langhaar [B-1] should be examined.

REFERENCE

(B-1) Henry L. Langhaar, *Energy Methods in Applied Mechanics*, Wiley, New York, 1962, pp. 308–328. (Also Krieger Publishing, Malabar, Florida, 1982.)

Appendix C

TYPICAL STRESS-STRAIN CURVES

Typical stress-strain curves are shown for the commonly used fiber-reinforced materials fiberglass-epoxy, boron-epoxy, and a representative graphite-epoxy. These curves are not accurate enough for design use!

C.1 FIBERGLASS-EPOXY STRESS-STRAIN CURVES

The curves for 3M XP251S fiberglass-epoxy are shown in Figures C-1 through C-5 [C-1]. Curves are given for both tensile and compressive behavior of the direct stresses. Note that the behavior in the fiber direction is essentially linear in both tension and compression. Transverse to the fiber direction, the behavior is nearly linear in tension, but very nonlinear in compression. The shear stress-strain curve is highly nonlinear. The Poisson's ratios (not shown) are essentially constant with values $\nu_{12} = .25$ and $\nu_{21} = .09$.

C.2 BORON-EPOXY STRESS-STRAIN CURVES

The curves for boron-epoxy are shown in Figures C-6 through C-11 [C-2]. As with fiberglass-epoxy, the behavior in the fiber direction is essentially linear in both tension and compression. In the direction transverse to the fibers, the behavior is nearly linear in tension and fairly nonlinear in compression. Finally, the behavior is highly nonlinear in shear. The Poisson's ratio, ν_{12}, decreases in tension and increases in compression.

C.3 GRAPHITE-EPOXY STRESS-STRAIN CURVES

The curves for Narmco 5605 graphite-epoxy shown in Figures C-12 through C-17 [C-2] are analogous in form to the boron-epoxy curves.

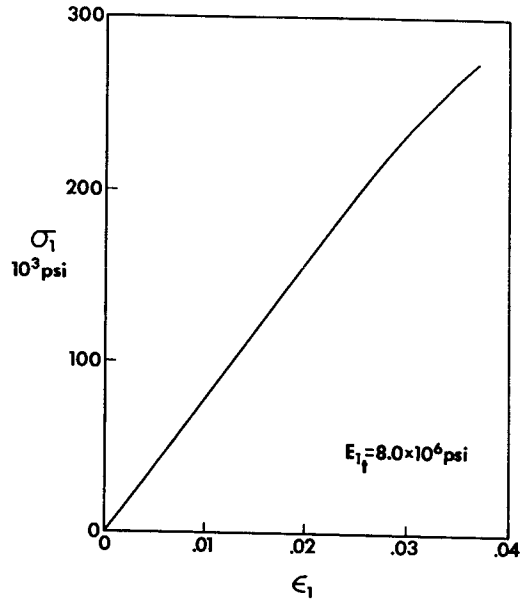

Figure C-1 Tensile $\sigma_1 - \varepsilon_1$ Curve for 3M XP251S Fiberglass-Epoxy *(Adapted from [C-1])*

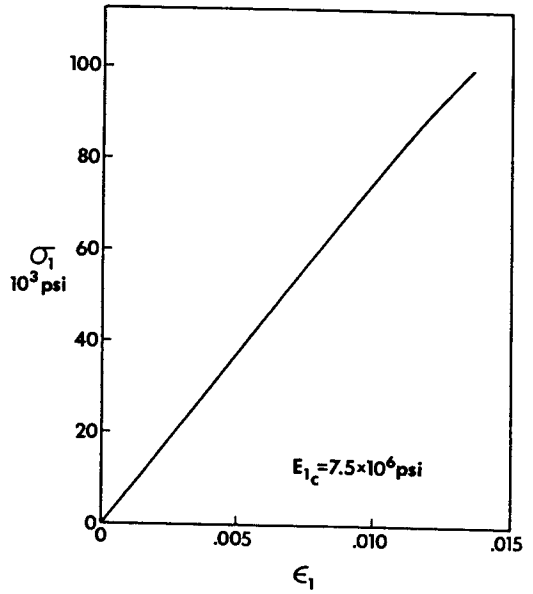

Figure C-2 Compressive $\sigma_1 - \varepsilon_1$ Curve for 3M XP251S Fiberglass-Epoxy *(Adapted from [C-1])*

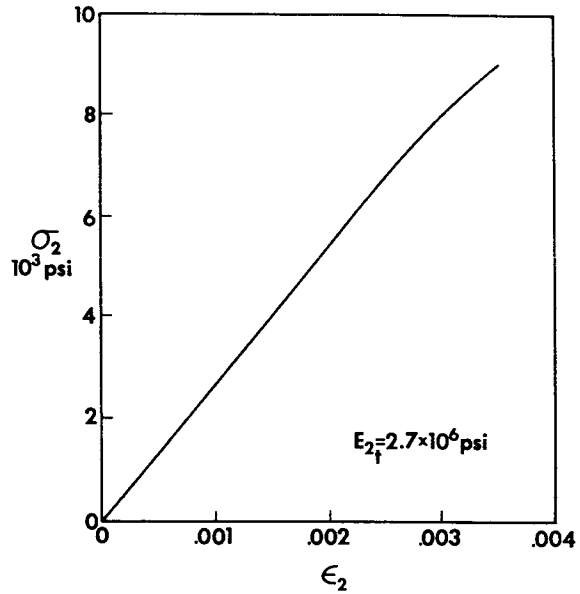

Figure C-3 Tensile $\sigma_2 - \varepsilon_2$ Curve for 3M XP251S Fiberglass-Epoxy *(Adapted from [C-1])*

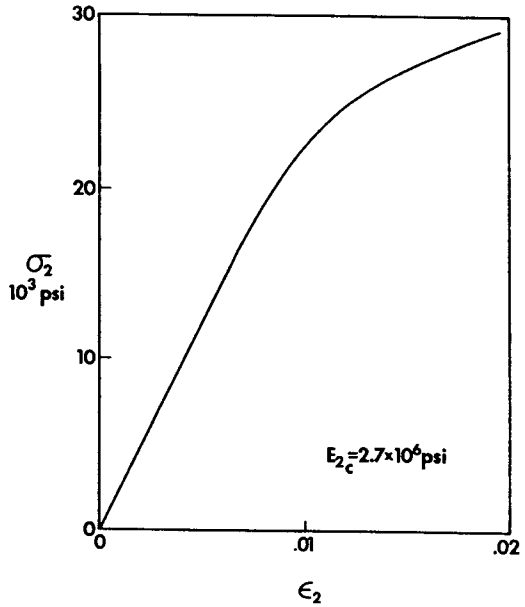

Figure C-4 Compressive $\sigma_2 - \varepsilon_2$ Curve for 3M XP251S Fiberglass-Epoxy *(Adapted from [C-1])*

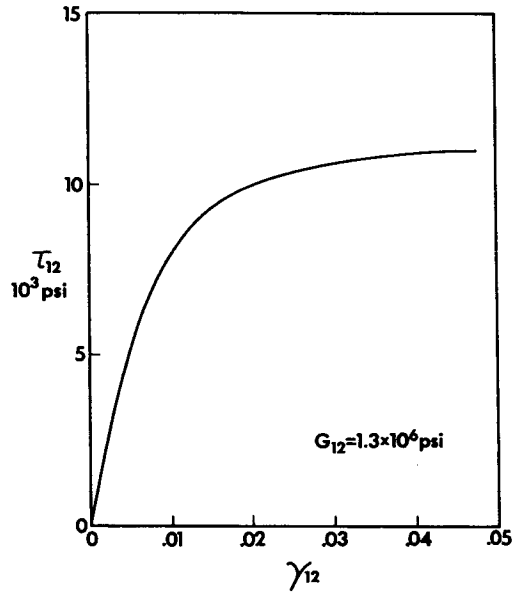

Figure C-5 Shear Stress-Strain Curve for 3M XP251S Fiberglass-Epoxy *(Adapted from [C-1])*

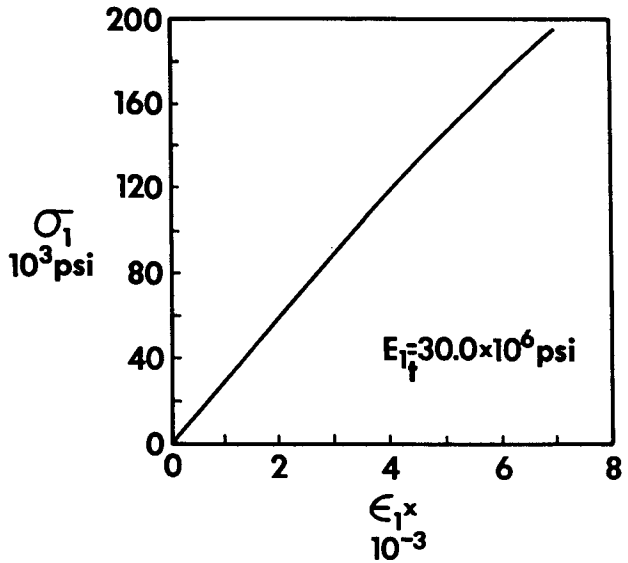

Figure C-6 Tensile $\sigma_1 - \varepsilon_1$ Curve for Boron-Epoxy *(Adapted from [C-2])*

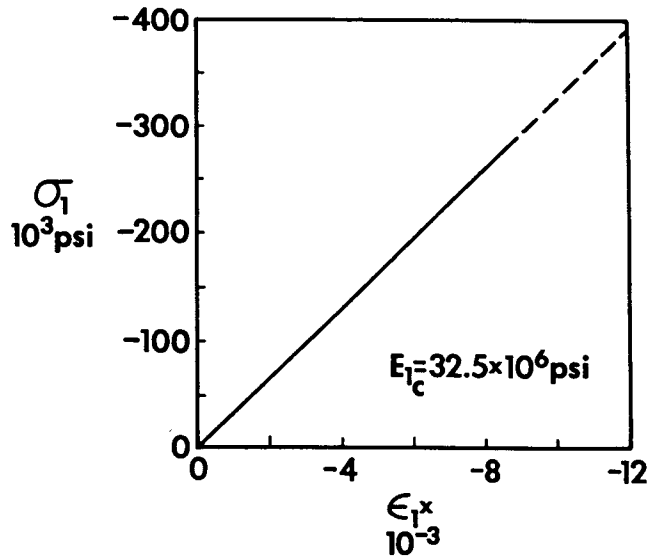

Figure C-7 Compressive $\sigma_1 - \varepsilon_1$ Curve for Boron-Epoxy *(Adapted from [C-2])*

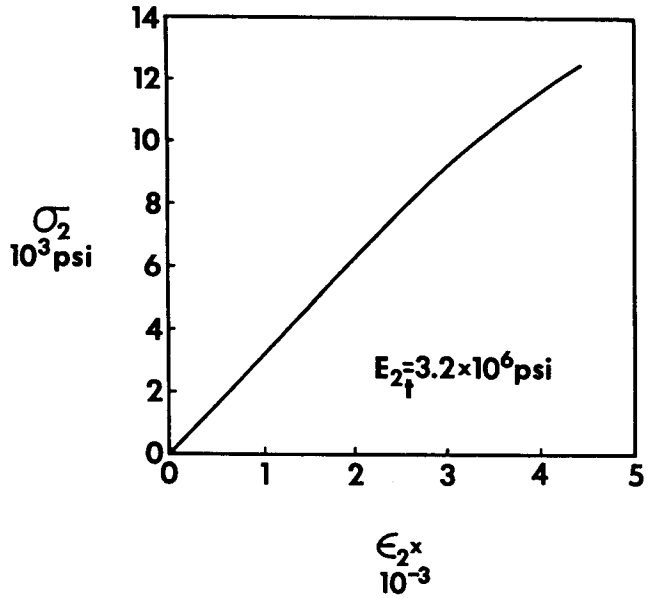

Figure C-8 Tensile $\sigma_2 - \varepsilon_2$ Curve for Boron-Epoxy *(Adapted from [C-2])*

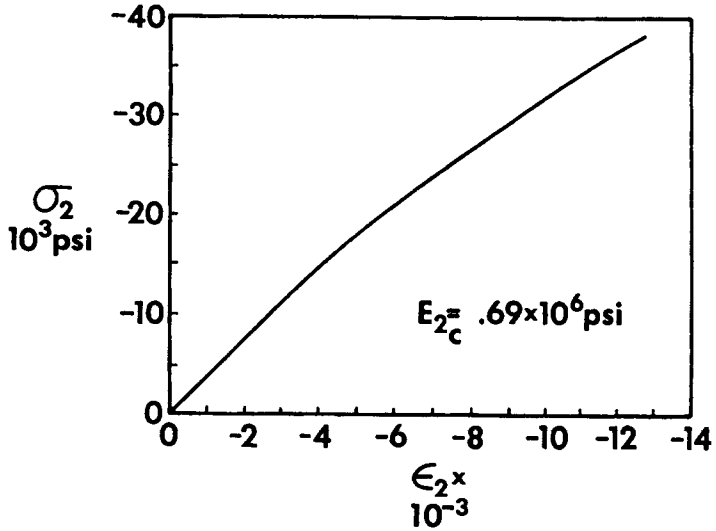

Figure C-9 Compressive $\sigma_2 - \varepsilon_2$ Curve for Boron-Epoxy *(Adapted from [C-2])*

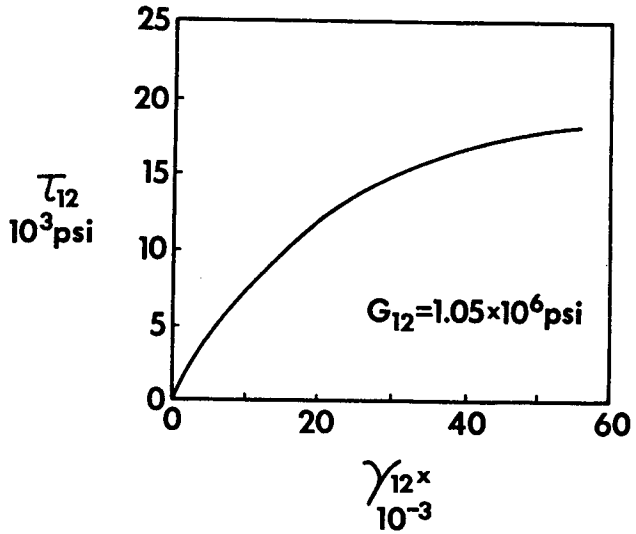

Figure C-10 Shear Stress-Strain Curve for Boron-Epoxy *(Adapted from [C-2])*

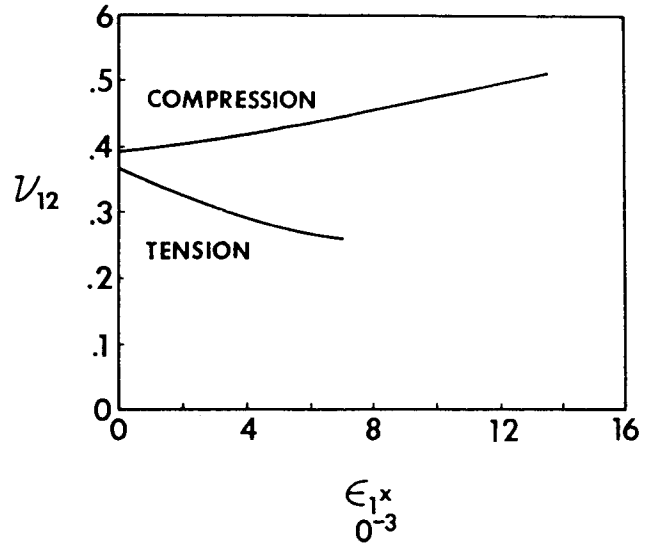

Figure C-11 Poisson's Ratio Curves for Boron-Epoxy *(Adapted from [C-2])*

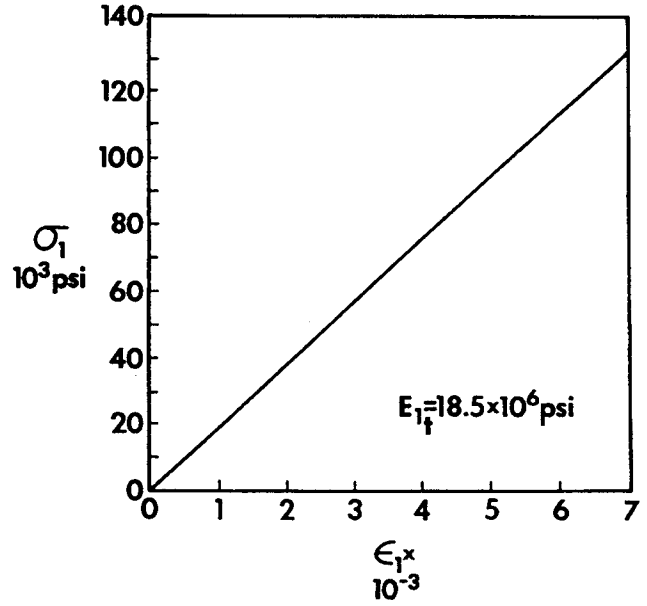

Figure C-12 Tensile $\sigma_1 - \varepsilon_1$ Curve for Narmco 5605 Graphite-Epoxy *(Adapted from [C-2])*

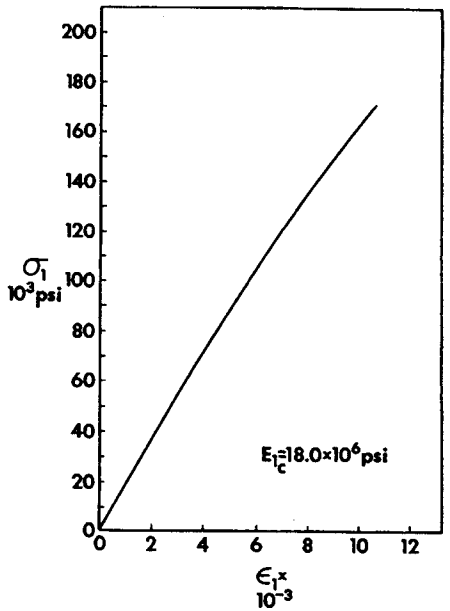

Figure C-13 Compressive $\sigma_1 - \varepsilon_1$ Curve for Narmco 5605 Graphite-Epoxy *(Adapted from [C-2])*

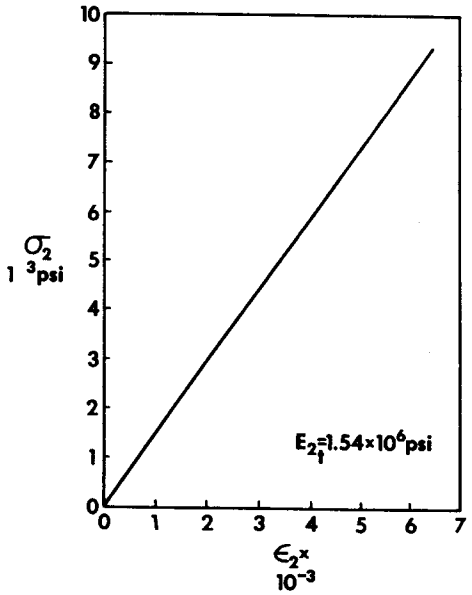

Figure C-14 Tensile $\sigma_2 - \varepsilon_2$ Curve for Narmco 5605 Graphite-Epoxy *(Adapted from [C-2])*

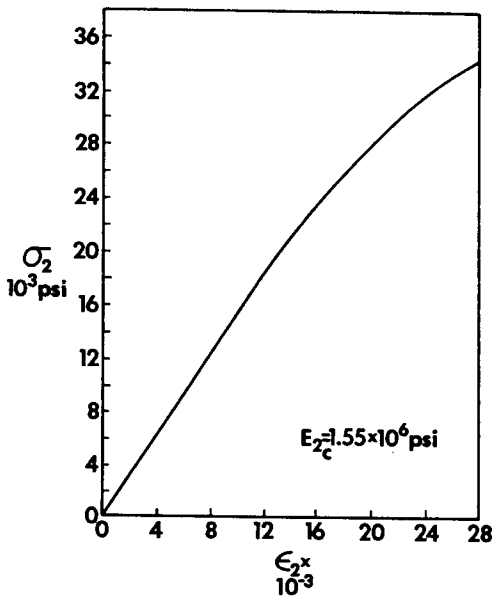

Figure C-15 Compressive $\sigma_2 - \varepsilon_2$ Curve for Narmco 5605 Graphite-Epoxy *(Adapted from [C-2])*

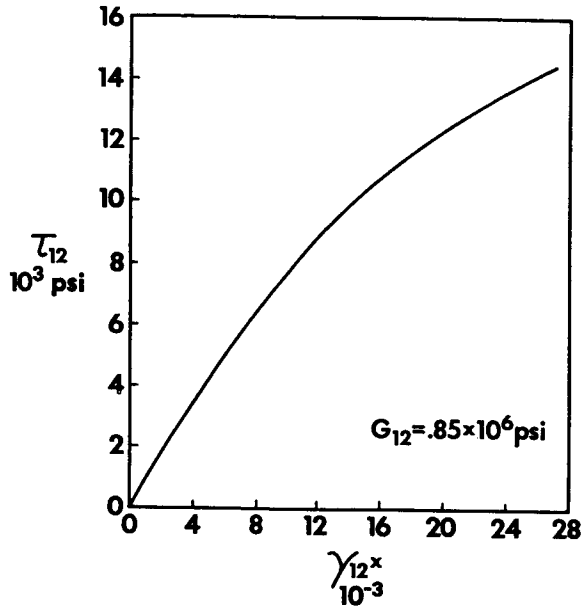

Figure C-16 Shear Stress-Strain Curve for Narmco 5605 Graphite-Epoxy *(Adapted from [C-2])*

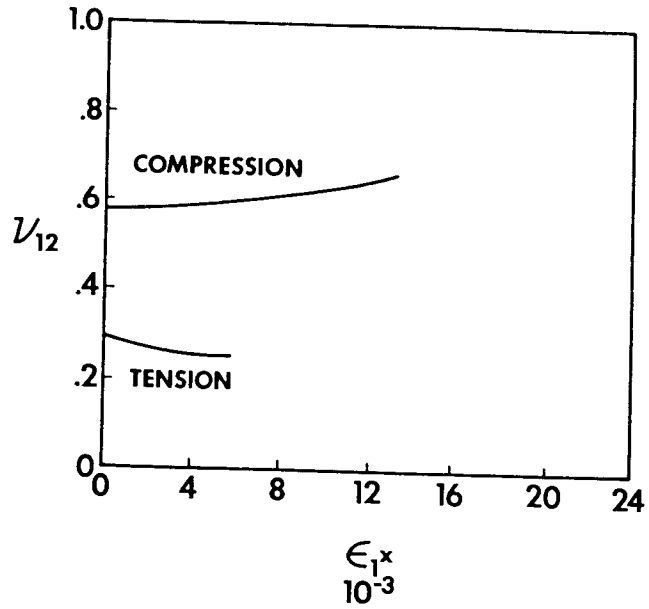

Figure C-17 Poisson's Ratio Curves for Narmco 5605 Graphite-Epoxy *(Adapted from [C-2])*

REFERENCES

C-1 *Plastics for Aerospace Vehicles, Part 1, Reinforced Plastics*, Military Handbook, MILHDBK-17A, January 1971.

C-2 J. E. Ashton, J. C. Halpin, and P. H. Petit, *Primer on Composite Materials: Analysis*, Technomic, Westport, Connecticut, 1969.

Appendix D

GOVERNING EQUATIONS FOR BEAM EQUILIBRIUM AND PLATE EQUILIBRIUM, BUCKLING, AND VIBRATION

D.1 INTRODUCTION

The equilibrium equations for a beam are derived to illustrate the derivation process and to serve as a review in preparation for addressing plates. Then, the plate equilibrium equations are derived for use in Chapter 5. Next, the plate buckling equations are discussed. Finally, the plate vibration equations are addressed. In each case, the pertinent boundary conditions are displayed. Nowhere in this appendix is reference needed to laminated beams or plates. All that is derived herein is applicable to any kind of beam or plate because only fundamental equilibrium, buckling, or vibration concepts are used.

D.2 DERIVATION OF BEAM EQUILIBRIUM EQUATIONS

Consider the differential element of a laterally and axially loaded beam as in Figure D-1. There, the axial force, shear force, moment, and lateral load are depicted along with the pertinent changes that occur along the length of the differential element.

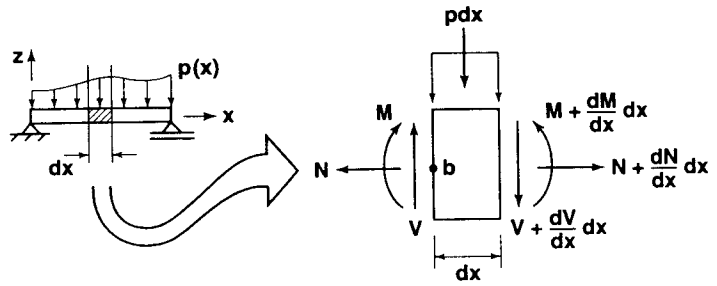

Figure D-1 Free-Body Diagram of a Beam Element

From force equilibrium in the x-direction,

$$-N+(N+\frac{dN}{dx})=0 \tag{D.1}$$

which simplifies to

$$\frac{dN}{dx}=0 \tag{D.2}$$

Therefore, unless axial loads are introduced along the beam, the axial force is constant.

From force equilibrium in the z-direction,

$$V-pdx-(V+\frac{dV}{dx}dx)=0 \tag{D.3}$$

which simplifies to

$$p=-\frac{dV}{dx} \tag{D.4}$$

Thus, the lateral loading causes a change in the shear force from point to point along the beam.

From moment equilibrium about point b in Figure D-1,

$$M+(pdx)\frac{dx}{2}+(V+\frac{dV}{dx}dx)dx-(M+\frac{dM}{dx}dx)=0 \tag{D.5}$$

Upon neglect of higher order terms in $(dx)^2$,

$$Vdx-(\frac{dM}{dx})dx=0 \tag{D.6}$$

whereupon

$$V=\frac{dM}{dx} \tag{D.7}$$

Thus, a shear force causes a change in the moment from point to point along the beam.

The boundary conditions on the ends of the beam are

$$\begin{array}{lll} N=\overline{N} & \text{or} & u=\overline{u} \\ M=\overline{M} & \text{or} & w'=\overline{w}' \\ V=\overline{V} & \text{or} & w=\overline{w} \end{array} \tag{D.8}$$

where u and w are displacements in the x- and z-directions, respectively, and the prime denotes a derivative with respect to x. The boundary conditions in the left-hand column are prescribed force (or moment) quantities, and the boundary conditions in the right-hand column are prescribed displacements or slopes. Only one of either the forces (or moment) or displacements can be prescribed. Thus, there are three boundary conditions at each end of the beam. For example, for the beam with a simply supported end in Figure D-2, there is no transverse deflection and no moment (free rotation), but two axial boundary conditions are possible.

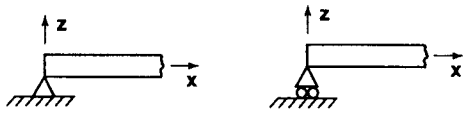

$w=0$ $\quad$ $w=0$
$M_x=0$ $\quad$ $M_x=0$
$u=0$ $\quad$ $N_x=0$

Figure D-2 Boundary Conditions for a Simply Supported End Beam

Alternatively, the beam end could have complete rotational restraint and no transverse displacement, i.e., clamped. However, a third boundary condition exists in Figure D-3 just as in Figure D-2. That is, an axial condition on displacement or force must exist in addition to the conditions usually thought of as comprising a clamped-end condition. Note that the block-like device at the end of the beam prevents rotation and transverse deflection. A similar device will be used later for plates. Whether all of the three boundary conditions can actually be enforced depends on the order of the differential equation set when (necessarily approximate) force-strain and moment-curvature relations are substituted in Equations (D.2), (D.4), and (D.7).

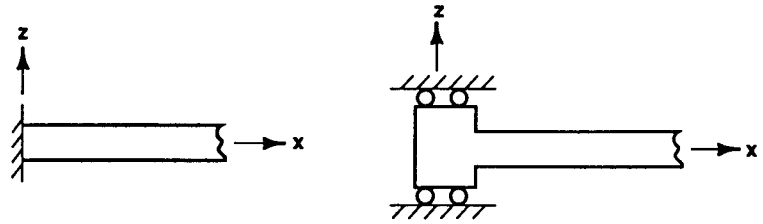

$w=0$ $\quad$ $w=0$
$w_{,x}=0$ $\quad$ $w_{,x}=0$
$u=0$ $\quad$ $N_x=0$

Figure D-3 Boundary Conditions for a Clamped-End Beam

Note that the shear equation, Equation (D.6), can be substituted in the transverse load equation, Equation (D.4), to get

$$p=-\frac{dV}{dx}=-\frac{d}{dx}(\frac{dM}{dx})=-\frac{d^2M}{dx^2} \tag{D.9}$$

or, upon substitution of the approximate moment-curvature relation,

$$M=-EIw'' \tag{D.10}$$

we get

$$p=EIw'''' \tag{D.11}$$

Thus, a fourth-order differential equation such as Equation (D.11) has four boundary conditions which are the second and third of the conditions in Equation (D.8) at each end of the beam. The first boundary condition in Equation (D.8) applies to the axial force equilibrium equation, Equation (D.2), or its equivalent in terms of displacement (u).

This review of the foregoing simple derivation will help you to understand the following derivation of the plate equilibrium equations. The major difference between plate and beam problems is that beams are one-dimensional and plates are two-dimensional. Therefore, beams have ordinary differential equations as governing equations whereas plates have partial differential equations. Moreover, in the derivation of the governing differential equations, there will necessarily be more force equilibrium and moment equilibrium equations for plates than for beams.

D.3 DERIVATION OF PLATE EQUILIBRIUM EQUATIONS

Consider the differential element of a plate with accompanying in-plane forces per unit width, N_x, N_y, and N_{xy}, and moments per unit width, M_x, M_y, and M_{xy}, plus the shear forces per unit width, Q_x and Q_y, subjected to the lateral pressure p(x,y). For emphasis, all force and moment quantities are expressed per unit of width of the plate element, i.e., they are all local intensities. The differential element is shown in Figure D-4 without the restraining forces and moments, i.e., the differential element in Figure D-4 is *not* a free-body diagram! Each of the three restraining systems, in-plane forces, lateral forces, and moments per unit width, is shown on a separate figure for the sake of clarity even though all act simultaneously. In Figures D-5, D-6, and D-7, respectively, the changes in forces and moments are expressed as partial derivatives times the pertinent differential element dimension.

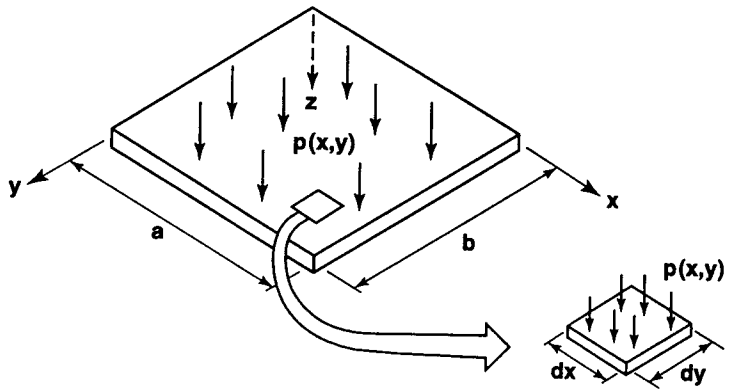

Figure D-4 Plate under Lateral Load

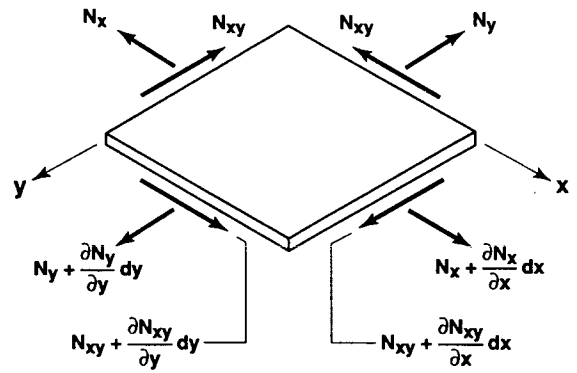

Figure D-5 In-Plane Forces on a Differential Element

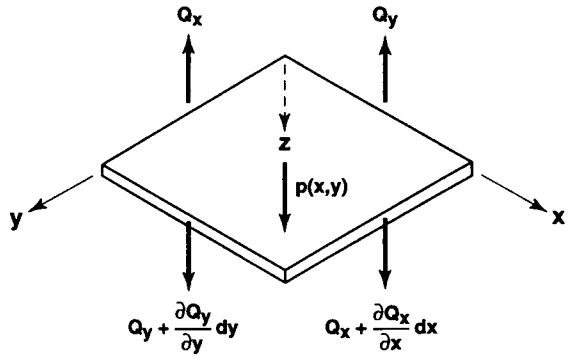

Figure D-6 Lateral Forces on a Differential Element

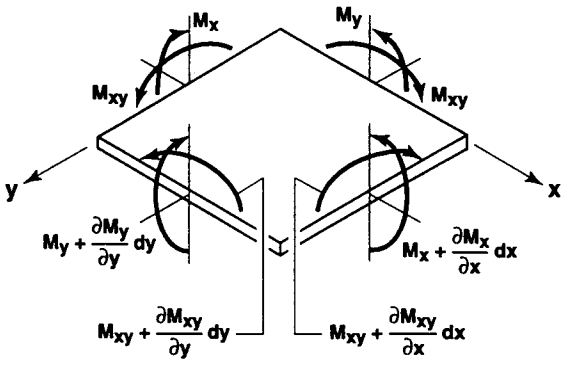

Figure D-7 Moments on a Differential Element

From Figure D-5 for in-plane forces, force equilibrium in the x-direction yields

$$-N_x dy - N_{xy} dx + (N_{xy} + \frac{\partial N_{xy}}{\partial y} dy)dx + (N_x + \frac{\partial N_x}{\partial x} dx)dy = 0 \quad \text{(D.12)}$$

Upon cancellation of like terms and division by dxdy,

$$\frac{\partial N_x}{\partial x} + \frac{\partial N_{xy}}{\partial y} = 0 \quad \text{(D.13)}$$

Similarly, force equilibrium in the y-direction yields

$$-N_{xy} dy - N_y dx + (N_y + \frac{\partial N_y}{\partial y} dy)dx + (N_{xy} + \frac{\partial N_{xy}}{\partial x} dx)dy = 0 \quad \text{(D.14)}$$

Upon cancellation of like terms and division by dxdy,

$$\frac{\partial N_{xy}}{\partial x} + \frac{\partial N_y}{\partial y} = 0 \quad \text{(D.15)}$$

From Figure D-6 for lateral forces, force equilibrium in the z-direction yields

$$-Q_x dy - Q_y dx + (Q_y + \frac{\partial Q_y}{\partial y} dy)dx + (Q_x + \frac{\partial Q_x}{\partial x} dx)dy + p\,dx\,dy = 0 \quad \text{(D.16)}$$

Upon cancellation of like terms and division by dxdy,

$$\frac{\partial Q_x}{\partial x} + \frac{\partial Q_y}{\partial y} + p = 0 \quad \text{(D.17)}$$

From moment equilibrium about the x-axis to which the moments of Figure D-7 and the lateral forces of Figure D-6 contribute (but not the in-plane forces of Figure D-5 because they are either parallel to or perpendicular to the x-axis),

$$M_{xy} dy + M_y dx - (M_y + \frac{\partial M_y}{\partial y} dy)dx - (M_{xy} + \frac{\partial M_{xy}}{\partial x} dx)dy - Q_x dy \frac{dy}{2} + (Q_y + \frac{\partial Q_y}{\partial y} dy)dxdy + (Q_x + \frac{\partial Q_x}{\partial x} dx)dy \frac{dy}{2} + p\,dx\,dy \frac{dy}{2} = 0 \quad \text{(D.18)}$$

Upon cancellation of like terms, neglect of higher order terms in $dx(dy)^2$, and division by dxdy,

$$Q_y = \frac{\partial M_{xy}}{\partial x} + \frac{\partial M_y}{\partial y} \quad \text{(D.19)}$$

Similarly, moment equilibrium about the y-axis yields

$$Q_x = \frac{\partial M_x}{\partial x} + \frac{\partial M_{xy}}{\partial y} \quad \text{(D.20)}$$

The equations for the shear forces, Q_x and Q_y, Equations (D.20) and (D.19), can be substituted in the z-direction force-equilibrium equation, Equation (D.17), to get

$$\frac{\partial}{\partial x}(\frac{\partial M_x}{\partial x} + \frac{\partial M_{xy}}{\partial y}) + \frac{\partial}{\partial y}(\frac{\partial M_{xy}}{\partial x} + \frac{\partial M_y}{\partial y}) + p = 0 \quad \text{(D.21)}$$

or

$$\frac{\partial^2 M_x}{\partial x^2} + 2\frac{\partial^2 M_{xy}}{\partial x \partial y} + \frac{\partial^2 M_y}{\partial y^2} = -p \quad \text{(D.22)}$$

The boundary conditions for a plate would appear to be

on edges x = constant:

$$\begin{aligned} N_x &= \bar{N}_x \quad \text{or} \quad u = \bar{u} \\ N_{xy} &= \bar{N}_{xy} \quad \text{or} \quad v = \bar{v} \\ M_x &= \bar{M}_x \quad \text{or} \quad \frac{\partial w}{\partial x} = \frac{\partial \bar{w}}{\partial x} \\ M_{xy} &= \bar{M}_{xy} \quad \text{or} \quad w_{,xy} = \bar{w}_{,xy} \\ Q_x &= \bar{Q}_x \quad \text{or} \quad w = \bar{w} \end{aligned} \quad \text{(D.23)}$$

on edges y = constant:

$$\begin{aligned} N_y &= \bar{N}_y \quad \text{or} \quad v = \bar{v} \\ N_{xy} &= \bar{N}_{xy} \quad \text{or} \quad u = \bar{u} \\ M_y &= \bar{M}_y \quad \text{or} \quad \frac{\partial w}{\partial y} = \frac{\partial \bar{w}}{\partial y} \\ M_{xy} &= \bar{M}_{xy} \quad \text{or} \quad w_{,xy} = \bar{w}_{,xy} \\ Q_y &= \bar{Q}_y \quad \text{or} \quad w = \bar{w} \end{aligned} \quad \text{(D.24)}$$

In plate theory, the problem is reduced from the deformation of a solid body to the deformation of a *surface* by use of the Kirchhoff hypothesis (normals to the undeformed middle surface remain straight and normal after deformation, etc., as discussed in Chapter 4). Then, we attempt to apply boundary conditions to that surface which is usually the middle surface of the plate. There should be no surprise that the boundary conditions for the unapproximated solid body are not the same as those for the solid approximated with a surface. The problem arises when these boundary conditions are applied to an approximate set of equilibrium equations that result when force-strain and moment-curvature

relations are substituted in Equations (D.13), (D.15), and (D.22). For example, if we substitute approximate moment-curvature relations,

$$M_x = \frac{Et^3}{12(1-\nu^2)}(\kappa_x + \nu\kappa_y)$$
$$M_y = \frac{Et^3}{12(1-\nu^2)}(\kappa_y + \nu\kappa_x) \qquad \text{(D.25)}$$
$$M_{xy} = \frac{Et^3}{24(1-\nu^2)}\kappa_{xy}$$

and approximate curvature expressions,

$$\kappa_x = -\frac{\partial^2 w}{\partial x^2}$$
$$\kappa_y = -\frac{\partial^2 w}{\partial y^2} \qquad \text{(D.26)}$$
$$\kappa_{xy} = -\frac{\partial^2 w}{\partial x \partial y}$$

then Equation (D.22) becomes

$$\frac{\partial^4 w}{\partial x^4} + 2\frac{\partial^4 w}{\partial x^2 \partial y^2} + \frac{\partial^4 w}{\partial y^4} = \frac{p}{D} \qquad \text{(D.27)}$$

This fourth-order partial differential equation can have only two boundary conditions on each edge for a total of eight boundary conditions. Thus, some step in the approximations leading to Equation (D.27) must limit the boundary conditions from those displayed in Equations (D.23) and (D.24) because there three boundary conditions occur for each edge for a total of twelve boundary conditions. This dilemma has been resolved historically by Kirchhoff who proved that the boundary conditions *consistent* with the approximate differential equation, Equation (D.27), are

$$K_x = Q_x - \frac{\partial M_{xy}}{\partial y} = \overline{K}_x \quad \text{or} \quad w = \overline{w}$$
$$M_x = \overline{M}_x \quad \text{or} \quad w_{,x} = \overline{w}_{,x} \qquad \text{(D.28)}$$
$$K_y = Q_y - \frac{\partial M_{xy}}{\partial x} = \overline{K}_y \quad \text{or} \quad w = \overline{w}$$
$$M_y = \overline{M}_y \quad \text{or} \quad w_{,y} = \overline{w}_{,y}$$

where K_x and K_y are called the Kirchhoff shear forces.

Note that the in-plane boundary conditions do not present such a dilemma. For example, if approximate force-strain relations

$$N_x = \frac{Et}{1-\nu^2}(u_{,x} + \nu v_{,y})$$
$$N_y = \frac{Et}{1-\nu^2}(v_{,y} + \nu u_{,x}) \qquad \text{(D.29)}$$
$$N_{xy} = \frac{Et}{2(1+\nu)}(u_{,y} + v_{,x})$$

are substituted in the in-plane equilibrium equations, Equations (D.13) and (D.15), then

$$u_{,xx} + \nu v_{,xy} + (1-\nu)(u_{,yy} + v_{,xy}) = 0$$
$$(1-\nu)(u_{,yx} + v_{,xx}) + v_{,yy} + \nu u_{,xy} = 0 \qquad \text{(D.30)}$$

This set of partial differential equations has two boundary conditions at each edge which are represented by the first two choices in Equations (D.23) and (D.24). When the geometric boundary condition of edge restraint in the z-direction is considered, the Kirchhoff shear force is not active as a boundary condition.

The types of boundary conditions that then exist for a simply supported edge with constant values of x are shown in Figure D-8 along with a geometric interpretation of their in-plane conditions. In all four simply supported edge boundary conditions, the knife-edge support prevents transverse displacement, w, and allows free rotation (about the plate middle surface which is difficult to visualize), so the moment is zero, i.e., $M_x = 0$. For S1 conditions, the base of the knife-edge support cannot move, so the in-plane displacements, u and v, must be zero. For S2 conditions, the knife-edge support rolls without resistance in the x-direction, but cannot move in the y-direction, so $N_x = 0$ ($u \neq 0$) and $v = 0$. For S3 conditions, the knife-edge support rolls without resistance in the y-direction, but cannot move in the x-direction, so $N_{xy} = 0$ ($v \neq 0$) and $u = 0$. Finally, for S4 conditions, the knife-edge support can roll without resistance in both the x- and y-directions, so $N_x = 0$ ($u \neq 0$) and $N_{xy} = 0$ ($v \neq 0$).

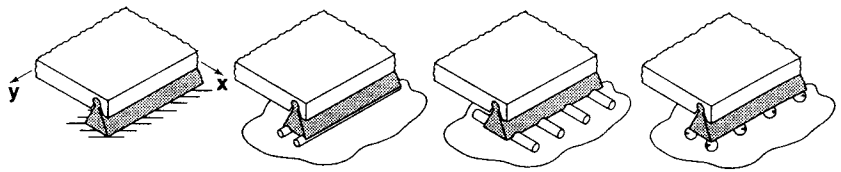

S1	S2	S3	S4
$w = 0$	$w = 0$	$w = 0$	$w = 0$
$M_x = 0$	$M_x = 0$	$M_x = 0$	$M_x = 0$
$u = 0$	$N_x = 0$	$u = 0$	$N_x = 0$
$v = 0$	$v = 0$	$N_{xy} = 0$	$N_{xy} = 0$

Figure D-8 Simply Supported Edge Boundary Conditions for a Plate

The analogous four boundary conditions for clamped edges are more difficult to perceive. The first impression for what constitutes a clamped edge might be the C1 condition of no displacements, u, v, and w, and no rotation, $\partial w/\partial x$. However, a clamped edge is commonly interpreted to mean only that the transverse displacement, w, and the edge rotation, $\partial w/\partial x$, are both zero *without specifying any in-plane displacement conditions.* Accordingly, the clamping fixture in Figures D-3 and D-9 restrains both transverse displacement, w, and edge rotation, $\partial w/\partial x$. The way the clamping fixture is itself supported determines the in-plane boundary conditions. Thus, if the clamping fixture cannot move in the x-y plane, then u = 0 and v = 0 for the C1 boundary condition. Or, if the clamping fixture can roll in the x-direction, then $N_x = 0$, but v = 0 because no displacement occurs in the y-direction for the C2 boundary condition. Next, if the clamping fixture can roll in the y-direction but not in the x-direction, then $N_{xy} = 0$ and u = 0. Finally, if the clamping fixture can roll in both the x- and y-directions as if supported on frictionless balls, then the in-plane forces must be zero, i.e., $N_x = 0$ and $N_{xy} = 0$.

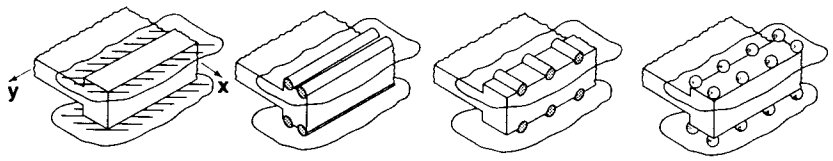

C1	C2	C3	C4
w = 0	w = 0	w = 0	w = 0
$w_{,x}$	$w_{,x}$	$w_{,x}$	$w_{,x}$
u = 0	$N_x = 0$	u = 0	$N_x = 0$
v = 0	v = 0	$N_{xy} = 0$	$N_{xy} = 0$

Figure D-9 Clamped-Edge Boundary Conditions for a Plate

Now recognize an apparent contradiction in classical plate theory. First, from force equilibrium in the z-direction, we saw transverse shear forces Q_x and Q_y must exist to equilibrate the lateral pressure, p. However, these shear forces can only be the resultant of certain transverse shearing stresses, i.e.,

$$Q_x = \int \tau_{xz} dz \qquad Q_y = \int \tau_{yz} dz \tag{D.31}$$

However, these transverse shearing stresses were neglected implicitly when we adopted the Kirchhoff hypothesis of lines that were normal to the undeformed middle surface remaining normal after deformation in Section 4.2.2 on classical lamination theory. That hypothesis is interpreted to mean that transverse shearing strains are zero, and, hence, by the stress-strain relations, the transverse shearing stresses are zero. The Kirchhoff hypothesis was also adopted as part of classical plate theory in Section 5.2.1.

The contradiction is that the transverse shearing stresses τ_{xz} and τ_{yz} must be nonzero as demonstrated with the equilibrium equations, yet we assume these stresses to be zero by virtue of the Kirchhoff hypothesis. Where does the truth lie? Of course, the equilibrium equations are fundamental to all our deliberations, so the transverse shearing stresses must exist. Accordingly, even though we have *supposedly* ignored the transverse shearing stresses, we can actually calculate their resultants by use of the equilibrium relations in Equations (D.19) and (D.20). However, we have no information on the distribution of the transverse shearing stresses through the thickness of the plate.

We can reexamine the beam problem to determine the distribution of the transverse shearing stress τ_{xz}. We know that the resultant of τ_{xz} is V which we obtain from Equation (D.7), i.e.,

$$V = \frac{dM}{dx} \tag{D.32}$$

The distribution of τ_{xz} for an isotropic beam of rectangular cross section comes from integration of the the stress-equilibrium equation

$$\tau_{xz,z} = -\sigma_{x,x} \tag{D.33}$$

to obtain

$$\tau_{xz} = \frac{V}{2I}\left[\frac{t^2}{4} - z^2\right] \tag{D.34}$$

which is the usual parabolic shear stress distribution.

However, the foregoing derivation is valid only for isotropic beams of rectangular cross section. For beams of nonrectangular cross section, the parabolic stress distribution is not correct. Also, for laminated beams, the parabolic distribution is most assuredly incorrect because of layer inhomogeneity. In fact, for laminated beams, we must expect different shapes of stress distribution in each layer as seen in Figure 6-19 for wide beams (there interpreted as cylindrical bending of a long strip, i.e., a special plate).

Accordingly, we find it difficult to determine the distribution of the transverse shearing stress in a beam, much less in a plate. Procedures for determining the approximate transverse shear stress distribution in plates are described in Section 6.5.2.

We have observed that the kinematics and the kinetics of the plate (and beam) problem are not consistent. However, such inconsistencies are an inherent part of mechanics of materials which must contain some inconsistencies; otherwise, mechanics of materials would be elasticity!

D.4 PLATE BUCKLING EQUATIONS

The plate buckling equations inherently cannot be derived from the equilibrium of a differential element. Instead, the buckling problem represents the departure from the equilibrium state when that state becomes unstable because the in-plane load is too high. The departure from the equilibrium state is accompanied by waves or buckles in the surface of the plate. That is, the plate cannot remain flat when the

buckling load is exceeded. Description of the process necessary to derive the buckling equations is far too lengthy to present here. Instead, see Jones [D-1], Timoshenko and Gere [D-2], or Brush and Almroth [D-3].

Instead of displacements, forces, and moments as in the equilibrium or bending problem, the buckling problem is formulated in terms of variations or changes in the displacements, forces, and moments from their values in the prebuckling equilibrium state. Thus, instead of u, v, w as displacements, we have δu, δv, δw as buckling displacements (in addition to the displacements that occurred in the equilibrium state prior to buckling). Such displacements might only consist of end shortening of a column, but no transverse displacement. Also, instead of N_x, N_y, N_{xy}, M_x, M_y, M_{xy}, we have δN_x, δN_y, δN_{xy}, δM_x, δM_y, δM_{xy}. The graphical depiction of the buckling boundary conditions is the same as for the equilibrium boundary conditions in Figures D-8 and D-9.

The buckling problem is *separate* from the equilibrium problem. Thus, the buckling boundary conditions are formulated somewhat differently from those of the equilibrium problem. For instance, all buckling boundary conditions are homogeneous, i.e., the right-hand sides of all the variable equations are zero. For example, along an edge x = constant:

$$\begin{aligned} \delta N_x &= 0 \quad \text{or} \quad \delta u = 0 \\ \delta M_x &= 0 \quad \text{or} \quad \partial(\delta w)/\partial x = 0 \\ \delta K_x &= 0 \quad \text{or} \quad \delta w = 0 \\ \delta N_{xy} &= 0 \quad \text{or} \quad \delta v = 0 \end{aligned} \tag{D.35}$$

The load in the buckling problem is introduced in the prebuckling equilibrium state, and the value of the load is the objective of the eigenvalue or proper value or characteristic value problem. That is, the buckling load *is* the eigenvalue, proper value or characteristic value of the buckling problem. The eigenvalue appears in the governing differential equations, but not in the boundary conditions.

D.5 PLATE VIBRATION EQUATIONS

The vibration problem is strictly analogous to the buckling problem. Accordingly, because of similar complexity, the derivation of the vibration equations is not attempted. The vibration boundary conditions are identical to the buckling boundary conditions.

REFERENCES

D-1 Robert M. Jones, *Buckling of Bars, Plates, and Shells*, to be published.

D-2 Stephen P. Timoshenko and James M. Gere, *Theory of Elastic Stability*, 2nd Edition, McGraw-Hill, New York, 1961.

D-3 D. O. Brush and B. O. Almroth, *Buckling of Bars, Plates, and Shells*, McGraw-Hill, New York, 1975.

Index

-A-

-B-

-C-

-D-

-E-

-F-

-G-

-H-

-I-

-J-

-K-

-L-

-M-

-N-

-O-

-P-

-Q-

-R-

-S-

-T-

-U-

-V-

-W-

-Y-

-Z-